CYTOKINES AND PAIN

EDITED BY: Waldiceu A. Verri, Felipe Almeida Pinho-Ribeiro and Larissa G. Pinto

PUBLISHED IN: Frontiers in Immunology and Frontiers in Neurology

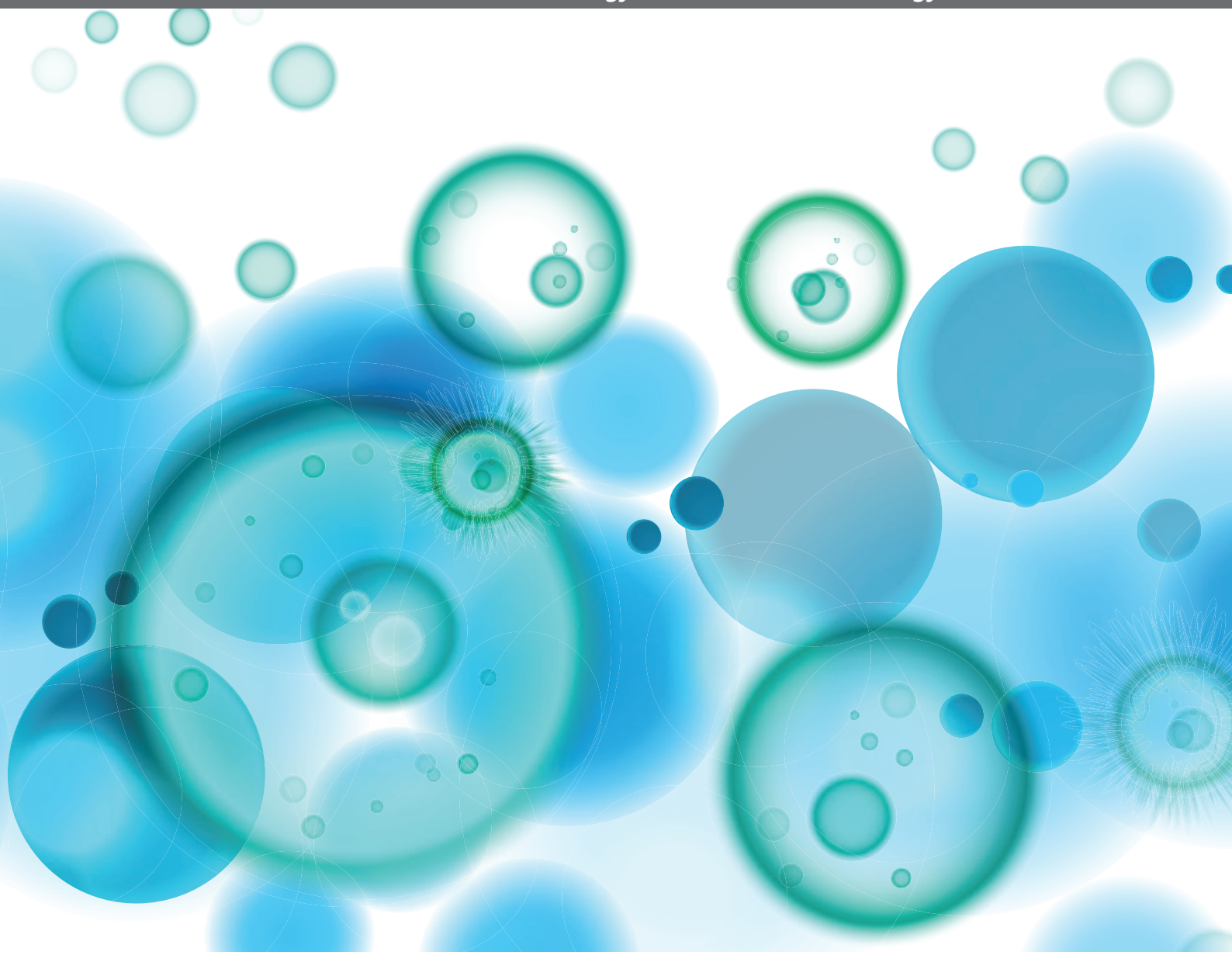

frontiers Research Topics

ISSN 1664-8714
ISBN 978-2-88971-860-3
DOI 10.3389/978-2-88971-860-3

About Frontiers

Frontiers is more than just an open-access publisher of scholarly articles: it is a pioneering approach to the world of academia, radically improving the way scholarly research is managed. The grand vision of Frontiers is a world where all people have an equal opportunity to seek, share and generate knowledge. Frontiers provides immediate and permanent online open access to all its publications, but this alone is not enough to realize our grand goals.

Frontiers Journal Series

The Frontiers Journal Series is a multi-tier and interdisciplinary set of open-access, online journals, promising a paradigm shift from the current review, selection and dissemination processes in academic publishing. All Frontiers journals are driven by researchers for researchers; therefore, they constitute a service to the scholarly community. At the same time, the Frontiers Journal Series operates on a revolutionary invention, the tiered publishing system, initially addressing specific communities of scholars, and gradually climbing up to broader public understanding, thus serving the interests of the lay society, too.

Dedication to Quality

Each Frontiers article is a landmark of the highest quality, thanks to genuinely collaborative interactions between authors and review editors, who include some of the world's best academicians. Research must be certified by peers before entering a stream of knowledge that may eventually reach the public - and shape society; therefore, Frontiers only applies the most rigorous and unbiased reviews.
Frontiers revolutionizes research publishing by freely delivering the most outstanding research, evaluated with no bias from both the academic and social point of view. By applying the most advanced information technologies, Frontiers is catapulting scholarly publishing into a new generation.

What are Frontiers Research Topics?

Frontiers Research Topics are very popular trademarks of the Frontiers Journals Series: they are collections of at least ten articles, all centered on a particular subject. With their unique mix of varied contributions from Original Research to Review Articles, Frontiers Research Topics unify the most influential researchers, the latest key findings and historical advances in a hot research area! Find out more on how to host your own Frontiers Research Topic or contribute to one as an author by contacting the Frontiers Editorial Office: frontiersin.org/about/contact

CYTOKINES AND PAIN

Topic Editors:
Waldiceu A. Verri, State University of Londrina, Brazil
Felipe Almeida Pinho-Ribeiro, Harvard Medical School, United States
Larissa G. Pinto, King's College London, United Kingdom

Citation: Verri, W. A., Pinho-Ribeiro, F. A., Pinto, L. G., eds. (2021). Cytokines and Pain. Lausanne: Frontiers Media SA. doi: 10.3389/978-2-88971-860-3

Table of Contents

frontiers in Immunology

EDITORIAL
published: 21 October 2021
doi: 10.3389/fimmu.2021.788578

Editorial: Cytokines and Pain

Larissa G. Pinto[1*†], *Felipe A. Pinho-Ribeiro*[2*†] *and Waldiceu A. Verri Jr*[3*†]

[1] Wolfson Centre for Age-Related Diseases, King's College London, London, United Kingdom, [2] Department of Immunology, Harvard Medical School, Boston, MA, United States, [3] Department of Pathology, Londrina State University, Londrina, Brazil

Keywords: pain, cytokine, neuro-immune communcation, microglia, astrocyte, interleukin, nociceptor, chemokine

Editorial on the Research Topic

Cytokines and Pain

OPEN ACCESS

Edited and reviewed by:
Robert Weissert,
University of Regensburg, Germany

****Correspondence:***
Larissa G. Pinto
larissa_garcia.pinto@kcl.ac.uk;
larifarm@gmail.com
Felipe A. Pinho-Ribeiro
felipe_ribeiro@hms.harvard.edu
Waldiceu A. Verri Jr
waldiceujr@yahoo.com.br;
waverri@uel.br

†ORCID:
Larissa G. Pinto
orcid.org/0000-0002-3619-907X
Felipe A. Pinho-Ribeiro
orcid.org/0000-0003-4264-9839
Waldiceu A. Verri Jr
orcid.org/0000-0003-2756-9283

Specialty section:
This article was submitted to Multiple Sclerosis and Neuroimmunology, a section of the journal Frontiers in Immunology

Received: *02 October 2021*
Accepted: *05 October 2021*
Published: *21 October 2021*

Citation:
Pinto LG, Pinho-Ribeiro FA and Verri WA Jr (2021) Editorial: Cytokines and Pain. Front. Immunol. 12:788578. doi: 10.3389/fimmu.2021.788578

Cytokines are released by immune and non-immune cells to orchestrate a great variety of physiological and disease processes. In special, cytokines can both directly and indirectly activate nociceptor sensory neurons modulating pain development. In turn, nociceptors also function as cellular regulators of the immune response in sterile and infectious diseases. All these aspects were within the aims of this Research Topic entitled "Cytokines and Pain". There were two review articles and nine research articles published. Starting with the two reviews, they used different approaches. Vanderwall and Milligan discuss the contribution of cytokines to pain as molecules that link the immune and nervous system cells from peripheral tissues to the spinal cord (SC) triggering pain with the underlying contribution of neuroimmune interactions. Another focus of the review is the current gene therapies targeting cytokines to reduce pathological pain. Sexual dimorphism in pain and some additional inflammatory pathways are discussed. Santos et al. address the contribution of cytokines to nociceptor activation at four levels; in the peripheral tissues, at the dorsal root ganglia (DRG) in which the cellular bodies and nucleus of primary afferent neurons reside, and at spinal cord (SC) and supra-SC levels. The discussion approaches cellular interactions and role of cytokines to pain at each level. Their table one also brings a comprehensive view of cytokine families, cellular sources, and roles in pain and diseases.

We organized the nine research papers in this editorial from the periphery to the CNS. Napimoga et al. investigated the inflammatory and nociceptive effects of secreted osteoclastogenic factor of activated T cells (SOFAT), a novel cytokine, in collagen-induced arthritis (CIA). The intra-articular injection of 10 ng of SOFAT induced a four days-lasting mechanical hyperalgesia. SOFAT levels were higher in joint samples of CIA mouse than naïve mouse, and in synovial samples of rheumatoid arthritis patients than in osteoarthritis patients. Thus, bringing the first insight about the role of SOFAT in pain and inflammation in arthritis.

Guo et al. demonstrate that the injection of NGF in the trigeminal ganglia (TG) reduces the bite force upon tooth movement, a surrogate measure of pain. Inhibiting NGF enhanced the bite force, indicating reduced pain. NGF and tooth movement increased CGRP and CCL19 expression in the TG as well as CCL19 injection in the TG induced pain. Anti-CCL19 inhibited tooth movement pain and NGF enhanced tooth movement pain. Thus, demonstrating a novel role for CCL19 in tooth movement- and NGF-dependent pain.

Gonçalves et al. asked what was maintaining pain in a model of antigen-induced monoarthritis (AIA) after articular inflammation resolution. Mechanical hyperalgesia was accompanied by c-Fos activation in the DRG by the 8th day when peripheral inflammation has already ended. At the DRG (L4 level) there was enhanced mRNA expression of TNF-α and TNFR2, and TNF-α levels. And

etanercept (a soluble TNFR2) inhibited the persistent pain. Thus, DRG TNF-α and TNFR2 explain the persistent pain in AIA after peripheral inflammation resolution.

Patients with Chagas disease caused by *Trypanosoma cruzi* report pain in the acute phase of the disease. Borghi et al. demonstrate for the first time that pain during *T. cruzi* infection involves the activation of DRG neurons and SC microglia and astrocytes. There is interaction of SC glial cells and neurons that *via* NFkB control the expression of CX3CR1, TNF-α and IL-1β since the inhibition of glial cells reduces the expression of those chemokines and cytokines both at the DRG and SC. Thus, unveiling a previously unknown mechanism of pain in *T. cruzi* infection.

Fonseca et al. identified the cytokine IL-27 as an important endogenous mediator that counteracts the development of neuropathic pain following spared nerve injury (SNI). Peripheral nerve injury induces IL-27 expression in the SC and DRG that activates IL-27 receptor-expressing cells (macrophages, microglia, and astrocytes), thus, triggering the production of IL-10 and controlling the intensity of pain. Piotrowska et al. observed that CXCL3 and CXCR2 co-localize with neurons in the SC of naïve and chronic constriction injury (CCI) animals. And that microglia could also be a source of CXCL3 in CCI. NVP CXCR2 20 (a selective CXCR2 receptor antagonist) treatment reduced SC production of CXCL3 and satellite glial cells activation in the DRG. Primary microglial and astroglial cultures corroborated microglia would be the main source of CXCL3. Thus, CXCL3/CXCR2 signaling has a role in CCI neuropathic pain that can be targeted by NVP CXCR2 20.

Nerve damage is also a key feature of multiple sclerosis (MS), an extremely debilitating neurodegenerative disease that is often accompanied by the development of chronic neuropathic pain. By analyzing the electroencephalography (EEG) of patients with central neuropathic pain and comparing the results with those from patients without neuropathic pain, Krupina et al. identified changes in the power spectral density (PSD) that were specific signatures of patients with neuropathic pain. The authors observed alterations in spectral EEG patterns and peak frequencies of MS patients with neuropathic pain, including increased PSD for the theta, beta1, and beta2 frequencies in most regions of interest. This work demonstrates the existence of putative alterations in cortical communication that are specific for MS patients with neuropathic pain and that could be the basis of the sensory dysfunction observed in these patients. The mechanisms involved in MS were also evaluated in a model of experimental autoimmune encephalomyelitis (EAE). Xiao et al. observed that HMGB1 (high mobility group box 1 protein) induced shh (sonic hedgehog) release in astrocytes culture, through RAGE (receptor for advanced glycation end-products)-mediated JNK, p38, and STAT3 phosphorylation. Furthermore, HMGB1 also promotes shh in EAE, and shh treatment was able to alleviate the progress of EAE in mice. Thus, this study suggests HMGB1/shh has a protective role in EAE.

Neural pain is an important symptom in leprosy patients. In a retrospective study, Angst et al. assessed serum levels of cytokines in leprosy patients with or without pain as well as diabetic neuropathy pain. The authors observed an increased level of IL-1β, TNF, TGF-β and IL-17 in leprosy patients with neuropathic or nociceptive pain when compared with painless leprosy patients. Moreover, serum levels of IL-6 were increased in both leprosy and diabetic neuropathic pain patients, being an interesting target to control pain. IL-1β was identified as a key cytokine associated with neural leprosy pain when compared to diabetic neuropathic pain and can be used as a biomarker for patient follow-up.

Concluding, the two review papers, seven research papers using animal models and two clinical research papers addressed peripheral, DRG, SC and supra-SC mechanisms focusing on cytokines and neuro-immune interaction mechanisms in pain.

AUTHOR CONTRIBUTIONS

All authors listed have made a substantial, direct, and intellectual contribution to the work and approved it for publication.

FUNDING

LP received funding from Versus Arthritis UK (grant 21522), Wellcome Trust UK (205006/Z/16/Z) and FAPESP/KCL Joint Grant (process number 2017/50419-9). WAVJ receives Brazilian grants from PPSUS funded by Decit/SCTIE/MS intermediated by CNPq with support of Fundação Araucária and SESA-PR (agreement 041/2017); Programa de Apoio a Grupos de Excelência (PRONEX) grant supported by SETI/Fundação Araucária and MCTI/CNPq, and Governo do Estado do Paraná (agreement 014/2017); and CNPq (#443180/2016-4; # 427946/2018-2; # 309633/2021-4; # 307186/2017-2).

Conflict of Interest: The authors declare that the research was conducted in the absence of any commercial or financial relationships that could be construed as a potential conflict of interest.

Publisher's Note: All claims expressed in this article are solely those of the authors and do not necessarily represent those of their affiliated organizations, or those of the publisher, the editors and the reviewers. Any product that may be evaluated in this article, or claim that may be made by its manufacturer, is not guaranteed or endorsed by the publisher.

frontiers in Immunology

ORIGINAL RESEARCH
published: 26 September 2019
doi: 10.3389/fimmu.2019.02198

Pharmacological Blockade of Spinal CXCL3/CXCR2 Signaling by NVP CXCR2 20, a Selective CXCR2 Antagonist, Reduces Neuropathic Pain Following Peripheral Nerve Injury

*Anna Piotrowska[1], Ewelina Rojewska[1], Katarzyna Pawlik[1], Grzegorz Kreiner[2], Agata Ciechanowska[1], Wioletta Makuch[1], Irena Nalepa[2] and Joanna Mika[1]**

[1] Department of Pain Pharmacology, Maj Institute of Pharmacology, Polish Academy of Sciences, Kraków, Poland,
[2] Department of Brain Biochemistry, Maj Institute of Pharmacology, Polish Academy of Sciences, Kraków, Poland

OPEN ACCESS

Edited by:
Waldiceu A. Verri, State University of Londrina, Brazil

Reviewed by:
Paulino Barragan-Iglesias, The University of Texas at Dallas, United States
Andrea Antonosante, University of L'Aquila, Italy

***Correspondence:**
Joanna Mika
joamika@if-pan.krakow.pl; joasia272@onet.eu

Specialty section:
This article was submitted to Cytokines and Soluble Mediators in Immunity, a section of the journal Frontiers in Immunology

Received: *06 July 2019*
Accepted: *30 August 2019*
Published: *26 September 2019*

Citation:
Piotrowska A, Rojewska E, Pawlik K, Kreiner G, Ciechanowska A, Makuch W, Nalepa I and Mika J (2019) Pharmacological Blockade of Spinal CXCL3/CXCR2 Signaling by NVP CXCR2 20, a Selective CXCR2 Antagonist, Reduces Neuropathic Pain Following Peripheral Nerve Injury. Front. Immunol. 10:2198. doi: 10.3389/fimmu.2019.02198

Recently, the role of CXCR2 in nociception has been noted. Our studies provide new evidence that the intrathecal administration of its CINC ligands (Cytokine-Induced Neutrophil Chemoattractant; CXCL1-3) induces pain-like behavior in naïve mice, and the effect occurring shortly after administration is associated with the neural location of CXCR2, as confirmed by immunofluorescence. RT-qPCR analysis showed, for the first time, raised levels of spinal CXCR2 after chronic constriction injury (CCI) of the sciatic nerve in rats. Originally, on day 2, we detected escalated levels of the spinal mRNA of all CINCs associated with enhancement of the protein level of CXCL3 lasting until day 7. Intrathecal administration of CXCL3 neutralizing antibody diminished neuropathic pain on day 7 after CCI. Interestingly, CXCL3 is produced in lipopolysaccharide-stimulated microglial, but not astroglial, primary cell cultures. We present the first evidence that chronic intrathecal administrations of the selective CXCR2 antagonist, NVP CXCR2 20, attenuate neuropathic pain symptoms and CXCL3 expression after CCI. Moreover, in naïve mice, this antagonist prevented CXCL3-induced hypersensitivity. However, NVP CXCR2 20 did not diminish glial activation, thus not enhancing morphine/buprenorphine analgesia. These results provide novel insight into the crucial role of CXCR2 in neuropathy based on CXCL3 modulation, which may become a potential therapeutic target in pain treatment.

Keywords: CXCL1, CXCL2, glia, microglia, astroglia

INTRODUCTION

Neuropathic pain, triggered by peripheral nerve injury, is associated with the plasticity of the nociceptive pathway, where this pain remains, even after the injured tissue has healed (1–5). Mainstream analgesics are not sufficiently successful in achieving selective palliation of neuropathic pain. In fact, these treatments only cause a greater number of side effects. To identify novel alternatives for more effective treatment, it is necessary to clarify the underlying mechanisms.

Cytokines, including interleukins and chemokines, are major inflammatory molecules that play an essential role in pain sensitization and have been recently investigated as key mediators in the induction and maintenance of neuropathic pain (6–12).

Chemokines are small cytokines (13), and their participation in neuropathic pain is not limited to their chemotactic activities because these factors also affect the functions of glial and neuronal cells. The evidence of the contribution of chemokines to neuropathic pain includes CX3CL1, CCL2, CCL5, CCL7 CXCL5, CXCL9, CXCL12, and XCL1, and their respective receptors: CCR2, CCR5, CXCR3, CXCR4, and XCR1 (2, 11, 14–28). It has recently been published that a blockade of CCR1 (27), CCR2 (25), CCR5 (28), and CXCR3 (29) restores the analgesic effects of morphine and/or buprenorphine under neuropathy. However, the question of the role of spinal CXCR2 and its endogenous ligands from the CXC (C-X-C motif) family, called cytokine-induced neutrophil chemoattractants (CINCs), belongs to future studies. Among CINCs, three types have been distinguished and are referred to as CINC-1 (chemokine CXC ligand 1, CXCL1; growth-regulated GRO protein alpha, GROα; melanoma growth stimulating activity alpha, MSGA-α; keratinocyte-derived chemokines, KC), CINC-2 (chemokine CXC ligand 3, CXCL3; growth-regulated GRO protein gamma, GROγ; macrophage inflammatory protein-2-beta, MIP2β), and CINC-3 (chemokine CXC ligand 2, CXCL2; growth-regulated protein beta, GROβ; macrophage inflammatory protein 2-alpha, MIP2α). In 2018, Gulati et al. (30) showed that the CINC family arose as a result of two rounds of gene duplication in the course of evolution. The family members are closely related to each other, and biological studies reported their differential tissue expression and regulation. Comparative studies on CXCR2 chemotactic activity have provided evidence of the highest efficacy for CXCL1 and intermediate efficacy for CXCL2 and CXCL3. A previous study showed that all CINCs are expressed by macrophages and play important roles in neutrophil infiltration (31). CINCs act specifically through CXCR2, a G protein-coupled receptor (32, 33), and induce calcium mobilization dose-dependently in CXCR2-transfected cells (34). *In vitro* studies proved that anti-CXCR2 serum almost entirely inhibits the neutrophil chemotactic activities of the three types of CINCs (34).

Therefore, the goal of our studies was to examine the comprehensive roles of all CINCs (CXCL1, CXCL2, and CXCL3) in the pathogenesis of neuropathic pain. Using RT-qPCR and Western blots, we assessed the changes in mRNA expression and protein levels of CXCR2 and its ligands in a rat spinal cord on days 2, 7, 14, and 28 after chronic constriction injury (CCI) of the sciatic nerve. We recognized the origin of CINCs in rat primary cultures of microglia and astroglia by Western blotting. In addition, we made an attempt to visualize the cellular location of CXCR2 and CXCL3 by immunohistochemistry in the lumbar spinal cord on day 7 after CCI. Furthermore, we determined the significance of CXCL1, CXCL2, and CXCL3 in nociceptive transmission in naive mice and the influence of CXCL3 neutralizing antibody in mice on day 7 after CCI. Additionally, another goal of our study involved the determination of how the blockade of CXCR2 signaling through the intrathecal administration of NVP CXCR2 20 affects neuropathic pain-related behavior, glia activation, and the levels of CXCR2 and its endogenous ligands in rats. Eventually, we examined if the CXCR2 antagonist might improve the effectiveness of opioids, such as morphine and buprenorphine in a neuropathic pain model.

MATERIALS AND METHODS

Animals

Adult male Wistar rats (250–300 g) and Albino Swiss mice (20–22 g) from Charles River Laboratories International, Inc. (Germany) were used in our experiments. The rats and mice were housed in cages lined with sawdust under a standard 12/12 h light/dark cycle (lights on at 8.00 a.m.) temperature of 22 ± 2°C with food and water available *ad libitum*. The animals were allowed to acclimate to the environment for ∼5 min prior to the behavioral testing. All experiments were performed according to the recommendations of the International Association for the Study of Pain (IASP) by Zimmermann (35) and the National Institutes of Health (NIH) Guide for the Care and Use of Laboratory Animals. The study protocol was approved by the II Local Bioethics Committee branch of the National Ethics Committee for Experiments on Animals based at the Maj Institute of Pharmacology, Polish Academy of Sciences (Krakow, Poland), permission number: 1277/2015 and 262/2017. Care was taken to minimize animal suffering and reduce the number of animals used (3R policy). Animal studies are reported in compliance with the ARRIVE guidelines (36, 37).

Intrathecal (*i.t.*) Injection

The rats were readied for *i.t.* injection: catheter implants were inserted according to the method described by Yaksh and Rudy (38) and our earlier publications (11, 39, 40). Just before the operation, each rat was anesthetized with sodium pentobarbital (60 mg/kg) administered intraperitoneally (*i.p.*). The *i.t.* catheter included a 13 cm-long polyethylene tubing (PE 10, Intramedic; Clay Adams, Parsippany, NJ, USA). Prior to the insertion for the injection the dead space of 10 μl was sterilized—immersed in 70% (v/v) ethanol and fully flushed with water. Subsequently, 7.8 cm of catheter was introduced through the atlanto-occipital membrane and into the subarachnoid space at the rostral level of the spinal cord lumbar enlargement (L4-L5). The first injection of water (10 μl) was slowly performed after implantation, and the catheter was tightened. All rats recovered after the surgery for 1 week before the establishment of a neuropathic pain model. Repeated *i.t.* drug administration can be achieved due to the catheter implantation. The studies are carried out in a rat model of neuropathic pain, because it allows studying changes in many mediators in one animal at the spinal cord and DRG level in parallel. Regarding the ethical principles of the 3R's, we are obliged to limit the suffering of animals. For this reason, in order to lower the number of animals (rats) subject to a catheter implantation, following the method described by Hylden and Wilcox (41), we performed single drug administrations in mice. Hamilton syringe and a thin needle were used to inject 5 μl of each chemokine between the L5-L6 vertebrae in the spinal cord. The tail reflex indicates the correct drug administration.

At the same time, we emphasize that both species of rodents, rats and mice, are commonly used to study the mechanisms of neuropathic pain.

Neuropathic Pain Model—Chronic Constriction Injury (CCI)

Seven days after the intrathecal catheter insertion in rats, chronic constriction injury to the sciatic nerve was performed according to the method of Bennett and Xie (42). The operation was performed in rats under sodium pentobarbital anesthesia (60 mg/kg; *i.p.*) and in mice under isoflurane anesthesia. An incision was performed under the hipbone, and the separation of biceps femoris and gluteus superficialis. After exposing the proper sciatic nerve, ligatures (4/0 silk) in rats and mice, four and three, respectively, were loosely tied around that nerve at 1-mm intervals until a little twitch in the operated hind limb was obtained. After the surgery, sustained tactile, and thermal hypersensitivity in the injured hind paw developed in each animal.

Drug Administration

All Substances Used in Rats

NVP CXCR2 20 (NVP, Tocris, Janki/Warsaw, Poland), morphine (M; TEVA, Kutno, Poland), and buprenorphine (B; Polfa Warszawa S.A., Warsaw, Poland). NVP CXCR2 20 was dissolved in DMSO, and morphine and buprenorphine were dissolved in water for injections (40, 43, 44). These substances were administered gently through the *i.t.* catheter in a volume of 5 μl, followed by an injection of 10 μl of water, which flushed the catheter. Before the drug injections, the baseline behaviors of the animals were determined using von Frey and cold plate tests. For the single *i.t.* treatment, the behavioral tests were conducted at 0.5, 1, 2, 4, 6 and 24 h after NVP CXCR2 20 injection at a dose of 10, 20, and 30 μg/5 μl. For the repeated *i.t.* treatment, the behavioral tests were carried out 120 (von Frey test) or 125 min (cold plate test) subsequent to NVP CXCR20 20 administration at the selected dose of 10 μg/5 μl according to the following scheme: preemptively at 16 and 1 h following CCI and then once daily for 7 days (28, 40, 45). The dose was chosen based on the results from single *i.t.* treatment behavioral results. For the co-treatment, on the 7th day post-CCI, single V-treated and NVP-treated rats received a single dose of morphine or buprenorphine (2.5 μg/5 μl) at 4 h after the NVP/vehicle injection, and then both behavioral tests were repeated (experimental schedule included in **Figure 9A**). The control groups received vehicle (injection of water or dimethyl sulfoxide, DMSO) according to the same schedule. Our previously study published by Rojewska et al. (46) demonstrated that water for injection- and DMSO-treated CCI-exposed rats developed similarly strong allodynia (11.8 ± 0.4 and 11.9 ± 1.3 g; respectively) and hyperalgesia (6.3 ± 0.5 vs. 6.6 ± 1.6 s; respectively), as demonstrated in the von Frey and cold plate tests. Also in 2016, Rojewska et al. (44) published that 100% DMSO did not influence on hypersensitivity in CCI-exposed rats. In current experiments, an attempt was made to prepare drugs at lower DMSO concentrations, but they precipitate.

All Substances Used in Mice

CXCL1, CXCL2, and CXCL3 proteins were obtained from R&D Systems (USA) and dissolved in water for injection. The reconstituted chemokines were intrathecally injected into naive mice at the following concentrations: 2, 400, and 800 ng/5 μl. The behavioral tests were performed at 1.5, 5, and 24 h following the administration of chemokine.

The CXCL3 neutralizing antibody was acquired from R&D Systems (USA) and further dissolved in water for injection. The reconstituted neutralizing antibodies were intrathecally injected into CCI-exposed mice at the following concentrations: 1, 4, and 8 μg/5 μl. The behavioral tests were carried out at 1.5, 5, 24, and 48 h after neutralizing antibody administration.

NVP CXCR2 20 was dissolved in DMSO and intrathecally injected into naive mice at a concentration of 60 μg/5 μl. The behavioral tests were performed at 2 h after CXCR2 antagonist administration. Single V-treated and NVP-treated mice received a single dose of CXCL3 (2 ng/5 μl) at 2 h after the NVP/vehicle injection, and then both behavioral tests were repeated after 1, 5, 5 and 24 h (experimental schedule included in **Figure 7A**).The animals were randomly assigned to groups, based on a single sequence of random assignments, simple randomization—odd/even methods (47, 48).

Behavioral Tests

Tactile Hypersensitivity Measurement (Von Frey Test)

In rats, tactile hypersensitivity was assessed in naive rats and rats subject to CCI with an automated von Frey apparatus (Dynamic Plantar Anesthesiometer, Cat. No. 37400, Ugo Basile, Italy) as previously described (11, 12, 43, 46). Five minutes before the experiment, each rat was placed in a plastic cage with a wire net floor to promote behavioral accommodation. The weight of the von Frey stimuli used in our experiments was up to 26 g. The mid-plantar ipsilateral and contralateral hind paw areas were tested, and the measurements were recorded automatically as described previously (46). No significantly different contralateral hind paw reactions were observed between the CCI and naive rats. Tactile hypersensitivity was assessed at 30 min after the final drug administration.

In mice, the response to non-noxious stimuli was evaluated with von Frey filaments—calibrated nylon monofilaments of increasing strength (from 0.6 to 6 g; Stoelting, USA). The filaments were successively applied to the plantar surfaces of the hind paws until withdrawal responses, as already described (23, 49, 50).

Thermal Hypersensitivity Measurement (Cold Plate Test)

In rats, thermal hypersensitivity was determined with a cold/hot plate analgesia meter (Cat. No. 05044/230 VAC, Columbus Instruments, USA) as described previously (11, 12, 43). The rats were placed on a cold stainless steel plate maintained at 5°C, and the latency to lift or shake the injured hind paw was measured. The cut-off latency was 30 s.

In mice, the response to noxious stimuli in the naïve and CCI-exposed animals was evaluated using a cold/hot plate analgesia meter (Cat. No. 35 100-001, Columbus Instruments, USA), as

previously described (24, 50). The mice were placed on the cold plate at a temperature of 2°C. The latency of hind paw elevation was recorded. The cut-off latency was 30 s.

Microglial and Astroglial Cell Cultures

Neonatal models of primary cultures of microglial and astroglial cells were used in our *in vitro* studies as shown previously (11, 12, 51). Both cell types cultures were prepared from 10 1-day-old Wistar rats according to the procedure by Zawadzka and Kaminska (52). The cells were taken from the cerebral cortex and put in poly-L-lysine-coated 75-cm^2 culture bottles at 3×10^5 cells/cm^2 density, in high-glucose DMEM with GlutaMAX (Gibco, New York, USA), heat-inactivated 10% fetal bovine serum, 0.1 mg/ml streptomycin, and 100 U/ml penicillin (Gibco, New York, USA). The cultures were maintained at 37°C in 5% CO_2. On day 4, the medium was changed. On day 9, the cultures were softly shaken and centrifuged to reclaim any loosely adherent microglia. On day 12, the medium was changed, and the microglia were retrieved again. Then, the medium was changed once more, and the cultures were left to grow on a rotary shaker at 37°C for 24 h (200 rpm) to remove the remaining non-adherent cells. The medium was then removed, and the astrocytes were cultured for 3 days and further trypsinized (0.005% trypsin EDTA solution, Sigma-Aldrich, St. Louis, USA). Microglia/astrocytes were seeded in culture medium onto 6-well plates at a final density of 1.2×10^6 cells per well for protein analysis. Primary microglial and astrocyte cell cultures were treated with NVP CXCR20 20 [100 nM] at 30 min before LPS (lipopolysaccharide from *Escherichia coli* 0111:B4; Sigma-Aldrich, St. Louis, USA) administration [100 ng/ml]. The LPS dose was selected basing on the literature (52, 53) and our experience (12, 44, 51). They were then incubated for 24 h for the Western blot analysis (11, 12, 39, 44, 51). We used immunostaining for IBA1 (a microglial marker, SC-327 225, Santa Cruz Biotechnology Inc., Santa Cruz, USA) and GFAP (an astrocyte marker, SC-166 458, Santa Cruz Biotechnology Inc., Santa Cruz, USA) to identify microglia and astrocytes in the cultures. We obtained highly homogeneous microglial and astroglial populations (more than 95% were positive for IBA1 and GFAP, respectively) Zawadzka and Kaminska (52). Only the minimal essential number of animals was used, and all of the procedures were performed according to the recommendations of IASP (35) and the NIH Guide for the Care and Use of Laboratory Animals. The study was carried out in accordance with the recommendations of the local Ethics Committee (Krakow, Poland), permission number: 1277/2015 and 262/2017.

Biochemical Tests

Analysis of Gene Expression by qRT-PCR

Ipsilateral fragments of the dorsal part of the lumbar (L4-L6) spinal cord were collected immediately after decapitation on days 2, 7, 14, and 28 after CCI. Total RNA was extracted with TRIzol reagent (Invitrogen; USA) compliant with the method by Chomczynski and Sacchi (54). A NanoDrop ND-1000 spectrometer (NanoDrop Technologies, Wilmington, USA) measured the RNA concentration in each sample. Reverse transcription was performed at 37°C for 60 min with Omniscript reverse transcriptase (Qiagen Inc., Hilden, Germany) and 1 μg of total RNA from the tissue. The reaction was performed in the presence of an RNAse inhibitor (rRNasin, Promega, Mannheim, Germany) and oligo (dT16) primers (Qiagen Inc., Hilden, Germany). The obtained cDNA templates were diluted 1:10 with H_2O, and ∼50 ng of cDNA templates from each animal were used for each quantitative real-time PCR (RT-qPCR) assay. RT-qPCR was performed with Assay-On-Demand TaqMan probes (Applied Biosystems, Foster City, CA, USA) on an iCycler device (Bio-Rad, Hercules, Warsaw, Poland) in compliance with the manufacturers' protocol. A standard dilution curve established the amplification efficiency in case of each assay. TaqMan primers and probes were used: Rn01527838_g1 (HPRT, hypoxanthine-guanine phosphoribosyltransferase); Rn02130551_s1 (CXCR2, chemokine (C-X-C motif) receptor 2); Rn00578225_m1 (CXCL1, CINC-1, chemokine (C-X-C motif) ligand 1); Rn00586403_m1 (CXCL2, CINC-3, Mip-2, chemokine (C-X-C motif) ligand 2); and Rn01414231_m1 (CXCL3, CINC-2, chemokine (C-X-C motif) ligand 3). A standard dilution curve established the amplification efficiency for each assay (between 1.7 and 2). The cycle threshold values were automatically calculated by CFX Manager v.2.1 software with the default parameters. The RNA content was calculated using the formula 2 (threshold cycle). The level of the HPRT transcript was not significantly changed in the CCI-exposed rats (55), and for this reason it served as an adequate housekeeping gene.

Analysis of the Protein Levels (Western Blot)

Ipsilateral fragments of the dorsal part of the lumbar (L4-L6) spinal cord and the DRG (L4-L6 polled into one sample) were collected immediately after decapitation on days 2, 7, 14 and 28 after CCI or at 6 h after the last injection of NVP CXCR2 20 on the 7th day after CCI. The cell lysates (in RIPA buffer with a protease inhibitor cocktail) from primary microglial and astroglial cultures for Western blot analysis were collected at 24 h after LPS stimulation. We collected the lysates from the cell cultures and tissues in RIPA buffer supplemented with a protease inhibitor cocktail. The reaction mixtures were cleared by centrifugation (14,000 × g for 30 min at 4°C). All samples (20 μg of protein from tissue and 10 μg of protein from primary cells) were heated in a loading buffer (4 × Laemmli Buffer, Bio-Rad, Warsaw, Poland) for 8 min at 98°C. Next, the samples were resolved on 4–15% Criterion™ TGX™ precast polyacrylamide gels (Bio-Rad, Warsaw, Poland) and placed on Immune-Blot PVDF membranes (Bio-Rad, Warsaw, Poland) with a semidry transfer (30 min, 25 V). Membranes were blocked with 5% non-fat dry milk (Bio-Rad, Warsaw, Poland) in Tris-buffered saline with 0.1% Tween 20 (TBST) for 1 h at RT, washed with TBST, and incubated with the following commercially available primary antibodies (reactivity of rat and specified by the producer of the observed molecular weight) overnight at 4°C: rabbit anti-Iba-1 (1:1,000, Proteintech, 10904-1-AP), anti-CXCR2 (1:2,000, LSBio, LS-C388292), anti-CXCL1 (1:200, LSBio, LS-C104778), anti-CXCL2 (1:200, Novus, MAB525), anti-CXCL3 (1:250, Novus, AF516), anti-GFAP (1:10,000, Novus, NB300-141), and mouse anti-GAPDH (1:5,000, Millipore, MAB374). Next, the membranes were incubated with 1:5,000 dilutions

of horseradish peroxidase-conjugated anti-rabbit or anti-mouse secondary antibodies for 1 h. We used the solutions from a SignalBoost™ Immunoreaction Enhancer Kit (Merck Millipore Darmstadt, Germany) in order to dilute the primary and secondary antibodies. The membranes underwent washing twice with TBST for 2 min each, and 3 times for 5 min each. In the final step, immune complexes were detected with the Clarity™ Western ECL Substrate (Bio-Rad, Warsaw, Poland) and visualized with a Fujifilm LAS-4000 FluorImager system. Fujifilm Multi Gauge software quantified the relative levels of immunoreactive bands. In **Figures 8D–F**, the blots are cropped which was shown with a dotted line on the representation bands below the figures.

Immunofluorescence Staining

Immunofluorescent staining was performed on lumbar (L4-L6) spinal cord samples from neuropathic rats on day 7 after CCI. The tissues were fixed in 4% PFA, embedded in paraffin blocks, cut at 7 μm thick slices on a rotary microtome (Leica, Germany), followed by immunofluorescent staining as described by Rafa-Zabłocka et al. (56). After deparaffinization followed by antigen retrieval (microwave method with citrate buffer), the sections were briefly incubated for 30 min in 5% normal pig serum (Vector Labs, USA) in a PBST buffer (0.2% Triton X-100 in phosphate-buffered saline). The sections were incubated overnight at 4°C with the following primary antibodies: anti-CXCR2 (1:100, LSBio, LS-C388292), anti-CXCL3 (1:100, Abcam, ab10064), anti-NeuN (neuronal marker, 1:500, Millipore, MAB377), anti-IBA1 (1:1,000, Abcam, ab139590), and anti-GFAP (1:500, Millipore, AB5541). Antigen-bound primary antibodies were visualized with anti-rabbit Alexa-488-, anti-mouse Alexa-594-, anti-goat Alexa-594-, and anti-chicken Alexa-594–coupled secondary antibodies. The stained sections were assessed and photographed under a fluorescence microscope (Nikon Eclipse 50i, Netherlands). The dorsal part of the lumbar spinal cord was visualized by using representative images of naive and CCI rats. The immunohistochemical study added new information regarding the possible co-localization of CXCR2 and CXCL3 with markers of neurons, micro- and astroglia. These data do not allow quantitative analyses of staining intensity since the experiments were designed to address co-localization only. Factors such as the number of animals per group refrain staining quantitation.

Statistical Analyses

The number of animals used in the behavioral and biochemical studies was selected based on an earlier study on a similar field (29). All graphs and analyses were prepared using GraphPad Prism 7 software. The data and statistical analysis comply with the recommendations on experimental design and analysis in pharmacology (57).

Behavioral Study

The data (**Figures 3A–F**, **4A–D**, **6A,B**, **7B,C**, **9B,C**) are presented in grams and seconds for each group, including the naive groups. The intergroup differences were analyzed via one-way analysis of variance (ANOVA), followed by Bonferroni's test for multiple comparisons. Bartlett's test for homogeneity of variances assessed if the assumption of equal variances was true before employing further statistical tests. Additionally, the results were evaluated using two-way ANOVA to determine the time × drug interaction, if applicable (**Figures 3**, **4**, **6**). In accordance with the 3R rule, the minimum number of animals necessary for conducting statistical analyzes was used in the research.

qRT-PCR and Western Blot Studies

In vivo studies: The results of the analyses (**Figures 1A–H**, **5A–I**) are presented as a fold change compared with the control group (naive rats) and were calculated for the ipsilateral side of the spinal cord and/or the DRG on days 2, 7, 14, and/or 28 after CCI or 4/6 h after the last injection of NVP CXCR2 20 on day 7 after CCI. The data are presented as the means ± SEM and represent the normalized averages derived from analyses of each group performed with the Multi Gauge analysis program. Intergroup differences were analyzed using ANOVA, followed by Bonferroni's multiple comparison tests. *In vitro studies:* In case of glial cell cultures, the results of the Western blot analyses (**Figures 8A–F**) are shown as a percentage of the control (vehicle-treated non-stimulated cells) shown as the means ± SEM of 3–4 independent experiments. The results were evaluated with a one-way analysis of variance (ANOVA) with Bonferroni's *post-hoc* test to see the differences between the treated groups. One of the graphs is presented as the relative protein level, and the result was evaluated using a *t*-test to assess the differences between the treatment groups (**Figure 8C**). The variability in the number of samples used in the studies is due to the lack of measurements for technical reasons.

RESULTS

The Time Course of Changes in the Levels of CXCR2, CXCL1, CXCL2, and CXCL3 mRNA and Protein in the Spinal Cord on the 2nd, 7th, 14th, and 28th Days After CCI in Rats

In the spinal cord, qRT-PCR analysis showed that the level of CXCR2 mRNA was upregulated 2.1-fold ($p < 0.001$), 2.3-fold ($p < 0.001$), and 2-fold ($p < 0.001$) at 2, 7, and 14 days after CCI, respectively (**Figure 1A**). The level of CXCL1 mRNA in the spinal cord was significantly enhanced (2.2-fold, $p < 0.001$) only on the 2nd day (**Figure 1B**). Similarly, the CXCL2 mRNA level was strongly increased (5.4-fold, $p < 0.001$) only on the 2nd day (**Figure 1C**). The level of CXCL3 mRNA was slightly enhanced (1.4-fold) at 2 days after CCI (**Figure 1D**).

In the spinal cord, the Western blot analysis showed that no significant changes in the levels of the CXCR2, CXCL1, and CXCL2 proteins were observed post-CCI (**Figures 1E–G**, respectively). A great increase in the level of CXCL3 protein was detected on the 2nd (1.4-fold, $p < 0.05$) and 7th (1.3-fold, $p < 0.05$) days after CCI (**Figure 1H**; **Data Sheet 1**).

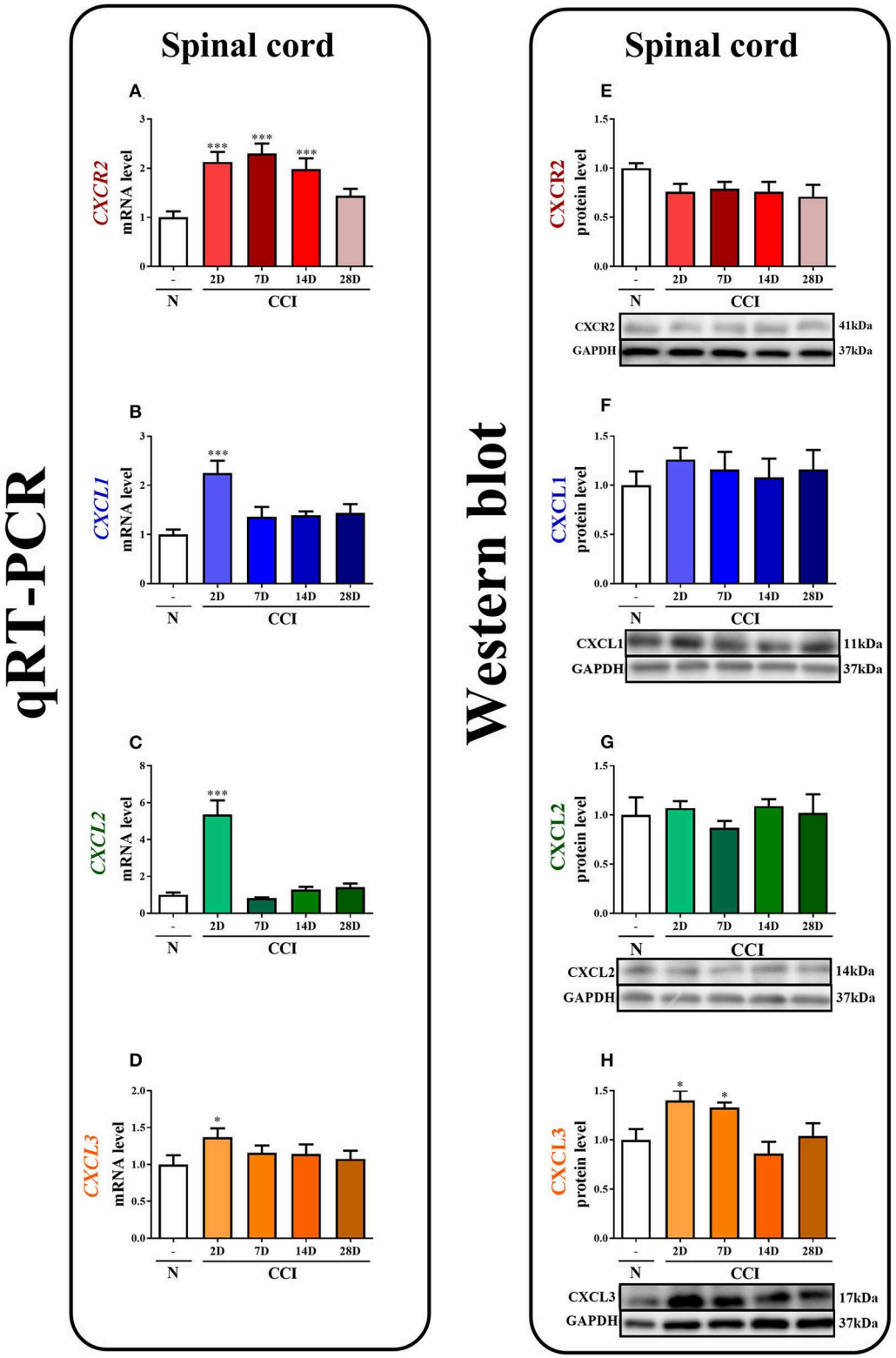

FIGURE 1 | The time course of changes in CXCR2, CXCL1, CXCL2, CXCL3 mRNAs **(A–D)** and proteins **(E–H)** in the spinal cord tissues on the 2nd, 7th, 14th, and 28th days after chronic constriction injury (CCI) in rats. The RT-qPCR and Western blot data are presented as the means ± SEM of 6–10 and 4–6 samples per group in each method, respectively. Intergroup differences were analyzed using ANOVA with Bonferroni's multiple comparisons test. $^{*}p < 0.05$, $^{***}p < 0.001$ indicate differences vs. naive rats. CCI, chronic constriction injury; N, naïve.

The Spinal Localization of CXCR2 and Its Ligand CXCL3 on the 7th Day After CCI in Rats

The immunofluorescent staining provided clear evidence that both CXCR2 and CXCL3, regardless of treatment (naive vs. CCI) co-localize with neurons, as shown by double staining using the neuronal marker, NeuN (**Figures 2A–D**, upper rows). Co-staining with microglia marker, IBA1, and astroglia marker, GFAP, showed lack of co-localization of CXCR2 or CXCL3 with Iba1 or GFAP (**Figures 2A–D**, middle and bottom rows), however in CCI-induced animals there were possible to find a few, singular cells co-stained with CXCL3 and IBA1 (**Figure 2D**, indicated by arrows), revealing that at least under enhanced inflammatory response some CXCL3-positive cells may also expressed activated microglia.

The Influence of the Single Intrathecal Administration of CXCL1, CXCL2, and CXCL3 on Nociceptive Transmission in Naive Mice

The single intrathecal administration of different doses of CXCL1, CXCL2, and CXCL3 induced the development of

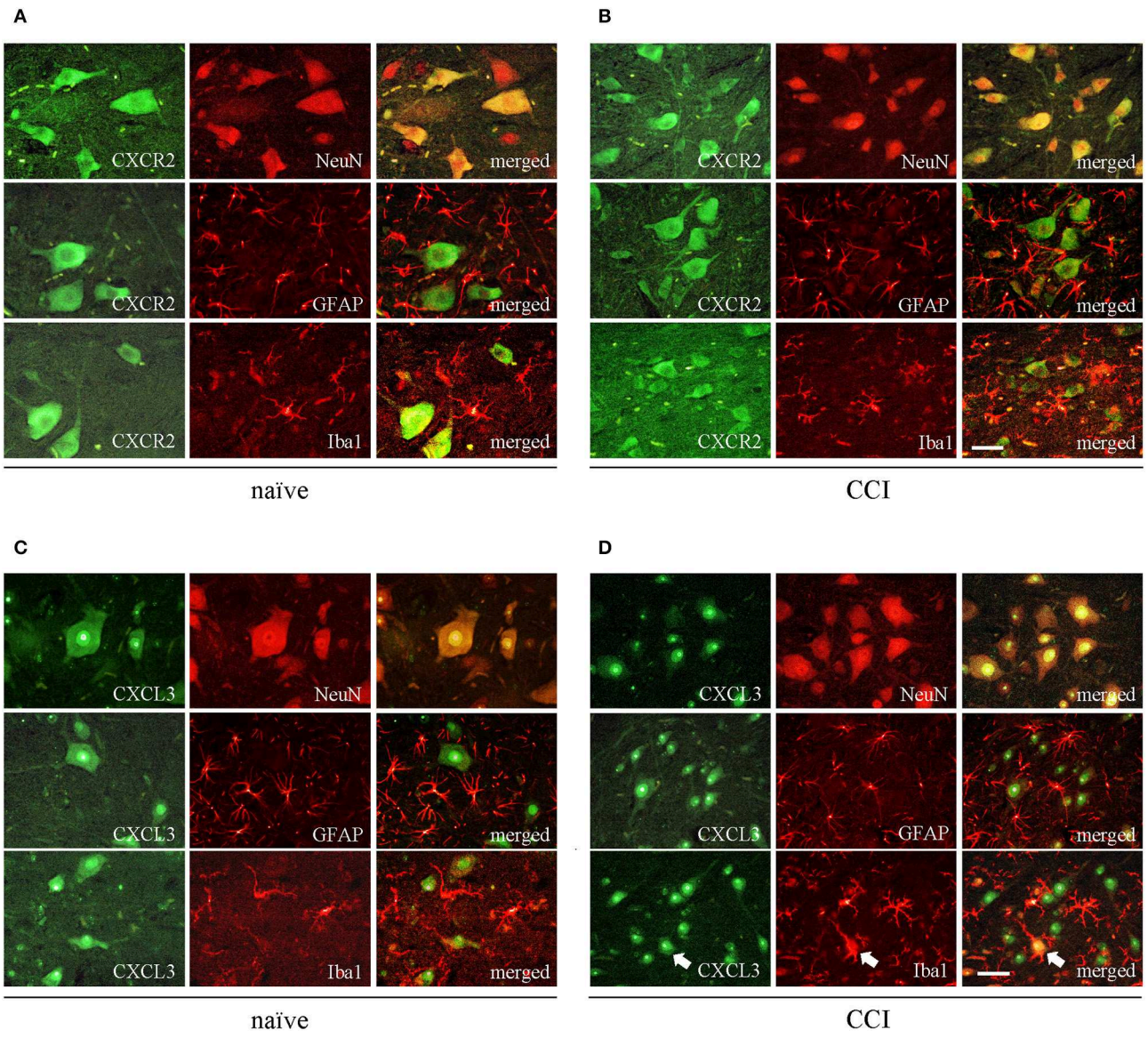

FIGURE 2 | The spinal localization of CXCR2 and its ligand CXCL3 in naive and CCI-exposed rats. Immunofluorescent staining was performed on paraffin-embedded 7 μm **(A,B)** co-staining of CXCR2 (green) and neuronal marker NeuN (red; upper row); astroglial marker GFAP (red, middle row), and microglial marker IBA1 (red, bottom row). **(C,D)** co-staining of CXCL3 (green) and neuronal marker NeuN (red; upper row); astroglial marker GFAP (red, middle row), and microglial marker IBA1 (red, bottom row). White arrows indicate representative CXCL3-positive cells that co-localize with IBA1-positive cells. Scale bar for all pictures: 25 μm.

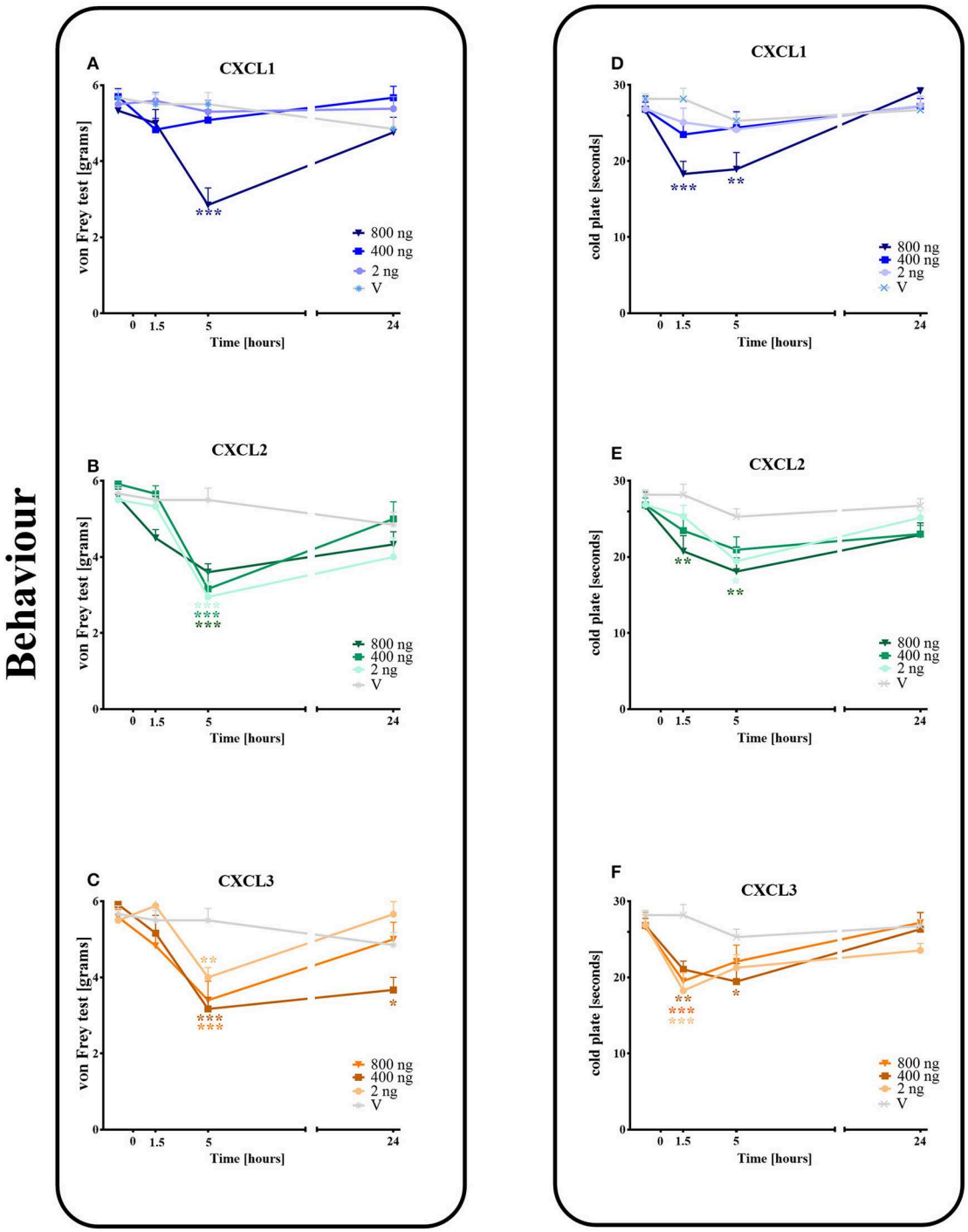

FIGURE 3 | Effects of single administrations of CXCL1, CXCL2, and CXCL3 **(A–F)** on nociceptive transmission in naive mice. The effects of single intrathecal administrations of CXCL1, CXCL2, CXCL3 (2, 400, or 800 ng/5 μl) on mechanical hypersensitivity (von Frey test, **A–C**) and thermal hypersensitivity (cold plate test, **D–F**) were measured at 1.5, 5, and 24 h after administration. Data are presented as the means ± SEM (6 mice per group). The results were evaluated using one-way ANOVA, followed by Bonferroni's test for comparisons of selected pairs measured separately at each time point. $^{*}p < 0.05$, $^{**}p < 0.01$, $^{***}p < 0.001$ for the comparison of vehicle-treated naive animals with all groups at the indicated time points. Additionally, the results were evaluated using two-way ANOVA to determine the time × drug interaction (please see results in Chapter 3.3). V, vehicle.

mechanical and thermal hypersensitivity, as measured using the von Frey (**Figures 3A–C**) and cold plate (**Figures 3D–F**) tests, respectively.

In the von Frey test, no significant pronociceptive effects were observed after a low dose of CXCL1 (2 ng/5 μl) at all studied time points (1.5–24 h). However, the high doses (400 and 800 ng) evoked mechanical hyperalgesia 1.5 h ($p < 0.001$) or 5 h ($p < 0.001$) after injection (**Figure 3A**). This effect vanished after 24 h. For CXCL2 and CXCL3, no significant reactions were observed at 1.5 h after the injection of all doses (2, 400, and 800 ng). However, at 5 h after the injection of CXCL2, the effects of all doses were strong ($p < 0.001$), which nevertheless disappeared altogether at 24 h (**Figure 3B**). Similarly, the pronociceptive effect of CXCL3 appeared later, and the strongest mechanical hypersensitivity was observed for all doses after 5 h ($p < 0.001$ for 400 ng; $p < 0.01$ for 800 ng; $p < 0.01$ for 2 ng). The effect faded after 24 h, except for one dose (400 ng) (**Figure 3C**). Two-way ANOVA confirmed a significant interaction [$F_{(9,110)} = 5.783$, $p < 0.0001$; $F_{(9,104)} = 2.689$, $p = 0.0075$; $F_{(9,104)} = 3.331$, $p = 0.0013$; respectively] between the investigated treatments for CXCL1, CXCL2, CXCL3, and the investigated time points. CXCL1, CXCL2, and CXCL3 significantly decreased the nociceptive threshold [$F_{(3,110)} = 6.268$, $p = 0.0006$; $F_{(3,104)} = 26.87$, $p < 0.0001$; $F_{(3,104)} = 20.32$, $p < 0.0001$], showing a pronociceptive dose-dependent effect of CXCL1, CXCL2, and CXCL3 in the von Frey test.

In the cold plate test, no significant pronociceptive effects were observed after low (2 ng/5 μl) and intermediate (400 ng/5 μl) doses of CXCL1 (**Figure 3D**) and after an intermediate (400 ng/5 μl) dose of CXCL2 (**Figure 3E**) at all studied time points (1.5–24 h). The mice displayed thermal hypersensitivity to stimuli at 1.5 h ($p < 0.001$) and 5 h ($p < 0.01$) after the injection of the highest dose of CXCL1 (800 ng), which nevertheless disappeared until 24 h (**Figure 3D**). Similarly, at 1.5 h ($p < 0.01$) and 5 h ($p < 0.01$) after CXCL2 injection, we observed the highest peak reaction for the highest dose and in addition to the low dose after 5 h ($p < 0.05$) (**Figure 3E**). All tested doses of the CXCL3 injection caused comparable reactions to thermal stimuli after 1.5 h ($p < 0.001$ for 2 and 800 ng; $p < 0.01$ for 400 ng). Only the reaction after the intermediate dose was also maintained after 5 h ($p < 0.01$) (**Figure 3F**). Two-way ANOVA confirmed a significant interaction [$F_{(9,124)} = 2.605$, $p = 0.0087$] between the investigated treatment for CXCL1 and the investigated time points. In the case of CXCL2 and CXCL3, two-way ANOVA did not show a time × drug interaction [$F_{(9,120)} = 0.8918$, $p = 0.5349$; $F_{(9,118)} = 1.905$, $p = 0.0577$, respectively]. CXCL1, CXCL2, and CXCL3 significantly decreased the nociceptive threshold [$F_{(3,124)} = 2.605$, $p = 0.0087$; $F_{(3,120)} = 9.048$, $p < 0.0001$; $F_{(3,118)} = 10.31$, $p < 0.0001$, respectively], showing a pronociceptive effect of CXCL1, CXCL2, and CXCL3 in the cold plate test.

Effect of the Single and Repeated Intrathecal Administrations of the CXCR2 Antagonist NVP CXCR2 20 on Mechanical and Thermal Hypersensitivity in the CCI-Induced Model of Neuropathic Pain

A single *i.t.* administration of NVP CXCR2 20 at concentrations of 10, 20 and 30 μg/5 μl was performed at 7 days after CCI. The influence of the NVP CXCR2 20 on the development of hypersensitivity to mechanical and thermal stimuli was measured by von Frey (**Figure 4A**) and cold plate (**Figure 4B**) tests, respectively, at 0.5, 1, 2, 4, 6, and 24 h after administration. NVP CXCR2 20 injection at the lowest dose did not diminish mechanical hypersensitivity (**Figure 4A**) and only slightly diminished thermal hypersensitivity (**Figure 4B**). However, higher doses showed significant analgesic effects at 2, 4 and 6 h after injection measurement by cold plate and von Frey tests (**Figures 4A,B**). Two-way ANOVA confirmed a significant interaction [$F_{(18,110)} = 4.054$, $P < 0.0001$; $F_{(18,133)} = 2.716$, $P = 0.0006$, respectively] between the investigated treatment and the investigated time points in von Frey and cold plate tests. The mechanical and thermal hypersensitivity were significantly diminished after NVP CXCR2 20 treatment [$F_{(6,110)} = 16.29$; $P < 0.0001$; $F_{(6,133)} = 25.58$; $P < 0.0001$; respectively]. Based on the obtained behavioral results and our pharmacological experience for the repeated treatment, we have chosen the dose of 10 μg/5 μl, so the lowest possible dose with analgesic effect to avoid side effects.

Repeated *i.t.* administration of NVP CXCR2 20 at a concentration of 10 μg/5 μl has analgesic effects in CCI-treated rats (**Figures 4C,D**). After CCI, all rats exhibited strong mechanical hypersensitivity in the paw ipsilateral to the injury (as demonstrated by the von Frey test results on days 2 and 7 after CCI ($p < 0.001$) (**Figure 4C**), and compared to the control group of naive animals, all rats exhibited potent thermal hypersensitivity (as demonstrated by the response latency in the cold plate test ($p < 0.001$; **Figure 4D**). NVP CXCR2 20 reduced mechanical ($p < 0.001$) (**Figure 4C**) and thermal ($p < 0.01$) hypersensitivity at 120 and 125 min after the last injection on day 2 after CCI (**Figure 4D**). On day 7 after CCI, NVP CXCR2 20 also diminished mechanical ($p < 0.01$) (**Figure 4C**) and thermal ($p < 0.01$) hypersensitivity (**Figure 4D**) at 125 min after the last injection.

The Influence of the Repeated Administration of NVP CXCR2 20 on CXCR2, IBA1, GFAP, CXCL1, CXCL2, and CXCL3 Protein Levels in the Spinal Cord and DRG at 7 Days After CCI in Rats

In the spinal cords of vehicle- and NVP-treated CCI-exposed rats, the level of the CXCR2 protein remained unchanged compared with that in the spinal cords of naive rats (**Figure 5A**). In the spinal cord of vehicle-treated, CCI-exposed rats, the levels of the IBA1 and GFAP proteins were increased (4.24-fold, $p < 0.01$; 2.5-fold, $p < 0.01$, respectively) compared with naïve rats (**Figures 5B,C**, respectively). NVP CXCR2 20 did not change the up-regulation of the IBA1 protein (5.3-fold in relation to control; **Figure 5B**) and GFAP protein (3.44-fold in relation to control; **Figure 5C**) levels in the spinal cord after CCI. No changes were observed in the spinal levels of the CXCL1 and CXCL2 proteins (**Figures 5D,F**, respectively), which corresponds well with the time-course study presented in **Figures 1F,G**. NVP CXCR2 20 also did not change the CXCL1 and CXCL2 protein levels (**Figures 5D,F**). Compared with naive rats, the level of the

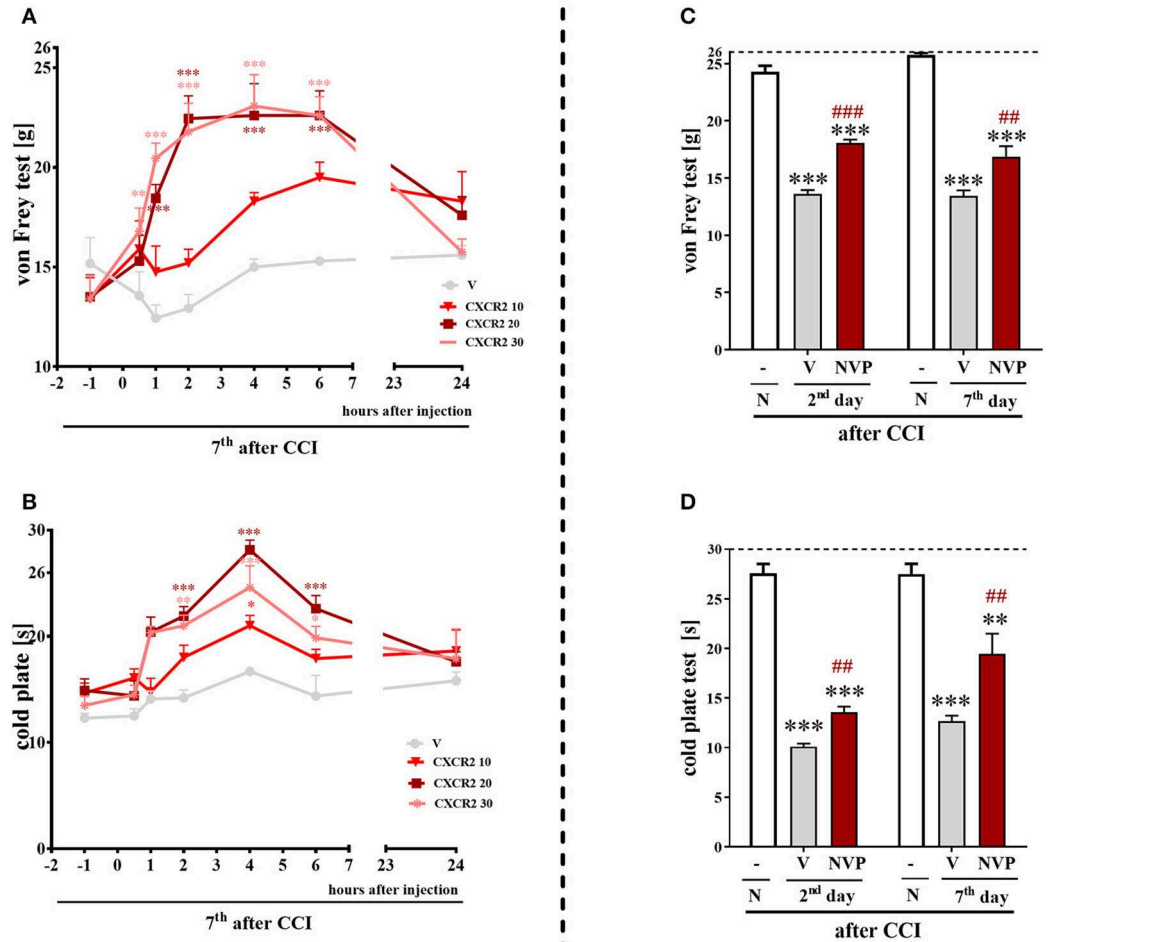

FIGURE 4 | Effects of single **(A,B)** (different doses: 10, 20, and 30 µg/5 µl) intrathecal NVP CXCR2 20 administration on mechanical (**A**; von Frey test) and thermal (**B**; cold plate test) hypersensitivity as measured 0.5, 1, 2, 4, 6, 24 h after NVP CXCR2 20 injection on day 7 in CCI-exposed rats. Effects of repeated **(C,D)** (one dose: 10 µg/5 µl *i.t.*; 16 h and 1 h before CCI and then once a day for 7 days) intrathecal NVP CXCR2 20 administration on mechanical (**C**; von Frey test) and thermal (**D**; cold plate test) hypersensitivity as on day 2 or 7 in CCI-exposed rats. Tactile and thermal hypersensitivity were assessed at 120 and 125 min after the last NVP CXCR2 20 injection, respectively. The horizontal dotted line shows the cut-off value. Data are presented as the means ± SEM of 10–18 rats after single administration and 8 rats after repeated administration per group. Intergroup differences were analyzed using ANOVA with Bonferroni's multiple comparisons test measured separately at each time point. $^{*}p < 0.05$, $^{**}p < 0.01$, $^{***}p < 0.001$ indicate differences between vs. naive rats. $^{\#\#}p < 0.01$, $^{\#\#\#}p < 0.001$ indicate differences between V- and NVP-treated, CCI-exposed rats. CCI, chronic constriction injury; N, naive; V, vehicle; NVP, NVP CXCR2 20. Additionally, the results presented on graphs A and B were additionally evaluated using two-way ANOVA to determine the time × drug interaction (please see results in chapter 3.4).

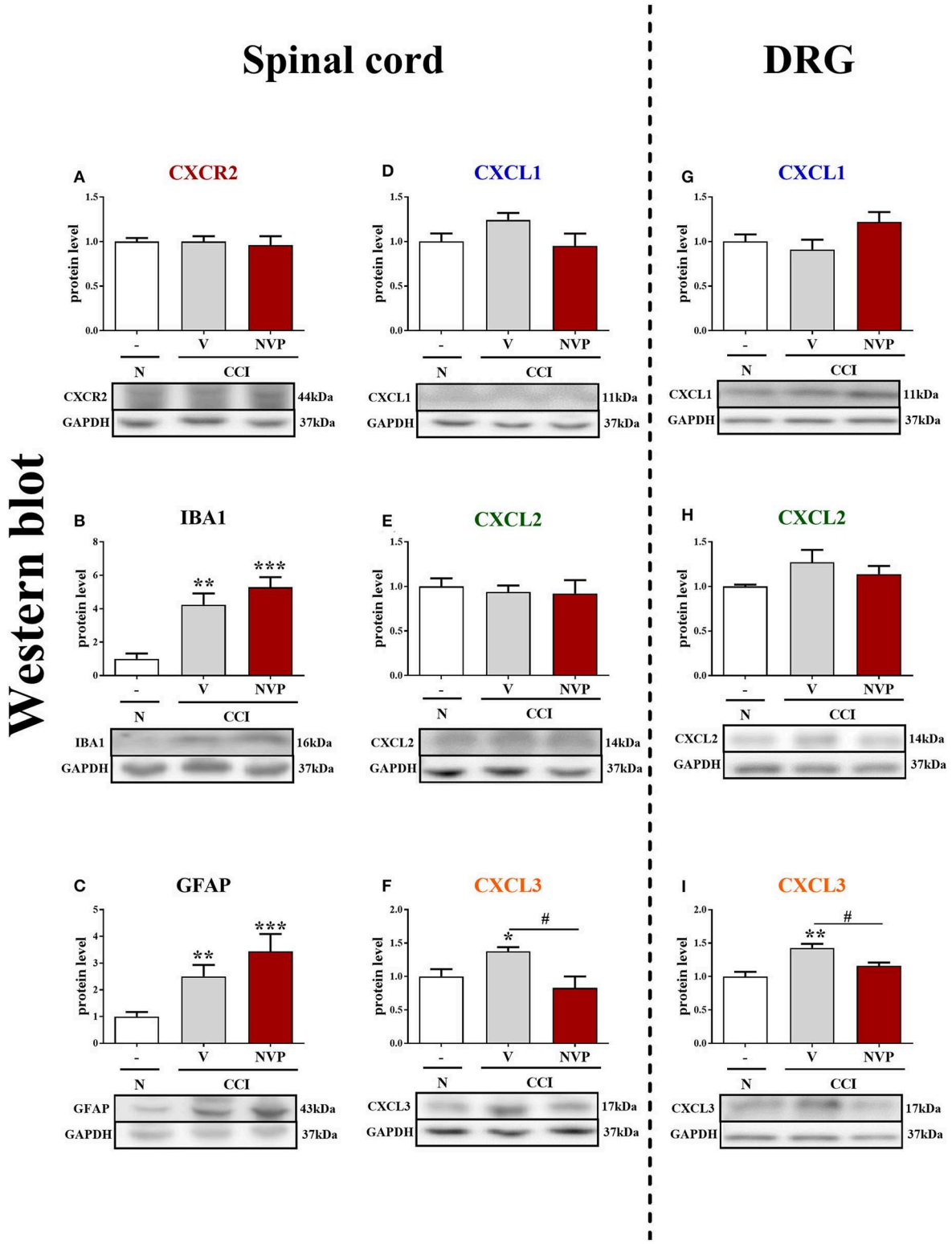

FIGURE 5 | Effects of the repeated administration of NVP CXCR2 20 (NVP; 10 μg/5 μl; *i.t.*; 16 h and 1 h before CCI and then once a day for 7 days) on the protein levels of CXCR2, IBA1, GFAP, CXCL1, CXCL2, and CXCL3 proteins **(A–I)** in the spinal cord **(A–F)** and DRG **(G–I)** on the 7th day after CCI in rats. The data are presented as the mean fold changes relative to the control ± SEM (5–6 samples per group). Intergroup differences were analyzed using ANOVA with Bonferroni's multiple comparisons test. $^{*}p < 0.05$, $^{**}p < 0.01$, $^{***}p < 0.001$ indicate differences vs. naive rats. $^{\#}p < 0.05$, indicate differences between V-treated and NVP-treated rats. CCI, chronic constriction injury; N, naive; V, vehicle; NVP, NVP CXCR2 20.

CXCL3 protein was increased 1.4-fold ($p < 0.05$) in vehicle-treated, CCI-exposed rats (**Figure 5F**), and importantly, NVP CXCR2 20 significantly attenuated CXCL3 protein expression to the level of control (1.7-fold; $p < 0.05$; **Figure 5F**).

In the DRG, as in the spinal cord, the levels of the CXCL1 and CXCL2 proteins remained unaltered in CCI-exposed rats, and NVP CXCR2 20 did not influence these factors (**Figures 5G,H**, respectively). The level of the CXCL3 protein was raised 1.4-fold ($p < 0.01$) in the vehicle-treated, CCI-exposed rats as compared to naive rats (**Figure 5I**), and again, the NVP CXCR2 20 significantly attenuated CXCL3 protein expression to the level of control (1.2-fold; $p < 0.05$) in the DRG (**Figure 5I**; **Data Sheet 2**).

The Influence of the Single Intrathecal Administration of CXCL3-Neutralizing Antibody on Pain-Related Behaviors on the 7th Day After CCI in Mice

CXCL3-neutralizing antibodies were administered (*i.t.*) once on day 7 after CCI at the following concentrations: 1, 4 and 8 μg/5 μl (**Figures 6A,B**). The control group, CCI-exposed mice received vehicle (V; water for injection). Reactions to mechanical and thermal stimuli were assessed by von Frey (**Figure 6A**) and cold plate (**Figure 6B**) tests, respectively.

In the von Frey test, all doses (1, 4, and 8 μg) of CXCL3-neutralizing antibodies (**Figure 6A**) diminished the pain-related behavior. For the 1 μg dose ($p < 0.001$), the effect was observed only in the 5th hour (**Figure 6A**), while for doses 4 and 8 μg, the effect was already observed after 1.5 h ($p < 0.01$, $p < 0.001$; respectively) and strongly persisted after 5 h ($p < 0.001$). The analgesic effects of neutralizing antibody for doses 1 and 4 μg were reversed after 24 h and for the 8 μg dose only after 48 h, as measured by von Frey test (**Figure 6A**). Two-way ANOVA confirmed a significant interaction [$F_{(8, 103)} = 5{,}555$, $p < 0.0001$] between the investigated treatment for CXCL3-neutralizing antibody and investigated time points. The CXCL3-neutralizing antibody significantly increased the nociceptive threshold [$F_{(4, 103)} = 12{,}65$, $p < 0.0001$], showing an antinociceptive dose-dependent effect of the CXCL3-neutralizing antibody in the von Frey test.

In the cold plate test, after all doses (1, 4, and 8 μg) of CXCL3-neutralizing antibodies were used, the pain-related behavior was diminished (**Figure 6B**). This strong analgesic effect could be seen after 1.5 and 5 h for all tested doses (1, 4, and 8 μg) ($p < 0.05$; $p < 0.001$; $p < 0.001$, respectively) (**Figure 6B**). This effect was still observed after 24 h, but only for the highest dose, 8 μg ($p < 0.01$) (**Figure 6B**). The analgesic effects of 1 and 4 μg doses were reversed after 24 h as measured by the cold plate test (**Figure 6B**). Two-way ANOVA confirmed a significant interaction [$F_{(12, 111)} = 2{,}723$ $p = 0.0029$] between the investigated treatment for CXCL3-neutralizing antibody and the investigated time points. The CXCL3-neutralizing antibody significantly increased the nociceptive threshold [$F_{(4, 111)} = 9{,}512$ $p < 0.0001$], showing

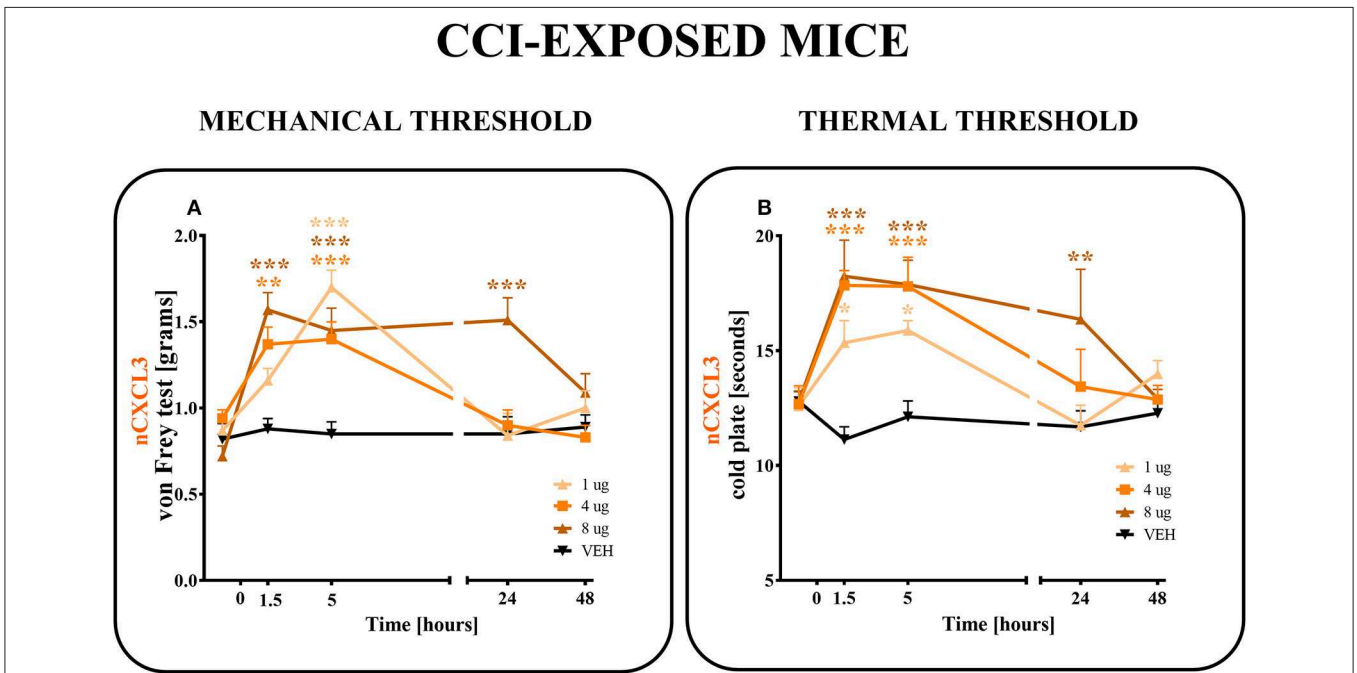

FIGURE 6 | Effects of single administrations of CXCL3 neutralizing antibody **(A,B)** on nociceptive transmission in CCI-exposed mice. The effects of single intrathecal administrations of CXCL3 neutralizing antibody (1, 4, or 8 μg/5 μl) on mechanical hypersensitivity (von Frey test, **A**) and thermal hypersensitivity (cold plate test, **B**) were measured at 1.5, 5, 24, and 48 h after administration at 7 days after CCI. Data are presented as the means ± SEM (6–8 mice per group). The results were evaluated using one-way ANOVA followed by Bonferroni's test for comparisons of selected pairs. $^{*}p < 0.05$, $^{**}p < 0.01$, $^{***}p < 0.001$ for the comparison of CCI-exposed vehicle-treated animals with all groups at the indicated time points. Additionally, the results were evaluated using two-way ANOVA to determine the time × drug interaction (please see results in chapter 3.6). V, vehicle.

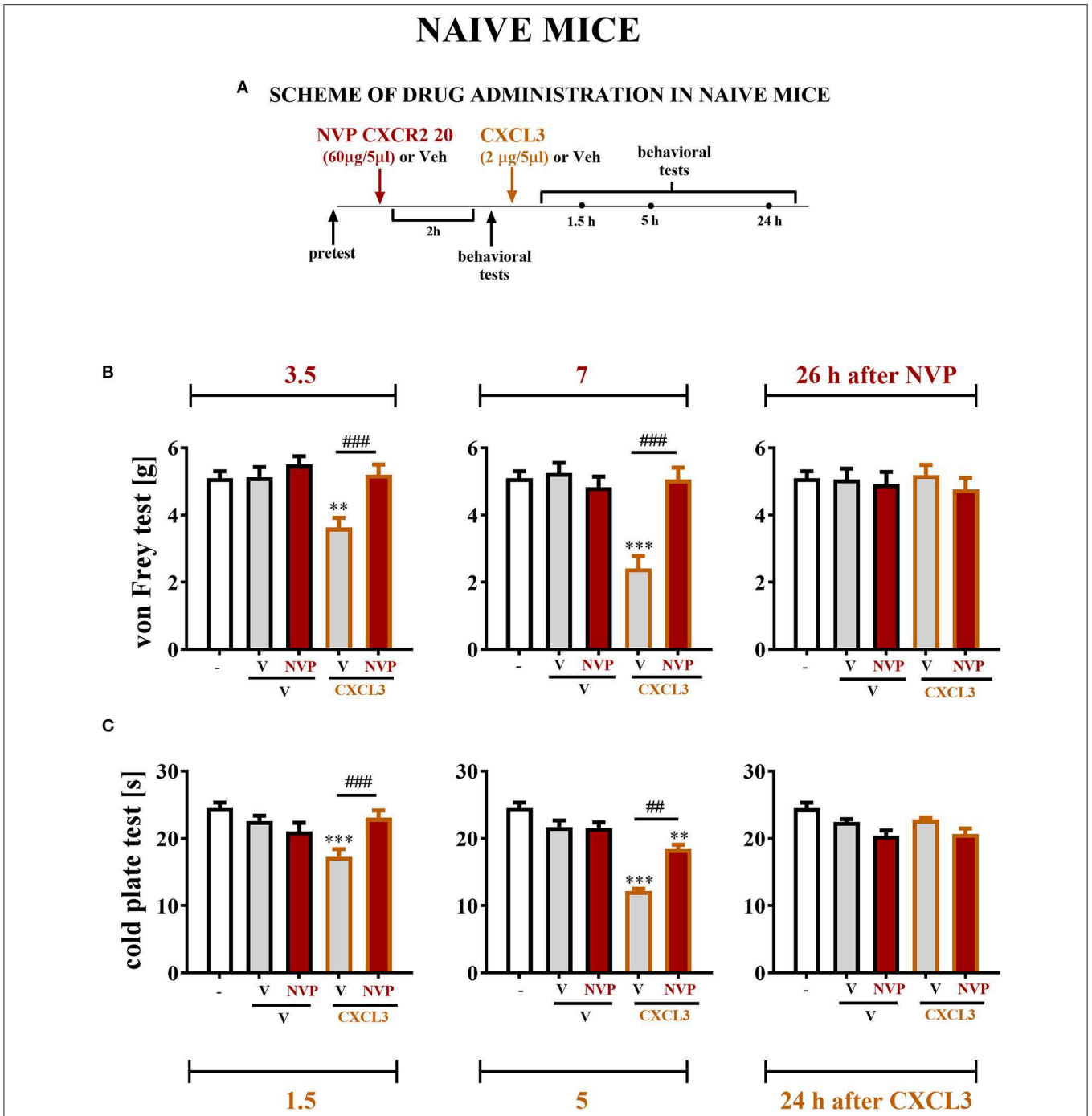

FIGURE 7 | Effects of single NVP CXCR2 20 administration on a single CXCL3 injection and nociceptive transmission in naive mice **(B,C)**. Single intrathecal administrations of vehicle (V) or NVP CXCR2 20 (60 µg/5 µl) were performed 120 min before a single intrathecal administration of V or CXCL3 (2 ng/5 µl). The effects of administrations on mechanical (von Frey test; **B**) and thermal (cold plate test; **C**) hypersensitivity were measured 3.5, 7 and 26 h after the NVP CXCR2 20 injection (1.5, 5, and 24 h after the CXCL3) **(A)**. Data are presented as the means ± SEM (6–8 mice per group). The results were evaluated using one-way ANOVA followed by Bonferroni's test for comparisons of selected pairs. $^{**}p < 0.01$, $^{***}p < 0.001$ indicate differences in comparison with V+V-treated animals at the indicated time points. $^{\#\#}p < 0.01$, $^{\#\#\#}p < 0.001$ indicate differences in comparison with V+CXCL3-treated animals at the indicated time points. V, vehicle; NVP, NVP CXCR2 20.

an antinociceptive dose-dependent effect of CXCL3-neutralizing antibody in the cold plate test.

The control antibody administration did not influence the development of tactile (e.g., pretest for V-treated group 0.67 ± 0.05 g vs. IgG-treated group 0.74 ± 0.07 g; 4 h after *i.t.* administration: V-treated group 0.83 ± 0.09 g vs. IgG-treated group 0.8 ± 0.08 g) or thermal (e.g., pretest for V-treated group 7.66 ± 0.5 s vs. IgG-treated group 7.71 ± 0.6 s; 4 h after *i.t.*

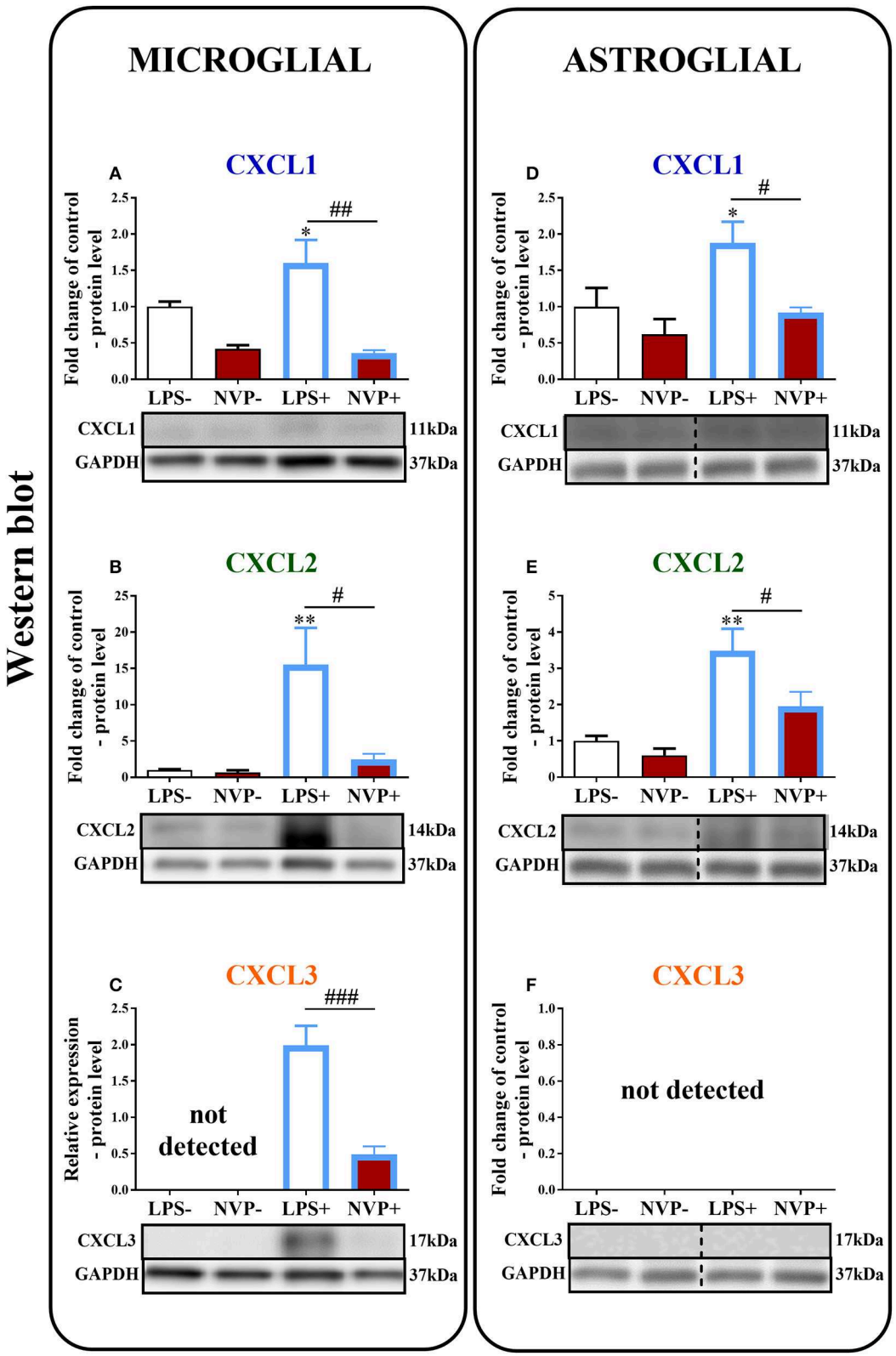

FIGURE 8 | Effects of on NVP CXCR2 20 levels of the CXCL1, CXCL2, and CXCL3 proteins **(A–F)** in primary rat microglial **(A–C)** and astroglial **(D–F)** cell cultures. Samples were analyzed 24 h after cells were stimulated with LPS. The data are presented as the fold change relative to the control and relative protein levels. *Fold change relative to control*: the Western blot data are presented as the means ± SEM and represent the normalized averages derived from analyses of 3–4

(Continued)

FIGURE 8 | independent experiments. Intergroup differences were analyzed using ANOVA with Bonferroni's multiple comparisons test. $^{*}p < 0.05$, $^{**}p < 0.01$, $^{***}p < 0.001$ indicate differences in comparison with the control group (vehicle-treated non-stimulated cells); $^{\#}p < 0.05$, $^{\#\#}p < 0.01$, $^{\#\#\#}p < 0.001$ indicate differences between vehicle-treated and NVP-treated LPS-stimulated cells. *Relative protein level:* Inter-group differences in relative protein level were analyzed using a t-test. $^{\#\#\#}p < 0.001$ indicates differences compared to the vehicle-treated LPS-stimulated cells. LPS-, vehicle-treated non-stimulated cells; NVP-, NVP-treated non-stimulated cells, LPS+, vehicle-treated LPS-stimulated cells; NVP+, NVP-treated LPS-stimulated cells. In **(D–F)** the blots are cropped which was shown with a dotted line on the representation bands below the figures.

administration: V-treated group 7.96 ± 0.5 s vs. IgG-treated group 8.4 ± 0.47 s) hypersensitivity.

The Influence of Single Intrathecal Administration of CXCL3 Preceded by NVP CXCR2 20 Injection on Nociceptive Transmission in Naive Mice

The reactions to non-noxious (**Figure 7B**) and noxious (**Figure 7C**) stimuli in naive, vehicle + vehicle–treated and vehicle + NVP–treated (60 μg/5 μl) mice were similar (**Figures 7B,C**). At 2 h after substance administration, behavioral tests were conducted, and the mice received CXCL3 (2 ng/5 μl) following the testing (**Figure 7A**). The behavioral tests were performed at 1.5, 5, and 24 h after CXCL3 injection (3.5, 7, and 26 h after NVP CXCR2 20 administration) (**Figure 7A**). The vehicle + CXCL3–treated group (800 ng/5 μl) developed mechanical and thermal hypersensitivity (**Figures 7B,C**, respectively), which was prevented by pretreatment with NVP CXCR2 20 (**Figures 7B,C**).

The Influence of NVP CXCR2 20 on the Levels of the CXCL1, CXCL2, and CXCL3 Proteins in Rat Microglial and Astroglial Cell Cultures at 24 h After Lipopolysaccharide Stimulation

In microglial cell cultures, we observed an expressive increase in the levels of CXCL1 (1.6-fold, $p < 0.05$; **Figure 8A**) and CXCL2 (15.6-fold, $p < 0.01$; **Figure 8B**) proteins at 24 h after LPS stimulation. CXCL3 protein levels were not detected in non-stimulated cells, but we observed strongly increased CXCL3 protein levels in LPS-stimulated microglia (**Figure 8C**). NVP CXCR2 20 decreased the CXCL1 (4.4-fold, $p < 0.01$; **Figure 8A**), CXCL2 (6.3-fold, $p < 0.05$; **Figure 8B**), and CXCL3 (4.3-fold, $p < 0.001$; **Figure 8C**) protein levels in LPS-stimulated cells compared with those in vehicle-treated LPS-stimulated microglia.

In astroglial cell cultures, we observed a considerable increase in the levels of the CXCL1 (1.9-fold, $p < 0.05$; **Figure 8D**) and CXCL2 (3.5-fold, $p < 0.01$; **Figure 8E**) proteins at 24 h after LPS stimulation. NVP CXCR2 20 decreased the CXCL1 (2-fold, $p < 0.05$; **Figure 8D**) and CXCL2 (1.8-fold, $p < 0.05$; **Figure 8E**) protein levels in LPS-stimulated cells compared with those in vehicle-treated LPS-stimulated microglia. CXCL3 protein levels were not detected in astrocytes (in non-stimulated or LPS-treated) (**Figure 8F**; **Data Sheet 3**).

The Influence of Single Administrations of NVP CXCR2 20 on Opioid Effectiveness on the 7th Day Post-CCI in Rats

In the von Frey test, single injections of the respective opioids caused similar analgesic effects as single injections of NVP CXCR2 20 (10 μg/5 μl). The combined administration of NVP CXCR2 20 and morphine (2.5 μg/5 μl) or buprenorphine (2.5 μg/5 μl) did not change the effectiveness of the individual substances (**Figure 9B**).

In the cold plate test, single injections of the respective opioids caused similar analgesic effects as single injections of NVP CXCR2 20 (10 μg/5 μl). The single administration of the combination of NVP CXCR2 20 and morphine (2.5 μg/5 μl) or buprenorphine (2.5 μg/5 μl) did not change their efficacy (**Figure 9C**).

DISCUSSION

First, we observed that intrathecal injections of CINCs induced pain-related behaviors in naive mice, which is related to the CXCR2 neuronal response. Second, RT-qPCR and Western blot results of the time course changes in chemokines indicated CXCL3 involvement in the development of neuropathic pain, whereas only the mRNA expression of the two other ligands was increased in the initial phase. Moreover, the neutralizing antibody for CXCL3 reduced neuropathic pain symptoms in mice on day 7 after CCI. Third, immunofluorescence staining indicated that in the spinal cord, CXCR2 and CXCL3 are expressed mainly in neurons as measured at 7 days after sciatic nerve injury. Fourth, we proved that a potent and selective CXCR2 receptor antagonist, NVP CXCR2 20, reduces the symptoms of neuropathic pain and the CCI-upregulated levels of CXCL3 in the spinal cord and DRG and prevents the development of hypersensitivity to stimuli after CXCL3 administration. Finally, we provided evidence that the chronic intrathecal administration of NVP CXCR2 20 did not attenuate microglial activation, and this is probably the reason why these compounds do not enhance morphine/buprenorphine analgesia, which was observed in our previous studies on the CXCR3 antagonist (±)-NBI-74330 (29). Notably, to the best of our knowledge, this study is the first to present the comparison of these three chemokines in a single experiment involving a neuropathic pain model. Our findings provide evidence that, out of all investigated CINCs, spinal CXCL3 plays an important role in CXCR2 signaling in neuropathic pain.

Our results obtained in a neuropathic pain model are consistent with other findings (58–61), which suggests that CXCR2 is important for nociception transmission. First, it was shown that the expression of CXCR2 becomes upregulated in

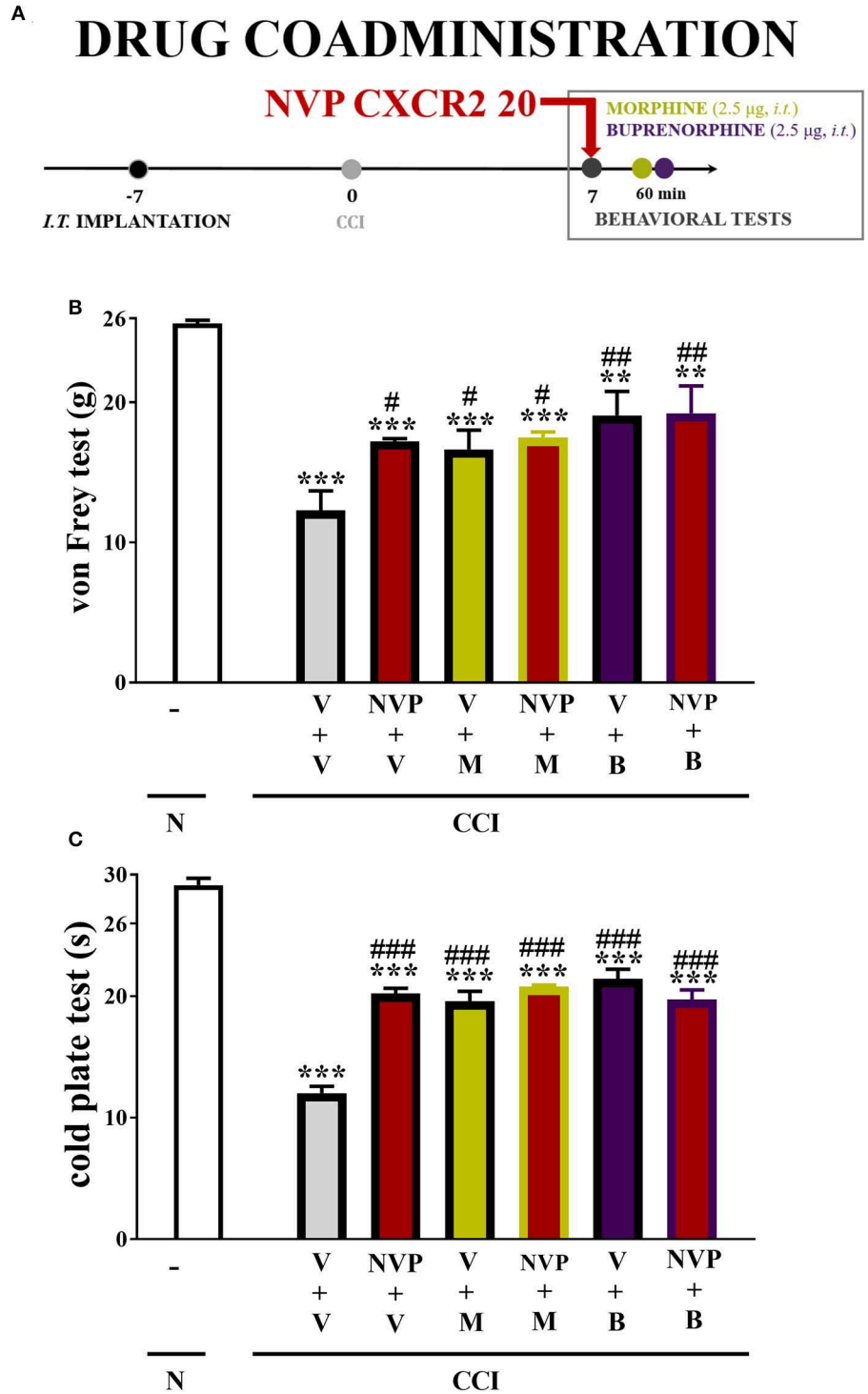

FIGURE 9 | Scheme of drug co-administration **(A)**. Effects of single **(B,C)** administration of NVP CXCR2 20 (NVP; 10 μg/5 μl; single dose *i.t.*; on the 7th day post-CCI) **(A)** on pain-related behaviors (von Frey test **A**; cold plate test **B**) and the analgesic effects of morphine (M; 2.5 μg/5 μl; single dose *i.t.*; on the 7th day post-CCI, 4 h after NVP or V injection) and buprenorphine (B; 2.5 μg/5 μl; single dose *i.t.*; on the 7th day post-CCI, 4 h after NVP or V injection) on CCI-exposed rats. The data are presented as the means ± SEM of 6 rats per group. Intergroup differences were analyzed using ANOVA with Bonferroni's multiple comparisons test. $^{**}p < 0.01$, $^{***}p < 0.001$ indicate differences compared with naïve rats. $^{\#}p < 0.05$, $^{\#\#}p < 0.01$, $^{\#\#\#}p < 0.001$ indicate differences compared V+V-treated, CCI-exposed rats. B, buprenorphine; CCI, chronic constriction injury; M, morphine; N, naive; NVP, NVP CXCR2 20; V, vehicle.

macrophages and neutrophils infiltrated locally at a nerve injury site (62). Immunohistochemical studies demonstrated that under neuropathic conditions, the majority of spinal CXCR2 molecules are located on dorsal horn neurons (15, 63); however, their upregulation also occurs in non-neuronal cells (15, 63, 64). Second, it has recently been published that under homeostatic conditions, spinal microglia do not express CXCR2, but it can be upregulated upon its activation in central nervous system (CNS) pathologies, such as Alzheimer's disease, multiple sclerosis, traumatic brain or nerve injuries, and inflammation, including Complete Freund's Adjuvant injection (15, 65–70). Our immunohistochemical staining proved the presence of spinal CXCR2 in neurons. Our results show the upregulation of CXCR2 mRNA on days 2, 7, and 14 after CCI in rats, which is in line with Xu et al. (26). The protein changes in CXCR2 are not measurable, which is not surprising because many GPCRs may rapidly internalize upon agonist stimulation and subsequently become replaced by newly synthesized receptors. Like other GPCRs, CXCR2 is rapidly internalization following a burst of agonist-mediated signaling. The mechanism appears to be similar to that used by many other GPCRs (71). During receptor activation, the induction of internalization of CXCR2 depends on the interactions between the N-terminal of the chemokine and the N-domain of the chemokine receptor (72). After agonist removal, internalized CXCR2 is associated with different cellular trafficking regulators and may be recycled to the cell surface, thereby enabling a subsequent round of signaling (71, 73) or may enter lysosomal sorting pathway of CXCR2 (74). These various receptor-mediated events are directly dependent on the CXCL1 or CXCL2 concentration (75), and dysregulation of these processes e.g., in the pathogenesis of neuropathic pain could switch the cell phenotype. Changes in ligand levels during neuropathic pain may lead to disorders in receptor activation and signaling, but this requires further study. In our recent studies using the CCR4 antagonist (Kujacz et al., submitted), we observed an increase in mRNA levels, in parallel with no change in protein levels in the neuropathic pain model. However, blocking these receptors causes strong analgesic effects—this requires further molecular studies—while the importance of these receptors in the nociceptive transmission is beyond doubt, as is CXCR2. The neuronal location of CXCR2 suggested by some authors (15, 63, 70, 76) correlates well with our behavioral results and explains why intrathecally injected CXCR2 ligands induce very fast and strong pain-like behavior in naive mice. Kiguchi et al. (62) reported that the administration of the histone acetyltransferase inhibitor anacardic acid suppressed the upregulation of CXCR2 at an injured sciatic nerve site after its partial ligation. Liang et al. (77) showed that the spinal administration of the CXCR2/CXCR1 antagonist, SCH527123, potently reversed sensitization after traumatic brain injury. Our study provides, for the first time, evidence that intrathecal injections of a potent and selective CXCR2 antagonist, NVP CXCR2 20, reduce neuropathic pain symptoms by modulating the release of CXCL3 at the spinal cord and DRG level. Based on these results and previously published data, we propose that the spinal blockade of CXCR2 signaling may produce efficient analgesic effects under neuropathy.

CXCL1 was the first discovered endogenous ligand of CXCR2. However, its role in nociception remains unclear. Our results indicate that in naive mice, the intrathecal administration of a high dose (800 ng) of CXCL1 causes hypersensitivity to mechanical and/or thermal stimuli, which suggests a confirmed spinal neuronal location of CXCR2. In 2007, Li et al. (78) reported that injuries of the spinal cord and sciatic nerve induce the upregulation of CXCL1 in DRG neurons (76) at 3 but not 7 days after surgery. Subsequently, it was shown that CXCL1 sensitizes primary neurons by triggering an increase in calcium ion influx, modulating potassium and sodium currents (15, 59, 79–81). In the CNS, however, CXCL1 astrocyte expression has already been shown in animal models after brain (82) and spinal cord (15, 83) injury, as well as in humans with multiple sclerosis (84). This observation was later confirmed by *in vitro* results showing that CXCL1 is released from primary astroglial cells following TNFα (15, 85) and IL-1beta (84) stimulation. Similarly, we showed the LPS-induced release of CXCL1 from primary astroglia cultures and, for the first time, microglial cells. Nevertheless, under neuropathic pain conditions, CXCL1 mRNA does not increase in parallel with microglia activation (10, 25, 44). We observed a spinal increase in CXCL1 mRNA only on day 2 after sciatic nerve injury, similar to Manjavachi et al. (86) after partial sciatic nerve ligation in Swiss mice. In our experiments, the spinal protein changes of CXCL1 in Wistar rats remained undetectable, which corresponds to the results in BALB/c mice after spinal nerve transection (87). Nevertheless, after spinal nerve ligation, some authors observed elevated CXCL1 protein levels in Sprague-Dawley rats and Albino Swiss mice (15, 88). Such discrepancies may arise due to the applied model of neuropathic pain or as a result of the specific genomic characteristics of the abovementioned rodent strains.

CXCL1 is 90% identical in amino acid sequence to its related chemokine, CXCL2. Based on our data, we were the first to indicate that, similar to other CINCs, the intrathecal administration of CXCL2 causes the rapid development of hypersensitivity to thermal and mechanical stimuli in naive mice, which confirms the spinal neuronal location of CXCR2. In 2012, Haraguchi et al. (89) showed that CXCL2 is produced in an injured sciatic nerve by partial ligation and suggested that this chemokine is secreted by monocytes and acts as chemotactic for leukocytes, which was confirmed by Kiguchi et al. (62). These authors observed that CXCL2 mRNA became elevated in an injured sciatic nerve during the first 24 h after damage, but no further changes were detected until day 14. Similarly, we showed an increase in CXCL2 mRNA at the spinal cord level only shortly (day 2) after sciatic nerve injury. However, the spinal protein level of CXCL2 did not change after injury, suggesting that under neuropathy, CXCL2 plays an important role in the PNS (peripheral nervous system) rather than the CNS. The lack of spinal CXCL2 upregulation was unexpected, since earlier *in vitro* studies showed an increase in CXCL2 in activated mouse primary microglia (89), which is in agreement with our *in vitro* results obtained in rat microglia and astroglia cultures. Nonetheless, we did not observe any spinal upregulation of CXCL2 protein in parallel with glial activation under neuropathic pain, as measured on days 2–28. Based on the literature and our current data,

we hypothesize that the induction of the CXCL2/CXCR2 axis is extremely important at the periphery after nerve injury but probably not at the spinal cord level.

CXCL3 is another member of CINCs, and it is the least researched chemokine in the context of nociception processes. Despite the fact that structural details and receptor binding interactions in the case of CXCL1 and CXCL2 have been elucidated for years, the information regarding the structural and biophysical characteristics of CXCL3 became available as late as 2018, when Gulati et al. (30) successfully cloned, expressed, and purified the recombinant CXCL3. The authors revealed that although the overall structural and oligomerization features of CXCL3 and CXCL1/2 are similar, prominent differences can be observed on their characteristic surface structures, thus indicating a functional divergence. CXCL3/CXCR2 signaling exerts its functions through a number of signaling pathways, including p38MAPK, ERK1/2, and JAK2/STAT3 (90, 91). The involvement of these pathways in the development of neuropathy has been known for many years, also in our model (11, 39, 40). CXCL3 is strongly expressed in a number of tumorous conditions (30, 92); however, its role in the context of neuropathy has yet to be studied. Our results regarding time course changes of mRNA and protein indicate that of all CINCs, CXCL3 is the most important in the development of neuropathic pain, and its protein level undergoes upregulation up to 7 days. In addition, our results regarding naive mice showed for the first time that intrathecal CXCL3 administrations cause hypersensitivity to mechanical and/or thermal stimuli, appearing quickly after injection and lasting up to 24 h because of its location in neurons, what can be confirmed by immunofluorescent staining. What is more, the antibody neutralization of endogenous CXCL3 results in reductions of these symptoms in mice on day 7 after CCI. Moreover, we showed that CXCL3-induced pain behavior is abolished by pretreatment with NVP CXCR2 20, which proves an important role for CXCR2 in the effects of this chemokine. CXCL1 and CXCL2 are strongly related to each other, both structurally and functionally. They play a pivotal role in the immune response by recruiting and activating neutrophils in PNS with the highest concentration 1–3 days after injury (93, 94). CXCL3 helps neutrophil recruitment to inflamed areas and functions as an important mediator of macrophage chemotaxis (95). Our results provide the first evidence that spinal CXCL3 plays an important role in the development of neuropathic pain, since its protein is the only protein whose upregulation can be observed 2–7 days after CCI. Within the same time frame, we were able to observe the strongest microglia activation (10, 44). Additionally, our *in vitro* studies were the first to indicate the release of CXCL3 by stimulated microglial primary cells. In the case of CINCs, it is not expressed in the microglia at rest, and LPS strongly induces its release, suggesting that CXCL3 may act as a proinflammatory factor in activated microglia by insults (e.g., infection, injury, stress). Our immunohistochemical staining indicates mainly the neuronal origin of CXCL3 in the spinal cord, however, what's interesting, we observe the release of CXCL3 by activated microglial cells on day 7 after injury. The *in vitro* and *in vivo* results suggest that the microglia cells are able to produce this compound in some circumstances, which requires further in-depth research. On the other hand, CXCL3, as a strongly pronociceptive mediator, is not produced by astrocytes, which play an important role in restoring homeostasis in the CNS (96, 97). Our results indicate for the first time an important contribution of CXCL3 both in the initiation and development of neuropathic pain, and modulation of CXCL3 release can have beneficial effects, which may help in relieving the symptoms of neuropathic pain.

While opioids are commonly used in the treatment of chronic pain, in neuropathic pain they exhibit rather weak effectiveness (98). Previous reports suggest that, the CXCR2 receptor is capable of forming heterodimers with opioid receptors, and a change in the conformation of receptors may have an effect on their activation or ligand binding (99). The interaction of CXCR2 with DOR has been confirmed so far (99), which, however, may not be sufficient and significant for the effectiveness of morphine and buprenorphine during neuropathic pain. In the literature, it is well-established that microglial activation is essential for opioid analgesia under neuropathic pain (8, 100–103). It has been shown that the activation of microglia and subsequent increased level of pronociceptive cytokines, which have anti-opioid properties, e.g., IL-1beta (104), IL-18 (10) decreased opioid effectiveness and the development of morphine tolerance (8, 105). Recently, we have shown that blockade of CCR2 [RS504393, (25)], CCR5 [maraviroc, (28)], and CXCR3 [(±)-NBI-74330]; (29) can restore the analgesic activities of morphine and/or buprenorphine. Therefore, initially, it was surprising that the CXCR2 antagonist NVP CXCR2 20 did not enhance the analgesia of these opioids. However, in contrast to the antagonists of CCR2, CCR5, and CXCR3 (25, 28, 29), repeated administration of NVP CXCR2 20 did not diminish spinal microglia activation as well as important kinases associated with the activation of these cells, e.g., p38MAPK, ERK1/2 (own unpublished results). Our earlier findings support the view that activated spinal microglia through the modulation of the production of cytokines, including chemokines, are important not only in the development of neuropathic pain but also in a diverse efficacy of opioid analgesics (106–109).

CONCLUSIONS

As far as we are concerned, our study is the first to show strong pronociceptive properties of CXCL3. Moreover, chronic administrations of the CXCR2 antagonist (NVP CXCR2 20) can diminish hypersensitivity (and simultaneously CXCL3 expression) at the spinal cord and DRG level in a rat neuropathic pain model. Importantly, NVP CXCR2 20 does not influence microglia or astroglia activation, and probably for this reason, this substance is not responsible for increasing opioid analgesia under neuropathic pain. In summary, neuronal spinal CXCL3-CXCR2 signaling plays a crucial role in the pathogenesis of neuropathy after peripheral nerve injury, and we propose this site of action as a promising target for enabling the inhibition of its development in patients suffering from neuropathic pain. However, more research is needed on the role of all CXCR2 ligands (including CXCL8), not just those of the CINC family.

DATA AVAILABILITY

The datasets generated for this study are available on request to the corresponding author.

ETHICS STATEMENT

The number of animals was limited to the necessary minimum. The experiments were carried out in compliance with IASP recommendations (35), NIH Guide for Care and Use of Laboratory Animals and approved by the 2nd Local Ethical Committee on Animal Testing in Maj Institute of Pharmacology, Polish Academy of Sciences (12 Smetna Str., 31-343 Krakow, Poland; permission number: 1277/2015 and 262/2017).

AUTHOR CONTRIBUTIONS

All authors have made substantial contributions to the conception, design of the study, analysis and interpretation of data for the present study, final approval of the version to be published, and agreement to be accountable for all aspects of the research in ensuring that questions related to the accuracy or integrity of any part of the study is appropriately investigated and resolved. AP, ER, KP, GK, AC, WM, and JM made the experiments. AP and JM planned the study. AP, ER, KP, GK, AC, WM, IN, and JM analyzed and interpreted the results, drafted the manuscript, and accepted the finalized version.

FUNDING

This study was supported by the National Science Center, Poland grants OPUS 11 2016/21/B/NZ4/00128 and PRELUDIUM 12 2016/23/N/NZ7/00356 and statutory funds of the Maj Institute of Pharmacology Polish Academy of Sciences. AP is a Ph.D. student funded by a scholarship from the National Center of Scientific Leading sponsored by the Ministry of Science and Higher Education, Republic of Poland. AP was supported by the Foundation for Polish Sciences (FNP), the L'Oréal–UNESCO for Women in Science program in Poland.

ACKNOWLEDGMENTS

We are grateful to Magdalena Zychowska and Dominika Piłat for technical support. The English was corrected by American Journal Experts (certificate no. 92FE-C852-52F1-76FD-37D4).

SUPPLEMENTARY MATERIAL

The Supplementary Material for this article can be found online at: https://www.frontiersin.org/articles/10.3389/fimmu.2019.02198/full#supplementary-material

REFERENCES

1. DeLeo JA, Yezierski RP. The role of neuroinflammation and neuroimmune activation in persistent pain. *Pain*. (2001) 90:1–6. doi: 10.1016/S0304-3959(00)00490-5
2. Gao YJ, Ji RR. Chemokines, neuronal-glial interactions, and central processing of neuropathic pain. *Pharmacol Ther*. (2010) 126:56–68. doi: 10.1016/j.pharmthera.2010.01.002
3. Kiguchi N, Kobayashi Y, Kishioka S. Chemokines and cytokines in neuroinflammation leading to neuropathic pain. *Curr Opin Pharmacol*. (2012) 12:55–61. doi: 10.1016/j.coph.2011.10.007
4. Amy Old E, Clark AK, Malcangio M. The role of glia in the spinal cord in neuropathic and inflammatory pain. *Handb Exp Pharmacol*. (2015) 227:145–70. doi: 10.1007/978-3-662-46450-2_8
5. Burke D, Fullen BM, Stokes D, Lennon O. Neuropathic pain prevalence following spinal cord injury: a systematic review and meta-analysis. *Eur J Pain*. (2016) 21:29–44. doi: 10.1002/ejp.905
6. Milligan ED, Soderquist RG, Malone SM, Mahoney JH, Hughes TS, Langer SJ, et al. Intrathecal polymer-based interleukin-10 gene delivery for neuropathic pain. *Neuron Glia Biol*. (2006) 2:293–308. doi: 10.1017/S1740925X07000488
7. Miyoshi K, Obata K, Kondo T, Okamura H, Noguchi K. Interleukin-18-mediated microglia/astrocyte interaction in the spinal cord enhances neuropathic pain processing after nerve injury. *J Neurosci*. (2008) 28:12775–87. doi: 10.1523/JNEUROSCI.3512-08.2008
8. Mika J, Zychowska M, Popiolek-Barczyk K, Rojewska E, Przewlocka B. Importance of glial activation in neuropathic pain. *Eur J Pharmacol*. (2013) 716:106–19. doi: 10.1016/j.ejphar.2013.01.072
9. Zychowska M, Rojewska E, Przewlocka B, Mika J. Mechanisms and pharmacology of diabetic neuropathy - experimental and clinical studies. *Pharmacol Rep*. (2013) 65:1601–10. doi: 10.1016/S1734-1140(13)71521-4
10. Pilat D, Piotrowska A, All E, Rojewska E, Jurga A, Slusarczyk J, et al. Blockade of IL-18 signaling diminished neuropathic pain and enhanced the efficacy of morphine and buprenorphine. *Mol Cell Neurosci*. (2016) 71:114–24. doi: 10.1016/j.mcn.2015.12.013
11. Piotrowska A, Kwiatkowski K, Rojewska E, Makuch W, Mika J. Maraviroc reduces neuropathic pain through polarization of microglia and astroglia - evidence from *in vivo* and *in vitro* studies. *Neuropharmacology*. (2016) 108:207–19. doi: 10.1016/j.neuropharm.2016.04.024
12. Piotrowska A, Kwiatkowski K, Rojewska E, Slusarczyk J, Makuch W, Basta-Kaim A, et al. Direct and indirect pharmacological modulation of CCL2/CCR2 pathway results in attenuation of neuropathic pain — *in vivo* and *in vitro* evidence. *J Neuroimmunol*. (2016) 297:9–19. doi: 10.1016/j.jneuroim.2016.04.017
13. Bajetto A, Bonavia R, Barbero S, Florio T, G. S. Chemokines and their receptors in the central nervous system. *Front Neuroendocr*. (2001) 22:147–84. doi: 10.1006/frne.2001.0214
14. Abbadie C, Bhangoo S, De Koninck Y, Malcangio M, Melik-Parsadaniantz S, White FA. Chemokines and pain mechanisms. *Brain Res Rev*. (2009) 60:125–34. doi: 10.1016/j.brainresrev.2008.12.002
15. Zhang Z-J, Cao D-L, Zhang X, Ji R-R, Gao Y-J. Chemokine contribution to neuropathic pain: respective induction of CXCL1 and CXCR2 in spinal cord astrocytes and neurons. *Pain*. (2013) 154:2185–97. doi: 10.1016/j.pain.2013.07.002
16. Bhangoo SK, Ripsch MS, Buchanan DJ, Miller RJ, White FA. Increased chemokine signaling in a model of HIV1-associated peripheral neuropathy. *Mol Pain*. (2009) 5:48. doi: 10.1186/1744-8069-5-48
17. Ren K DR. Interactions between the immune and nervous systems in pain. *Nat Med*. (2010) 16:1267–76. doi: 10.1038/nm.2234
18. Van Steenwinckel J, Reaux-Le Goazigo A, Pommier B, Mauborgne A, Dansereau M-A, Kitabgi P, et al. CCL2 released from neuronal synaptic vesicles in the spinal cord is a major mediator of local inflammation and pain after peripheral nerve injury. *J Neurosci*. (2011) 31:5865–75. doi: 10.1523/JNEUROSCI.5986-10.2011

19. Biber K, Boddeke E. Neuronal CC chemokines: the distinct roles of CCL21 and CCL2 in neuropathic pain. *Front Cell Neurosci*. (2014) 8:1–10. doi: 10.3389/fncel.2014.00210
20. Souza GR, Talbot J, Lotufo CM, Cunha FQ, Cunha TM, Ferreira SH. Fractalkine mediates inflammatory pain through activation of satellite glial cells. *Proc Natl Acad Sci USA*. (2013) 110:11193–8. doi: 10.1073/pnas.1307445110
21. Xu J, Zhu M-D, Zhang X, Tian H, Zhang J-H, Wu X-B, et al. NFκB-mediated CXCL1 production in spinal cord astrocytes contributes to the maintenance of bone cancer pain in mice. *J Neuroinflammation*. (2014) 11:38. doi: 10.1186/1742-2094-11-38
22. Zhu X, Cao S, Zhu M, Liu J, Chen J, Gao YJ. Contribution of chemokine CCL2/CCR2 signaling in the dorsal root ganglion and spinal cord to the maintenance of neuropathic pain in a rat model of lumbar disc herniation. *J Pain*. (2014) 15:516–26. doi: 10.1016/j.jpain.2014.01.492
23. Zychowska M, Rojewska E, Pilat D, Mika J. The role of some chemokines from the CXC subfamily in a mouse model of diabetic neuropathy. *J Diabetes Res*. (2015) 2015:1–13. doi: 10.1155/2015/750182
24. Zychowska M, Rojewska E, Piotrowska A, Kreiner G, Mika J. Microglial inhibition influences XCL1/XCR1 expression and causes analgesic effects in a mouse model of diabetic neuropathy. *Anesthesiology*. (2016) 125:573–89. doi: 10.1097/ALN.0000000000001219
25. Kwiatkowski K, Piotrowska A, Rojewska E, Makuch W, Mika J. The RS504393 influences the level of nociceptive factors and enhances opioid analgesic potency in neuropathic rats. *J Neuroimmune Pharmacol*. (2017) 12:402–19. doi: 10.1007/s11481-017-9729-6
26. Xu Y, Zhang Q, Xue W, Zeng S, Zhang Z, Zhang X, et al. CXC chemokine receptor 4 (CXCR4) antagonist, a novel pathway to prevent chronic allograft nephropathy. *Ann Transplant*. (2016) 21:728–34. doi: 10.12659/AOT.899492
27. Rojewska E, Zychowska M, Piotrowska A, Kreiner G, Nalepa I, Mika J. Involvement of macrophage inflammatory protein-1 family members in the development of diabetic neuropathy and their contribution to effectiveness of morphine. *Front Immunol*. (2018) 9:494. doi: 10.3389/fimmu.2018.00494
28. Kwiatkowski K, Piotrowska A, Rojewska E, Makuch W, Jurga A, Slusarczyk J, et al. Beneficial properties of maraviroc on neuropathic pain development and opioid effectiveness in rats. *Prog Neuro-Psychopharmacol Biol Psychiatry*. (2016) 64:68–78. doi: 10.1016/j.pnpbp.2015.07.005
29. Piotrowska A, Rojewska E, Pawlik K, Kreiner G, Ciechanowska A, Makuch W, et al. Pharmacological blockade of CXCR3 by (±)-NBI-74330 reduces neuropathic pain and enhances opioid effectiveness - evidence from *in vivo* and *in vitro* studies. *Biochim Biophys Acta Mol Basis Dis*. (2018) 1864:3418–3437. doi: 10.1016/j.bbadis.2018.07.032
30. Gulati K, Gangele K, Agarwal N, Jamsandekar M, Kumar D, Poluri KM. Molecular cloning and biophysical characterization of CXCL3 chemokine. *Int J Biol Macromol*. (2018) 107:575–84. doi: 10.1016/j.ijbiomac.2017.09.032
31. Shibata F. The role of rat cytokine-induced neutrophil chemoattractants (CINCs) in inflammation. *Yakugaku Zasshi*. (2002) 122:263–8. doi: 10.1248/yakushi.122.263
32. Gershengorn MC, Geras-Raaka E, Varma A, Clark-Lewis I. Chemokines activate Kaposi's sarcoma-associated herpesvirus G protein-coupled receptor in mammalian cells in culture. *J Clin Invest*. (1998) 102:1469–72. doi: 10.1172/JCI4461
33. Gouwy M, Struyf S, Leutenez L, Pörtner N, Sozzani S, Van Damme J. Chemokines and other GPCR ligands synergize in receptor-mediated migration of monocyte-derived immature and mature dendritic cells. *Immunobiology*. (2014) 219:218–29. doi: 10.1016/j.imbio.2013.10.004
34. Shibata F, Konishi K, Nakagawa H. Identification of a common receptor for three types of rat cytokine-induced neutrophil chemoattractants (CINCs). *Cytokine*. (2000) 12:1368–73. doi: 10.1006/cyto.2000.0739
35. Zimmermann M. Ethical guidelines for investigations of experimental pain in conscious animals. *Pain*. (1983) 16:109–10. doi: 10.1016/0304-3959(83)90201-4
36. Kilkenny C, Parsons N, Kadyszewski E, Festing MFW, Cuthill IC, Fry D, et al. Survey of the quality of experimental design, statistical analysis and reporting of research using animals. *PLoS ONE*. (2009) 4:e7824. doi: 10.1371/journal.pone.0007824
37. McGrath JC, Lilley E. Implementing guidelines on reporting research using animals (ARRIVE etc.): new requirements for publication in BJP. *Br J Pharmacol*. (2015) 172:3189–93. doi: 10.1111/bph.12955
38. Yaksh TL, Rudy TA. Chronic catheterization of the spinal subarachnoid space. *Physiol Behav*. (1976) 17:1031–6. doi: 10.1016/0031-9384(76)90029-9
39. Popiolek-Barczyk K, Kolosowska N, Piotrowska A, Makuch W, Rojewska E, Jurga AM, et al. Parthenolide relieves pain and promotes M2 microglia/macrophage polarization in rat model of neuropathy. *Neural Plast*. (2015) 2015:1–15. doi: 10.1155/2015/676473
40. Rojewska E, Popiolek-Barczyk K, Kolosowska N, Piotrowska A, Zychowska M, Makuch W, et al. PD98059 influences immune factors and enhances opioid analgesia in model of neuropathy. *PLoS ONE*. (2015) 10:e0138583. doi: 10.1371/journal.pone.0138583
41. Hylden JLK, Wilcox GL. Intrathecal morphine in mice: a new technique. *Eur J Pharmacol*. (1980) 67:313–6. doi: 10.1016/0014-2999(80)90515-4
42. Bennett GJ, Xie YK. A peripheral mononeuropathy in rat that produces disorders of pain sensation like those seen in man. *Pain*. (1988) 33:87–107. doi: 10.1016/0304-3959(88)90209-6
43. Makuch W, Mika J, Rojewska E, Zychowska M, Przewlocka B. Effects of selective and non-selective inhibitors of nitric oxide synthase on morphine- and endomorphin-1-induced analgesia in acute and neuropathic pain in rats. *Neuropharmacology*. (2013) 75:445–57. doi: 10.1016/j.neuropharm.2013.08.031
44. Rojewska E, Piotrowska A, Makuch W, Przewlocka B, Mika J. Pharmacological kynurenine 3-monooxygenase enzyme inhibition significantly reduces neuropathic pain in a rat model. *Neuropharmacology*. (2016) 102:80–91. doi: 10.1016/j.neuropharm.2015.10.040
45. Jurga AM, Rojewska E, Piotrowska A, Makuch W, Pilat D, Przewlocka B, et al. Blockade of toll-like receptors (TLR2, TLR4) attenuates pain and potentiates buprenorphine analgesia in a rat neuropathic pain model. *Neural Plast*. (2016) 2016:1–12. doi: 10.1155/2016/5238730
46. Rojewska E, Makuch W, Przewlocka B, Mika J. Minocycline prevents dynorphin-induced neurotoxicity during neuropathic pain in rats. *Neuropharmacology*. (2014) 86:301–10. doi: 10.1016/j.neuropharm.2014.08.001
47. Altman DG, Bland MJ. Treatment allocation in controlled trials: Why randomise? *BMJ*. (1999) 318:1209. doi: 10.1136/bmj.318.7192.1209
48. Suresh K. An overview of randomization techniques: An unbiased assessment of outcome in clinical research. *J Hum Reprod Sci*. (2011) 4:8–11. doi: 10.4103/0974-1208.82352
49. Mika J, Wawrzczak-Bargiela A, Osikowicz M, Makuch W, Przewlocka B. Attenuation of morphine tolerance by minocycline and pentoxifylline in naive and neuropathic mice. *Brain Behav Immun*. (2009) 23:75–84. doi: 10.1016/j.bbi.2008.07.005
50. Osikowicz M, Mika J, Makuch W, Przewlocka B. Glutamate receptor ligands attenuate allodynia and hyperalgesia and potentiate morphine effects in a mouse model of neuropathic pain. *Pain*. (2008) 139:117–26. doi: 10.1016/j.pain.2008.03.017
51. Piotrowska A, Popiolek-Barczyk K, Pavone F MJ. Comparison of the expression changes after botulinum toxin type A and minocycline administration in lipopolysaccharide-stimulated rat microglial and astroglial cultures. *Front Cell Infect Microbiol*. (2017) 7:1–17. doi: 10.3389/fcimb.2017.00141
52. Zawadzka M, Kaminska B. A novel mechanism of FK506-mediated neuroprotection: downregulation of cytokine expression in glial cells. *Glia*. (2005) 49:36–51. doi: 10.1002/glia.20092
53. Przanowski P, Dabrowski M, Ellert-Miklaszewska A, Kloss M, Mieczkowski J, Kaza B, et al. The signal transducers Stat1 and Stat3 and their novel target Jmjd3 drive the expression of inflammatory genes in microglia. *J Mol Med*. (2014) 92:239–54. doi: 10.1007/s00109-013-1090-5
54. Chomczynski P, Sacchi N. Single-step method of RNA isolation by acid guanidinium thiocyanate-phenol-chloroform extraction. *Anal Biochem*. (1987) 162:156–9. doi: 10.1016/0003-2697(87)90021-2
55. Mika J, Rojewska E, Makuch W, Przewlocka B. Minocycline reduces the injury-induced expression of prodynorphin and pronociceptin in the dorsal root ganglion in a rat model of neuropathic pain. *Neuroscience*. (2010) 165:1420–8. doi: 10.1016/j.neuroscience.2009.11.064

56. Rafa-Zabłocka K, Kreiner G, Baginska M, Kuśmierczyk J, Parlato R, Nalepa I. Transgenic mice lacking CREB and CREM in noradrenergic and serotonergic neurons respond differently to common antidepressants on tail suspension test. *Sci Rep.* (2017) 7:1–11. doi: 10.1038/s41598-017-14069-6
57. Curtis MJ, Bond RA, Spina D, Ahluwalia A, Alexander SPA, Giembycz MA, et al. Experimental design and analysis and their reporting: new guidance for publication in BJP. *Br J Pharmacol.* (2015) 72:3461–71. doi: 10.1111/bph.12856
58. Manjavachi MN, Quintão NL, Campos MM, Deschamps IK, Yunes RA, Nunes RJ, et al. The effects of the selective and non-peptide CXCR2 receptor antagonist SB225002 on acute and long-lasting models of nociception in mice. *Eur J Pain.* (2010) 14:23–31. doi: 10.1016/j.ejpain.2009.01.007
59. Carreira EU, Carregaro V, Teixeira MM, Moriconi A, Aramini A, Verri WA, et al. Neutrophils recruited by CXCR1/2 signalling mediate post-incisional pain. *Eur J Pain.* (2013) 17:654–63. doi: 10.1002/j.1532-2149.2012.00240.x
60. Zhou Y, Li RJ, Li M, Liu X, Zhu HY, Ju Z, et al. Overexpression of GRK6 attenuates neuropathic pain via suppression of CXCR2 in rat dorsal root ganglion. *Mol Pain.* (2016) 12:1–13. doi: 10.1177/1744806916646381
61. Brandolini L, Benedetti E, Ruffini PA, Russo R, Cristiano L, Antonosante A, et al. CXCR1/2 pathways in paclitaxel-induced neuropathic pain. *Oncotarget.* (2017) 8:23188–201. doi: 10.18632/oncotarget.15533
62. Kiguchi N, Kobayashi Y, Maeda T, Fukazawa Y, Tohya K, Kimura M, et al. Epigenetic augmentation of the macrophage inflammatory protein 2/C-X-C chemokine receptor type 2 axis through histone H3 acetylation in injured peripheral nerves elicits neuropathic pain. *J Pharmacol Exp Ther.* (2012) 340:577–87. doi: 10.1124/jpet.111.187724
63. Horuk R, Martin AW, Wang Z, Schweitzer L, Gerassimides A, Guo H, et al. Expression of chemokine receptors by subsets of neurons in the central nervous system. *J Immunol.* (1997) 158:2882–90.
64. Sun Y, Sahbaie P, Liang DY, Li WW, Li XQ, Shi XY, et al. Epigenetic regulation of spinal CXCR2 signaling in incisional hypersensitivity in mice. *Anesthesiology.* (2013) 119:1198–208. doi: 10.1097/ALN.0b013e31829ce340
65. Filipovic R, Jakovcevski I, Zecevic N. GRO-alpha and CXCR2 in the human fetal brain and multiple sclerosis lesions. *Dev Neurosci.* (2003) 25:279–90. doi: 10.1159/000072275
66. Popivanova BK, Koike K, Tonchev AB, Ishida Y, Kondo T, Ogawa S, et al. Accumulation of microglial cells expressing ELR motif-positive CXC chemokines and their receptor CXCR2 in monkey hippocampus after ischemia-reperfusion. *Brain Res.* (2003) 970:195–204. doi: 10.1016/S0006-8993(03)02343-6
67. Vallès A, Grijpink-Ongering L, de Bree FM, Tuinstra T, Ronken E. Differential regulation of the CXCR2 chemokine network in rat brain trauma: Implications for neuroimmune interactions and neuronal survival. *Neurobiolo Dis.* (2006) 22:312–22. doi: 10.1016/j.nbd.2005.11.015
68. Semple BD, Bye N, Ziebell JM, Morganti-Kossmann MC. Deficiency of the chemokine receptor CXCR2 attenuates neutrophil infiltration and cortical damage following closed head injury. *Neurobiol Dis.* (2010) 40:394–403. doi: 10.1016/j.nbd.2010.06.015
69. Ryu JK, Cho T, Choi HB, Jantaratnotai N, McLarnon JG. Pharmacological antagonism of interleukin-8 receptor CXCR2 inhibits inflammatory reactivity and is neuroprotective in an animal model of Alzheimer's disease. *J Neuroinflammation.* (2015) 12:1–13. doi: 10.1186/s12974-015-0339-z
70. Cao DL, Zhang ZJ, Xie RG, Jiang BC, Ji RR, Gao YJ. Chemokine CXCL1 enhances inflammatory pain and increases NMDA receptor activity and COX-2 expression in spinal cord neurons via activation of CXCR2. *Exp Neurol.* (2014) 261:328–36. doi: 10.1016/j.expneurol.2014.05.014
71. Rose JJ, Foley JF, Murphy PM, Venkatesan S. On the mechanism and significance of ligand-induced internalization of human neutrophil chemokine receptors CXCR1 and CXCR2. *J Biol Chem.* (2004) 279:24372–86. doi: 10.1074/jbc.M401364200
72. Prado GN, Suetomi K, Shumate D, Maxwell C, Ravindran A, Rajarathnam K, et al. Chemokine signaling specificity: Essential role for the N-terminal domain of chemokine receptor. *Biochemistry.* (2007) 46:8961–8. doi: 10.1021/bi7004043
73. Yang W, Wang D, Richmond A. Role of clathrin-mediated endocytosis in CXCR2 sequestration, resensitization, and signal transduction. *J Biol Chem.* (1999) 274:11328–33. doi: 10.1074/jbc.274.16.11328
74. Neel NF, Schutyser E, Sai J, Fan GH, Richmond A. Chemokine receptor internalization and intracellular trafficking. *Cytokine Growth Factor Rev.* (2005) 16:637–58. doi: 10.1016/j.cytogfr.2005.05.008
75. Sawant KV, Xu R, Cox R, Hawkins H, Sbrana E, Kolli D, et al. Chemokine CXCL1-mediated neutrophil trafficking in the lung: role of CXCR2 activation. *J Innate Immun.* (2015) 7:647–58. doi: 10.1159/000430914
76. Cao DL, Qian B, Zhang ZJ, Gao YJ, Wu XB. Chemokine receptor CXCR2 in dorsal root ganglion contributes to the maintenance of inflammatory pain. *Brain Res Bull.* (2016) 127:219–25. doi: 10.1016/j.brainresbull.2016.09.016
77. Liang DY, Shi X, Liu P, Sun Y, Sahbaie P, Li WW, et al. The chemokine receptor CXCR2 supports nociceptive sensitization after traumatic brain injury. *Mol Pain.* (2017) 13:1–12. doi: 10.1177/1744806917730212
78. Li H, Xie W, Strong JA, Zhang JM. Systemic antiinflammatory corticosteroid reduces mechanical pain behavior, sympathetic sprouting, and elevation of proinflammatory cytokines in a rat model of neuropathic pain. *Anesthesiology.* (2007) 107:469–77. doi: 10.1097/01.anes.0000278907.37774.8d
79. Yang RH, Strong JA, Zhang JM. NF-kappaB mediated enhancement of potassium currents by the chemokine CXCL1/growth related oncogene in small diameter rat sensory neurons. *Mol Pain.* (2009) 5:1–12. doi: 10.1186/1744-8069-5-26
80. Dong, F, Du.YR, Xie W, Strong JA, He XJ, Zhang JM. Increased function of the TRPV1 channel in small sensory neurons after local inflammation or *in vitro* exposure to the pro-inflammatory cytokine GRO/KC. *Neurosci Bull.* (2012) 28:155–64. doi: 10.1007/s12264-012-1208-8
81. Silva RL, Lopes AH, Guimarães RM, Cunha TM. CXCL1/CXCR2 signaling in pathological pain: role in peripheral and central sensitization. *Neurobiol Dis.* (2017) 105:109–16. doi: 10.1016/j.nbd.2017.06.001
82. Katayama T, Tanaka H, Yoshida T, Uehara T, Minami M. Neuronal injury induces cytokine-induced neutrophil chemoattractant-1 (CINC-1) production in astrocytes. *J Pharmacol Sci.* (2009) 109:88–93. doi: 10.1254/jphs.08298FP
83. Pineau I, Sun L, Bastien D, Lacroix S. Astrocytes initiate inflammation in the injured mouse spinal cord by promoting the entry of neutrophils and inflammatory monocytes in an IL-1 receptor/MyD88-dependent fashion. *Brain Behav Immun.* (2010) 24:540–53. doi: 10.1016/j.bbi.2009.11.007
84. Omari KM, John G, Lango R, Raine CS. Role for CXCR2 and CXCL1 on glia in multiple sclerosis. *Glia.* (2006) 53:24–31. doi: 10.1002/glia.20246
85. Chen G, Park CK, Xie RG, Berta T, Nedergaard M, Ji RR. Connexin-43 induces chemokine release from spinal cord astrocytes to maintain late-phase neuropathic pain in mice. *Brain.* (2014) 137:2193–209. doi: 10.1093/brain/awu140
86. Manjavachi MN, Costa R, Quintão NL, Calixto JB. The role of keratinocyte-derived chemokine (KC) on hyperalgesia caused by peripheral nerve injury in mice. *Neuropharmacology.* (2014) 79:17–27. doi: 10.1016/j.neuropharm.2013.10.026
87. Cao L, Malon JT. Anti-nociceptive role of CXCL1 in a murine model of peripheral nerve injury-induced neuropathic pain. *Neuroscience.* (2018) 372:225–36. doi: 10.1016/j.neuroscience.2017.12.048
88. Liu X, Liu H, Xu S, Tang Z, Xia W, Cheng Z, et al. Spinal translocator protein alleviates chronic neuropathic pain behavior and modulates spinal astrocyte-neuronal function in rats with L5 spinal nerve ligation model. *Pain.* (2016) 157:103–16. doi: 10.1097/j.pain.0000000000000339
89. Haraguchi K, Kawamoto A, Isami K, Maeda S, Kusano A, Asakura K, et al. TRPM2 contributes to inflammatory and neuropathic pain through the aggravation of pronociceptive inflammatory responses in mice. *J Neurosci.* (2012) 32:3931–41. doi: 10.1523/JNEUROSCI.4703-11.2012
90. Al-Alwan LA, Chang Y, Mogas A, Halayko AJ, Baglole CJ, Martin JG, et al. Differential roles of CXCL2 and CXCL3 and their receptors in regulating normal and asthmatic airway smooth muscle cell migration. *J Immunol.* (2013) 191:2731–41. doi: 10.4049/jimmunol.1203421
91. Zhang L, Zhang L, Li H, Ge C, Zhao F, Tian H, et al. CXCL3 contributes to CD133+CSCs maintenance and forms a positive feedback regulation loop with CD133 in HCC via Erk1/2 phosphorylation. *Sci Rep.* (2016) 6:1–10. doi: 10.1038/srep27426
92. Han KQ, He XQ, Ma MY, Guo XD, Zhang XM, Chen J, et al. Inflammatory microenvironment and expression of chemokines in

hepatocellular carcinoma. *World J Gastroenterol.* (2015) 21:4864–74. doi: 10.3748/wjg.v21.i16.4864
93. Fleming JC, Norenberg MD, Ramsay DA, Dekaban GA, Marcillo AE, Saenz AD, et al. The cellular inflammatory response in human spinal cords after injury. *Brain.* (2006) 129:3249–69. doi: 10.1093/brain/awl296
94. Schomberg D, Olson J. Immune responses of microglia in the spinal cord: contribution to pain states. *Exp Neurol.* (2012) 234:262–70. doi: 10.1016/j.expneurol.2011.12.021
95. Furuichi K, Wada T, Kaneko S, Murphy PM, Furuichi K, Wada T, et al. Roles of chemokines in renal ischemia/reperfusion injury. *Front Biosci.* (2008) 13:4021–8. doi: 10.2741/2990
96. Milligan ED, Watkins LR. Pathological and protective roles of glia in chronic pain. *Nat Rev Neurosci.* (2009) 10:23–36. doi: 10.1038/nrn2533
97. Jha MK, Lee WH, Suk K. Functional polarization of neuroglia: implications in neuroinflammation and neurological disorders. *Biochem Pharmacol.* (2016) 103:1–16. doi: 10.1016/j.bcp.2015.11.003
98. Szczudlik A, Dobrogowski J, Wordliczek J, Stępień A, Krajnik M, Leppert W, et al. Diagnosis and management of neuropathic pain: review of literature and recommendations of the polish association for the study of pain and the polish neurological society - part one. *Neurol Neurochir Pol.* (2014) 48:262–71. doi: 10.1016/j.pjnns.2014.07.011
99. Parenty G, Appelbe S, Milligan G. CXCR2 chemokine receptor antagonism enhances DOP opioid receptor function via allosteric regulation of the CXCR2-DOP receptor heterodimer. *Biochem J.* (2008) 412:245–56. doi: 10.1042/BJ20071689
100. Watkins LR, Hutchinson MR, Rice KC, Maier SF. The "Toll" of opioid-induced glial activation: improving the clinical efficacy of opioids by targeting glia. *Trends Pharmacol Sci.* (2009) 30:581–91. doi: 10.1016/j.tips.2009.08.002
101. Hutchinson MR, Shavit Y, Grace PM, Rice KC, Maier SF, Watkins LR. Exploring the neuroimmunopharmacology of opioids: an integrative review of mechanisms of central immune signaling and their implications for opioid analgesia. *Pharmacol Rev.* (2011) 63:772–810. doi: 10.1124/pr.110.004135
102. Wen YR, Tan PH, Cheng JK, Liu YC, Ji RR. Microglia: a promising target for treating neuropathic and postoperative pain, and morphine tolerance. *J Formos Med Assoc.* (2011) 110:487–94. doi: 10.1016/S0929-6646(11)60074-0
103. Popiolek-Barczyk K, Mika J. Targeting the microglial signaling pathways: new insights in the modulation of neuropathic pain. *Curr Med Chem.* (2016) 23:2908–28. doi: 10.2174/0929867323666160607120124
104. Pilat D, Rojewska E, Jurga AM, Piotrowska A, Makuch W, Przewlocka B, et al. IL-1 receptor antagonist improves morphine and buprenorphine efficacy in a rat neuropathic pain model. *Eur J Pharmacol.* (2015) 764:240–8. doi: 10.1016/j.ejphar.2015.05.058
105. Raghavendra V, Tanga F, Rutkowski MD, DeLeo JA. Anti-hyperalgesic and morphine-sparing actions of propentofylline following peripheral nerve injury in rats: mechanistic implications of spinal glia and proinflammatory cytokines. *Pain.* (2003) 104:655–64. doi: 10.1016/S0304-3959(03)00138-6
106. Mika J. Modulation of microglia can attenuate neuropathic pain symptoms and enhance morphine effectiveness. *Pharmacol Rep.* (2008) 60:297–307.
107. Mika J, Popiolek-Barczyk K, Rojewska E, Makuch W, Starowicz K, Przewlocka B. Delta-opioid receptor analgesia is independent of microglial activation in a rat model of neuropathic pain. *PLoS ONE.* (2014) 9:1–14. doi: 10.1371/journal.pone.0104420
108. Happel C, Steele AD, Finley MJ, Kutzler MA, Rogers TJ. DAMGO-induced expression of chemokines and chemokine receptors: the role of TGF-beta1. *J Leukoc Biol.* (2008) 83:956–63. doi: 10.1189/jlb.1007685
109. Szabo I, Chen XH, Xin L, Adler MW, Howard OMZ, Oppenheim JJ, et al. Heterologous desensitization of opioid receptors by chemokines inhibits chemotaxis and enhances the perception of pain. *Proc Natl Acad Sci USA.* (2002) 99:10276–81. doi: 10.1073/pnas.102327699

Conflict of Interest Statement: The authors declare that the research was conducted in the absence of any commercial or financial relationships that could be construed as a potential conflict of interest.

frontiers in Immunology

REVIEW
published: 23 December 2019
doi: 10.3389/fimmu.2019.03009

Cytokines in Pain: Harnessing Endogenous Anti-Inflammatory Signaling for Improved Pain Management

Arden G. Vanderwall[1,2]* *and Erin D. Milligan*[1]*

[1] Department of Neurosciences, University of New Mexico School of Medicine, Albuquerque, NM, United States, [2] Department of Anesthesiology and Critical Care, University of New Mexico School of Medicine, Albuquerque, NM, United States

Current pain therapeutics offer inadequate relief to patients with chronic pain. A growing literature supports that pro-inflammatory cytokine signaling between immune, glial, and neural cells is integral to the development of pathological pain. Modulation of these communications may hold the key to improved pain management. In this review we first offer an overview of the relationships between pro-inflammatory cytokine and chemokine signaling and pathological pain, with a focus on the actions of cytokines and chemokines in communication between glia (astrocytes and microglia), immune cells (macrophages and T cells), and neurons. These interactions will be discussed in relation to both peripheral and central nervous system locations. Several novel non-neuronal drug targets for controlling pain are emerging as highly promising, including non-viral IL-10 gene therapy, which offer the potential for substantial pain relief through localized modulation of targeted cytokine pathways. Preclinical investigation of the mechanisms underlying the success of IL-10 gene therapy revealed the unexpected discovery of the powerful anti-nociceptive anti-inflammatory properties of D-mannose, an adjuvant in the non-viral gene therapeutic formulation. This review will include gene therapeutic approaches showing the most promise in controlling pro-inflammatory signaling via increased expression of anti-inflammatory cytokines like interleukin-10 (IL-10) or IL-4, or by directly limiting the bioavailability of specific pro-inflammatory cytokines, as with tumor necrosis factor (TNF) by the TNF soluble receptor (TNFSR). Approaches that increase endogenous anti-inflammatory signaling may offer additional opportunities for pain therapeutic development in patients not candidates for gene therapy. Promising novel avenues discussed here include the disruption of lymphocyte function-associated antigen (LFA-1) activity, antagonism at the cannabinoid 2 receptor (CB2R), and toll-like receptor 4 (TLR4) antagonism. Given the partial efficacy of current drugs, new strategies to manipulate neuroimmune and cytokine interactions hold considerable promise.

Keywords: cytokines, chemokines, gene therapy, chronic pain, IL-10, IL-4, TNF-α, CCL2

OPEN ACCESS

Edited by:
Waldiceu A. Verri,
State University of Londrina, Brazil

Reviewed by:
Sebastien Talbot,
Université de Montréal, Canada
Niels Eijkelkamp,
University Medical Center Utrecht, Netherlands

***Correspondence:**
Arden G. Vanderwall
avanderwall@salud.unm.edu
Erin D. Milligan
emilligan@salud.unm.edu

Specialty section:
This article was submitted to Cytokines and Soluble Mediators in Immunity, a section of the journal Frontiers in Immunology

Received: *25 September 2019*
Accepted: *09 December 2019*
Published: *23 December 2019*

Citation:
Vanderwall AG and Milligan ED (2019) Cytokines in Pain: Harnessing Endogenous Anti-Inflammatory Signaling for Improved Pain Management. Front. Immunol. 10:3009. doi: 10.3389/fimmu.2019.03009

INTRODUCTION

Pain is the evolutionarily protective perception of a nociceptive stimulus indicative of actual or potential bodily harm. However, when pain occurs outside the window of usefulness it is termed pathological. It is considered chronic when it lasts 3 months or greater (1). Chronic pain is a global problem affecting more than 1.5 billion people, and in 2015 was the leading cause of disability in

most countries (2, 3). Unfortunately, clinically available medications offer insufficient long-term analgesia in many pain patients (4). Furthermore, as is the case with opioids like morphine, they can be associated with unwanted effects (e.g., sedation and constipation), rapid onset of tolerance, a high potential for abuse, and even risk of death (5).

Physiologic pain is mediated by neuron-to-neuron signaling with classical neurotransmitters and neuropeptides like glutamate, calcitonin-gene related protein (CGRP), and substance P (6). However, considerable evidence indicates that neurons are not alone in the development of pathological pain. Rather, numerous immunological pathways mediated by glia (e.g., astrocytes and microglia), immune cells, and pro-inflammatory cytokines and chemokines modify neuronal communication leading to pathological pain (7–9). Current pain therapeutics neglect the actions of these non-neuronal contributors. Therefore, development of interventions designed to target neuroimmune communication will likely improve patient outcomes.

The goal of this review is to provide an overview of the immune contributions to pathological pain with a particular focus on the role of cytokines and chemokines. The authors discuss advances in gene therapeutics and novel small molecule therapeutics that relieve chronic pain through modification of neuroimmune cytokine signaling pathways.

OVERVIEW OF IMMUNE CONTRIBUTIONS TO PATHOLOGICAL PAIN

Peripheral Immune Actions in Pathological Pain

Following peripheral nerve injury or infection, receptors referred to as pattern recognition receptors expressed on immune cells are activated. Specifically, pattern recognition receptors are triggered by pathogen associated molecular patterns (PAMPs), exogenous signals indicative of pathogen invasion, or by danger associated molecular patterns (DAMPs), endogenous signals indicative of sterile tissue injury. Common pattern recognition receptors include toll-like receptors (TLRs) and Nod-like receptors (NLRs) (10). Ligand interaction with TLRs and NLRs activate pro-inflammatory intracellular pathways mediated by transcription factors like nuclear factor-κB (NF-κB) and activator protein-1 (AP-1), as well as activation of the inflammasome. This leads to increased synthesis of pro-inflammatory cytokines, including tumor necrosis factor-α (TNF-α), interleukin (IL)-6, and IL-1β. Additionally, chemotactic cytokines, referred to as chemokines, like C-C motif chemokine ligand 2 (CCL2; aka MCP-1) and C-X3-C Motif Chemokine Ligand 1 (CX3CL1; aka Fractalkine), and other immune mediators like nitric oxide (NO) are also produced (9).

Within 3 days of injury, macrophages and neutrophils are recruited to the site and secrete cytokines which aid helper T cells and B cells as well as sensitize peripheral nociceptors (11). These inflammatory mediators include pro-inflammatory cytokines like TNF-α, IL-1β, IL-6, and IL-17, nerve growth factor (NGF), serotonin, histamine, and prostaglandins like prostaglandin E2 (PGE2) (12). Activated immune cells also release anti-inflammatory molecules, such as the cytokine IL-10 and pro-resolution mediators derived from omega-3 unsaturated fatty acids (e.g., resolvins, protectins, and maresins) as a method of autoregulation in the healing process and reestablishment of homeostasis (12–14).

Interestingly, sensory neurons express receptors for many of these mediators, such as cytokine receptors (IL-1βR, TNF-αR, IL-6R, and IL-17RA), NGF receptors (TrkA), and G protein coupled receptors for serotonin, histamine, and PGE2 (12, 15). Recent reports of single cell RNA-sequencing using peripheral nociceptors located in dorsal root ganglia (DRG) have identified numerous potential neuronally expressed cytokine and chemokine receptor targets, further supporting that direct immune modulation of neuronal action is a likely driver of pathological pain (16). Activation of these receptors expressed by nearby nociceptive neurons (e.g., C fibers and Aδ fibers) leads to enhanced membrane excitability and sensitization to subsequent stimulation (15, 17). This process is termed peripheral sensitization and results in primary nociceptors that become overly responsive to previously subthreshold levels of peripheral stimulus (6).

Peripheral nerve sensitization can in turn lead to enhanced nociceptor release of excitatory neurotransmitters at their terminal synapses within the spinal cord dorsal horn, a site of significant sensory signal modulation. This enhanced signaling within the dorsal horn further sensitizes second order sensory neurons through a mechanism known as central sensitization, a neurobiological plasticity process first characterized by Woolf in the early 1980s (18). Following development of central sensitization, nociceptive neurons now potently signal to higher order structures in the brain and brainstem, resulting in pathological pain perception including hyperalgesia (enhanced response to normally noxious stimuli) and allodynia (pain in response to normally non-noxious stimuli, such as to light touch) (19). Furthermore, expansion of receptive fields is often observed, resulting in pain perception from stimulation of uninjured tissue (secondary hyperalgesia) (6, 19). Pathological pain can arise if these nociceptive pathways remain excitable beyond the period of healing.

Central Immune Actions in Pathological Pain

Astrocytes arise from neuroepithelium and are found throughout the brain and spinal cord (20), outnumbering neurons and accounting for 40–50% of all central nervous system (CNS) glia (21). In contrast, microglia have mesodermal hematopoietic origin, constituting only 5–10% of all glia, and are considered the resident mononuclear phagocytes of the CNS (7, 20).

As with injury or infection of the CNS, damage to peripheral nerves incites glia in the spinal cord dorsal horn to express increased markers of activation (22). These spinal glia assume "activated" phenotypes, with changes in morphology (e.g., switch from highly ramified to amoeboid appearance) as well as upregulation of astrocytic activation markers like glial fibrillary acidic protein (GFAP), and microglial activation markers like

complement receptor 3 (CR3), cluster of differentiation 11b (CD11b), or ionized calcium binding adaptor molecule 1 (Iba1) (8, 23, 24). Of note, the recently identified microglial-specific marker transmembrane protein 119 (TMEM119) (25) may offer newfound utility in discriminating between microglia vs. macrophages/monocytes (26–28), as prior markers are expressed by both.

Glial Activation in Pathological Pain

Lumbar astrocytes undergo changes in morphology and increased GFAP expression, indicating a state of increased activation following chronic constriction injury (CCI) of the rat sciatic nerve (29). Since this initial study demonstrating anatomical evidence that spinal glia play a role in pain modulation, later studies documented that spinal glia are closely associated with neural synapses, express many of the same neurotransmitter receptors as neurons, and are known to assume "activated" phenotypes in response to abnormal or heightened neuronal signaling (8, 9, 15, 23, 30–32). Astrocytes and microglia express pain-relevant neurotransmitter receptors, like AMPA (α-amino-3-hydroxy-5-methyl-4-isoxazolepropionic acid) receptors, metabotropic glutamate receptors (mGluR), purinergic receptors (e.g., $P2X_4R$ or $P2X_7R$), or neurokinin 1 receptors (NK1R), which are activated by neurotransmitters released from presynaptic nerve terminals. These neurotransmitters include glutamate, ATP and substance P (9). Following peripheral nerve damage, neurons also release chemokines like CCL2 (33) and CX3CL1(34), and other immune mediators like colony-stimulating factor 1 (CSF-1) (35) and ATP (36, 37). These released factors potently activate astrocytes and microglia (9), which in turn release pro-inflammatory cytokines (e.g., IL-1β, TNF-α, and IL-6) (38), chemokines (e.g., CCL2) (33), ATP, excitatory amino acids (EAAs), and NO (7). As in the periphery, dorsal horn neurons express receptors for many of these factors, including the pro-inflammatory cytokines, IL-1β, TNF-α, IL-6, and IL-17 (12, 15). Activation of neuronally-expressed cytokine receptors modifies neuronal function. For example, the pro-inflammatory cytokines TNF-α and IL-1β enhance excitatory synaptic transmission and suppress inhibitory synaptic transmission in neurons of spinal cord lamina II (31, 39). Whereas, TNF-α enhances spontaneous excitatory post-synaptic current (sEPSC) frequency, IL-6 reduces frequency of the spontaneous inhibitory post-synaptic current (sIPSC). Notably, IL-1β is able to enhance both sEPSC frequency and amplitude while reducing sIPSC frequency and amplitude. Additionally, TNF-α and IL-1β enhance excitatory AMPA- and NMDA-induced currents, and IL-1β and IL-6 suppress inhibitory GABA- and glycine-induced currents (39). Therefore, activation of these cytokine receptors further sensitizes local neurons leading to a feed-forward cycle of nociceptive signaling.

Trafficking Immune Cells and Pathological Pain

Macrophages in Pathological Pain

While it is clear that peripheral immune cells migrate to local sites of nerve damage, a growing body of evidence supports that they also traffic to more remote pain-relevant neural tissues and play a role in the development of pathological pain. For instance, macrophages are recruited to sites remote from the initial insult, such as to the spinal cord (40, 41) and DRG (41–43), following peripheral nerve trauma in response to chemotactic factors like CCL2 (42–44) and CX3CL1 (33, 45) derived from injured neurons with their cell bodies or central projections in these distant locations. Macrophages present in the DRG are most likely important for maintenance of chronic pain. This is supported by evidence that depletion of peripheral macrophages partially reverses established paclitaxel-induced or nerve ligation-induced mechanical hyperalgesia and reduces TNF-α expression in DRG (43, 46).

T Cells in Pathological Pain

In addition to macrophages, T cells may also be important in the mechanisms that underlie pathological pain. For instance, activated $CD4^+$ T cells, specifically Th1 and Th17 cells, migrate to associated lumbar DRG and/or the lumbar spinal cord dorsal horn in animal models of sciatic nerve transection (47–49), spared nerve injury (50, 51), partial sciatic nerve ligation (52, 53), and sciatic nerve chronic constriction injury (54).

Increased T cell trafficking in these animal models of neuropathic pain has been associated with concurrent increases in pro-inflammatory T cell-related cytokine signaling. For example, Costigan et al. identified T cell infiltration of the spinal cord dorsal horn following a spared nerve injury (SNI) in rats with concurrent increases in spinal interferon-γ (IFN-γ) expression (50). IFN-γ is the signature pro-inflammatory cytokine released by activated Th1 cells (55). In a related study, neuropathic pain resulting from spared nerve injury is significantly diminished in both Rag1 knockout ($Rag1^{-/-}$; T-cell deficient) mice and IFN-γ receptor null mutant mice as compared to wildtype controls (50).

T helper cell-mediated IL-17 expression also appears to be important for pain pathology. Compared to wild-type mice, IL-17 knockout mice display significantly less mechanical hypersensitivity as well as decreased T cell accumulation at both the site of partial sciatic nerve ligation and within the relevant lumbar DRG (L3-L5) (52). Similarly, increased $CD4^+$ T cells were observed in the rat spinal cord in a model of spinal nerve ligation (e.g., peripheral nerve damage), with double-positive $CD4^+$/IL-17^+ T cells located in superficial laminae of the spinal cord dorsal horn by immunofluorescence staining (51). This was accompanied by significant upregulation of IL-17, IL-1β, and IL-6 (51).

Sexual Dimorphism in Pathological Pain

Much of what is known about the mechanisms of pain was identified in male animal models. However, recent reports indicate that mechanisms of pain may differ between the sexes (56, 57). While microglial activation is required for preclinical models of pathological pain in males, this does not seem to be the case for females who instead appear to be more vulnerable to the actions of T cells (54, 58–61).

Recent work from Noor et al. demonstrates that males and females exhibit divergent T cell-associated actions within

discrete pain-relevant anatomic regions in a rodent model of sciatic neuropathy (54). During neuropathy, females display more profound Th17 specific responses with higher levels of IL-17A than males, both at the injured nerve and in the corresponding lumbar spinal cord. When neuropathic animals were treated with a β2-integrin antagonist, BIRT377, pain-relieved females expressed dramatically reduced IL-17A levels in sciatic and lumbar spinal cord tissues as compared to their male counterparts (for further discussion, see section "Lymphocyte Function-Associated antigen-1" below). This not only supports a role for IL-17A in mechanisms of neuropathic pain, it offers evidence of a T cell differentiation bias toward a pro-inflammatory status that is significantly greater in females than males (54).

There is growing evidence that other cytokines may also be differentially regulated in males vs. females following peripheral nerve injury. For instance, recent RNA-seq analysis of lumbar DRG following rat sciatic CCI identified that the cytokine CSF-1 is 1.7 times higher in females than males (62).

GENE THERAPEUTIC MODULATION OF CYTOKINES FOR CONTROL OF PATHOLOGICAL PAIN

Gene Therapeutic Approaches and Challenges

Gene therapy offers the advantage of anatomically targeted long-duration expression of a desired protein, thereby limiting possible unwanted systemic effects observed in other types of pharmacologic interventions. Currently available gene therapeutic approaches aim to treat disease through modification of gene expression by cells, often via viral transduction or non-viral transfection, though newer gene editing approaches, such as through CRISPR/Cas9, may become more common (63). To date, there are three FDA approved gene therapies, including Spinraza (nusinersen; anti-sense oligonucleotide for treatment of spinal muscular atrophy type 1) (64, 65), Kymriah (tisagenlecleucel; CAR T-cell therapy for treatment of B-cell precursor acute lymphoblastic leukemia) (66), and Luxturna (voretigene neparvovec; adeno-associated virus-mediated delivery of RPE65 for treatment of RPE65-mediated inherited retinal dystrophy) (67). Various gene therapies first began to enter clinical trials in the 1990s, but these early forays were plagued by unexpected toxicities, limited clinical benefit, and even cases of patient deaths (63). Further investigations revealed obstacles to using viral vectors, including insertional mutagenesis, immune-targeted destruction of genetically modified cells, and potentially fatal immunogenicity associated with the viral vectors themselves (68–70). While more modern viral vector approaches aim to limit these toxicities, non-viral approaches have become an appealing alternative. Specifically, viral approaches rely on viral vectors to mediate cellular transfection and subsequent gene expression. In contrast, non-viral gene therapies gain cellular access through a wide variety of mechanisms ranging from simple cellular uptake of naked plasmid DNA, to more formal packaging of genetic material within carriers like liposomes, polymers, or basic proteins to facilitate transfection (69–72). These packaging modifications are often aimed at limiting immune detection, protecting the payload (e.g., plasmid DNA) from degradation by endonucleases, targeting to the therapy to cells of interest, as well as promoting cellular entry (73).

Given that sustained functional suppression of pain-relevant pro-inflammatory cytokines may ameliorate chronic pain conditions, gene therapeutic expression of targets leading to improved anti-inflammatory function has been explored. A summary of reports in which gene therapeutics encoding anti-inflammatory mediators induce pain relief observed in pre-clinical pain models and in which changes in inflammatory mediators were also evaluated is provided here (**Table 1**).

Gene Therapy for Pathological Pain

Interleukin-4 Signaling

Interleukin-4 (IL-4) is an important regulator of immunity, with diverse roles in processes, such as T-cell proliferation, activated B-cell stimulation, activation of macrophages, chronic inflammation, and wound repair (88). IL-4 is primarily produced by macrophages, T-cells (especially Th2 cells), mast cells, eosinophils, and basophils (89). This cytokine exerts a variety of effects through actions at two receptor subtypes. The IL-4R-I receptor is expressed by T cells, and B cells, monocytes/macrophages, and fibroblasts (90), and is involved in the regulation of maturation and proliferation of Th2 cells, and in IgE synthesis by B cells (88).

IL-4 signaling has been shown to decrease the production and actions of several pain-relevant pro-inflammatory mediators. For instance, IL-4 suppresses NLR protein 3 (NLRP3) inflammasome-dependent caspase-1 activation and the subsequent IL-1β secretion by macrophages (91). NLRP3 serves as a sensor protein capable of initiating assembly of the intracellular inflammasome protein complex, resulting in caspase-1 activation and consequent conversion of pro-IL-1β to mature bioactive IL-1β (92, 93). IL-4 has also been shown to increase expression of endogenous IL-1 receptor antagonist (IL-1ra) mRNA and protein (94), thus diminishing the actions of pro-inflammatory IL-1β. Additionally, IL-4 directly inhibits the induction of nitric oxide synthase (NOS) and levels of cyclooxygenase 2 (COX-2), thereby decreasing the production of NO and PGE2, respectively (95).

In contrast to IL-10, which is predominantly characterized as an anti-inflammatory cytokine, IL-4 exerts some pro-inflammatory actions. In vascular endothelial cells, IL-4 induces expression of CCL2 and IL-6 (96). It also synergistically increases IL-1β, TNF-α, and vascular cell adhesion protein 1 (VCAM-1; a.k.a. CD106) in lipopolysaccharide-stimulated vascular endothelium (96). IL-4-induced IL-6 expression is mediated via a reactive oxygen species (ROS)-dependent mechanism in human aortic endothelial cells (96).

IL-4 Gene Therapy as a Pain Therapeutic

Despite some evidence that it can serves as a facilitator of pro-inflammatory cytokine expression (97–99), IL-4 is an attractive candidate for treatment of pathological pain due to its broad spectrum of anti-inflammatory actions. Additionally, IL-4

TABLE 1 | Anti-inflammatory gene therapies for treatment of pathological pain.

Target	References	Vector/Delivery	Model organism	Pain model	Inflammatory mediators
IL-4	Hao et al. (74)	HSV/Subcutaneous	Male Sprague-Dawley Rats	L5 Spinal Nerve Ligation	**Lumbar Spinal Cord DH:** ↓ IL-1β, p-p38, PGE2 **Lumbar DRG:**↑ IL-4
TNFSR	Peng et al. (75)	HSV/Subcutaneous	Female Sprague-Dawley Rats	Spinal Cord Injury	**Lumbar Spinal Cord:** ↓ TNF-α, p-p38 **Lumbar Spinal Cord DH:** ↓ p-p38
	Hao et al. (76)	HSV/Subcutaneous	Sprague-Dawley Rats	Sciatic Nerve Ligation	**Lumbar Spinal Cord DH**: ↓ TNF-α, IL-1β, p-p38
	Huang et al. (77)	HSV/Subcutaneous	Male Sprague-Dawley Rats	Perineural HIV gp120	**Lumbar Spinal Cord DH:** ↓ TNFα, CXCL12, CXCR4, ↑ TNFSR **Lumbar DRG:** ↓ TNF, CXCL12, CXCR4, ↑ TNFSR
	Ortmann and Chattopadhyay (78)	HSV/Subcutaneous	Sprague-Dawley Rats	Diabetic Neuropathy	**Lumbar Spinal Cord DH:** ↓ TNF-α, p-p38 **Lumbar DRG:** ↓ TNF-α, p-p38, ↑ TNFSR **Sciatic Nerve:** ↓ TNF-α
IL-10	Milligan et al. (79)	Adenovirus/Intrathecal	Male Sprague-Dawley Rats	Sciatic Inflammatory Neuropathy	**CSF:** ↓ IL-1β, ↑ IL-10
	Lau et al. (80)	HSV/Subcutaneous	Male Sprague-Dawley Rats	Spinal Cord Injury	**Lumbar Spinal Cord DH:** ↓ TNF-α
	Zheng et al. (81)	HSV/Subcutaneous	Male Sprague-Dawley Rats	Perineural HIV gp120 with DDC	**Lumbar Spinal Cord DH:** ↓ TNF-α, p-p38, CXCL12, CXCR4 **Lumbar DRG:** ↓ TNF-α, p-p38, CXCL12, CXCR4
	Zheng et al. (82)	HSV/Subcutaneous	Male Sprague-Dawley Rats	Perineural HIV gp120	**Lumbar Spinal Cord DH:** ↓ TNF-α, p-p38, CXCL12, CXCR4 **Lumbar DRG:** ↓ TNF-α, p-p38, CXCL12, CXCR4
	Milligan et al. (83)	Naked Plasmid DNA/Intrathecal	Male Sprague-Dawley Rats	Sciatic CCI	**Lumbar Spinal Cord DH:** ↑ IL-10 **Cauda Equina:**↑ IL-10
	Ledeboer et al. (84)	Naked Plasmid DNA/Intrathecal	Male Sprague-Dawley Rats	Chemotherapy-induced Peripheral Neuropathy	**Lumbar DRG:** ↓ IL-1β, p-p38, TNF-α; ↑ IL-10 **Meninges:** ↑ IL-10
	Sloane et al. (85)	Naked Plasmid DNA/Intrathecal	Male Sprague-Dawley Rats	Sciatic CCI	**CSF:** ↑ IL-10
	Soderquist et al. (86)	PLGA Encapsulated Plasmid DNA/Intrathecal	Male Sprague-Dawley Rats	Sciatic CCI	**Lumbar Spinal Cord:** ↑ IL-10 **CSF:** ↑ IL-10
	Dengler et al. (87)	Naked Plasmid DNA with D-mannose Pre-treatment/Intrathecal	Male Sprague-Dawley Rats	Sciatic CCI	**Lumbar Spinal Cord:** ↓ IL-1β, ↑ IL-10 **Lumbar DRG:** ↑ IL-10
	Vanderwall et al. (28)	Naked Plasmid DNA co-injected with D-mannose/Intrathecal	Male IL-10 Knockout Mice	Sciatic CCI	**Lumbar Spinal Cord:**↓ TNFα, CCL2; no change IL-1β, TGF-β1 **Lumbar DRG:** ↓ TNF; ↑ IL-10, TGF-β1, IL-10Rα; no change IL-1β **Cauda Equina:** ↑ IL-10 **Sciatic nerve:** ↑ TNF, IL-1β, CCL2, IFN-γ, IL-6, CXCL1, TGF-β1; no change IL-12p70

This table includes data from reports in which gene therapeutics encoded anti-inflammatory mediators that induced pain relief in pre-clinical pain models and also evaluated changes in inflammatory mediators (e.g., cytokines, chemokines, transcription factors, etc.) in pain-relevant tissues. Relative changes are indicated in the level of inflammatory mediators identified in tissues collected from pain relieved vs. control animals.

CXCL1 (C-X-C motif chemokine ligand 1; aka KC/GRO), CXCL12 (C-X-C motif chemokine ligand 12; pro-inflammatory chemokine), CXCR4 (C-X-C motif chemokine receptor 4), DDC (2′,3′-dideoxycytidine; nucleoside reverse transcriptase inhibitor), IL-10Rα (IL-10 Receptor α), IL-12p70 (Interleukin-12 p70; bioactive form), PLGA (Poly lactic-co-glycolic acid).

deficiency in naïve IL-4 knockout mice exhibit increased tactile allodynia (100). However, IL-4 protein replacement therapy is precluded from use for systemic administration due to IL-4's short protein half-life as well as its pleiotropic effects on immune and vascular function (74). Therefore, gene therapeutic approaches offer the best avenue for application.

IL-4 gene therapy has been examined for control of neuropathic pain in an animal model of spinal nerve ligation. Work by Hao et al. demonstrated that herpes simplex viral vector-mediated expression of IL-4 administered after the onset of mechanical allodynia results in 5 weeks of pain relief with concurrent increases in IL-4 protein expression in DRG (74).

Similar effects were observed following a repeat injection. Interestingly, prophylactic treatment at 1 week prior to sciatic nerve ligation appeared to delay the onset of mechanical allodynia by about 5 weeks (74).

IL-4 gene therapy has also been examined in an animal model of painful inflammatory arthritis (101). Intra-articular injection of IL-4 gene therapy using a retroviral vector led to a reduction in paw swelling and decreased radiographic evidence of bone destruction, though differences only achieved significance about 2 weeks post-injection and paw edema measurements were not assessed throughout the entire timecourse of the inflammatory model (101), which can last several months (102), so duration of effect is speculative. Potential sex differences in IL-4 efficacy as a therapeutic to control chronic pathological pain has not been reported.

Tumor Necrosis Factor and Pathological Pain

Tumor necrosis factor-α (TNF-α) is a classic pro-inflammatory cytokine that exerts actions on two cell-surface receptors which are either constitutively expressed (TNFR1, p55-R) or inducible (TNFR2, p75-R), with most cells expressing constitutively low levels of TNFR1 (103). TNF-α signaling regulates apoptotic pathways, NF-κB-induced inflammation, and stress-induced activation of protein kinases (103, 104). Of note, TNF-α drives a positive regulatory feedback loop in which TNF-induced NF-κB signaling drives further expression of TNF-α (104).

Approaches that interfere with TNF-α signaling hold promise for the treatment of neuropathic pain, as demonstrated by pre-clinical work in animal models. Many studies have demonstrated that pain behaviors can be attenuated by local or spinal administration of agents that antagonize TNF-α (105–108). TNF soluble receptor (TNFSR), commercially known as etanercept, is previously approved by the FDA for treatment of painful inflammatory conditions including rheumatoid arthritis, psoriatic arthritis, and ankylosing spondylitis (109). While preclinical trials with recombinant TNFSR have shown promise, randomized clinical trials have had limited success (109). Clinical translation may be limited by the potential loss of beneficial neuroprotective and neuroregenerative properties of TNF-α, and by its impermeability at the blood-brain-barrier (9). Interestingly, while TNFR1-mediated signaling is associated with neurotoxicity, TNFR2 signaling may by neuroprotective (110–112). Some controversy over the roles of TNFR1 vs. TNFR2 in chronic pain remains (113). The role of TNF-α in pathological pain has been extensively reviewed elsewhere (104, 113).

TNFSR Gene Therapy as a Pain Therapeutic

Gene therapeutic approaches may bypass some of the obstacles faced by application of recombinant TNFSR. When applied subcutaneously to the hindpaw 1 week following sciatic nerve ligation, herpes simplex virus (HSV)-mediated TNFSR is associated with transient improvements in mechanical allodynia and reversal of thermal latency (76). HSV-mediated TNFSR has also been shown to improve pain behaviors in models of diabetic neuropathy, spinal cord injury, HIV gp120-mediated inflammation of the sciatic nerve, and neuropathy secondary to antiretroviral therapy (75, 77, 78).

Interleukin-10

Interleukin-10 Pleiotropically Inhibits Pro-inflammatory Signaling

Interleukin-10 (IL-10) is a powerful anti-inflammatory cytokine that binds to the IL-10 receptor (IL-10R), with IL-10R1 (a.k.a. IL-10Rα) being the high affinity subunit necessary for signal transduction (114). Importantly, the IL-10R1 subunit is expressed by astrocytes, microglia, oligodendrocytes, endothelial cells, and trafficking leukocytes (115). Despite IL-10 R1 having been identified by RNA-sequencing analysis of lumbar spinal and DRG neurons in several reports (16), these findings have not yet been convincingly validated by confirmed neuronal protein expression. Two separate reports provide evidence of IL-10R1 protein expression in embryonic (E16-18) rat neurons *in vitro* (116, 117). Post-natal rodent protein analyses have been somewhat mixed, with one report identifying IL-10R1 protein expression in DRG neurons (118), and another report failing to identify IL-10R1 in brains (115). Due to ongoing uncertainty of neuronal IL-10 receptor expression, it remains possible that the pain-relieving actions of IL-10 and other anti-inflammatory cytokines may provide therapeutic benefit through actions at neuronal receptors.

IL-10 pleiotropically inhibits the actions of many pro-inflammatory factors by numerous mechanisms briefly described here, but thoroughly discussed elsewhere [for review, see (119, 120)]. IL-10 signaling leads to decreased bioavailability of pro-inflammatory cytokine proteins through upregulation of both IL-1ra and TNF-α decoy receptor (119). This is also accomplished through reduced gene transcription, decreased mRNA stability, and reduced translation for pro-inflammatory cytokines and chemokines, many of which are downstream of toll-like receptor 4 (TLR4) (121, 122). Additionally, IL-10 destabilizes mRNA transcripts for the pro-inflammatory cytokines TNF-α and IL-1β (119, 123). IL-10 signaling also induces suppressor of cytokine signaling 1 (SOCS1) and SOCS3 production, thereby further suppressing pro-inflammatory cytokine production by targeting the p65 NF-κB subunit (a key transcriptional regulator in the inflammatory process) for degradation (124).

The anti-inflammatory effects of IL-10 come about by blocking downstream signaling of TLR4, the actions of which normally promote a pro-inflammatory environment critical for the development of neuropathic pain (125). For instance, IL-10 inhibits translation of MyD88, an adaptor protein used by TLR4 that leads to pro-inflammatory cytokine production and release (126). IL-10 also increases ubiquitination and subsequent proteasomal degradation of MyD88-dependent signaling molecules (127). Interestingly, IL-10 induces microRNA-146b, which negatively regulates TLR4-mediated pro-inflammatory cytokine and chemokine induction, with targets including IL-6, TNF-α, IL-8, CCL3, CCL2, CCL7, and CXCL10 (128). IL-10 signaling also increases transcription of numerous effector proteins that inhibit TLR-induced downstream signaling molecules. For instance, IL-10 increases expression of Abin-3 and DUSP-1, leading to inhibition of p38 MAP kinase (MAPK)

phosphorylation as well as increased nuclear translocation and DNA binding of p50/p50 homodimers of NF-κB, a form of NF-κB insufficient for induction of pro-inflammatory cytokine transcription (129).

IL-10 Gene Therapy as a Pain Therapeutic

Several studies indicate that under some chronic pain states, patients suffer from suppressed IL-10 expression (114). Similarly, animal studies also support a link between IL-10 dysregulation and pathological pain. Following peripheral nerve injury, IL-10 is briefly upregulated in what is thought to be a compensatory effort for homeostatic conditions to return. However, as pathological pain develops, IL-10 expression falls below baseline levels in pain-relevant anatomic locations (130–134). Direct application of IL-10 protein to the site of pathology is capable of producing immediate symptom relief, effects are often transient and may require repeated injections (79). These findings support that returning IL-10 expression to near-basal levels may be key to treatment for pathological pain.

Like IL-4, IL-10 has a short half-life, thus making gene therapy a desirable route of administration, particularly in patients requiring local IL-10 expression, such as in individuals with low back radiculopathy. Initial studies utilized viral vectors for lumbar spinal (intrathecal) delivery of the IL-10 gene, including non-replicating adenovirus, adeno-associated virus, and herpes simplex viral vectors. While potent pain relief was observed in animal models of chronic sciatic pain, effects were short-lived (79–82, 135, 136). The transience of the pain relief in these studies may be a result of possible complications associated with the use of a viral vector itself, such as an immune response following exposure to viral antigens (68, 120). To circumvent these possible viral obstacles, non-viral IL-10 gene therapy was explored.

Paradoxically, though non-viral gene therapies are considered the least efficient methods of gene transfer, spinal non-viral IL-10 gene therapy has been repeatedly demonstrated to provide profound and long-lasting pain relief in a variety of animal models (28, 83–87, 114, 137–139). Spinal non-viral IL-10 gene delivery in neuropathic animals produces pain relief through elevated peri-spinal IL-10 production with corresponding reduction of pro-inflammatory mediators (84, 87, 138, 140). The intriguing possibility that the protein derived from the IL-10 transgene could be capable of dimerizing with available endogenous IL-10 protein followed by receptor binding was considered a potential mechanism for the observed enduring efficacy of this unique non-viral approach. Prior work identified a non-silent point mutation in the IL-10 gene being applied in the previously published reports, and there had been some concern that it might disrupt the ability of plasmid-derived IL-10 to engage endogenous IL-10 (28). However, a recent report demonstrates that non-viral IL-10 gene therapy applied to neuropathic IL-10 knockout mice following sciatic chronic constriction injury provides long-lasting relief of allodynia, indicating that endogenous IL-10 is not required for these effects (28). Expression of the IL-10 transgene expression in pain-relieved IL-10 knockout mice was identified in lumbar DRG with concurrent increases in anti-inflammatory transforming growth factor (TGF)-β1 and decreases in pro-inflammatory TNF-α mRNA. While no IL-10 transgene was identified in the lumbar spinal cord, anti-inflammatory changes in the DRG appear to drive concordant decreases in lumbar TNF-α, CCL2, and markers of both astrocytic (GFAP) and microglial (TMEM119) activation (28). This provides compelling evidence that modification of cytokines within the DRG may be sufficient for relief of spinal mechanisms of neuropathic pain following peripheral nerve damage. To date, sex differences in IL-10 efficacy for treating chronic pathological pain have not been reported.

Non-viral IL-10 gene therapy holds significant promise for clinical translation. At this time the non-viral IL-10 gene therapy XT-150 is currently in phase I/II clinical trials (ClinicalTrials.gov Identifiers: NCT03282149; NCT03769662; NCT03477487).

Adjuvants for Non-viral Gene Therapy

While non-viral IL-10 gene therapy has been shown to effectively relieve pathological pain in numerous animal models, initial studies required repeated large doses of DNA, thereby making clinical translation less feasible. To ameliorate the dose limitations, various carriers for non-viral gene therapy have been explored but are limited by adverse effects or added levels of complexity (71, 72, 141). Co-delivered adjuvants may offer a simpler alternative to carrier-type approaches.

D-mannose as an Adjuvant for Non-viral Gene Therapy

D-mannose is an inexpensive and commonly available dietary supplement (142) that has been assessed via phase III clinical trial for prevention of recurrent urinary tract infections (ClinicalTrials.gov Identifier: NCT01808755) (143). D-mannose is a known mannose receptor agonist. The mannose receptor (MR; CD206) is a c-type lectin receptor that functions in endocytosis and pathogen recognition (144). MR is expressed by macrophages, dendritic cells, and microvascular endothelial cells (145), as well as astrocytes, microglia, Schwann cells, and some neurons (146–148). MR is commonly used as a macrophage marker, though increased expression of MR is often associated with anti-inflammatory macrophages (149).

D-mannose was initially explored for use as an adjuvant due to the hypothesis that it may increase intracellular uptake of naked plasmid (87). Interestingly, D-mannose greatly increases gene therapeutic efficacy allowing for long-lasting pain relief following a single co-injection of D-mannose with plasmid DNA encoding the gene for IL-10 in neuropathic rats (87). Work by Dengler et al. also suggests that D-mannose exposure itself increases anti-inflammatory signaling, possibly through actions of endogenous IL-10. However, work by Vanderwall et al. identifies that D-mannose-mediated anti-inflammatory effects do not require IL-10, as intrathecal D-mannose alone induces transient pain relief in IL-10 knockout mice (28).

Historically MR was not considered to possess signaling ability due to the receptor's absence of a clear intracellular signaling motif. Further, if signaling was identified, it was reported as pro-inflammatory in nature. However, many of these studies were performed under inflammatory states which likely predispose MR toward pro-inflammatory signaling pathways (150–152). New evidence supports that MR activation is also

capable of increasing anti-inflammatory cytokines under the right conditions (144, 153). For instance, treatment of dendritic cells with "activating" anti-MR monoclonal antibodies potently increases endogenous IL-10 and IL-1ra while decreasing IL-1β and TNF-α production (154). Furthermore, D-mannose treatment prior to LPS stimulation of RAW 264.7 mouse macrophages reduces release of pro-inflammatory TNF-α, IL-1β, and NO, but increases IL-10 secretion (87).

While D-mannose was initially explored as an adjuvant for gene therapy, its modulation of pain-relevant cytokine signaling pathways make it a novel pain therapeutic in its own right. D-mannose and MR-mediated anti-inflammatory signaling may be clinically relevant for the treatment of a variety of chronic pain conditions due to its engagement of both IL-10-independent and IL-10-mediated anti-inflammation (28, 87). These characteristics may make D-mannose useful for pain relief in patients with known IL-10 gene polymorphisms that would prevent normal IL-10 production in response to other therapeutic approaches. It may also be beneficial for treatment of pain pathologies associated with decreased IL-10 expression, like fibromyalgia (114, 155).

HARNESSING ENDOGENOUS ANTI-INFLAMMATORY CAPACITY FOR TREATMENT OF CHRONIC PAIN

While gene therapy offers many advantages in for treatment of chronic pain, it may not be appropriate for all patients. Therapeutics must balance between homeostasis vs. immunocompromise. For example, excessive or mistimed IL-10 secretion can inhibit a sufficient pro-inflammatory response to pathogens like *Leishmania* spp. (leishmaniasis), *Plasmodium* spp. (malaria), *T. cruzi* (Chagas disease), *Mycobacterium* spp. (tuberculosis), and lymphocytic choriomeningitis virus (lymphocytic choriomeningitis), effectively enabling the pathogens to escape immune control (156). This can result in fatal or chronic infections.

Whereas gene therapeutics are designed to be expressed independently of host transcriptional regulation, therapeutics that engage expression of endogenous anti-inflammatory functions may instead allow for dampened pro-inflammatory signaling without detriment to the body's immune-activating homeostatic mechanisms. A number of therapeutics exist that support the intriguing approach of harnessing the cell's anti-inflammatory processes. We have chosen only a subset based on recent preclinical evidence of altering glial and immune cell proinflammatory activation and corresponding regulation of anti-inflammatory cytokine production. Several promising targets for treatment of chronic neuropathic pain through engagement of endogenous anti-inflammatory capacity are reviewed below.

Cannabinoid Receptors

The two best characterized cannabinoid receptors are CB1R and CB2R, both of which belong to the G-protein coupled receptor (GPCR) superfamily and couple to the inhibitory $G_{i/o}$ and G_i proteins, respectively (157). CB1R was first discovered as the receptor for Δ9-tetrahydrocannabinol (THC), the major psychoactive ingredient in *Cannabis sativa* (158). Peripherally, CB1R is primarily expressed by neurons within the heart, small intestine, urinary bladder and vas deferens, while centrally CB1R is expressed at the highest concentrations by neurons in the cerebellum, hippocampus, basal ganglia and cerebral cortex (157, 159, 160). Clinical application of CB1R agonists are limited by development of tolerance, psychotropic effects (e.g., cognitive impairment, catalepsy, and negative impacts on learning and memory), and risk of hypothermia (157).

CB2R is abundantly expressed by peripheral immune cells (e.g., lymphocytes, neutrophils, and macrophages), and at lower levels within the CNS primarily on microglia, but has also been identified on some neurons (e.g., in the hippocampus, cortex, and substantia nigra) (159–163). CB_2R signaling, while less well-understood, appears to primarily promote anti-inflammatory effects (164), and lack the unwanted psychotropic effects observed with CB1R activation (132). CB2R agonism has been associated with increased expression of IL-10 and decreased production of pro-inflammatory mediators like TNF-α, CCL2, and nitric oxide (164). These characteristics make CB2R a potential target for pain therapeutic development.

CB2R agonists reduce pathological pain with corresponding decreases in pro-inflammatory signaling in several animal pain models, including chronic constriction injury (132), paw incision (165), L5 spinal nerve transection (166), diabetic peripheral neuropathy (167), and chemotherapy induced neuropathic pain (168–171). The pre-clinical and clinical use of cannabinoid receptor agonists in pain has been well-reviewed elsewhere (157, 172–174).

A key CB2R ligand used in these studies, AM1710, does not cross the blood brain barrier and is 57-fold more selective for the CB2R than CB1R (175). Intrathecal AM1710 was shown to both reverse bilateral mechanical hypersensitivity in a model of peripheral nerve injury, and to prevent bilateral mechanical hypersensitivity in a model if spinal gp120 inflammatory pain. While IL-10 immunoreactivity was decreased in neuropathic animals, relief of mechanical sensitivity was associated with a return to basal levels of IL-10 expression (132). This supports that targeting the body's endogenous anti-inflammatory capabilities may relieve pathological pain through re-establishment of homeostatic conditions.

More recently, several orphan receptors, including the GPCRs GPR18, GPR55, and GPR119, have been identified as putative members of the cannabinoid receptor family, with growing evidence that GPR18 and GPR55 may be novel targets for therapeutic modulation of chronic pain (160). GPR18 is expressed in spleen, lymphocytes, neutrophils, macrophages, and lymph nodes (176–179), while GPR55 is expressed in tonsil, spleen, and by CNS neurons (160, 180, 181). The immune-relevant roles of these receptors is not well-understood, though there is some evidence to suggest that GPR55 may alleviate inflammatory pain through altered expression of IL-4, IL-10, and IFN-γ (180).

Lymphocyte Function-Associated Antigen-1

Lymphocyte function-associated antigen-1 (LFA-1; CD11a/CD18) is a β2-integrin expressed on myeloid cells, T cells, and microglia (182–184). LFA-1 is most widely understood to be important for the leukocyte–endothelial cell interaction, which involves leukocytic rolling, firm adhesion, transmigration, and sub-endothelial migration (185). In addition to the widely characterized roles of LFA-1 in cell adhesion and migration, evidence reveals that LFA-1 expression levels following immune challenge are inversely correlated with serum IL-10 expression in experimental mice (186). Reports demonstrate LFA-1 engagement with T cells results in T cell activation, T cell differentiation, and stabilization of T cell cytokine mRNA transcripts including TNF-α (186–189). For example, LFA-1 deficient mice are resistant to LPS-induced acute liver injury, and the mechanism appears to rely on increased IL-10 expression (186). *In vitro* pretreatment of RAW 264.7 macrophages with BIRT-377, an LFA-1 antagonist, prior to LPS stimulation results in a dose-dependent increase in IL-10 protein with a simultaneous decrease in IL-1β and TNF-α (190). Activation of LFA-1 beyond T cell interaction stimulates a variety of downstream signaling cascades in a context-dependent manner modified by the local cytokine milieu (191). In point of fact, these recent reports demonstrate *in vivo* pro-inflammatory cytokine contribution driven by activated LFA-1 on innate immune cells (e.g., macrophages) and T cells during chronic disease.

The dual actions of LFA-1 in cell migration and pro-inflammatory cytokine signaling make it a reasonable target for development of pain therapeutics. The role of LFA-1 in pathological pain was first explored in work by Noor et al. that revealed prenatal alcohol exposure (PAE) predisposes adult rats to develop neuropathic pain in response to a minor injury. They found that LFA-1 expression is increased on microglia and trafficking immune cells in the lumbar spinal cords and on peripheral immune cells of neuropathic PAE rats (192). It was later identified that intrathecal or intravenous administration of BIRT-377, a small molecule non-competitive LFA-1 antagonist, relieves allodynia in neuropathic rats, which was associated with decreased immunoreactivity for spinal markers of glial activation and IL-1β and concurrent increases in IL-10 immunoreactivity (193, 194). Additionally, BIRT-377 intravenous administration in female neuropathic rats reduces Th17 cytokines and elevates FOXP3, a T cell-specific transcription factor necessary for inducing the generation of T regulatory cells characterized by their secretion of IL-10 [(193); Noor et al., under review].

Given the potential for sexual dimorphism in pathological pain, it is noteworthy that intravenous administration of BIRT-377 relieves sciatic neuropathic pain in both male and female mice to a similar degree (54). Pain relief in neuropathic mice of both sexes was concurrent with reductions in pro-inflammatory IL-1β and TNF-α and increases in anti-inflammatory IL-10 and TGF-β1. Interestingly, female-derived T cell cytokines were found to be transcriptionally regulated by LFA-1 antagonism, as demonstrated by reduced pro-inflammatory IL-17A production and increases in IL-10, TGF-β, as well as FOXP3 (54).

The Potential Role of TLR4 Underlying Opioid-Induced Hyperalgesia

A common and unfortunate clinical side effect of chronic opioid use is the development of a paradoxical increase in pain sensitivity, termed opioid-induced hyperalgesia (195–201). Studies demonstrate in both humans and animal models that a number of key factors affect the development of opioid-induced hyperalgesia including anatomical projections from supra-spinal regions onto spinal pain projection neurons (an axonal route where pain facilitation can occur), variants in the mu-opioid receptor, sex differences, prior experience with pain, and even local activation of microglia and astrocytes (201). Given this work's emphasis on glial and immune factors, a brief review of the literature that supports opioid-induced hyperalgesia resulting from the production of pro-inflammatory immune mediators (e.g., cytokines, chemokines, and NO) that produce hyperalgesia (202) is provided below.

TLR4 actions may play a role in opioid-induced hyperalgesia. For instance, TLR4 signaling blockade attenuates opioid-induced hypersensitivity due to morphine or morphine metabolites (e.g., M3G) (203–208). Further, inhibition of glial activation (e.g., with pharmacologic glial inhibitors like minocycline and ibudilast, or by utilization of a microglial targeted Designer Receptor Exclusively Activated by a Designer Drug [DREADD] system) or direct inhibition of specific pro-inflammatory mediators (e.g., TNF-α, IL-1β, IL-6, CX_3CL1, NOS, and p38 MAPK) after repeated morphine attenuates opioid-induced hyperalgesia (207–212).

Not only do opioids induce hyperalgesia, recent work by Grace et al., implicates that repeated opioid exposure prolongs neuropathic pain symptoms. They showed that morphine administered to neuropathic rats leads to persistent nociceptive sensitization through induction of spinal microglial NLRP3 inflammasome via activation of TLR4. This sensitization can be prevented or reversed. Naloxone is famous for its application as a rescue agent in cases of opioid overdose. While (–)-naloxone has antagonistic actions at both the μ-opioid receptor and TLR4, the (+)-naloxone isomer retains only the ability to block TLR4 signaling due to (–)-naloxone stereoselectivity at the μ-opioid receptor (213, 214). TLR4-mediated signaling has been repeatedly implicated in opioid tolerance and opioid-induced hyperalgesia (203–208, 215). These findings indicate that use of (+)-naloxone as an adjuvant to opioid therapy may enable opioid-analgesia while limiting the negative effects caused by TLR4-mediated pro-inflammatory signaling that would ordinarily result in opioid tolerance and opioid-induced hyperalgesia.

Finally, given the growing literature that supports pro-inflammatory cytokine actions in the development of opioid-induced hyperalgesia, gene therapeutics that aim to decrease such pro-inflammatory factors or increase anti-inflammatory cytokines may offer a novel tool for both the study and treatment of this unwanted side effect.

CONCLUDING REMARKS

The worldwide opioid crisis has brought public awareness to the concept that clinically available therapeutics for pain management are not adequate and come with significant health risks. To address this, new approaches must be developed, but this cannot occur without a better understanding of the underlying mechanisms of various chronic pain pathologies. There is now a greater appreciation for actions by non-neuronal support and immune cells, including astrocytes, microglia, and leukocytes that mediate the development and maintenance of chronic pain. Here we have described what is known about the methods of immunological communication between neurons, glia, and immune cells leading to pathological pain, with a focus on the role of pro- and anti-inflammatory cytokines. We also offer potential targets for development of novel non-opioid pain therapeutics that aim to relieve pathological pain by augmenting the body's own anti-inflammatory potential. Future studies will continue to benefit from exploring the roles of neuro-immune interactions and allow for improved patient outcomes.

AUTHOR CONTRIBUTIONS

AV and EM contributed to all aspects of the manuscript.

FUNDING

This work was supported by National Institute of Alcohol Abuse and Alcoholism R21-AA023051: Exploration of neural immune mechanisms, pain, and prenatal alcohol exposure. National Institute of Alcohol Abuse and Alcoholism R01-AA025967: Prenatal alcohol exposure potentiates pain via lifelong spinal immune changes, National Institute of Alcohol Abuse and Alcoholism T32-AA014127: Graduate student training grant in prenatal alcohol exposure, National Institute of Alcohol Abuse and Alcoholism P50-AA022534: Fetal ethanol-induced behavioral deficits: mechanisms diagnosis and intervention, and National Institute of Drug Abuse R01-DA018156: Spinal neuroimmune mechanisms underlying interleukin-10 gene therapy for pain control.

REFERENCES

1. Treede RD, Rief W, Barke A, Aziz Q, Bennett MI, Benoliel R, et al. Chronic pain as a symptom or a disease: the IASP classification of chronic pain for the international classification of diseases (ICD-11). *Pain.* (2019) 160:19–27. doi: 10.1097/j.pain.0000000000001384
2. Yaqub F. Pain in the USA: states of suffering. *Lancet.* (2015) 386:839. doi: 10.1016/S0140-6736(15)00041-0
3. GBD 2015 Disease and Injury Incidence and Prevalence Collaborators. Global, regional, and national incidence, prevalence, and years lived with disability for 310 diseases and injuries, 1990–2015: a systematic analysis for the Global Burden of Disease Study 2015. *Lancet.* (2016) 388:1545–602. doi: 10.1016/S0140-6736(16)31678-6
4. Med I. *Relieving Pain in America: A Blueprint for Transforming Prevention, Care, Education, and Research*. Washington, DC: National Academy of Sciences (2011). p. 1–364.
5. Lembke A, Humphreys K, Newmark J. Weighing the risks and benefits of chronic opioid therapy. *Am Fam Physician.* (2016) 93:982–90. doi: 10.1001/jamapsychiatry.2016.1390
6. Basbaum AI, Bautista DM, Scherrer G, Julius D. Cellular and molecular mechanisms of pain. *Cell.* (2009) 139:267–84. doi: 10.1016/j.cell.2009.09.028
7. Watkins LR, Hutchinson MR, Ledeboer A, Wieseler-Frank J, Milligan ED, Maier SF. Glia as the "bad guys": implications for improving clinical pain control and the clinical utility of opioids. *Brain Behav Immun.* (2007) 21:131–46. doi: 10.1016/j.bbi.2006.10.011
8. Milligan ED, Watkins LR. Pathological and protective roles of glia in chronic pain. *Nat Rev Neurosci.* (2009) 10:23–36. doi: 10.1038/nrn2533
9. Grace PM, Hutchinson MR, Maier SF, Watkins LR. Pathological pain and the neuroimmune interface. *Nat Rev Immunol.* (2014) 14:217–31. doi: 10.1038/nri3621
10. Takeuchi O, Akira S. Pattern recognition receptors and inflammation. *Cell.* (2010) 140:805–20. doi: 10.1016/j.cell.2010.01.022
11. Totsch SK, Sorge RE. Immune system involvement in specific pain conditions. *Mol Pain.* (2017) 13:1744806917724559. doi: 10.1177/1744806917724559
12. Chavan SS, Pavlov VA, Tracey KJ. Mechanisms and therapeutic relevance of neuro-immune communication. *Immunity.* (2017) 46:927–42. doi: 10.1016/j.immuni.2017.06.008
13. Xu ZZ, Zhang L, Liu T, Park JY, Berta T, Yang R, et al. Resolvins RvE1 and RvD1 attenuate inflammatory pain via central and peripheral actions. *Nat Med.* (2010) 16:592–7, 591p following 597. doi: 10.1038/nm.2123
14. Ji R-R, Xu Z-Z, Gao Y-J. Emerging targets in neuroinflammation-driven chronic pain. *Nat Rev Drug Discov.* (2014) 13:533. doi: 10.1038/nrd4334
15. Scholz J, Woolf CJ. The neuropathic pain triad: neurons, immune cells and glia. *Nat Neurosci.* (2007) 10:1361–8. doi: 10.1038/nn1992
16. Crosson T, Roversi K, Balood M, Othman R, Ahmadi M, Wang JC, et al. Profiling of how nociceptor neurons detect danger–new and old foes. *J Intern Med.* (2019) 286:268–89. doi: 10.1111/joim.12957
17. Littlejohn G. Neurogenic neuroinflammation in fibromyalgia and complex regional pain syndrome. *Nat Rev Rheumatol.* (2015) 11:639. doi: 10.1038/nrrheum.2015.100
18. Woolf CJ. Evidence for a central component of post-injury pain hypersensitivity. *Nature.* (1983) 306:686–8. doi: 10.1038/306686a0
19. Latremoliere A, Woolf CJ. Central sensitization: a generator of pain hypersensitivity by central neural plasticity. *J Pain.* (2009) 10:895–926. doi: 10.1016/j.jpain.2009.06.012
20. Rowitch DH, Kriegstein AR. Developmental genetics of vertebrate glial-cell specification. *Nature.* (2010) 468:214–22. doi: 10.1038/nature09611
21. Lee JC, Mayer-Proschel M, Rao MS. Gliogenesis in the central nervous system. *Glia.* (2000) 30:105–21. doi: 10.1002/(SICI)1098-1136(200004)30:2<105::AID-GLIA1>3.0.CO;2-H
22. Watkins LR, Maier SF. Immune regulation of central nervous system functions: from sickness responses to pathological pain. *J Intern Med.* (2005) 257:139–55. doi: 10.1111/j.1365-2796.2004.01443.x
23. Watkins LR, Milligan ED, Maier SF. Spinal cord glia: new players in pain. *Pain.* (2001) 93:201–5. doi: 10.1016/S0304-3959(01)00359-1
24. Echeverry S, Shi XQ, Zhang J. Characterization of cell proliferation in rat spinal cord following peripheral nerve injury and the relationship with neuropathic pain. *Pain.* (2008) 135:37–47. doi: 10.1016/j.pain.2007.05.002
25. Bennett ML, Bennett FC, Liddelow SA, Ajami B, Zamanian JL, Fernhoff NB, et al. New tools for studying microglia in the mouse and human CNS. *Proc Natl Acad Sci USA.* (2016) 113:E1738–46. doi: 10.1073/pnas.1525528113
26. Satoh J, Kino Y, Asahina N, Takitani M, Miyoshi J, Ishida T, et al. TMEM119 marks a subset of microglia in the human brain. *Neuropathology.* (2016) 36:39–49. doi: 10.1111/neup.12235
27. Zrzavy T, Hametner S, Wimmer I, Butovsky O, Weiner HL, Lassmann H. Loss of 'homeostatic' microglia and patterns of their activation in active multiple sclerosis. *Brain.* (2017) 140:1900–13. doi: 10.1093/brain/awx113
28. Vanderwall AG, Noor S, Sun MS, Sanchez JE, Yang XO, Jantzie LL, et al. Effects of spinal non-viral interleukin-10 gene therapy formulated with d-mannose in neuropathic interleukin-10 deficient mice: behavioral

characterization, mRNA and protein analysis in pain relevant tissues. *Brain Behav Immun.* (2018) 69:91–112. doi: 10.1016/j.bbi.2017.11.004
29. Garrison CJ, Dougherty PM, Kajander KC, Carlton SM. Staining of glial fibrillary acidic protein (GFAP) in lumbar spinal cord increases following a sciatic nerve constriction injury. *Brain Res.* (1991) 565:1–7. doi: 10.1016/0006-8993(91)91729-K
30. De Leo JA, Tawfik VL, Lacroix-Fralish ML. The tetrapartite synapse: path to CNS sensitization and chronic pain. *Pain.* (2006) 122:17–21. doi: 10.1016/j.pain.2006.02.034
31. Ji RR, Chamessian A, Zhang YQ. Pain regulation by non-neuronal cells and inflammation. *Science.* (2016) 354:572–7. doi: 10.1126/science.aaf8924
32. Li T, Chen X, Zhang C, Zhang Y, Yao W. An update on reactive astrocytes in chronic pain. *J Neuroinflammation.* (2019) 16:140. doi: 10.1186/s12974-019-1524-2
33. Zhang ZJ, Jiang BC, Gao YJ. Chemokines in neuron-glial cell interaction and pathogenesis of neuropathic pain. *Cell Mol Life Sci.* (2017) 74:3275–91. doi: 10.1007/s00018-017-2513-1
34. Zhuang ZY, Kawasaki Y, Tan PH, Wen YR, Huang J, Ji RR. Role of the CX3CR1/p38 MAPK pathway in spinal microglia for the development of neuropathic pain following nerve injury-induced cleavage of fractalkine. *Brain Behav Immun.* (2007) 21:642–51. doi: 10.1016/j.bbi.2006.11.003
35. Guan Z, Kuhn JA, Wang X, Colquitt B, Solorzano C, Vaman S, et al. Injured sensory neuron-derived CSF1 induces microglial proliferation and DAP12-dependent pain. *Nat Neurosci.* (2016) 19:94–101. doi: 10.1038/nn.4189
36. Tsuda M, Shigemoto-Mogami Y, Koizumi S, Mizokoshi A, Kohsaka S, Salter MW, et al. P2X4 receptors induced in spinal microglia gate tactile allodynia after nerve injury. *Nature.* (2003) 424:778. doi: 10.1038/nature01786
37. Beggs S, Trang T, Salter MW. P2X4R$^+$ microglia drive neuropathic pain. *Nat Neurosci.* (2012) 15:1068–73. doi: 10.1038/nn.3155
38. Chen G, Zhang Y-Q, Qadri YJ, Serhan CN, Ji R-R. Microglia in pain: detrimental and protective roles in pathogenesis and resolution of pain. *Neuron.* (2018) 100:1292–311. doi: 10.1016/j.neuron.2018.11.009
39. Kawasaki Y, Zhang L, Cheng JK, Ji RR. Cytokine mechanisms of central sensitization: distinct and overlapping role of interleukin-1beta, interleukin-6, and tumor necrosis factor-alpha in regulating synaptic and neuronal activity in the superficial spinal cord. *J Neurosci.* (2008) 28:5189–94. doi: 10.1523/JNEUROSCI.3338-07.2008
40. Hu P, Bembrick AL, Keay KA, Mclachlan EM. Immune cell involvement in dorsal root ganglia and spinal cord after chronic constriction or transection of the rat sciatic nerve. *Brain Behav Immun.* (2007) 21:599–616. doi: 10.1016/j.bbi.2006.10.013
41. Raoof R, Willemen HLDM, Eijkelkamp N. Divergent roles of immune cells and their mediators in pain. *Rheumatology.* (2017) 57:429–40. doi: 10.1093/rheumatology/kex308
42. Kwon MJ, Shin HY, Cui Y, Kim H, Thi AHL, Choi JY, et al. CCL2 mediates neuron–macrophage interactions to drive proregenerative macrophage activation following preconditioning injury. *J Neurosci.* (2015) 35:15934–47. doi: 10.1523/JNEUROSCI.1924-15.2015
43. Zhang H, Li Y, De Carvalho-Barbosa M, Kavelaars A, Heijnen CJ, Albrecht PJ, et al. Dorsal root ganglion infiltration by macrophages contributes to paclitaxel chemotherapy-induced peripheral neuropathy. *J Pain.* (2016) 17:775–86. doi: 10.1016/j.jpain.2016.02.011
44. Schreiber RC, Krivacic K, Kirby B, Vaccariello SA, Wei T, Ransohoff RM, et al. Monocyte chemoattractant protein (MCP)-1 is rapidly expressed by sympathetic ganglion neurons following axonal injury. *Neuroreport.* (2001) 12:601–6. doi: 10.1097/00001756-200103050-00034
45. Huang ZZ, Li D, Liu CC, Cui Y, Zhu HQ, Zhang WW, et al. CX3CL1-mediated macrophage activation contributed to paclitaxel-induced DRG neuronal apoptosis and painful peripheral neuropathy. *Brain Behav Immun.* (2014) 40:155–65. doi: 10.1016/j.bbi.2014.03.014
46. Barclay J, Clark AK, Ganju P, Gentry C, Patel S, Wotherspoon G, et al. Role of the cysteine protease cathepsin S in neuropathic hyperalgesia. *Pain.* (2007) 130:225–34. doi: 10.1016/j.pain.2006.11.017
47. Cao L, Deleo JA. CNS-infiltrating CD4$^+$ T lymphocytes contribute to murine spinal nerve transection-induced neuropathic pain. *Eur J Immunol.* (2008) 38:448–58. doi: 10.1002/eji.200737485
48. Cao L, Beaulac H, Eurich A. Differential lumbar spinal cord responses among wild type, CD4 knockout, and CD40 knockout mice in spinal nerve L5 transection-induced neuropathic pain. *Mol Pain.* (2012) 8:88. doi: 10.1186/1744-8069-8-88
49. Draleau K, Maddula S, Slaiby A, Nutile-Mcmenemy N, De Leo J, Cao L. Phenotypic identification of spinal cord-infiltrating CD4(+) T lymphocytes in a murine model of neuropathic pain. *J Pain Relief Suppl.* (2014) 3:003. doi: 10.4172/2167-0846.S3-003
50. Costigan M, Moss A, Latremoliere A, Johnston C, Verma-Gandhu M, Herbert TA, et al. T-cell infiltration and signaling in the adult dorsal spinal cord is a major contributor to neuropathic pain-like hypersensitivity. *J Neurosci.* (2009) 29:14415–22. doi: 10.1523/JNEUROSCI.4569-09.2009
51. Sun C, Zhang J, Chen L, Liu T, Xu G, Li C, et al. IL-17 contributed to the neuropathic pain following peripheral nerve injury by promoting astrocyte proliferation and secretion of proinflammatory cytokines. *Mol Med Rep.* (2017) 15:89–96. doi: 10.3892/mmr.2016.6018
52. Kim CF, Moalem-Taylor G. Interleukin-17 contributes to neuroinflammation and neuropathic pain following peripheral nerve injury in mice. *J Pain.* (2011) 12:370–83. doi: 10.1016/j.jpain.2010.08.003
53. Lopes DM, Malek N, Edye M, Jager SB, Mcmurray S, Mcmahon SB, et al. Sex differences in peripheral not central immune responses to pain-inducing injury. *Sci Rep.* (2017) 7:16460. doi: 10.1038/s41598-017-16664-z
54. Noor S, Sun MS, Vanderwall AG, Havard MA, Sanchez JE, Harris NW, et al. LFA-1 antagonist (BIRT377) similarly reverses peripheral neuropathic pain in male and female mice with underlying sex divergent peripheral immune proinflammatory phenotypes. *Neuroimmunol Neuroinflamm.* (2019) 6:10. doi: 10.20517/2347-8659.2019.18
55. Castro F, Cardoso AP, Gonçalves RM, Serre K, Oliveira MJ. Interferon-gamma at the crossroads of tumor immune surveillance or evasion. *Front Immunol.* (2018) 9:847. doi: 10.3389/fimmu.2018.00847
56. Mapplebeck JC, Beggs S, Salter MW. Molecules in pain and sex: a developing story. *Mol Brain.* (2017) 10:9. doi: 10.1186/s13041-017-0289-8
57. Rosen S, Ham B, Mogil JS. Sex differences in neuroimmunity and pain. *J Neurosci Res.* (2017) 95:500–8. doi: 10.1002/jnr.23831
58. Sorge RE, Lacroix-Fralish ML, Tuttle AH, Sotocinal SG, Austin JS, Ritchie J, et al. Spinal cord Toll-like receptor 4 mediates inflammatory and neuropathic hypersensitivity in male but not female mice. *J Neurosci.* (2011) 31:15450–4. doi: 10.1523/JNEUROSCI.3859-11.2011
59. Sorge RE, Mapplebeck JC, Rosen S, Beggs S, Taves S, Alexander JK, et al. Different immune cells mediate mechanical pain hypersensitivity in male and female mice. *Nat Neurosci.* (2015) 18:1081–3. doi: 10.1038/nn.4053
60. Taves S, Berta T, Liu DL, Gan S, Chen G, Kim YH, et al. Spinal inhibition of p38 MAP kinase reduces inflammatory and neuropathic pain in male but not female mice: sex-dependent microglial signaling in the spinal cord. *Brain Behav Immun.* (2016) 55:70–81. doi: 10.1016/j.bbi.2015.10.006
61. Mapplebeck JCS, Dalgarno R, Tu Y, Moriarty O, Beggs S, Kwok CHT, et al. Microglial P2X4R-evoked pain hypersensitivity is sexually dimorphic in rats. *Pain.* (2018) 159:1752–63. doi: 10.1097/j.pain.0000000000001265
62. Stephens KE, Zhou W, Ji Z, Chen Z, He S, Ji H, et al. Sex differences in gene regulation in the dorsal root ganglion after nerve injury. *BMC Genomics.* (2019) 20:147. doi: 10.1186/s12864-019-5512-9
63. Dunbar CE, High KA, Joung JK, Kohn DB, Ozawa K, Sadelain M. Gene therapy comes of age. *Science.* (2018) 359:eaan4672. doi: 10.1126/science.aan4672
64. Finkel RS, Mercuri E, Darras BT, Connolly AM, Kuntz NL, Kirschner J, et al. Nusinersen versus sham control in infantile-onset spinal muscular atrophy. *N Engl J Med.* (2017) 377:1723–32. doi: 10.1056/NEJMoa1702752
65. Mercuri E, Darras BT, Chiriboga CA, Day JW, Campbell C, Connolly AM, et al. Nusinersen versus sham control in later-onset spinal muscular atrophy. *N Engl J Med.* (2018) 378:625–35. doi: 10.1056/NEJMoa1710504
66. Maude SL, Laetsch TW, Buechner J, Rives S, Boyer M, Bittencourt H, et al. Tisagenlecleucel in children and young adults with B-cell lymphoblastic leukemia. *N Engl J Med.* (2018) 378:439–48. doi: 10.1056/NEJMoa1709866
67. Russell S, Bennett J, Wellman JA, Chung DC, Yu Z-F, Tillman A, et al. Efficacy and safety of voretigene neparvovec (AAV2-hRPE65v2) in patients with RPE65-mediated inherited retinal dystrophy: a randomised, controlled, open-label, phase 3 trial. *Lancet.* (2017) 390:849–60. doi: 10.1016/S0140-6736(17)31868-8

68. Wood MJA, Charlton HM, Wood KJ, Kajiwara K, Byrnes AP. Immune responses to adenovirus vectors in the nervous system. *Trends Neurosci.* (1996) 19:497–501. doi: 10.1016/S0166-2236(96)10060-6
69. Glover DJ, Lipps HJ, Jans DA. Towards safe, non-viral therapeutic gene expression in humans. *Nat Rev Genet.* (2005) 6:299–310. doi: 10.1038/nrg1577
70. Mingozzi F, High KA. Immune responses to AAV in clinical trials. *Curr Gene Ther.* (2011) 11:321–30. doi: 10.2174/156652311796150354
71. Jayant RD, Sosa D, Kaushik A, Atluri V, Vashist A, Tomitaka A, et al. Current status of non-viral gene therapy for CNS disorders. *Expert Opin Drug Deliv.* (2016) 13:1433–45. doi: 10.1080/17425247.2016.1188802
72. Slivac I, Guay D, Mangion M, Champeil J, Gaillet B. Non-viral nucleic acid delivery methods. *Expert Opin Biol Ther.* (2017) 17:105–18. doi: 10.1080/14712598.2017.1248941
73. Yin H, Kanasty RL, Eltoukhy AA, Vegas AJ, Dorkin JR, Anderson DG. Non-viral vectors for gene-based therapy. *Nat Rev Genet.* (2014) 15:541. doi: 10.1038/nrg3763
74. Hao S, Mata M, Glorioso JC, Fink DJ. HSV-mediated expression of interleukin-4 in dorsal root ganglion neurons reduces neuropathic pain. *Mol Pain.* (2006) 2:6. doi: 10.1186/1744-8069-2-6
75. Peng XM, Zhou ZG, Glorioso JC, Fink DJ, Mata M. Tumor necrosis factor-alpha contributes to below-level neuropathic pain after spinal cord injury. *Ann Neurol.* (2006) 59:843–51. doi: 10.1002/ana.20855
76. Hao S, Mata M, Glorioso JC, Fink DJ. Gene transfer to interfere with TNFα signaling in neuropathic pain. *Gene Ther.* (2007) 14:1010. doi: 10.1038/sj.gt.3302950
77. Huang W, Zheng W, Ouyang H, Yi H, Liu S, Zeng W, et al. Mechanical allodynia induced by nucleoside reverse transcriptase inhibitor is suppressed by p55TNFSR mediated by herpes simplex virus vector through the SDF1alpha/CXCR4 system in rats. *Anesth Analg.* (2014) 118:671–80. doi: 10.1213/ANE.0000000000000079
78. Ortmann KLM, Chattopadhyay M. Decrease in neuroimmune activation by HSV-mediated gene transfer of TNFα soluble receptor alleviates pain in rats with diabetic neuropathy. *Brain Behav Immun.* (2014) 41:144–51. doi: 10.1016/j.bbi.2014.05.009
79. Milligan ED, Langer SJ, Sloane EM, He L, Wieseler-Frank J, O'connor K, et al. Controlling pathological pain by adenovirally driven spinal production of the anti-inflammatory cytokine, interleukin-10. *Eur J Neurosci.* (2005) 21:2136–48. doi: 10.1111/j.1460-9568.2005.04057.x
80. Lau D, Harte SE, Morrow TJ, Wang S, Mata M, Fink DJ. Herpes simplex virus vector-mediated expression of interleukin-10 reduces below-level central neuropathic pain after spinal cord injury. *Neurorehabil Neural Repair.* (2012) 26:889–97. doi: 10.1177/1545968312445637
81. Zheng W, Huang W, Liu S, Levitt RC, Candiotti KA, Lubarsky DA, et al. IL-10 mediated by herpes simplex virus vector reduces neuropathic pain induced by HIV gp120 combined with ddC in rats. *Mol Pain.* (2014) 10:49. doi: 10.1186/1744-8069-10-49
82. Zheng W, Huang W, Liu S, Levitt RC, Candiotti KA, Lubarsky DA, et al. Interleukin 10 mediated by herpes simplex virus vectors suppresses neuropathic pain induced by human immunodeficiency virus gp120 in rats. *Anesth Analg.* (2014) 119:693–701. doi: 10.1213/ANE.0000000000000311
83. Milligan ED, Sloane EM, Langer SJ, Hughes TS, Jekich BM, Frank MG, et al. Repeated intrathecal injections of plasmid DNA encoding interleukin-10 produce prolonged reversal of neuropathic pain. *Pain.* (2006) 126:294–308. doi: 10.1016/j.pain.2006.07.009
84. Ledeboer A, Jekich BM, Sloane EM, Mahoney JH, Langer SJ, Milligan ED, et al. Intrathecal interleukin-10 gene therapy attenuates paclitaxel-induced mechanical allodynia and proinflammatory cytokine expression in dorsal root ganglia in rats. *Brain Behav Immun.* (2007) 21:686–98. doi: 10.1016/j.bbi.2006.10.012
85. Sloane E, Langer S, Jekich B, Mahoney J, Hughes T, Frank M, et al. Immunological priming potentiates non-viral anti-inflammatory gene therapy treatment of neuropathic pain. *Gene Ther.* (2009) 16:1210–22. doi: 10.1038/gt.2009.79
86. Soderquist RG, Sloane EM, Loram LC, Harrison JA, Dengler EC, Johnson SM, et al. Release of plasmid DNA-encoding IL-10 from PLGA microparticles facilitates long-term reversal of neuropathic pain following a single intrathecal administration. *Pharm Res.* (2010) 27:841–54. doi: 10.1007/s11095-010-0077-y
87. Dengler EC, Alberti LA, Bowman BN, Kerwin AA, Wilkerson JL, Moezzi DR, et al. Improvement of spinal non-viral IL-10 gene delivery by D-mannose as a transgene adjuvant to control chronic neuropathic pain. *J Neuroinflammation.* (2014) 11:92. doi: 10.1186/1742-2094-11-92
88. Busch-Dienstfertig M, González-Rodríguez S. IL-4, *JAK-STAT* signaling, and pain. *JAK-STAT.* (2013) 2:e27638. doi: 10.4161/jkst.27638
89. Gadani SP, Cronk JC, Norris GT, Kipnis J. IL-4 in the brain: a cytokine to remember. *J Immunol.* (2012) 189:4213–9. doi: 10.4049/jimmunol.1202246
90. Andrews A-L, Holloway JW, Holgate ST, Davies DE. IL-4 receptor α is an important modulator of IL-4 and IL-13 receptor binding: implications for the development of therapeutic targets. *J Immunol.* (2006) 176:7456–61. doi: 10.4049/jimmunol.176.12.7456
91. Hwang I, Yang J, Hong S, Ju Lee E, Lee S-H, Fernandes-Alnemri T, et al. Non-transcriptional regulation of NLRP3 inflammasome signaling by IL-4. *Immunol Cell Biol.* (2015) 93:591–9. doi: 10.1038/icb.2014.125
92. Lu A, Wu H. Structural mechanisms of inflammasome assembly. *FEBS J.* (2015) 282:435–44. doi: 10.1111/febs.13133
93. Xue Y, Enosi Tuipulotu D, Tan WH, Kay C, Man SM. Emerging activators and regulators of inflammasomes and pyroptosis. *Trends Immunol.* (2019) 40:1035–52. doi: 10.1016/j.it.2019.09.005
94. Vannier E, Miller LC, Dinarello CA. Coordinated antiinflammatory effects of interleukin 4: interleukin 4 suppresses interleukin 1 production but up-regulates gene expression and synthesis of interleukin 1 receptor antagonist. *Proc Natl Acad Sci USA.* (1992) 89:4076–80. doi: 10.1073/pnas.89.9.4076
95. Hart PH, Vitti GF, Burgess DR, Whitty GA, Piccoli DS, Hamilton JA. Potential antiinflammatory effects of interleukin 4: suppression of human monocyte tumor necrosis factor alpha, interleukin 1, and prostaglandin E2. *Proc Natl Acad Sci USA.* (1989) 86:3803–7. doi: 10.1073/pnas.86.10.3803
96. Lee YW, Lee WH, Kim PH. Oxidative mechanisms of IL-4-induced IL-6 expression in vascular endothelium. *Cytokine.* (2010) 49:73–9. doi: 10.1016/j.cyto.2009.08.009
97. Pousset F, Cremona S, Dantzer R, Kelley K, Parnet P. Interleukin-4 and interleukin-10 regulate IL1-beta induced mouse primary astrocyte activation: a comparative study. *Glia.* (1999) 26:12–21. doi: 10.1002/(SICI)1098-1136(199903)26:1<12::AID-GLIA2>3.0.CO;2-S
98. Van Kampen C, Gauldie J, Collins SM. Proinflammatory properties of IL-4 in the intestinal microenvironment. *Am J Physiol Gastrointest Liver Physiol.* (2005) 288:G111–7. doi: 10.1152/ajpgi.00014.2004
99. Park KW, Baik HH, Jin BK. Interleukin-4-induced oxidative stress via microglial NADPH oxidase contributes to the death of hippocampal neurons *in vivo*. *Curr Aging Sci.* (2008) 1:192–201. doi: 10.2174/1874609810801030192
100. Uceyler N, Topuzoglu T, Schiesser P, Hahnenkamp S, Sommer C. IL-4 deficiency is associated with mechanical hypersensitivity in mice. *PLoS ONE.* (2011) 6:e28205. doi: 10.1371/journal.pone.0028205
101. Boyle DL, Nguyen KHY, Zhuang S, Shi Y, Mccormack JE, Chada S, et al. Intra-articular IL-4 gene therapy in arthritis: anti-inflammatory effect and enhanced Th2activity. *Gene Ther.* (1999) 6:1911–8. doi: 10.1038/sj.gt.3301049
102. Pearson CM, Wood FD. Studies of polyarthritis and other lesions induced in rats by injection of mycobacterial adjuvant. I. General clinical and pathologic characteristics and some modifying factors. *Arthritis Rheum.* (1959) 2:440–59. doi: 10.1002/1529-0131(195910)2:5<440::AID-ART1780020510>3.0.CO;2-N
103. Sedger LM, Mcdermott MF. TNF and TNF-receptors: From mediators of cell death and inflammation to therapeutic giants–past, present and future. *Cytokine Growth Factor Rev.* (2014) 25:453–72. doi: 10.1016/j.cytogfr.2014.07.016
104. Zhang J-M, An J. Cytokines, inflammation, and pain. *Int Anesthesiol Clin.* (2007) 45:27–37. doi: 10.1097/AIA.0b013e318034194e
105. Lindenlaub T, Teuteberg P, Hartung T, Sommer C. Effects of neutralizing antibodies to TNF-alpha on pain-related behavior and nerve regeneration in mice with chronic constriction injury. *Brain Res.* (2000) 866:15–22. doi: 10.1016/S0006-8993(00)02190-9
106. Sommer C, Lindenlaub T, Teuteberg P, Schafers M, Hartung T, Toyka KV. Anti-TNF-neutralizing antibodies reduce pain-related behavior in two

different mouse models of painful mononeuropathy. *Brain Res.* (2001) 913:86–9. doi: 10.1016/S0006-8993(01)02743-3
107. Sommer C, Schafers M, Marziniak M, Toyka KV. Etanercept reduces hyperalgesia in experimental painful neuropathy. *J Peripher Nerv Syst.* (2001) 6:67–72. doi: 10.1046/j.1529-8027.2001.01010.x
108. Svensson CI, Schafers M, Jones TL, Powell H, Sorkin LS. Spinal blockade of TNF blocks spinal nerve ligation-induced increases in spinal P-p38. *Neurosci Lett.* (2005) 379:209–13. doi: 10.1016/j.neulet.2004.12.064
109. Hung AL, Lim M, Doshi TL. Targeting cytokines for treatment of neuropathic pain. *Scand J Pain.* (2017) 17:287–93. doi: 10.1016/j.sjpain.2017.08.002
110. Fontaine V, Mohand-Said S, Hanoteau N, Fuchs C, Pfizenmaier K, Eisel U. Neurodegenerative and neuroprotective effects of tumor necrosis factor (TNF) in retinal ischemia: opposite roles of TNF receptor 1 and TNF receptor 2. *J Neurosci.* (2002) 22:RC216. doi: 10.1523/JNEUROSCI.22-07-j0001.2002
111. Yang L, Lindholm K, Konishi Y, Li R, Shen Y. Target depletion of distinct tumor necrosis factor receptor subtypes reveals hippocampal neuron death and survival through different signal transduction pathways. *J Neurosci.* (2002) 22:3025–32. doi: 10.1523/JNEUROSCI.22-08-03025.2002
112. Figiel I. Pro-inflammatory cytokine TNF-alpha as a neuroprotective agent in the brain. *Acta Neurobiol Exp (Wars).* (2008) 68:526–34.
113. Leung L, Cahill CM. TNF-alpha and neuropathic pain–a review. *J Neuroinflammation.* (2010) 7:27. doi: 10.1186/1742-2094-7-27
114. Milligan ED, Penzkover KR, Soderquist RG, Mahoney MJ. Spinal interleukin-10 therapy to treat peripheral neuropathic pain. *Neuromodulation.* (2012) 15:520–6; discussion 526. doi: 10.1111/j.1525-1403.2012.00462.x
115. Gonzalez P, Burgaya F, Acarin L, Peluffo H, Castellano B, Gonzalez B. Interleukin-10 and interleukin-10 receptor-I are upregulated in glial cells after an excitotoxic injury to the postnatal rat brain. *J Neuropathol Exp Neurol.* (2009) 68:391–403. doi: 10.1097/NEN.0b013e31819dca30
116. Zhou Z, Peng X, Insolera R, Fink DJ, Mata M. Interleukin-10 provides direct trophic support to neurons. *J Neurochem.* (2009) 110:1617–27. doi: 10.1111/j.1471-4159.2009.06263.x
117. Chen H, Lin W, Zhang Y, Lin L, Chen J, Zeng Y, et al. IL-10 promotes neurite outgrowth and synapse formation in cultured cortical neurons after the oxygen-glucose deprivation via JAK1/STAT3 pathway. *Sci Rep.* (2016) 6:30459. doi: 10.1038/srep30459
118. Shen K-F, Zhu H-Q, Wei X-H, Wang J, Li Y-Y, Pang R-P, et al. Interleukin-10 down-regulates voltage gated sodium channels in rat dorsal root ganglion neurons. *Exp Neurol.* (2013) 247:466–75. doi: 10.1016/j.expneurol.2013.01.018
119. Moore KW, De Waal Malefyt R, Coffman RL, O'garra A. Interleukin-10 and the interleukin-10 receptor. *Annu Rev Immunol.* (2001) 19:683–765. doi: 10.1146/annurev.immunol.19.1.683
120. Kwilasz AJ, Grace PM, Serbedzija P, Maier SF, Watkins LR. The therapeutic potential of interleukin-10 in neuroimmune diseases. *Neuropharmacology.* (2015) 96:55–69. doi: 10.1016/j.neuropharm.2014.10.020
121. Kishore R, Tebo JM, Kolosov M, Hamilton TA. Cutting edge: clustered AU-rich elements are the target of IL-10-mediated mRNA destabilization in mouse macrophages. *J Immunol.* (1999) 162:2457–61.
122. Murray PJ. The primary mechanism of the IL-10-regulated antiinflammatory response is to selectively inhibit transcription. *Proc Natl Acad Sci USA.* (2005) 102:8686–91. doi: 10.1073/pnas.0500419102
123. Lobo-Silva D, Carriche GM, Castro AG, Roque S, Saraiva M. Balancing the immune response in the brain: IL-10 and its regulation. *J Neuroinflammation.* (2016) 13:297. doi: 10.1186/s12974-016-0763-8
124. Yoshimura A, Naka T, Kubo M. SOCS proteins, cytokine signalling and immune regulation. *Nat Rev Immunol.* (2007) 7:454–65. doi: 10.1038/nri2093
125. Tanga FY, Nutile-Mcmenemy N, Deleo JA. The CNS role of Toll-like receptor 4 in innate neuroimmunity and painful neuropathy. *Proc Natl Acad Sci USA.* (2005) 102:5856–61. doi: 10.1073/pnas.0501634102
126. Dagvadorj J, Naiki Y, Tumurkhuu G, Hassan F, Islam S, Koide N, et al. Interleukin-10 inhibits tumor necrosis factor-α production in lipopolysaccharide-stimulated RAW 264.7 cells through reduced MyD88 expression. *Innate Immun.* (2008) 14:109–15. doi: 10.1177/1753425908089618
127. Chang J, Kunkel SL, Chang C-H. Negative regulation of MyD88-dependent signaling by IL-10 in dendritic cells. *Proc Natl Acad Sci USA.* (2009) 106:18327–32. doi: 10.1073/pnas.0905815106
128. Curtale G, Mirolo M, Renzi TA, Rossato M, Bazzoni F, Locati M. Negative regulation of Toll-like receptor 4 signaling by IL-10-dependent microRNA-146b. *Proc Natl Acad Sci USA.* (2013) 110:11499–504. doi: 10.1073/pnas.1219852110
129. Sabat R, Grutz G, Warszawska K, Kirsch S, Witte E, Wolk K, et al. Biology of interleukin-10. *Cytokine Growth Factor Rev.* (2010) 21:331–44. doi: 10.1016/j.cytogfr.2010.09.002
130. Jancalek R, Dubovy P, Svizenska I, Klusakova I. Bilateral changes of TNF-alpha and IL-10 protein in the lumbar and cervical dorsal root ganglia following a unilateral chronic constriction injury of the sciatic nerve. *J Neuroinflammation.* (2010) 7:11. doi: 10.1186/1742-2094-7-11
131. Jancalek R, Svizenska I, Klusakova I, Dubovy P. Bilateral changes of IL-10 protein in lumbar and cervical dorsal root ganglia following proximal and distal chronic constriction injury of peripheral nerve. *Neurosci Lett.* (2011) 501:86–91. doi: 10.1016/j.neulet.2011.06.052
132. Wilkerson JL, Gentry KR, Dengler EC, Wallace JA, Kerwin AA, Armijo LM, et al. Intrathecal cannabilactone CB(2)R agonist, AM1710, controls pathological pain and restores basal cytokine levels. *Pain.* (2012) 153:1091–106. doi: 10.1016/j.pain.2012.02.015
133. Wilkerson JL, Gentry KR, Dengler EC, Wallace JA, Kerwin AA, Kuhn MN, et al. Immunofluorescent spectral analysis reveals the intrathecal cannabinoid agonist, AM1241, produces spinal anti-inflammatory cytokine responses in neuropathic rats exhibiting relief from allodynia. *Brain Behav.* (2012) 2:155–77. doi: 10.1002/brb3.44
134. Khan J, Ramadan K, Korczeniewska O, Anwer MM, Benoliel R, Eliav E. Interleukin-10 levels in rat models of nerve damage and neuropathic pain. *Neurosci Lett.* (2015) 592:99–106. doi: 10.1016/j.neulet.2015.03.001
135. Milligan ED, Sloane EM, Langer SJ, Cruz PE, Chacur M, Spataro L, et al. Controlling neuropathic pain by adeno-associated virus driven production of the anti-inflammatory cytokine, interleukin-10. *Mol Pain.* (2005) 1:9. doi: 10.1186/1744-8069-1-9
136. Beutler AS, Reinhardt M. AAV for pain: steps towards clinical translation. *Gene Ther.* (2009) 16:461. doi: 10.1038/gt.2009.23
137. Milligan ED, Soderquist RG, Malone SM, Mahoney JH, Hughes TS, Langer SJ, et al. Intrathecal polymer-based interleukin-10 gene delivery for neuropathic pain. *Neuron Glia Biol.* (2006) 2:293–308. doi: 10.1017/S1740925X07000488
138. Sloane E, Ledeboer A, Seibert W, Coats B, Van Strien M, Maier SF, et al. Anti-inflammatory cytokine gene therapy decreases sensory and motor dysfunction in experimental multiple sclerosis: MOG-EAE behavioral and anatomical symptom treatment with cytokine gene therapy. *Brain Behav Immun.* (2009) 23:92–100. doi: 10.1016/j.bbi.2008.09.004
139. Grace PM, Loram LC, Christianson JP, Strand KA, Flyer-Adams JG, Penzkover KR, et al. Behavioral assessment of neuropathic pain, fatigue, and anxiety in experimental autoimmune encephalomyelitis (EAE) and attenuation by interleukin-10 gene therapy. *Brain Behav Immun.* (2017) 59:49–54. doi: 10.1016/j.bbi.2016.05.012
140. Soderquist RG, Milligan ED, Harrison JA, Chavez RA, Johnson KW, Watkins LR, et al. PEGylation of interleukin-10 for the mitigation of enhanced pain states. *J Biomed Mater Res A.* (2010) 93:1169–79. doi: 10.1002/jbm.a.32611
141. Oliveira AV, Rosa Da Costa AM, Silva GA. Non-viral strategies for ocular gene delivery. *Mater Sci Eng C Mater Biol Appl.* (2017) 77:1275–89. doi: 10.1016/j.msec.2017.04.068
142. Hu X, Shi YN, Zhang P, Miao M, Zhang T, Jiang B. d-Mannose: properties, production, and applications: an overview. *Compr Rev Food Sci Food Saf.* (2016) 15:773–85. doi: 10.1111/1541-4337.12211
143. Porru D, Parmigiani A, Tinelli C, Barletta D, Choussos D, Franco CD, et al. Oral D-mannose in recurrent urinary tract infections in women: a pilot study. *J Clin Urol.* (2014) 7:208–13. doi: 10.1177/2051415813518332
144. Martinez-Pomares L. The mannose receptor. *J Leukoc Biol.* (2012) 92:1177–86. doi: 10.1189/jlb.0512231

145. Taylor PR, Gordon S, Martinez-Pomares L. The mannose receptor: linking homeostasis and immunity through sugar recognition. *Trends Immunol.* (2005) 26:104–10. doi: 10.1016/j.it.2004.12.001
146. Burudi EM, Riese S, Stahl PD, Regnier-Vigouroux A. Identification and functional characterization of the mannose receptor in astrocytes. *Glia.* (1999) 25:44–55. doi: 10.1002/(SICI)1098-1136(19990101)25:1<44::AID-GLIA5>3.0.CO;2-C
147. Burudi EM, Regnier-Vigouroux A. Regional and cellular expression of the mannose receptor in the post-natal developing mouse brain. *Cell Tissue Res.* (2001) 303:307–17. doi: 10.1007/s004410000311
148. Baetas-Da-Cruz W, Alves L, Pessolani MC, Barbosa HS, Regnier-Vigouroux A, Corte-Real S, et al. Schwann cells express the macrophage mannose receptor and MHC class II. Do they have a role in antigen presentation? *J Peripher Nerv Syst.* (2009) 14:84–92. doi: 10.1111/j.1529-8027.2009.00217.x
149. Gordon S. Alternative activation of macrophages. *Nat Rev Immunol.* (2003) 3:23–35. doi: 10.1038/nri978
150. Fernandez N, Alonso S, Valera I, Vigo AG, Renedo M, Barbolla L, et al. Mannose-containing molecular patterns are strong inducers of cyclooxygenase-2 expression and prostaglandin E2 production in human macrophages. *J Immunol.* (2005) 174:8154–62. doi: 10.4049/jimmunol.174.12.8154
151. Lopez-Herrera A, Liu Y, Rugeles MT, He JJ. HIV-1 interaction with human mannose receptor (hMR) induces production of matrix metalloproteinase 2 (MMP-2) through hMR-mediated intracellular signaling in astrocytes. *Biochim Biophys Acta.* (2005) 1741:55–64. doi: 10.1016/j.bbadis.2004.12.001
152. Tachado SD, Zhang J, Zhu J, Patel N, Cushion M, Koziel H. Pneumocystis-mediated IL-8 release by macrophages requires coexpression of mannose receptors and TLR2. *J Leukoc Biol.* (2007) 81:205–11. doi: 10.1189/jlb.1005580
153. Hussell T, Bell TJ. Alveolar macrophages: plasticity in a tissue-specific context. *Nat Rev Immunol.* (2014) 14:81–93. doi: 10.1038/nri3600
154. Chieppa M, Bianchi G, Doni A, Del Prete A, Sironi M, Laskarin G, et al. Cross-linking of the mannose receptor on monocyte-derived dendritic cells activates an anti-inflammatory immunosuppressive program. *J Immunol.* (2003) 171:4552–60. doi: 10.4049/jimmunol.171.9.4552
155. Üçeyler N, Valenza R, Stock M, Schedel R, Sprotte G, Sommer C. Reduced levels of antiinflammatory cytokines in patients with chronic widespread pain. *Arthritis Rheum.* (2006) 54:2656–64. doi: 10.1002/art.22026
156. Couper KN, Blount DG, Riley EM. IL-10: the master regulator of immunity to infection. *J Immunol.* (2008) 180:5771–7. doi: 10.4049/jimmunol.180.9.5771
157. Wilkerson JL, Milligan ED. The central role of glia in pathological pain and the potential of targeting the cannabinoid 2 receptor for pain relief. *ISRN Anesthesiol.* (2011) 2011:19. doi: 10.5402/2011/593894
158. Mechoulam R, Gaoni Y. A total synthesis of dl-Δ1-tetrahydrocannabinol, the active constituent of Hashish. *J Am Chem Soc.* (1965) 87:3273–5. doi: 10.1021/ja01092a065
159. Svizenska I, Dubovy P, Sulcova A. Cannabinoid receptors 1 and 2 (CB1 and CB2), their distribution, ligands and functional involvement in nervous system structures–a short review. *Pharmacol Biochem Behav.* (2008) 90:501–11. doi: 10.1016/j.pbb.2008.05.010
160. Guerrero-Alba R, Barragán-Iglesias P, González-Hernández A, Valdez-Moráles EE, Granados-Soto V, Condés-Lara M, et al. Some prospective alternatives for treating pain: the endocannabinoid system and its putative receptors GPR18 and GPR55. *Front Pharmacol.* (2019) 9:1496. doi: 10.3389/fphar.2018.01496
161. Galiègue S, Mary S, Marchand J, Dussossoy D, Carrière D, Carayon P, et al. Expression of central and peripheral cannabinoid receptors in human immune tissues and leukocyte subpopulations. *Eur J Biochem.* (1995) 232:54–61. doi: 10.1111/j.1432-1033.1995.tb20780.x
162. Walter L, Franklin A, Witting A, Wade C, Xie Y, Kunos G, et al. Nonpsychotropic cannabinoid receptors regulate microglial cell migration. *J Neurosci.* (2003) 23:1398–405. doi: 10.1523/JNEUROSCI.23-04-01398.2003
163. Stempel AV, Stumpf A, Zhang H-Y, Özdogan T, Pannasch U, Theis A-K, et al. Cannabinoid type 2 receptors mediate a cell type-specific plasticity in the hippocampus. *Neuron.* (2016) 90:795–809. doi: 10.1016/j.neuron.2016.03.034
164. Turcotte C, Blanchet M-R, Laviolette M, Flamand N. The CB(2) receptor and its role as a regulator of inflammation. *Cell Mol Life Sci.* (2016) 73:4449–70. doi: 10.1007/s00018-016-2300-4
165. Romero-Sandoval A, Eisenach JC. Spinal cannabinoid receptor type 2 activation reduces hypersensitivity and spinal cord glial activation after paw incision. *Anesthesiology.* (2007) 106:787–94. doi: 10.1097/01.anes.0000264765.33673.6c
166. Romero-Sandoval A, Nutile-Mcmenemy N, Deleo JA. Spinal microglial and perivascular cell cannabinoid receptor type 2 activation reduces behavioral hypersensitivity without tolerance after peripheral nerve injury. *Anesthesiology.* (2008) 108:722–34. doi: 10.1097/ALN.0b013e318167af74
167. Toth CC, Jedrzejewski NM, Ellis CL, Frey, WHII. Cannabinoid-mediated modulation of neuropathic pain and microglial accumulation in a model of murine type I diabetic peripheral neuropathic pain. *Mol Pain.* (2010) 6:16. doi: 10.1186/1744-8069-6-16
168. Rahn EJ, Makriyannis A, Hohmann AG. Activation of cannabinoid CB1 and CB2 receptors suppresses neuropathic nociception evoked by the chemotherapeutic agent vincristine in rats. *Br J Pharmacol.* (2007) 152:765–77. doi: 10.1038/sj.bjp.0707333
169. Rahn EJ, Zvonok AM, Thakur GA, Khanolkar AD, Makriyannis A, Hohmann AG. Selective activation of cannabinoid CB2 receptors suppresses neuropathic nociception induced by treatment with the chemotherapeutic agent paclitaxel in rats. *J Pharmacol Exp Ther.* (2008) 327:584–91. doi: 10.1124/jpet.108.141994
170. Deng L, Guindon J, Vemuri VK, Thakur GA, White FA, Makriyannis A, et al. The maintenance of cisplatin- and paclitaxel-induced mechanical and cold allodynia is suppressed by cannabinoid CB2 receptor activation and independent of CXCR4 signaling in models of chemotherapy-induced peripheral neuropathy. *Mol Pain.* (2012) 8:71. doi: 10.1186/1744-8069-8-71
171. Rahn EJ, Deng L, Thakur GA, Vemuri K, Zvonok AM, Lai YY, et al. Prophylactic cannabinoid administration blocks the development of paclitaxel-induced neuropathic nociception during analgesic treatment and following cessation of drug delivery. *Mol Pain.* (2014) 10:27–27. doi: 10.1186/1744-8069-10-27
172. Rahn EJ, Hohmann AG. Cannabinoids as pharmacotherapies for neuropathic pain: from the bench to the bedside. *Neurotherapeutics.* (2009) 6:713–37. doi: 10.1016/j.nurt.2009.08.002
173. Davis MP. Cannabinoids in pain management: CB1, CB2 and non-classic receptor ligands. *Expert Opin Investig Drugs.* (2014) 23:1123–40. doi: 10.1517/13543784.2014.918603
174. Donvito G, Nass SR, Wilkerson JL, Curry ZA, Schurman LD, Kinsey SG, et al. The endogenous cannabinoid system: a budding source of targets for treating inflammatory and neuropathic pain. *Neuropsychopharmacology.* (2018) 43:52–79. doi: 10.1038/npp.2017.204
175. Rahn EJ, Thakur GA, Wood JAT, Zvonok AM, Makriyannis A, Hohmann AG. Pharmacological characterization of AM1710, a putative cannabinoid CB2 agonist from the cannabilactone class: antinociception without central nervous system side-effects. *Pharmacol Biochem Behav.* (2011) 98:493–502. doi: 10.1016/j.pbb.2011.02.024
176. Gantz I, Muraoka A, Yang YK, Samuelson LC, Zimmerman EM, Cook H, et al. Cloning and chromosomal localization of a gene (GPR18) encoding a novel seven transmembrane receptor highly expressed in spleen and testis. *Genomics.* (1997) 42:462–6. doi: 10.1006/geno.1997.4752
177. Vassilatis DK, Hohmann JG, Zeng H, Li F, Ranchalis JE, Mortrud MT, et al. The G protein-coupled receptor repertoires of human and mouse. *Proc Natl Acad Sci USA.* (2003) 100:4903–8. doi: 10.1073/pnas.0230374100
178. Burstein SH, Mcquain CA, Ross AH, Salmonsen RA, Zurier RE. Resolution of inflammation by N-arachidonoylglycine. *J Cell Biochem.* (2011) 112:3227–33. doi: 10.1002/jcb.23245
179. Chiang N, Dalli J, Colas RA, Serhan CN. Identification of resolvin D2 receptor mediating resolution of infections and organ protection. *J Exp Med.* (2015) 212:1203–17. doi: 10.1084/jem.20150225
180. Staton PC, Hatcher JP, Walker DJ, Morrison AD, Shapland EM, Hughes JP, et al. The putative cannabinoid receptor GPR55 plays a role in mechanical hyperalgesia associated with inflammatory and neuropathic pain. *Pain.* (2008) 139:225–36. doi: 10.1016/j.pain.2008.04.006
181. Marichal-Cancino BA, Fajardo-Valdez A, Ruiz-Contreras AE, Mendez-Díaz M, Prospero-García O. Advances in the physiology of GPR55 in the central nervous system. *Curr Neuropharmacol.* (2017) 15:771–8. doi: 10.2174/1570159X14666160729155441
182. Akiyama H, Mcgeer PL. Brain microglia constitutively express beta-2 integrins. *J Neuroimmunol.* (1990) 30:81–93. doi: 10.1016/0165-5728(90)90055-R

183. Moneta ME, Gehrmann J, Topper R, Banati RB, Kreutzberg GW. Cell adhesion molecule expression in the regenerating rat facial nucleus. *J Neuroimmunol.* (1993) 45:203–6. doi: 10.1016/0165-5728(93)90181-W
184. Evans R, Patzak I, Svensson L, De Filippo K, Jones K, Mcdowall A, et al. Integrins in immunity. *J Cell Sci.* (2009) 122:215–25. doi: 10.1242/jcs.019117
185. Evans BJ, Mcdowall A, Taylor PC, Hogg N, Haskard DO, Landis RC. Shedding of lymphocyte function–associated antigen-1 (LFA-1) in a human inflammatory response. *Blood.* (2006) 107:3593–9. doi: 10.1182/blood-2005-09-3695
186. Emoto M, Emoto Y, Brinkmann V, Miyamoto M, Yoshizawa I, Stäber M, et al. Increased resistance of LFA-1-deficient mice to lipopolysaccharide-induced shock/liver injury in the presence of TNF-α and IL-12 is mediated by IL-10: a novel role for LFA-1 in the regulation of the proinflammatory and anti-inflammatory cytokine balance. *J Immunol.* (2003) 171:584–93. doi: 10.4049/jimmunol.171.2.584
187. Wang JG, Collinge M, Ramgolam V, Ayalon O, Fan XC, Pardi R, et al. LFA-1-Dependent HuR nuclear export and cytokine mRNA stabilization in T cell activation. *J Immunol.* (2006) 176:2105–13. doi: 10.4049/jimmunol.176.4.2105
188. Suzuki J-I, Yamasaki S, Wu J, Koretzky GA, Saito T. The actin cloud induced by LFA-1–mediated outside-in signals lowers the threshold for T-cell activation. *Blood.* (2007) 109:168–75. doi: 10.1182/blood-2005-12-020164
189. Wang Y, Kai H, Chang F, Shibata K, Tahara-Hanaoka S, Honda S-I, et al. A critical role of LFA-1 in the development of Th17 cells and induction of experimental autoimmune encephalomyelytis. *Biochem Biophys Res Commun.* (2007) 353:857–62. doi: 10.1016/j.bbrc.2006.12.104
190. Lam N, Ornatowski W, Alberti LB, Wilkerson JL, Moezzi D, Sun MS, et al. The role of leukocyte accumulation and diminished spinal IL-10 expression in chronic neuropathy. Program No. 166.12. In: *2013 Neuroscience Meeting Planner*. San Diego, CA: Society for Neuroscience (2013).
191. Verma NK, Kelleher D. Not just an adhesion molecule: LFA-1 contact tunes the T lymphocyte program. *J Immunol.* (2017) 199:1213–21. doi: 10.4049/jimmunol.1700495
192. Noor S, Sanchez JJ, Vanderwall AG, Sun MS, Maxwell JR, Davies S, et al. Prenatal alcohol exposure potentiates chronic neuropathic pain, spinal glial and immune cell activation and alters sciatic nerve and DRG cytokine levels. *Brain Behav Immun.* (2017) 61:80–95. doi: 10.1016/j.bbi.2016.12.016
193. Noor S, Sanchez JJ, Pervin Z, Sanchez JE, Sun MS, Epler L, et al. Neuropathic pain susceptibility in prenatal alcohol exposed (PAE) females is mediated by the proinflammatory actions of lymphocyte function-associated antigen (LFA)-1 on immune and glial cells. Program No. 666.18. In: *2018 Neuroscience Meeting Planner*. San Diego, CA: Society for Neuroscience (2018).
194. Sanchez JJ, Sanchez JE, Noor S, Ruffaner-Hanson CD, Davies S, Wagner CR, et al. Targeting the β2-integrin LFA-1, reduces adverse neuroimmune actions in neuropathic susceptibility caused by prenatal alcohol exposure. *Acta Neuropathol Commun.* (2019) 7:54. doi: 10.1186/s40478-019-0701-y
195. Doverty M, White JM, Somogyi AA, Bochner F, Ali R, Ling W. Hyperalgesic responses in methadone maintenance patients. *Pain.* (2001) 90:91–6. doi: 10.1016/S0304-3959(00)00391-2
196. Vanderah TW, Suenaga NMH, Ossipov MH, Malan TP, Lai J, Porreca F. Tonic descending facilitation from the rostral ventromedial medulla mediates opioid-induced abnormal pain and antinociceptive tolerance. *J Neurosci.* (2001) 21:279–86. doi: 10.1523/JNEUROSCI.21-01-00279.2001
197. Ossipov MH, Lai J, King T, Vanderah TW, Porreca F. Underlying mechanisms of pronociceptive consequences of prolonged morphine exposure. *Biopolymers.* (2005) 80:319–24. doi: 10.1002/bip.20254
198. Angst MS, Clark JD. Opioid-induced hyperalgesia: a qualitative systematic review. *Anesthesiology.* (2006) 104:570–87. doi: 10.1097/00000542-200603000-00025
199. Hay JL, White JM, Bochner F, Somogyi AA, Semple TJ, Rounsefell B. Hyperalgesia in opioid-managed chronic pain and opioid-dependent patients. *J Pain.* (2009) 10:316–22. doi: 10.1016/j.jpain.2008.10.003
200. Hay JL, Kaboutari J, White JM, Salem A, Irvine R. Model of methadone-induced hyperalgesia in rats and effect of memantine. *Eur J Pharmacol.* (2010) 626:229–33. doi: 10.1016/j.ejphar.2009.09.056
201. Roeckel L-A, Le Coz G-M, Gavériaux-Ruff C, Simonin F. Opioid-induced hyperalgesia: cellular and molecular mechanisms. *Neuroscience.* (2016) 338:160–82. doi: 10.1016/j.neuroscience.2016.06.029
202. Lacagnina MJ, Watkins LR, Grace PM. Toll-like receptors and their role in persistent pain. *Pharmacol Ther.* (2018) 184:145–58. doi: 10.1016/j.pharmthera.2017.10.006
203. Hutchinson MR, Zhang Y, Shridhar M, Evans JH, Buchanan MM, Zhao TX, et al. Evidence that opioids may have toll-like receptor 4 and MD-2 effects. *Brain Behav Immun.* (2010) 24:83–95. doi: 10.1016/j.bbi.2009.08.004
204. Lewis SS, Hutchinson MR, Rezvani N, Loram LC, Zhang Y, Maier SF, et al. Evidence that intrathecal morphine-3-glucuronide may cause pain enhancement via toll-like receptor 4/MD-2 and interleukin-1beta. *Neuroscience.* (2010) 165:569–83. doi: 10.1016/j.neuroscience.2009.10.011
205. Ferrini F, Trang T, Mattioli TAM, Laffray S, Del'guidice T, Lorenzo LE, et al. Morphine hyperalgesia gated through microglia-mediated disruption of neuronal Cl? homeostasis. *Nat Neurosci.* (2013) 16:183–92. doi: 10.1038/nn.3295
206. Grace PM, Ramos KM, Rodgers KM, Wang X, Hutchinson MR, Lewis MT, et al. Activation of adult rat CNS endothelial cells by opioid-induced toll-like receptor 4 (TLR4) signaling induces proinflammatory, biochemical, morphological, and behavioral sequelae. *Neuroscience.* (2014) 280:299–317. doi: 10.1016/j.neuroscience.2014.09.020
207. Johnson JL, Rolan PE, Johnson ME, Bobrovskaya L, Williams DB, Johnson K, et al. Codeine-induced hyperalgesia and allodynia: investigating the role of glial activation. *Transl Psychiatry.* (2014) 4:e482. doi: 10.1038/tp.2014.121
208. Grace PM, Strand KA, Galer EL, Urban DJ, Wang X, Baratta MV, et al. Morphine paradoxically prolongs neuropathic pain in rats by amplifying spinal NLRP3 inflammasome activation. *Proc Natl Acad Sci USA.* (2016) 113:E3441–50. doi: 10.1073/pnas.1602070113
209. Raghavendra V, Rutkowski MD, Deleo JA. The role of spinal neuroimmune activation in morphine tolerance/hyperalgesia in neuropathic and sham-operated rats. *J Neurosci.* (2002) 22:9980–9. doi: 10.1523/JNEUROSCI.22-22-09980.2002
210. Johnston IN, Milligan ED, Wieseler-Frank J, Frank MG, Zapata V, Campisi J, et al. A role for proinflammatory cytokines and fractalkine in analgesia, tolerance, and subsequent pain facilitation induced by chronic intrathecal morphine. *J Neurosci.* (2004) 24:7353–65. doi: 10.1523/JNEUROSCI.1850-04.2004
211. Hutchinson MR, Coats BD, Lewis SS, Zhang Y, Sprunger DB, Rezvani N, et al. Proinflammatory cytokines oppose opioid-induced acute and chronic analgesia. *Brain Behav Immun.* (2008) 22:1178–89. doi: 10.1016/j.bbi.2008.05.004
212. Tumati S, Largent-Milnes TM, Keresztes A, Ren J, Roeske WR, Vanderah TW, et al. Repeated morphine treatment-mediated hyperalgesia, allodynia and spinal glial activation are blocked by co-administration of a selective cannabinoid receptor type-2 agonist. *J Neuroimmunol.* (2012) 244:23–31. doi: 10.1016/j.jneuroim.2011.12.021
213. Hutchinson MR, Zhang Y, Brown K, Coats BD, Shridhar M, Sholar PW, et al. Non-stereoselective reversal of neuropathic pain by naloxone and naltrexone: involvement of toll-like receptor 4 (TLR4). *Eur J Neurosci.* (2008) 28:20–9. doi: 10.1111/j.1460-9568.2008.06321.x
214. Lewis SS, Loram LC, Hutchinson MR, Li C-M, Zhang Y, Maier SF, et al. (+)-Naloxone, an opioid-inactive toll-like receptor 4 signaling inhibitor, reverses multiple models of chronic neuropathic pain in rats. *J Pain.* (2012) 13:498–506. doi: 10.1016/j.jpain.2012.02.005
215. Eidson LN, Murphy AZ. Blockade of toll-like receptor 4 attenuates morphine tolerance and facilitates the pain relieving properties of morphine. *J Neurosci.* (2013) 33:15952–63. doi: 10.1523/JNEUROSCI.1609-13.2013

Conflict of Interest: The authors declare that the research was conducted in the absence of any commercial or financial relationships that could be construed as a potential conflict of interest.

frontiers in Immunology

ORIGINAL RESEARCH
published: 20 January 2020
doi: 10.3389/fimmu.2019.03120

Sensory Ganglia-Specific TNF Expression Is Associated With Persistent Nociception After Resolution of Inflammation

William Antonio Gonçalves[1], Barbara Maximino Rezende[2], Marcos Paulo Esteves de Oliveira[1], Lucas Secchim Ribeiro[3], Victor Fattori[4], Walison Nunes da Silva[5], Pedro Henrique Dias Moura Prazeres[5], Celso Martins Queiroz-Junior[1], Karina Talita de Oliveira Santana[6], Walyson Coelho Costa[1], Vinícius Amorim Beltrami[1], Vivian Vasconcelos Costa[1], Alexander Birbrair[5], Waldiceu A. Verri Jr.[4†], Fernando Lopes[7], Thiago Mattar Cunha[8], Mauro Martins Teixeira[9], Flávio Almeida Amaral[9‡] and Vanessa Pinho[1‡]*

[1] Departamento de Morfologia, Instituto de Ciências Biológicas (ICB), Universidade Federal de Minas Gerais (UFMG), Belo Horizonte, Brazil, [2] Departamento de Enfermagem Básica, Escola de Enfermagem da Universidade Federal de Minas Gerais (UFMG), Belo Horizonte, Brazil, [3] Biomediziniches Zentrum (BMZ), Institut für Angeborene Immunität, Rheinische Friedrich-Wilhelms-Universität Bonn, Venusberg, Germany, [4] Departamento de Patologia, Center of Biological Sciences, Londrina State University, Londrina, Brazil, [5] Departamento de Patologia, Instituto de Ciências Biológicas (ICB), Universidade Federal de Minas Gerais (UFMG), Belo Horizonte, Brazil, [6] Departamento de Genética, Ecologia e Evolução, Instituto de Ciências Biológicas (ICB), Universidade Federal de Minas Gerais (UFMG), Belo Horizonte, Brazil, [7] Institute of Parasitology and Department of Microbiology and Immunology, McGill University, Montreal, QC, Canada, [8] Departamento de Farmacologia, Faculdade de Medicina de Ribeirão Preto, Universidade de São Paulo (USP), Ribeirão Preto, Brazil, [9] Departamento de Bioquímica e Imunologia, Instituto de Ciências Biológicas (ICB), Universidade Federal de Minas Gerais (UFMG), Belo Horizonte, Brazil

OPEN ACCESS

Edited by:
Diana Boraschi, Istituto di Biochimica delle Proteine (IBP), Italy

Reviewed by:
Detlef Neumann, Hannover Medical School, Germany
Fons Van De Loo, Radboud University Medical Center, Netherlands

***Correspondence:**
Vanessa Pinho
vpinho@icb.ufmg.br

†ORCID:
Waldiceu A. Verri Jr.
orcid.org/0000-0003-2756-9283

‡These authors have contributed equally to this work

Specialty section:
This article was submitted to Cytokines and Soluble Mediators in Immunity, a section of the journal Frontiers in Immunology

Received: *11 October 2019*
Accepted: *20 December 2019*
Published: *20 January 2020*

Citation:
Gonçalves WA, Rezende BM, Oliveira MPE, Ribeiro LS, Fattori V, Silva WN, Prazeres PHDM, Queiroz-Junior CM, Santana KTO, Costa WC, Beltrami VA, Costa VV, Birbrair A, Verri WA Jr, Lopes F, Cunha TM, Teixeira MM, Amaral FA and Pinho V (2020) Sensory Ganglia-Specific TNF Expression Is Associated With Persistent Nociception After Resolution of Inflammation. Front. Immunol. 10:3120. doi: 10.3389/fimmu.2019.03120

Joint pain is a distressing symptom of arthritis, and it is frequently persistent even after treatments which reduce local inflammation. Continuous production of algogenic factors activate/sensitize nociceptors in the joint structures and contribute to persistent pain, a challenging and difficult condition to treat. TNF is a crucial cytokine for the pathogenesis of several rheumatic diseases, and its inhibition is a mainstay of treatment to control joint symptoms, including pain. Here, we sought to investigate the inflammatory changes and the role of TNF in dorsal root ganglia (DRG) during persistent hypernociception after the resolution of acute joint inflammation. Using a model of antigen-induced arthritis, the peak of joint inflammation occurred 12–24 h after local antigen injection and was characterized by an intense influx of neutrophils, pro-inflammatory cytokine production, and joint damage. We found that inflammatory parameters in the joint returned to basal levels between 6 and 8 days after antigen-challenge, characterizing the resolving phase of joint inflammation. Mechanical hyperalgesia was persistent up to 14 days after joint insult. The persistent nociception was associated with the inflammatory status of DRG after cessation of acute joint inflammation. The late state of neuroinflammation in the ipsilateral side was evidenced by gene expression of TNF, TNFR2, IL-6, IL-1β, CXCL2, COX2, and iNOS in lumbar DRG (L3-L5) and leukocyte adhesion in the lumbar intumescent vessels between days 6 and 8. Moreover, there were signs of resident macrophage activation in DRG, as evidenced by an increase in Iba1-positive cells. Intrathecal or

systemic injection of etanercept, an agent clinically utilized for TNF neutralization, at day 7 post arthritis induction, alleviated the persistent joint hyperalgesia by specific action in DRG. Our data suggest that neuroinflammation in DRG after the resolution of acute joint inflammation drives continuous neural sensitization resulting in persistent joint nociception in a TNF-dependent mechanism.

Keywords: resolution of inflammation, arthritis, pain, TNF, neuroinflammation, dorsal root ganglia

INTRODUCTION

The inflammatory process, a protective response against various infectious and sterile noxious stimuli, is responsible for the elimination of the stressor agent resulting in a return to tissue homeostasis (1, 2). However, continuous inflammation is associated with persistent harmful stimuli or failed inflammatory resolution (3–5). The resolution of inflammation is a well-controlled process resulting in a reduction of leukocyte accumulation and an increase in neutrophil apoptosis, macrophages reprogramming, and functional recovery of tissue. In joint inflammation, pain is an important cardinal signal associated with loss of function. Previous studies have demonstrated that articular hyperalgesia may persist after resolution of inflammation in a model of antigen induced-arthritis (6, 7). The mechanism which coordinates this persistent articular pain following inflammatory cessation is unknown.

Joint pain is initiated by the activation of specialized neuronal fibers called nociceptors, these include afferent C and Aδ fibers (8–11). These peripheral sensory nerve terminals in the joints detect a plethora of algogenic molecules during inflammation, including several immune mediators, such as cytokines released by activated resident and migrated cells, in different contexts of arthritis (12–14). In this context, the elicited response to nociceptive stimuli is exacerbated (15) resulting in an increased intensity and frequency of transduced action potentials from the affected joint neurons to the central nervous system, which modulate the pain pathways (16). Patients affected by arthritis can experience persistent pain in the joint without any obvious signs of inflammatory activity (17–20). The response in the central nervous system is one of the most studied mechanisms underlying this phenomenon, and both spinal cord neuroinflammation and microglial cell activation drive hyperresponsivity of nociceptive pathways (16, 21–23).

TNF is a crucial cytokine for the development of articular pain during arthritis (12, 24). The neutralization of TNF by anti-TNF drugs is an important pharmacological strategy for decreasing disease activity and joint pain (25, 26). Experimentally, the neutralization of spinal TNF by intrathecal treatment with infliximab, an anti-TNF monoclonal antibody, decreased joint nociception in a mouse model of antigen-induced arthritis (AIA) (27). Moreover, the intraarticular injection of etanercept, a fusion protein based on the TNF receptor type 2 (TNFR2), reduces the responsivity of articular nociceptors to mechanical stimulation. This suggests that TNF acts in peripheral neuronal terminals during inflammatory phases in AIA (28, 29). However, despite central and peripheral mechanisms producing articular pain, the role of TNF in driving persistent joint pain in the dorsal root ganglia (DRG) after resolution of joint inflammation is still poorly understood.

The hyperalgesia observed during active joint inflammation is associated with the actions of TNF in the peripheral sites (6) and hyperexpression of its receptors, TNFR1 and TNFR2, in the DRG (30, 31). Furthermore, nociceptive responses decrease following TNF neutralization by systemic injection of anti-TNF drug (6) or etanercept (30, 31). However, the specific site where this cytokine was neutralized, leading to pain relief has, until now, remained unknown. In addition, the role of TNF in maintaining pain during the late stages of an inflammatory response when the productive phase of cell recruitment and cytokine production have subsided remains unknown. Therefore, in this work we aimed to investigate the role of TNF expressed in the DRG in driving persistent joint nociception even during the resolving phase of joint inflammation in an experimental model of arthritis in mice.

METHODS

Animals

Seven to twelve-week-old male age-matched C57Bl/6 mice (20 to 25 g) were used in animal experiments. These animals were housed in ventilated micro isolator cages in a temperature-controlled room (22 to 25°C), under a 12 h light/dark cycle with *ad libitum* access to water and food. All procedures were approved by the animal ethics committee of the Federal University of Minas Gerais (51/2018).

Antigen-Induced Arthritis

The immunization procedure was performed as previously described (7, 32). Anesthetised (100 μl of a mixture of 100 mg/kg of ketamine and 15 mg/kg of xylazine, intraperitoneally) mice were sensitized by intradermal (i.d.) injection of 500 μg of methylated bovine serum albumin (mBSA) dissolved in an emulsion containing 50 μl of phosphate buffer solution (PBS) and 50 μl of complete Freund's adjuvant (CFA; 1 mg/mL of *Mycobacterium tuberculosis*). For AIA induction, 14 days after emulsion injection, the right knees of mice were challenged with an intra-articular injection solution containing 10 μg of mBSA dissolved in 10 μl of sterile PBS.

Analysis of Cell Accumulation in the Joint

Groups of mice were culled with an overdose of anesthesia (100 μl of a mixture of 180 mg/kg of ketamine and 24 mg/kg of xylazine, intraperitoneally) and the knee joint cavity was

surgically exposed and washed with 10 μL of PBS contained 3% (w/v) of bovine serum albumin. The total number of leukocytes were determined using a Neubauer chamber and Turk's solution. Neutrophil and mononuclear cell counts were performed using Cytospin (Shandon III) preparations by evaluating the percentage of each leukocyte type on a slide stained with Panoptic solutions (Laborclin, PR, Brazil) and subsequently differentiated by light microscopy for quantification.

Histology

Tibiofemoral joint samples were collected for histopathological evaluation. The samples were fixed in 10% (v/v) buffered formalin (pH 7.4), decalcified in 14% EDTA (w/v) for 4 weeks, embedded in paraffin, sectioned, placed in slides, and stained with H&E. The H&E sections were examined and scored by a pathologist in a blinded manner for the following parameters: inflammatory infiltrate intensity, severity of synovial membrane hyperplasia, presence of inflammatory cells in the synovial space, and bone resorption. The grades were summed to obtain a histologic score (ranging from 0 to 12) as previously described (33).

Intravital Microscopy

After AIA induction, synovial (34) or spinal cord venules were exposed for the quantification of rolling and adhesion leukocytes by intravital microscopy. For knee joint analysis, the quadriceps tendon was carefully sectioned and rebounded to the opening target area presenting venules underlying the synovial tissue. For the spinal cord analysis, we used a laminectomy of vertebrates that involved lumbar intumescence exposing dorsal microvasculature of the dorsal horn of the spinal cord. Following the surgery, the knee was slightly flexed, or mice were correctly positioned allowing examination of articular or spinal microcirculation, respectively, using a 20-fold objective from intravital microscope (ECLIPSE 50i; Nikon). A digital camera (DS-Qi1MC; Nikon) was used to capture images. Registration of experiment were performed using Nikon imaging software. Rolling leukocytes were defined as cells that moved at a velocity less than that of the erythrocytes within a given vessel. The rolling cell flux was measured in venules with 20–40 μm, determined as the number of rolling cells that passed by a given point per minute. Leukocytes were considered to be adherent if they remained stationary for ≥30 s, and total leukocyte adhesion was quantified as the number of adherent cells in the intravascular space within an area of 100 μm.

Hyperalgesia Articular Evaluation

For environmental adaptation, mice were placed in acrylic cages (12 x 10 x 17 cm in height) with a wire-grid floor, in a noised controlled room, for 60 min. After this time, exploratory behavior manifestation was abrogated, and all mice remained quiet allowing for nociceptive response evaluation. To identify the withdrawal threshold, we used an electronic von Frey algesimeter (INSIGHT Instruments, Ribeirão Preto, SP, Brazil). Using a hand-held force transducer, fitted with a polypropylene tip (4.15 mm), the observer applied a vertical and constant force in central plantar surface of mice paw. This procedure was intended to produce an articular mechanical stimulus for knee flexion. The sufficient force in grams (g) to trigger a paw withdrawal movement, the characteristic aversive behavior to avoid the incident stress, was recorded by an electronic component of the apparatus. The withdrawal threshold was calculated by replicating the procedure in triplicate for each mouse (and averages were expressed in absolute values). Basal response was measured 24 h before saline or mBSA injections. After AIA induction, the nociceptive response was measured within 24 h, and subsequent time points with 48 h of interval.

Intrathecal Injection

Intrathecal injection was performed in intervertebral space between the fifth and sixth lumbar vertebrates (L5/L6). A volume of 5 μL was injected with a 30G needle in anesthetised animals. The injection was considered correct when mice presented a tail reflex after needle insertion (35).

Gene Expression by qRT-PCR

DRG and spinal cords were collected for mRNA expression analyses. Briefly, mice were anesthetised and culled at different time points after AIA induction or PBS challenge. Subsequently, vertebrae laminectomy was performed to allow removal of the lumbar DRG (L3-L5) and its respective spinal cord segments. These segments were separated in ipsi- and contralateral portions, or only the dorsal horn section of the ipsilateral portion. We used Trizol reagent (Invitrogen Life Technologies Corporation- Carlsbad, CA, USA) for total RNA extraction from collected tissues according to the manufacturer's instructions. Total RNA purity was determined using a Nanodrop 1000 spectrophotometer (Thermo Scientific- Waltham, MA, USA). The wavelength absorption rate (260/230 nm and 280 /260 nm) between 1.8 and 2.0, respectively, was presented for all samples. A mix containing the reserve transcriptase, SuperScript III, ribonuclease recombinant inhibitor (RNAse Out; Invitrogen Life Technologies Corporation- Carlsbad, CA, USA) and dithiothreitol (DTT; 1 mM) were used for reverse transcription of total RNA into cDNA. For quantitative PCR the Power SYBR Master Mix reagent (Invitrogen Life Technologies Corporation- Carlsbad, CA, USA) and initiators pars (Integrated DNA Technologies- Coralville, IA, EUA) plus cDNA were placed into a 96-well plate in duplicate. Next, a 7500 Fast Real-Time PCR System (Applied Biosystems, Waltham, MA, EUA) was used for performing the programmed reaction: initial heating at 95 °C for 10 min, following by 40 cycles at 95°C for 60 seconds and 60°C for 1 min. The 2-ΔΔCT method (36) was used to calculate the cycle threshold (CT), and the fold change was normalized to glyceraldehyde 3-phosphate dehydrogenase (GAPDH) levels and expressed as fold change compared to the PBS-treated controls.

Western Blot

Lumbar DRG were homogenized in a lysate solution buffer (1% Triton X-100, 100 mM Tris/ HCl, pH 8.0, 10% (v/v) glycerol, 5 mM EDTA, 200 mM NaCl, 1 mM DTT, 1 mM PMSF, 2.5 μg/mL leupeptin, 5 μg/mL aprotinin, 1 mM sodium orthovanadate). Each poll of ganglia contained L4 from three different animals. The lysate protein concentration was quantified with a Bradford

assay (Bio-Rad, Hercules, CA, USA). Sodium dodecyl sulfate polyacrylamide gel electrophoresis (SDS-PAGE) was carried with 30 μg of proteins per sample. After separation by SDS-PAGE, proteins were transferred onto a nitrocellulose membrane (Hybond ECL, GE Healthcare). The membrane was then incubated with a goat monoclonal primary antibody against TNF (1:1000, Cat: sc1348, Santa Cruz Biotechnology, Inc) and GAPDH (HRP conjugate; 1:1000, Cat: #3686, Cell Signaling, Inc) over night at 4°C. After incubation with the anti-TNF primary antibody, the membrane was washed 3 times for 5 min each wash with PBS 0.1% Tween-20 before being incubated with a rabbit anti-goat IgG-HRP secondary antibody (1:3000, Cat: sc2768, Santa Cruz Biotechnology, Inc) for 3 h at room temperature. Immunoreactive bands were visualized on photosensitive film after exposure to enhanced chemiluminescence (ECL) solution.

ELISA

The protein concentration of cytokines from articular tissue, namely the infrapatellar fat pad, meniscus, synovial membrane, joint capsule, patella, patellar tendon, and synovia, was measured at different time points after AIA induction. The collected tissues were mixed in a homogenizer (Quiagen, Biotecnologia Brasil Ltda, São Paulo, SP, Brazil) for 5 min with a solution that contained antiproteases (0.1 mM PMSF), 0.1 nM benzethonium chloride, 10 mM EDTA, 20 Kallikrein inhibitor units, aprotinin A, and 0.05% (v/v) Tween-20. The samples were centrifuged for 10 min at 10,000 rpm at 4°C. The supernatants were analyzed by enzyme-linked immunosorbent assay (ELISA). The concentrations of analyzed cytokines were measured according to the manufacturer's instructions (R&D systems). Colorimetric reactions were analyzed with a spectrophotometer at 492 nm.

Immunofluorescence

L4 DRGs were dissected, post-fixed, and incubated overnight with 30% (w/v) sucrose. DRGs were embedded in optimum cutting temperature, and 20 μm sections were cut in a cryostat and processed for immunofluorescence. The primary antibodies used in this study were: anti-cfos (1:500, cat #MA1-21190, Thermo Fisher Scientific, Waltham, MA, USA) and anti-Iba 1 (1:100, cat #PA5-21274, Thermo Fisher Scientific, Waltham, MA, USA). Secondary antibodies were: Alexa Fluor 647 (1:500, cat #A32733, Thermo Fisher Scientific, Waltham, MA, USA), Alexa Fluor 488 (1:1000, cat #A11001, Thermo Fisher Scientific, Waltham, MA, USA. DAPI (1:1000, Thermo Fisher Scientific, Waltham, MA, USA) was used as a nucleus marker. The coverslips were fixed on slides with Fluormount (00-4958-02, Thermo Fisher Scientific, Waltham, MA, USA). Imaging was performed using a confocal microscope (Leica TCS SP8, Leica Microsystems, Mannheim, Germany). The fluorescence intensity was quantified using LAS X Software (Leica Microsystems, Mannheim, Germany) and macrophages present in DRG were quantified by counting the total iba1 positive marked cells in the histological sections.

Statistical Analysis

Graph-Pad Prism version 6 was used for statistical analysis. Data are expressed as the means ± SEM. Comparisons among the groups were performed by unpaired Student's t test or ANOVA, followed by Dunnett *post-hoc* analysis. Two-way ANOVA was adopted to compare the nociceptive response among the groups and/or doses at different times in the curve. The *post-hoc* tests were determined in accordance with recommendation of utilized statistical software. Statistical significance was set as $p < 0.05$.

RESULTS

Temporal Characterization of Resolution of Acute Joint Inflammation in the AIA Model

The AIA model is characterized by a rapid and massive accumulation of leukocytes, mostly neutrophils, into the challenged joint (6, 7). The time course and intensity of the inflammatory response in this model is shown in **Figure 1**. We found that there was a peak of neutrophil accumulation in the articular cavity at 12 h and 1 day after AIA induction. Moreover, mononuclear cells peaked 2 days after intraarticular challenge (**Figure 1A**). The intravital analysis of the joint microvasculature showed an increase in rolling cells from 12 h after joint insult that was still elevated after up to 2 days (**Figure 1B**). The increase in adherent cells started from 6 h after AIA induction (**Figure 1C**). Importantly, 4 days after AIA induction, the number of rolling and adherent cells returned to basal levels.

Leukocyte depuration and pro-inflammatory cytokine clearance are important steps for the efficient resolution of acute joint inflammation and return to tissue homeostasis (37, 38). Here, neutrophils were gradually removed from inflamed cavity between 2 and 6 days after arthritis induction. Mononuclear cells depuration started at a later time point. However, both cells types had been eliminated from the joint at day 8 after AIA induction (**Figure 1A**), characterizing an effective resolution of acute joint inflammation. The levels of TNF in the articular tissue increased 12 to 48 h after AIA induction, but returned to the control levels within 4 to 8 days (**Figure 1D**). In addition, levels of IL-1β and IL-6 were increased at 12 h and 1 day after AIA induction and returned to basal levels on day 2 (**Figures 1E,D**).

The histopathological analysis corroborated previous findings, indicating an intense leukocyte infiltrate, predominantly of neutrophils, both in the synovial tissue and cavity at 1 day and 2 days post-challenge (**Figures 2A,B**). Focal hyperplasia of the synovial membrane and scarce lacunae of bone resorption were also detected. Altogether, this set of results evidences a regression of tissue inflammation in this acute model of arthritis, indicating a complete resolution of acute joint inflammation 8 days after arthritis induction.

Prolonged Joint Nociception During the Resolving Phase of Arthritis Is Associated With an Inflammatory State in DRG

Mechanical joint nociception reached its peak at 2 days after joint challenge. However, although there was complete resolution of acute joint inflammation at day 8 post arthritis induction, mechanical joint nociception was persistent until day 14, returning to basal levels at day 16 (**Figure 3A**). In parallel, we confirmed the activation of the sensorial system in DRG

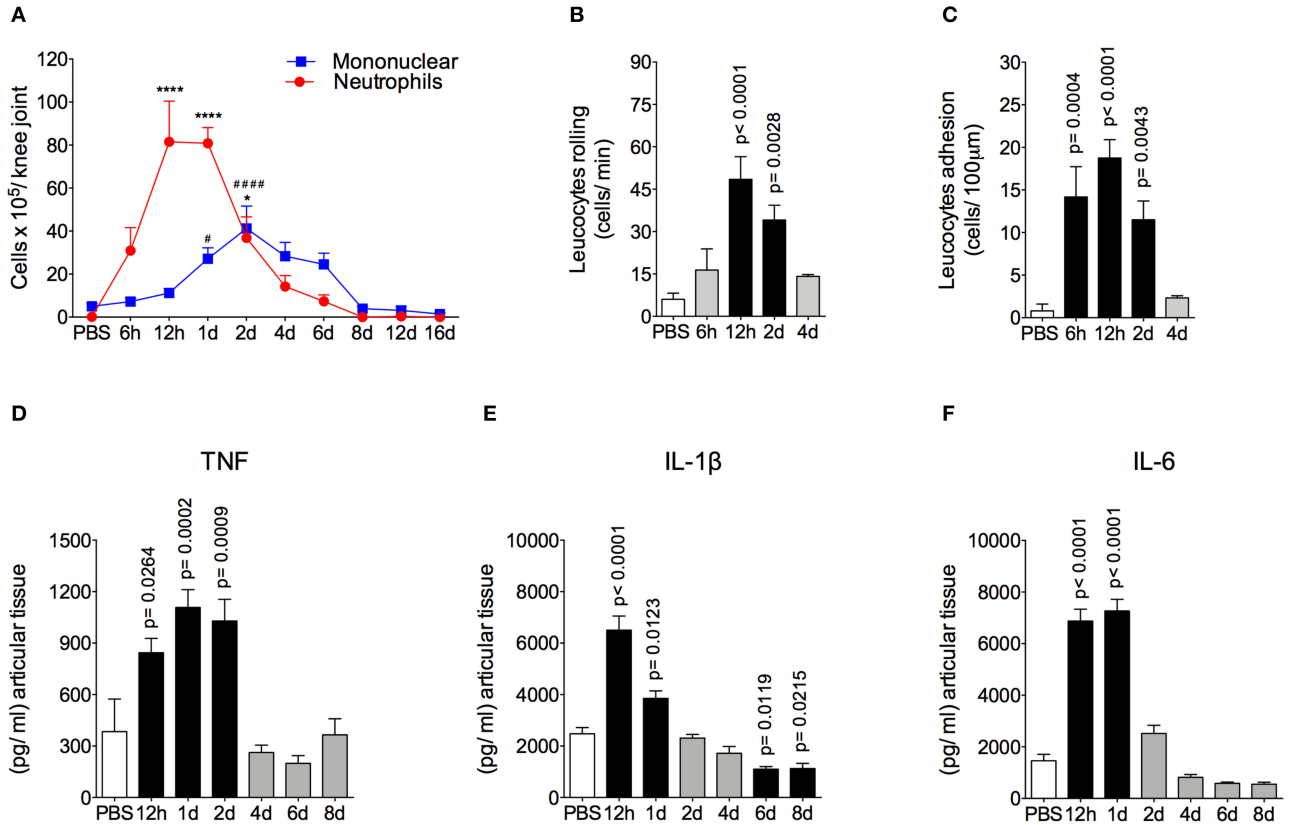

FIGURE 1 | Time course of inflammatory response in AIA model. **(A)** Number of neutrophils and mononuclear cells in the knee joint cavity at different time points after injection of 10 µg of mBSA (10 µg/10 µl of PBS), as well as 12 h after injection of 10 µl of sterile phosphate buffered saline (PBS) into the knee joints of immunized mice ($n = 4$–6). **(B)** Rolling and **(C)** adhesion of leukocytes in knee joint microvasculature ($n = 5$). Concentration of **(D)** TNF, **(E)** IL-1β and **(F)** IL-6 in the joint tissue homogenate were evaluated by ELISA ($n = 5$). The results are represented as mean ± SEM; $^{*}p < 0.05$, ****(to neutrophils), and #### (to mononuclear cells) $p <$ 0.0001 (A) or $p =$ specified value in the graph **(B–F)** compared to control group (PBS) using one-way ANOVA following by Dunnett *post-hoc* analysis.

by evaluating c-Fos expression after the inflammatory phase of AIA (**Figures 3B,C**). These findings suggest that sensory neuron excitability might be altered even after the resolution of acute joint inflammation. Several pain conditions can induce neuroinflammation in the sensory ganglion (21). DRG are the anatomical site where the cellular bodies of C and Aδ thin fibers, which sense nociceptive stimulus, are found. We observed an increase in Iba1^{+} cells (resident macrophage marker) in the DRG at 6 and 8 days (**Figures 4A,B**). This macrophage activation was accompanied by increased IL-1β gene expression at 8 days after AIA induction (**Figure 4C**). Moreover, expression of IL-6, CXCL1, COX2, and iNOS genes in the lumbar DRG (L3-L5) were also upregulated 6 and 8 days post joint challenge (**Figures 4D–G**). We also detected an increase in IL-10 gene expression at the same time points (**Figure 4H**). These results demonstrate that resolution of acute joint inflammation is restricted to the peripheral site in the first days after AIA induction and is followed by a transient inflammatory state in the sensory ganglia at later time points.

In summary, after resolution of acute inflammation in the challenged joint of immunized mice, there is an inflammatory environment in the DRG. This persistent local inflammatory state may be providing the nociceptive trigger factors that potentially sensitize neurons that maintain increased joint hyperalgesia following natural remission of AIA.

Prolonged Joint Nociception Is Dependent on TNF in the Sensory Ganglia

TNF, a pro-nociceptive cytokine, is directly involved in various pain disorders, including joint pain in different forms of arthritis, due to central and peripheral actions (6, 27). However, without conditional peripheral inflammation, TNF has not been shown to elicit persistent pain in arthritis. Following the resolution of acute inflammation in the joint, there was an increase in TNF and TNFR2 gene expression 6 and 8 days after AIA induction in lumbar DRG (L3-5; **Figures 5A,B,D**). Moreover, increased TNF protein expression was detected in L4 DRG at day 8 (**Figures 5E,F**). However, this was not seen in the L3 or L5 DRG (data not shown). Additionally, there was no increase in TNFR1 gene expression (**Figure 5C**).

In order to demonstrate the active contribution of TNF expression in DRG for joint mechanical nociception, we neutralized TNF by intrathecal injection of etanercept at day 7 after AIA induction. This treatment permanently reversed

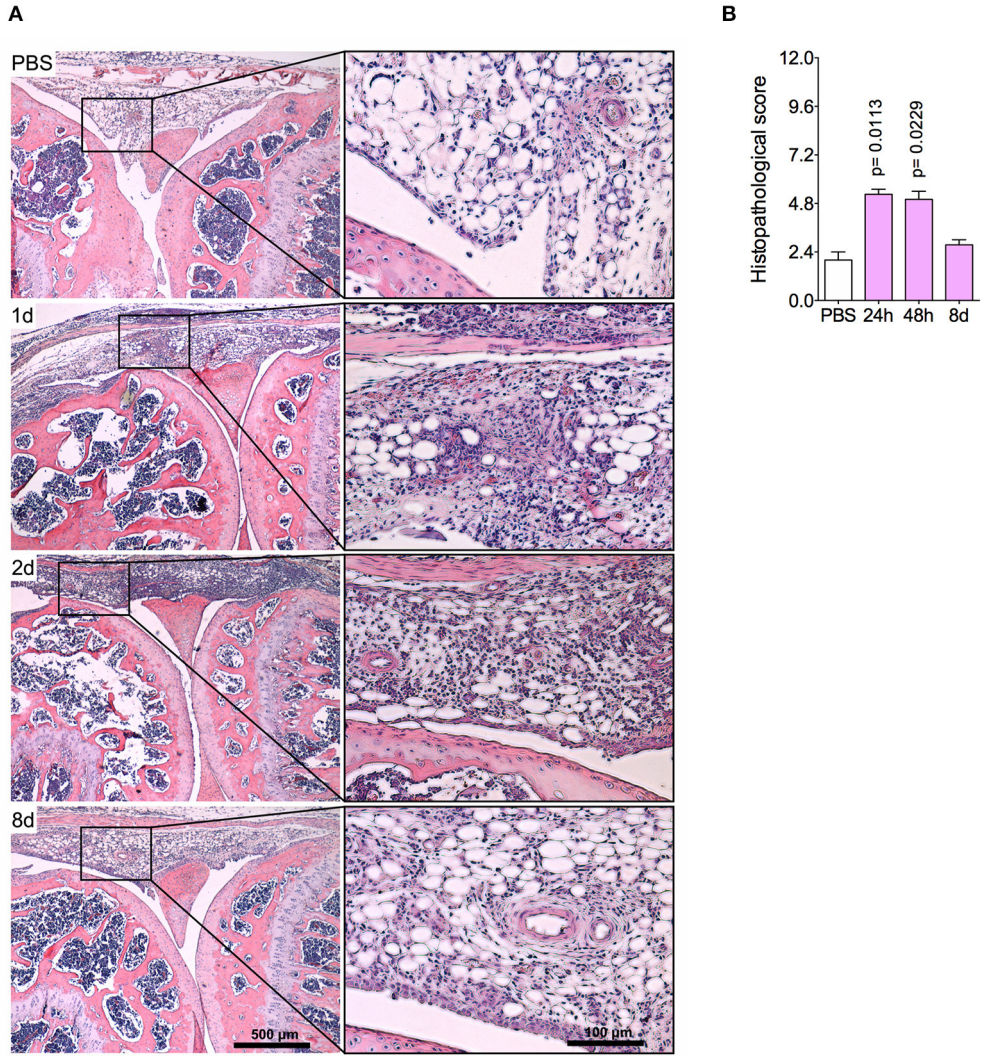

FIGURE 2 | Histopathological analyses of the knee joint in AIA model. Immunized mice received either i.a. injection of mBSA (10 µg/10 µl of PBS) to AIA induction or PBS (10 µl) in control group. **(A)** Representative histological slide to H&E of challenged knee joint. **(B)** Histopathological score quantification of **(A)**. Knee joint samples from the control group were extracted 24 h after i.a. injection ($n = 4–5$). The results are represented as mean ± SEM; p = specified value in the graph compared to control group (PBS) using one-way ANOVA following by Dunnett *post-hoc* analysis.

the nociceptive response of AIA mice (**Figure 6**). Intrathecal injection allows injected substance to spread through the subarachnoid space to reach the DRG body-rich area (39, 40). However, this route also permits injected substances to access the spinal cord structures (e.g., the dorsal horn) (40). To eliminate the hypothesis that the anti-nociceptive effect of etanercept was due to its action in the surficial laminae of the dorsal horn of the spinal cord, we investigated TNF expression at this site. No changes were observed in TNF gene expression on the ipsilateral spinal cord (**Figures 7A,B**) or dorsal horn (**Figures 7C,D**) during the time points evaluated in this model. Additionally, neither TNFR1 nor TNFR2 gene expression were increased in the dorsal horn of the spinal cord (**Figures 7E,F**, respectively). In addition, there were no changes in IBA-1 and GFAP gene expression (**Figures 8B,C**), indicating normal activity of microglia and astrocytes within the dorsal horn of the spinal cord (**Figure 8A**). Although there were no changes in these two activating glial cells markers, there was slight vascular activation in the spinal cord. We observed an increase in leukocyte adhesion in the posterior region of lumbar intumescence by intravital microscopy (**Figures 8D,E**). The analyzed vessels are located near the dorsal roots of the sensitive ganglia that penetrate the dorsal horn of the spinal cord.

Therefore, we have demonstrated that TNF affects neutralization after intrathecal etanercept administration, specifically in the DRG but not in the nociceptive spinal cord regions. In a separate experiment, etanercept was given systemically 7 days after AIA induction. Similar to the intrathecal treatment, systemic neutralization of TNF also reversed joint nociception (**Figure 9A**). DRG have an extensive and fenestrated

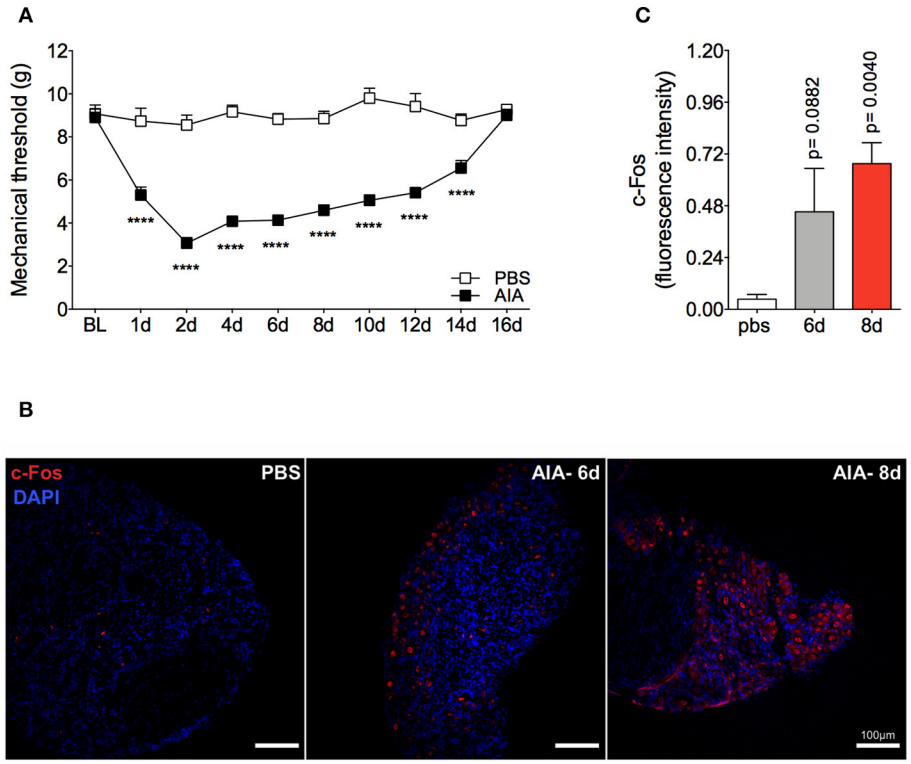

FIGURE 3 | Persistent articular nociception in AIA model. Immunized mice received either i.a. injection of mBSA (10 µg/10 µl of PBS) to AIA induction or PBS (10 µl) in the control group. **(A)** Time course of nociceptive responses was recorded by electronic von Frey algesimeter. BL (baseline) ($n = 6$). **(B)** Confocal microscopy slides show c-Fos positive neurons within DRG (L4) 8 days after AIA induction and **(C)** its quantification. DRG samples from the control group were extracted 8 days after i.a. injection ($n = 5$–6). The results are represented as mean ± SEM; $^{****}p < 0.0001$ **(A)** or $p =$ specified value in the graph **(C)** compared to control group (PBS) using two-way ANOVA following by Sidak *post-hoc* analysis **(A)** or by Dunnett *post-hoc* analysis **(C)**.

vasculature (41). To determine whether systemic anti-TNF treatment could reach the DRG structure, we evaluated vascular permeability in the DRG. Intravenous injection of Evans blue penetrated DRG, confirming its vascular permeability to high molecular weight molecules (**Figure 9B**). These results indicate a consistent possibility for systemic treatment with TNF inhibitors for pain relief even in the remission phase of joint inflammation due to the blockade of persistent TNF expression in the DRG.

DISCUSSION

Joint pain is a common and debilitating symptom in arthritic patients and different molecules produced in inflammatory environment directly activate peripheral sensory innervation, reducing the threshold for the nociceptor signal transduction. Using an acute model of arthritis in mice, we demonstrated here that joint nociception is detected for several days after complete resolution of acute joint inflammation and that acute neutrophilic inflammation in an AIA model was spontaneously resolved. In line with previous studies, the decreased number of neutrophils in our model is directly correlated to the resolving phase of joint inflammation and tissue repair (7). Here, there was also a decrease of cytokine production and improvement of tissue injury. These results highlighted that AIA presents an orchestrated series of events that eventually lead to self-limited resolution of inflammation (38). However, our results showed that nociception was persistent for several days after neutrophilic resolution in the challenged knee. Of note, this sensorial response was not triggered by peripheral action of sensitizing cytokines, TNF, IL-1β and IL-6, which are important mediators of the hyperalgesia evoked by AIA (6, 42–44). This persistent articular nociception was associated with continuous activation of non-neuronal cells and inflammatory status in the DRG, with crucial participation of TNF. The blockade of TNF with etanercept delivered by intrathecal or systemic routes was able to reverse the persistent nociception evoked by TNF in the DRG. It has been demonstrated that T cells may be involved in the transition from acute to chronic pain after inflammatory stimulus, indicating a role in pain maintenance of several inflammatory diseases (45). However, in our model, the number of mononuclear cells, which includes monocytes and lymphocytes, present after AIA did not differ from the basal level of cells from cavities injected with PBS. Thus, lymphocytes do not appear to be involved in pain maintenance in our model. Together, our findings suggest that delayed and continuous TNF production in the sensorial ganglia may drive persistent joint pain after the resolution of acute inflammation associated with arthritis.

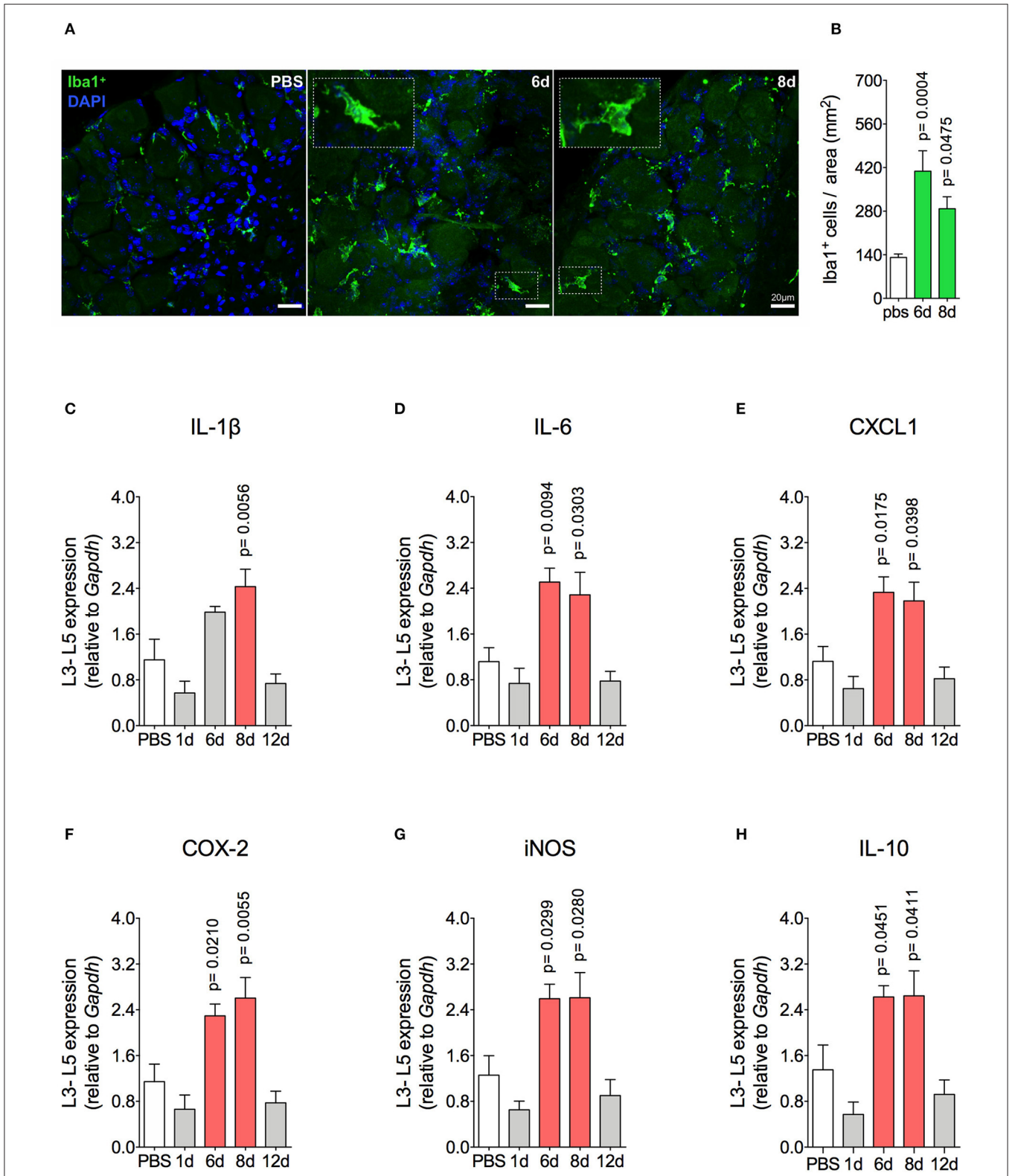

FIGURE 4 | Resident macrophage activation and inflammatory molecules gene expression characterizes inflammatory status of DRG after resolution of inflammation in AIA model. Immunized mice received either i.a. injection of mBSA (10 μg/10 μl of PBS) to AIA induction or PBS (10 μl) in control group. **(A)** Confocal microscopy slides show marked Iba1$^+$ cells within DRG (L4) 8 days after AIA induction and **(B)** its quantification ($n = 5$). Time course of gene expression of **(C)** IL-1β, **(D)** IL-6, **(E)** CXCL1, **(F)** COX-2, **(G)** iNOS, and **(H)** IL-10 within lumbar DRG (L3–L5). DRG samples from the control group were extracted 8 days after i.a. injection ($n = 5$). The results are represented as mean ± SEM; p = specified value in the graph compared to control group (PBS) using ANOVA following by Dunnett *post-hoc* analysis.

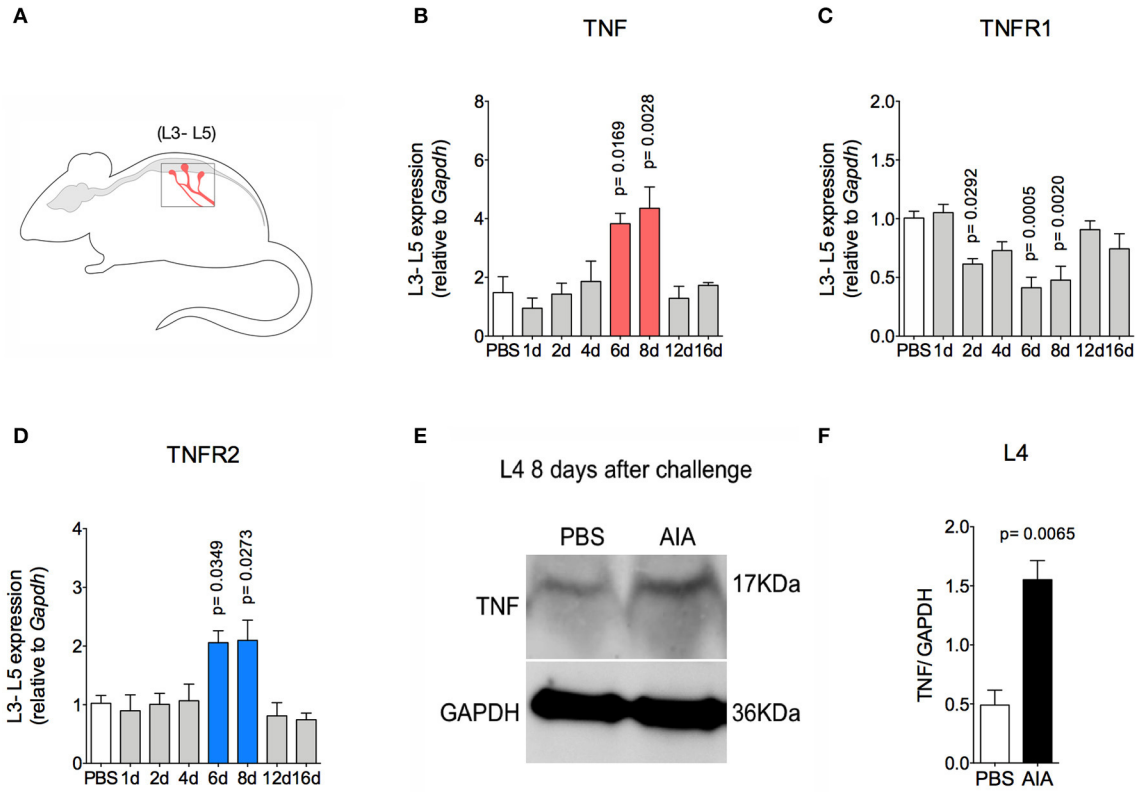

FIGURE 5 | TNF expression within DRG after resolution of inflammation in AIA model. Immunized mice received either i.a. injection of mBSA (10 μg/10 μl of PBS) to AIA induction or PBS (10 μl) in control group. **(A)** Lumbar DRG (L3–L5) extracted at different time points after AIA (specified in the graphs **B–D**). **(B)** TNF and its receptors **(C)** TNFR1 and **(D)** TNFR2 gene expression evaluation ($n = 5$). **(E)** TNF expressed protein within DRG (L4) 8 days after AIA by western blot. **(F)** Densitometry referring to **(E)** ($n = 3$). DRG samples from the control group were extracted 8 days after i.a. injection. The results are represented as mean ± SEM; $p =$ specified value in the graph compared to control group (PBS) using ANOVA following by Dunnett *post-hoc* **(B–D)** or two tailed unpaired *T*-test **(F)**.

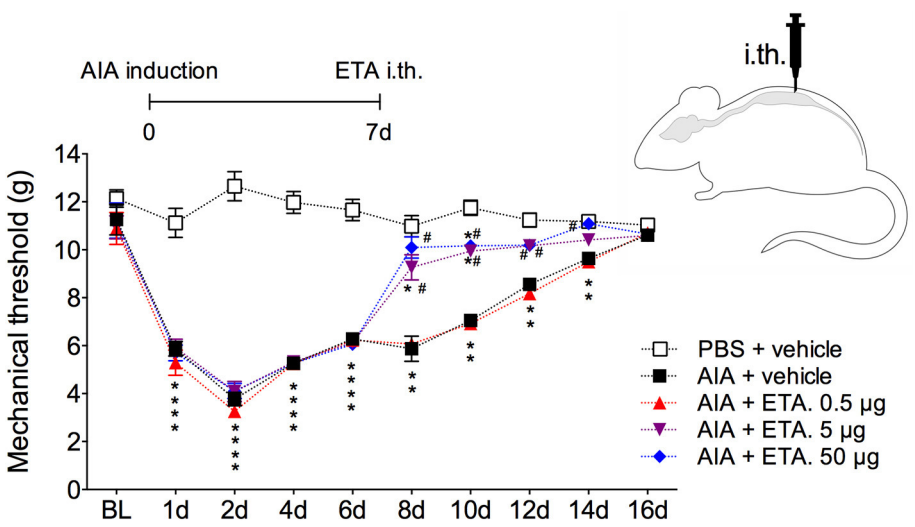

FIGURE 6 | Persistent nociception is reversed after neutralization of TNF within DRG by intrathecal injection of etanercept. Immunized mice received either i.a. injection of mBSA (10 μg/10 μl of PBS) to AIA induction or PBS (10 μl) in control group. Time course of nociceptive response was recorded by electronic von Frey algesimeter. Etanercept (ETA; 0.5, 5, or 50 μg) was intrathecally (i.th.) administered on the 7th day after AIA. BL (baseline) ($n = 7$). The results are represented as mean ± SEM; *Compared to the control group (PBS) or $^{\#}$compared to AIA + vehicle group when $p < 0.05$ using two-way ANOVA following by Dunnett *post-hoc* analysis.

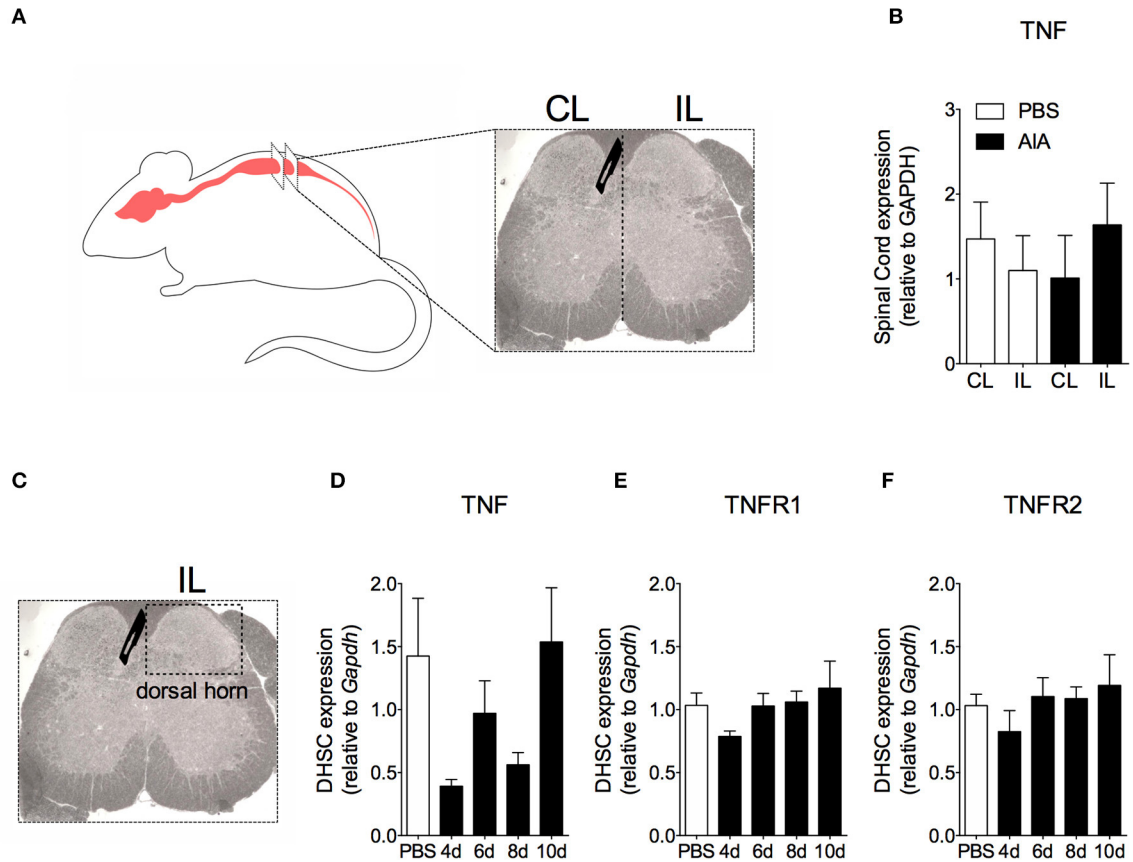

FIGURE 7 | Time course of TNF and its receptors TNFR1 and TNFR2 gene expression within the spinal cord in AIA model. Immunized mice received either i.a. injection of mBSA (10 μg/10 μl of PBS) to AIA induction or PBS (10 μl) in control group. **(A)** Contralateral (CL) and ipsilateral (IL) lumbar intumescence. **(B)** Relative evaluation of TNF gene expression in CL and IL spinal cord of AIA and control mice 8 days after AIA induction ($n = 5$). **(C)** Dorsal horn of the spinal cord (DHSC). **(D)** TNF and its receptors **(E)** TNFR1 and **(F)** TNFR2 gene expression evaluation in the dorsal horn extracted at different time points ($n = 8$). Samples of the spinal cord of the control group were extracted 8 days after i.a. injection. The results are represented as mean ± SEM; ($n = 5$–8) to statistical analyses was used ANOVA following by Dunnett *post-hoc* analyses.

There have been a number of studies which have tried to decipher neuro-immune interactions in the nociceptive apparatus and how that leads to increased pain sensitivity (21, 46). Changes in the DRG environment that explain persistent pain following arthritis remission are not fully understood. Hence, we had asked whether inflammatory stimuli in the DRG after the resolution of acute joint inflammation in AIA could be associated with persistent joint nociception. Our results show an increase in Iba1$^+$ cells in DRG associated with elevated TNF, IL-1β, IL-6, COX2, and iNOS gene expression *in situ*. Our observations are consistent with the role of inflammatory molecules for the sensitization of neurons in DRG and the development of hyperalgesia (47–53). Interestingly, this neuroinflammation within the DRG was corroborated with the activation of leukocyte-endothelium interactions in the lumbar intumescence.

The presence of TNF in peripheral and central structures is fundamental for joint pain in arthritis (6, 14, 27, 44). During joint inflammation in experimental models of arthritis, up-regulated TNF in the spinal cord is implicated in increased articular nociception (27, 54). Quadros et al. (27) demonstrated that challenging the joints of immunized mice with a high dose of mBSA produce marked articular hypernociception that is associated with increased TNF expression and microglial activation in the spinal cord. These authors have also shown that TNF neutralization by intrathecal administration of infliximab, or spinal prevention of microglial activation by minocycline or fluorocitrate injection, ameliorates AIA-induced hypernociception. Similarly, reversion of persistent pain hypersensitivity in a model of collagen antigen-induced arthritis was induced by spinal inhibition of microglia and astrocyte activation after intrathecal minocycline and pentoxifylline administration, respectively (55). In contrast, we did not observe spinal overexpression of TNF, TNFR1, and TNFR2, nor did we observe overexpression of Iba1$^+$ and GFAP$^+$ cells, which are glial cell activation markers, during the persistent joint nociception. Therefore, we eliminated the hypothesis that etanercept could neutralize TNF produced in the spinal

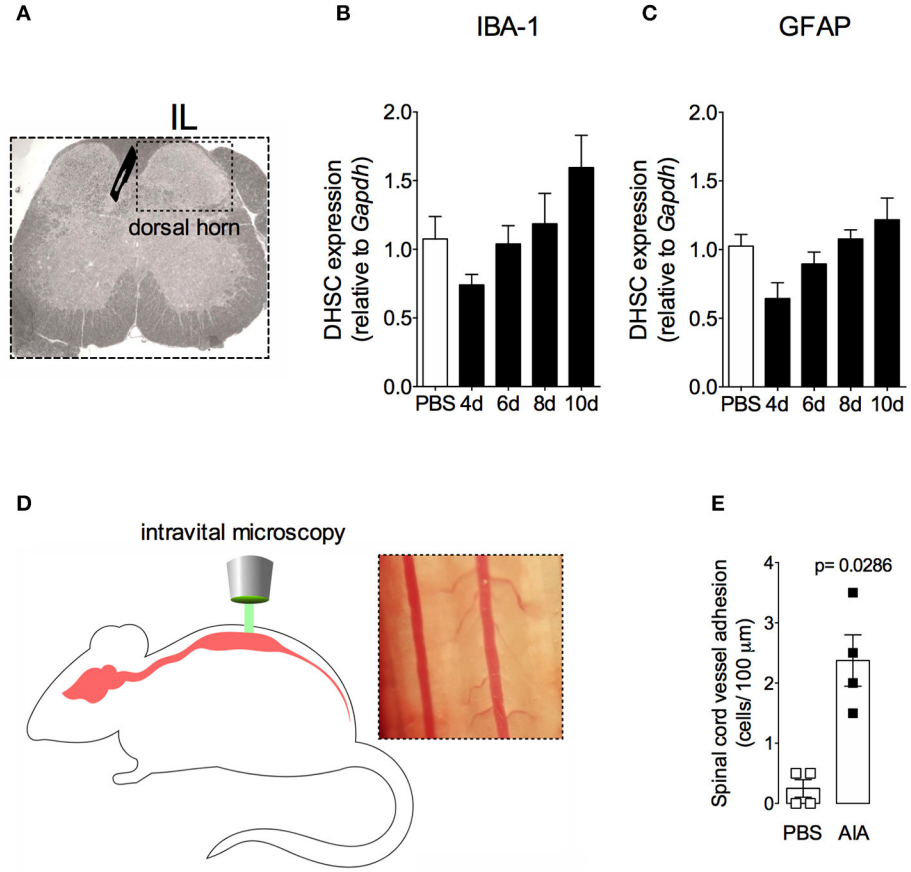

FIGURE 8 | Non-reactive status of glial cells and leucocytes adhesion in the spinal cord after resolution of acute inflammation in AIA model. Immunized mice received either i.a. injection of mBSA (10 µg/10 µl of PBS) to AIA induction or PBS (10 µl) in control group. **(A)** Dorsal horn of the spinal cord (DHSC). **(B)** Iba1 and **(C)** GFAP relative evaluation of gene expression in the dorsal horn extracted at different time points ($n = 8$). Dorsal horn samples from the control group were extracted 8 days after i.a. injection. The results are represented as mean ± SEM; to statistical analyses was used ANOVA following by Dunnett *post-hoc* analyses. A laminectomy was performed 8 days after i.a. injection of mBSA or PBS to evaluate **(E)** adherent leucocytes (**D**, representative photo on right) in dorsal microvasculature of lumbar intumescence (**D**, schematic picture on left) by intravital microscopy ($n = 4$). The results are represented as mean ± SEM; ($n = 8$) p = specified value in the graph compared to control group (PBS) using two tailed unpaired *T*-test.

cord. However, intrathecal injection of etanercept after a complete resolution of acute joint inflammation was able to reverse persistent joint nociception. To explain our findings, we evaluated TNF expression in the DRG. We found increased TNF expression in the sensory ganglia after resolution of acute inflammation in the challenged joint. The action of TNF in the DRG is expected to produce a pro-nociceptive effect (21), and its overexpression in this sensorial organ is involved with pathological pain sensitization in models of neuropathic pain (56), acute herpetic neuralgia (57), and diabetes neuropathy (58). Thus, our work suggest that the source of TNF is Iba1^{+} macrophages within DRG 6 and 8 days post AIA. At these time points, we also observed both elevated TNF gene expression in lumbar ganglions (L3-L5) and increased amounts of TNF in L4 DRG. Our observations are consistent with a previous study showing that TNF expression in the DRG environment is produced by macrophages (47, 59). As a result, we suggested that articular hyperalgesia remaining after the resolving phase in AIA is triggered by overexpression of TNF, possibly from non-neuronal cells activated in the DRG.

Within the DRG, inflammatory conditions also enhances TNFR1 expression in either non-neuronal cells and nociceptors, while increased TNFR2 expression is restricted in non-neuronal cells (59). In arthritis, the profile of changes in TNF receptors in DRG is not clear in the literature. In a model of arthritis induced by complete Freund's adjuvant, Inglis et al. (30) had demonstrated that both TNFR1 and TNFR2 expression were increased in neurons and infiltered macrophages into the DRG, respectively. However, Boettger et al. (28) showed expression of both receptors on small- and medium-sized DRG neurons, but the proportion of TNFR1 and TNFR2 positives cells did not alter the course of AIA. Here, TNFR1 gene expression in DRG was decreased after the resolving phase 6 and 8 days after AIA. On the other hand, increased TNFR2 gene expression was observed in DRG 8 days after

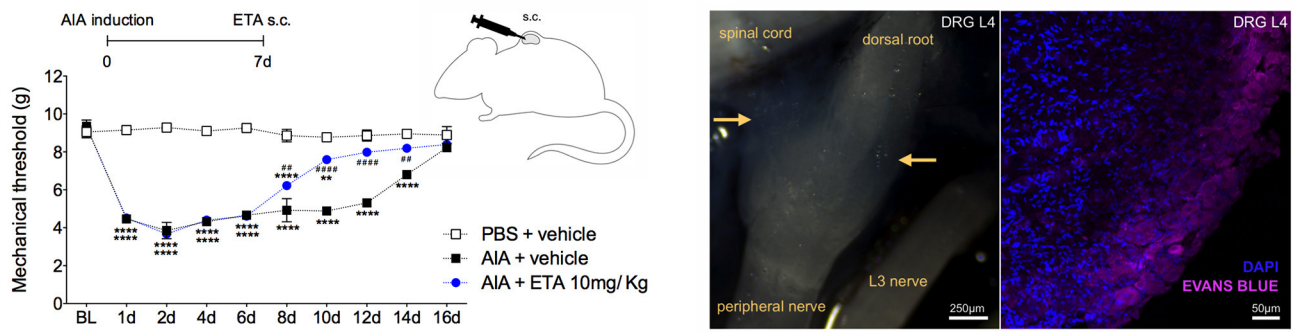

FIGURE 9 | Articular hypernociception induced by TNF in the DRG is reversed after systemic injection of etanercept. Immunized mice received either i.a. injection of mBSA (10 μg/10 μl of PBS) to AIA induction or PBS (10 μl) in the control group. Etanercept (ETA; 10 mg/ Kg) was subcutaneously administered 7 days after AIA after the inflammatory phase in the joint. **(A)** Nociceptive response was recorded by electronic von Frey algesimeter. BL (baseline) ($n = 5$). **(B)** Arthritic mice received an intravenous injection of Evans Blue 8 days after AIA induction to DRG permeability evaluation. (**B,** left) Yellow rows indicate accumulation of Evans Blue around intact L4 DRG. (**B,** right) Confocal microscopy slide shows marked Evans Blue accumulated in body reach area of DRG (purple) and nuclei by DAPI (blue) within L4 DRG from AIA mice. The results are represented as mean ± SEM.; *Compared to control group (PBS) or #compared to AIA + vehicle group when $p < 0.05$ using two-way ANOVA following by Tukey *post-hoc* analysis (a).

AIA induction. In fact, macrophages infiltrating the DRG during arthritis express TNFR2 and are associated with articular pain (30, 31). In addition, these TNFR2 expressing immune cells could be a second pathway to neuronal modulation by TNF (30). Since local and systemic neutralization of TNF by etanercept decreased the persistent articular hypernociception, our data suggest that expression of both TNF and TNFR2 in DRG might be necessary to maintain hypernociception. Of note, TNF produced peripherally contributes to inflammation and sensitizes nociceptive endings in the joints structures (6, 13). Therefore, systemically delivered etanercept could target articular tissue. We also evaluated the antinociceptive effect of this drug when TNF levels returned to basal level in articular sites. Thus, we eliminated the hypothesis that decreased nociceptive response after systemic administration of etanercept could be associated with articular TNF neutralization. Taken together, systemic administration of etanercept may be beneficial against clinical manifestation of both articular inflammation and pain. These perspective highlight the potential advantages for systemic drug administration in clinician practice, that includes easy application and widespread actions of injected agents (39). In order to improve the clinical translation, the use of humanized chimeric mouse models needs to be explored.

In conclusion, we have demonstrated that natural resolution may not contribute to pain recovery once TNF remains active in the DRG. However, whether exogenous treatment with pro-resolving mediators decrease the levels of TNF in the DRG and alleviate pain still needs to be clarified. Our data show that TNF targeting DRG represents a mechanism independent of spinal sensitization which elicits articular hypernociception after resolution of acute joint inflammation.

DATA AVAILABILITY STATEMENT

The raw data supporting the conclusions of this article will be made available by the authors, without undue reservation, to any qualified researcher.

ETHICS STATEMENT

The animal study was reviewed and approved by the Animal ethics committee of Federal University of Minas Gerais.

AUTHOR CONTRIBUTIONS

WG, TC, MT, FA, and VP designed the study, performed the data analysis, and wrote the manuscript. WG prepared all figures. WG, BR, MO, LR, VF, WS, PP, CQ-J, KS, WC, VB, VC, AB, WV, and FL conducted the experiments and reviewed the manuscript.

FUNDING

This work was supported by grants from Conselho Nacional de Desenvolvimento Científico e Tecnológico (CNPq, Brazil), Fundação de Amparo à Pesquisa do Estado de Minas Gerais (FAPEMIG, Brazil), Pró-Reitoria de Pesquisa da Universidade Federal de Minas Gerais-PRPq, and Coordenação de Aperfeiçoamento de Pessoal de Nível Superior (CAPES).

ACKNOWLEDGMENTS

We would like to thank Rosemeire Oliveira, Ilma Marçal, and Danuza Montijo Diniz for their technical assistance.

REFERENCES

1. Medzhitov R. Origin and physiological roles of inflammation. *Nature*. (2008) 454:428–35. doi: 10.1038/nature07201
2. Medzhitov R. Inflammation 2010: new adventures of an old flame. *Cell*. (2010) 140:771–6. doi: 10.1016/j.cell.2010.03.006
3. Chen Z, Bozec A, Ramming A, Schett G. Anti-inflammatory and immune-regulatory cytokines in rheumatoid arthritis. *Nat Rev Rheumatol*. (2019) 15:9–17. doi: 10.1038/s41584-018-0109-2
4. Nikoopour E, Schwartz JA, Singh B. Therapeutic benefits of regulating inflammation in autoimmunity. *Inflamm Allergy - Drug Targets*. (2008) 7:203–10. doi: 10.2174/187152808785748155
5. Shen HH, Yang YX, Meng X, Luo XY, Li XM, Shuai ZW, et al. NLRP3: a promising therapeutic target for autoimmune diseases. *Autoimmun Rev*. (2018) 17:694–702. doi: 10.1016/j.autrev.2018.01.020
6. Sachs D, Coelho FM, Costa VV, Lopes F, Pinho V, Amaral FA, et al. Cooperative role of TNF-alpha, IL-1beta and neutrophils in a novel behavioural model that concomitantly demonstrates articular inflammation and hypernociception in mice. *Br J Pharmacol*. (2010) 162:72–83. doi: 10.1111/j.1476-5381.2010.00895.x
7. Lopes F, Coelho FM, Costa VV, Vieira ÉLM, Sousa LP, Silva TA, et al. Resolution of neutrophilic inflammation by H2O2 in antigen-induced arthritis. *Arthritis Rheum*. (2011) 63:2651–60. doi: 10.1002/art.30448
8. Schaible H-G, Grubb BD. Afferent and spinal mechanisms of joint pain. *Pain*. (1993) 55:5–54. doi: 10.1016/0304-3959(93)90183-P
9. Ebinger M, Schmidt RF, Heppelmann B. Composition of the medial and posterior articular nerves of the mouse knee joint. *Somatosens Mot Res*. (2001) 18:62–5. doi: 10.1080/08990220020021357
10. Kelly S, Dunham JP, Murray F, Read S, Donaldson LF, Lawson SN. Spontaneous firing in C-fibers and increased mechanical sensitivity in A-fibers of knee joint-associated mechanoreceptive primary afferent neurones during MIA-induced osteoarthritis in the rat. *Osteoarthr Cartil*. (2012) 20:305–13. doi: 10.1016/j.joca.2012.01.002
11. Schaible HG, Schmidt RF. Activation of groups III and IV sensory units in medial articular nerve by local mechanical stimulation of knee joint. *J Neurophysiol*. (2017) 49:35–44. doi: 10.1152/jn.1983.49.1.35
12. Cook AD, Christensen AD, Tewari D, McMahon SB, Hamilton JA. Immune cytokines and their receptors in inflammatory pain. *Trends Immunol*. (2018) 39:240–55. doi: 10.1016/j.it.2017.12.003
13. Schaible HG. Nociceptive neurons detect cytokines in arthritis. *Arthritis Res Ther*. (2014) 16:470. doi: 10.1186/s13075-014-0470-8
14. Schaible H-G, Von Banchet GS, Boettger MK, Bräuer R, Gajda M, Richter F, et al. The role of proinflammatory cytokines in the generation and maintenance of joint pain. *Ann N Y Acad Sci*. (2010) 1193:60–9. doi: 10.1111/j.1749-6632.2009.05301.x
15. Schaible HG, Schmidt RF. Effects of an experimental arthritis on the sensory properties of fine articular afferent units. *J Neurophysiol*. (1985) 54:1109–22. doi: 10.1152/jn.1985.54.5.1109
16. Schaible HG, Ebersberger A, Segond Von Banchet G. Mechanisms of pain in arthritis. *Ann N Y Acad Sci*. (2002) 966:343–54. doi: 10.1111/j.1749-6632.2002.tb04234.x
17. Koop SMW, ten Klooster PM, Vonkeman HE, Steunebrink LMM, van de Laar MAFJ. Neuropathic-like pain features and cross-sectional associations in rheumatoid arthritis. *Arthritis Res Ther*. (2015) 17:237. doi: 10.1186/s13075-015-0761-8
18. Boyden SD, Hossain IN, Wohlfahrt A, Lee YC. Non-inflammatory causes of pain in patients with rheumatoid arthritis. *Curr Rheumatol Rep*. (2016) 18:30. doi: 10.1007/s11926-016-0581-0
19. Lee YC, Frits ML, Iannaccone CK, Weinblatt ME, Shadick NA, Williams DA, et al. Subgrouping of patients with rheumatoid arthritis based on pain, fatigue, inflammation, and psychosocial factors. *Arthritis Rheumatol*. (2014) 66:2006–14. doi: 10.1002/art.38682
20. Lee YC, Cui J, Lu B, Frits ML, Iannaccone CK, Shadick NA, et al. Pain persists in DAS28 rheumatoid arthritis remission but not in ACR/EULAR remission: a longitudinal observational study. *Arthritis Res Ther*. (2011) 13:R83. doi: 10.1186/ar3353
21. Ji RR, Chamessian A, Zhang YQ. Pain regulation by non-neuronal cells and inflammation. *Science*. (2016) 354:572–7. doi: 10.1126/science.aaf8924
22. Christianson CA, Corr M, Firestein GS, Mobargha A, Yaksh TL, Svensson CI. Characterization of the acute and persistent pain state present in K/BxN serum transfer arthritis. *Pain*. (2010) 151:394–403. doi: 10.1016/j.pain.2010.07.030
23. Bas DB, Su J, Sandor K, Agalave NM, Lundberg J, Codeluppi S, et al. Collagen antibody-induced arthritis evokes persistent pain with spinal glial involvement and transient prostaglandin dependency. *Arthritis Rheum*. (2012) 64:3886–96. doi: 10.1002/art.37686
24. Beckham JC, Caldwell DS, Peterson BL, Pippen AMM, Currie MS, Keefe FJ, et al. Disease severity in rheumatoid arthritis: Relationships of plasma tumor necrosis factor-α, soluble interleukin 2-receptor, soluble CD4/CD8 ratio, neopterin, and fibrin D-dimer to traditional severity and functional measures. *J Clin Immunol*. (1992) 12:353–61. doi: 10.1007/BF00920793
25. Seymour HE, Worsley A, Smith JM, Thomas SHL. Anti-TNF agents for rheumatoid arthritis. *Br J Clin Pharmacol*. (2001) 51:201–8. doi: 10.1046/j.1365-2125.2001.00321.x
26. Moreland LW, Baumgartner SW, Schiff MH, Tindall EA, Fleischmann RM, Weaver AL, et al. Treatment of rheumatoid arthritis with a recombinant human tumor necrosis factor receptor (p75)-Fc fusion protein. *N Engl J Med*. (1997) 337:141–7. doi: 10.1056/NEJM199707173370301
27. Quadros AU, Pinto LG, Fonseca MM, Kusuda R, Cunha FQ, Cunha TM. Dynamic weight bearing is an efficient and predictable method for evaluation of arthritic nociception and its pathophysiological mechanisms in mice. *Sci Rep*. (2015) 5:14648. doi: 10.1038/srep14648
28. Boettger MK, Hensellek S, Richter F, Gajda M, Stöckigt R, Von Banchet GS, et al. Antinociceptive effects of tumor necrosis factor alpha neutralization in a rat model of antigen-induced arthritis: Evidence of a neuronal target. *Arthritis Rheum*. (2008) 58:2368–78. doi: 10.1002/art.23608
29. Richter F, Natura G, Löser S, Schmidt K, Viisanen H, Schaible HG. Tumor necrosis factor causes persistent sensitization of joint nociceptors to mechanical stimuli in rats. *Arthritis Care Res*. (2010) 62:3806–14. doi: 10.1002/art.27715
30. Inglis JJ, Nissim A, Lees DM, Hunt SP, Chernajovsky Y, Kidd BL. The differential contribution of tumour necrosis factor to thermal and mechanical hyperalgesia during chronic inflammation. *Arthritis Res Ther*. (2005) 7:R807–16. doi: 10.1186/ar1743
31. Segond von Banchet G, Boettger MK, Fischer N, Gajda M, Bräuer R, Schaible HG. Experimental arthritis causes tumor necrosis factor-α-dependent infiltration of macrophages into rat dorsal root ganglia which correlates with pain-related behavior. *Pain*. (2009) 145:151–9. doi: 10.1016/j.pain.2009.06.002
32. Brackertz D, Mitchell GF, Mackay IR. Antigen-induced arthritis in mice. I. Induction of arthritis in various strains of mice. *Arthritis Rheum*. (1977) 20:841–50. doi: 10.1002/art.1780200314
33. Queiroz-Junior CM, Madeira MFM, Coelho FM, Costa VV, Bessoni RLC, Sousa LF et al. Experimental arthritis triggers periodontal disease in mice: involvement of TNF-α and the oral Microbiota. *J Immunol*. (2011) 187:3821–30. doi: 10.4049/jimmunol.1101195
34. Veihelmann A, Szczesny G, Nolte D, Krombach F, Refior HJ, Messmer K. A novel model for the study of synovial microcirculation in the mouse knee joint *in vivo*. *Res Exp Med*. (1998) 198:43–54. doi: 10.1007/s004330050088
35. Mestre C, Pélissier T, Fialip J, Wilcox G, Eschalier A. A method to perform direct transcutaneous intrathecal injection in rats. *J Pharmacol Toxicol Methods*. (1994) 32:197–200. doi: 10.1016/1056-8719(94)90087-6
36. Livak KJ, Schmittgen TD. Analysis of relative gene expression data using real-time quantitative PCR and the 2-ΔΔCT method. *Methods*. (2001) 25:402–8. doi: 10.1006/meth.2001.1262
37. Sugimoto MA, Sousa LP, Pinho V, Perretti M, Teixeira MM. Resolution of inflammation: what controls its onset? *Front Immunol*. (2016) 7:160. doi: 10.3389/fimmu.2016.00160
38. Perez DA, Vago JP, Athayde RM, Reis AC, Teixeira MM, Sousa LP, et al. Switching off key signaling survival molecules to switch on the resolution of inflammation. *Mediators Inflamm*. (2014) 2014:829851. doi: 10.1155/2014/829851
39. Berta T, Qadri Y, Tan PH, Ji RR. Targeting dorsal root ganglia and primary sensory neurons for the treatment of chronic pain. *Expert Opin Ther Targets*. (2017) 21:695–703. doi: 10.1080/14728222.2017.1328057
40. Joukal M, Klusáková I, Dubový P. Direct communication of the spinal subarachnoid space with the rat dorsal root ganglia. *Ann Anat*. (2016) 205:9–15. doi: 10.1016/j.aanat.2016.01.004

41. Jimenez-Andrade JM, Herrera MB, Ghilardi JR, Vardanyan M, Melemedjian OK, Mantyh PW. Vascularization of the dorsal root ganglia and peripheral nerve of the mouse: Implications for chemical-induced peripheral sensory neuropathies. *Mol Pain*. (2008) 4:10. doi: 10.1186/1744-8069-4-10
42. Ebbinghaus M, Segond von Banchet G, Massier J, Gajda M, Bräuer R, Kress M, et al. Interleukin-6-dependent influence of nociceptive sensory neurons on antigen-induced arthritis. *Arthritis Res Ther*. (2015) 17:334. doi: 10.1186/s13075-015-0858-0
43. Krock E, Jurczak A, Svensson CI. Pain pathogenesis in rheumatoid arthritis—what have we learned from animal models? *Pain*. (2018) 159 (Suppl.1):S98–109. doi: 10.1097/j.pain.0000000000001333
44. Verri WA, Cunha TM, Parada CA, Poole S, Cunha FQ, Ferreira SH. Hypernociceptive role of cytokines and chemokines: targets for analgesic drug development? *Pharmacol Ther*. (2006) 112:116–38. doi: 10.1016/j.pharmthera.2006.04.001
45. Laumet G, Ma J, Robison AJ, Kumari S, Heijnen CJ, Kavelaars A. T cells as an emerging target for chronic pain therapy. *Front Mol Neurosci*. (2019) 12:216. doi: 10.3389/fnmol.2019.00216
46. Baral P, Udit S, Chiu IM. Pain and immunity: implications for host defence. *Nat Rev Immunol*. (2019) 19:433–47. doi: 10.1038/s41577-019-0147-2
47. Leisengang S, Ott D, Murgott J, Gerstberger R, Rummel C, Roth J. Primary cultures from rat dorsal root ganglia: responses of neurons and glial cells to somatosensory or inflammatory stimulation. *Neuroscience*. (2018) 394:1–13. doi: 10.1016/j.neuroscience.2018.10.018
48. Araldi D, Ferrari LF, Lotufo CM, Vieira AS, Athié MCP, Figueiredo JG, et al. Peripheral inflammatory hyperalgesia depends on the COX increase in the dorsal root ganglion. *Proc Natl Acad Sci USA*. (2013) 110:3603–8. doi: 10.1073/pnas.1220668110
49. Fehrenbacher JC, Burkey TH, Nicol GD, Vasko MR. Tumor necrosis factor α and interleukin-1β stimulate the expression of cyclooxygenase II but do not alter prostaglandin E 2 receptor mRNA levels in cultured dorsal root ganglia cells. *Pain*. (2005) 113:113–22. doi: 10.1016/j.pain.2004.09.031
50. Morioka N, Inoue A, Hanada T, Kumagai K, Takeda K, Ikoma K, et al. Nitric oxide synergistically potentiates interleukin-1β-induced increase of cyclooxygenase-2 mRNA levels, resulting in the facilitation of substance P release from primary afferent neurons: involvement of cGMP-independent mechanisms. *Neuropharmacology*. (2002) 43:868–76. doi: 10.1016/S0028-3908(02)00143-0
51. Inoue A, Ikoma K, Morioka N, Kumagai K, Hashimoto T, Hide I, et al. Interleukin-1beta induces substance P release from primary afferent neurons through the cyclooxygenase-2 system. *J Neurochem*. (1999) 73:2206–13. doi: 10.1046/j.1471-4159.1999.02206.x
52. Qin X, Wan Y, Wang X. CCL2 and CXCL1 trigger calcitonin gene-related peptide release by exciting primary neciceptive neurons. *J Neurosci Res*. (2005) 82:51–62. doi: 10.1002/jnr.20612
53. Cao DL, Qian B, Zhang ZJ, Gao YJ, Wu XB. Chemokine receptor CXCR2 in dorsal root ganglion contributes to the maintenance of inflammatory pain. *Brain Res Bull*. (2016) 127:219–25. doi: 10.1016/j.brainresbull.2016.09.016
54. Bao L, Zhu Y, Elhassan AM, Wu Q, Xiao B, Zhu J, et al. Adjuvant-induced arthritis: IL-1 beta, IL-6 and TNF-alpha are up-regulated in the spinal cord. *Neuroreport*. (2001) 12:3905–8. doi: 10.1097/00001756-200112210-00010
55. Fernandez-Zafra T, Gao T, Jurczak A, Sandor K, Hore Z, Agalave NM, et al. Exploring the transcriptome of resident spinal microglia after collagen antibody-induced arthritis. *Pain*. (2019) 160:224–36. doi: 10.1097/j.pain.0000000000001394
56. Souza GR, Talbot J, Lotufo CM, Cunha FQ, Cunha TM, Ferreira SH. Fractalkine mediates inflammatory pain through activation of satellite glial cells. *Proc Natl Acad Sci USA*. (2013) 110:11193–8. doi: 10.1073/pnas.1307445110
57. Silva JR, Lopes AH, Talbot J, Cecilio NT, Rossato MF, Silva RL, et al. Neuroimmune–glia interactions in the sensory ganglia account for the development of acute herpetic Neuralgia. *J Neurosci*. (2017) 37:6408–22. doi: 10.1523/JNEUROSCI.2233-16.2017
58. Chen T, Li H, Yin Y, Zhang Y, Liu Z, Liu H. Interactions of Notch1 and TLR4 signaling pathways in DRG neurons of *in vivo* and *in vitro* models of diabetic neuropathy. *Sci Rep*. (2017) 7:14923. doi: 10.1038/s41598-017-15053-w
59. Li Y, Ji A, Weihe E, Schäfer MK. Cell-specific expression and lipopolysaccharide-induced regulation of tumor necrosis factor alpha (TNFalpha) and TNF receptors in rat dorsal root ganglion. *J Neurosci*. (2004) 24:9623–31. doi: 10.1523/JNEUROSCI.2392-04.2004

Conflict of Interest: The authors declare that the research was conducted in the absence of any commercial or financial relationships that could be construed as a potential conflict of interest.

frontiers in Neurology

ORIGINAL RESEARCH
published: 21 January 2020
doi: 10.3389/fneur.2019.01380

Central Neuropathic Pain and Profiles of Quantitative Electroencephalography in Multiple Sclerosis Patients

Nataliya A. Krupina[1], *Maxim V. Churyukanov*[2,3]*, *Mikhail L. Kukushkin*[4] and *Nikolay N. Yakhno*[5]

[1] Laboratory of General Pathology of the Nervous System, The Institute of General Pathology and Pathophysiology, Moscow, Russia, [2] I.M. Sechenov First Moscow State Medical University (Sechenov University), Moscow, Russia, [3] Clinic of Pain Study and Treatment, B.V. Petrovsky Russian Scientific Surgery Center, Moscow, Russia, [4] Laboratory of Fundamental and Applied Problems of Pain, The Institute of General Pathology and Pathophysiology, Moscow, Russia, [5] Scientific and Research Department of Neurology, I.M. Sechenov First Moscow State Medical University (Sechenov University), Moscow, Russia

OPEN ACCESS

Edited by:
Felipe Almeida Pinho Ribeiro, Harvard Medical School, United States

Reviewed by:
Bonaventura Casanova, University and Polytechnic Hospital of La Fe, Spain
Antonio Ivano Triggiani, National Institutes of Health (NIH), United States
Aleksandra Vuckovic, University of Glasgow, United Kingdom

***Correspondence:**
Maxim V. Churyukanov
mchurukanov@gmail.com

Specialty section:
This article was submitted to Multiple Sclerosis and Neuroimmunology, a section of the journal Frontiers in Neurology

Received: 07 May 2019
Accepted: 13 December 2019
Published: 21 January 2020

Citation:
Krupina NA, Churyukanov MV, Kukushkin ML and Yakhno NN (2020) Central Neuropathic Pain and Profiles of Quantitative Electroencephalography in Multiple Sclerosis Patients. Front. Neurol. 10:1380. doi: 10.3389/fneur.2019.01380

Pain has a significant impact on the quality of life of patients with multiple sclerosis (MS). However, the neurophysiological mechanisms of central neuropathic pain in a MS course are not known. We hypothesized that changes in power spectral density (PSD) that take place in the electroencephalography (EEG) of MS patients with and without the central neuropathic pain (CNP) would differ. The study aimed to assess the features of quantitative EEG using the PSD indicator along with peak frequencies in the standard frequency bands in MS patients with and without CNP. We have analyzed the quantitative spectral content of the EEG at a resting state in 12 MS patients with CNP, 12 MS patients without CNP, and 12 gender- and age-matched healthy controls using fast Fourier transformation. Based on the ANOVA, at the group level, the theta band absolute and relative PSD showed an increase, whereas alpha band relative PSD showed a decrease in MS patients both with and without CNP. However, only in MS with CNP group, the absolute and relative PSD in the beta1 and beta2 bands increased and exceeded that in patients without pain. Only MS patients with CNP demonstrated the significantly increased absolute PSD for the theta, beta1, and beta2 frequency bands in most regions of interest. In the theta band, MS patients with CNP displayed the increase in absolute spectral power for the mid-temporal derivation of the right hemisphere and the increase in relative spectral power for the prefrontal derivation of this hemisphere. In the beta1 band, the increase in absolute spectral power was observed for the three temporal derivations of the right hemisphere, whereas in the beta2 band, for the occipital, parietal, and temporal lobes of both hemispheres. In the alpha band, only a relative spectral power decrease was revealed for the occipital lobes of both hemispheres and parietal lobe of the right hemisphere. In MS patients with CNP, the frequencies of the dominant spectral power (peak frequencies) in the high-frequency beta band were higher than in the healthy control in posterior areas of the left hemisphere. Data could represent central nervous system alterations related to central neuropathic pain in MS patients that lead to the disturbances in cortical communication.

Keywords: multiple sclerosis, central neuropathic pain, quantitative EEG, spectral power, peak frequency

INTRODUCTION

Pain has a significant impact on the quality of life of patients with multiple sclerosis (MS) (1–6). According to various data, pain occurs in 50–85% of MS patients, of whom 30–58% suffers from central neuropathic pain (CNP) (7–10). However, so far, it is unclear whether central neuropathic pain affects the multiple sclerosis electroencephalography (EEG) patterns, and, if so, how.

The International Association for the Study of Pain defines neuropathic pain as pain originating from a lesion or disease of the somatosensory nervous system (11). There is no definite view of the genesis of CNP, including MS (12–14). The lesions of spinothalamic–cortical tracts and failure to conduct nociceptive information are believed to be determinants for CNP development (15, 16). This view was based on the results of the studies where clinical and neurophysiological methods were used (9, 17). The predisposing role of psychological and behavioral factors for CNP in MS patients is a matter of debate (18).

MS pathophysiology contains two dissimilar arms: the inflammatory demyelination and the neurodegeneration running in parallel (3). Axonal damage along with neuronal loss occurs from the beginning of disease process and leads to progressive and permanent disability. MS potentially affects human CNS at all levels. Magnetic resonance imaging studies show cortical and corpus callosum damages in MS patients (19, 20). As a result of axonal damage and widespread gray matter pathology, one can expect a deficit in cortico-cortical and cortico-subcortical connectivity leading to EEG alterations. Numerous studies point to EEG abnormalities in 20–60% (21, 22) or even in 40–79% of MS patients (23). More typical findings are an increase in slow frequencies (theta and delta) and a decrease in the alpha band especially related to cognitive dysfunctions; occasionally, paroxysmal activity, and focal slow waves or localized flattened EEG activity may be found (22–25). Different works have looked at possible relationships between EEG activity and some aspects of the MS disease. There are conflicting data on the correlation between EEG changes and the disability score in MS patients (26, 27). In recent studies assessing cognitive impairment in MS, changes in the high EEG spectrum (beta2 and gamma) localized to the anterior regions of the right hemisphere and bilaterally to the posterior areas of the scalp were revealed (28, 29). No significant correlations between quantitative EEG (QEEG) changes and the other variables analyzed, including behavioral performance, were observed. In general, EEG spectral power is considered to be of little use in MS (30).

As for CNP, EEG changes in patients with neuropathic pain are thought to occur due to the development of thalamocortical dysrhythmias (15, 31–34). EEG analysis for neuropathic pain revealed changes not only in the standard frequency ranges in general but also in some subbands. In patients with neurogenic pain, Sarnthein and Jeanmonod (35) determined the EEG power peak in the standard theta band (θ, 4–9 Hz), when the alpha peak in the standard alpha band (α, 9–13 Hz) was reduced or even not present. Vuckovic et al. (36) identified predictors of neuropathic pain in patients with spinal cord injury showing the reduction in the EEG reactivity to opening eyes in the alpha band and reduced alpha power. Slowing of the dominant peak and EEG spectral power overactivations in the theta (with maximal differences in the high theta frequencies) and beta (in the low beta frequencies, beta1 band) power localized to multiple pain-associated areas were the most apparent characteristics in patients with neurogenic pain (37, 38). Under painful stimulation, healthy volunteers demonstrated a most pronounced decrease in alpha amplitude and several changes evidenced for the increase in the high beta frequencies (18.5–24 Hz) (32). Neurofeedback training for treatment of central neuropathic pain showed the association between pain reduction and suppression of theta power in the standard band and beta2 power in the 20–30 Hz band (39). A number of EEG studies have also shown the association between neuropathic pain and beta/gamma overactivations (32–34). However, changes in the power spectral density in the gamma frequency range are often associated with the attentional processing and cognitive impairment (28, 40). In patients with severe chronic neuropathic pain, higher pain ratings correlated consistently positive with EEG power values, while larger psychopathology correlated with lower frequency values (4).

Given the above, patients with MS and patients with CNP have several similar changes in the EEG. First of all, one might draw attention to an increase in spectral power in the theta range and a decrease in the alpha activity. However, only patients with CNP demonstrated an increase in the spectral power in the high-frequency bands. The question remains how the neuropathic pain could change the EEG pattern characteristic for MS, and vice versa, that is, what is the interaction between MS and chronic neuropathic pain as judging by the EEG indices? How will thalamocortical dysrhythmia related to CNP manifest in patients with multiple sclerosis? What mechanisms can underlie the influences if they appeared? Comparative neurophysiological studies in MS with and without CNP may be a new approach to improving our knowledge of both MS and CNP genesis. We consider the present study as the first step in finding answers to questions posed.

This work aimed to identify the features of QEEG using the PSD indicator along with peak frequencies in the standard frequency bands in MS patients with and without CNP.

MATERIALS AND METHODS

Patients and Healthy Controls

This study was carried out in accordance with the recommendations of the Ethical Committee of the Institute of General Pathology and Pathophysiology (the project approval protocol Number 5 of November 25, 2016) and was approved by the Ethical Committee (final approval protocol Number 1a of April 03, 2018). All participants signed informed consent after a complete explanation of the study in accordance with the Helsinki Declaration of 1964 with all subsequent amendments.

All the patients underwent complex assessment, which included a clinical neurological examination. Neurological impairment was estimated according to Kurtzke's Expanded Disability Status Scale (EDSS scores) (41).

Diagnosis of definite MS was based on clinical and neuroradiological data, according to the criteria of McDonald et al. (42).

Inclusion criteria for our study were clinical remission of the disease in the last 1 month before the study and the absence of corticosteroid treatment for at least 1 month. No cases of epilepsy were diagnosed in MS patients included.

The group of MS patients was divided into two clinical subgroups based on CNP presence. MS patients were classified as either having CNP or not. Most of the patients reported pain in more than one anatomical location. The most commonly reported pain areas were lower extremities and the upper extremities. Five patients reported pain on the left side of the body and five on the right side, and two patients experienced pain both on the right and on the left. Assessment took place according to the complaints of pain with descriptors for the neuropathic pain, symptoms of CNS lesion that is sensation disorders (hypoesthesia, hyperesthesia, paresthesia, or dysesthesia) in a body territory with decreased or increased sensation to touch, pinprick, warmth or cold at bedside examination, and had no history or clinical evidence of peripheral neuropathic pain. Furthermore, nociceptive musculoskeletal, spasticity-related, and visceral pain conditions had to be either excluded. Pain syndrome was assessed using the 10-point Visual Analog Scale (VAS). The mean VAS score for the group of MS patients with CNP was 5.4 ± 0.6 (mean ± SEM).

Exclusion criteria for MS patients with and without CNP were the same: other known neurological diseases (including peripheral nerve damage), cancer, renal disease, severe psychiatric disease, diabetes mellitus, and Mini-Mental State Examination score <24 (43).

Among comorbid disorders, some patients in MS groups with and without CNP had occasional tension headaches, migraines, arterial hypertension, biliary dyskinesia, irritable bowel syndrome, peptic ulcer disease, and psoriasis.

The healthy control (HC) group included volunteers with no history of neurological disorders and not allowed to suffer from any pain.

The characteristics of the groups examined are given in **Table 1**. All study participants were right-handed.

EEG Recording

EEG was administered to MS patients during remission, usually after the course of corticosteroids. MS patients with CNP did not complain of pain sensations during EEG recording.

All participants underwent EEG while subjects were sitting in a dark room, fully awake but with the eyes closed. Unipolar recordings were performed from 16 electrodes (Fp1, Fp2, F3, F4, F7, F8, C3, C4, T3, T4, T5, T6, P3, P4, O1, O2) according to the International 10–20 system. Linked-ear reference was used for recording. Impedances were below 10 kΩ in all electrodes processed in the further analysis. EEG signals were registered using the "Neuro-KM21" system (analog-to-digital converter with amplifier; sampling rate, 200 Hz, 0.5–30 Hz band pass filter, notch filter at 50 Hz; Russia) and continuously viewed on a PC monitor.

Twenty minutes of EEG were recorded, including resting wakeful eyes closed state (usually 3–4 min) followed by routine activation maneuvers according to standard clinical EEG protocol. In present work, we focused our analysis on the spontaneous EEG before EEG activation, i.e., on a resting state eyes closed EEG activity since it has been shown that clinical dysfunction altered resting-state networks in MS (45). The electroencephalographer was blind to the diagnosis of the subject at the time of recording, processing, and interpretation of electrophysiological data.

EEG Processing

EEGs were reviewed and analyzed offline with the commercial software "BRAINSYS" (Version 2.0 for Windows, Russia) (46). EEG was visually inspected, and segments contaminated with eye movements, electromyography, or other artifacts of technical origin were manually removed. Preprocessed EEG data were then processed using the BRAINSYS algorithm for advanced artifact search when the EEG amplitude is considered as a random variable, and its deviation from the zero lines by 4–5 SD serves as criteria for identifying an artifact. These marked sites were additionally inspected.

Data were segmented into 4-s epochs (without overlapping); for each participant, 15–25 free of artifact segments were included in further analyses: (mean ± SEM; 20.2 ± 1.0 epochs of 80.8 ± 4.2 s duration on the average). Epoch's number did not

TABLE 1 | Baseline characteristics of the groups.

Groups (number of participants)	Males/females	The average age, years (min – max)	The number of patients with a clinical type of the disease course	The average duration of the disease, years	EDSS scores
MS with CNP ($n = 12$)	3/9	36.6 ± 3.2 (23–57)	RRMS – 10 PPMS – 2	7.2 ± 1.2	2.8 [2.0; 3.0]
MS without CNP ($n = 12$)	4/8	42.9 ± 2.8 (30–55)	RRMS – 9 PPMS – 1 SPMS – 2	7.2 ± 1.8	2.5 [2.0; 3.0]
Healthy control (HC) ($n = 12$)	4/8	40.3 ± 4.0 (22–65)	–	–	–

RRMS, relapsing-remitting multiple sclerosis; PPMS, primary progressive multiple sclerosis; SPMS, secondary progressive multiple sclerosis, according to Lublin and Reingold (44). The average age and the average duration of the disease presented as Mean ± S.E.M; EDSS scores—as Median with lower and upper quartiles.

significantly differ between groups: 23.3 ± 2.0, 20.3 ± 1.8, and 17.4 ± 1.6 in MS group with CNP, MS group without CNP, and HC, correspondingly [$F_{(2,33)} = 2{,}740$; $p = 0.079$].

Analysis of the power spectral density of electrical activity (EA) of the brain was carried out according to fast Fourier transform algorithm, in the frequencies of five physiological ranges: δ (delta, 0.5–4.0 Hz), θ (theta, 4.0–8.0 Hz), α (alpha, 8.0–13.0 Hz), $\beta 1$ (beta1, 13.0–20.0 Hz), and $\beta 2$ (beta2, 20.0–30.0 Hz).

In every frequency band, we identified the following characteristics: absolute power spectral density (aPSD, μV^2), relative power spectral density (rPSD, %) defined by the ratio of the absolute power spectral density in the actual frequency band to the overall absolute spectral power computed as the sum of power spectral density' values within all empirically defined bands of interest (in percent), and peak frequency—the frequency of the dominant spectral power in the frequency band (Hz—*per se* the frequency of the amplitude maximum of spectral power in the band). Simultaneous evaluation of aPSD and rPSD increases the information content of the analysis since rPSD allows evaluating the contribution of each rhythm component to the total EEG power in the analyzed segment.

Data Analysis and Statistics

All statistics were calculated with statistical package "STATISTICA 7.0" for Windows and "BRAINSYS" software. We tested all variables comparing between patients and controls for normal distribution by the Kolmogorov–Smirnov test. If they proved to be normally distributed, we applied the parametric tests for independent samples; otherwise, we used the non-parametric tests.

Logarithmic transformation was used for any power spectral density value to achieve a valid normal distribution of these data and allow an ANOVA analysis (47); for absolute spectral power, we calculated Ln(aPSD); for relative spectral power:

$$\text{Ln (rPSD)} = \text{Ln}[(\text{power (\%)})/(100 - \text{power (\%)})] \quad (1)$$

where Ln is the natural logarithm and power (%) is the relative spectral power (%).

Ln(absolute spectral power) and Ln[(relative spectral power)/(100 – relative spectral)] for absolute and relative spectral power, respectively. The homogeneity of variances in compared samples was verified with Bartlett's test. Differences in spectral power between groups were assessed using analysis of variance (ANOVA) followed by pairwise *post-hoc* comparison using Duncan test to account for multiple comparisons. Regional normalized power spectral density values were used as dependent variable of the ANOVAs. The three-way ANOVA factors were the following: group [levels (3): MS with CNP, MS without CNP, healthy control; independent variable], region of interest (ROI) [levels (8): prefrontal (Fp1, Fp2), frontal (F3, F4), central (C3, C4), parietal (P3, P4), occipital (O1, O2), anterior temporal (F7, F8), mid-temporal (T3, T4), and posterior temporal (T5, T6); independent variable], and hemisphere [levels (2): left and right; independent variable]. For the test statistics of ANOVA, we calculated eta-squared (η^2) as effect size (ES) measurement using the standard formula (48, 49):

$$\eta^2 = \text{SS}_{\text{Effect}}/\text{SS}_{\text{Total}} \quad (2)$$

where $\text{SS}_{\text{Effect}}$ is the sum of squares of effect and SS_{Total} is the total sum of squares.

ES interpretation was the following: ES $\leq$ 0.02 indicates a weak effect, 0.02 $<$ ES $\leq$ 0.13 indicates a moderate effect, and ES $>$ 0.13 indicates a strong effect (50). When ANOVA showed 0.050 $< p \leq$ 0.085 and ES was moderate, we considered a trend.

Differences in peak frequency between groups were estimated using Kruskal–Wallis ANOVA followed by multiple comparisons of mean ranks (two-tailed). For the test statistics of Kruskal–Wallis H, we calculated eta-squared (η^2) and Cohen's d (d_{Cohen}) as effect size (ES) measurement using an ES calculator (51). Cohen's d of 0.20–0.40 indicates a small effect, 0.50–0.70 indicates a medium-sized effect, and 0.80–1.0 and more indicates a large effect; eta-squared of 0.010–0.039 indicates a small effect, 0.060–0.110 indicates a medium-sized effect, and 0.140–0.200 indicates a large effect (51, 52). When ANOVA showed 0.050 $< p \leq$ 0.085 and Cohen's d was more than 0.8 or η^2 was more than 0.140, we considered a trend.

Differences between groups (EDSS, the clinical score of neurological signs) were evaluated using Wilcoxon–Mann–Whitney rank sum test (two groups). Pearson chi-square (χ^2 criterion) was applied to test the difference between the two groups in terms of percentages of female/male (gender index). The non-parametric Spearman's rank correlation coefficient rho (ρ_S) with false discovery rate control (53) to correct for multiple comparisons was used for correlation analyzes. All the tests were two-tailed. The α level was set at 0.05.

RESULTS

Sample Characteristics

In all the groups, neither the mean age [$F_{(2,33)} = 0.899$; $p = 0.416$, one-way ANOVA] nor the gender index ($p > 0.05$, χ^2 criterion) significantly differed (see **Table 1**). Thus, the controls were age- and gender-matched clinically normal subjects. MS groups with and without CNP were fully comparable in the frequency of the occurrence of the disease course and comorbid disorders. The mean number of years since MS diagnosis in groups with and without CNP also did not significantly differ [$F_{(1,22)} = 0{,}001$; $p = 0.982$, one-way ANOVA] same as the disease severity as judged by EDSS scores ($p = 0.843$, Wilcoxon–Mann–Whitney test).

Analysis of EEG Power Spectra

Analysis of Absolute Power Spectral Density

In the δ band, the three-way ANOVA showed a group effect on aPSD of the scalp EEG [$F_{(2,528)} = 3.501$, $p = 0.031$; $\eta^2 = 0.012$]. Only in MS with CNP group, absolute spectral powers significantly increased as compared with HC: according to the *post-hoc* Duncan test, $p = 0.011$ (**Figure 1A**). The main effect of the ROI factor was significant [$F_{(7,528)} = 4.177$, $p < 0.001$; $\eta^2 = 0.051$] and revealed higher aPSD in the prefrontal region as compared with occipital, posterior, and mid-temporal regions (in

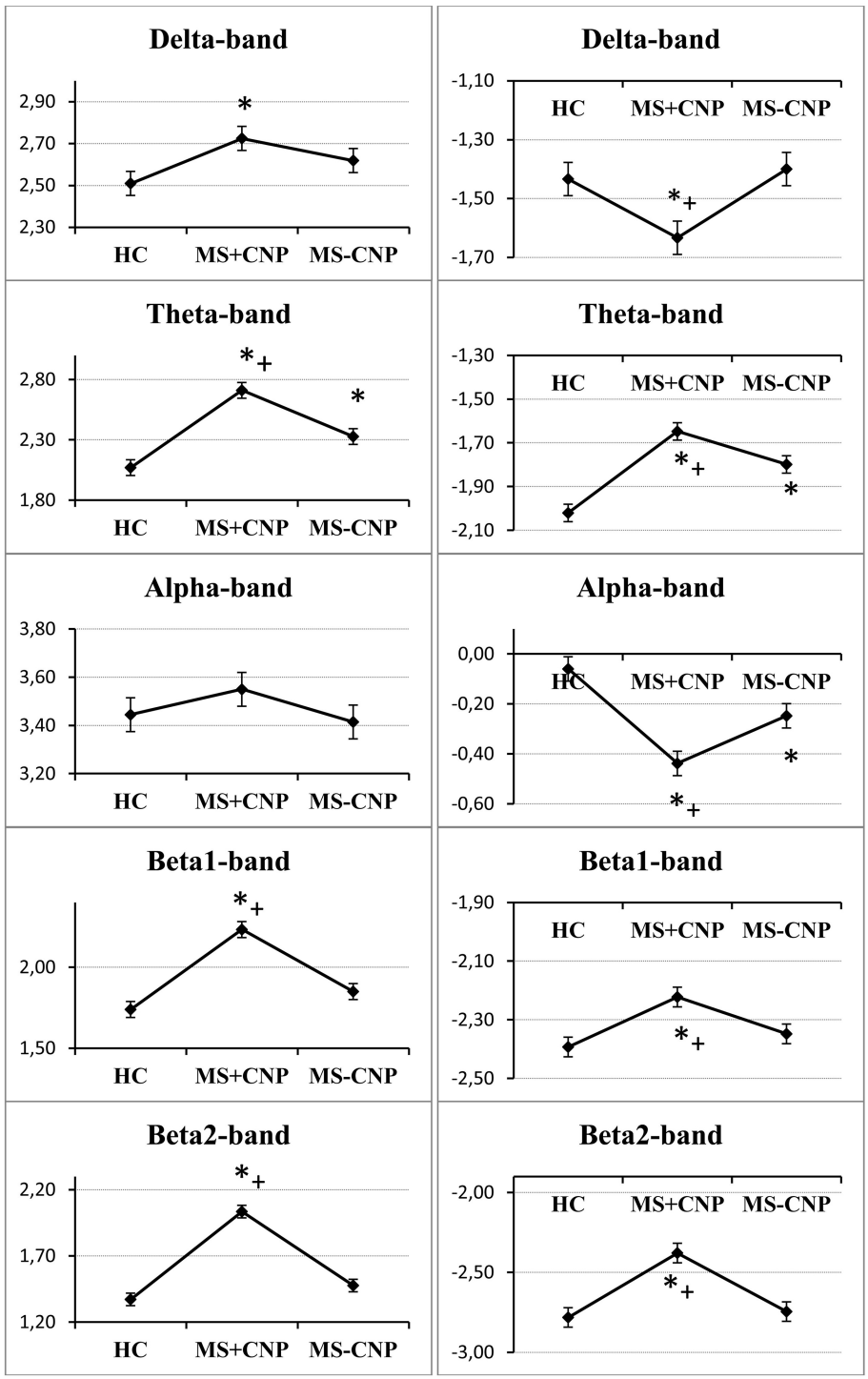

FIGURE 1 | Group factor effects on the absolute and relative power spectral density in the five frequencies ranges. **(A)** A vertical row on the left side, the vertical axis on the graphics indicate normalized absolute power spectral density; **(B)** a vertical row on the right side, the vertical axis on the graphics indicate normalized relative power spectral density. HC, healthy control; MS + CNP, multiple sclerosis patients with CNP; MS-CNP, multiple sclerosis patients without CNP. $^{*}p < 0.05$ as compared with the HC group; $^{+}p < 0.05$ as compared with MS patients without CNP (three-way ANOVA followed by *post-hoc* Duncan test).

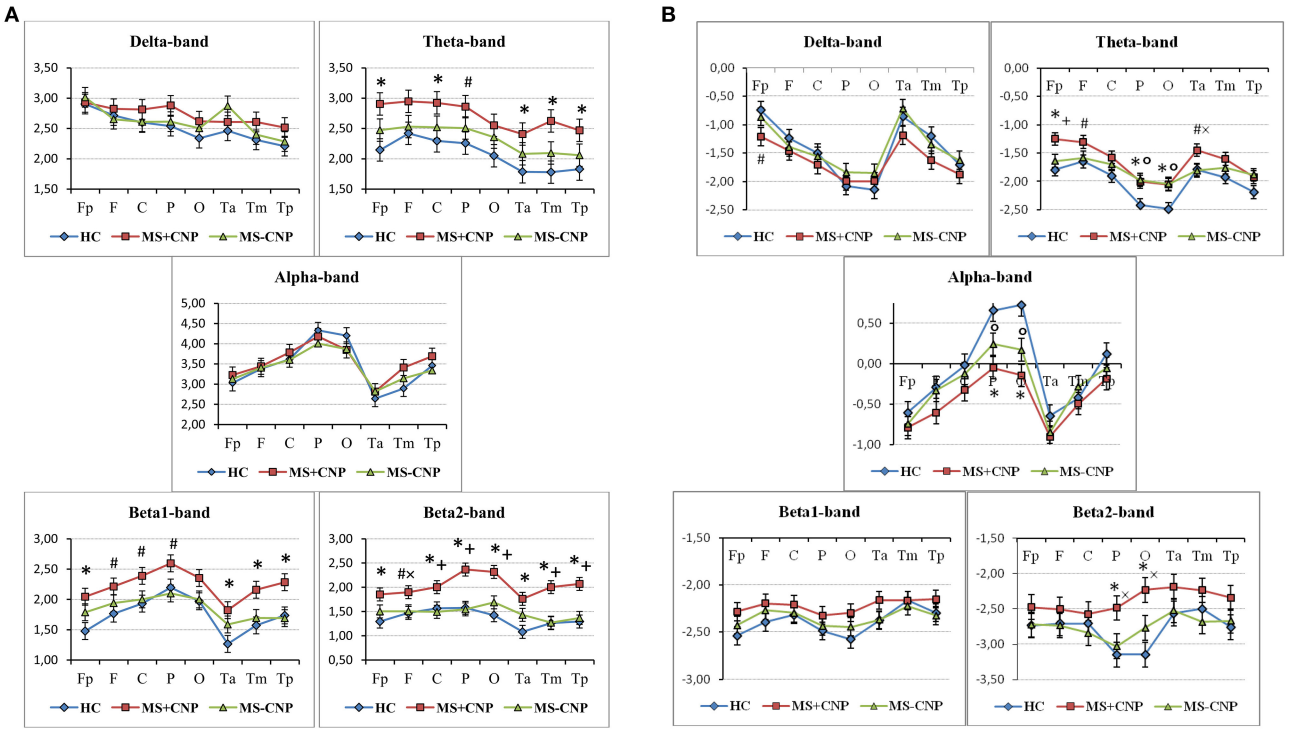

FIGURE 2 | Topographical differences between the groups in the absolute **(A)** and relative **(B)** power spectral density in the five frequencies ranges. The graphics show the normalized PSD values in the following ROI: prefrontal (Fp), frontal (F), central (C), parietal (P), occipital (O), anterior temporal (Ta), mid-temporal (Tm), and posterior temporal (Tp). HC, healthy control; MS + CNP, multiple sclerosis patients with CNP; MS-CNP, multiple sclerosis patients without CNP. $^{*}p < 0.05$, $^{\#}p < 0.08$—comparing the MS + CNP group vs. the HC group; $^{+}p < 0.05$, $^{\times}p<0.08$—comparing the MS + CNP group vs. MS-CNP group; $p < 0.05$—comparing the MS-CNP group vs. the HC group (three-way ANOVA followed by *post-hoc* Duncan test).

all cases, $p < 0.05$) with the least power in the posterior temporal region. However, we did not observe significant differences between aPSD in any of the ROIs (**Figure 2A**) and derivations in MS groups and HC. The hemisphere factor did not affect aPSD either in the δ band or in the other frequency ranges studied.

In the θ band, aPSD in both MS groups increased as compared with HC [group factor: $F_{(2,\ 528)} = 24.372$, $p < 0.001$, three-way ANOVA; $\eta^2 = 0.080$; in both cases, $p < 0.01$] (**Figure 1A**). Besides, power density in MS with CNP group exceeded that in MS without CNP group ($p < 0.001$, Duncan test). ROI factor [$F_{(7,\ 528)} = 4.349$, $p < 0.001$; $\eta^2 = 0.050$] showed the decreased power density in the temporal regions as compared with the other areas except for the occipital cortex (in all cases, $p < 0.05$, Duncan test). MS patients with CNP demonstrated increased absolute power density for the prefrontal, central, parietal (a trend), and all temporal regions as compared with the HC group (**Figure 2A**). Besides, we revealed higher aPSD for the mid-temporal derivation of the right hemisphere (T4) as compared with the control (results of *post-hoc* analysis are presented in **Figure 3**). We saw no difference between MS patients with and without CNP or MS patients without CNP and HC in any ROI and derivation.

In the α band, ANOVA showed no group effect on EEG aPSD [$F_{(2,\ 528)} = 1.026$, NS; $\eta^2 = 0.003$] (**Figure 1A**). ROI effect was significant [$F_{(7,\ 528)} = 16.490$, $p < 0.001$; $\eta^2 = 0.175$] that expectedly manifested as a higher EEG power in the occipital and parietal regions compared with other brain regions. Between-group differences were not revealed (**Figure 2A**).

In the $\beta 1$ band, only MS patients in group with CNP showed increased EEG aPSD compared with HC and MS patients without CNP as accounted by the ANOVA main effect group factor [$F_{(2,\ 528)} = 27.635$, $p < 0.001$; $\eta^2 = 0.084$; in both cases; Duncan test, $p < 0.001$] (**Figure 1A**). ANOVA main effect for ROI factor was significant [$F_{(7,\ 528)} = 8.332$, $p < 0.001$; $\eta^2 = 0.089$]: in anterior temporal region, aPSD was lower than in frontal, central, parietal, and occipital regions; also, in prefrontal and mid-temporal regions, it was lower than in central, parietal, and occipital regions (in most cases, $p < 0.001$). *Post-hoc* Duncan test revealed differences in power spectral density between the groups. MS patients with CNP showed a statistically significant increase in aPSD in prefrontal and all temporal regions and a trend to increase aPSD in frontal, parietal, and occipital regions as compared with the HC group (**Figure 2A**). In addition, in the posterior (T6), mid- (T4), and anterior temporal derivations (F8) of the right hemisphere, the spectral power in MS with CNP group was higher than in HC (see **Figure 3**). In the posterior temporal derivation (T6), absolute power in MS patients without CNP tended ($p = 0.059$) to be lower than in MS patients with CNP. We did not reveal any statistically significant differences for this band between MS without CNP and HC groups.

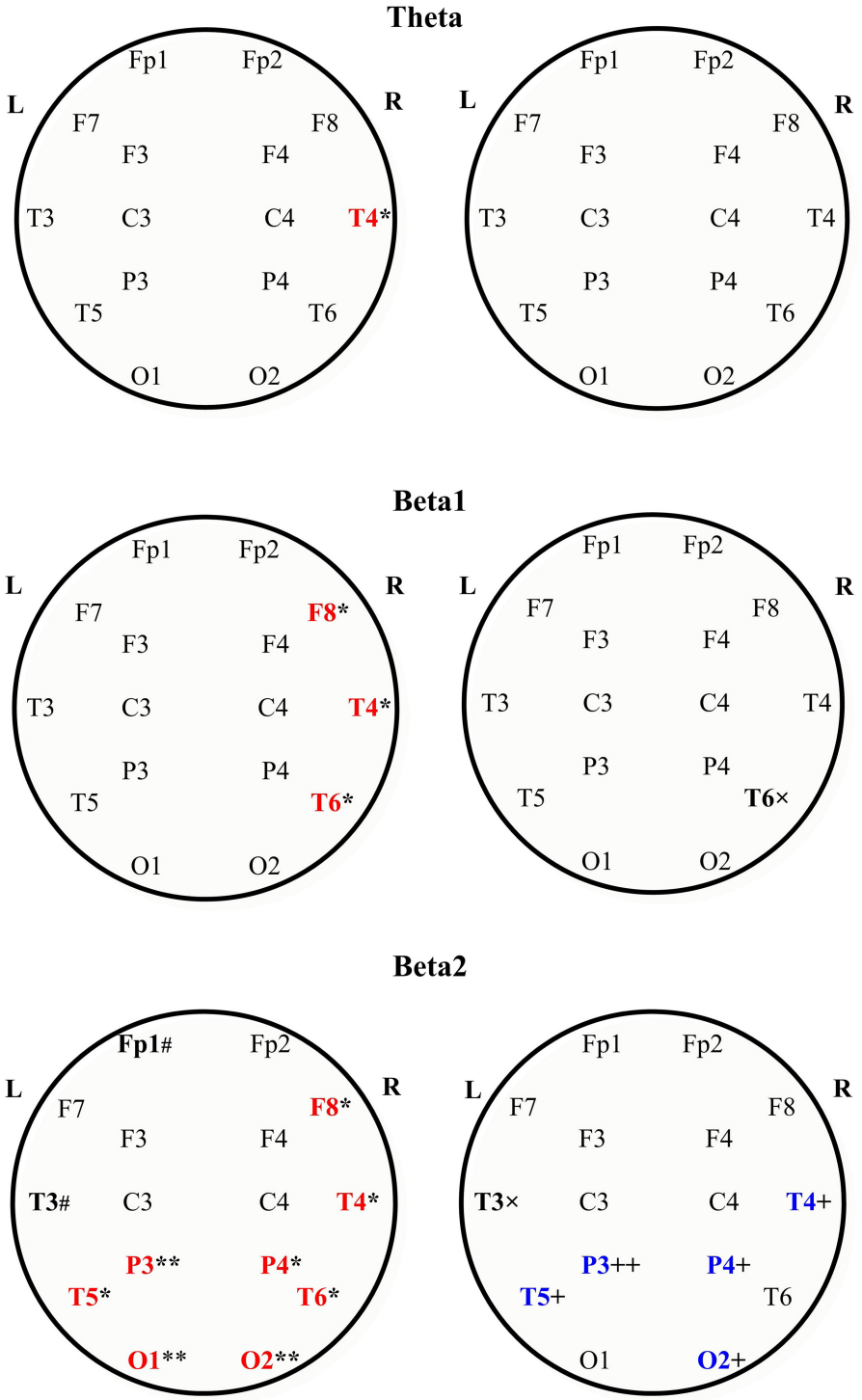

FIGURE 3 | Absolute power spectral density of the scalp EEG in the theta (the upper row), beta1 the middle row), and beta2 bands (the bottom row) in MS patients with and without central neuropathic pain. Topographic view of each scalp electrode positions used in this study. Heads are shown in top view. L, left hemisphere; R, right hemisphere. In each row: MS with CNP—to the left; MS without CNP—to the right. The large bold letters represent the following: red—the channels where the absolute spectral power increased as compared with control; blue—the channels where the absolute spectral power decreased as compared with MS patients with CNP; black—the channels where a trend toward difference with one of the groups was revealed. Boundaries of frequency ranges, Hz; see Materials and Methods; $n = 12$ for each group. *post-hoc* results for spectral analysis of the frequency bands (Duncan test) are shown. Statistically significant differences: $^{*}p < 0.05$; $^{**}p < 0.01$ as compared with control; $^{+}p < 0.05$; $^{++}p < 0.01$ as compared with MS patients with CNP. # Indicates a trend ($0.05 < p < 0.06$) to increase as compared with control; × indicates a trend ($0.05 < p < 0.06$) to decrease as compared with MS with CNP. See the **Supplementary Table** for more information.

In the $\beta 2$ band, similar to the $\beta 1$ band, EEG aPSD increased in MS with CNP group compared with MS without CNP group and HC [ANOVA main effect for group factor: $F_{(2, 528)} = 56.856$, $p < 0.001$; $\eta^2 = 0.167$; in both cases, Duncan test: $p < 0.001$] (**Figure 1A**). ANOVA showed a significant ROI effect [$F_{(7, 528)} = 3.374$, $p = 0.002$; $\eta^2 = 0.035$]: in anterior temporal region, power density was lower than in the central, parietal, and occipital regions (in most cases, $p < 0.05$, Duncan test). In the most ROIs, aPSD increased as compared with HC (**Figure 2A**); also, in central, parietal, occipital, mid-, and posterior temporal regions, absolute power density was higher than in the MS without CNP group. In MS with CNP group, we noted an upward trend for aPSD in the frontal region compared with the HC and MS without CNP groups. In the cortical derivations (excluding central, frontal, and prefrontal in both hemispheres and anterior temporal derivation in the left hemisphere), spectral power exceeded the corresponding values in the HC group (see **Figure 3**). In the mid- and posterior temporal, parietal, and occipital derivations, EEG aPSD in MS without CNP group was lower than in MS with CNP group (except for the occipital derivation of the left hemisphere and the posterior temporal derivation of the right hemisphere). Similar to the other frequency bands, aPSD in MS patients without CNP did not significantly differ from the HC group in any region and derivation.

ANOVA showed no statistically significant interaction effect on EEG aPSD for group × ROI, group × hemisphere, ROI × hemisphere, and group × ROI × hemisphere in any frequency band.

Analysis of Relative Power Spectral Density

In the δ band, EEG rPSD decreased in MS with CNP group compared with HC and MS without CNP groups as accounted by the ANOVA main effect group [$F_{(2, 528)} = 4.979$; $p = 0.007$; $\eta^2 = 0.014$; according to *post-hoc* Duncan test, $p = 0.013$ and $p = 0.005$, respectively] (**Figure 1B**). Relative power density increased from the posterior areas of the cortex to the anterior regions as accounted by the ANOVA main effect ROI [$F_{(7, 528)} = 20.333$; $p < 0.001$; $\eta^2 = 0.206$]. We did not observe significant differences between rPSD in any of the ROIs (**Figure 2B**) and derivations in MS groups and HC. The δ-band rPSD showed no significant main effect for hemisphere [$F_{(1, 528)} = 0.210$; NS].

In the θ band, rPSD, similar to aPSD, increased in both MS groups as compared with HC [ANOVA main effect group factor: $F_{(2, 528)} = 22.146$, $p < 0.001$; $\eta^2 = 0.064$; in both cases, $p < 0.001$] (**Figure 1B**). Power density in MS with CNP group also exceeded that in MS without CNP group ($p = 0.007$). Three-way ANOVA main effect for ROI factor [$F_{(7, 528)} = 15.668$, $p < 0.001$; $\eta^2 = 0.158$] showed decreased rPSD in posterior areas compared with central, prefrontal, and frontal regions; in posterior temporal region, rPSD were lower than in anterior and mid-temporal regions (in most comparisons, $p < 0.01$, Duncan test). In the prefrontal region, rPSD in MS with CNP patients was higher than in the HC group and stronger than in MS without CNP patients (**Figure 2B**). In the anterior temporal region, a trend toward an increase in rPSD was observed in the MS with CNP group compared with the other groups. In parietal and occipital regions, spectral power exceeded control values in both MS groups. Between groups, a statistically significant difference was only found for the anterior frontal derivation in the right hemisphere (Fp2): the relative power density in MS patients with CNP was higher than that in the HC group (**Figure 4**). In MS without CNP group, *post-hoc* Duncan test showed a trend to increase rPSD as compared with HC in the occipital derivations of the left hemisphere ($p = 0.082$). There were no significant differences in rPSD in any of the derivations between MS groups with and without CNP. The θ-band rPSD showed no significant main effect for hemisphere [$F_{(1, 528)} = 0.090$; NS].

In the α band, in contrast, a decrease in relative spectral power in MS groups with and without CNP as compared with HC was found as accounted by the ANOVA main effect group [$F_{(2, 528)} = 15.033$; $p < 0.001$; $\eta^2 = 0.040$; according to Duncan test, $p < 0.001$ and $p = 0.007$, respectively] (**Figure 1B**). In MS patients with CNP, relative PSD also was lower than in MS patients without CNP ($p = 0.006$, Duncan test). ROI effect was significant and strong [$F_{(7, 528)} = 25.973$; $p < 0.001$; $\eta^2 = 0.239$]: power density, as expected, was decreasing toward the frontal areas. In both MS groups, rPSD in parietal and occipital regions decreased as compared with the HC group (**Figure 2B**). However, the detailed analysis showed that only in MS patients with CNP, rPSD was significantly less than in HC in the occipital derivations of both hemispheres and parietal lobe of the right hemisphere (see **Figure 4**), whereas in MS patients without CNP, rPSD in occipital derivations only showed a trend to decrease as compared with the control (for O1, $p = 0.082$; for O2, $p = 0.084$, Duncan test). MS groups with and without CNP did not statistically differ from each other in any ROIs and derivations. The α-band rPSD showed no significant main effect for hemisphere [$F_{(1, 528)} = 1.550$; NS].

In the $\beta 1$ band, the main effect of the group factor was found [$F_{(2, 528)} = 6.937$; $p = 0.001$; $\eta^2 = 0.024$]. According to Duncan test, relative PSD in MS with CNP group exceeded power density in HC and MS without CNP group: $p < 0.001$ and $p = 0.008$, respectively (**Figure 1B**). ANOVA main effect for ROI factor [$F_{(7, 528)} = 2.761$, $p = 0.008$; $\eta^2 = 0.034$] showed the strongest power in the mid-temporal region as compared with prefrontal and posterior areas (in most comparisons, $p < 0.01$, Duncan test). MS groups did not differ between themselves in any ROIs (**Figure 2B**) and derivations. The $\beta 1$-band rPSD showed no significant main effect for hemisphere [$F_{(1, 528)} = 0.012$; NS].

In the $\beta 2$ band, similar to the effect in $\beta 1$ band, rPSD in MS patients with CNP increased as compared with HC ($p < 0.001$) and MS patients without CNP ($p < 0.001$) as accounted by the ANOVA main effect group [$F_{(2, 527)} = 13.293$; $p < 0.001$; $\eta^2 = 0.045$] (**Figure 2B**). In addition, the main effect for ROI factor was statistically significant [$F_{(7, 527)} = 2.116$; $p = 0.040$; $\eta^2 = 0.026$] with the least power in parietal region. Relative PSD in the parietal and occipital regions was stronger in MS with CNP patients as compared with the control and tended to exceed rPSD in MS patients without CNP (**Figure 2B**). Moreover, in MS with CNP group, relative PSD in both occipital derivations (O1 and O2) exceeded control values (see **Figure 4**). The $\beta 2$-band rPSD showed a significant although weak ANOVA main effect for hemisphere [$F_{(1, 527)} = 2.116$; $p = 0.040$; $\eta^2 = 0.026$] with the

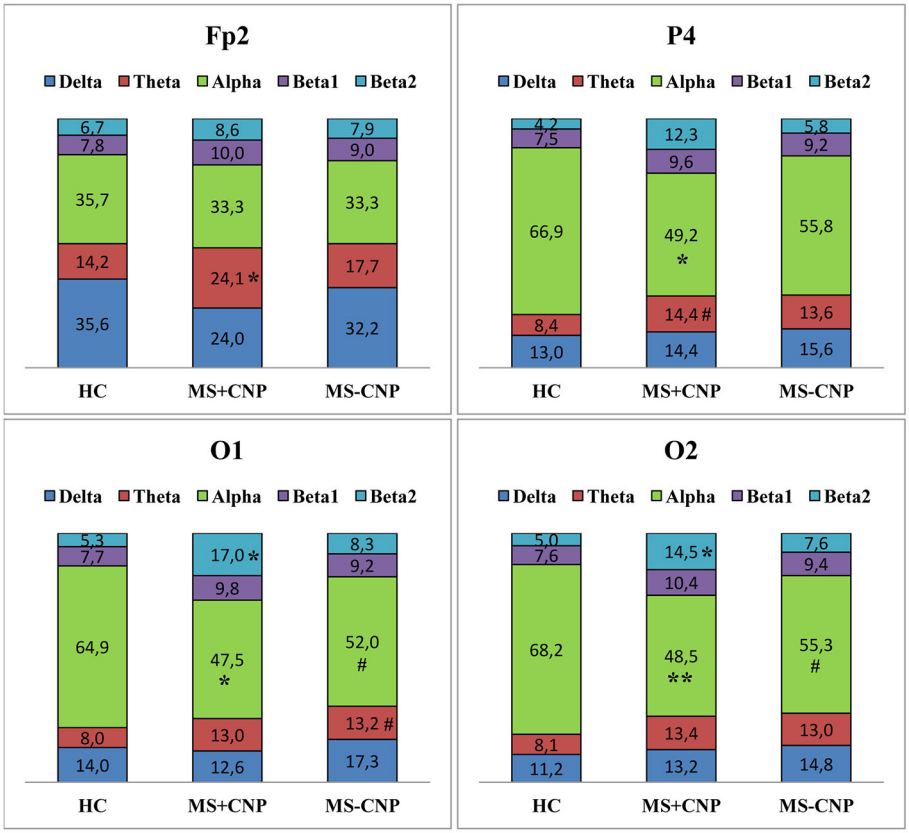

FIGURE 4 | Relative power spectral density (%) of the scalp EEG for Fp2, P4, O1, and O2 electrodes positions in MS patients with and without central neuropathic pain. HC, healthy control; MS + CNP, multiple sclerosis patients with CNP; MS-CNP, multiple sclerosis patients without CNP. *Post-hoc* results for spectral analysis of the frequency bands (Duncan test) are shown. Statistically significant differences: $^{*}p < 0.05$; $^{**}p < 0.01$ as compared with control; # indicates a trend ($0.05 < p \leq 0.084$) as compared with control. See the **Supplementary Table** for more information.

stronger power in the left hemisphere ($p = 0.039$, Duncan test). In MS with CNP group, rPSD in both hemispheres was stronger than in the other groups: in all cases ($p < 0.05$, Duncan test).

ANOVA did not show any statistically significant interaction effect on EEG rPSD for group × ROI, group × hemisphere, ROI × hemisphere, and group × ROI × Hemisphere in any frequency band.

Analysis of Peak Frequency

Table 2 shows the changes in peak frequency. In the δ band, in the MS with CNP group, peak frequencies in the left frontal area (F3) were higher than in the control group. In the MS without CNP group, in contrast, peak frequency in a posterior temporal derivation of the left hemisphere (T5) was lower than in the control group. Peak frequency in MS patients without CNP was lower than in MS patients with CNP in a variety of derivations—the right posterior temporal (T6) and both mid-temporal (T3, T4), the right frontal (F4) and occipital (O2), and both central (C3, C4) derivations.

In the $\beta 2$ band, in the MS with CNP group, peak frequencies in the occipital, parietal, and posterior temporal derivations of the left hemisphere (O1, P3, and T5) were higher than in the control group. In addition, we saw a strong tendency to increase peak frequency for the frontal derivation of the left hemisphere (F7) in comparison with the control group.

No changes of peak frequency were detected in the other frequency bands.

Analysis of Correlations

We failed to reveal any statistically significant correlations between absolute spectral power in the five frequency bands and the intensity of pain on the VAS scale in MS patients with CNP.

We also did not find any correlation between absolute or relative spectral power for any derivations in the frequency bands and EDSS score in MS patients with and without CNP.

DISCUSSION

The present study used a new approach to the analysis of EEG peculiarities in patients with MS, based on whether they have CNP. Although the theta band absolute PSD showed an increase in MS patients both with and without CNP (see **Figure 1A**), the power in the theta as well as beta1, and beta2 ranges in MS

TABLE 2 | Peak frequency (Hz) in the δ and β2-bands in patients with multiple sclerosis.

Electrodes	Results of Kruskal-Wallis ANOVA H (2, $N = 36$); p		Effect size η^2; d_{Cohen}		Healthy control		MS with CNP		MS without CNP	
	δ	β_2	δ	β_2	δ	β_2	δ	β_2	δ	β_2
O1	5.72; 0.06	7.72; 0.02	0.113; 0.713	0.173; 0.916	1.5 (0.8)	21.4 (2.0)	2.2 (0.8)	**24.6 (2.5)***	1.8 (0.9)	22.6 (2.5)
O2	7.81; 0.02	5.61; 0.06	0.176; 0.924	0.109; 0.701	1.7 (0.8)	21.8 (2.3)	2.0 (0.7)	24.2 (2.5)	**1.4 (1.0)**$^{+}$	22.4 (2.8)
P3	5.20; 0.07	9.92; 0.01	0.097; 0.655	0.240; 1.124	2.0 (1.1)	21.5 (2.3)	2.3 (0.8)	**25.2(1.8)****	1.5 (0.8)	22.6 (2.5)
P4	1.63; 0.44	0.02; 0.99	0.011; 0.214	0.060; 0.505	1.9 (0.9)	22.0 (2.5)	2.1 (0.8)	22.7 (2.8)	1.8(0.9)	22.0 (2.2)
C3	7.35; 0.03	0.16; 0.92	0.162; 0.880	0.056; 0.486	1.8 (0.8)	22.2 (2.5)	2.3 (0.7)	22.9 (2.7)	**1.6 (0.7)**$^{+}$	22.6 (2.5)
C4	10.78; 0.00	0.35; 0.84	0.266; 1.204	0.050; 0.460	1.8 (0.8)	22.1 (2.6)	2.4 (0.7)	22.5 (2.7)	**1.3 (0.6)**$^{++}$	21.2 (1.6)
F3	6.89; 0.03	4.16; 0.12	0.148; 0.834	0.066; 0.529	1.6 (0.8)	22.2 (2.4)	**2.3 (0.7)***	24.3 (2.4)	1.7 (1.0)	22.1 (2.3)
F4	6.83; 0.03	0.35; 0.84	0.146; 0.828	0.050; 0.459	1.6(0.9)	21.9 (2.3)	2.3 (0.7)	22.9 (2.8)	**1.5 (1.1)**$^{+}$	22.0 (2.0)
Fp1	5.21; 0.07	4.00; 0.14	0.097; 0.656	0.061; 0.508	1.2 (0.6)	22.2 (2.6)	1.6 (0.5)	24.4 (2.4)	1.3 (0.9)	22.4 (2.6)
Fp2	3.63; 0.16	1.19; 0.55	0.049; 0.455	0.024; 0.316	1.4 (0.5)	22.7 (3.2)	1.9 (0.9)	23.4 (2.7)	1.3 (0.4)	21.6 2.0
T5	6.57; 0.04	7.06; 0.03	0.138; 0.802	0.153; 0.851	2.1 (0.9)	22.4 (2.4)	1.9 (0.7)	**24.7 (2.1)***	**1.3 (0.6)***	22.7 (2.4)
T6	6.10; <0.05	0.91; 0.64	0.124; 0.753	0.033; 0.370	1.5 (0.9)	22.3 (2.4)	2.1 (0.9)	23.2 (2.8)	**1.3 (0.5)**$^{+}$	22.2 (2.3)
T3	6.26; 0.04	2.21; 0.33	0.129; 0.770	0.006; 0.161	1.7 (0.8)	22.4 (2.2)	1.9 (0.7)	24.0 (2.6)	**1.2 (0.6)**$^{+}$	22.4 (2.6)
T4	10.95; 0.00	0.09; 0.95	0.271; 1.220	0.058; 0.495	1.6 (0.9)	23.0 (2.6)	2.2 (0.7)	23.0 (2.7)	**1.2 (0.4)**$^{++}$	22.4 (2.2)
F7	4.00; 0.14	6.73; 0.03	0.061; 0.508	0.143; 0.818	1.3 (0.6)	22.6 (3.2)	1.7 (0.7)	**25.0 (2.1)**$^{\&}$	1.2 (0.4)	22.7 (2.4)
F8	0.35; 0.84	3.86; 0.15	0.050; 0.459	0.056; 0.488	1.3 (0.6)	22.5 (3.1)	1.3 (0.7)	24.1 (2.3)	1.4 (0.8)	22.6 (2.1)

Peak frequency is shown as Mean (Standard Deviation). $^{*}p < 0.05$; $^{**}p < 0.05$; $^{\&}p = 0.052$ as compared with ≪Control≫; $^{+}p < 0.05$; $^{++}p < 0.01$ as compared with ≪MS with CNP≫ by multiple comparisons of mean ranks (2-tailed). Statistically significant differences are shown in bold.

with CNP group exceeded that in patients without pain. Only MS patients with CNP demonstrated the significantly increased absolute spectral powers for the theta, beta1, and beta2 frequency bands in most regions of interest (see **Figure 2A**). Moreover, in the beta2 frequency range, the power exceeded that in patients without pain in almost all the regions examined. Detailed analysis of derivations showed the peculiarities of the differences between MS patients with and without CNP: only MS patients with CNP demonstrated the increased absolute spectral powers for the theta and beta1 frequency bands in the temporal lobes of the right hemisphere, and the increased powers for the beta2 band in the occipital, parietal, and temporal lobes of both hemispheres (see **Figure 3**).

On the basis of EEG and functional low-resolution electromagnetic tomography, peak overactivation mainly within the theta (6–9 Hz) and low beta frequency bands (12–16 Hz) localized to multiple pain-associated areas (primarily to insular, anterior cingulate, prefrontal, and inferior posterior parietal cortices, as well as to primary, secondary, and supplementary somatosensory cortices) and slight overactivation in the high beta frequency band (16–30 Hz) localized to the occipital lobe have been reported for neurogenic pain patients (38). Only using EEG, we observed similar overactivation for the theta (4.0–8.0 Hz) and beta1 (13.0–20.0 Hz) bands in the right hemisphere and the beta2 (20.0–30.0 Hz) band in the posterior areas (including occipital lobes) in MS patients with CNP. Of interest, the main changes in theta and low beta bands frequency ranges were found in the right hemisphere, although there was an equal number of patients with pains on the left and right sides in the group. Below, we consider the possible ways and mechanisms of the revealed EEG changes.

Vazquez-Marrufo et al. (28) identified the increase in high-frequency bands [for beta (22–30 Hz) and gamma (31–45 Hz), not for low beta (13–21 Hz) or theta (5–8 Hz) bands] in both the occipital regions (O1 and O2) and the frontal right hemisphere region (F4) in the relapsing–remitting multiple sclerosis (RRMS) group of patients when the subjects were being stressed during a visuospatial task. Although the authors did not report neuropathic pain in patients, we assume CNP to be a stress factor, the effect of which reflects in the increment of high bands in the EEG.

The increment of high bands could be caused in different ways, for example, by the increase in anxiety (54) [especially in the central part of frontal cortex (55)], by administration of some psychotropic drugs (56, 57) or by physiological artifacts—due to muscle activity in temporal lobes (28). In our research, MS patients with and without CNP did not differ in anxiety (58, 59). All included patients were free of any psychotropic medication during the participation in the study at least for a month. Besides, the changes in the high-frequency band were observed not only in temporal but also in occipital, parietal, central, frontal, and prefrontal regions, which allows discarding muscle influence. Thus, the increment of the beta2 band might be an additional indicator for CNP in MS patients.

The lack of correlation between the degree of disability score and EEG values in any of the brain areas and spectral power bands in MS patients with and without CNP in the present study in principle agreed with the results reported by the other authors for MS patients, regardless CNP (26, 28). Thus, it is unlikely that the overactivation of beta and theta bands in the cortex associated with neurological impairment.

ANOVA revealed the decrease in relative power spectral density in the alpha band in MS patients in posterior areas regardless of the pain. The effect was stronger in MS with CNP group (see **Figures 1B**, **2B**). This finding is in good agreement with the data of Babiloni et al. (60), who demonstrated abnormal cortical sources of resting state in MS patients with both RRMS and SP subtypes compared to the HC group: increase in delta (higher amplitude) and decreased in alpha (lower amplitude) rhythms as estimated by LORETA (normalized relative current density at the cortical voxels). Decrement in the relative spectral power in the alpha band in the posterior brain areas of the right hemisphere, which we identified with a detailed analysis in MS patients with CNP, may testify to a reorganization of the brain EA, which appears as the increase in spectral power in the theta and beta bands in the right hemisphere. This assumption conforms to functional MRI exploration, where patients at the earliest stage of MS showed significantly higher activation in the right frontopolar cortex, the bilateral lateral prefrontal cortices, and the right cerebellum during a cognitive task (13). Lenne et al. (61) found a significant decrease in mutual information in a network of brain areas in patients with RRMS during resting condition. Interhemispheric and right hemisphere mutual information was significantly lower in patients with MS than in control subjects that can reflect the global disconnection of cortico-cortical or cortico-subcortical areas in RRMS. However, the authors did not report whether any patients suffered from CNP.

In the present study, the clinical course of the disease was defined as RRMS in most patients, and there were no cognitively deficient patients according to Mini-Mental State Examination in both experimental groups. However, only MS patients with CNP showed the increase in EA power in the theta band and the low beta band for temporal lobes of the right hemisphere as well as a significant decrease in relative power spectral density in the alpha band in the occipital region.

According to the concept of thalamocortical dysrhythmia, the chronic neurogenic pain mechanism may be triggered at thalamic levels when a decreased excitatory input into the thalamus results in a shifted mode of thalamocortical processing, consisting of a functionally disconnected rhythmic activity at both slow (theta, 4–9 Hz) and fast (beta, 12–30 Hz/gamma, 30–80 Hz) rhythms (33, 36–38). In experiments, Hughes and Crunelli (62) demonstrated that the thalamus could act as an independent pacemaker of α and θ rhythms. Thus, the shifts in the EEG revealed in our study, namely, a decrease in PSD in the alpha band and, on the contrary, an increase in PSD in the theta band, could associate with thalamic deactivation (dysfunction). We said above that all the examined patients were right-handed subjects. Recent MR studies have revealed neuroanatomical features and specifics of the cerebral asymmetry in right-handers. Barrick et al. (63) showed gray matter rightward asymmetry of the thalamus and inferior parietal lobe. MRI diffusion tensor imaging tractography revealed a lateralized right-sided upper brainstem–thalamic function as part of the dominant right-sided cortical/subcortical vestibular system in healthy right-handed subjects (64). Right-lateralized white matter connectivity between the temporoparietal junction and insula was found in the right-handers (65). The authors suggested that disruption of the temporoparietal junction–insula pathway in the right hemisphere affects the salience system in persons with chronic pain. We suggest that the dysfunction in pain connectome-including areas (e.g., thalamus, insula, inferior parietal lobe) in the right-handed MS patients with CNP may manifest by the EEG changes in the right hemisphere.

As for the QEEG analysis in the alpha band, MS patients with and without CNP had no statistically significant difference for the absolute power spectral density and peak frequency compared to each other and the HC group in any regions of the scalp. The findings are contrary to the data of Kim et al. (66) who showed the alpha peak in the EEG to be reduced or not present in MS patients with neuropathic pain: alpha peak frequencies were lower than in the age-matched healthy control within the thalamus and the posterior insula and in the posterior cingulate cortex of the default mode network (the pain connectome-including areas). In previous studies of the other authors, the "slowing down" phenomenon manifesting as a shift toward a lower dominant frequency in patients with neuropathic pain was also noted (36, 67). What could the reason be for the lack of a difference in the alpha band in our study? One of the explanations comes from the early research that has demonstrated significant improvement in the clinical state of the patients with MS and a marked increase in the mean alpha frequency in the parietooccipital region after short intensive immunosuppressive therapy (27). In our study, all the patients, including those with CNP, had previously received corticosteroid therapy that resulted in neurological improvement and could consequently normalize alpha activity. In addition, we cannot exclude that RRMS subtype affects EEG changes that primarily relate to CNP.

Of note, with increasing relative PSD in the $\beta 2$ band in the left hemisphere, β2-peak frequencies increased in the left hemisphere only in MS patients with pain. To interpret the facts mentioned above, we can use the findings of the study, which shows that the left hemisphere closely relates to desynchronizing mesencephalic structures, whereas the right hemisphere, on the contrary, refers to synchronizing diencephalic brain structures (68). Authors assumed that, in a case of CNS disorder, functional state of diencephalon and brainstem structures would determine the role of each hemisphere in compensatory processes. In our studies, the changes in peak frequency in the high beta band in the left hemisphere may provide an additional indicator of disorders of the cortico-subcortical integration in MS patients with CNP and testify for the mid-stem dysfunction. In these patients, the modification of EA in the right hemisphere could be a compensatory response. In general, changes in a resting-state EEG in MS with CNP could reflect the disturbances in cortical communication. This suggestion partly conforms to the data on the decrease in mutual information in brain EA in patients with RRMS (61). Authors suppose that averaged interhemispheric mutual information obtained in a resting state is a marker for the neurological damage induced by RRMS. Meanwhile, in our study, we saw the signs of putative alterations in cortical communication only in patients with CNP.

Remarkably, spectral power in MS patients with CNP differed from the control and rarely from MS patients without CNP.

Spectral power of EA in MS patients without CNP did not significantly differ from the control except for the group effect on absolute and relative PSD in the theta band and group and ROI effects on relative PSD in the alpha band. The fact is that EEG in MS patients without central neuropathic pain tended to change similarly to EEG in MS patients with CNP in the theta and alpha ranges (see **Figures 2**, **4**) but hardly ever reached the significant difference from the other groups. Thus, spectral power in MS patients without CNP occupy an intermediate position between spectral power in MS patients with CNP and the control. We should keep in mind that all of the patients completed the course of treatment before testing and showed significant improvement in suppressing both MS symptoms and neuropathic pain. Several studies reported more severe MS, as assessed by EDSS in patients with neuropathic pain (8, 69). In the present study, in MS patients with and without CNP, EDSS score did not differ, which confirms clinical improvement. Significant EA changes in MS patients with CNP assume to consider central neuropathic pain as a stressful factor that enhances spectral power (not peak frequency) alterations typical for MS.

We have previously observed the increase in absolute spectral power in the high-frequency bands in other types of pathology, associated with a malfunction in the nervous regulation, for example, in patients with brain–gut dysregulation burdened by CNP (70, 71). We cannot exclude that the beta bands increment in the EEG might be a marker of CNS pathology that appears as neuropathic and psychosomatic disorders. The difference between spectral EEG patterns and peak frequencies in MS patients with and without CNP could represent CNS alterations related to central neuropathic pain in MS patients.

However, a small number of patients in the groups with the well-known high variability of MS courses are a potential limitation of the study. Another limitation lies within EEG recording after the course of corticosteroids in MS patients, although the period after corticosteroid withdrawal was at least a month. We could not find direct experimental evidence that corticosteroid therapy can affect the main EEG frequencies. However, polysomnographic recordings showed that during prolonged treatment with corticosteroids (for 10 days), early RRMS patients demonstrated several sleep–EEG alterations, in particular, changes in REM sleep, slow-wave sleep, and some others (72). Among the limitations of this study, we also consider a small number of EEG electrodes and a low number of the epochs analyzed. A sound conclusion requires further research.

DATA AVAILABILITY STATEMENT

All datasets generated for this study are included in the article/**Supplementary Material**.

ETHICS STATEMENT

This study was carried out in accordance with the recommendations of the Ethical Committee of the Institute of General Pathology and Pathophysiology (the project approval protocol Number 5 of November 25, 2016) and was approved by the Ethical Committee (final approval protocol Number 1a of April 03, 2018). All participants signed informed consent after a complete explanation of the study in accordance with the Helsinki Declaration of 1964 with all subsequent amendments.

AUTHOR CONTRIBUTIONS

NK: substantial contributions to acquisition of data, to analysis and interpretation of data. MC: substantial contributions to acquisition of data, to analysis, and drafting the article. MK: substantial contributions to conception and design, revising the article critically for important intellectual content. NY: substantial contributions to conception and design, final approval of the version to be published.

ACKNOWLEDGMENTS

We thank Mr. Viktor Komkov for the technical assistance.

SUPPLEMENTARY MATERIAL

The Supplementary Material for this article can be found online at: https://www.frontiersin.org/article/10.3389/fneur.2019.01380/full#supplementary-material

REFERENCES

1. Ghajarzadeh M, Jalilian R, Sahraian MA, Moghadasi AN, Azimi A, Mohammadifar M, et al. Pain in patients with multiple sclerosis. *Maedica*. (2018) 13:125–30. doi: 10.26574/maedica.2018.13.2.125
2. Green R, Cutter G, Friendly M, Kister I. Which symptoms contribute the most to patients' perception of health in multiple sclerosis? *Mult Scler J Exp Transl Clin*. (2017) 3:2055217317728301. doi: 10.1177/2055217317728301
3. Minagar A. *Multiple Sclerosis: An Overview of Clinical Features, Pathophysiology, Neuroimaging, and Treatment Options*. Colloquium series on Integrated Systems Physiology: From Molecule to Function to Disease. Granger DN and Granger JP, series editors. San Rafael, CA: Morgan & Claypool Life Sciences (2014). doi: 10.4199/C00116ED1V01Y201408ISP055
4. Schmidt S, Naranjo JR, Brenneisen C, Gundlach J, Schultz C, Kaube H, et al. Pain ratings, psychological functioning and quantitative EEG in a controlled study of chronic back pain patients. *PLoS ONE*. (2012) 7:e31138. doi: 10.1371/journal.pone.0031138
5. Bermejo PE, Oreja-Guevara C, Díez-Tejedor E. Pain in multiple sclerosis: prevalence, mechanisms, types and treatment. *Rev Neurol*. (2010) 50:101–8. [In Spanish]. doi: 10.33588/rn.5002.2008613
6. Schmidt TE, Yakhno NN. *Multiple Sclerosis*. Moscow: Medicina (2003). [In Russian].
7. Moisset X, Ouchchane L, Guy N, Bayle DJ, Dallel R, Clavelou P. Migraine headaches and pain with neuropathic characteristics: comorbid conditions in patients with multiple sclerosis. *Pain*. (2013) 154:2691–9. doi: 10.1016/j.pain.2013.07.050
8. Truini A, Galeotti F, La Cesa S, Di Rezze S, Biasiotta A, Di Stefano G, et al. Mechanisms of pain in multiple sclerosis: a combined clinical and neurophysiological study. *Pain*. (2012) 153:2048–54. doi: 10.1016/j.pain.2012.05.024

9. Österberg A, Boivie J, Thuomas KA. Central neuropathic pain in multiple sclerosis - prevalence and clinical characteristics. *Eur J Pain.* (2005) 9:531–42. doi: 10.1016/j.ejpain.2004.11.005
10. Svendsen KB, Jensen TS, Hansen HJ, Bach FW. Sensory function and quality of life in patients with multiple sclerosis and pain. *Pain.* (2005) 114:473–81. doi: 10.1016/j.pain.2005.01.015
11. International Association for the Study of Pain. *IASP Taxonomy*. International Association for the Study of Pain (2014). Available online at: https://www.iasp-pain.org/terminology?navItemNumber=576#Centralneropathicpain (accessed August 22, 2019).
12. Canavero S, Bonicalzi V. *Central Neuropathic Pain: Pathophysiology, Diagnosis and Management*. New York, NY: Cambridge University Press (2007). p. 22.
13. Audoin B, Ibarrola D, Ranjeva JP, Confort-Gouny S, Malikova I, Ali-Chérif A, et al. Compensatory cortical activation observed by fMRI during a cognitive task at the earliest stage of MS. *Hum Brain Mapp.* (2003) 20:51–8. doi: 10.1002/hbm.10128
14. Kukushkin ML. Pathophysiological mechanisms of pain syndromes. *Bol'.* (2003) 1:5–12. [In Russian]. Available online at: https://elibrary.ru/download/elibrary_23774684_20182626.pdf
15. Walton KD, Llinás RR. Chapter 13: Central pain as a thalamocortical dysrhythmia: a thalamic efference disconnection? In: Kruger L, Light AR, editors. *Translational Pain Research: From Mouse to Man. Frontiers in Neuroscience*. Boca Raton, FL: CRC Press (2010), p. 301-14. doi: 10.1201/9781439812105-c13
16. Wang G, Thompson SM. Maladaptive homeostatic plasticity in a rodent model of central neuropathic pain: thalamic hyperexcitability after spinothalamic tract lesions. *J Neurosci.* (2008) 28:11959–69. doi: 10.1523/JNEUROSCI.3296-08.2008
17. Toropina GG, Shmidt TE. Pain in multiple sclerosis. *Nevrologicheskij zhurnal.* (2003) 1:40–45. [In Russian]. Available online at: https://elibrary.ru/item.asp?id=17239945
18. Osborne TL, Jensen MP, Ehde DM, Hanley MA, Kraft G. Psychosocial factors associated with pain intensity, pain-related interference, and psychological functioning in persons with multiple sclerosis and pain. *Pain.* (2007) 127:52–62. doi: 10.1016/j.pain.2006.07.017
19. Lucchinetti CF, Popescu BF, Bunyan RF, Moll NM, Roemer SF, Lassmann H, et al. Inflammatory cortical demyelination in early multiple sclerosis. *N Engl J Med.* (2011) 365:2188–97. doi: 10.1056/NEJMoa1100648
20. Pelletier J, Suchet L, Witjas T, Habib M, Guttmann CR, Salamon G, et al. A longitudinal study of callosal atrophy and interhemispheric dysfunction in relapsing-remitting multiple sclerosis. *Arch Neurol.* (2001) 58:105–11. doi: 10.1001/archneur.58.1.105
21. Poser CM, Brinar VV. Epilepsy and multiple sclerosis. *Epilepsy Behav.* (2003) 4:6–12. doi: 10.1016/S1525-5050(02)00646-7
22. Iragui-Madoz VJ. Electrophysiology of multiple sclerosis. In: Daly DD, Pedley TA, editors. *Current Practice of Clinical Electroencephalography*. 2nd ed. New York, NY: Raven (1990). p. 708–38.
23. Leocani L, Comi G. Neurophysiological investigations in multiple sclerosis. *Curr Opin Neurol.* (2000) 13:255–61. doi: 10.1097/00019052-200006000-00004
24. Leocani L, Locatelli T, Martinelli V, Rovaris M, Falautano M, Filippi M, et al. Electroencephalographic coherence analysis in multiple sclerosis: correlation with clinical, neuropsychological, and MRI findings. *J Neurol Neurosurg Psychiatry.* (2000) 69:192–8. doi: 10.1136/jnnp.69.2.192
25. Harrer G, Harrer H, Kofler B, Haas R. Multiple sclerosis and the electroencephalogram (computer EEG studies). [Article in German]. *Wien Med Wochenschr.* (1985) 135:38–40.
26. Pakalnis A, Drake ME Jr, Dadmehr N, Weiss K. Evoked potentials and EEG in multiple sclerosis. *Electroencephalogr Clin Neurophysiol.* (1987) 67:333–6. doi: 10.1016/0013-4694(87)90120-9
27. Colon E, Hommes OR, de Weerd, JP. Relation between EEG and disability scores in multiple sclerosis. *Clin Neurol Neurosurg.* (1981) 83:163–8. doi: 10.1016/0303-8467(81)90018-4
28. Vazquez-Marrufo M, Gonzalez-Rosa JJ, Vaquero E, Duque P, Borges M, Gomez C, et al. Quantitative electroencephalography reveals different physiological profiles between benign and remitting-relapsing multiple sclerosis patients. *BMC Neurol.* (2008) 8:44. doi: 10.1186/1471-2377-8-44
29. Vazquez-Marrufo M, Gonzalez-Rosa JJ, Vaquero E, Duque P, Escera C, Borges M, et al. Abnormal ERPS and high frequency bands power in multiple sclerosis. *Intern J Neurosci.* (2008) 118:27–38. doi: 10.1080/00207450601041906
30. Facchetti D, Mai R, Colombo A, Capra R, Marciano N, Gasparotti R, et al. Limited clinical significance of traditional and quantitative EEG in multiple sclerosis. *Acta Neurol Belg.* (1994) 94:245–50.
31. Liu CC, Franaszczuk P, Crone NE, Jouny C, Lenz FA. Studies of properties of "Pain Networks" as predictors of targets of stimulation for treatment of pain. *Front Integr Neurosci.* (2011) 5:80. doi: 10.3389/fnint.2011.00080
32. Chen AC, Rappelsberger P. Brain and human pain: topographic EEG amplitude and coherence mapping. *Brain Topogr.* (1994) 7:129–40. doi: 10.1007/BF01186771
33. Llinás R1, Urbano FJ, Leznik E, Ramírez RR, van Marle HJ. Rhythmic and dysrhythmic thalamocortical dynamics: GABA systems and the edge effect. *Trends Neurosci.* (2005) 28:325–33. doi: 10.1016/j.tins.2005.04.006
34. Michels L, Moazami-Goudarzi M, Jeanmonod D. Correlations between EEG and clinical outcome in chronic neuropathic pain: surgical effects and treatment resistance. *Brain Imaging Behav.* (2011) 5:329–48. doi: 10.1007/s11682-011-9135-2
35. Sarnthein J, Jeanmonod D. High thalamocortical theta coherence in patients with neurogenic pain. *NeuroImage.* (2008) 39:1910–7. doi: 10.1016/j.neuroimage.2007.10.019
36. Vuckovic A, Jajrees M, Purcell M, Berry H, Fraser M. Electroencephalographic predictors of neuropathic pain in subacute spinal cord injury. *J Pain.* (2018) 19:e1-1256.e17. doi: 10.1016/j.jpain.2018.04.011
37. Sarnthein J, Stern J, Aufenberg C, Rousson V, Jeanmonod D. Increased EEG power and slowed dominant frequency in patients with neurogenic pain. *Brain.* (2006) 129(Pt 1):55–64. doi: 10.1093/brain/awh631
38. Stern J, Jeanmonod D, Sarnthein J. Persistent EEG overactivation in the cortical pain matrix of neurogenic pain patients. *NeuroImage.* (2006) 31:721–31. doi: 10.1016/j.neuroimage.2005.12.042
39. Hassan MA, Fraser M, Conway BA, Allan DB, Vuckovic A. The mechanism of neurofeedback training for treatment of central neuropathic pain in paraplegia: a pilot study. *BMC Neurol.* (2015) 15:200. doi: 10.1186/s12883-015-0445-7
40. Mably AJ, Colgin LL. Gamma oscillations in cognitive disorders. *Curr Opin Neurobiol.* (2018) 52:182–7. doi: 10.1016/j.conb.2018.07.009
41. Kurtzke JF. Rating neurological impairment in multiple sclerosis: an expanded disability status scale (EDDS). *Neurology.* (1983) 33:1444–52. doi: 10.1212/WNL.33.11.1444
42. McDonald IW, Compston A, Edah G, Goodkin D, Hartung HP, Lublin FD, et al. Recommended diagnostic criteria for multiple sclerosis: guidelines from the international panel on the diagnostic of multiple sclerosis. *Ann Neurol.* (2001) 50:121–7. doi: 10.1002/ana.1032
43. Folstein MF, Folstein SE, McHugh PR. "Mini-mental state." A practical method for grading the cognitive state of patients for the clinician. *J Psychiatr Res.* (1975) 12:189–98. doi: 10.1016/0022-3956(75)90026-6
44. Lublin FD, Reingold SC. Defining the clinical course of multiple sclerosis: result of an international survey. National Multiple Sclerosis Society (USA). Advisory Committee on Clinical Trials of New Agents in Multiple Sclerosis. *Neurology.* (1996) 46:907–11. doi: 10.1212/WNL.46.4.907
45. Tewarie P, Schoonheim MM, Stam CJ, van der Meer ML, van Dijk BW, Barkhof F, et al. Cognitive and clinical dysfunction, altered MEG resting-state networks and thalamic atrophy in multiple sclerosis. *PLoS ONE.* (2013) 8:e69318. doi: 10.1371/journal.pone.0069318
46. Mitrofanov AA. *Computer Analysis and Topographic Mapping of Electrical Brain Activity with a Neurometric Bank of EEG Data (Application Description).* (Moscow) (2005). p. 63 [In Russian].
47. Gasser T, Bächer P, Möcks J. Transformation towards the normal distribution of broad band spectral parameters of the EEG. *Electroencephalogr Clin Neurophysiol.* (1982) 53:119–24. doi: 10.1016/0013-4694(82)90112-2
48. Yigit S, Mendes M. Which effect size measure is appropriate for one-way and two-way ANOVA models? A monte carlo simulation study. *Rev Stat J.* (2018) 16:295–313. Available online at: https://www.researchgate.net/publication/319207513_Which_Effect_Size_Measure_is_Appropriate_for_One-Way_and_Two-Way_ANOVA_Models_A_Monte_Carlo_Simulation_Study

49. Levine T, Hullett C. Eta squared, partial eta squared, and misreporting of effect size in communication research. *Hum Commun Res.* (2002) 28:612–25. doi: 10.1111/j.1468-2958.2002.tb00828.x
50. Draper SW. *Effect Size*. (2011). Available online at: http://www.psy.gla.ac.uk/~steve/best/effect.html
51. *Psychometrica. Freeware. Computation of Effect Sizes*. Available online at: https://www.psychometrica.de/effect_size#
52. Cohen J. *Statistical Power Analysis for the Behavioral Sciences (2. Auflage).* Hillsdale, NJ: Erlbaum (1988).
53. Benjamini Y, Hochberg, Y. Controlling the false discovery rate: a practical and powerful approach to multiple testing. *J R Statist Soc. B.* (1995) 57:289–300. doi: 10.1111/j.2517-6161.1995.tb02031.x
54. Sviderskaia NE, Prudnikov VN, Antonov AG. Characteristics of EEG signs of anxiety in human. *Zh Vyssh Nerv Deiat Im I P Pavlova.* (2001) 51:158–65. [In Russian]. Available online at: https://elibrary.ru/item.asp?id=14959936
55. Roohi-Azizi M, Azimi L, Heysieattalab S, Aamidfar M. Changes of the brain's bioelectrical activity in cognition, consciousness, and some mental disorders. *Med J Islam Repub Iran*. (2017) 31:53. doi: 10.14196/mjiri.31.53
56. Adamaszek M, Khaw AV, Buck U, Andresen B, Thomasius R.Evidence of neurotoxicity of ecstasy: sustained effects on electroencephalographic activity in polydrug users. *PLoS ONE*. (2010) 5:e14097. doi: 10.1371/journal.pone.0014097
57. Coutin-Churchman P, Añez P, Uzcátegui M, Alvarez L, Vergara F, Mendez L, et al. Quantitative spectral analysis of EEG in psychiatry revisited: drawing signs out of numbers in a clinical setting. *Clin Neurophysiol.* (2003) 114:2294–306. doi: 10.1016/S1388-2457(03)00228-1
58. Churyukanov MV, Alexeev VV, Kukushkin ML, Krupina NA, Toropina GG, Yakhno NN. Clinical, psychological and neurophysiological aspects of central neuropathic pain in multiple sclerosis. *Eur J Pain Suppl.* (2011) 5:141. doi: 10.1016/S1754-3207(11)70484-9
59. Churukanov MV, Alekseev VV, Kukushkin ML, Toropina GG, Yakhno NN. The clinical and electrophysiological particulars of patients with central neuropathic pain in multiple sclerosis. *Rossiyskiy Zhurnal Boli (Russian Journal of Pain, formerly known as Bol').* (2011) 3–4:8–12. [In Russian]. Available online at: https://painrussia.ru/russian-Journal-of-Pain/32%2011.pdf
60. Babiloni C, Del Percio C, Capotosto P, Noce G, Infarinato F, Muratori C, et al. Cortical sources of resting state electroencephalographic rhythms differ in relapsing-remitting and secondary progressive multiple sclerosis. *Clin Neurophysiol.* (2016) 127:581–90. doi: 10.1016/j.clinph.2015.05.029
61. Lenne B, Blanc JL, Nandrino JL, Gallois PH, Hautecœur P, Pezard L. Decrease of mutual information in brain electrical activity of patients with relapsing-remitting multiple sclerosis. *Behav Neurol.* (2013) 27:201–12. doi: 10.3233/BEN-120278
62. Hughes SW, Crunelli V. Just a phase they're going through: the complex interaction of intrinsic high-threshold bursting and gap junctions in the generation of thalamic alpha and theta rhythms. *Int J Psychophysiol.* (2007) 64:3–17. doi: 10.1016/j.ijpsycho.2006.08.004
63. Barrick TR, Mackay CE, Prima S, Maes F, Vandermeulen D, Crow TJ, et al. Automatic analysis of cerebral asymmetry: an exploratory study of the relationship between brain torque and planum temporale asymmetry. *Neuroimage.* (2005) 24:678–91. doi: 10.1016/j.neuroimage.2004.09.003
64. Dieterich M, Kirsch V, Brandt T. Right-sided dominance of the bilateral vestibular system in the upper brainstem and thalamus. *J Neurol.* (2017) 264(Suppl. 1):55–62. doi: 10.1007/s00415-017-8453-8
65. Kucyi A, Moayedi M, Weissman-Fogel I, Hodaie M, Davis KD. Hemispheric asymmetry in white matter connectivity of the temporoparietal junction with the insula and prefrontal cortex. *PLoS ONE*. (2012)7:e35589. doi: 10.1371/journal.pone.0035589
66. Kim JA, Bosma RL, Hemington KS, Rogachov A, Osborne NR, Cheng JC, et al. Neuropathic pain and pain interference are linked to alpha-band slowing and reduced beta-band magnetoencephalography activity within the dynamic pain connectome in patients with multiple sclerosis. *Pain*. (2019) 160:187–97. doi: 10.1097/j.pain.0000000000001391
67. Vuckovic A, Hasan MA, Fraser M, Conway BA, Nasseroleslami B, Allan DB. Dynamic oscillatory signatures of central neuropathic pain in spinal cord injury. *J Pain.* (2014) 15:645–55. doi: 10.1016/j.jpain.2014.02.005
68. Boldyreva GN, Sharova EV, Dobronravova IS. The role of cerebral regulatory structures in formation of the human EEG. *Fiziol Cheloveka.* (2000) 26:19–34. [In Russian]. doi: 10.1007/BF02760368
69. Hadjimichael O, Kerns RD, Rizzo MA, Cutter G, Vollmer T. Persistent pain and uncomfortable sensations in persons with multiple sclerosis. *Pain.* (2007) 127:35–41. doi: 10.1016/j.pain.2006.07.015
70. Krupina NA, Khadzegova FR, Maychuk EU, Kukushkin ML, Kryzhanovskii GN. Analysis of brain electrical activity in patients with irritable bowel syndrome. *Bol'.* (2008) 2:6–12. [In Russian]. Available online at: https://elibrary.ru/item.asp?id=11580755
71. Krupina NA, Malakhova EV, Loranskaya ID, Kukushkin ML, Kryzhanovskii GN. Analysis of brain electrical activity in patients with gallbladder dysfunction. *Bol'.* (2005) 3:34–41. [In Russian]. Available online at: https://elibrary.ru/item.asp?id=20165641
72. Antonijevic IA, Steiger A. Depression-like changes of the sleep-EEG during high dose corticosteroid treatment in patients with multiple sclerosis. *Psychoneuroendocrinology.* (2003) 28:780–95. doi: 10.1016/S0306-4530(02)00085-9

Conflict of Interest: The authors declare that the research was conducted in the absence of any commercial or financial relationships that could be construed as a potential conflict of interest.

frontiers in Immunology

ORIGINAL RESEARCH
published: 24 January 2020
doi: 10.3389/fimmu.2020.00023

Cytokine Levels in Neural Pain in Leprosy

Débora Bartzen Moraes Angst[1,2]*, *Roberta Olmo Pinheiro*[1], *Joyce Soares da Silva Vieira*[1], *Roberta Arnoldi Cobas*[3], *Mariana de Andréa Vilas-Boas Hacker*[1], *Izabela Jardim Rodrigues Pitta*[1,2], *Louise Mara Giesel*[1], *Euzenir Nunes Sarno*[1] and *Márcia Rodrigues Jardim*[1,2,4]

[1] Leprosy Laboratory, Oswaldo Cruz Foundation (Fiocruz), Rio de Janeiro, Brazil, [2] Postgraduate Program in Neurology of Federal University of Rio de Janeiro State (UNIRIO), Rio de Janeiro, Brazil, [3] Endocrinology Discipline of the Faculty of Medical Sciences, State University of Rio de Janeiro (UERJ), Rio de Janeiro, Brazil, [4] Neurology Discipline of the Faculty of Medical Sciences, State University of Rio de Janeiro (UERJ), Rio de Janeiro, Brazil

Pain is a frequent symptom in leprosy patients. It may be predominantly nociceptive, as in neuritis, or neuropathic, due to injury or nerve dysfunction. The differential diagnosis of these two forms of pain is a challenge in clinical practice, especially because it is quite common for a patient to suffer from both types of pain. A better understanding of cytokine profile may serve as a tool in assessing patients and also help to comprehend pathophysiology of leprosy pain. Patients with leprosy and neural pain ($n = 22$), neuropathic pain ($n = 18$), neuritis (nociceptive pain) ($n = 4$), or no pain ($n = 17$), further to those with diabetic neuropathy and neuropathic pain ($n = 17$) were recruited at Souza Araujo Out-Patient Unit (Fiocruz, Rio de Janeiro, RJ, Brazil). Serum levels of IL1β, IL-6, IL-10, IL-17, TNF, CCL-2/MCP-1, IFN-γ, CXCL-10/IP-10, and TGF-β were evaluated in the different Groups. Impairment in thermal or pain sensitivity was the most frequent clinical finding (95.5%) in leprosy neuropathy patients with and without pain, but less frequent in Diabetic Group (88.2%). Previous reactional episodes have occurred in patients in the leprosy and Pain Group ($p = 0.027$) more often. Analysis of cytokine levels have demonstrated that the concentrations of IL-1β, TNF, TGF-β, and IL-17 in serum samples of patients having leprosy neuropathy in combination with neuropathic or nociceptive pain were higher when compared to the samples of leprosy neuropathy patients without pain. In addition, these cytokine levels were significantly augmented in leprosy patients with neuropathic pain in relation to those with neuropathic pain due to diabetes. IL-1β levels are an independent variable associated with both types of pain in patients with leprosy neuropathy. IL-6 concentration was increased in both groups with pain. Moreover, CCL-2/MCP-1 and CXCL-10/IP-10 levels were higher in patients with diabetic neuropathy over those with leprosy neuropathy. In brief, IL-1β is an independent variable related to neuropathic and nociceptive pain in patients with leprosy, and could be an important biomarker for patient follow-up. IL-6 was higher in both groups with pain (leprosy and diabetic patients), and could be a therapeutic target in pain control.

Keywords: leprosy, nociceptive pain, neuropathic pain, cytokines, diabetes, neuropathy

OPEN ACCESS

Edited by:
Larissa Garcia Pinto, King's College London, United Kingdom

Reviewed by:
Edessa Negera Gobena, London School of Hygiene and Tropical Medicine, University of London, United Kingdom
Aparecida Tiemi Nagao-Dias, Federal University of Ceara, Brazil

***Correspondence:**
Débora Bartzen Moraes Angst
deborabma@gmail.com

Specialty section:
This article was submitted to Multiple Sclerosis and Neuroimmunology, a section of the journal Frontiers in Immunology

Received: *30 September 2019*
Accepted: *07 January 2020*
Published: *24 January 2020*

Citation:
Angst DBM, Pinheiro RO, Vieira JSdS, Cobas RA, Hacker MA, Pitta IJR, Giesel LM, Sarno EN and Jardim MR (2020) Cytokine Levels in Neural Pain in Leprosy. Front. Immunol. 11:23. doi: 10.3389/fimmu.2020.00023

INTRODUCTION

Despite ongoing efforts to eradicate leprosy in Brazil, it remains an endemic disease and a public health challenge (1). Nerve trunk involvement in leprosy results in debilitating deformities in 20% of all patients (2). The accompanying neural pain, experienced by up to 70% of these patients, presents as nociceptive (neuritis) or neuropathic pain resulting from damage or disease of sensory pathway (2–5). Currently, pain is a functional disability not regarded an inability when leprosy patients are monitored by the Brazilian Department of Health. As a result, the disability of leprosy patients may be underestimated.

Leprosy is a chronic infectious disease caused by *Mycobacterium leprae*, an intracellular pathogen that preferentially infects macrophages and Schwann cells.

Mycobacterium leprae alters mitochondrial glucose metabolism in Schwann cell (SC). This affects the complicated modulation of Schwann cell and axons, resulting in a reduction of axonal metabolism, demyelination, and loss of axons (6).

Schwann cells also play an important role in pain modulation. SC can proliferate and secrete soluble mediators which control Wallerian degeneration and regeneration. Amongst the soluble mediators are pro-inflammatory cytokines that function as chemoattractant, but may also sensitize nociceptors (7).

Some studies have indicated cytokines as possible pain biomarkers. A number of preclinical and clinical studies are being developed (8) by using biomarkers in a correlation with patients with pain. For example, IL-6 is a prominently pro-inflammatory cytokine secreted by mast cells, macrophages, lymphocytes, neurons, and glial cells (9). Under certain conditions, however, it can modulate anti-inflammatory responses (10).

In animal models, IL-6 has been shown to mediate neuropathic pain development (11). In fact, some studies have demonstrated that patients with neuropathic pain due to intervertebral disc herniation or the carpal tunnel syndrome had increased serum IL-6 and TNF (12, 13). Similar reports of increased serum IL-6 have occurred in patients with post-herpetic neuralgia, which have also correlated quantitatively with pain intensity in neuralgia (14). In rats, TNF seems to be responsible for the neuropathic pain caused by nerve injury (15). In animal models of neuropathic pain, the involvement of proinflammatory cytokines such as TNF, IL-1β, and IL-6 after peripheral nerve involvement has been well-documented (15, 16). Regional complex pain syndromes, peripheral neuropathy, and neuropathic pain associated with spinal cord injury are known to be associated with increased serum IL-6 and TNF levels (17–19).

IL-1β is a pluripotent cytokine produced and secreted under conditions of stress by immune cells including macrophages, monocytes, and microglia (9). This cytokine is one of many agents involved in neuropathic pain, and its production may also be related to the presence of specific immunological markers (4).

A study with rats and mice undergoing transient focal demyelination of sciatic nerve have reported increased expression of CCL-2/MCP-1 and CXCL-10/IP-10 receptors (20).

Although prior studies have investigated pain in leprosy (2, 21, 22), no study has currently provided alternatives to better differentiate nociceptive from neuropathic pain.

In addition, the evaluation of cytokines in most studies was limited to the pain resulting from acute inflammatory episodes known as leprosy reactions. However, high levels of pro-inflammatory cytokines during a reaction episode can mistake the accurate understanding of the mechanisms involved in leprosy pain. Furthermore, the treatment of pain is not specific, highlighting the need of studies focusing on the examination of neural pain mediators and mechanisms. The present report has investigated the cytokine profile in serum samples of leprosy patients with pain.

METHODOLOGY

Study Design

This retrospective cross-sectional study is based on data collected from Souza Araujo Out-Patient Unit (ASA) (Fiocruz, Rio de Janeiro, RJ, Brazil) and Diabetes Outpatient Clinic of Pedro Ernesto University Hospital (State University of Rio de Janeiro, Rio de Janeiro, RJ, Brazil). Medical records and a database of leprosy neuropathy patients evaluated at ASA from January 1998 to December 2017 were also the source of data collection, together with data regarding histopathology of nerve biopsy to determine neuropathy etiology. During the aforementioned period of time, 662 biopsies were performed. Within the biopsied patients, 311 were diagnosed with leprosy. Out of the 311 leprosy patients, 89 had pain during the evaluation prior to nerve biopsy, while 222 had no pain. All the biopsied patients having confirmed leprosy neuropathy in combination with neural pain were selected to the study. The other patients were selected to take part into two comparative groups, namely, one group consisting of painless leprosy neuropathy patients, the other group consisting of patients with diabetic neuropathy in combination with neuropathic pain. The total number of patients was divided up into three groups, as follows:

Group A: Leprosy Neuropathic Pain Group (89 patients); Group B: Painless Leprosy Neuropathy Comparative Group (50 patients); and Group C: Diabetic Neuropathic Pain Comparative Group with Type II Diabetes Mellitus (23 patients).

Patients with comorbidities known to cause peripheral neuropathy such as rheumatologic diseases, alcoholism, hypothyroidism, diabetes (except Group C patients), B12 hypovitaminosis, HIV or viral hepatitis, patients in corticosteroid treatment or in reaction, further to patients with incomplete medical records or without a laboratory-stored blood sample were excluded from this study. Accordingly, 106 patients were excluded. Out of them, 67 patients were excluded from Group A, 33 patients were excluded from Group B, and 6 patients from Group C. After applying the exclusion criteria, 56 patients have remained in the study: 22 in Group A; 17 in Group B; and 17 in Group C.

The following flowchart describes the methodology used in the present study (**Figure 1**). As soon as the inclusion and exclusion criteria were met, epidemiological, clinical, immunological, and neurophysiological data were collected. Epidemiological, clinical, and immunological data were obtained

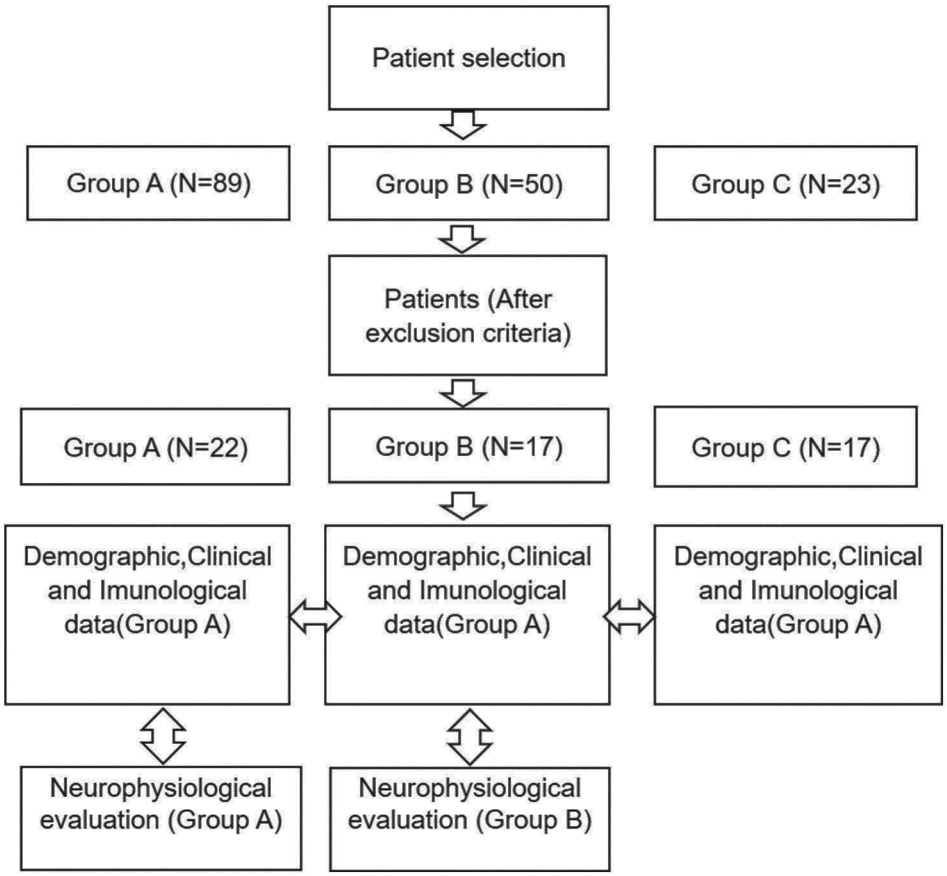

FIGURE 1 | Methodology flowchart. Group A: Leprosy neuropathic pain group; Group B: painless leprosy neuropathy comparative group; Group C: diabetic neuropathic pain comparative group with type II diabetes mellitus.

from all patients. Neurophysiological data were not collected from diabetic patients, considering these patients were not submitted to such examinations.

Case Definitions

Neuropathic pain was defined as pain caused by damage or disease affecting the somatosensory nervous system, according to International Association for the Study of Pain. Neuropathic pain diagnosis was based on European Federation of Neurological Societies (EFNS) guidelines (23). Patients were selected in case of pain classified as probable or definite. "Probable" neuropathic pain requires supporting evidence obtained from a clinical examination of sensory signs. Probable criteria was confirmed by physical examination. "Definite" neuropathic pain requires an objective diagnostic test to confirm the somatosensory nervous system lesion or disease. Definite criteria was confirmed by electromyography. All patients having neuropathic pain in combination with leprosy have filled-in definite criteria. All patients having neuropathic pain in combination with diabetes have filled-in probable criteria. Nociceptive pain was defined as the pain resulting from nociceptor activation, secondary to tissue damage or potential tissue-damaging stimuli. Nociceptive pain is the most important pathological mechanism related to neuritis, defined as the presence of one or more nerves with enlargement, pain, or loss of function (24).

Clinical Evaluation

Information on the neurological examination performed prior to nerve biopsies was gathered from medical records. The type of pain (stinging, burning, electric shocklike, cold, other), pain intensity (numerical pain rating scale from 0 to 10 or 11 point scale) (25), and pain location were recorded. Furthermore, the presence of neural thickening, previous reactional episodes (type I or II), further to information on sensitive and motor neurological examination were gathered from database.

Type 1 reaction or reversal reaction (RR) is a type IV delayed hypersensitivity reaction characterized by ulcerative, red, swollen skin lesions followed by fever (26). Type II reaction, or erithema nodosum leprosum (ENL), is an acute inflammatory condition, characterized by nodules and painful, raised red papules. These nodules are accompanied by neuritis, uveitis, iridocyclitis, episcleritis, arthritis, dactilitis, lympohadenitis, and/or orquitis. Fever, prostration, anorexia and other constitutional symptoms are frequent (27).

Neurophysiological Evaluation

Data were collected from examinations performed via a 4-channel Nihon-Koden-Neuropack S1 equipment, in accordance with standard procedures (28). Amplitude, velocity, and latency were recorded for the median, radial, ulnar, and sural sensory nerves, further to the median, ulnar, and peroneal motor nerves.

According to the results, the following six pathophysiological classifications were determined:

(a) No injury, or normal: when the findings were within the reference values;
(b) Axonal injury: when there was a sharp decrease in compound muscle action potential (CMAP) amplitude (more than 30% of the lower limit), or a moderate decrease with a slight reduction in conduction velocity (>70% the lower limit of normality), or a slight prolongation of latency (<130% the upper limit of normality);
(c) Demyelinating lesion: when there was a sharp decrease in conduction velocity (below 70% the lower limit of normal), or an evident prolongation of CMAP latencies (>130% the upper limit of normal) with slightly reduced amplitude including the presence/absence of demyelination markers such as conduction block (CB) and temporal dispersion (TD);
(d) Demyelinating lesion with secondary axonal damage, or mixed lesion: when there was either axonal or demyelinating impairment, i.e., sharp decrease in amplitudes with greatly reduced velocities and quite prolonged latencies, further to demyelination markers, such as CB and TD, with a sharp reduction in amplitudes;
(e) Not fulfilled: sensory or motor alterations that did not fit the criteria above; and
(f) Unclassified/unresponsive: in case of absent sensory and motor responses (29).

The clinical and neurophysiological diagnosis of neuropathy was defined as a clinically or neurophysiologically detectable impairment of sensory and/or motor nerve.

Histopathological Evaluation

The selection of which sensory nerves to be biopsied in each patient was based on the findings regarding their clinical and neurophysiological involvement. Nerve biopsies were performed in accordance with institutional protocol and leprosy etiology in pure neural leprosy patients, and confirmed by Antunes et al. (30).

Serum Cytokine Levels

Serum samples used to measure cytokine concentrations were stored at −70°C, according to Good Laboratory Practices. Serum concentrations of IL1-β, IL-6, IL-10, IL-17, TNF, CCL-2/MCP-1, IFN-γ, CXCL-10/IP-10, and TGF-β in the samples were evaluated via ELISA, as specified by the manufacturer (eBioscience-San Diego, CA, United States). Serum levels were measured in picograms per mL (pg/mL).

Data Analysis

All the collected patient data were recorded on the database spreadsheets commonly used in outpatient clinic. Data analysis was performed using SPSS statistics 22 program. A descriptive analysis of explanatory variables described below was performed. Comparisons between groups were carried out by means of Chi-square and Fisher's tests for categorical variables, and Kruskal–Wallis test for continuous variables. A logistic regression using a stepwise method was performed to evaluate any possible pain variables.

Explanatory Variables:

The following variables were analyzed:

(a) Demographic data: age (in years), gender (female or male), and ethnicity (white, brown, or black);
(b) Clinical data: clinical form of leprosy (in groups A and B) according to Ridley and Jopling (31) criteria, pain intensity (by means of the numerical pain scale from 0 to 10, wherein 0 is the absence of pain and 10 refers to the most intense one), pain characteristics (burning, stinging, electric shocklike, stabbing), pain extension (localized in up to two or more nerves), the presence of neural thickening, reactional episodes, sensory alterations according to the size of affected fibers (small or large involvement), and motor alterations;
(c) Nerve conduction study: lesion pattern (axonal, demyelinating, demyelinating with secondary axonal degeneration, not fulfilled, or unclassified/unresponsive);
(d) Cytokine and chemokine serum concentrations: The concentrations of IL1-β, IL-6, IL-10, IL-17, TNF, CCL-2/MCP-1, IFN-γ, CXCL-10/IP-10, and TGF-β were recorded in picograms per mL (pg/mL).

Ethical Considerations

Our research was carried out in compliance with the International Compilation of Human Research Standards, and approved by the Ethics Committee of Oswaldo Cruz Foundation. Approval number: 2.972.967 CAAE 94630718.7.0000.5248. All patients have signed informed consent before any procedure.

RESULTS

Demographic Characteristics

Demographic data of the three Groups are described in **Table 1**. The mean age was significantly higher in type II Diabetes Group than in Leprosy Group. There was no statistically significant difference between the mean ages in Leprosy Groups with or without pain (45 and 47 years old, respectively).

Clinical Characteristics

A history of previous reactional episodes was noted in 6 patients (27.3%) from Group A and none from Group B, a statistically significant finding ($p = 0.019$). Neural thickening was noted in both Groups at a similar frequency. Out of patients from Group A, 18 (81.8%) had neuropathic pain and 4 had neuritis (**Table 2**).

As to pain characteristics among leprosy patients, the most frequently mentioned was a burning sensation (50%), followed

TABLE 1 | Demographic data of group A (leprosy neuropathy with neural pain), group B (leprosy neuropathy without pain), group C (diabetic neuropathy with neuropathic pain).

Demographic data		Group A	Group B	Group C	*p*-Value
Gender	Female	9 (40.9%)	8 (47.1%)	9 (52.9%)	0.755
	Male	13 (59.1%)	9 (52.9%)	8 (47.1%)	
Ethnicity	White	9 (42.9%)	10 (58.8%)	6 (35.3%)	0.482
	Brown	5 (23.8%)	1 (5.9%)	3 (17.6%)	
	Black	7 (33.3%)	6 (35.3%)	8 (47.1%)	
Age	Mean (years)	45.2	47.4	74.0	<0. 00001

TABLE 2 | Clinical characteristics of patients with leprosy neuropathy.

Clinical characteristics		Group A	Group B	*p*-Value
Clinical form	NP	13 (65%)	17 (100%)	N.A
	LL	5 (25%)	0	
	BB	1 (5%)	0	
	BL	1 (5%)	0	
Leprosy reactional episodes	Yes	6 (27.3%)	0	0.027
	No	16 (72.6%)	17 (100%)	
Neural thickening	Yes	8 (36.4%)	6 (35.3%)	0.945
	No	14 (63.5%)	11 (64.7%)	

N.A, not applicable; NP, neural pure leprosy form; LL, lepromatous leprosy form; BB, boderline borderline form; BL, boderline lepromatous form.

TABLE 3 | Description of neural pain characteristics in group A ($N = 22$).

Intensity	Mean	7.95 (±2.20)
	Severe (more than 7)	17 (81%)
Type of pain	Burning Sensation	11 (50%)
	Electric Shock Sensation	9 (40.9%)
	Other	2 (9%)
Number of nerves affected by pain	Less than 2 nerves	9 (40.9%)
	More than 2 nerves	13 (59.1%)

by pain similar to an electric shock (40.9%). Pain was considered severe (intensity higher than 7) in 81% of all cases; and most of patients have experienced pain in more than 2 nerves according to their neuroanatomical distribution. These findings are summarized in **Table 3**.

Nerve thickening was present in 36.4% of Group A and 35.3% of Group B patients. Sensory changes characterized by small fibers impairment (such as impaired thermal and pain sensitivities) were present in 95.5% (21 patients) of Group A, 88.2% (15 patients) of Group B, and 70.6% (12 patients) of Group C. Large fibers involvement (characterized by impaired vibration sensitivity) was noted in 18.2% (4 patients) of Group A, 11.8% (2 patients) of Group B, and 100% (17 patients) of Group C. The involvement of large-caliber fibers was significantly higher in Diabetic Group ($p < 0.00001$), whereas there was no statistically significant difference between Groups A and B ($p = 0.883$ and $p = 0.582$, respectively). Motor impairment was noted in 59.1% of Group A and 47.1% of Group B ($p = 0.455$) (**Table 4**).

TABLE 4 | Principal neurological examination in patients with leprosy neuropathy with (Group A) and without pain (Group B).

Nerve involvement		Group A $N = 18$	Group B $N = 17$	*p*-Value
Small fiber	Yes	21 (95.5%)	15 (88.2%)	0.426
	No	1 (4.5%)	2 (11.8%)	
Large fiber	Yes	4 (18.2%)	2 (11.8%)	0.582
	No	18 (81.8%)	15 (88.2%)	
Motor Involvement	Yes	13 (59.1%)	8 (47.1%)	0.455
	No	14 (63.6%)	11 (64.7%)	

Serum Cytokines in Patients With Pain

Mean values for IL-1β, TNF, TGF-β, and IL-17 cytokine concentrations were higher in the Group of leprosy neuropathy in combination with neural pain than in the other Groups. Regarding mean values, IL-10 concentrations in Group A were lower than in Groups B and C, with a statistically significant difference between Groups A and C ($p = 0.001$). IL-1β concentrations were significantly higher in Group A than in Groups B and C ($p = 0.0001$ in both comparisons). No difference was noted between Groups B and C ($p = 0.46$).

IL-6 concentrations were higher in patients with diabetic neuropathy in combination with neuropathic pain, further to those with leprosy neuropathy in combination with neural pain in a comparison with leprosy neuropathy patients without pain. This difference was considered statistically significant ($p = 0.041$). Even so, no difference was found between Groups A and C ($p = 0.75$); and TNF was higher in Group A than in Group B. There was no statistical difference between Groups A and B ($p = 1.0$), however Groups A and C were significantly different ($p = 0.02$). Mean values of IL-17 were significantly higher in Group A than in Group B ($p = 0.01$). However, there was no statistical difference in the other group comparisons, although CCL-2/MCP-1 mean values had been higher in Group C than in the other Groups. There was a significant difference when comparing CCL2/MCP-1 values in Group C to Groups A and B ($p = 0.001$ and $p = 0.01$ respectively). No difference was noted between Groups A and B; but the differences between IFN-γ values in Group C ($p = 0.0001$) were higher and significant when compared to the ones in Group A.

CXCL-10/IP-10 concentrations were higher in Diabetes Group, intermediate in Group B, and lower in Group A. These data were statistically significant between Groups A and B ($p = 0.02$) and Groups A and C ($p = 0.0001$). The opposite have occurred with regard to TGF-β concentration levels, which were higher in Group A and significant between both Groups A and B ($p = 0.01$), further to Groups A and C ($p = 0.0001$). **Figure 2** shows the differences in cytokine serum concentrations between the Groups and their significance in each comparison. Logistic regression was performed to Groups A and B regarding variables, age, clinical form, presence of previous history of reaction, nerve conduction pattern, and serum concentration levels of cytokines. IL-1β levels plays the rule of an independent variable when comparing Groups A and B.

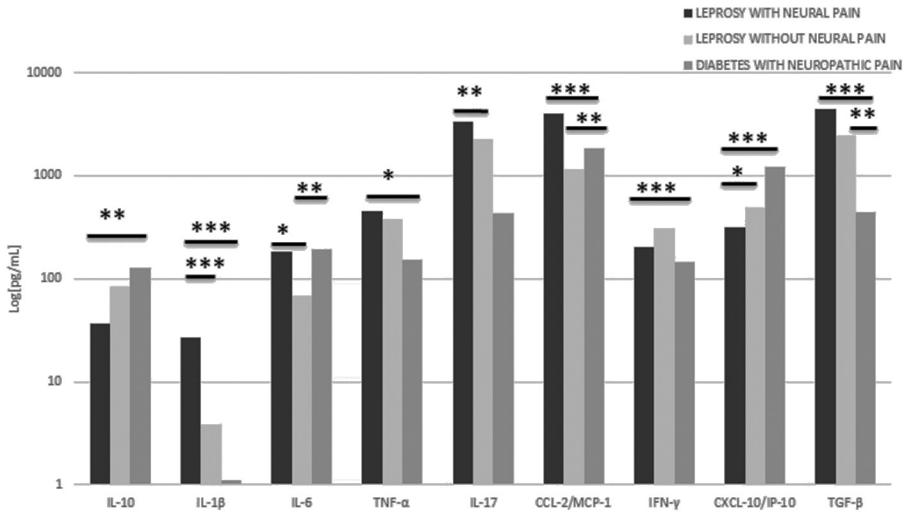

FIGURE 2 | Mean values of serum cytokines in all groups. The graph shows the very high concentration of serum IL-1b levels in the neural pain leprosy group compared to the other groups. Statistically significant differences between groups with leprosy with and without pain were also found regarding IL-6, IL-17, CCL-2/MCP-1, CXCL-10/IP-10 concentrations. $^{*}p < 0.05$, $^{**}p < 0.005$, and $^{***}p < 0.0005$.

In Neural Pain Group, 18 patients had neuropathic pain and 4 had neuritis. Serum concentrations were averaged in patients with neuropathic pain and neuritis. Similar mean concentrations were found for IL-17, IL-10, IL-6, IL-1β, TNF, and TGF-β cytokines. The concentrations of CCL-2/MCP-1, IFN-γ and, CXCL10 / IP-10 were slightly higher in patients with neuropathic pain, as opposed to those with neuritis. In view of the small number of participants having neuritis, a mere descriptive analysis of concentrations was performed.

DISCUSSION

Neural pain is a quite common symptom in leprosy patients. In a cross-sectional study by Santos et al. (32), the 260 participants included in their report were diagnosed with leprosy; out of them, 195 patients (75%) presented with pain during evaluation, resulting in a lower life quality index. Considering these data as a whole, leprosy pain is definitely a public health problem. Data on the prevalence of neuropathic pain in leprosy fluctuates widely, from 11 to 78.9%, depending on the study (3, 4, 33). The presence of neuropathic pain depends on the moment it is detected, the antimicrobial treatment situation, and the clinical form of the disease (2, 5). In the present study, neural pain prior to the diagnostic biopsy was evidenced in 89 out of the 311 (28.6%) patients treated for leprosy.

Chances are that neuropathic pain is even more common subsequently to multidrug treatment (MDT), as demonstrated by a different kind of study (4, 5, 34). A study by Nascimento et al. (35) has reported cases in which symptoms of neuropathic pain have begun many years after the end of treatment. Another study has traced the slow development of symptoms in a group of six patients who had already finished treatment at least 10 years before the appearance of any typical sensory signs or symptoms (36).

Previous reactional episodes were not noted in Painless Neuropathy Group, but in the Group of leprosy neuropathy in combination with neural pain, which consists mostly of multibacillary patients. Many authors believe that the reactional episodes accompanying leprosy are among the risk factors for neuropathic pain (2, 4, 22, 32, 37).

In the present study, during neurological examination, small fiber neuropathy was the most frequent finding among leprosy patients. These data are similar to the ones previously described (2, 32). Unmyelinated and poorly myelinated fibers could be affected (38). Small fiber neuropathy correlates with neuropathic pain by means of physiology (39, 40). On the other hand, large-caliber sensory fiber involvement is uncommon in leprosy neuropathy (2).

As to nerve conduction studies, despite the absence of statistically significant differences between the groups with and without pain, there was a tendency toward prevalence of demyelinating form in the group with pain. Jardim et al. (41) have described that, in the early stages of infection, nerve conduction alterations of demyelination are commonly noted. The remarkable absence of evocative sensory and motor responses in the group of patients without pain denotes more severe nerve impairment in this group.

Many studies have shown that cytokines are higher in leprosy type I and II reactional episodes, defined as systemic inflammatory complications in leprosy. One study suggests that TNF and IL-10 could possibly predict the occurrence of type I and II reactions, respectively, while increased IL-1β and IFN-γ might also predict the occurrence of both reactional types acting as biomarkers (42). The increase of cytokine levels during reactional episodes has also been described by other authors (43–45).

Again, the present study ascertains that IL-1β is an independent variable related to neural pain group. Although most patients in the present study have neither presented

with acute neuritis nor experienced acute reactional episodes, a process of silent neuritis cannot be ruled out (4/56 patients presented with neuritis). Proinflammatory cytokines such as TNF and IL-1β are effective to directly stimulate and sensitize Aδ fibers and type C fibers (46). In rats with neuropathic pain due to chemotherapy-induced neuropathy, these abnormal, spontaneous discharges of A and C fibers are associated with neuropathic pain pathogenesis (47). Increased levels of IL-1β in leprosy and neural pain patients may also be associated with an analogous mechanism, wherein the increased inflammatory response maintains the nociceptive stimulus by peripheral sensitization.

Moreover, increased levels of TNF, TGF-β, and IL-17 in leprosy and neural pain patients have also been detected. One report has shown that, in leprosy, TNF and TGF-β induce apoptosis in Schwann cells, with a consequent damage to peripheral nerve (48). Although no statistical difference in TNF levels in Groups A and B has been found, a difference was noted between Groups A and C, indicating that such a cytokine may be associated with the pathophysiological mechanisms of nerve damage in leprosy, but not in a non-infectious clinical condition like diabetes. TGF-β was significantly higher in leprosy and neural pain group. Studies have reported an increase of this protein in multibacillary patients (25% of group A). Therefore, such a difference may be related to the clinical form and the extent of nerve damage. Higher TGF-β expression in patients with the lepromatous form of the disease is associated with a higher frequency of apoptosis in the lesions (48, 49), further to fibrogenesis (50).

IL-17 levels were increased in Pain Group. The association between higher IL-17 and pain has been previously described in relation to both nociceptive (51) and neuropathic pains (52–54). This cytokine seems to be involved in the maintenance of neuropathic pain due to the activation of astrocytes and the secretion of proinflammatory cytokines (55).

Lower levels of IL-10, an anti-inflammatory cytokine, were noted in the group of patients with leprosy neuropathy in combination with neural pain. IL-10 causes the negative regulation of proinflammatory cytokines (56), presenting reduced levels in chronic pain (19). However, higher values of IL-10 were noted to patients with neuropathic pain as a result of diabetes. The intake of metformin or the use of insulin may increase IL-10 levels in diabetic patients, so that it may have been a confounding factor. Furthermore, increased IL-6 concentrations in the groups of patients with pain secondary to leprosy and diabetes were noted.

IL-6 has been related to postherpetic neuralgia, neuropathic pain secondary to disc herniation, and the carpal tunnel syndrome (12, 13). It may also be a biomarker for chronic pain (8). IFN-γ levels were surprisingly low in leprosy patients. Increased levels of this cytokine have been previously described in the paucibacillary and pure neural forms (42, 57). High IFN-γ levels were noted within diabetic patients, seeming to be related to the pathophysiology of type II diabetes (58). Higher concentrations were found in patients with neuropathic pain secondary to leprosy as opposed to neuritic patients, when comparing patients with neuropathic pain and neuritis. In a study with rats, increased IFN-γ concentrations have been described as key elements in the pathophysiology of neuropathic pain due to hyperexcitability of dorsal horn (59).

Increased CCL2/MCP-1 and CXCL-10/IP-10 levels were noted in diabetic patients with neuropathic pain. Studies indicate that CCL-2/MCP-1 may regulate the excitability in neurons of dorsal ganglion root (DRG) as it is associated with the development of chronic, painful hypersensitivity states (60, 61). A study in rats and mice undergoing transient focal demyelination of sciatic nerve has demonstrated an increased expression of CCL-2/MCP-1 and CXCL-10/IP-10 receptors (20). Patients with neuropathic pain, secondary to leprosy neuropathy, have also had higher concentrations over patients with neuritis, what may be linked to an analogous mechanism of GER hyperexcitability (62).

Furthermore, the present study reaffirms that the immunological profile of patients with neural pain has shown an increased level of pro-inflammatory cytokines. IL-1β is an independent variable related to neural pain and may be an important biomarker for patient follow-up. The lack of differences in neurological examination may indicate that the cytokine profile is more closely related to pain than to nerve damage itself.

Regarding serum levels comparison within the different groups, increased levels of IL-6 were noted in patients with neural pain secondary to leprosy and type II diabetes mellitus in combination with neuropathic pain, indicating that IL-6 may be a pain biomarker. Anti-IL-6 drugs have been investigated as possible targets to pain control. A new drug called tocilizumab has been used in cases of inflammatory arthritis and acute optic neuritis followed by inflammatory and neuropathic pains, respectively (63, 64). An additional study has demonstrated that the new drug was effective to alleviate depression, fatigue, and pain (65).

Finally, the fact that this is a retrospective study is an important limitation. Many patients were excluded due to lack of data or absence of blood samples, which greatly reduced the sample of patients. Moreover, the fact that data were collected from assessments of different examiners is another limitation.

In conclusion, further prospective studies with larger numbers of patients are needed to confirm the role of cytokines in neural pain. However, this study highlights a possible biomarker for follow-up and brings new perspectives in the management of patients with neural pain in leprosy.

DATA AVAILABILITY STATEMENT

The datasets generated for this study are available on request to the corresponding author.

ETHICS STATEMENT

The studies involving human participants were reviewed and approved by the Oswaldo Cruz Foundation. The

patients/participants provided their written informed consent to participate in this study.

AUTHOR CONTRIBUTIONS

DA, ES, MJ, and RP formulated the study questions. DA, MJ, RP, MH, and JV designed the study protocol. DA, RP, JV, RC, MH, IP, LG, ES, and MJ conducted the experiment. ES, MJ, and RP supervised the study. DA and MH analyzed the data. DA drafted the manuscript. ES, MJ, and RP revised the manuscript. All authors contributed to the interpretation of the data, read and approved the final version for publication and agreed to be accountable for all aspects of the work in ensuring that questions related to the accuracy or integrity of any part of the work are appropriately investigated and resolved.

FUNDING

This work was supported by the Brazilian National Council for Scientific and Technological Development (CNPq) [grant number 303834/2017-0]; the Carlos Chagas Filho Foundation for Research Support of the State of Rio de Janeiro (FAPERJ) [grant number 203675]; the Brazilian Coordination for the Improvement of Higher Education Personnel (CAPES) and PIBIC Fiocruz (Scientific Training Institutional Program at Fiocruz).

REFERENCES

1. Ribeiro MDA, Silva JCAO, Brito S. Estudo epidemiológico da hanseníase no Brasil: reflexão sobre as metas de eliminação. *Rev Panamer Salud Pública*. (2018) 2018:42. doi: 10.26633/RPSP.2018.42
2. Giesel LM, Pitta IJR, Silveira RC, Andrade LR, Vital RT, Nery JAC, et al. Clinical and neurophysiological features of leprosy patients with neuropathic pain. *Am J Trop Med Hyg*. (2018) 98:1609–13. doi: 10.4269/ajtmh.17-0817
3. Haroun OM, Hietaharju A, Bizuneh E, Brandsma JW, Tesfaye F, Haanpää M, et al. Investigation of neuropathic pain in treated leprosy patients in ethiopia: a cross-sectional study. *Pain*. (2012) 153:1620–4. doi: 10.1016/j.pain.2012.04.007
4. Raicher I, Stump PR, Baccarelli R, Marciano LHS, Ura S, Virmond MCL, et al. Neuropathic pain in leprosy. *Clindermatol*. (2016) 34:59–65. doi: 10.1016/j.clindermatol.2015.10.012
5. Raicher I, Stump PR, Harnik SB, Alves RO, Baccarelli R, Marciano L, et al. Neuropathic pain in leprosy: symptom profile characterization and comparison with neuropathic pain of other etiologies. *Pain Rep*. (2018) 3:E638. doi: 10.1097/PR9.0000000000000638
6. Medeiros RC, Girardi KD, Cardoso FK, Mietto BS, Pinto TG, Gomez LS, et al. Subversion of schwann cell glucose metabolism by *Mycobacterium leprae*. *J Biol Chem*. (2016) 291:21375–87. doi: 10.1074/jbc.M116.725283
7. Campana WM. Schwann cells: activated peripheral glia and their role in neuropathic painBrain. *Behav Immun*. (2007) 21:522–7. doi: 10.1016/j.bbi.2006.12.008
8. Bäckryd E. Pain in the blood? Envisioning mechanism-based diagnoses and biomarkers in clinical pain medicine. *Diagnostics*. (2015) 5:84–95. doi: 10.3390/diagnostics5010084
9. Turner MD, Nedjai B, Hurst T, Pennington DJ. Cytokines and chemokines: at the crossroads of cell signalling and inflammatory disease. *Biochim Biophys Acta*. (2014) 1843:2563–82. doi: 10.1016/j.bbamcr.2014.05.014
10. Arruda JL, Sweitzer S, Rutkowski MD, Deleo JA. Intrathecal anti-IL-6 antibody and IgG attenuates peripheral nerve injury-induced mechanical allodynia in the rat: possible immune modulation in neuropathic pain. *Brain Res*. (2000) 879:216–25. doi: 10.1016/S0006-8993(00)02807-9
11. Ozaktay AC, Kallakuri S, Takebayashi T, Cavanaugh JM, Asik I, Deleo JA, et al. Effects of interleukin-1 beta, interleukin-6, and tumor necrosis factor on sensitivity of dorsal root ganglion and peripheral receptive field in rats. *Eur Spine J*. (2006) 15:1529–37. doi: 10.1007/s00586-005-0058-8
12. Kraychete DC, Sakata RK, Machado A, Bacellar A, Jesus RC, Carvalho EM. Proinflammatory cytokines in patients with neuropathic pain treated with tramadol. *Rev Brasil Anestesiol*. (2009) 59:483–91. doi: 10.1590/S0034-70942009000300004
13. Andrade P, Hoogland G, Garcia MA, Steinbusch HW, Daemen MA, Visser-Vandewalle V. Elevated IL-1b and IL-6 levels in lumbar herniated discs in patients with sciatic pain. *Eur Spine J*. (2013) 22:714–20. doi: 10.1007/s00586-012-2502-x
14. Zhu SM, Liu YM, An ED, Chen QL. Influence of systemic immune and cytokine responses during the acute phase of zoster on the development of postherpetic neuralgia. *J Zhejiang Univ Sci B*. (2009) 10:625–30. doi: 10.1631/jzus.B0920049
15. Shubayev V, Myers R. Axonal transport of Tnf-A in painful neuropathy: distribution of ligand tracer and tnf receptors. *J Neuroimmunol*. (2001) 114:48–56. doi: 10.1016/S0165-5728(00)00453-7
16. Kawasaki Y, Xu Z, Wang X, Park J, Zhuang Z, Tan P, et al. Distinct roles of matrix metalloproteases in the early- and late-phase development of neuropathic pain. *Nat Med*. (2008) 14:331–6. doi: 10.1038/nm1723
17. Alexander GM, Peterlin BL, Perreault MJ, Grothusen JR, Schwartzman RJ. Changes in plasma cytokines and their soluble receptors in complex regional pain syndrome. *J Pain*. (2012) 13:10–20. doi: 10.1016/j.jpain.2011.10.003
18. Birkkein F, Schmelz M, Schifter S, Weber M. The important role of neuropeptides in complex regional pain syndrome. *Neurology*. (2001) 57:2179–84. doi: 10.1212/WNL.57.12.2179
19. Davies AL, Hayes KC, Dekaban GA. Clinical correlates of elevated serum concentrations of cytokines and autoantibodies in patients with spinal cord injury. *Arch Phys Med Rehabil*. (2007) 88:1384–93. doi: 10.1016/j.apmr.2007.08.004
20. Bhangoo S, Ren D, Miller RJ, Henry KJ, Lineswala J, Hamdouchi C, et al. Delayed functional expression of neuronal chemokine receptors following focal nerve demyelination in the rat: a mechanism for the development of chronic sensitization of peripheral nociceptors. *Mol Pain*. (2007) 3:38. doi: 10.1186/1744-8069-3-38
21. Véras LS, Vale RG, Mello DB, Castro JA, Lima V, Silva KN. Degree of disability, pain levels, muscle strength, and electromyographic function in patients with Hansen's disease with common peroneal nerve damage. *Rev Soc Bras Med Trop*. (2012) 45:375–9. doi: 10.1590/S0037-86822012000300018
22. Chen S, Qu J, Chu T. Prevalence and characteristics of neuropathic pain in the people affected by leprosy in China. *Lepr Rev*. (2012) 83:195–201.
23. Cruccu G, Sommer C, Anand P, Attal N, Baron R, Garcia-Larrea L, et al. EFNS guidelines on neuropathic pain assessment: revised. *Eur J Neurol*. (2010) 17:1010–8. doi: 10.1111/j.1468-1331.2010.02969.x
24. Nicholson B. Differential diagnosis: nociceptive and neuropathic pain. *Am J Manage Care*. (2006) 12:S256–62.
25. Von Korff M, Jensen MP, Karoly P. Assessing global pain severity by self-report in clinical and health services research. *Spine*. (2000) 25:3140–51. doi: 10.1097/00007632-200012150-00009
26. Jardim MR, Antunes SL, Santos AR, Nascimento OJ, Nery JA, Sales AM, et al. Criteria for diagnosis of pure neural leprosy. *J Neurol*. (2003) 250:606–809. doi: 10.1007/s00415-003-1081-5
27. Jardim M, Chimelli L, Faria SC, Fernandes PV, Da Costa Néri JA, Sales AM, et al. Clinical, electroneuromyographic and morphological studies of pure neural leprosy in a Brazilian referral center. *Lepr Rev*. (2004) 75, 242–253.
28. Delisa JA, Lee HJ, Baran EM, Lai K-S. *Manual of Nerve Conduction Velocity and Clinical Neurophysiology*. Philadelphia, PA: Lippincott Williams & Wilkins (1994).
29. Tankisi H, Pugdahl K, Fuglsang-Frederiksen A, Johnsen B, de Carvalho M, Fawcett PR, et al. (2005). Pathophysiology inferred from electrodiagnostic nerve tests and classification of polyneuropathies. suggested guidelines. *Clin Neurophysiol*. 116:1571–80. doi: 10.1016/j.clinph.2005.04.003
30. Antunes SL, Chimelli L, Jardim MR, Vital RT, Nery JA, Cortereal S, et al. Histopathological examination of nerve samples from pure

neural leprosy patients: obtaining maximum information to improve diagnostic efficiency. *Mem Inst Oswaldo Cruz*. (2012) 107:246–53. doi: 10.1590/S0074-02762012000200015
31. Ridley DS, Jopling WH. Classification of leprosy according to immunity. A five-group system. *Int J Lepr Other Mycobact Dis.* (1966) 34:255–73.
32. Santos VS, Santana JCV, Castro FDN, Oliveira LS, Santana JCV, Feitosa VLC, et al. Pain and quality of life in leprosy patients in an endemic area of Northeast Brazil: a cross-sectional study. *Infect Dis Pover*. (2016) 5:18. doi: 10.1186/s40249-016-0113-1
33. Ramos JM, Alonso-Castañeda B, Eshetu D, Lemma D, Reyes F, Belinchón I, et al. Prevalence and characteristics of neuropathic pain in leprosy patients treated years ago. *Pathog Glob Health.* (2014) 108:186–90. doi: 10.1179/2047773214Y.0000000140
34. Stump PR, Baccarelli R, Marciano LH, Lauris JR, Teixeira MJ, Ura S, et al. Neuropathic pain in leprosy patients. *Int J Lepr Other Mycobact Dis*. (2004) 72:134–8. doi: 10.1489/1544-581X(2004)072<0134:NPILP>2.0.CO;2
35. Nascimento O, de Freitas M, Escada T, Marques W, Cardoso F, Pupe C, et al. Leprosy late-onset neuropathy: an uncommon presentation of leprosy. *Arquiv Neuro Psiquiatr*. (2012) 70:404–6. doi: 10.1590/S0004-282X2012000600004
36. Rosenberg N, Faber WR, Vermeulen M. Unexplained delayed nerve impairment in leprosy after treatment. *Lepr Rev*. (2003) 74:357–65.
37. Lasry-Levy E, Hietaharju A, Pai V, Ganapati R, Rice ASC, Haanpää M, et al. Neuropathic pain and psychologicalmorbidity in patients with treated leprosy:across-sectional prevalence study in Mumbai. *PLoS Negl Trop Dis*. (2011) 5:981. doi: 10.1371/journal.pntd.0000981
38. Shelley BP, Shenoy MM. Revisiting Hansen's disease: recognizing the many neurodermatologic faces and its diagnostic challenges. *Arch Med Health Sci*. (2018) 6:157. doi: 10.4103/amhs.amhs_57_18
39. De Greef BTA, Hoeijmakers JGJ, Gorissen-Brouwers CML, Geerts M, Faber CG, Merkies ISJ. Associated conditions in small fiber neuropathy - a large cohort study and review of the literature. *Eur J Neurol*. (2018) 25:348–55. doi: 10.1111/ene.13508
40. Cazzato D, Lauria G. Small fibre neuropathy. *Curr Opin Neurol*. (2017) 30:490–9. doi: 10.1097/WCO.0000000000000472
41. Jardim MR, Vital R, Hacker MA, Nascimento M, Balassiano SL, Sarno EN, et al. Leprosy neuropathy evaluated by ncs is independent of the patient's infectious state. *Clin Neurol Neurosurg*. (2015) 131:5–10. doi: 10.1016/j.clineuro.2015.01.008
42. Madan NK, Agarwal K, Chander R. Serum cytokine profile in leprosy and its correlation with clinico-histopathological profile. *Lepr Rev*. (2011) 82:371–82.
43. Pisa P, Gennene M, Söder O, Ottenhoff T, Hansson M, Kiessling R. Serum tumor necrosis factor levels and disease dissemination in leprosy and leishmaniasis. *J Infect Dis*. (1990) 161:988–91. doi: 10.1093/infdis/161.5.988
44. Sarno EN, Grau GE, Vieira LMM, Nery JA. Serum levels of tumor necrosis factor-alpha and interleukin-1b during leprosy reactional states. *Clin Exp Immunol*. (1991) 84:103–8. doi: 10.1111/j.1365-2249.1991.tb08131.x
45. Parida SK, Grau GE, Zaheer SA, Mukherjee R. Serum tumor necrosis factor and interleukin 1 in leprosy and during lepra reactions. *Clin Immunol Immunopathol*. (1992) 63:23–7. doi: 10.1016/0090-1229(92)90088-6
46. Schafers M, Sorkin L. Effect of cytokines on neuronal excitability. *Neurosci Lett*. (2008) 437:188–93. doi: 10.1016/j.neulet.2008.03.052
47. Tanner KD, Levine JD, Topp KS. Microtubule disorientation and axonal swelling in unmyelinated sensory axons during vincristine-induced painful neuropathy in rat. *J Comp Neurol.* (1998) 395:481–92. doi: 10.1002/(SICI)1096-9861(19980615)395:4<481::AID-CNE5>3.0.CO;2-Y
48. Oliveira RB, Sampaio EP, Aarestrup F, Teles RM, Silva TP, Oliveira AL. Cytokines and mycobacterium leprae induce apoptosis in human Schwann Cells. *J Neuropathol Exp Neurol*. (2005) 64:882–90. doi: 10.1097/01.jnen.0000182982.09978.66
49. Aarão TLS, De Sousa JR, Falcão A, Falcão L, Quaresma J. Nerve growth factor and pathogenesis of leprosy: review and update. *Front Immunol*. (2018) 9:939. doi: 10.3389/fimmu.2018.00939
50. Petito RB, Amadeu TP, Pascarelli BM, Jardim MR, Vital RT, Sarno EN, et al. Transforming growth factor-beta1 may be a key mediator of the fibrogenic properties of neural cells in Leprosy. *J Neuropathol Exp Neurol.* (2013) 72:351–66. doi: 10.1097/NEN.0b013e31828bfc60
51. Lubberts E. Il-17/Th17 targeting: on the road to prevent chronic destructive arthritis? *Cytokine*. (2008) 41:84–91. doi: 10.1016/j.cyto.2007.09.014
52. Noma N, Khan J, Chen IF, Markman S, Benoliel R, Hadlaq E, et al. Interleukin-17 levels in rat models of nerve damage and neuropathic pain. *Neurosci Lett*. (2011) 493:86–91. doi: 10.1016/j.neulet.2011.01.079
53. Day YJ, Liou JT, Lee CM, Lin YC, Mao CC, Chou AH, et al. Lack of interleukin-17 leads to a modulated micro-environment and amelioration of mechanical hypersensitivity after peripheral nerve injury in mice. *Pain.* (2014) 155:1293–302. doi: 10.1016/j.pain.2014.04.004
54. Zheng H, Zhang Z, Luo N, Liu Y, Chen Q, Yan H. Increased Th17 cells and IL-17 in rats with traumatic optic neuropathy. *Mol Med Rep.* (2014) 10:1954–8. doi: 10.3892/mmr.2014.2448
55. Sun C, Zhang J, Chen L, Liu T, Xu G, Li C, et al. IL-17 contributed to the neuropathic pain following peripheral nerve injury by promoting astrocyte proliferation and secretion of proinflammatory cytokines. *Mol Med Rep*. (2017) 5:89–96. doi: 10.3892/mmr.2016.6018
56. Austin PJ, Moalem-Taylor G. The neuro-immune balance in neuropathic pain: involvement of inflammatory immune cells, immune-like glial cells and cytokines. *J Neuroimmunol.* (2010). 229:26–50. doi: 10.1016/j.jneuroim.2010.08.013
57. Belgaumkar VA, Gokhale NR, Mahajan PM, Bharadwaj R, Pandit DP, Deshpande S. Circulating cytokine profiles in leprosy patients. *Lepr Rev*. (2007) 78:223–30.
58. Tsiavou A, Hatziagelaki E, Chaidaroglou A, Koniavitou K, Degiannis D, Raptis SA. Correlation between intracellular interferon-gamma (IFN-gamma) production by CD4+ and CD8+ lymphocytes and IFN-gamma gene polymorphism in patients with type 2 diabetes mellitus and latent autoimmune diabetes of adults (lada). *Cytokine*. (2005) 21:135–41. doi: 10.1016/j.cyto.2005.02.011
59. Tsuda M, Masuda T, Kitano J, Shimoyama H, Tozaki-Saitoh H, Inoue K. IFN-gamma receptor signaling mediates spinal microglia activation driving neuropathic pain. *Proc Natl Acad Sci USA*. (2009) 106:8032–7. doi: 10.1073/pnas.0810420106
60. Abbadiea C, Lindia JA, Cumiskey AM, Peterson LB, Mudgett JS, Bayne EK, et al. Impaired neuropathic pain responses in mice lacking the chemokine receptor CCR2. *Proc Natl Acad Sci USA*. (2003) 100:7947–52. doi: 10.1073/pnas.1331358100
61. Jung H, Miller RJ. Activation of the nuclear factor of activated T-cells (NFAT) mediates upregulation of CCR2 chemokine receptors in dorsal root ganglion (DRG) neurons: a possible mechanism for activity-dependent transcription in DRG neurons in association with neuropathic pain. *Mol Cell Neurosci.* (2008) 37:170–7. doi: 10.1016/j.mcn.2007.09.004
62. Zang ZJ, Cao DL, Zhang X, Ji RR, Gao YJ. Chemokine contribution to neuropathic pain: respective induction of CXCL1 and CXCR2 in spinal cord astrocytes and neurons. *Pain*. (2013) 154:2185–97. doi: 10.1016/j.pain.2013.07.002
63. Araki M, Matsuoka T, Yamamura T. Efficacy of the anti-Il-6 receptor antibody tocilizumab in neuromyelitis optica: a pilot study. *Neurology*. (2014) 82:1302–6. doi: 10.1212/WNL.0000000000000317
64. Jones G, Panova E. New insights and long-term safety of tocilizumab in rheumatoid arthritis. *Ther Adv Musculoskelet Dis*. (2018) 10:195–9. doi: 10.1177/1759720X18798462
65. Behrens F, Englbrecht M, Biewer WA, Burmester GR, Feuchtenberger M, Flacke JP, et al. SAT0182 Tocilizumab S.C. – Improvement of the depressiveness, fatigue and pain in Ra therapy. *Ann Rheum Dis.* (2018) 77:952. doi: 10.1136/annrheumdis-2018-eular.2176

Conflict of Interest: The authors declare that the research was conducted in the absence of any commercial or financial relationships that could be construed as a potential conflict of interest.

frontiers in Immunology

REVIEW
published: 28 January 2020
doi: 10.3389/fimmu.2019.03061

Neuraxial Cytokines in Pain States

Gilson Gonçalves dos Santos[1†], *Lauriane Delay*[1†], *Tony L. Yaksh*[1] *and Maripat Corr*[2*]

[1] *Department of Anesthesiology, University of California, San Diego, La Jolla, CA, United States,* [2] *Division of Rheumatology, Allergy and Immunology, University of California, San Diego, La Jolla, CA, United States*

A high-intensity potentially tissue-injuring stimulus generates a homotopic response to escape the stimulus and is associated with an affective phenotype considered to represent pain. In the face of tissue or nerve injury, the afferent encoding systems display robust changes in the input–output function, leading to an ongoing sensation reported as painful and sensitization of the nociceptors such that an enhanced pain state is reported for a given somatic or visceral stimulus. Our understanding of the mechanisms underlying this non-linear processing of nociceptive stimuli has led to our appreciation of the role played by the functional interactions of neural and immune signaling systems in pain phenotypes. In pathological states, neural systems interact with the immune system through the actions of a variety of soluble mediators, including cytokines. Cytokines are recognized as important mediators of inflammatory and neuropathic pain, supporting system sensitization and the development of a persistent pathologic pain. Cytokines can induce a facilitation of nociceptive processing at all levels of the neuraxis including supraspinal centers where nociceptive input evokes an affective component of the pain state. We review here several key proinflammatory and anti-inflammatory cytokines/chemokines and explore their underlying actions at four levels of neuronal organization: (1) peripheral nociceptor termini; (2) dorsal root ganglia; (3) spinal cord; and (4) supraspinal areas. Thus, current thinking suggests that cytokines by this action throughout the neuraxis play key roles in the induction of pain and the maintenance of the facilitated states of pain behavior generated by tissue injury/inflammation and nerve injury.

Keywords: cytokine, chemokine, pain, neuroimmune crosstalk, neuraxis

OPEN ACCESS

Edited by:
Waldiceu A. Verri,
State University of Londrina, Brazil

Reviewed by:
R. R. Ji,
Duke University, United States
Djane Braz Duarte,
University of Brasilia, Brazil

***Correspondence:**
Maripat Corr
mpcorr@ucsd.edu

[†] *These authors have contributed equally to this work*

Specialty section:
This article was submitted to Cytokines and Soluble Mediators in Immunity, a section of the journal Frontiers in Immunology

Received: *14 October 2019*
Accepted: *16 December 2019*
Published: *28 January 2020*

Citation:
Gonçalves dos Santos G, Delay L, Yaksh TL and Corr M (2020) Neuraxial Cytokines in Pain States. Front. Immunol. 10:3061. doi: 10.3389/fimmu.2019.03061

INTRODUCTION

High-intensity mechanical or thermal stimuli will selectively increase the activity of populations of primary afferents, referred to as nociceptors, with the frequency of discharge reflecting the intensity of the stimulus. This input drives activation of second-order neurons, many of which project to the brain. The consequence of this input is to drive a pain state, which at its simplest results in a protective response (e.g., withdrawal of the affected limb) mediated by spinal and supraspinal organization (e.g., nociception) and then at higher-order levels of processing drives a state of negative affect (e.g., pain/suffering) (1). Of note, it is appreciated that in the face of persistent afferent input, as after tissue or nerve injury, there is an increased activation of the afferent and the second-order spinofugal neuron, which drives an enhanced pain response. Such "hyperalgesic" states variously reflect increased responsiveness of the primary afferent and/or the second-order projection neurons, leading to the enhanced pain report. The biology of systems underlying this change in input–output functionality of the spinal dorsal horn has been the subject of considerable interest. One underlying element of this facilitated processing reflects the role played by cytokine signaling in system function.

Classically, three considerations have characterized the actions of cytokines.

(1) They are peptides released from immunocompetent cells, notably T cells and monocyte family members (2).
(2) This increased production and release is driven by pathological conditions such as tissue injury and infection, which initiate activation of these inflammatory cells.
(3) Their perceived role is largely to engage immune signaling and pathologic targets, serving as entities involved in autocrine, paracrine, and endocrine signaling.

Advances in our understanding of cytokine biology have considerably expanded this original profile. It is now clear that aside from immune cells (resident and recruited macrophages, lymphocytes, and mast cells present throughout the neuraxis), cytokines are released from peripheral afferents (Schwann cells and peripheral termini of sensory fibers), as well as from cells within the dorsal root ganglia (DRG) and spinal cord (3). As will be reviewed, this release can indeed be initiated by injury or inflammation, and also by neuronal activity otherwise driven by these injury conditions (4). Cytokine signaling is now known to exert direct effects upon neural signaling through eponymous receptors located on neurons, microglia, and astrocytes, in the spinal parenchyma and in the DRG and brain. Further, while neuronal activation might be the result of receptor-mediated and direct cell-to-cell contact-dependent mechanisms (e.g., gap junction contacts in DRG neurons and satellite cells) (5), soluble extracellular molecules serve to create broader gradients of paracrine- and autocrine-like regulatory networks. These cytokines thus comprise a communication network between immune and neuronal cells. In the context of high-frequency afferent traffic generated by tissue injury, a wave of inflammatory cytokines acts on the terminals of sensory nerve fibers (nociceptors), triggering activation of corresponding pain pathways while neuronal activation leads to a reciprocal activation of a variety of cytokine-generating cells (3). Of note, prolonged inflammation alters nociceptive processing in such a fashion as to yield a persistent pain phenotype even after the inflammation and wounding has resolved, creating a "neuropathic"-like phenotype (6).

A further intriguing complexity is that several of these cytokines, as will be reviewed below, act through signaling to suppress excitatory signaling (e.g., they have an anti-inflammatory phenotype). Finally, current work raises the likelihood that signaling secondary to sustained cytokine and chemokine release and the recruitment of migratory effector cells into the DRG and spinal cord can initiate a feedback loop that results in neuronal injury and subsequently chronic pain. Thus, the balance between repair and proinflammatory factors may determine the rate of progression and outcome of a neurodegenerative process.

Cytokines thus play important roles at the systems level in regulating the functionality of neuraxial systems regulating neurodevelopment, neuroinflammation, and synaptic transmission. Here, we seek to provide an overview focused on a curated list of cytokines identified in the context of neuronal modulation and damage, to play a role in changes in pain processing after tissue and nerve injury, and discuss roles that cytokines play at the interface of the neuronal and immune system interfaces divided across four levels of neuronal organization: (1) peripheral termini; (2) DRG; (3) spinal cords; and (4) supraspinal areas.

CYTOKINE FAMILIES

Cytokines, from the combination of two Greek words *cyto* (cell) and *kinos* (movement), are defined as a family of low-molecular-weight bioactive proteins or glycoproteins secreted by immune cells and non-neuronal cells (e.g., epithelial cells, fibroblasts, and Schwann cells). Interferon was the first cytokine discovered more than 60 years ago (7). In the absence of a unified classification, cytokines are classified by numeric order of discovery, by kinetic or functional role in inflammatory/immune responses, by primary cell of origin, or by structural homologies shared with related molecules (8). According to structural homologies, cytokines can by classified into groups: tumor necrosis factors (TNFs), interleukins (ILs), interferons (IFNs), colony-stimulating factors, transforming growth factors (TGFs), and *chemo*attractant cyto*kines*, also called chemokines.

Chemokines are small proteins that direct the movement of circulating leukocytes and immune cells. They constitute a family of more than 50 structurally homologous proteins classified in four families according to the location of N-terminal cysteine residues (i.e., CXC, CC, CX3C, or XC). Chemokines affect cells by activating surface receptors that are seven-transmembrane domain G-protein-coupled receptors (GPCRs) and have been implicated in a wide range of inflammatory diseases, such as multiple sclerosis and atherosclerosis (9). These ligands and their respective receptors participate in neuronal and microglial crosstalk (10, 11). The temporal expression of chemokines and their receptors may directly or indirectly contribute to the development of acute pain and the maintenance of chronic pain states.

Historically, cytokines were simply classified according to the functional T-helper (Th) cell group (Th1 or Th2) that produced them. However, recent studies show that cytokines and chemokine display anti-inflammatory and proinflammatory properties producing inhibitory and stimulatory effects in the immune system. As shown in **Table 1**, properties of a cytokine are dependent on the microenvironment, and most have dual effects according to their context (38, 112, 113). For example, IL-1β is considered a proinflammatory cytokine and can increase neuronal sensitization (17, 18), but it can also regulate inhibitory neurotransmission (15, 16). IL-10 is typically considered to be an immunosuppressive cytokine, which attenuates proinflammatory cytokine release and can reduce antigen presentation. However, IL-10 can also support the activation and proliferation of B cells (39), which can sustain autoimmune attacks. One of the most complex cytokines is TGF-β, which under certain conditions is involved in the differentiation of regulatory T cells (Treg) or in conjunction with IL-6 can drive the differentiation of proinflammatory T cells that produce IL-17 (Th17) (38). Hence, cytokines are characterized by (1) pleiotropy (i.e., a specific

TABLE 1 | Dual effects of cytokines involved in chronic pain*.

Cytokines	Major source	Receptors	Antinociceptive properties	Pronociceptive properties	Diseases	Biologic DMARD (year approved)
INTERLEUKINS						
IL-1β	Macrophages, mast cells, Schwann cells, microglia, astrocytes (12)	IL-1R1 IL-1R2 IL-1Ra	At physiological level, acts as a neuromodulator of LTP (13), assists host defense against infection (14), and can regulate inhibitory neurotransmission (15, 16)	↑Neuronal sensitization (17, 18), ↑mechanosensitivity of C fibers (19), ↑TRPV1 receptor expression in DRG neurons (20), ↑release of proinflammatory cytokines (14)	RA, OA, neuropathic pain, IBD, MS, AD, atherosclerosis (14, 21)	Anakinra (2001) Rilonacept (2008) Canakinumab (2009)
IL-4	Activated T cells (22)	IL-4R1 IL-4R2	↑T cell proliferation, activation of B cells, macrophages, inflammation, and wound repair (22)	Promote the differentiation of monocytes into DCs that support Th1 cell response (23), exacerbate a Th1-dependent model of colitis (24)	Atopic dermatitis Asthma, chronic itch, AD, MS (25–28)	Benralizumab (2017) Dupilumab (2017)
IL-5	Eosinophils, T_H2 cells, mast cells, NK cells (29)	IL-5R	None	Promote allergic response via ↑eosinopoiesis (29)	Asthma, headache (30, 31)	Mepolizumab (2015) Reslizumab (2016)
IL-6	Monocytes, macrophages (32)	IL-6R sIL-6R gp130	Regenerative processes (classical signaling via IL-6R) (33)	Recruitment of mononuclear cells, inhibition of T cells apoptosis, and Treg cell differentiation (trans-signaling via sIL-6R) (33), ↑TRPV1 in DRG (34), sensitization of nociceptive C-fibers (35)	Arthritis, cancer pain (33, 34, 36, 37)	Tocilizumab (2010) Siltuximab (2014) Sarilumab (2017)
IL-10	Macrophages, DCs, B cells, mast cells, T cells (38)	IL-10R1 IL-10R2	Immunosuppressive activity↓ of proinflammatory release,↓ antigen presentation, ↑release of anti-inflammatory cytokines (39),↑spinal microglial expression of β-endorphin (40) IL-10-deficient mice developed mechanical allodynia (41)	↑Activation and proliferation of immune cells (39), ↑IFN-γ production (42), ↑MHCII expression on B cells, inhibition of the suppression of B cells (38)	RA, MS, SLE, psoriasis, IBS, IBD, post-operative pain, pelvic pain, neuropathic pain (40, 43)	None
IL-13	Th2 cells, CD8+ T cells, mast cells, eosinophils, basophils (44)	IL-13Rα1	Inhibition of the release of proinflammatory cytokines and prostaglandins (45), modulation of pain-facilitating macrophages (46)	Drive skin inflammation (26), potent growth and differentiation factor for B cells (47)	Asthma, breast cancer, chronic itch, RA (26, 45, 48)	Dupilumab (2017) Lebrikizumab (2017)
IL-17	T cells (T_h17), fibroblasts (49)	Il17RA	Anti-inflammatory effect in the development of experimental autoimmune uveitis (50), maintenance of the epithelial tight junction barrier in the intestinal epithelium during inflammation (51), protection against bacterial-inflammation-induced bone loss (51)	↑Transcription of proinflammatory cytokines (49), direct activation of nociceptors (52), induced hyperalgesia by a TND-dependent neutrophil infiltration (53, 54)	Psoriasis, arthritis (55–57)	Ustekinumab (2009) Secukinumab (2015) Ixekizumab (2016) Brodalumab (2017)
IL-18	Monocytes, macrophages, microglia, astrocytes (58, 59)	IL-18R	None	↑Allodynia and hyperalgesia after intrathecal injection (60) induces astroglial activation (58) and mediates microglia/astrocyte and microglia/neuron interactions (58, 61)	RA, SLE, psoriasis, IBD, bone cancer, neuropathic pain (58, 59, 61)	None
IL-27	Activated APC (62)	IL-27 Rα/WSX-1 TCCR gp130	Suppression of inflammatory immunity via polarization of Tregs (63), ↓expansion of Th17 and IL-17 levels (63–66), and inhibition of osteoclastogenesis (67)	Trigger IFN-γ production by naïve $CD4^+$ T cells (62)	Asthma, cancer, metabolic disorders, arthritis (68)	None
IL-33	Macrophage, mast cell, astrocyte, microglia, oligodendrocyte (69)	ST2 (IL1RL1) IL-1RAcP	Single intrathecal treatment with sST2 reduces ongoing CCI-induced hyperalgesia (70)	Oligodendrocytes release IL-33 that activates both astrocytes and microglia to further produce TNF-α and IL-1β (70) and contribute to spinal pain processing (71)	RA, cancer (72–74)	None

(Continued)

TABLE 1 | Continued

Cytokines	Major source	Receptors	Antinociceptive properties	Pronociceptive properties	Diseases	Biologic DMARD (year approved)
IL-35	T_{reg}, B cells (75, 76)	IL-35R	Suppression of T-cell proliferation (77) ↓Expression of proinflammatory cytokines, ↓spinal neuronal apoptosis via inhibiting JNK signaling pathways, ↑production of IL-10 (78)	Release of proinflammatory cytokines from mononuclear cells *in vitro* (79)	RA, MS, neuropathic pain (78, 80)	None
TUMOR NECROSIS FACTOR						
TNF-α	Macrophages, astrocytes, microglia (81–83)	TNFR1 TNFR2	Nerve demyelination (via TNFR1 signaling) (84)	↑Neuronal sensitization and CGRP release (85–87), stimulation of oligodendrocyte regeneration (via TNFR2 signaling) (84)	RA, cancer, diabetes, IBD (88)	Etanercept (1988) Infliximab (1998) Adalimumab (2002) Certolizumab pegol (2008) Golimumab (2009)
TRANSFORMING GROWTH FACTOR						
TGF-β1	Macrophages, Th3 cells (38)	TGF-βR1 TGF-βR2	Development, differentiation, and polarization of Treg (38); inhibition of spinal microgliosis and spinal and astrocyte activation (89)	In association with IL-6, drive the differentiation of Th17 cells to a proinflammatory state (38)	Neurological disorders, arthritis, neuropathic pain, chronic pancreatitis (89–92)	Galunisertib (2019)
INTERFERON						
IFN-1α	Macrophages, monocytes, T cells, glial cells, neurons (93)	IFN-α/βR	Analgesic properties: ↓glutamate and substance P release (94)	Potentialization of excitatory synaptic transmission (93)	SLE (95)	None
IFN-γ	$CD4^+$ T cells, astrocytes, microglia (38, 96)	IFN-γR	Neuroprotective role and regulation of immunity (97, 98)	Recruitment and activation of microglia (99), ↑excitatory synaptic transmission (94)	Neuropathic pain, lupus, RA, MS, IBD, HLH (99–102)	Emapalumab (2018)
CHEMOKINES						
CCL2/MCP-1	Macrophages, monocytes (103)	CCR2	Global suppressive effects on T-cell trafficking and differentiation (38)	Activation of microglia (104), ↑activity of NMDA receptors in dorsal horn neurons (11), recruitment of macrophages (103)	OA, MS, asthma RA, cancer pain, IBD (38, 103)	None
CXCL1/GRO-α	Macrophages, astrocytes (105)	CXCR2	None	Involve in astroglial–neuronal interaction, central sensitization via NMDA receptors activity (106), attract polymorphonuclear cells toward inflammatory sites (105)	Neuropathic pain (106, 107)	None
CXCL8/IL-8	Macrophages, monocytes, T cells $CD8^+$, osteoclasts (108)	CXCR1 CXCR2	Participate in tissue homeostasis (e.g., skin, lung, and joint) via angiogenesis, neutrophil migration, and recruitment (109)	Neutrophil recruitment (109) and angiogenesis (110) in pathological conditions, direct activation of nociceptors in arthralgia (68, 108)	Atherosclerosis, cancer, IBD (109, 111)	None

**For biologic treatment agents, the date in parentheses represents the initial U.S. approval according to the Food and Drug Administration (FDA). AD, Alzheimer's disease; APC, antigen-presenting cells; DCs, dendritic cells; DRG, dorsal root ganglia; GRO, growth-related oncogene; HLH, hemophagocytic lymphohistiocytosis; IBD, intestinal bowel disease; IFN, interferon; IL, interleukin; MCP, macrophage inflammatory protein; MS, multiple sclerosis; NK, natural killer; NMDA, N-methyl-d-aspartate; RA, rheumatoid arthritis; OA, osteoarthritis; SLE, systemic lupus erythematosus; TGF, transforming growth factor; TNF, tumor necrosis factor; TRPV1, transient receptor potential cation channel subfamily V type 1.*

cytokine can affect several types of cells), (2) redundancy (i.e., overlapping functions), and (3) cascading signal activation (i.e., one cytokine stimulates the production of additional cytokines) (113, 114).

Physiologically, cytokines are involved in multiple biological functions such as cell differentiation, survival, growth, and metabolism (115). Although broad characterizations of cytokine behavior were aligned with adaptive immune functions, cytokine responses of the innate immune system are important to prevent damage during and following autoimmune attack, inflammation, and infections. In pathological conditions, the imbalance of cytokines participates in the development of the disease and progression leading to damage (114). In the context of the nervous system, some cytokines are considered to function as pain mediators as well as messengers of the immune system. This level of pleiotropy underscores the elegant role these molecules play in communication between the immune system and the nervous system.

SIGNALING PATHWAYS

Although the receptors for individual cytokines display specificity for their respective ligands, the subsequent signaling

pathways often converge, resulting in nuclear translocation of transcription factors and a secondary transcription of additional downstream mediators. Common signaling pathways activated following cytokine receptor ligation and activation include (1) nuclear factor-κB (NF-κB), (2) the mitogen-activated protein kinases (MAPKs), (3) the Janus kinase (JAK) and signal transducer and activator of transcription (STAT), and (4) the Smad family signaling pathways (114, 116).

NF-κB Signaling

The most widely studied signaling cascade associated with cytokine signaling is the NF-κB (NF kappa light chain enhancer of activated B cells) family (117). These are a family of highly conserved transcription factors including NF-κB2 p52/p100, NF-κB1 p50/p105, c-Rel, RelA/p65, and RelB, which form functional dimers. Receptors that can activate this cascade include IL-1R and the TNF receptors. In the cytoplasm, NF-κB family members are bound to IκB. In the classical or canonical pathways, proinflammatory cytokine receptors activate an IκB kinase complex (IKKβ, IKKα, and NEMO), which phosphorylates IκB proteins, leading to IκB degradation and the release and translocation of the NF-κB/Rel complexes to the nucleus. In the nucleus, these transcription factors can induce gene transcription alone or in combination with other transcription factors including AP-1 and STATs (118).

Some of the target genes include other proinflammatory cytokines, like IL-6 and IL-8. In some instances, there is an alternative pathway through signaling of cytokine receptors like the lymphotoxin-β receptor (LTβR and TNFRSF3) (119). These activate Nck-interacting kinase [NIK; MAPK kinase kinase (MAPKKK) 14], which in turn activates IKKα complexes that phosphorylate NF-κB2 p100. Phosphorylation of NF-κB2 p100 then leads to its ubiquitination and proteasomal processing to NF-κB2 p52/RelB complexes that translocate to the nucleus and induce target gene expression (117).

MAPK Signaling

The MAPKs are generally divided into the p38 stress-activated protein kinase (SAPK)/Jun amino-terminal kinase (JNK) and extracellular signal-regulated kinase (ERK) pathways (120). These kinase pathways are activated by a variety of environmental stresses, growth factors, GPCR agonists, and inflammatory cytokines. In the MAPK cascades, there are tiered activation steps. The membrane proximal MAPKKK kinases (MAPKKKKs) or GTPases activate MAPKKK, which mediate phosphorylation and activation of MAPK kinases (MAPKKs), which in turn phosphorylate and activate MAPK. p38 MAPK is activated by MKK3/MKK6 and is involved in the regulation of HSP27, MAPKAPK-2 (MK2), MAPKAPK-3 (MK3), and several transcription factors including ATF-2, Stat1, the Max/Myc complex, MEF-2, Elk-1, and indirectly CREB via activation of MSK1 (121).

Stress signals are delivered to the JNK family cascade by small GTPases of the Rho family (Rac, Rho, and cdc42). As with the other MAPKs, the membrane proximal kinase is a MAPKKK, typically MEKK1–MEKK4, or a member of the mixed lineage kinases (MLKs) that phosphorylate and activate MKK4 (SEK) or MKK7 and that phosphorylate the SAPK/JNK kinases, which then translocate to the nucleus where they can regulate the activity of multiple other transcription factors (122).

The ERK signaling cascade is activated by receptors involved in growth and differentiation including receptor tyrosine kinases (RTKs), integrins, and ion channels. The receptors signal through cascades that include small GTP-binding proteins (Ras and Rap1), which in turn activate a MAPKKK (Raf), a MAPKK (MEK1/MEK2), and then Erk MAPK (123). Erk dimers can regulate targets in the cytosol and also translocate to the nucleus where they phosphorylate a variety of transcription factors regulating gene expression related to growth, migration, and differentiation. As an example of signaling complexity for cytokines, TNF acts through two receptors, TNFR1 and TNFR2, which drive MAP kinase activation and enhance inflammatory responses by secondary IL-1, IL-6, and IL-8 release following the transcription of their target genes (124).

Activation of neuronal TNF receptors drives MAPK activation, which enhances inflammatory response by increasing IL-1, IL-6, and IL-8 release. IL-1 for instance is involved with cyclooxygenase (COX) upregulation within the DRG, inducing neuronal sensitization. Moreover, sensitization of ion channels in neuronal cells is involved with pain processing (125). IL-6 has been shown to induce JAK and protein kinase C (PKC) activation, which enhances the ion channel transient receptor potential (TRP) cation channel subfamily V member (TRPV1) sensitivity. In fact, JAK and PKC inhibitors decrease TRPV1 sensitization (126, 127). However, not only does this sensitization apply for the primary afferent, but it also seems that cytokines can induce neuronal sensitization in other anatomical levels such as cells in the DRG, dorsal horn of the spinal cord, and supraspinal areas (128). In fact, peripheral inflammation increases the expression of IL-1β and COX in the DRG, cascades known to be involved with neuronal network sensitization (18). It is thus noteworthy that TNF and IL-1β induced sensitization of cells in the dorsal horn and increased pain hypersensitivity (hyperalgesia) by enhancing α-amino-3-hydroxy-5-methyl-4-isoxazolepropionic acid (AMPA)- or *N*-methyl-D-aspartate (NMDA)-induced currents. Further, IL-1β and IL-6 suppressed typical inhibitory gamma-aminobutyric acid (GABA)- and glycine-induced currents (17). Accordingly, TNF and IL-1β enhanced NMDA receptor phosphorylation in the trigeminal nucleus in mesencephalic (trigeminal nucleus) and also increased NMDA current in the hippocampus (129).

Smad Signaling

The Smad family of transcription factors is largely downstream of the TGF-β and bone morphogenetic protein (BMP) superfamilies (130). In general, signaling is initiated with ligand-induced activation of serine/threonine receptor kinases and phosphorylation of the cytoplasmic signaling molecules Smad2/Smad3 for the TGF-β/activin pathway, and Smad1/Smad5/Smad9 for the BMP pathway. Activated Smads regulate diverse biological effects by partnering with other transcription factors, resulting in transcription of specific cell state-associated target genes (131). This family has inherent

regulatory negative feedback loops with inhibitory Smads (I-Smads) 6 and 7, which are also induced by both TGF-β and BMP signaling. The TGF-β and BMP pathways are cross-regulated by MAPK signaling. Moreover, in certain contexts, TGF-β signaling can also affect the Erk, SAPK/JNK, and p38 MAPK pathways independent of Smad activation (116).

JAK/STAT Signaling

Over 50 cytokines and growth factors use the JAK/STAT pathway for signaling. After receptor ligation, the JAK proteins are phosphorylated, and activated JAKs then phosphorylate STAT monomers, leading to dimerization, nuclear translocation, and DNA binding. Although there are four JAKs (JAK1, JAK2, JAK3, and TYK2) and seven STATs (STAT1, STAT2, STAT3, STAT4, STAT5a, STAT5b, and STAT6) in mammals, the number of potential combinations alone does not fully explain the pleiotropy in signaling (22, 34, 132). For example, IL-6R and IL-10R signaling both result in STAT3 activation through JAK activation; however, one cytokine is mostly proinflammatory, and the other is considered anti-inflammatory. There may be differences in STAT use for some cytokines, whereas other cytokines like IL-27 strongly activate more than one STAT protein (STAT1 and STAT3). To add to the complexity, multiple STATs may bind to the same target site due to shared specificities. In addition STAT proteins can be phosphorylated on serine residues to influence their DNA binding pattern, and STAT signaling influences epigenetic changes. Some STAT proteins have extra nuclear functions, for instance, at the mitochondrion level (133, 134).

Cytokine-Induced Peripheral Transcription

While it is well-documented that nuclear translocation of transcription factors is initiated by cytokine signaling, it has recently been demonstrated that cytokines also can induce nociceptive plasticity by local protein synthesis in the *peripheral* processes of sensory afferents (135). It is well-established that IL-6 expression is increased in arthritis and peripheral nerve injury. Likewise, nerve growth factor (NGF) levels are elevated in inflammatory and neuropathic pain states (36). IL-6- and NGF-induced mechanical hyperalgesia is reversed by rapamycin (135). Moreover, the IL-6R signals through the ERK pathway and the NGF receptor signals primarily through the AKT/mTOR pathway leading to phosphorylation of the CAP-binding protein eIF4E. Finally, phosphorylation of eIF4E enhances rapid changes in the translational control of gene expression in sensory neurons, and this effect is linked to mechanical allodynia (136). Although cytokines can induce nociceptive plasticity by local protein synthesis in the peripheral processes of sensory afferents, it remains unclear how these pathways directly intersect with the activities of ion channels or GPCR. In **Figure 1**, we schematically illustrate these pathways and actions in the cell body of a nociceptor (**Figure 1A**) and the peripheral terminus (**Figure 1B**).

PERIPHERAL NOCICEPTOR TERMINAL

Irritants or immunogens such as carrageenan administered in the hindpaw induce a transient hyperalgesia that is prevented by non-steroidal anti-inflammatory drugs (NSAIDs). However, inflammatory mediators such as prostaglandins into the same site induced prolonged hyperalgesia, described as latent or "primed" state, that is not prevented by NSAIDs (85, 137). In the same manner, during chronic pathophysiological conditions such as arthritis, cytokines induce neuronal sensitization and priming of the primary afferent (85), of the DRG (18), and as reviewed below at supraspinal levels (128). Indeed, in an arthritic murine model [K/BxN passive serum transfer (138)], the mouse shows an early phase characterized by inflammation, increased TNF production, and pain and a late phase characterized by the inflammation's resolution, decreased TNF, but persistent pain (41). These data suggest that cytokines play a role in priming peripheral nociceptors.

Peripheral termini of nociceptors form arborization-like structures in the skin, muscles, bone, joints, and viscera (139). These locations, in proximity to many different cells (e.g., keratinocytes and immune cells), facilitate the immune modulation of nociceptor function. Among the many different inflammatory diseases, arthritic diseases like rheumatoid arthritis (RA) have been studied for the pathophysiology of localized peripheral inflammation and pain. Notably, arthritic diseases have been described to involve an imbalance of cytokines (114, 140). In RA, studies highlight an early alteration of cytokine and chemokine levels months to years before the onset of joint swelling, particularly in patients with arthralgia (i.e., joint pain without observable clinical signs of disease such as joint redness or swelling) (48, 141, 142). Serum cytokine profiles also differ in RA patients with specific autoantibodies. Anti-citrullinated peptide autoantibodies (ACPAs) are present in a major subset of RA patients (around 60–70%) (143), are serological markers for the diagnosis of RA (144), and are prognostic factors for more aggressive joint diseases (145). In the sera of RA patients with ACPAs, there was an increase in the IL-5, IFN-1α, TNF, and IL-13 levels. In contrast, there were specific increases in eotaxin and RANTES (i.e., regulated on activation normal T cell expressed and secreted) levels in the sera of RA patients who did not have any detectable ACPAs (48). In animal models of arthritis, including antigen-induced arthritis (AIA), collagen antibody-induced arthritis (CAIA), and collagen-induced arthritis (CIA), IL-6 has been implicated as a key factor in peripheral pain mechanisms (36). Direct IL-6 or IL-6/sIL-6R administration into knee joints in rodents induced a long-lasting sensitization of nociceptive C-fibers, contributing to mechanical hypersensitivity (35).

In models of inflammatory pain, such as carrageenan administration in the hindpaw, infiltration of macrophages and the local release of TNF play a key role in the development and sensitization of peripheral afferents (85). Activation of neuronal TNF receptors increases the production of IL-1β, IL-6, and CCL2 [formerly known as monocyte chemoattractant protein-1 (MCP-1)]. Both IL-1β and IL-6 have been shown to have activity in acute inflammatory and chronic pain (146–148). Indeed IL-1β enhanced pain transduction and conduction via modulation of ion channels such as TRP ankyrin 1 (TRPA1), TRPV1, and Nav1.7. CCL2 also contributes to macrophage recruitment (104, 149). Thus, these factors serve to perpetuate a feedback loop

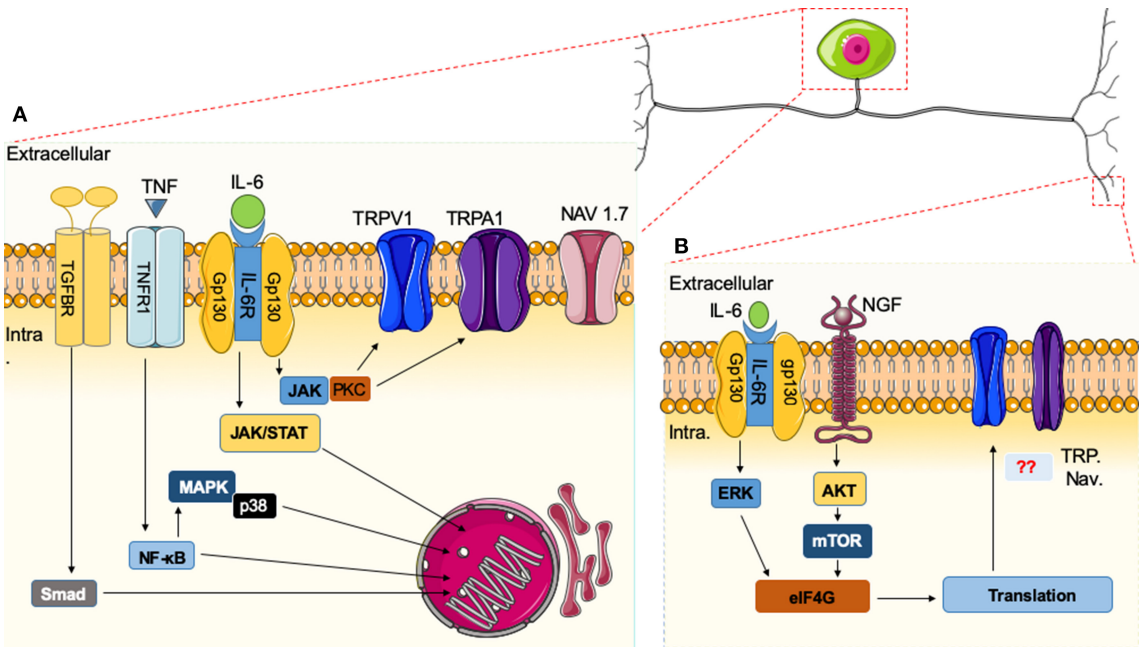

FIGURE 1 | Immune system and nociceptor activation. **(A)** Cytokines released in the vicinity of the cell body of nociceptors can induce specific receptor activation and signaling cascades. Upon activation of nuclear factor (NF)-κB, mitogen-activated protein kinase (MAPK)/Janus kinase (JAK), and Smad transcription factors present in the cytoplasm are phosphorylated and translocated to the nucleus, leading to the expression of target genes, resulting in biological responses. Alternatively, downstream modulators like protein kinase C (PKC) can sensitize neurons through effects on ion channels (e.g., TRPV1 or Na^+ channels). **(B)** In the peripheral terminus, there are additional cytokines that signal through the extracellular signal-regulated kinase (ERK) pathway and the AKT/mTOR pathways leading to phosphorylation of eIF4E, which can regulate local protein synthesis in the peripheral processes of sensory afferents. It remains unknown how these pathways directly intersect with the activities of ion channels.

between neuronal sensitization and cytokine production during tissue injury or inflammation.

Other studies have suggested that additional cytokines play key roles in the induction of inflammatory pain in models of arthritis, including IL-8, IL-17, and IL-27 (55, 58, 68). The chemokine IL-8 and its receptor CXCR2 are involved in sensitization of afferent nociceptors in ACPA-induced arthralgia. Interestingly, recent studies demonstrated that a single injection of human IgG ACPA or monoclonal murinized IgG ACPA antibodies isolated from RA patients is capable of initiating pain without paw swelling when injected into rodents (68). This effect of ACPAs is associated with osteoclast activation, at least *in vitro*, which via the release of the chemokine CXCL1 (an analog to human IL-8) mediates their pronociceptive effects (68, 108). IL-8 has also been implicated in conditions such as chronic low back pain (LBP). Krock et al. showed a specific upregulation of this chemokine in the cerebrospinal fluid of LBP patients with degenerating disks and a reduction of disk degeneration and chronic back pain in a mouse model (148). In a neuropathic orofacial pain condition, the burning mouth syndrome, patients present an elevated level of plasma IL-8, and this signature directly correlates with pain and depressive symptomatology (150). Hence, IL-8 has been implicated in the periphery for several different pain phenotypes.

As described above, IL-6 has pleiotropic roles associated with pain and inflammation. Another cytokine that also shares the gp130 common receptor chain and signals through the JAK/STAT pathway is IL-27. IL-27 is a heterodimer formed by the Epstein–Barr virus-induced gene 3 (EBI3) and IL-27 p28 subunits, which binds to a receptor composed of the gp130 common receptor chain and IL-27Rα (i.e., WSX-1 or TCCR) (62). Sasaguri et al. showed that IL-27 signaling constitutively contributes to control of thermal (heat and cold) and mechanical sensitivity (151). In an arthritis model, IL-27 attenuates disease development and histological disease severity (i.e., cell infiltration in the joint, synovial hyperplasia, and joint erosion) by reducing the expansion of Th17 cells and IL-17 levels (63–66), which can reduce nociception (**Table 1**). In osteoimmunology, IL-27 plays a critical role in limiting bone erosion by inhibiting osteoclastogenesis (67). Osteoclast activity is directly involved in pain development and reduced with the use of osteoclast inhibitors such as bisphosphonates or denosumab (152). The suggested mechanisms of this action include mechanical stabilization in bone pain from trauma and also changes in pH and acidosis in bone pain from cancer. Nociception could be promoted by acidosis in which H^+ protons can directly activate specific ionic or receptors sensitive to protons such as TRPV1 and the acid-sensing ion channel (ASIC) family (153, 154).

DORSAL ROOT GANGLIA

It has become apparent that the excitability of the afferent input circuitry reflects the functional complexity of the DRG system. DRG neurons are supplied by a fenestrated vasculature that lies outside the blood–brain barrier (BBB), slowing the passage of molecules that are normally excluded from the neuraxis (155). This exposure of the afferent cell bodies to circulating products, including cytokines, may partly explain why circulating neurotoxic agents (e.g., chemotherapeutics) preferentially accumulate and injure cells within the DRG, inducing a sensory rather than a motor neuropathy (156). DRG neurons are additionally supported by satellite glial cells (SGCs), which envelop them and display gap junction linkages between these two cell types (157). During inflammation, SGCs display enhanced activation, increased TNF production, and neuronal excitability (73). An increase of gap junctions has been observed in pain-generating conditions, and this correlates with enhanced neuronal excitability (157). Importantly, peripheral inflammation or nerve injury causes DRG neuronal sensitization, leading to a spreading activation of SGCs through gap junctions and to the expression and release of IL-1β from SGCs.

Current work highlights an important role of macrophages in response to inflammation and cytokine signaling. A major source of endogenous cytokine production is from these resident and migratory DRG macrophages. In arthritic conditions (e.g., osteoarthritis and RA), macrophages infiltrate into the DRG and acquire a phenotype resembling that of TNF-stimulated macrophages, suggesting a role of these cells in the maintenance of arthritic pain (158). *In vitro*, macrophages stimulated with TNF promote release of calcitonin gene-related peptide (CGRP) by nociceptors, which is consistent with their pronociceptive effect (159). *In vivo*, TNF is involved with sensitization of nociceptive fibers and elicits a rapid increase of CGRP release from the peripheral termini of nociceptors (86, 87). Other than macrophages, during inflammation, SGCs become activated, increasing TNF production, and enhancing neuronal excitability (73). In neuropathic pain, a key role of TNF in the DRG has been demonstrated by lentivirus-mediated silencing of TNF in DRG, which attenuated the pain phenotype and reduced neuronal cell death in mice with an L5 transection (160).

DRG cells produce additional cytokines such as IL-1β and IL-6 and chemokines such as CCL2 or CXCL1 within the DRGs that are involved in pain signaling (3, 161). Interestingly in osteoarthritis, a high CCL2 production is associated with elevated numbers of macrophages in the DRG and a high level of CGRP in DRG neurons (162, 163). Mice lacking the CCR2 receptor (global knockout) fail to develop mechanical allodynia in nerve injury models (164). Accordingly, we suggest that during inflammation, a neuro-crosstalk can occur in the DRG where inflammation triggers cytokine and chemokine release from local/infiltrating macrophages and neurons, contributing to development and maintenance of facilitated states of excitability in the local DRG circuit. Such enhanced excitability would contribute to an enhanced afferent input into dorsal horn second-order neurons.

Several cytokines, IL-6 for example, can excite DRG neurons directly by rapid effects that do not require gene transcription but are likely to involve phosphorylation of different ion channels, such as the TRP family. IL-6 is a pleiotropic cytokine with a pivotal role in the pathophysiology of arthritis and pain sensitization through increasing neuronal calcium mobilization, action potential generation, and ion channel sensitization. IL-6 acting through IL-6R and gp130 drives JAK and PKC activation, which enhances TRPV1, inducing excitability of nociceptive $TRPV1^+$ DRG neurons (34, 124). Correspondingly JAK and PKC inhibitors decrease TRPV1 sensitization (34).

Gap junctions in the DRG can provide direct communications between neuronal cell bodies and SGCs. An increase in gap junctions has been observed in pain condition and seems to enhance neuronal excitability and thus elicit pain (157). Importantly, peripheral inflammation or nerve injury causes sensitization of neurons, innervating peripheral tissues, and spreading of activation of SGCs through gap junctions, which leads to the expression and release of IL-1β from SGCs. IL-1β has been shown to increase TRPV1 expression in DRG neurons. Moreover, IL-1RI antagonism reduces thermal hyperalgesia antigen-induced arthritis (20). IL-1β has been shown to act in a p38 MAPK-dependent manner, to increase the excitability of nociceptors. Indeed, IL-1β relieves resting slow inactivation of tetrodotoxin-resistant voltage-gated sodium channels and also enhances persistent TTX-resistant current near the threshold (165). These IL-1β actions on nociceptors have facilitatory effects in neurotransmission, which at least in part explains the hyperalgesic effect seen with the direct application of IL-1β or the endogenous production and release of IL-1β within the DRG.

Beyond the effect of IL-1β on ion channel sensitization, it has been shown that intraplantar IL-1β can induce persistent hyperalgesia, which is dependent on GPCR kinase 2 (GRK2) and IL-10 downregulation. GRK2 plays a regulatory role in the inflammatory response as studied in arthritis models. Reduction of GRK2 in peripheral macrophages markedly prolonged hyperalgesia and pain behavior in response to an intraplantar injection of IL-1β or the inflammatory agent carrageenan (166). The reduction of GRK2 in macrophages is associated with the transition from acute to persistent hyperalgesia due to the lack of IL-10 production. Moreover, local anti-IL-10 treatment in the paw did not influence IL-1β-induced hyperalgesia, indicating that IL-10 signaling in the spinal cord or DRG is required for spontaneous resolution of hyperalgesia. Corroborating these data, our group recently showed that mice deficient in IL-10 rapidly developed mechanical allodynia that did not recover, suggesting that this cytokine also plays a key role in the acute and chronic phases of pain-like behavior (41).

These data suggest that beyond changes in the peripheral terminus nociceptor, the DRG plays an important role in the development of pain states. Thus, cytokines produced by local cells or released into the DRG are involved with the facilitation of nociceptive stimulus, inducing subsequent dorsal horn spinal activity.

SPINAL CORD

The peripheral nociceptor forms an excitatory synapse with second-order neurons in the dorsal horn of the spinal

cord to initiate transmission in the central nervous system (CNS). This synapse can be modulated by local interneurons, microglia, and astrocytes. These last cells constitute a component serving to alter the input–output function of the dorsal horn. Inflammatory cytokines maintain enhanced pain signaling through modulating the central terminals of nociceptors and/or spinal cord neurons. In naïve animals, intrathecal delivery of cytokines can induce a direct pronociceptive effect, leading to mechanical, and/or thermal hyperalgesia, which has been observed after intrathecal injection of IL-1β (15, 16, 167, 168), IL-18 (60), TNF (15, 16, 167), IL-6 (15), CXCL1 (107), CX3CL1/fractalkine (169), or CCL2/MCP-1 (170) among others. Conversely, a pronociceptive phenotype is reduced in mice lacking such cytokine or chemokine signaling or after the administration of anti-cytokine antibodies or cytokine receptor antagonists. In pathologic conditions, chronic intrathecal administration of IL-1 receptor antagonist (IL-1ra) prevents pain induced by nerve injury in mice, and a single intrathecal injection of IL-1ra induced a long-lasting attenuation of mechanical hypersensitivity in the same model (171). Intrathecally, coadministration of IFN-β and anti-TNF antibodies permanently reversed mechanical allodynia in males in the murine K/BxN serum transfer model of RA (41). Moreover, intrathecal delivery of cytokines such as TGF-β or IL-13 can also induce an antinociceptive effect in neuropathic pain condition (46, 89, 158). TGF-β can inhibit excitatory synaptic transmission in the spinal cord (172) and neuropathic pain along with glial activation and neuroinflammation in the spinal cord (89, 172).

Considering that cytokines play a role in the development and maintenance of pain at the spinal cord level, we raise the question of where these neuraxial cytokines are produced and where they act. Microglia serve as spinal-resident macrophage-like cells and display a rapid response to increased afferent traffic and to pathological changes in the CNS. Spinal microglial activation has been demonstrated in several pain conditions [for review, see (173), including mononeuropathies after peripheral nerve injury (174), polyneuropathies after chemotherapy (175, 176), or in diabetic models (177), chronic inflammatory pain (178), and cancer pain (179), although some data are conflicting (180)]. Microglia participate notably in the regulation of neuroinflammation that contributes to the pathogenesis of pain (173). Signals that activate microglia converge on intracellular signaling cascades frequently involving the phosphorylation of p38 MAPK, triggering production and release of TNF, IL-1β, and IL-18; increased expression of COX; and subsequent synthesis of prostaglandin E2 (PGE_2) (18, 181, 182). These neuromodulators then lead to enhanced dorsal horn excitability, which ultimately serves to enhance receptive fields, increase output of the pain-relevant sensory message to supraspinal areas, and enhance pain behavior.

Astrocytes have a key role in neurotransmitter recycling, regulation of blood flow, energy metabolism, synaptogenesis, and synaptic transmission (183–187). Astrocytes signal physically through gap junctions (e.g., connexin Cx43), facilitating intercellular transmission (188, 189). Moreover, it has been demonstrated that upregulation of Cx43 triggers release of chemokines, ATP, and glutamate, which ultimately induces nociceptor sensitization (185, 186). Astrocytes have been shown to play both beneficial and detrimental roles, depending on the nature of the injury or disease, that differ in their functions (190). Thus, spinal cord astrocytes can generate IFN-α, which have an antinociceptive effect mediated through the mu opioid receptor (94). In addition, recent data from our group have shown that the post-inflammatory allodynia from an arthritis model may be robustly regulated by downstream effectors activated through IFN-β and interferon-inducible factors, including IL-10 and IL-1ra (41). In this model, the allodynia only subsided when anti-TNF therapy was combined with supplemental IFN-β, indicating that chronic pain treatment might require modulation of multiple pathways (41).

Astrocytes can also modulate pain through IL-33 production. IL-33 is a member of the IL-1 superfamily but is active after transcription and is deactivated by caspase cleavage. It binds to the ST2 (Il1rl1) receptor, encoded by the *IL1RL1* gene, and the coreceptor IL-1 receptor accessory protein (IL-1RAcP). After receptor engagement, the MyD88 signal cascade is activated similarly as after IL-1R and IL-18R activation. This cytokine has a pronociceptive effect with intrathecal injection (191, 192). In addition, inhibiting the IL-33/ST2 pathway reduced nociceptive behavior in murine models of pain, including cancer and chemically induced inflammation (72, 192, 193).

The effects of the intrathecal injection of cytokines cited above directly support the key roles played by spinal cord cytokines in pain states. As these cytokines are not acting independently, it is not surprising that these agents display important interactions in different pain states reflecting their facilitatory and suppressive interactions. As an example, intrathecal administration of recombinant IL-27 induced antinociception dependent on IL-10 during the maintenance phase of peripheral neuropathy (194). Also, intrathecal delivery of IL-35 in an experimental murine model of autoimmune encephalomyelitis (EAE) reduced pain behaviors (i.e., facial allodynia and grimacing), which was noted to occur through an upregulation of an inflammatory cytokine, IL-10 (195). IL-35 has been very recently highlighted as a candidate target for diabetic neuropathic pain (DNP) treatment (78). In fact, in a streptozotocin-induced DNP rat model, other than a protective effect against inflammatory response, IL-35 injected intrathecally reduced allodynia via inhibition of JNK signaling (78).

Second-order dorsal horn neurons express cytokine receptors such as TNFR1, TNFR2, IL-1R, and IL-6R. Cytokine released at the spinal cord level by resident cells (e.g., microglia/astrocytes) can induce sensitization of the secondary neuron, leading to supraspinal areas of activation where pain is processed and perceived as an uncomfortable sensation (139). In fact, IL-6, TNF, and IL-β enhance spontaneous post-synaptic current (sEPSCs) in the spinal cord by both increasing excitatory synaptic neurotransmission and suppressing inhibitory synaptic transmissions (160). Taken together, these studies show that therapeutically targeting peripheral inflammation will not necessarily affect persistent pain. However, modulating multiple pathways at the spinal level might be an effective way to

prevent the development of chronic pain and to alleviate ongoing pain.

SUPRASPINAL AREAS

Changes in higher-order functions such as anxiety or depression are critical components of pain phenotypes, especially in the context of a chronic pain state (196, 197). Studies in animal models (99, 198, 199) and *in vivo* positron emission tomography (PET) associated with magnetic resonance imaging (MRI) in humans (200, 201) are consistent with the fact that chronic pain states lead to an alteration of glial function in the brain. Current thinking emphasizes the critical role that cytokines can play in regulating depressive states, through their effects upon key aminergic pharmacological systems regulating depressive states such as increased monoamine transporter activity (202), reduced cofactor availability (203), and reduced expression of glutamate transporters and increased glutamate release from astrocytes (204).

Cytokines play key roles in supraspinal modulation of pain transduction. Consistent with this assertion are the findings that intracerebroventricular (ICV) injection of TNF, IL-1β, and IL-6 induced hyperalgesia (205–207) and that blocking these cytokines in the brain reduced the behaviorally defined expression of a pain state (208). Of note, mechanistically, it is not clear whether this pain state reflects the role of an enhanced supraspinal response to the ascending pain stimulus or an activation of descending facilitatory/loss of descending inhibitory system (209).

Microglial activation (Iba1 marker) after nerve injury is observed in specific brain regions involved in pain and affect. These regions include not only the thalamus and somatosensory cortex but also limbic regions considered to be affiliated with the affective component of the pain response (210). Importantly, as in the spinal cord, glial cells are thought to be a major source of cytokines and chemokines in the brain (204), and the activation of these cells is considered to play a key role in anxiety and depression, comorbidities associated with chronic pain states (211, 212). Other works support the involvement of microglial activation in prefrontal cortex, amygdala, and hippocampal neurons associated with an overproduction of TNF in neuropathic pain and chronic-pain-associated depression (211, 213). Moreover, upregulation of IL-10 and IL-1β is found in the contralateral–ventrolateral orbital cortex (VLO) of rats with spared nerve injury (SNI), and IL-1β expression and glutamatergic neurotransmission are enhanced in the prefrontal cortex (PFC) of mice with neuropathic pain (214).

Cytokine activation in the brain on the affective-motivation component of pain processing is an exciting component of the role played by cytokines in pain processing. Considerable work has demonstrated that circulating inflammatory markers (e.g., IL-1β, TNF, IL-6, and C-reactive protein) are important covariates for depression and anxiety in humans (215, 216).

CYTOKINES AS THERAPEUTIC TARGETS

Although not the focus of this review, it would seem remiss not to briefly comment on some of the advances seen with the advent of approved biologic therapies. As described previously, cytokines and chemokines have a key role in disease-associated pain and therapies exerting an action on cytokine release or activity, which is really effective [**Table 1**; (182, 183)]. Accumulating data suggest that in a variety of pain states, there is a strong covariance between circulating proinflammatory cytokine messages and the pain states in fibromyalgia (217) or painful (vs. non-painful) neuropathies (218, 219). Of note, TNF antagonism improved depressive symptoms in patients with high baseline inflammatory biomarkers (220). While these endpoints do not directly impact upon pain signaling, they provide an important covariate between chronic pain and comorbidities that can enhance the chronic pain states (221).

The bulk of clinical data describe the relief of pain in the treatment of inflammatory states like RA using agents that block the activity of key cytokines like IL-6 and TNF. Conventional synthetic disease-modifying antirheumatic drugs (csDMARDs) such as methotrexate or sulfasalazine can attenuate cytokine release (222–226), but the biologic disease-modifying antirheumatic drugs (bDMARDs), which have a direct effect on the function and levels of circulating cytokines, have been shown to be more effective alone or in combination with csDMARDs [**Table 1**; (124, 227–229)]. The success of these agents is reflected in the development of agents with similar targets. Notable groups of agents include anti-TNF (including infliximab, adalimumab, certolizumab pegol, etanercept, or golimumab) and anti-IL-6 or IL-6 receptor antagonists (i.e., tocilizumab, sarilumab, clazakizumab, and olokizumab) (115). However, remission of inflammation by clinical parameters has not universally been associated with complete relief of pain, and residual pain with neuropathic features can persist (178). More recently, agents that intercede with signaling, notably the JAK inhibitors, may add to the armamentarium of agents that can reduce pain as well as inflammation (230, 231). The development of therapeutic agents that target individual cytokines and their signaling pathways is a promising and exciting area that has been extensively reviewed by others (232, 233). These therapies hold significant promise for the future, and further investigations into their level of anatomic activity will hopefully yield insights into individualized therapeutic plans.

CONCLUSION

The primary emphasis of this review has been on reviewing the role of cytokines at the levels of the peripheral terminus, the DRG, the spinal dorsal horn, and supraspinal circuits (**Figure 2**). Although pain arises from different conditions, some mechanistic components are conserved across pain states:

(i) Peripheral nerve fibers (nociceptors) are directly exposed to circulating products like cytokines and detect environmental stimuli (thermal, mechanical, or chemical

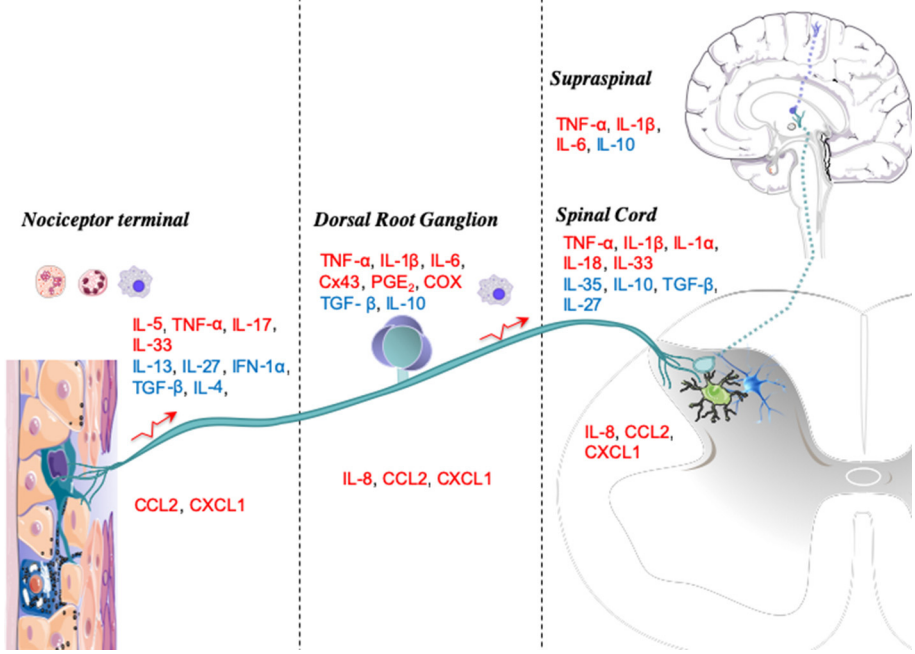

FIGURE 2 | Anatomic levels of cytokine interactions with nociceptive processing. Upon injury or infection, mediators such as immune cytokines are released locally by resident or blood-derived immune cells. The peripheral terminals of nociceptors, dorsal root ganglia (DRGs), and spinal cords have several receptors for these mediators, which activate signaling cascades that modulate nociceptive activity. Cytokines are displayed as pronociceptive (red) or antinociceptive (blue).

nature) and stimulate excitation of second-order neurons at the spinal cord.

(ii) In the DRG, the somata of nociceptors are surrounded by SGCs and macrophages. As noted, the DRG lies outside of the conventional BBB restriction, leading it to be directly exposed to these circulating proteins and other danger signals. These peripheral stimuli drive cytokine secretion from SGCs and macrophages, contributing to inflammatory signaling cascades and persistent pain.

(iii) The dorsal horn in the spinal cord receives information from nociceptors.

(iv) The incoming information is processed by complex circuits involving excitatory and inhibitory interneurons and transmitted to projection neurons to several supraspinal areas in the CNS. Spinal cord astrocytes and microglia are described as key cells in the mechanism of pain processing in several pain models (234).

In **Figure 2**, we graphically summarize key cytokines that play a role in these four major neuraxial components (i.e., the peripheral terminal, DRG, spinal cord, and brain). At each anatomic level, we note the relevance of the several local systems (neuronal, glial, and inflammatory cells) that contribute both as a source of cytokines and as a target for these molecules functioning in an autocrine-/paracrine-like fashion.

This review serves to emphasize the multiple levels at which cytokines may be released and act to alter the nociceptive phenotype and reflect the role of a local paracrine or autocrine function. It is clear, however, that this position does not exclude the likelihood that the circulating cytokine profile observed in a variety of inflammatory and injury states might contribute to the abnormal pain and depression though a circulating delivery. Of note, the presence of these circulating proinflammatory products and the accessibility of these products to neuraxial components such as the peripheral terminal and the DRG point to potential interactions. The ability of glia such as astrocytes and perivascular macrophages to sample circulating products, along with the evident role played by glia in CNS function, points to the likelihood that circulating products can modify function throughout the neuraxis. We therefore conclude that targeting inflammatory cytokine and chemokine signaling may provide additional strategies in the therapeutic intervention of chronic pain. However, we note that despite recent promising advances, any single agent is unlikely to be uniformly effective, and future studies in this area are warranted.

AUTHOR CONTRIBUTIONS

All authors contributed to the drafting and revision of the manuscript.

FUNDING

This work was funded in part by grants from NIH/NINDS 1 R01 NS099338 (TY) and 1 R01 NS102432-01.

REFERENCES

1. Catani M, Dell'Acqua F, Thiebaut de Schotten M. A revised limbic system model for memory, emotion and behaviour. *Neurosci Biobehav Rev*. (2013) 37:1724–37. doi: 10.1016/j.neubiorev.2013.07.001
2. Rittner HL, Machelska H, Stein C. Immune system, pain and analgesia. In: Masland RH, editor. *The Senses: A Comprehensive Reference*. New York, NY: Elsevier (2008). p. 407–27.
3. Miller RJ, Jung H, Bhangoo SK, White FA. Cytokine and chemokine regulation of sensory neuron function. *Handb Exp Pharmacol*. (2009) 194:417–49. doi: 10.1007/978-3-540-79090-7_12
4. Baral P, Udit S, Chiu IM. Pain and immunity: implications for host defence. *Nat Rev Immunol*. (2019) 19:433–47. doi: 10.1038/s41577-019-0147-2
5. Lapato AS, Tiwari-Woodruff SK. Connexins and pannexins: at the junction of neuro-glial homeostasis & disease. *J Neurosci Res*. (2018) 96:31–44. doi: 10.1002/jnr.24088
6. Woller SA, Eddinger KA, Corr M, Yaksh TL. An overview of pathways encoding nociception. *Clin Exp Rheumatol*. (2017) 35(Suppl. 1):40–6.
7. Isaacs A, Lindenmann J. Virus interference. I. The interferon. *Proc R Soc London Ser B Biol Sci*. (1957) 147:258–67. doi: 10.1098/rspb.1957.0048
8. McInnes IB. *Cytokines*. New York, NY: Elsevier (2017). doi: 10.1016/B978-0-323-31696-5.00026-7
9. Charo IF, Ransohoff RM. The many roles of chemokines and chemokine receptors in inflammation. *N Engl J Med*. (2006) 354:610–21. doi: 10.1056/NEJMra052723
10. Abbadie C, Bhangoo S, De Koninck Y, Malcangio M, Melik-Parsadaniantz S, White FA. Chemokines and pain mechanisms. *Brain Res Rev*. (2009) 60:125–34. doi: 10.1016/j.brainresrev.2008.12.002
11. Gao Y-J, Ji R-R. Chemokines, neuronal-glial interactions, and central processing of neuropathic pain. *Pharmacol Ther*. (2010) 126:56–68. doi: 10.1016/j.pharmthera.2010.01.002
12. Ren K, Dubner R. Interactions between the immune and nervous systems in pain. *Nat Med*. (2010) 16:1267–76. doi: 10.1038/nm.2234
13. Hewett SJ, Jackman NA, Claycomb RJ. Interleukin-1β in central nervous system injury and repair. *Eur J Neurodegener Dis*. (2012) 1:195–211.
14. Dinarello CA. Overview of the IL-1 family in innate inflammation and acquired immunity. *Immunol Rev*. (2018) 281:8–27. doi: 10.1111/imr.12621
15. Kawasaki Y, Zhang L, Cheng J-K, Ji R-R. Cytokine mechanisms of central sensitization: distinct and overlapping role of interleukin-1beta, interleukin-6, and tumor necrosis factor-alpha in regulating synaptic and neuronal activity in the superficial spinal cord. *J Neurosci*. (2008) 28:5189–94. doi: 10.1523/JNEUROSCI.3338-07.2008
16. Gruber-Schoffnegger D, Drdla-Schutting R, Hönigsperger C, Wunderbaldinger G, Gassner M, Sandkühler J. Induction of thermal hyperalgesia and synaptic long-term potentiation in the spinal cord lamina I by TNF-α and IL-1β is mediated by glial cells. *J Neurosci*. (2013) 33:6540–51. doi: 10.1523/JNEUROSCI.5087-12.2013
17. Liu T, Jiang CY, Fujita T, Luo SW, Kumamoto E. Enhancement by interleukin-1β of AMPA and NMDA receptor-mediated currents in adult rat spinal superficial dorsal horn neurons. *Mol Pain*. (2013) 9:16. doi: 10.1186/1744-8069-9-16
18. Araldi D, Ferrari LF, Lotufo CM, Vieira AS, Athié MCP, Figueiredo JG, et al. Peripheral inflammatory hyperalgesia depends on the COX increase in the dorsal root ganglion. *Proc Natl Acad Sci*. (2013) 110:3603–8. doi: 10.1073/pnas.1220668110
19. Cook AD, Christensen AD, Tewari D, McMahon SB, Hamilton JA. Immune cytokines and their receptors in inflammatory pain. *Trends Immunol*. (2018) 39:240–55. doi: 10.1016/j.it.2017.12.003
20. Ebbinghaus M, Uhlig B, Richter F, Von Banchet GS, Gajda M, Bräuer R, et al. The role of interleukin-1β in arthritic pain: main involvement in thermal, but not mechanical, hyperalgesia in rat antigen-induced arthritis. *Arthritis Rheum*. (2012) 64:3897–907. doi: 10.1002/art.34675
21. Ren K, Torres R. Role of interleukin-1beta during pain and inflammation. *Brain Res Rev*. (2009) 60:57–64. doi: 10.1016/j.brainresrev.2008.12.020
22. Busch-Dienstfertig M, González-Rodríguez S. IL-4, JAK-STAT signaling, and pain. *JAK-STAT*. (2014) 2:e27638. doi: 10.4161/jkst.27638
23. Major J, Fletcher JE, Hamilton TA. IL-4 pretreatment selectively enhances cytokine and chemokine production in lipopolysaccharide-stimulated mouse peritoneal macrophages. *J Immunol*. (2002) 168:2456–63. doi: 10.4049/jimmunol.168.5.2456
24. Fort MM, Lesley R, Davidson NJ, Menon S, Brombacher F, Leach MW, et al. IL-4 exacerbates disease in a Th1 cell transfer model of colitis. *J Immunol*. (2001) 166:2793–800. doi: 10.4049/jimmunol.166.4.2793
25. Gadani SP, Cronk JC, Norris GT, Kipnis J. IL-4 in the brain: a cytokine to remember. *J Immunol*. (2012) 189:4213–9. doi: 10.4049/jimmunol.1202246
26. Oetjen LK, Mack MR, Feng J, Whelan TM, Niu H, Guo CJ, et al. Sensory neurons co-opt classical immune signaling pathways to mediate chronic itch. *Cell*. (2017) 171:217–28.e13. doi: 10.1016/j.cell.2017.08.006
27. Kim J, Kim BE, Leung DYM. Pathophysiology of atopic dermatitis: clinical implications. *Allergy asthma Proc*. (2019) 40:84–92. doi: 10.2500/aap.2019.40.4202
28. Steinke JW, Borish L. Th2 cytokines and asthma. Interleukin-4: its role in the pathogenesis of asthma, and targeting it for asthma treatment with interleukin-4 receptor antagonists. *Respir Res*. (2001) 2:66–70.
29. Bagnasco D, Ferrando M, Varricchi G, Puggioni F, Passalacqua G, Canonica GW. Anti-Interleukin 5 (IL-5) and IL-5Ra biological drugs: efficacy, safety, and future perspectives in severe eosinophilic asthma. *Front Med*. (2017) 4:135. doi: 10.3389/fmed.2017.00135
30. Munno I, Centonze V, Marinaro M, Bassi A, Lacedra G, Causarano V, et al. Cytokines and migraine: increase of IL-5 and IL-4 plasma levels. *Headache*. (1998) 38:465–7. doi: 10.1046/j.1526-4610.1998.3806465.x
31. Talbot S, Foster SL, Woolf CJ. Neuroimmunity: physiology and pathology. *Annu Rev Immunol*. (2016) 34:421–47. doi: 10.1146/annurev-immunol-041015-055340
32. Gabay C. Interleukin-6 and chronic inflammation. *Arthritis Res Ther*. (2006) 8 (Suppl. 2):S3. doi: 10.1186/ar1917
33. Schett G. Physiological effects of modulating the interleukin-6 axis. *Rheumatology*. (2018) 57:ii43–50. doi: 10.1093/rheumatology/kex513
34. Fang D, Kong L-Y, Cai J, Li S, Liu X-D, Han J-S, et al. Interleukin-6-mediated functional upregulation of TRPV1 receptors in dorsal root ganglion neurons through the activation of JAK/PI3K signaling pathway: roles in the development of bone cancer pain in a rat model. *Pain*. (2015) 156:1124–44. doi: 10.1097/j.pain.0000000000000158
35. Brenn D, Richter F, Schaible H-G. Sensitization of unmyelinated sensory fibers of the joint nerve to mechanical stimuli by interleukin-6 in the rat: an inflammatory mechanism of joint pain. *Arthritis Rheum*. (2007) 56:351–9. doi: 10.1002/art.22282
36. Krock E, Jurczak A, Svensson CI. Pain pathogenesis in rheumatoid arthritis-what have we learned from animal models? *Pain*. (2018) 159(Suppl. 1):S98–109. doi: 10.1097/j.pain.0000000000001333
37. Choy EHS, Calabrese LH. Neuroendocrine and neurophysiological effects of interleukin 6 in rheumatoid arthritis. *Rheumatology*. (2018) 57:1885–95. doi: 10.1093/rheumatology/kex391
38. Shachar I, Karin N. The dual roles of inflammatory cytokines and chemokines in the regulation of autoimmune diseases and their clinical implications. *J Leukoc Biol*. (2013) 93:51–61. doi: 10.1189/jlb.0612293
39. Iyer SS, Cheng G. Role of interleukin 10 transcriptional regulation in inflammation and autoimmune disease. *Crit Rev Immunol*. (2012) 32:23–63. doi: 10.1615/CritRevImmunol.v32.i1.30
40. Wu H-Y, Mao X-F, Tang X-Q, Ali U, Apryani E, Liu H, et al. Spinal interleukin-10 produces antinociception in neuropathy through microglial β-endorphin expression, separated from antineuroinflammation. *Brain Behav Immun*. (2018) 73:504–19. doi: 10.1016/j.bbi.2018.06.015
41. Woller SA, Ocheltree C, Wong SY, Bui A, Fujita Y, Gonçalves dos Santos G, et al. Neuraxial TNF and IFN-beta co-modulate persistent allodynia in arthritic mice. *Brain Behav Immun*. (2019) 76:151–8. doi: 10.1016/j.bbi.2018.11.014
42. Lauw FN, Pajkrt D, Hack CE, Kurimoto M, van Deventer SJH, van der Poll T. Proinflammatory effects of IL-10 during human endotoxemia. *J Immunol*. (2000) 165:2783–9. doi: 10.4049/jimmunol.165.5.2783
43. Tian G, Li J-L, Wang D-G, Zhou D. Targeting IL-10 in auto-immune diseases. *Cell Biochem Biophys*. (2014) 70:37–49. doi: 10.1007/s12013-014-9903-x

44. Fasoulakis Z, Kolios G, Papamanolis V, Kontomanolis EN. Interleukins associated with breast cancer. *Cureus*. (2018) 10:e3549. doi: 10.7759/cureus.3549
45. McCann B, Miaskowski C, Koetters T, Baggott C, West C, Levine JD, et al. Associations between pro- and anti-inflammatory cytokine genes and breast pain in women prior to breast cancer surgery. *J Pain*. (2012) 13:425–37. doi: 10.1016/j.jpain.2011.02.358
46. Kiguchi N, Sakaguchi H, Kadowaki Y, Saika F, Fukazawa Y, Matsuzaki S, et al. Peripheral administration of interleukin-13 reverses inflammatory macrophage and tactile allodynia in mice with partial sciatic nerve ligation. *J Pharmacol Sci*. (2017) 133:53–56. doi: 10.1016/j.jphs.2016.11.005
47. Justiz Vaillant AA, Qurie A. *Interleukin*. Treasure Island, FL: StatPearls Publishing (2019).
48. Chalan P, Bijzet J, van den Berg A, Kluiver J, Kroesen B-J, Boots AMH, et al. Analysis of serum immune markers in seropositive and seronegative rheumatoid arthritis and in high-risk seropositive arthralgia patients. *Sci Rep*. (2016) 6:26021. doi: 10.1038/srep26021
49. Moynes DM, Vanner SJ, Lomax AE. Participation of interleukin 17A in neuroimmune interactions. *Brain Behav Immun*. (2014) 41:1–9. doi: 10.1016/j.bbi.2014.03.004
50. Ke Y, Liu K, Huang G-Q, Cui Y, Kaplan HJ, Shao H, et al. Anti-inflammatory role of IL-17 in experimental autoimmune uveitis. *J Immunol*. (2009) 182:3183–90. doi: 10.4049/jimmunol.0802487
51. McGeachy MJ, Cua DJ, Gaffen SL. The IL-17 family of cytokines in health and disease. *Immunity*. (2019) 50:892–906. doi: 10.1016/j.immuni.2019.03.021
52. Richter F, Natura G, Ebbinghaus M, von Banchet GS, Hensellek S, König C, et al. Interleukin-17 sensitizes joint nociceptors to mechanical stimuli and contributes to arthritic pain through neuronal interleukin-17 receptors in rodents. *Arthritis Rheum*. (2012) 64:4125–34. doi: 10.1002/art.37695
53. Pinto LG, Cunha TM, Vieira SM, Lemos HP, Verri WA, Cunha FQ, et al. IL-17 mediates articular hypernociception in antigen-induced arthritis in mice. *Pain*. (2010) 148:247–56. doi: 10.1016/j.pain.2009.11.006
54. McNamee KE, Alzabin S, Hughes JP, Anand P, Feldmann M, Williams RO, et al. IL-17 induces hyperalgesia via TNF-dependent neutrophil infiltration. *Pain*. (2011) 152:1838–45. doi: 10.1016/j.pain.2011.03.035
55. Mens LJJ, Sande MGH, Menegatti S, Chen S, Blijdorp ICJ, Jong HM, et al. Brief report: interleukin-17 blockade with secukinumab in peripheral spondyloarthritis impacts synovial immunopathology without compromising systemic immune responses. *Arthritis Rheumatol*. (2018) 70:1994–2002. doi: 10.1002/art.40581
56. Chiricozzi A, Krueger JG. IL-17 targeted therapies for psoriasis. *Expert Opin Investig Drugs*. (2013) 22:993–1005. doi: 10.1517/13543784.2013.806483
57. McInnes IB, Mease PJ, Ritchlin CT, Rahman P, Gottlieb AB, Kirkham B, et al. Secukinumab sustains improvement in signs and symptoms of psoriatic arthritis: 2 year results from the phase 3 FUTURE 2 study. *Rheumatology*. (2017) 56:1993–2003. doi: 10.1093/rheumatology/kex301
58. Miyoshi K, Obata K, Kondo T, Okamura H, Noguchi K. Interleukin-18-mediated microglia/astrocyte interaction in the spinal cord enhances neuropathic pain processing after nerve injury. *J Neurosci*. (2008) 28:12775–87. doi: 10.1523/JNEUROSCI.3512-08.2008
59. Dinarello CA, Novick D, Kim S, Kaplanski G. Interleukin-18 and IL-18 binding protein. *Front Immunol*. (2013) 4:289. doi: 10.3389/fimmu.2013.00289
60. Yang Y, Li H, Li T-T, Luo H, Gu X-Y, Lü N, et al. Delayed activation of spinal microglia contributes to the maintenance of bone cancer pain in female Wistar rats via P2X7 receptor and IL-18. *J Neurosci*. (2015) 35:7950–63. doi: 10.1523/JNEUROSCI.5250-14.2015
61. Liu S, Liu Y-P, Lv Y, Yao J-L, Yue D-M, Zhang M-Y, et al. IL-18 Contributes to bone cancer pain by regulating glia cells and neuron interaction. *J Pain*. (2018) 19:186–95. doi: 10.1016/j.jpain.2017.10.003
62. Pflanz S, Timans JC, Cheung J, Rosales R, Kanzler H, Gilbert J, et al. IL-27, a heterodimeric cytokine composed of EBI3 and p28 protein, induces proliferation of naive CD4+ T cells. *Immunity*. (2002) 16:779–90. doi: 10.1016/S1074-7613(02)00324-2
63. Pickens SR, Chamberlain ND, Volin M V, Mandelin AM, Agrawal H, Matsui M, et al. Local expression of interleukin-27 ameliorates collagen-induced arthritis. *Arthritis Rheum*. (2011) 63:2289–98. doi: 10.1002/art.30324
64. Niedbala W, Cai B, Wei X, Patakas A, Leung BP, McInnes IB, et al. Interleukin 27 attenuates collagen-induced arthritis. *Ann Rheum Dis*. (2008) 67:1474–9. doi: 10.1136/ard.2007.083360
65. Jones GW, Bombardieri M, Greenhill CJ, McLeod L, Nerviani A, Rocher-Ros V, et al. Interleukin-27 inhibits ectopic lymphoid-like structure development in early inflammatory arthritis. *J Exp Med*. (2015) 212:1793–802. doi: 10.1084/jem.20132307
66. Jones GW, Hill DG, Cardus A, Jones SA. IL-27: a double agent in the IL-6 family. *Clin Exp Immunol*. (2018) 193:37–46. doi: 10.1111/cei.13116
67. Kalliolias GD, Zhao B, Triantafyllopoulou A, Park-Min K-H, Ivashkiv LB. Interleukin-27 inhibits human osteoclastogenesis by abrogating RANKL-mediated induction of nuclear factor of activated T cells c1 and suppressing proximal RANK signaling. *Arthritis Rheum*. (2010) 62:402–13. doi: 10.1002/art.27200
68. Wigerblad G, Bas DB, Fernades-Cerqueira C, Krishnamurthy A, Nandakumar KS, Rogoz K, et al. Autoantibodies to citrullinated proteins induce joint pain independent of inflammation via a chemokine-dependent mechanism. *Ann Rheum Dis*. (2016) 75:730–8. doi: 10.1136/annrheumdis-2015-208094
69. Fattori V, Hohmann MSN, Rossaneis AC, Manchope MF, Alves-Filho JC, Cunha TM, et al. Targeting IL-33/ST2 signaling: regulation of immune function and analgesia. *Expert Opin Ther Targets*. (2017) 21:1141–52. doi: 10.1080/14728222.2017.1398734
70. Zarpelon AC, Rodrigues FC, Lopes AH, Souza GR, Carvalho TT, Pinto LG, et al. Spinal cord oligodendrocyte-derived alarmin IL-33 mediates neuropathic pain. *FASEB J*. (2016) 30:54–65. doi: 10.1096/fj.14-267146
71. Liu S, Mi W-L, Li Q, Zhang M-T, Han P, Hu S, et al. Spinal IL-33/ST2 signaling contributes to neuropathic pain via neuronal CaMKII-CREB and astroglial JAK2-STAT3 cascades in mice. *Anesthesiology*. (2015) 123:1154–69. doi: 10.1097/ALN.0000000000000850
72. Zhao J, Zhang H, Liu S-B, Han P, Hu S, Li Q, et al. Spinal interleukin-33 and its receptor ST2 contribute to bone cancer-induced pain in mice. *Neuroscience*. (2013) 253:172–82. doi: 10.1016/j.neuroscience.2013.08.026
73. Ji R-R, Chamessian A, Zhang Y-Q. Pain regulation by non-neuronal cells and inflammation. *Science*. (2016) 354:572–7. doi: 10.1126/science.aaf8924
74. Fattori V, Amaral FA, Verri WA. Neutrophils and arthritis: role in disease and pharmacological perspectives. *Pharmacol Res*. (2016) 112:84–98. doi: 10.1016/j.phrs.2016.01.027
75. Collison LW, Workman CJ, Kuo TT, Boyd K, Wang Y, Vignali KM, et al. The inhibitory cytokine IL-35 contributes to regulatory T-cell function. *Nature*. (2007) 450:566–9. doi: 10.1038/nature06306
76. Wang R-X, Yu C-R, Dambuza IM, Mahdi RM, Dolinska MB, Sergeev Y V, et al. Interleukin-35 induces regulatory B cells that suppress autoimmune disease. *Nat Med*. (2014) 20:633–41. doi: 10.1038/nm.3554
77. Huang A, Cheng L, He M, Nie J, Wang J, Jiang K. Interleukin-35 on B cell and T cell induction and regulation. *J Inflamm*. (2017) 14:16. doi: 10.1186/s12950-017-0164-5
78. Jiang Y, Wang J, Li H, Xia L. IL-35 alleviates inflammation progression in a rat model of diabetic neuropathic pain via inhibition of JNK signaling. *J Inflamm*. (2019) 16:19. doi: 10.1186/s12950-019-0217-z
79. Filková M, Vernerová Z, Hulejová H, Prajzlerová K, Veigl D, Pavelka K, et al. Pro-inflammatory effects of interleukin-35 in rheumatoid arthritis. *Cytokine*. (2015) 73:36–43. doi: 10.1016/j.cyto.2015.01.019
80. Bello RO, Chin VK, Abd Rachman Isnadi MF, Abd Majid R, Atmadini Abdullah M, Lee TY, et al. The role, involvement and function(s) of interleukin-35 and interleukin-37 in disease pathogenesis. *Int J Mol Sci*. (2018) 19:E1149. doi: 10.3390/ijms19041149
81. Parameswaran N, Patial S. Tumor necrosis factor-a signaling in macrophages. *Crit Rev Eukaryot Gene Expr*. (2010) 20:87–103. doi: 10.1615/CritRevEukarGeneExpr.v20.i2.10
82. Chung IY, Benveniste EN. Tumor necrosis factor-alpha production by astrocytes. Induction by lipopolysaccharide, IFN-gamma, and IL-1 beta. *J Immunol*. (1990) 144:2999–3007.
83. Berta T, Park C-K, Xu Z-Z, Xie R-G, Liu T, Lü N, et al. Extracellular caspase-6 drives murine inflammatory pain via microglial TNF-α secretion. *J Clin Invest*. (2014) 124:1173–86. doi: 10.1172/JCI72230

84. Dong Y, Fischer R, Naudé PJW, Maier O, Nyakas C, Duffey M, et al. Essential protective role of tumor necrosis factor receptor 2 in neurodegeneration. *Proc Natl Acad Sci USA*. (2016) 113:12304–9. doi: 10.1073/pnas.1605195113
85. Parada CA, Yeh JJ, Joseph EK, Levine JD. Tumor necrosis factor receptor type-1 in sensory neurons contributes to induction of chronic enhancement of inflammatory hyperalgesia in rat. *Eur J Neurosci*. (2003) 17:1847–52. doi: 10.1046/j.1460-9568.2003.02626.x
86. Qin X, Wan Y, Wang X. CCL2 and CXCL1 trigger calcitonin gene-related peptide release by exciting primary neciceptive neurons. *J Neurosci Res*. (2005) 82:51–62. doi: 10.1002/jnr.20612
87. Kidd BL, Urban LA. Mechanisms of inflammatory pain. *Br J Anaesth*. (2001) 87:3–11. doi: 10.1093/bja/87.1.3
88. Bradley J. TNF-mediated inflammatory disease. *J Pathol*. (2008) 214:149–60. doi: 10.1002/path.2287
89. Echeverry S, Shi XQ, Haw A, Liu H, Zhang ZW, Zhang J. Transforming growth factor-β1 impairs neuropathic pain through pleiotropic effects. *Mol Pain*. (2009) 5:16. doi: 10.1186/1744-8069-5-16
90. Zhang X, Zheng H, Zhu HY, Hu S, Wang S, Jiang X, et al. Acute effects of transforming growth factor-β1 on neuronal excitability and involvement in the pain of rats with chronic pancreatitis. *J Neurogastroenterol Motil*. (2016) 22:333–43. doi: 10.5056/jnm15127
91. Kashima R, Hata A. The role of TGF-β superfamily signaling in neurological disorders. *Acta Biochim Biophys Sin*. (2018) 50:106–20. doi: 10.1093/abbs/gmx124
92. Cheon H, Yu S-J, Yoo DH, Chae IJ, Song GG, Sohn J. Increased expression of pro-inflammatory cytokines and metalloproteinase-1 by TGF-beta1 in synovial fibroblasts from rheumatoid arthritis and normal individuals. *Clin Exp Immunol*. (2002) 127:547–52. doi: 10.1046/j.1365-2249.2002.01785.x
93. Qin Z-F, Hou D-Y, Fang Y-Q, Xiao H-J, Wang J, Li K-C. Interferon-alpha enhances excitatory transmission in substantia gelatinosa neurons of rat spinal cord. *Neuroimmunomodulation*. (2012) 19:235–40. doi: 10.1159/000335167
94. Liu C-C, Gao Y-J, Luo H, Berta T, Xu Z-Z, Ji R-R, et al. Interferon alpha inhibits spinal cord synaptic and nociceptive transmission via neuronal-glial interactions. *Sci Rep*. (2016) 6:34356. doi: 10.1038/srep34356
95. Choubey D, Moudgil KD. Interferons in autoimmune and inflammatory diseases: regulation and roles. *J Interferon Cytokine Res*. (2011) 31:857–65. doi: 10.1089/jir.2011.0101
96. Racz I, Nadal X, Alferink J, Banos JE, Rehnelt J, Martin M, et al. Interferon- is a critical modulator of CB2 cannabinoid receptor signaling during neuropathic pain. *J Neurosci*. (2008) 28:12136–45. doi: 10.1523/JNEUROSCI.3402-08.2008
97. Sun L, Li Y, Jia X, Wang Q, Li Y, Hu M, et al. Neuroprotection by IFN-γ via astrocyte-secreted IL-6 in acute neuroinflammation. *Oncotarget*. (2017) 8:40065–78. doi: 10.18632/oncotarget.16990
98. Savarin C, Hinton DR, Valentin-Torres A, Chen Z, Trapp BD, Bergmann CC, et al. Astrocyte response to IFN-γ limits IL-6-mediated microglia activation and progressive autoimmune encephalomyelitis. *J Neuroinflammation*. (2015) 12:79. doi: 10.1186/s12974-015-0293-9
99. Tsuda M, Masuda T, Kitano J, Shimoyama H, Tozaki-Saitoh H, Inoue K. IFN-gamma receptor signaling mediates spinal microglia activation driving neuropathic pain. *Proc Natl Acad Sci USA*. (2009) 106:8032–7. doi: 10.1073/pnas.0810420106
100. Miller CHT, Maher SG, Young HA. Clinical use of interferon-gamma. *Ann N Y Acad Sci*. (2009) 1182:69–79. doi: 10.1111/j.1749-6632.2009.05069.x
101. Theofilopoulos AN, Koundouris S, Kono DH, Lawson BR. The role of IFN-gamma in systemic lupus erythematosus: a challenge to the Th1/Th2 paradigm in autoimmunity. *Arthritis Res*. (2001) 3:136–41. doi: 10.1186/ar290
102. Miyake K, Nakashima H, Akahoshi M, Inoue Y, Nagano S, Tanaka Y, et al. Genetically determined interferon-gamma production influences the histological phenotype of lupus nephritis. *Rheumatology*. (2002) 41:518–24. doi: 10.1093/rheumatology/41.5.518
103. Deshmane SL, Kremlev S, Amini S, Sawaya BE. Monocyte chemoattractant protein-1 (MCP-1): an overview. *J Interferon Cytokine Res*. (2009) 29:313–26. doi: 10.1089/jir.2008.0027
104. Bäckryd E, Lind A-L, Thulin M, Larsson A, Gerdle B, Gordh T. High levels of cerebrospinal fluid chemokines point to the presence of neuroinflammation in peripheral neuropathic pain: a cross-sectional study of 2 cohorts of patients compared with healthy controls. *Pain*. (2017) 158:2487–95. doi: 10.1097/j.pain.0000000000001061
105. Silva RL, Lopes AH, Guimarães RM, Cunha TM. CXCL1/CXCR2 signaling in pathological pain: role in peripheral and central sensitization. *Neurobiol Dis*. (2017) 105:109–16. doi: 10.1016/j.nbd.2017.06.001
106. Cao D-L, Zhang Z-J, Xie R-G, Jiang B-C, Ji R-R, Gao Y-J. Chemokine CXCL1 enhances inflammatory pain and increases NMDA receptor activity and COX-2 expression in spinal cord neurons via activation of CXCR2. *Exp Neurol*. (2014) 261:328–36. doi: 10.1016/j.expneurol.2014.05.014
107. Zhang Z-J, Cao D-L, Zhang X, Ji R-R, Gao Y-J. Chemokine contribution to neuropathic pain: respective induction of CXCL1 and CXCR2 in spinal cord astrocytes and neurons. *Pain*. (2013) 154:2185–97. doi: 10.1016/j.pain.2013.07.002
108. Krishnamurthy A, Joshua V, Haj Hensvold A, Jin T, Sun M, Vivar N, et al. Identification of a novel chemokine-dependent molecular mechanism underlying rheumatoid arthritis-associated autoantibody-mediated bone loss. *Ann Rheum Dis*. (2016) 75:721–9. doi: 10.1136/annrheumdis-2015-208093
109. Russo RC, Garcia CC, Teixeira MM, Amaral FA. The CXCL8/IL-8 chemokine family and its receptors in inflammatory diseases. *Expert Rev Clin Immunol*. (2014) 10:593–619. doi: 10.1586/1744666X.2014.894886
110. Heidemann J, Ogawa H, Dwinell MB, Rafiee P, Maaser C, Gockel HR, et al. Angiogenic effects of interleukin 8 (CXCL8) in human intestinal microvascular endothelial cells are mediated by CXCR2. *J Biol Chem*. (2003) 278:8508–15. doi: 10.1074/jbc.M208231200
111. Simonini A, Moscucci M, Muller DWM, Bates ER, Pagani FD, Burdick MD, et al. IL-8 is an angiogenic factor in human coronary atherectomy tissue. *Circulation*. (2000) 101:1519–26. doi: 10.1161/01.CIR.101.13.1519
112. Üçeyler N, Sommer C. Cytokine regulation in animal models of neuropathic pain and in human diseases. *Neurosci Lett*. (2008) 437:194–8. doi: 10.1016/j.neulet.2008.03.050
113. de Oliveira CMB, Sakata RK, Issy AM, Gerola LR, Salomão R. Cytokines and pain. *Brazilian J Anesthesiol*. (2011) 61:255–65. doi: 10.1016/S0034-7094(11)70029-0
114. Sikandar S, Sommer C. Neurotrophins, Cytokines, and Pain. In: Wood JN, editor. *The Oxford Handbook of the Neurobiology of Pain*. Oxford University Press. doi: 10.1093/oxfordhb/9780190860509.013.25
115. Verri WA, Cunha TM, Parada CA, Poole S, Cunha FQ, Ferreira SH. Hypernociceptive role of cytokines and chemokines: Targets for analgesic drug development? *Pharmacol Ther*. (2006) 112:116–38. doi: 10.1016/j.pharmthera.2006.04.001
116. Heldin CH, Moustakas A. Signaling receptors for TGF-β family members. *Cold Spring Harb Perspect Biol*. (2016) 8:a022053 doi: 10.1101/cshperspect.a022053
117. Liu T, Zhang L, Joo D, Sun S-C. NF-κB signaling in inflammation. *Signal Transduct Target Ther*. (2017) 2:17023. doi: 10.1038/sigtrans.2017.23
118. Hayden MS, Ghosh S. Shared principles in NF-κB signaling. *Cell*. (2008) 132:344–62. doi: 10.1016/j.cell.2008.01.020
119. Sun S-C. The noncanonical NF-κB pathway. *Immunol Rev*. (2012) 246:125–40. doi: 10.1111/j.1600-065X.2011.01088.x
120. Cargnello M, Roux PP. Activation and function of the MAPKs and their substrates, the MAPK-activated protein kinases. *Microbiol Mol Biol Rev*. (2011) 75:50–83. doi: 10.1128/MMBR.00031-10
121. Cuadrado A, Nebreda AR. Mechanisms and functions of p38 MAPK signalling. *Biochem J*. (2010) 429:403–17. doi: 10.1042/BJ20100323
122. Kyriakis JM, Avruch J. Mammalian mitogen-activated protein kinase signal transduction pathways activated by stress and inflammation. *Physiol Rev*. (2001) 81:807–69. doi: 10.1152/physrev.2001.81.2.807
123. Caunt CJ, Finch AR, Sedgley KR, McArdle CA. Seven-transmembrane receptor signalling and ERK compartmentalization. *Trends Endocrinol Metab*. (2006) 17:276–83. doi: 10.1016/j.tem.2006.07.008
124. Kim GW, Lee NR, Pi RH, Lim YS, Lee YM, Lee JM, et al. IL-6 inhibitors for treatment of rheumatoid arthritis: Past, present, and future. *Arch Pharm Res*. (2015) 38:575–84. doi: 10.1007/s12272-015-0569-8
125. Moriyama T, Higashi T, Togashi K, Iida T, Segi E, Sugimoto Y, et al. Sensitization of TRPV1 by EP 1 and IP reveals peripheral

nociceptive mechanism of prostaglandins. *Mol Pain*. (2005) 1:3. doi: 10.1186/1744-8069-1-3
126. Schnizler K, Shutov LP, Van Kanegan MJ, Merrill MA, Nichols B, McKnight GS, et al. Protein kinase A anchoring via AKAP150 is essential for TRPV1 modulation by forskolin and prostaglandin E2 in mouse sensory neurons. *J Neurosci*. (2008) 28:4904–17. doi: 10.1523/JNEUROSCI.0233-08.2008
127. Vellani V, Mapplebeck S, Moriondo A, Davis JB, McNaughton PA. Protein kinase C activation potentiates gating of the vanilloid receptor VR1 by capsaicin, protons, heat and anandamide. *J Physiol*. (2001) 534:813–25. doi: 10.1111/j.1469-7793.2001.00813.x
128. Ta TT, Dikmen HO, Schilling S, Chausse B, Lewen A, Hollnagel JO, et al. Priming of microglia with IFN-γ slows neuronal gamma oscillations *in situ*. *Proc Natl Acad Sci USA*. (2019) 116:4637–42. doi: 10.1073/pnas.1813562116
129. Oka T, Aou S, Hori T. Intracerebroventricular injection of interleukin-1β enhances nociceptive neuronal responses of the trigeminal nucleus caudalis in rats. *Brain Res*. (1994) 656:236–44. doi: 10.1016/0006-8993(94)91466-4
130. Kitisin K, Saha T, Blake T, Golestaneh N, Deng M, Kim C, et al. Tgf-Beta signaling in development. *Sci STKE*. (2007) 2007:cm1. doi: 10.1126/stke.3992007cm1
131. Schmierer B, Hill CS. TGFbeta-SMAD signal transduction: molecular specificity and functional flexibility. *Nat Rev Mol Cell Biol*. (2007) 8:970–82. doi: 10.1038/nrm2297
132. Schwartz DM, Kanno Y, Villarino A, Ward M, Gadina M, O'Shea JJ. JAK inhibition as a therapeutic strategy for immune and inflammatory diseases. *Nat Rev Drug Discov*. (2017) 17:78. doi: 10.1038/nrd.2017.201
133. Levy DE, Darnell JE. STATs: transcriptional control and biological impact. *Nat Rev Mol Cell Biol*. (2002) 3:651–62. doi: 10.1038/nrm909
134. Meier JA, Larner AC. Toward a new STATe: the role of STATs in mitochondrial function. *Semin Immunol*. (2014) 26:20–8. doi: 10.1016/j.smim.2013.12.005
135. Kays J, Zhang YH, Khorodova A, Strichartz G, Nicol GD. Peripheral synthesis of an atypical protein kinase C mediates the enhancement of excitability and the development of mechanical hyperalgesia produced by nerve growth factor. *Neuroscience*. (2018) 371:420–32. doi: 10.1016/j.neuroscience.2017.12.030
136. Melemedjian OK, Asiedu MN, Tillu DV., Peebles KA, Yan J, Ertz N, et al. IL-6- and NGF-induced rapid control of protein synthesis and nociceptive plasticity via convergent signaling to the eIF4F complex. *J Neurosci*. (2010) 30:15113–23. doi: 10.1523/JNEUROSCI.3947-10.2010
137. Aley KO, Messing RO, Mochly-Rosen D, Levine JD. Chronic hypersensitivity for inflammatory nociceptor sensitization mediated by the ε isozyme of protein kinase C. *J Neurosci*. (2000) 20:4680–5. doi: 10.1523/JNEUROSCI.20-12-04680.2000
138. Korganow AS, Ji H, Mangialaio S, Duchatelle V, Pelanda R, Martin T, et al. From systemic T cell self-reactivity to organ-specific autoimmune disease via immunoglobulins. *Immunity*. (1999) 10:451–61. doi: 10.1016/S1074-7613(00)80045-X
139. Julius D. Molecular mechanisms of nociception. *Nature*. (2001) 413:203–10. doi: 10.1038/35093019
140. Gladman. *Les traumatismes et l'arthrite inflammatoire* (2008). Toronto, ON: Gouvernement de L'Ontario, Ministère du Travaul.
141. Deane KD, O'Donnell CI, Hueber W, Majka DS, Lazar AA, Derber LA, et al. The number of elevated cytokines and chemokines in preclinical seropositive rheumatoid arthritis predicts time to diagnosis in an age-dependent manner. *Arthritis Rheum*. Ontario: Gouvernement de L'Ontario, Ministère du Travaul (2010) 62:3161–72. doi: 10.1002/art.27638
142. Kokkonen H, Söderström I, Rocklöv J, Hallmans G, Lejon K, Rantapää Dahlqvist S. Up-regulation of cytokines and chemokines predates the onset of rheumatoid arthritis. *Arthritis Rheum*. (2010) 62:383–91. doi: 10.1002/art.27186
143. van Zanten A, Arends S, Roozendaal C, Limburg PC, Maas F, Trouw LA, et al. Presence of anticitrullinated protein antibodies in a large population-based cohort from the Netherlands. *Ann Rheum Dis*. (2017) 76:1184–90. doi: 10.1136/annrheumdis-2016-209991
144. Aletaha D, Neogi T, Silman AJ, Funovits J, Felson DT, Bingham CO, et al. 2010 Rheumatoid arthritis classification criteria: an American College of Rheumatology/European League Against Rheumatism collaborative initiative. *Arthritis Rheum*. (2010) 62:2569–81. doi: 10.1002/art.27584
145. Sokolove J, Pisetsky D. Bone loss, pain and inflammation: three faces of ACPA in RA pathogenesis. *Ann Rheum Dis*. (2016) 75:637–9. doi: 10.1136/annrheumdis-2015-208308
146. Zhang C, Ward J, Dauch JR, Tanzi RE, Cheng HT. Cytokine-mediated inflammation mediates painful neuropathy from metabolic syndrome. *PLoS ONE*. (2018) 13:e0192333. doi: 10.1371/journal.pone.0192333
147. Ramer MS, Thompson SWN, McMahon SB. Causes and consequences of sympathetic basket formation in dorsal root ganglia. *Pain*. (1999) 82(Suppl. 6):S111–20. doi: 10.1016/S0304-3959(99)00144-X
148. Krock E, Millecamps M, Anderson KM, Srivastava A, Reihsen TE, Hari P, et al. Interleukin-8 as a therapeutic target for chronic low back pain: upregulation in human cerebrospinal fluid and pre-clinical validation with chronic reparixin in the SPARC-null mouse model. *EBioMedicine*. (2019) 43:487–500. doi: 10.1016/j.ebiom.2019.04.032
149. Fuzzati-Armentero MT, Cerri S, Blandini F. Peripheral-central neuroimmune crosstalk in Parkinson's disease: what do patients and animal models tell Us? *Front Neurol*. (2019) 10:232. doi: 10.3389/fneur.2019.00232
150. Barry A, O'Halloran KD, McKenna JP, McCreary C, Downer EJ. Plasma IL-8 signature correlates with pain and depressive symptomatology in patients with burning mouth syndrome: Results from a pilot study. *J Oral Pathol Med*. (2018) 47:158–65. doi: 10.1111/jop.12666
151. Sasaguri T, Taguchi T, Murata Y, Kobayashi K, Iizasa S, Iizasa E, et al. Interleukin-27 controls basal pain threshold in physiological and pathological conditions. *Sci Rep*. (2018) 8:11022. doi: 10.1038/s41598-018-29398-3
152. Porta-Sales J, Garzón-Rodríguez C, Llorens-Torromé S, Brunelli C, Pigni A, Caraceni A. Evidence on the analgesic role of bisphosphonates and denosumab in the treatment of pain due to bone metastases: a systematic review within the European Association for Palliative Care guidelines project. *Palliat Med*. (2017) 31:5–25. doi: 10.1177/0269216316639793
153. Sun WH, Chen CC. Roles of proton-sensing receptors in the transition from acute to chronic pain. *J Dent Res*. (2016) 95:135–42. doi: 10.1177/0022034515618382
154. Mantyh PW. Mechanisms that drive bone pain across the lifespan. *Br J Clin Pharmacol*. (2019) 85:1103–13. doi: 10.1111/bcp.13801
155. Jimenez-Andrade JM, Herrera MB, Ghilardi JR, Vardanyan M, Melemedjian OK, Mantyh PW. Vascularization of the dorsal root ganglia and peripheral nerve of the mouse: Implications for chemical-induced peripheral sensory neuropathies. *Mol Pain*. (2008) 4:10. doi: 10.1186/1744-8069-4-10
156. Flatters SJL, Bennett GJ. Studies of peripheral sensory nerves in paclitaxel-induced painful peripheral neuropathy: evidence for mitochondrial dysfunction. *Pain*. (2006) 122:245–57. doi: 10.1016/j.pain.2006.01.037
157. Ravindra Deshmukh V. Gap junctions in the dorsal root ganglia. In: Aranda Abreu GE, editor. *Neurons - Dendrites and Axons*. London: Intechopen (2018). p. 1–22. doi: 10.5772/intechopen.82128
158. Raoof R, Willemen HLDM, Eijkelkamp N. Divergent roles of immune cells and their mediators in pain. *Rheumatology*. (2018) 57:429–40. doi: 10.1093/rheumatology/kex308
159. Schaible H-G, Von Banchet GS, Boettger MK, Bräuer R, Gajda M, Richter F, et al. The role of proinflammatory cytokines in the generation and maintenance of joint pain. *Ann N Y Acad Sci*. (2010) 1193:60–9. doi: 10.1111/j.1749-6632.2009.05301.x
160. Ogawa N, Kawai H, Terashima T, Kojima H, Oka K, Chan L, et al. Gene therapy for neuropathic pain by silencing of TNF-α expression with lentiviral vectors targeting the dorsal root ganglion in mice. *PLoS ONE*. (2014) 9:e92073. doi: 10.1371/journal.pone.0092073
161. McMahon SB, Cafferty WBJ, Marchand F. Immune and glial cell factors as pain mediators and modulators. *Exp Neurol*. (2005) 192:444–62. doi: 10.1016/j.expneurol.2004.11.001
162. Miller RE, Tran PB, Das R, Ghoreishi-Haack N, Ren D, Miller RJ, et al. CCR2 chemokine receptor signaling mediates pain in experimental osteoarthritis. *Proc Natl Acad Sci USA*. (2012) 109:20602–7. doi: 10.1073/pnas.1209294110
163. Zhang H, Li Y, de Carvalho-Barbosa M, Kavelaars A, Heijnen CJ, Albrecht PJ, et al. Dorsal root ganglion infiltration by macrophages contributes to paclitaxel chemotherapy-induced peripheral neuropathy. *J Pain*. (2016) 17:775–86. doi: 10.1016/j.jpain.2016.02.011

164. Abbadie C, Lindia JA, Cumiskey AM, Peterson LB, Mudgett JS, Bayne EK, et al. Impaired neuropathic pain responses in mice lacking the chemokine receptor CCR2. *Proc Natl Acad Sci USA*. (2003) 100:7947–52. doi: 10.1073/pnas.1331358100
165. Zhang P, Bi RY, Gan YH. Glial interleukin-1β upregulates neuronal sodium channel 1.7 in trigeminal ganglion contributing to temporomandibular joint inflammatory hypernociception in rats. *J Neuroinflammation*. (2018) 15:117. doi: 10.1186/s12974-018-1154-0
166. Willemen HLDM, Eijkelkamp N, Garza Carbajal A, Wang H, Mack M, Zijlstra J, et al. Monocytes/macrophages control resolution of transient inflammatory pain. *J Pain*. (2014) 15:496–506. doi: 10.1016/j.jpain.2014.01.491
167. Reeve AJ, Patel S, Fox A, Walker K, Urban L. Intrathecally administered endotoxin or cytokines produce allodynia, hyperalgesia and changes in spinal cord neuronal responses to nociceptive stimuli in the rat. *Eur J Pain*. (2000) 4:247–57. doi: 10.1053/eujp.2000.0177
168. Sung C-S, Wen Z-H, Chang W-K, Ho S-T, Tsai S-K, Chang Y-C, et al. Intrathecal interleukin-1β administration induces thermal hyperalgesia by activating inducible nitric oxide synthase expression in the rat spinal cord. *Brain Res*. (2004) 1015:145–53. doi: 10.1016/j.brainres.2004.04.068
169. Milligan E, Zapata V, Schoeniger D, Chacur M, Green P, Poole S, et al. An initial investigation of spinal mechanisms underlying pain enhancement induced by fractalkine, a neuronally released chemokine. *Eur J Neurosci*. (2005) 22:2775–82. doi: 10.1111/j.1460-9568.2005.04470.x
170. Tanaka T, Minami M, Nakagawa T, Satoh M. Enhanced production of monocyte chemoattractant protein-1 in the dorsal root ganglia in a rat model of neuropathic pain: possible involvement in the development of neuropathic pain. *Neurosci Res*. (2004) 48:463–9. doi: 10.1016/j.neures.2004.01.004
171. Gabay E, Wolf G, Shavit Y, Yirmiya R, Tal M. Chronic blockade of interleukin-1 (IL-1) prevents and attenuates neuropathic pain behavior and spontaneous ectopic neuronal activity following nerve injury. *Eur J Pain*. (2011) 15:242–8. doi: 10.1016/j.ejpain.2010.07.012
172. Chen G, Park C-K, Xie R-G, Ji R-R. Intrathecal bone marrow stromal cells inhibit neuropathic pain via TGF-β secretion. *J Clin Invest*. (2015) 125:3226–40. doi: 10.1172/JCI80883
173. Chen G, Zhang Y-Q, Qadri YJ, Serhan CN, Ji R-R. Microglia in pain: detrimental and protective roles in pathogenesis and resolution of pain. *Neuron*. (2018) 100:1292–311. doi: 10.1016/j.neuron.2018.11.009
174. Li Z, Wei H, Piirainen S, Chen Z, Kalso E, Pertovaara A, et al. Spinal versus brain microglial and macrophage activation traits determine the differential neuroinflammatory responses and analgesic effect of minocycline in chronic neuropathic pain. *Brain Behav Immun*. (2016) 58:107–17. doi: 10.1016/j.bbi.2016.05.021
175. Peters CM, Jimenez-Andrade JM, Jonas BM, Sevcik MA, Koewler NJ, Ghilardi JR, et al. Intravenous paclitaxel administration in the rat induces a peripheral sensory neuropathy characterized by macrophage infiltration and injury to sensory neurons and their supporting cells. *Exp Neurol*. (2007) 203:42–54. doi: 10.1016/j.expneurol.2006.07.022
176. Park HJ, Stokes JA, Pirie E, Skahen J, Shtaerman Y, Yaksh TL. Persistent hyperalgesia in the cisplatin-treated mouse as defined by threshold measures, the conditioned place preference paradigm, and changes in dorsal root ganglia activated transcription factor 3: the effects of gabapentin, ketorolac, and etanercept. *Anesth Analg*. (2013) 116:224–31. doi: 10.1213/ANE.0b013e31826e1007
177. Wang D, Couture R, Hong Y. Activated microglia in the spinal cord underlies diabetic neuropathic pain. *Eur J Pharmacol*. (2014) 728:59–66. doi: 10.1016/j.ejphar.2014.01.057
178. Christianson CA, Corr M, Firestein GS, Mobargha A, Yaksh TL, Svensson CI. Characterization of the acute and persistent pain state present in K/BxN serum transfer arthritis. *Pain*. (2010) 151:394–403. doi: 10.1016/j.pain.2010.07.030
179. Liu M, Yao M, Wang H, Xu L, Zheng Y, Huang B, et al. P2Y12 receptor-mediated activation of spinal microglia and p38MAPK pathway contribute to cancer-induced bone pain. *J Pain Res*. (2017) 10:417–26. doi: 10.2147/JPR.S124326
180. Imoto A, Mitsunaga S, Inagaki M, Aoyagi K, Sasaki H, Ikeda M, et al. Neural invasion induces cachexia *via* astrocytic activation of neural route in pancreatic cancer. *Int J Cancer*. (2012) 131:2795–807. doi: 10.1002/ijc.27594
181. Fitzsimmons BL, Zattoni M, Svensson CI, Steinauer J, Hua X-Y, Yaksh TL. Role of spinal p38α and β MAPK in inflammatory hyperalgesia and spinal COX-2 expression. *Neuroreport*. (2010) 21:313–7. doi: 10.1097/WNR.0b013e32833774bf
182. Rider P, Carmi Y, Cohen I. Biologics for targeting inflammatory cytokines, clinical uses, and limitations. *Int J Cell Biol*. (2016) 2016:9259646. doi: 10.1155/2016/9259646
183. Old EA, Clark AK, Malcangio M. The role of glia in the spinal cord in neuropathic and inflammatory pain. In: Schaible HG, editor. *Handbook of Experimental Pharmacology*. Vol. 227. Berlin; Heidelberg: Springer (2015). p. 145–70. doi: 10.1007/978-3-662-46450-2_8
184. Yoon H, Walters G, Paulsen AR, Scarisbrick IA. Astrocyte heterogeneity across the brain and spinal cord occurs developmentally, in adulthood and in response to demyelination. *PLoS ONE*. (2017) 12:e0180697. doi: 10.1371/journal.pone.0180697
185. Choi SR, Roh DH, Yoon SY, Choi HS, Kang SY, Han HJ, et al. Astrocyte sigma-1 receptors modulate connexin 43 expression leading to the induction of below-level mechanical allodynia in spinal cord injured mice. *Neuropharmacology*. (2016) 111:34–46. doi: 10.1016/j.neuropharm.2016.08.027
186. Chen G, Park CK, Xie RG, Berta T, Nedergaard M, Ji RR. Connexin-43 induces chemokine release from spinal cord astrocytes to maintain late-phase neuropathic pain in mice. *Brain*. (2014) 137(Pt 8):2193–209. doi: 10.1093/brain/awu140
187. Delpech JC, Herron S, Botros MB, Ikezu T. Neuroimmune crosstalk through extracellular vesicles in health and disease. *Trends Neurosci*. (2019) 42:361–72. doi: 10.1016/j.tins.2019.02.007
188. Ribeiro-Rodrigues TM, Martins-Marques T, Morel S, Kwak BR, Girão H. Role of connexin 43 in different forms of intercellular communication – gap junctions, extracellular vesicles and tunnelling nanotubes. *J Cell Sci*. (2017) 130:3619–30. doi: 10.1242/jcs.200667
189. Kotini M, Barriga EH, Leslie J, Gentzel M, Rauschenberger V, Schambon A, et al. Gap junction protein Connexin-43 is a direct transcriptional regulator of N-cadherin *in vivo*. *Nat Commun*. (2018) 9:3846. doi: 10.1038/s41467-018-06368-x
190. Zamanian JL, Foo LC, Nouri N, Zhou L, Barres BA, Xu L, et al. Genomic analysis of reactive astrogliosis. *J Neurosci*. (2012) 32:6391–410. doi: 10.1523/JNEUROSCI.6221-11.2012
191. Han P, Zhao J, Liu S-B, Yang C-J, Wang Y-Q, Wu G-C, et al. Interleukin-33 mediates formalin-induced inflammatory pain in mice. *Neuroscience*. (2013) 241:59–66. doi: 10.1016/j.neuroscience.2013.03.019
192. Han P, Liu S, Zhang M, Zhao J, Wang Y, Wu G, et al. Inhibition of spinal interlukin-33/ST2 signaling and downstream ERK and JNK pathways in electroacupuncture analgesia in formalin mice. *PLoS ONE*. (2015) 10:e0129576. doi: 10.1371/journal.pone.0129576
193. Zarpelon AC, Cunha TM, Alves-Filho JC, Pinto LG, Ferreira SH, McInnes IB, et al. IL-33/ST2 signalling contributes to carrageenin-induced innate inflammation and inflammatory pain: role of cytokines, endothelin-1 and prostaglandin E2. *Br J Pharmacol*. (2013) 169:90–101. doi: 10.1111/bph.12110
194. Fonseca MM, Santa-Cecilia F, Kusuda R, Ferreira D, Bezerra F, Ferreira M, et al. (153) the interleukin 27 (IL-27) protects mice from neuropathic pain development through up-regulation of anti-inflammatory cytokine IL-10. *J Pain*. (2017) 18:S14–15. doi: 10.1016/j.jpain.2017.02.059
195. Duffy SS, Keating BA, Perera CJ, Lees JG, Tonkin RS, Makker PGS, et al. Regulatory T cells and their derived cytokine, interleukin-35, reduce pain in experimental autoimmune encephalomyelitis. *J Neurosci*(2019) 39:2326–46. doi: 10.1523/JNEUROSCI.1815-18.2019
196. Kroenke K, Bair MJ, Damush TM, Wu J, Hoke S, Sutherland J, et al. Optimized antidepressant therapy and pain self-management in primary care patients with depression and musculoskeletal pain. *JAMA*. (2009) 301:2099. doi: 10.1001/jama.2009.723
197. Page GG, Opp MR, Kozachik SL. Reduced sleep, stress responsivity, and female sex contribute to persistent inflammation-induced mechanical hypersensitivity in rats. *Brain Behav Immun*. (2014) 40:244–51. doi: 10.1016/j.bbi.2014.02.013
198. Tsuda M, Shigemoto-Mogami Y, Koizumi S, Mizokoshi A, Kohsaka S, Salter MW, et al. P2X4 receptors induced in spinal microglia gate tactile

allodynia after nerve injury. *Nature*. (2003) 424:778–83. doi: 10.1038/nature01786
199. Ji R-R, Berta T, Nedergaard M. Glia and pain: Is chronic pain a gliopathy? *Pain*. (2013) 154:S10–28. doi: 10.1016/j.pain.2013.06.022
200. Loggia ML, Chonde DB, Akeju O, Arabasz G, Catana C, Edwards RR, et al. Evidence for brain glial activation in chronic pain patients. *Brain*. (2015) 138:604–15. doi: 10.1093/brain/awu377
201. Albrecht DS, Forsberg A, Sandstrom A, Bergan C, Kadetoff D, Protsenko E, et al. Brain glial activation in fibromyalgia - a multi-site positron emission tomography investigation. *Brain Behav Immun*. (2019) 75:72. doi: 10.1016/j.bbi.2018.09.018
202. Zhu C Bin, Blakely RD, Hewlett WA. The proinflammatory cytokines interleukin-1beta and tumor necrosis factor-alpha activate serotonin transporters. *Neuropsychopharmacology*. (2006) 31:2121–31. doi: 10.1038/sj.npp.1301029
203. Haroon E, Raison CL, Miller AH. Psychoneuroimmunology meets neuropsychopharmacology: translational implications of the impact of inflammation on behavior. *Neuropsychopharmacology*. (2012) 37:137–62. doi: 10.1038/npp.2011.205
204. Miller AH, Maletic V, Raison CL. Inflammation and its discontents: the role of cytokines in the pathophysiology of major depression. *Biol Psychiatry*. (2009) 65:732–41. doi: 10.1016/j.biopsych.2008.11.029
205. Oka T, Wakugawa Y, Hosoi M, Oka K, Hori T. Intracerebroventricular injection of tumor necrosis factor-αInduces thermal hyperalgesia in rats. *Neuroimmunomodulation*. (1996) 3:135–40. doi: 10.1159/000097238
206. Hori T, Oka T, Hosoi M, Aou S. Pain modulatory actions of cytokines and prostaglandin E2 in the brain. *Ann N Y Acad Sci*. (1998) 840:269–81. doi: 10.1111/j.1749-6632.1998.tb09567.x
207. Coelho A-M, Fioramonti J, Bueno L. Brain interleukin-1β and tumor necrosis factor-α are involved in lipopolysaccharide-induced delayed rectal allodynia in awake rats. *Brain Res Bull*. (2000) 52:223–8. doi: 10.1016/S0361-9230(00)00269-0
208. Wei F, Guo W, Zou S, Ren K, Dubner R. Supraspinal glial-neuronal interactions contribute to descending pain facilitation. *J Neurosci*. (2008) 28:10482–95. doi: 10.1523/JNEUROSCI.3593-08.2008
209. Zeidan F, Salomons T, Farris SR, Emerson NM, Adler-Neal A, Jung Y, et al. Neural mechanisms supporting the relationship between dispositional mindfulness and pain. *Pain*. (2018) 159:2477–85. doi: 10.1097/j.pain.0000000000001344
210. Taylor AMW, Mehrabani S, Liu S, Taylor AJ, Cahill CM. Topography of microglial activation in sensory- and affect-related brain regions in chronic pain. *J Neurosci Res*. (2017) 95:1330–5. doi: 10.1002/jnr.23883
211. Barcelon EE, Cho W-H, Jun SB, Lee SJ. Brain microglial activation in chronic pain-associated affective disorder. *Front Neurosci*. (2019) 13:213. doi: 10.3389/fnins.2019.00213
212. Yirmiya R, Rimmerman N, Reshef R. Depression as a microglial disease. *Trends Neurosci*. (2015) 38:637–58. doi: 10.1016/j.tins.2015.08.001
213. Liu Y, Zhou L-J, Wang J, Li D, Ren W-J, Peng J, et al. TNF-α differentially regulates synaptic plasticity in the hippocampus and spinal cord by microglia-dependent mechanisms after peripheral nerve injury. *J Neurosci*. (2017) 37:871–81. doi: 10.1523/JNEUROSCI.2235-16.2016
214. Shao Q, Li Y, Wang Q, Zhao J. IL-10 and IL-1β Mediate neuropathic-pain like behavior in the ventrolateral orbital cortex. *Neurochem Res*. (2015) 40:733–9. doi: 10.1007/s11064-015-1521-5
215. Roman M, Irwin MR. Novel neuroimmunologic therapeutics in depression: a clinical perspective on what we know so far. *Brain Behav Immun*. (2019) 83:7–21. doi: 10.1016/j.bbi.2019.09.016
216. Lee SM, Te S, Breen EC, Olmstead R, Irwin MR, Cho JH. Circulating versus lipopolysaccharide-induced inflammatory markers as correlates of subthreshold depressive symptoms in older adults. *World J Biol Psychiatry*. (2019) 1–8. doi: 10.1080/15622975.2019.1671608. [Epub ahead of print].
217. Bäckryd E, Tanum L, Lind AL, Larsson A, Gordh T. Evidence of both systemic inflammation and neuroinflammation in fibromyalgia patients, as assessed by a multiplex protein panel applied to the cerebrospinal fluid and to plasma. *J Pain Res*. (2017) 10:515–25 doi: 10.2147/JPR.S128508
218. Üçeyler N, Rogausch JP, Toyka K V., Sommer C. Differential expression of cytokines in painful and painless neuropathies. *Neurology*. (2007) 69:42–9. doi: 10.1212/01.wnl.0000265062.92340.a5
219. Langjahr M, Schubert A-L, Sommer C, Üçeyler N. Increased pro-inflammatory cytokine gene expression in peripheral blood mononuclear cells of patients with polyneuropathies. *J Neurol*. (2018) 265:618–27. doi: 10.1007/s00415-018-8748-4
220. Raison CL, Rutherford RE, Woolwine BJ, Shuo C, Schettler P, Drake DF, et al. A randomized controlled trial of the tumor necrosis factor antagonist infliximab for treatment-resistant depression: the role of baseline inflammatory biomarkers. *Arch Gen Psychiatry*. (2013) 70:31–41. doi: 10.1001/2013.jamapsychiatry.4
221. Medina-Rodriguez EM, Lowell JA, Worthen RJ, Syed SA, Beurel E. Involvement of innate and adaptive immune systems alterations in the pathophysiology and treatment of depression. *Front Neurosci*. (2018) 12:547. doi: 10.3389/fnins.2018.00547
222. Brown PM, Pratt AG, Isaacs JD. Mechanism of action of methotrexate in rheumatoid arthritis and the search for biomarkers. *Nat Rev Rheumatol*. (2016) 12:731–42. doi: 10.1038/nrrheum.2016.175
223. Davila L, Ranganathan P. Pharmacogenetics: implications for therapy in rheumatic diseases. *Nat Rev Rheumatol*. (2011) 7:537–50. doi: 10.1038/nrrheum.2011.117
224. Smedegård G, Björk J. Sulphasalazine: mechanism of action in rheumatoid arthritis. *Br J Rheumatol*. (1995) 34(Suppl. 2):7–15. doi: 10.1093/rheumatology/XXXIV.suppl_2.7
225. Tian H, Cronstein BN. Understanding the mechanisms of action of methotrexate: implications for the treatment of rheumatoid arthritis. *Bull NYU Hosp Jt Dis*. (2007) 65:168–73.
226. Kaltsonoudis E, Papagoras C, Drosos AA. Current and future role of methotrexate in the therapeutic armamentarium for rheumatoid arthritis. *Int J Clin Rheumtol*. (2012) 7:179–89. doi: 10.2217/ijr.12.10
227. Radner H, Aletaha D. Anti-TNF in rheumatoid arthritis: an overview. *Wiener Medizinische Wochenschrift*. (2015) 165:3–9. doi: 10.1007/s10354-015-0344-y
228. Gabay C, Hasler P, Kyburz D, So A, Villiger P, von Kempis J, et al. Biological agents in monotherapy for the treatment of rheumatoid arthritis. *Swiss Med Wkly*. (2014) 144:w13950. doi: 10.4414/smw.2014.13950
229. Calabrò A, Caterino AL, Elefante E, Valentini V, Vitale A, Talarico R, et al. One year in review 2016: novelties in the treatment of rheumatoid arthritis. *Clin Exp Rheumatol*. (2016) 34:357–72.
230. Fleischmann R, Kremer J, Cush J, Schulze-Koops H, Connell CA, Bradley JD, et al. Placebo-controlled trial of tofacitinib monotherapy in rheumatoid arthritis. *N Engl J Med*. (2012) 367:495–507. doi: 10.1056/NEJMoa1109071
231. Lee EB, Fleischmann R, Hall S, Wilkinson B, Bradley JD, Gruben D, et al. Tofacitinib versus methotrexate in rheumatoid arthritis. *N Engl J Med*. (2014) 370:2377–86. doi: 10.1056/NEJMoa1310476
232. Smolen JS, Landewé R, Bijlsma J, Burmester G, Chatzidionysiou K, Dougados M, et al. EULAR recommendations for the management of rheumatoid arthritis with synthetic and biological disease-modifying antirheumatic drugs: 2016 update. *Ann Rheum Dis*. (2017) 76:935–38. doi: 10.1136/annrheumdis-2016-210715
233. Senolt L. Emerging therapies in rheumatoid arthritis: focus on monoclonal antibodies. *F1000Research*. (2019) 8:1549. doi: 10.12688/f1000research.18688.1
234. Borghi SM, Fattori V, Pinho-Ribeiro FA, Domiciano TP, Miranda-Sapla MM, Zaninelli TH, et al. Contribution of spinal cord glial cells to *L. amazonensis* experimental infection-induced pain in BALB/c mice. *J Neuroinflammation*. (2019) 16:113. doi: 10.1186/s12974-019-1496-2

Conflict of Interest: The authors declare that the research was conducted in the absence of any commercial or financial relationships that could be construed as a potential conflict of interest.

frontiers in Immunology

ORIGINAL RESEARCH
published: 28 January 2020
doi: 10.3389/fimmu.2019.03059

IL-27 Counteracts Neuropathic Pain Development Through Induction of IL-10

*Miriam M. Fonseca[1†], Marcela Davoli-Ferreira[1,2], Flávia Santa-Cecília[1], Rafaela M. Guimarães[1,2], Francisco F. B. Oliveira[1], Ricardo Kusuda[1], David W. Ferreira[1], José C. Alves-Filho[1], Fernando Q. Cunha[1] and Thiago M. Cunha[1]**

[1] Department of Pharmacology, Center for Research in Inflammatory Diseases (CRID), Ribeirão Preto Medical School, University of São Paulo (USP), Ribeirão Preto, Brazil, [2] Graduate Program in Basic and Applied Immunology, Ribeirão Preto Medical School, University of São Paulo (USP), Ribeirão Preto, Brazil

OPEN ACCESS

Edited by:
Felipe Almeida Pinho Ribeiro, Harvard Medical School, United States

Reviewed by:
Felipe J. Nobre Lelis, Brigham and Women's Hospital and Harvard Medical School, United States
Rafael Gonzalez-Cano, Boston Children's Hospital and Harvard Medical School, United States
Larissa Staurengo-Ferrari, University of California, San Francisco, United States

***Correspondence:**
Thiago M. Cunha
thicunha@fmrp.usp.br

†Present address:
Miriam M. Fonseca, Pain Mechanisms Laboratory, Department of Anesthesiology, Wake Forest School of Medicine, Winston-Salem, NC, United States

Specialty section:
This article was submitted to Multiple Sclerosis and Neuroimmunology, a section of the journal Frontiers in Immunology

Received: 16 October 2019
Accepted: 16 December 2019
Published: 28 January 2020

Citation:
Fonseca MM, Davoli-Ferreira M, Santa-Cecília F, Guimarães RM, Oliveira FFB, Kusuda R, Ferreira DW, Alves-Filho JC, Cunha FQ and Cunha TM (2020) IL-27 Counteracts Neuropathic Pain Development Through Induction of IL-10. Front. Immunol. 10:3059. doi: 10.3389/fimmu.2019.03059

Neuroimmune–glia interactions have been implicated in the development of neuropathic pain. Interleukin-27 (IL-27) is a cytokine that presents regulatory activity in inflammatory conditions of the central nervous system. Thus, we hypothesized that IL-27 would participate in the neuropathic pain process. Here, we found that neuropathic pain caused by peripheral nerve injury (spared nerve injury model; SNI), was enhanced in IL-27-deficient$^{(-/-)}$ mice, whereas nociceptive pain is similar to that of wild-type mice. SNI induced an increase in the expression of IL-27 and its receptor subunit (*Wsx1*) in the sensory ganglia and spinal cord. IL-27 receptor was expressed mainly in resident macrophage, microglia, and astrocytes of the sensory ganglia and spinal cord, respectively. Finally, we identify that the antinociceptive effect of IL-27 was not observed in IL-10$^{-/-}$ mice. These results provided evidence that IL-27 is a cytokine produced after peripheral nerve injury that counteracts neuropathic pain development through induction of the antinociceptive cytokine IL-10. In summary, our study unraveled the role of IL-27 as a regulatory cytokine that counteracts the development of neuropathic pain after peripheral nerve damage. In conclusion, they indicate that immunotherapies based on IL-27 could emerge as possible therapeutic approaches for the prevention of neuropathic pain development after peripheral nerve injury.

Keywords: neuropathic pain, cytokines, IL-27, IL-10, glial cells, macrophages

INTRODUCTION

Chronic neuropathic pain is caused by diseases or lesions affecting the somatosensory nervous system. Often resistant to different types of therapies, neuropathic pain affects ∼3–17% of the chronic pain population in the world (1). Many studies have shown that neuroimmune response in nociceptive pathway has an important role for the development of neuropathic pain (2–4). Different forms of injury to the peripheral nervous systems, evoked by traumatic, metabolic, or toxic events, can lead to abnormal neuronal response from the site of damage to the sensory ganglia and then the central nervous system (CNS), inducing an intense neuroinflammation response in these sites (5, 6). Non-neuronal cells, including satellite glial cells, macrophages, microglia, and astrocytes, along the nociceptive pathway can be activated, which influence the neuronal excitability and consequently participate in the establishment of chronic pain states (7–9). In the local of

nerve injury, sensory ganglia, and spinal cord, non-neuronal cells can release a diverse range of proinflammatory mediators, which may directly or indirectly amplify pain signaling (10, 11). On the other hand, in order to control the inflammatory and nociceptive responses, these cells can also release anti-inflammatory mediators, such as IL-4, IL-10, IL-13, and transforming growth factor beta (TGF-β) and pro-resolving mediators such as resolvins, lipoxins, protectins, and maresins, which regulate the response to nerve damage and might attenuate pain behavior in animal models of chronic pain (12–16). Another cytokine that appears to control the inflammatory response in the periphery and CNS is interleukin-27 (IL-27) (17).

IL-27 is a member of the IL-6/IL-12 heterodimeric cytokine family, formed by two subunits, Epstein–Barr virus-induced gene 3 (EBI3) and p28. It binds to a receptor composed of gp130 (shared with other cytokine receptors, including IL-6R) and IL-27Rα (also known as WSX-1 or TCCR), which is specific for IL-27 (18, 19). IL-27 is generally produced by antigen-presenting cells, such as macrophages and dendritic cells; however, some studies suggest that it can be released by astrocytes and microglia in CNS (20, 21), and the signaling for IL-27 subunit production is induced by immune stimuli and different pathogens (18, 22). IL-27 is remarkably characterized by immunosuppressive and anti-inflammatory functions mediated by the production of IL-10 and suppression of IL-17 expression (20, 23, 24). IL-27 can suppress the differentiation of naïve T cells toward IL-17-producing T cells (Th17). It also promotes differentiation of activated T cells to T cells able to secrete IL-10 in an antigen-specific manner, named type 1 regulatory (Tr1) T cells (25, 26).

The immunomodulatory activity of IL-27 has been demonstrated in several *in vivo* models. WSX-1-deficient mice develop an excessive inflammatory response during infections and in autoimmune disease models (27, 28). In a model of infection in the CNS induced by the JHM strain of mouse hepatitis virus, IL-27 promotes the production of IL-10, which is essential for controlling inflammation response (29). In addition, in a murine model of experimental encephalomyelitis (EAE), treatment with recombinant IL-27 delays the onset of EAE and improves the clinical signs of the disease (30). Furthermore, IL-27 has demonstrated potential therapeutic action in the rheumatoid arthritis model (31–33). Although many studies are showing the importance of IL-27 in neuroimmune-mediated diseases, there is no study investigating its role in the pathophysiology of neuropathic pain. Herein, we showed that IL-27 is upregulated in the dorsal root ganglia (DRGs) and spinal cord of mice after peripheral nerve injury (spared nerve injury, SNI). Moreover, we showed that IL-27 counteracted the development of neuropathic pain through the induction of IL-10 production.

Abbreviations: CNS, central nervous system; CX3CR1, motif chemokine receptor 1; DRG, dorsal root ganglion; EAE, experimental autoimmune encephalomyelitis; EBI3, epstein–barr virus-induced 3; ELISA, enzyme-linked immunosorbent assay; GFAP, glial fibrillary acidic protein; i.p, intraperitoneal injection; i.t, intrathecally injection; IBA-1 (*Aif1*), ionized calcium-binding adapter molecule 1; IL-4, interleukin 4; IL-10, interleukin 10; IL-13, interleukin 13; IL-17, interleukin 17; IL-18, interleukin 18; IL-1β, interleukin 1 beta; IL-27, interleukin 27; IL-27r, recombinant mouse IL-27 protein; mg, milligram; PBS, phosphate-buffered saline; PFA, paraformaldehyde; pg, picogram; Sham, false-operated animals; SNI, spared nerve injury; TGF-β, transforming growth factor beta; Th17, T helper 17 cell; TNFα, tumor necrosis factor alpha; Tr1, type 1 regulatory cells; WT, wild type.

METHODS

Animals

The experiments were performed in C57BL/6 wild-type (WT) male mice (6–8 weeks old) and C57BL/6 mice deficient ($^{-/-}$) in the following proteins: IL-27 (EBI3) (34) and IL-10 (35), as well as in transgenic animals expressing the green fluorescent protein (GFP) in cells that express CX3C chemokine receptor 1 (CX3CR1$^{GFP/+}$) (36). Local colonies of transgenic mice were then established and maintained on a C57BL/6 background at the animal care facility of Ribeirão Preto Medical School, University of São Paulo. The controls and transgenic mice were not littermates. The animals were taken to the testing room at least 1 h before the experiments. Food and water were available *ad libitum*. All behavioral tests were performed between 8:00 a.m. and 5:00 p.m.

Drugs and Chemicals

The following drugs were obtained from the sources indicated: recombinant mouse IL-27 (NS0-expressed) protein (IL-27r) (2799-ML-010, R&D, Minneapolis, USA) and diazepam (D0899, Sigma, St Louis, MO, USA). Acetone (Fisher Chemical, Gell, Belgium). Formalin solution (1%) was prepared using 37% formaldehyde (Fisher Chemical Gell, Belgium) in 0.9% sodium chloride saline solution (Baxter hospitalar, São Paulo, Brazil). To prepare 1 L of phosphate-buffered saline (PBS), 0.1 M was used with 9 g of NaCl, 0.122 g of KH_2PO_4, and 0.814 g of Na_2HPO_4 (Sigma-Aldrich, St. Louis, NO, USA) in distilled water (pH = 7.4).

Neuropathic Pain Model

A model of persistent peripheral neuropathic pain, the spared nerve injury (SNI), was induced as previously described (37). Briefly, under isoflurane anesthesia, the sciatic nerve and their three terminal branches (the sural, common peroneal, and tibial nerves) were exposed at lower-thigh level by blunt dissection through the biceps femoris muscle. The common peroneal and tibial nerves were tightly ligated with 6.0 silk, while the sural nerve was spared. The nerves distal to the ligature were sectioned. The experimental control group consisted of false-operated animals (Sham). In these animals, there was exposure of the sciatic nerve similarly to the SNI group, but without any manipulation of nerves. Muscle and skin were closed in layers. Then, mechanical pain hypersensitivity and cold allodynia were evaluated on specific days.

Behavioral Nociceptive Tests

An investigator blinded to group allocation performed all the behavior tests.

Formalin Assay

We assessed formalin-evoked nociception by injection of 20 μl of formalin (1%) into the dorsal surface of the right hind paw of two groups of male mice: IL-27$^{-/-}$ and WT-naive mice. The time in seconds spent licking or flinching the injected paw was recorded and expressed as the total time of nociceptive behaviors in the early phase (0–10 min) and late phase (10–50 min) after formalin injection (38).

Hot Plate Test

The noxious thermal thresholds of the hind paws were examined in IL-27$^{-/-}$ and WT-naive mice via hot plate test using an electrically heated surface (Ugo Basile, model 35100, Gemonio VA, Italy) at different temperatures (48, 50, 52, and 56°C). For each specified temperature, each animal was placed on the heated plate, and time responses to the thermal stimulus (jumping, withdrawal, and licking of the hind or front paws) were recorded in seconds. The cutoff time used was 20 s to avoid possible injury in the animal paws (39).

Acetone Test

In different days after SNI, IL-27$^{-/-}$, and WT mice were placed in a clear plastic box with a wire mesh floor and allowed to habituate for 30 min prior to testing. Then, 50 μl fluid (acetone) was sprayed on the plantar surface of the right hind paw using a syringe of 1 ml (Tuberculin slip tip, BD, Franklin Lake, NJ, USA). Paw withdrawal response, defined as flinching, licking, or biting of the limb, was measured within 1 min after the application of acetone (40). The acetone test was measured after the paw mechanical withdrawal threshold test was done.

Mechanical Nociception Test

The mechanical nociceptive threshold was evaluated in WT, IL-27$^{-/-}$, and IL-10$^{-/-}$ mice that were placed on an elevated wire grid, and the plantar surface of the ipsilateral hind paw was stimulated perpendicularly with a series of von Frey filaments (Stoelting, Chicago, IL, USA), with logarithmically increasing stiffness (0.008–2.0 g) (41). The withdrawal frequency was calculated as a percentage of withdrawals after 10 applications of 0.008 g von Frey filament in the right hind paw.

Rota-rod Test

To discard possible non-specific muscle relaxant or sedative effects of recombinant mouse IL-27, mice motor performance was evaluated on the rota-rod test (42). The apparatus consisted of a bar with a diameter of 2.5 cm, subdivided into six compartments by disks 25 cm in diameter (Ugo Basile, Model 7600). The bar rotated at a constant speed of 22 rotations per minute. WT-naive animals were selected 24 h previously by eliminating those mice that did not remain on the bar for two consecutive periods of 120 s. Then, those animals were treated intrathecally with vehicle (saline) or recombinant IL-27 (100 ng) in a final volume of 5 μl using a BD Ultra-Fine® (29G) insulin syringe (BD, Franklin Lakes, NJ, USA). Diazepam (5 mg/kg, intraperitoneal) was used as a positive control. To inject diazepam solution, 1 ml sub-Q syringe and needle 26G x 5/8 (BD, Franklin Lakes, NJ, USA) were used. The cutoff time used was 120 s.

Intrathecal Injection

Under isoflurane (2%) anesthesia, recombinant IL-27 (100 ng) or vehicle (saline) was administered intrathecally (i.t.) in WT and IL-10$^{-/-}$ mice. The technique used for intrathecal injection was described by Papir-Kricheli et al. (43), modified by holding the mice securely in one hand by the pelvic girdle and inserting a BD Ultra-Fine® (29G) insulin syringe (BD, Franklin Lakes, NJ, USA) directly on the subarachnoid space (close to L4–L5 segments) of the spinal cord. A sudden lateral movement of the tail indicated proper placement of the needle in the intrathecal space. For all administrations, 5-μl volume was used. Then, the syringe was held in the specific position for a few seconds and progressively removed to avoid any outflow of the drug.

Quantitative Real-Time PCR

At the indicated times after nerve injury, mice were anesthetized and then perfused with 0.1 M PBS. DRGs and spinal cord, ipsilateral to the lesion, were collected from the region correspondent to lumbar segments (L3–L5) and homogenized in TRI Reagent® (Life Technologies Corporation, Carlsbad, CA, USA) reagent at 4°C. Then, total cellular mRNA was purified from whole tissues, according to the manufacturer's instructions. After FACS sorting procedure, ∼25,000 cells were used to isolate mRNA using RNeasy micro kit® (Qiagen, Hiden, Germany). To convert the mRNA in cDNA, high-capacity cDNA Reverse Transcription Kit (Thermo Fisher Scientific, Graiciuno, Vilnius, LT) was used. The level of each gene was normalized to the levels of the mouse *Gapdh* gene, and the results were analyzed by the method of quantitative relative expression $2^{-\Delta\Delta CT}$ as previously described (44). Primer pairs for mouse *Gapdh*, *Aif1*, *Gfap*, *Tnf*, *Il1b*, *Ebi3*, *p28*, *Wsx1*, *Il12p35*, and *Il10* were as follows:

Gapdh fwd: 5′-CATCTTCTTGTGCAGTGCCA-3′
Gapdh rev: 5′-CGGCCAAATCCGTTCAC-3′
Aif1 fwd: 5′-TGAGGAGCCATGAGCCAAAG-3′
Aif1 rev: 5′-GCTTCAAGTTTGGACGGCAG-3′
Gfap fwd: 5′-AGGGCGAAGAAAACCGCATCACC-3′
Gfap rev: 5′-TCTAAGGGAGAGCTGGCAGGGCT-3′
Tnf fwd: 5′-TGTGCTCAGAGCTTTCAACAA-3′
Tnf rev: 5′-CTTGATGGTGGTGCATGAGA-3′
Il1b fwd: 5′-TGACAGTGATGATGAGAATGACCTGTTC-3′
Il1b rev: 5′-TTGGAAGCAGCCCTTCATCT-3′
Il27 (*Ebi3*) fwd: 5′-TGCCATGCTTCTCGGTATCC-3′
Il27 (*Ebi3*) rev: 5′-AGGGTCCGGCTTGATGATTC-3′
Il27 (*p28*) fwd: 5′-GGCTATGTCCACAGCTTTGCT-3′
Il27 (*p28*) rev: 5′-CGAAGTGTGGTAGCGAGGAA-3′
Wsx1: Taqman®: Mm00497259_m1
Il12p35 fwd: 5′-AAGACATCACACGGGACCAAA-3′
Il12p35 rev: 5′-CAGGCAACTCTCGTTCTTGTGTA-3′
Il10 fwd: 5′-AACAAAGGACCAGCTGGACAAC-3′
Il10 rev: 5′-GCAACCCAAGTAACCCTTAAAGTC-3′

Immunofluorescence

At day 10 after surgery, WT and CX3CR1$^{GFP/+}$ mice were deeply anesthetized with ketamine and xylazine and perfused

transcardially with phosphate buffer 0.1 M, followed by fresh 4% paraformaldehyde (PFA) in PBS 0.1 M (pH 7.4). After the perfusion, segments of spinal cord lumbar correspondent L3, L4, and L5 were dissected out, post-fixed for 2 h in PFA, and then replaced with 30% sucrose overnight. Transverse spinal sections (free-floating, 60 μm) were cut in a cryostat. The floating sections were used for immunofluorescence assays as previously described (45). Then, the sections were incubated overnight at 4°C with polyclonal primary antibodies: anti-WSX-1 (1:250) (5996—Abcam), anti-GFAP (1:500) conjugated with alexa fluor 488 (MAB 3042X—Millipore), anti-NeuN (1:250) (MAB377—Millipore), and anti-GFP (1:500) conjugated with FITC (ab6662—Abcam), for the tissue from CX3CR1$^{GFP/+}$ mice. After washing, the sections were then incubated with the appropriate secondary antibody solution for 2 h at room temperature; all secondary solutions were diluted 1:500: Alexa fluor 594, Alexa fluor 488, or Alexa fluor 647 (Invitrogen). The sections were washed with PBS as described earlier, mounted on glass slides, and covered with coverslips with Fluromount^{TM} Aqueous Mounting Medium (Sigma). The sections of spinal cord were acquired using a SP5 confocal laser scanning microscope (Leica, Wetzlar, Germany). Colocalization was ensured with confocal Z stacks at 1-μm intervals and visualization in three-dimensional orthogonal planes.

Cell Sorting

Cell sorting of CD11b^{+} and CD45^{-} cells from DGRs was performed as described previously (46). Briefly, the ipsilateral DRGs (L3, L4, and L5 pooled from eight animals) were collected at day 10 from WT or IL-27$^{-/-}$ mice submitted to SNI or Sham surgery, as well as from WT mice submitted to SNI and treated for five consecutive days (starting on day 10 up to day 14) with recombinant IL-27 (100 ng/in a final volume of 5 μl) or vehicle (i.t). DRGs were incubated in 5 ml of RPMI medium containing 2 mg/ml of collagenase type II (Sigma Aldrich) for 1 h at 37°C. After this time, the tissues were passed through a cell strainer (40 μm), followed by centrifugation with RPMI medium containing 10% fetal bovine serum (FBS, Gibco). Cells obtained were resuspended in 0.1 M PBS containing 10% of rabbit serum, to avoid non-specific background staining, and specific monoclonal antibodies for 30 min at 4°C. The following monoclonal antibodies (BD Biosciences) were used for staining: CD45-BV421 (clone 30-F11), Ly6G-FITC (clone 1A8), and CD11b-APCCy7 (clone M1/70); the antibodies were diluted 1:250. Cells were isolated using FACSAria III (BD Biosciences), and then the pellets obtained were resuspended in lysis buffer to isolate mRNA. For all of the experiments, sample purity was ∼70% for CD11b+ Ly6G- cells and ∼90% for CD45- cells. The data were analyzed using FlowJo 10 software (Treestar, Ashland, USA). The gating strategy used to perform cell sorting from sensory ganglia is depicted in **Figure S1**.

Cytokine Measurement by ELISA

At 7 and 10 days after nerve injury, mice were anesthetized and then perfused with 0.1 M PBS. The ipsilateral DRGs and lumbar segments of the spinal cord (L3, L4, and L5 pooled from two animals) from WT or IL-27$^{-/-}$ mice were collected and homogenized in lysis buffer containing protease inhibitors (to each 10 mg of tissue, 100 μl of lysis buffer was used); the supernatant without dilution was used to measure IL-10. Mouse DuoSet ELISA kit to IL-10 was purchased from R&D Systems and performed as instructed by the manufacturer. The results are expressed as picogram (pg) of cytokines per milligram (mg) of tissue protein. The protein concentration of the lysate was determined using a Pierce^{TM} bicinchoninic acid assay protein assay kit (Thermo Scientific, Rockford, IL, USA).

Data Analyses and Statistics

Data are reported as means ± SEM. The normality of the distribution of data was analyzed by D'Agostino and Pearson tests. Two-way ANOVA followed by Bonferroni's *t*-test was used to compare the groups and doses at different times (curves) when the responses (nociception) were measured. The factors analyzed were treatment, time, and time vs. treatment interaction. Alternatively, if the responses (nociception, protein expression, mRNA expression) were measured only once after stimulus injection, the differences between responses were evaluated by one-way ANOVA followed by Bonferroni's *t*-test (for three or more groups), comparing all pairs of columns. For comparisons of groups across two groups, an unpaired Student *t*-test was used. $P < 0.05$ were considered significant. Statistical analysis was performed with GraphPad Prism (GraphPad Software, San Diego, CA, USA).

RESULTS

IL-27 Counteracts the Development of Neuropathic Pain but Is Not Involved in Basal Control of Nociception Threshold

We first characterized the physiological nociceptive response of IL-27$^{-/-}$ mice. WT and IL-27$^{-/-}$ mice were assessed behaviorally after acute peripheral application of different stimuli. IL-27$^{-/-}$ mice exhibited the same intensity of mechanical pain threshold (using von Frey filament) and thermal pain threshold (temperatures of 48, 50, 52, and 56°C) compared to WT mice (**Figures 1A–C**). Furthermore, IL-27$^{-/-}$ mice also showed no difference in nociceptive behaviors in the early and late phase of the formalin test compared to WT mice (**Figure 1D**). These data indicate that, under normal physiological conditions, IL-27 is not involved in acute nociception. Next, we determined whether IL-27 plays a role in the development of chronic neuropathic pain induced by SNI. The injured WT mice (WT-SNI) showed an increase in mechanical hypersensitivity (more percentage of frequency response), starting on day 3 and reaching the maximal response at day 10, which persists until day 21 compared to sham-operated WT mice (WT-Sham). In contrast, IL-27$^{-/-}$ mice submitted to SNI (IL-27$^{-/-}$-SNI) displayed a significant increase in mechanical hypersensitivity after nerve injury on day 5 until day 10 compared to WT-SNI mice (**Figure 1E**). Similarly, WT-SNI mice showed an increase in cold hypersensitivity, starting on day 3 until day 21, compared to Sham-WT mice. Furthermore, IL-27$^{-/-}$-SNI animals also showed increased levels of cold

hypersensitivity when compared to WT-SNI mice (**Figure 1F**). Taken together, these data indicate that IL-27 signaling might be negatively controlling the development of neuropathic pain but is not involved in the detection of mechanical, thermal, and chemical nociception in basal conditions.

Peripheral Nerve Injury Triggers an Increase in the Expression of IL-27 and Its Receptor-Specific Subunit, WSX-1, in Spinal Cord and Dorsal Root Ganglia

To explore the role of IL-27 signaling in the development of neuropathic pain, we evaluated the levels of mRNA expression of IL-27 subunits (*p28* and *Ebi3*) and *Wsx1*, a specific subunit of its receptor, in ipsilateral lumbar DRGs (L3–L5) and spinal cord of WT animals after SNI induction. We detected that *p28* expression was upregulated between days 7 and 14 in the DRGs and spinal cord of WT-SNI mice compared to WT-Sham mice (**Figures 2A,E**). *Ebi3* expression increased either in DRGs and spinal cord after SNI at all times evaluated (**Figures 2B,F**). *Wsx1* expression was also upregulated in the DRGs (10 days after SNI) and at day 7 in the spinal cord of WT-SNI mice compared to WT-Sham mice (**Figures 2C,G**). To exclude the participation of IL-35 cytokine because it is formed by EBI3 and IL12p35, we analyzed the gene expression of *Il12p35* in the same tissues; however, we did not detect any difference in all times analyzed (**Figures 2D,H**). Altogether these results indicate that after peripheral nerve injury, IL-27 and its specific receptor subunit, but not IL-35, are upregulated in the sensory ganglia and spinal cord.

WSX-1 Is Expressed in Microglia and Astrocytes in the Spinal Cord and in the Macrophages of DRGs After Peripheral Nerve Injury

Next, we sought to analyze which cell type might be expressing the IL-27 receptor in the sensory ganglia and spinal cord after peripheral nerve injury. In naïve animals, the immunoreactivity for WXS-1 is very low in the dorsal horn of the spinal cord (**Figure 3A**), corroborating the mRNA data; however, WSX-1 expression is upregulated in the spinal cord at 10 days after SNI. WSX-1 is expressed in the spinal cord cells that also express CX3CR1 and GFAP, but not NeuN (**Figure 3B**). Thus, these data suggest that after peripheral nerve injury, WXS-1 expression might be upregulated in microglia and astrocytes, but not in neurons of the spinal cord.

In an attempt to evaluate in which cell type WSX-1 might be expressed in sensory ganglia, at day 10 after SNI or Sham surgeries, DRGs were harvested and $CD45^-$ and $CD11b^+$ $Ly6G^-$ cells (macrophages) were purified using FACS sorting. Then, we analyzed *Wsx1* gene expression in these cells. It was found that *Wsx1* mRNA was only detected in $CD11b^+$ $Ly6G^-$ cells, and the expression was upregulated after SNI in these cells compared to cells from Sham-operated mice (**Figure 3C**). These results suggest that, in the sensory ganglia, *Wsx1* is mainly expressed in macrophages, and peripheral nerve injury induces an increase in its expression.

The Impact of IL-27 Deficiency in the Activation of Immune/Glial Cells and Cytokine Production in the DRGs and Spinal Cord After Peripheral Nerve Injury

Peripheral nerve injury induces the activation of resident macrophages in the sensory ganglia and glial cells (microglia and astrocytes) in spinal cord that account for the development of neuropathic pain through the production of pro-inflammatory cytokines such as TNF and IL-1β (2, 4, 47, 48). Since the expression of IL-27 receptor is mainly observed in glial/immune cells of the spinal cord and DRGs after peripheral nerve injury, we hypothesize that the role of IL-27 in counteracting neuropathic pain might be through regulating these neuroimmune–glia processes. Thus, we analyzed the gene expression of *Aif1* (IBA-1) and *Gfap* as indicators of the macrophages/microglial cell and satellite glial/astrocyte activation in the DRGs and spinal cord, respectively. In all times and tissues evaluated, the expression of *Aif1* and *Gfap* in IL-$27^{-/-}$-SNI mice was not different from WT-SNI mice (**Figures 4A,E,B,F**). Furthermore, the expression of *Tnf* and *Il1b* was also not different between IL-$27^{-/-}$-SNI and WT-SNI mice (**Figures 4C,D,G,H**).

There is evidence that the immunoregulatory role of IL-27 is dependent on its ability to induce IL-10 production (23, 28, 29). Furthermore, IL-10 is a well-known anti-nociceptive cytokine that reduces the development of pathological pain, including neuropathic pain (49–51). Based on these evidences, we analyzed next the interference of IL-27 deficiency on IL-10 production in DRGs and spinal cord after peripheral nerve injury. Notably, it was found that the expression of IL-10 (mRNA and protein) in the DRGs and spinal cord was reduced in IL-$27^{-/-}$-SNI mice when compared to WT-SNI mice (**Figures 5A–D**). Collectively, these results indicate that IL-27 is a triggering mechanism of IL-10 production after peripheral nerve injury; however, it has minimum effect on immune/glial cell activation and pro-nociceptive cytokine production.

Exogenous IL-27 Reduced Neuropathic Pain Through the Induction of IL-10

Since IL-$27^{-/-}$ animals presented higher signs of neuropathic pain, it might indicate that exogenous IL-27 would be a useful tool to reduce neuropathic pain. In this context, we analyzed whether the intrathecal administration of recombinant IL-27 could affect the mechanical pain hypersensitivity induced by SNI. Previously, we conducted a long series of experiments in an attempt to find the best dose and time for recombinant IL-27 treatments (data not shown). We found that on day 10 after SNI induction, the treatment of animals intrathecally with recombinant IL-27 (100 ng/site), twice a day, was able to reduce mechanical pain hypersensitivity (**Figure 6A**). It is noteworthy that this dose of recombinant IL-27 neither changed the mechanical withdrawal threshold of naive mice nor caused motor impairment, discarding possible non-specific muscle relaxant or sedative effects of recombinant IL-27 (**Figures 6B,C**).

Next, we sought to evaluate whether the antinociceptive effect of exogenous IL-27 on neuropathic pain would be dependent on IL-10. For this, WT and IL-$10^{-/-}$ mice were submitted

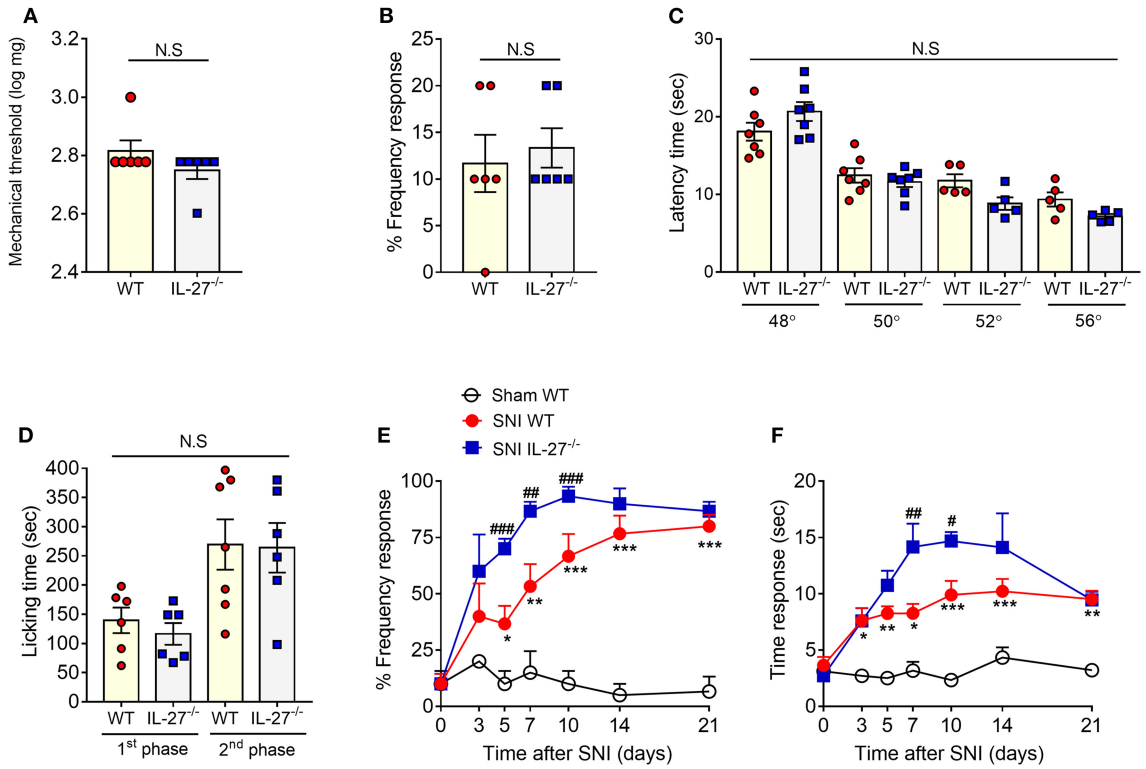

FIGURE 1 | IL-27 signaling is not involved in nociceptive pain but protects the animals in neuropathic pain condition. Different behavior tests were realized in WT and IL-27$^{-/-}$ mice: mechanical nociceptive threshold using von Frey filaments **(A)** ($n = 6$). Percentage of withdrawal frequency using von Frey filaments **(B)** ($n = 6$). Thermal nociceptive threshold using hot plate test at different temperatures **(C)** ($n = 6$). Total duration (seconds) of nociceptive behavior for 0–10 min (first phase) and for 10 up to 50 min (second phase) after administration of formalin in the paw **(D)** ($n = 6$). Mechanical nociception test using percentage of withdrawal frequency **(E)** ($n = 8$) and acetone test **(F)** ($n = 8$), in which values represent withdrawal threshold before (day 0) and up to 21 days after nerve injury (SNI) or in sham-operated mice. Data are presented as means ± S.E.M. $^{*}P < 0.05$, $^{**}P < 0.01$, $^{***}P < 0.001$ vs. Sham-WT and $^{\#}P < 0.05$, $^{\#\#}P < 0.01$, $^{\#\#\#}P < 0.001$ vs. SNI-WT. Data were analyzed by *t*-test **(A–D)** and two-way ANOVA followed by Bonferroni post-test **(E,F)**.

to peripheral nerve injury (SNI), and at day 10 after surgery we detected mechanical hypersensitivity development in these animals. Different groups of mice were treated with daily doses of recombinant IL-27 (100 ng/site) or vehicle up to day 14 (**Figure 7A**). As already shown, the treatment with recombinant IL-27 reduced the mechanical pain hypersensitivity in WT-SNI. However, this antinociceptive effect of IL-27 has not been observed in IL-10$^{-/-}$-SNI mice (**Figure 7B**). Corroborating these data, the treatment of WT-SNI mice with recombinant IL-27 promoted an upregulation of *Il10* expression in the DRGs and spinal cord when compared to mice submitted to SNI treated with vehicle (**Figures 7C,D**). Supporting our previous finding that IL-27 receptor is mainly expressed in CD11b^{+} cells in the DRGs (**Figure 3C**), we found that the upregulatory effect of recombinant IL-27 treatment on IL-10 expression is only observed in CD11b^{+} cells compared to non-immune cells (CD45^{-} cells) (**Figure 7E**). Lastly, we sought to confirm that IL-10 cytokine expression after peripheral nerve injury depends on IL-27 action in myeloid cells in the DRGs. WT and IL-27$^{-/-}$ mice were submitted to SNI or Sham surgeries. At day 10 after injury, DRGs were collected, and CD45^{-} (non-immune cells) and CD11b^{+} cells (macrophages) were isolated by FACS sorting. Then, we analyzed the gene expression of *Il10* in these types of cells. It was found that only CD11b^{+} cells from WT animals submitted to SNI expressed *Il10*, which was reduced in CD11b^{+} cells from IL-27$^{-/-}$ SNI animals (**Figure 7F**). Altogether these results indicate that the antinociceptive effect of exogenous and endogenous IL-27 upon neuropathic pain caused by peripheral nerve injury depends on the induction of IL-10 expression on myeloid cells in the DRGs.

DISCUSSION

Neuropathic pain is a challenging condition often refractory to different therapies. It is well-known that neuroimmune–glia interactions play a crucial role in the development of neuropathic pain. In this context, understanding the function of each cytokine in neuropathic pain pathophysiology might provide potential opportunities to amplify the arsenal of treatment options available (52). The main signaling molecules of the immune system are cytokines, which can be largely categorized as either pro- or anti-inflammatory. Elevated pro-inflammatory cytokine signal has been associated with symptoms of pain after nerve injury, whereas cytokines such as IL-10 and IL-4 are

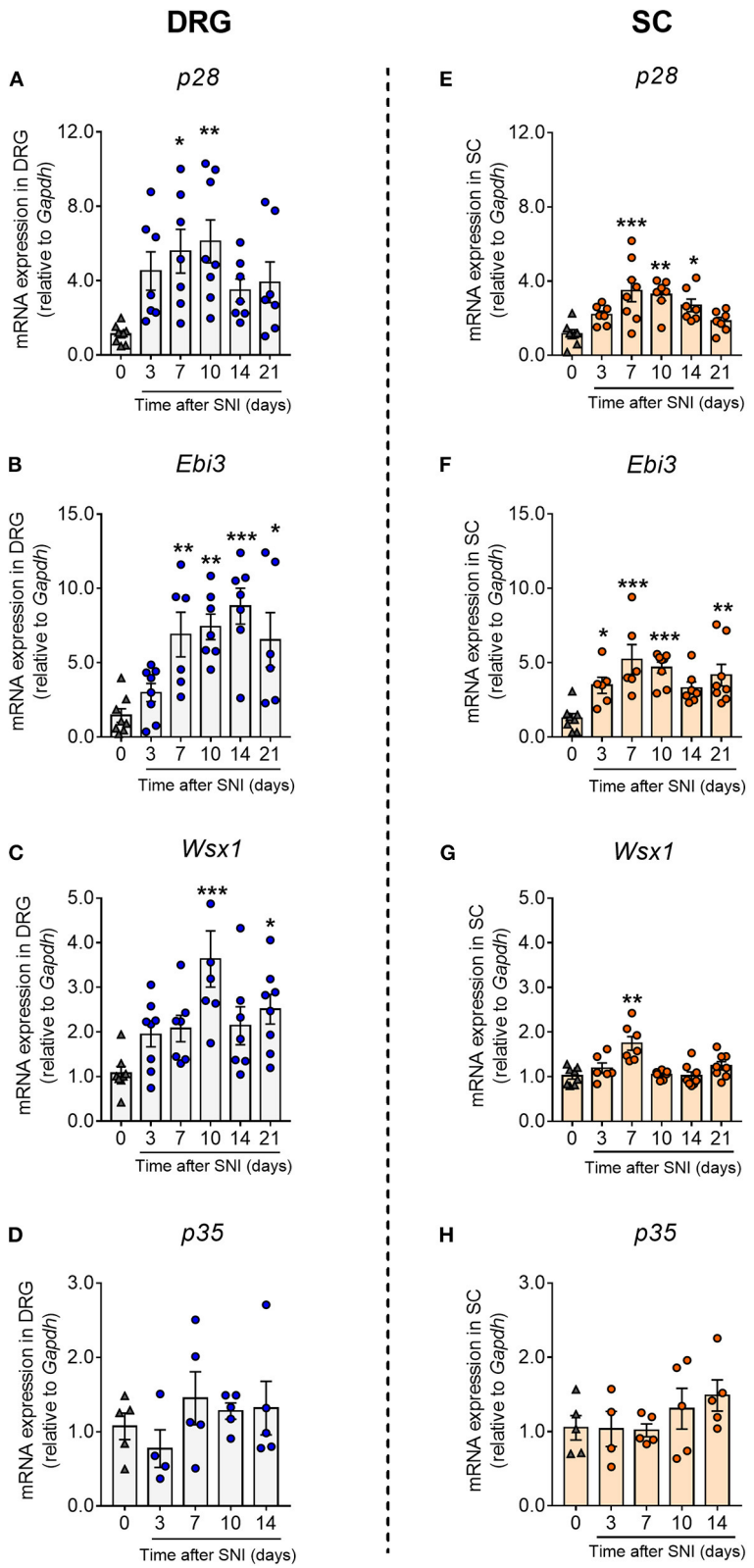

FIGURE 2 | Peripheral nerve injury upregulated the expression of IL-27 and its receptor in spinal cord and dorsal root ganglia. Real-time PCR analysis on days 3, 7, 10, 14, and 21 after SNI or sham-operated (0) in WT mice: *p28* **(A)**, *Ebi3* **(B)**, *Wsx1* **(C)**, and *Il12p35* **(D)** in DRGs; *p28* **(E)**, *Ebi3* **(F)**, *Wsx-1* **(G)**, and *Il12p35* **(H)** in spinal cord, relative expression to *Gapdh* levels ($n = 5–8$). Data are presented as means ± S.E.M. $^{*}P < 0.05$, $^{**}P < 0.01$, $^{***}P < 0.001$ vs. Sham-operated. Data were analyzed by one-way ANOVA followed by Bonferroni post-test.

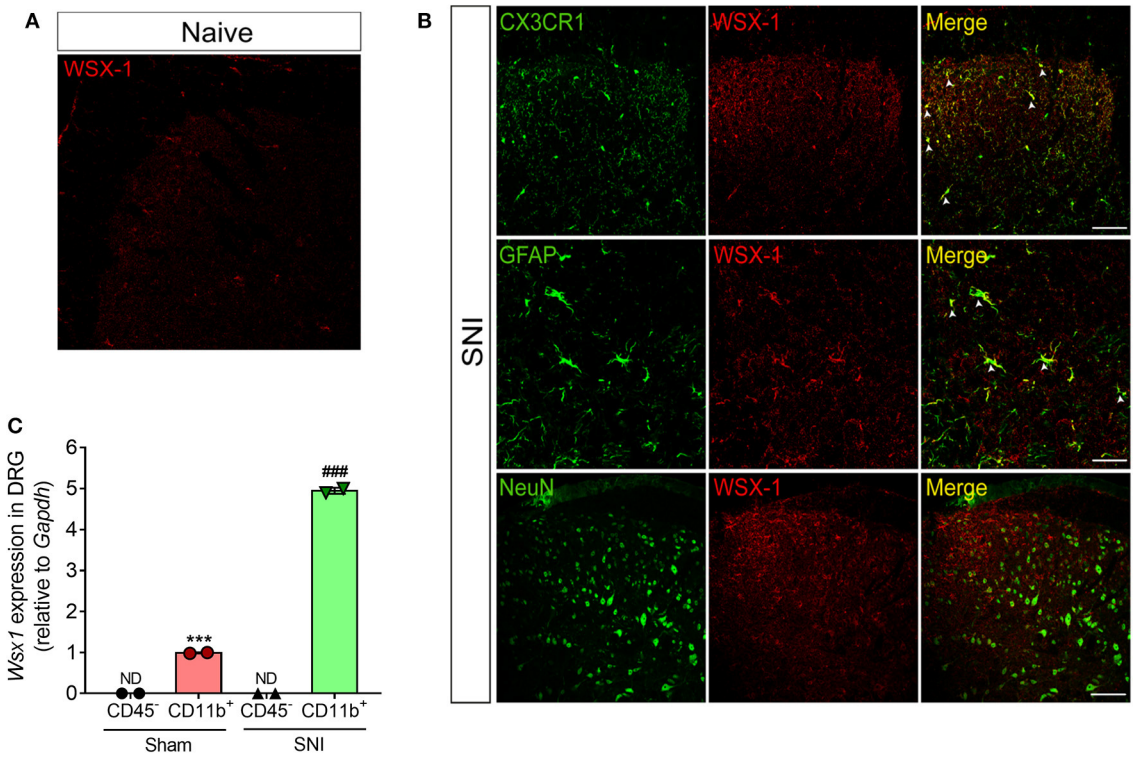

FIGURE 3 | Peripheral nerve injury induces WSX-1 expression in glial cells in spinal cord and in macrophage of DRGs. Representative confocal images of spinal cord at day 10 after SNI in CX3CR1$^{GFP/+}$ and WT mice. **(A)** Spinal cord from CX3CR1$^{GFP/+}$-naive mice labeled with WSX-1 (*red*). **(B)** Sections from CX3CR1$^{GFP/+}$ and WT mice were double-labeled marked with WSX-1 (*magenta* or *red*; middle panels), GFAP (*green*; left and middle panels), or NeuN (*green*; left panel, above). The merged images are shown in the right panels (*yellow* indicates double-positive cells, followed by *arrows*). Scale bars, 25 uM ($n = 4$). **(C)** Real-time PCR analysis of *Wsx1* expression relative to *Gapdh* levels in CD45$^-$ and CD11b$^+$ cells isolated, by FACS sorting, from DRGs of SNI or Sham-operated WT mice at day 10 after surgery ($n = 2$, pool from eight animals for each). Data are presented as means ± S.E.M. $^{***}P < 0.001$ vs. CD45$^-$ from Sham. $^{###}P < 0.001$ vs. CD11b$^+$ from Sham. ND, not detected. Data were analyzed by one-way ANOVA followed by Tukey post-test.

associated with the downregulation of the immune system and neuropathic pain relief (47, 52–54). Here, we provided evidence that IL-27 counteracts neuropathic pain development through the induction of anti-inflammatory cytokine IL-10.

Our findings demonstrate that IL-27 protects animals against the development of mechanical and cold pain hypersensitivity after peripheral nerve injury, two major symptoms of neuropathic pain. On the other hand, our data indicate that IL-27 did not participate in the nociceptive pain caused by different stimuli modalities, which was different from a previous report showing that the deficiency of IL-27 and its signaling constitutively control thermal and mechanical nociceptive thresholds (19). Although the explanation for these differences is not immediately apparent, it could be due to the difference in the source of the mutant mice. Nevertheless, our data show that the expression of IL-27 receptor is very low in the nociceptive pathway at naïve condition, favoring the idea that IL-27 would have little or no participation in nociceptive pain. Despite this controversy, it was shown that IL-27-deficient mice present higher mechanical sensitivity when submitted to inflammatory and neuropathic pain models compared to WT animals (19), supporting our data. Furthermore, the data showing that peripheral nerve injury induced upregulation of IL-27 subunits (EBI3 and p28) and its receptor subunit (WSX-1) in important structures of the nociceptive pathway (DRGs and spinal cord) argue in favor of the regulatory role of IL-27 in the development of neuropathic pain.

The neuroimmune–glia interactions across the pain pathway play a crucial role in the development of neuropathic pain (4). For instance, peripheral nerve injury triggers the activation/proliferation of macrophages in the DRGs and glial cells (microglia and astrocytes) in the spinal cord (4). These glial cells mediate the development of neuropathic pain through the production of several neuroactive molecules (55–58). It is noteworthy that IL-27 receptor-specific subunit WXS-1 (17) is expressed in different leukocyte populations such as macrophages (18, 59, 60), microglia, and astrocytes from the brain of multiple sclerosis patients (21). Our results extend these findings, indicating that after peripheral nerve injury, WSX-1 expression in the DRGs and spinal cord was mainly observed in immune or glial cells. Based on those findings and on the fact that IL-27 is an important immunoregulatory cytokine (24, 28), we analyzed whether IL-27 counteracts neuropathic pain development through the modulation of macrophage/glial

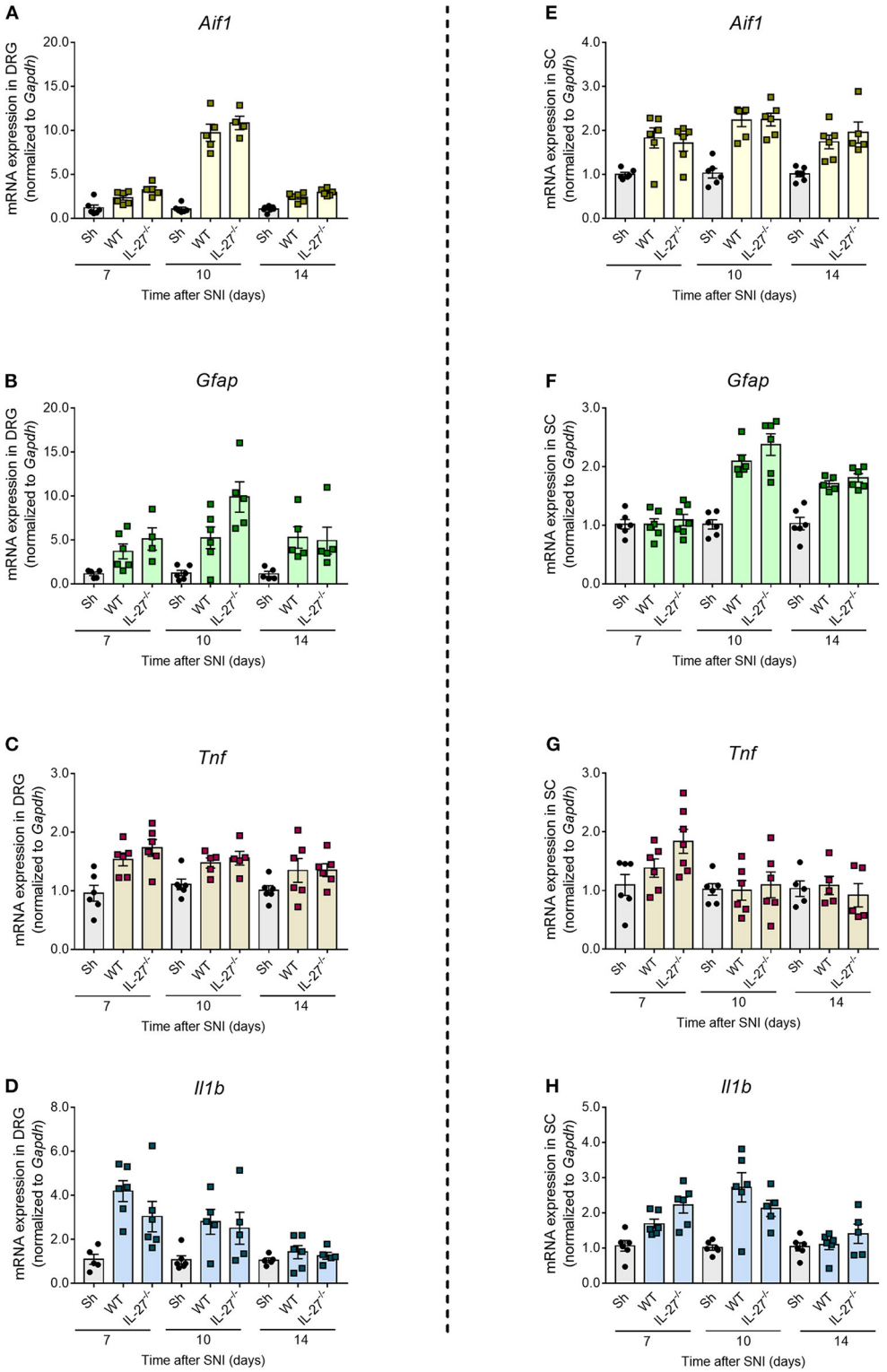

FIGURE 4 | Activation of immune/glial cells and cytokine expression in the DRGs and spinal cord after peripheral nerve injury in the absence of IL-27. Real-time PCR analysis of the expression of glial markers and pro-inflammatory cytokines relative to *Gapdh* at days 7, 10, and 14 after SNI or Sham surgery in WT and IL-27$^{-/-}$ mice: **(A)** *Aif1,* **(B)** *Gfap,* **(C)** *Tnf*, and **(D)** *Il1b* expressions in DRGs, **(E)** *Aif1,* **(F)** *Gfap,* **(G)** *Tnf*, and **(H)** *Il1b* expressions in spinal cord ($n = 7$). Data are presented as means ± S.E.M. Data were analyzed by one-way ANOVA followed by Bonferroni post-test.

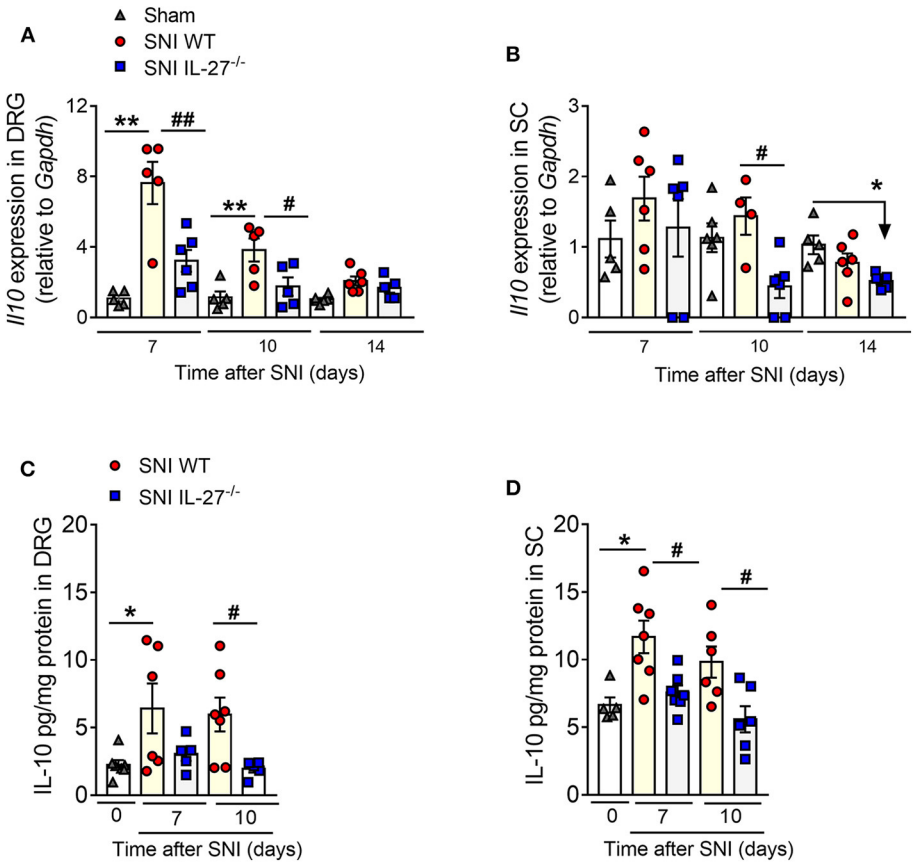

FIGURE 5 | The impact of IL-27 deficiency in anti-inflammatory cytokine expression after peripheral nerve injury. WT and IL-27$^{-/-}$ mice were submitted to SNI or Sham surgeries, and at days 7, 10, and 14, tissues were collected to real-time PCR analysis: **(A,B)** *Il10* expression relative to *Gapdh* in DRGs and in the spinal cord, respectively. **(C,D)** Level of IL-10 measured by ELISA in DRGs and in the spinal cord, respectively, on days 10 and 14 after SNI or Sham-operated (day 0) in WT and IL-27$^{-/-}$ mice. Data are presented as means ± S.E.M (n = 5–7). $^{*}P < 0.05$ and $^{**}P < 0.01$ vs. Sham-WT. $^{\#}P < 0.05$ and $^{\#\#}P < 0.01$ vs. SNI-WT **(A,B)**. $^{*}P < 0.05$ and $^{**}P < 0.01$ vs. Sham-operated (day 0). $^{\#}P < 0.05$ and $^{\#\#}P < 0.01$ vs. SNI-WT **(C,D)**. Data were analyzed by one-way ANOVA followed by Bonferroni post-test.

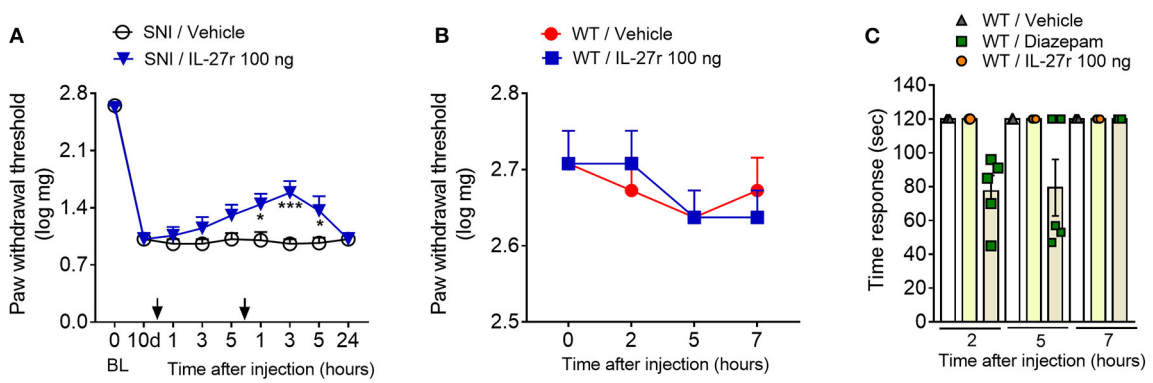

FIGURE 6 | Recombinant IL-27 intrathecally injected partially reverses mechanical hypersensitivity after peripheral nerve injury. **(A)** WT animals were submitted to SNI surgery and at day 10 were treated i.t. with recombinant IL-27 (IL-27r) or vehicle, and the treatments were repeated after ~5 h; mechanical threshold was evaluated using von Frey filaments (n = 8). **(B)** Effect of recombinant IL-27 in the basal mechanical threshold in WT-naive animals (n = 6). **(C)** Rota-rod test was realized to discard possible non-specific muscle relaxant or sedative effects of recombinant IL-27 in WT-naive animals (n = 5). Data are presented as means ± S.E.M. **(A)** $^{*}P <$ 0.05, $^{***}P < 0.001$ vs. SNI-vehicle. **(C)** $^{*}P < 0.05$ vs. WT-vehicle. Data were analyzed by two-way ANOVA followed by Bonferroni post-test.

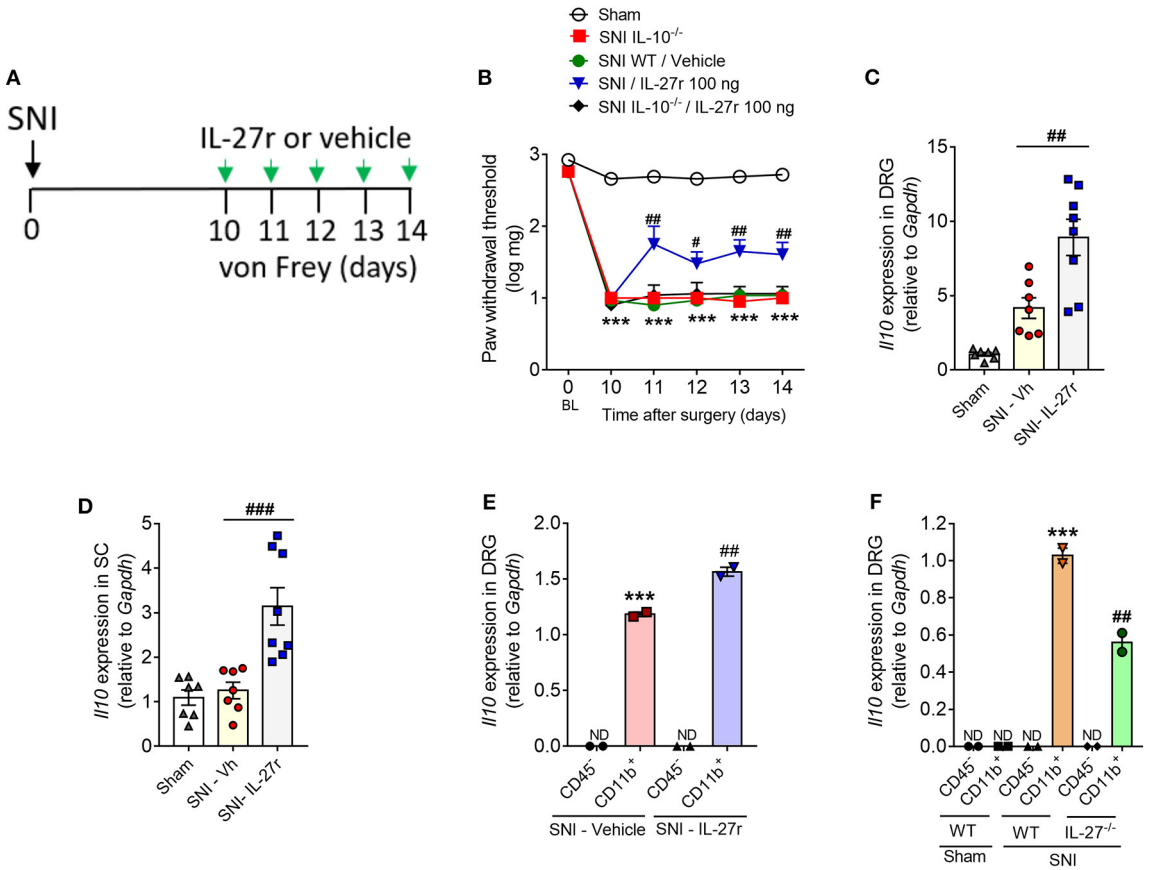

FIGURE 7 | Exogenous IL-27 reduced neuropathic pain through the induction of IL-10. **(A)** WT and IL-10$^{-/-}$ mice were submitted to SNI (day 0), and on day 10 up to day 14, different groups of animals were treated with recombinant IL-27 or vehicle (i.t) daily. **(B)** Paw withdrawal thresholds were evaluated using von Frey filament before (day 0) and up to 14 days after SNI ($n = 8$). ***$p < 0.001$ vs. Sham-operated mice; $^{\#}p < 0.05$ and $^{\#\#}p < 0.01$ vs. WT-SNI. Real-time PCR analysis of *Il10* expression relative to *Gapdh* in WT mice submitted to SNI or Sham surgeries and treated with recombinant IL-27 (SNI-IL27r) or vehicle (SNI-Vh) on day 10 until day 14 **(C)** in DRGs and **(D)** in the spinal cord ($n = 7$–8). ***$P < 0.001$ vs. Sham-operated; $^{\#\#}P < 0.05$ and $^{\#\#\#}P < 0.001$ vs. SNI-Vh. **(E)** Using the same protocol of treatment, CD45^{-} and CD11b^{+} cells were isolated from DRGs, by FACS sorting, and levels of *Il10* relative to *Gapdh* expression were quantified using real-time PCR ($n = 2$, pool from eight animals for each). ***$P < 0.001$ vs. CD45^{-} SNI-vehicle. $^{\#\#}P < 0.05$ vs. CD11b^{+} from SNI-vehicle; *ND* not detected. **(F)** At 10 days after SNI or Sham surgeries, cells were isolated from DRGs of WT and IL-27$^{-/-}$ and real-time PCR analysis of *Il10* expression relative to *Gapdh* was realized ($n = 2$, pool from eight animals for each). ***$P < 0.05$ vs. CD45^{-} from SNI-WT; $^{\#\#}P < 0.05$ vs. CD11b^{+} from Sham-WT; ND, not detected. Data are presented as means ± S.E.M. Data were analyzed by two-way ANOVA followed by Bonferroni post-test **(B)** or by one-way ANOVA followed by Tukey post-test **(C–F)**.

cell (microglia and astrocytes) activation in the DRGs and spinal cord, respectively. However, no significant changes in the expression of macrophage/glial cell activation markers and their derived pro-nociceptive cytokines (TNF and IL-1β) were detected after peripheral nerve injury in the DRGs and spinal cord from IL-27 null mice compared to WT mice. Thus, although IL-27 receptor seems to be confined in macrophage/microglia and astrocyte after peripheral nerve injury, IL-27 effect on neuropathic pain process appears to be independent on the regulation of these cells' activation/proliferation. These data corroborate with the previous study showing no role for IL-27 signaling in spinal cord microgliosis after peripheral nerve injury (19).

Concomitantly to the production of pro-inflammatory molecules by immune and glial cells at the sensory ganglia and spinal cord after peripheral nerve injury, there is also evidence suggesting the production of anti-inflammatory/anti-nociceptive molecules (12, 13, 50). Among these molecules, IL-10 seems to be one of the most important (15, 61, 62). The antinociceptive role of IL-10 has been extensively explored in different models of pathological pain (63–66). We found that the regulatory role of IL-27 in the development of neuropathic pain is dependent on IL-10 production in the DRGs and spinal cord. At least in the DRGs, IL-27 triggers the induction of IL-10 in macrophages. It is important to point out that IL-10 upregulation after peripheral nerve injury was not exclusively dependent on IL-27 since IL-10 production was not abrogated in IL-27 null mice. Thus, other direct or indirect mechanisms might be involved in the induction of IL-10, such as A2A and A3 adenosine receptor activation (67, 68). In addition, our data corroborate with a recent finding showing that the antinociceptive effect of IL-10 is not dependent on inhibition

of neuroinflammation (69). Therefore, it is plausible to suggest that IL-10 might reduce neuropathic pain by acting directly on sensitive neurons. In fact, IL-10R1 is expressed in neurons, and its activation directly regulates the functions of the primary sensory neurons (70, 71).

The use of exogenous IL-27 has been recognized as a novel biological tool to treat a vast range of inflammatory and autoimmune disease (28, 30, 31, 72, 73). In addition to the endogenous involvement of IL-27 in counteracting peripheral nerve injury-induced neuropathic pain development, exogenously administered recombinant IL-27 was also able to reduce neuropathic pain. It is noteworthy that the effective dose of recombinant IL-27 did not alter the mechanical pain threshold, in contrast to previous findings (19). These might be explained by the different dose or route (intrathecal vs. systemic) of IL-27 administration. In addition, the dose of recombinant IL-27 used did not cause any sedative/motor impairment. Then, these data might indicate that IL-27 could be a useful tool to prevent/reduce neuropathic pain in clinical settings.

In summary, our study unraveled the role of IL-27 as a regulatory cytokine that counteracts the development of neuropathic pain through the induction of anti-nociceptive cytokine IL-10. In conclusion, these data provide new insights into the neuroimmune–glia interaction mechanisms involved in the development of neuropathic pain. Finally, they indicate that immunotherapies based on IL-27 could emerge as possible therapeutic approaches for the prevention of neuropathic pain development after peripheral nerve injury.

DATA AVAILABILITY STATEMENT

The datasets generated for this study are available on request to the corresponding author.

ETHICS STATEMENT

Animal care and handling procedures were in accordance with the International Association for the Study of Pain guidelines (74) for those animals used in pain research, and they were approved by the Committee for Ethics in Animal Research of Ribeirão Preto Medical School -USP (Process no 211/2014).

AUTHOR CONTRIBUTIONS

MF designed and performed most of the experiments, analyzed the data, and wrote the manuscript. MD-F and FS-C designed and assisted in performing the experiments. RG, RK, FO, and DF assisted in performing some experiments. FC and JA-F reviewed the manuscript and provided expert discussion of the project. TC conceived the study, supervised the overall project, and wrote the manuscript. All authors contributed to manuscript revision and read and approved the submitted version.

FUNDING

The research leading to these results has received funding from São Paulo Research Foundation (FAPESP) under grant agreements no 2011/19670-0 (Thematic project) and 2013/08216-2 (Center for Research in Inflammatory Disease).

ACKNOWLEDGMENTS

The authors gratefully acknowledge the technical assistance of Sergio R. Rosa, Ieda Santos, and Katia Santos.

SUPPLEMENTARY MATERIAL

The Supplementary Material for this article can be found online at: https://www.frontiersin.org/articles/10.3389/fimmu.2019.03059/full#supplementary-material

Figure S1 | Representative gating strategies for flow cytometry analysis. After the specified days, DRGs were collected from mice, and $CD45^-$ (non-immune cells) and macrophages ($CD11b^+Ly6G^-$) were isolated using FACS sorting. FSC-H/FSC-A preliminary gate was performed for all cytometry analysis to exclude cell debris and cell doublets. Next, $CD45^+$ cells were gated on two populations, $CD11b^+Ly6G^+$ and $CD11b^+Ly6G^-$. Then, $CD45^-$ and $CD45^+C11b^+Ly6G^-$ were sorted. For all of the experiments, the sample purity was ∼70% for $CD11b^+Ly6G^-$ cells and ∼90% for $CD45^-$ cells. We use ∼25,000 cells to isolate mRNA in each group of experiment.

REFERENCES

1. van Hecke O, Austin SK, Khan RA, Smith BH, Torrance N. Neuropathic pain in the general population: a systematic review of epidemiological studies. *Pain.* (2014) 155:654–62. doi: 10.1016/j.pain.2013.11.013
2. Marchand F, Perretti M, McMahon SB. Role of the immune system in chronic pain. *Nat Rev Neurosci.* (2005) 6:521–32. doi: 10.1038/nrn1700
3. Grace PM, Hutchinson MR, Maier SF, Watkins LR. Pathological pain and the neuroimmune interface. *Nat Rev Immunol.* (2014) 14:217–31. doi: 10.1038/nri3621
4. Ji RR, Chamessian A, Zhang YQ. Pain regulation by non-neuronal cells and inflammation. *Science.* (2016) 354:572–7. doi: 10.1126/science.aaf8924
5. Basbaum AI, Bautista DM, Scherrer G, Julius D. Cellular and molecular mechanisms of pain. *Cell.* (2009) 139:267–84. doi: 10.1016/j.cell.2009.09.028
6. Ji RR, Xu ZZ, Gao YJ. Emerging targets in neuroinflammation-driven chronic pain. *Nat Rev Drug Discov.* (2014) 13:533–48. doi: 10.1038/nrd4334
7. Hu P, McLachlan EM. Macrophage and lymphocyte invasion of dorsal root ganglia after peripheral nerve lesions in the rat. *Neuroscience.* (2002) 112:23–38. doi: 10.1016/S0306-4522(02)00065-9
8. Liu FY, Sun YN, Wang FT, Li Q, Su L, Zhao ZF, et al. Activation of satellite glial cells in lumbar dorsal root ganglia contributes to neuropathic pain after spinal nerve ligation. *Brain Res.* (2012) 1427:65–77. doi: 10.1016/j.brainres.2011.10.016
9. Peng J, Gu N, Zhou LB, Eyo U, Murugan M, Gan WB, et al. Microglia and monocytes synergistically promote the transition from acute to chronic pain after nerve injury. *Nat Commun.* (2016) 7:1–13. doi: 10.1038/ncomms12029
10. Watkins LR, Maier SF. Glia: a novel drug discovery target for clinical pain. *Nat Rev Drug Discov.* (2003) 2:973–85. doi: 10.1038/nrd1251

11. Inoue K. The function of microglia through purinergic receptors: neuropathic pain and cytokine release. *Pharmacol Ther*. (2006) 109:210–26. doi: 10.1016/j.pharmthera.2005.07.001
12. Xu ZZ, Zhang L, Liu T, Park JY, Berta T, Yang R, et al. Resolvins RvE1 and RvD1 attenuate inflammatory pain via central and peripheral actions. *Nat Med.* (2010) 16:592–7. doi: 10.1038/nm.2123
13. Üçeyler N, Topuzoglu T, Schiesser P, Hahnenkamp S, Sommer C. IL-4 deficiency is associated with mechanical hypersensitivity in mice. *PLoS ONE.* (2011) 6:e28205. doi: 10.1371/journal.pone.0028205
14. Chen G, Park CK, Xie RG, Ji RR. Intrathecal bone marrow stromal cells inhibit neuropathic pain via TGF-β secretion. *J Clin Invest.* (2015) 125:3226–40. doi: 10.1172/JCI80883
15. Khan J, Ramadan K, Korczeniewska O, Anwer MM, Benoliel R, Eliav E. Interleukin-10 levels in rat models of nerve damage and neuropathic pain. *Neurosci Lett.* (2015) 592:99–106. doi: 10.1016/j.neulet.2015.03.001
16. Bobinski F, Teixeira JM, Sluka KA, Santos ARS. Interleukin-4 mediates the analgesia produced by low-intensity exercise in mice with neuropathic pain. *Pain.* (2018) 159:437–50. doi: 10.1097/j.pain.0000000000001109
17. Pflanz S, Timans JC, Cheung J, Rosales R, Kanzler H, Gilbert J, et al. IL-27, a heterodimeric cytokine composed of EBI3 and p28 protein, induces proliferation of naive CD4+ T cells. *Immunity.* (2002) 16:779–90. doi: 10.1016/S1074-7613(02)00324-2
18. Pflanz S, Hibbert L, Mattson J, Rosales R, Vaisberg E, Bazan JF, et al. WSX-1 and glycoprotein 130 constitute a signal-transducing receptor for IL-27. *J Immunol.* (2004) 172:2225–31. doi: 10.4049/jimmunol.172.4.2225
19. Sasaguri T, Taguchi T, Murata Y, Kobayashi K, Iizasa S, Iizasa E, et al. Interleukin-27 controls basal pain threshold in physiological and pathological conditions. *Sci Rep.* (2018) 8:11022. doi: 10.1038/s41598-018-29398-3
20. Lee YS, Amadi-Obi A, Yu CR, Egwuagu CE. Retinal cells suppress intraocular inflammation (uveitis) through production of interleukin-27 and interleukin-10. *Immunology.* (2011) 132:492–502. doi: 10.1111/j.1365-2567.2010.03379.x
21. Sénécal V, Deblois G, Beauseigle D, Schneider R, Brandenburg J, Newcombe J, et al. Production of IL-27 in multiple sclerosis lesions by astrocytes and myeloid cells: modulation of local immune responses. *Glia.* (2016) 64:553–69. doi: 10.1002/glia.22948
22. Yoshida H, Hunter CA. The immunobiology of interleukin-27. *Annu Rev Immunol.* (2015) 33:417–43. doi: 10.1146/annurev-immunol-032414-112134
23. Fitzgerald DC, Zhang GX, El-Behi M, Fonseca-Kelly Z, Li H, Yu S, et al. Suppression of autoimmune inflammation of the central nervous system by interleukin 10 secreted by interleukin 27-stimulated T cells. *Nat Immunol.* (2007) 8:1372–9. doi: 10.1038/ni1540
24. Villarino AV, Larkin J III, Saris CJ, Caton AJ, Lucas S, Wong T, et al. Positive and negative regulation of the IL-27 receptor during lymphoid cell activation. *J Immunol.* (2005) 174:7684–91. doi: 10.4049/jimmunol.174.12.7684
25. Stumhofer JS, Hunter CA. Advances in understanding the anti-inflammatory properties of IL-27. *Immunol Lett.* (2008) 117:23–30. doi: 10.1016/j.imlet.2008.01.011
26. Yoshida H, Nakaya M, Miyazaki Y. Interleukin 27: a double-edged sword for offense and defense. *J Leukoc Biol.* (2009) 86:1295–303. doi: 10.1189/jlb.0609445
27. Hölscher C, Hölscher A, Rückerl D, Yoshimoto T, Yoshida H, Mak T, et al. The IL-27 receptor chain WSX-1 differentially regulates antibacterial immunity and survival during experimental tuberculosis. *J Immunol.* (2005) 174:3534–44. doi: 10.4049/jimmunol.174.6.3534
28. Batten M, Li J, Yi S, Kljavin NM, Danilenko DM, Lucas S, et al. Interleukin 27 limits autoimmune encephalomyelitis by suppressing the development of interleukin 17-producing T cells. *Nat Immunol.* (2006) 7:929–36. doi: 10.1038/ni1375
29. de Aquino MT, Kapil P, Hinton DR, Phares TW, Puntambekar SS, Savarin C, et al. IL-27 limits central nervous system viral clearance by promoting IL-10 and enhances demyelination. *J Immunol.* (2014) 193:285–94. doi: 10.4049/jimmunol.1400058
30. Fitzgerald DC, Ciric B, Touil T, Harle H, Grammatikopolou J, Das Sarma J, et al. Suppressive effect of IL-27 on encephalitogenic Th17 cells and the effector phase of experimental autoimmune encephalomyelitis. *J Immunol.* (2007) 179:3268–75. doi: 10.4049/jimmunol.179.5.3268
31. Niedbala W, Cai B, Wei X, Patakas A, Leung BP, McInnes IB, et al. Interleukin 27 attenuates collagen-induced arthritis. *Ann Rheum Dis.* (2008) 37:1474–9. doi: 10.1136/ard.2007.083360
32. Pickens S R, Chamberlain ND, Volin MV, Mandelin AM II, Agrawal H, Matsui M, et al. Local expression of interleukin-27 ameliorates collagen-induced arthritis. *Arthritis Rheum.* (2011) 63:2289–98.doi: 10.1002/art.30324
33. Tanida S, Yoshitomi H, Ishikawa M, Kasahara T, Murata K, Shibuya H, et al. IL-27-producing CD14(+) cells infiltrate inflamed joints of rheumatoid arthritis and regulate inflammation and chemotactic migration. *Cytokine.* (2011) 55:237–44. doi: 10.1016/j.cyto.2011.04.020
34. Nieuwenhuis EE, Neurath MF, Corazza N, Iijima H, Trgovcich J, Wirtz S, et al. Disruption of T helper 2-immune responses in epstein–barr virus-induced Gene 3-deficient mice. *Proc Natl Acad Sci USA.* (2002) 99:16951–6. doi: 10.1073/pnas.252648899
35. Kühn R, Löhler J, Rennick D, Rajewsky K, Müller W. Interleukin-10-deficient mice develop chronic enterocolitis. *Cell.* (1993) 75:263–74. doi: 10.1016/0092-8674(93)80068-P
36. Jung S, Aliberti J, Graemmel P, Sunshine MJ, Kreutzberg GW, Sher A, et al. Analysis of fractalkine receptor CX(3)CR1 function by targeted deletion and green fluorescent protein reporter gene insertion. *Mol Cell Bio.* (2000) 20:4106–14. doi: 10.1128/MCB.20.11.4106-4114.2000
37. Decosterd I, Woolf CJ. Spared nerve injury: an animal model of persistent peripheral neuropathic pain. *Pain.* (2000) 87:149–58. doi: 10.1016/S0304-3959(00)00276-1
38. Hunskaar S, Hole K. The formalin test in mice: dissociation between inflammatory and non-inflammatory pain. *Pain.* (1987) 30:103–14. doi: 10.1016/0304-3959(87)90088-1
39. Kuraishi Y, Harada Y, Aratani S, Satoh M, Takagi H. Separate involvement of the spinal noradrenergic and serotonergic systems in morphine analgesia: the differences in mechanical and thermal algesic tests. *Brain Res.* (1983) 273:245–52. doi: 10.1016/0006-8993(83)90849-1
40. Choi Y, Yoon YW, Na HS, Kim SH, Chung JM. Behavioral signs of ongoing pain and cold allodynia in a rat model of neuropathic pain. *Pain.* (1994) 59:369–76. doi: 10.1016/0304-3959(94)90023-X
41. Cunha TM, Verri WA Jr, Vivancos GG, Moreira IF, Reis S, Parada CA, et al. An electronic pressure-meter nociception paw test for mice. *Braz J Med Biol Res.* (2004) 37:401–7. doi: 10.1590/S0100-879X2004000300018
42. Ribeiro RA, Vale ML, Thomazzi SM, Paschoalato AB, Poole S, Ferreira SH, et al. Involvement of resident macrophages and mast cells in the writhing nociceptive response induced by zymosan and acetic acid in mice. *Eur J Pharmacol.* (2000) 387:111–8. doi: 10.1016/S0014-2999(99)00790-6
43. Papir-Kricheli D, Frey J, Laufer R, Gilon C, Chorev M, Selinger Z, et al. Behavioural effects of receptor-specific substance P agonists. *Pain.* (1987) 31:263–76. doi: 10.1016/0304-3959(87)90041-8
44. Livak KJ, Schmittgen TD. Analysis of relative gene expression data using real-time quantitative PCR and the 2[-delta delta C(T)] method. *Methods.* (2001) 25:402–8. doi: 10.1006/meth.2001.1262
45. Sorge RE, Mapplebeck JC, Rosen S, Beggs S, Taves S, Alexander JK, et al. Different immune cells mediate mechanical pain hypersensitivity in male and female mice. *Nat Neurosci.* (2015) 18:1081–3. doi: 10.1038/nn.4053
46. Santa-Cecília FV, Ferreira DW, Guimaraes RM, Cecilio NT, Fonseca MM, Lopes AH, et al. The NOD2 signaling in peripheral macrophages contributes to neuropathic pain development. *Pain.* (2009) 160:102–16. doi: 10.1097/j.pain.0000000000001383
47. Austin PJ, Moalem-Taylor G. The neuro-immune balance in neuropathic pain: involvement of inflammatory immune cells, immune-like glial cells and cytokines. *J Neuroimmunol.* (2010) 229:26–50. doi: 10.1016/j.jneuroim.2010.08.013
48. Lee HL, Lee KM, Son SJ, Hwang SH, Cho HJ. Temporal expression of cytokines and their receptors mRNAs in a neuropathic pain model. *Neuroreport.* (2004) 15:2807–11.
49. Milligan ED, Langer SJ, Sloane EM, He L, Wieseler-Frank J, O'Connor K, et al. Controlling pathological pain by adenovirally driven spinal production of the anti-inflammatory cytokine, interleukin-10. *Eur J Neurosci.* (2005) 21:2136–48. doi: 10.1111/j.1460-9568.2005.04057.x
50. Jancálek R, Dubový P, Svízenská I, Klusáková I. Bilateral changes of TNF-alpha and IL-10 protein in the lumbar and cervical dorsal root ganglia following

a unilateral chronic constriction injury of the sciatic nerve. *J Neuroinflam.* (2010) 7:11. doi: 10.1186/1742-2094-7-11
51. Milligan ED, Penzkover KR, Soderquist RG, Mahoney MJ. Spinal interleukin-10 therapy to treat peripheral neuropathic pain. *Neuromodulation.* (2012) 15:520–6. doi: 10.1111/j.1525-1403.2012.00462.x
52. Hung AL, Lim M, Doshi TL. Targeting cytokines for treatment of neuropathic pain. *Scand J Pain.* (2017) 17:287–93. doi: 10.1016/j.sjpain.2017.08.002
53. Thacker MA, Clark AK, Marchand F, McMahon SB. Pathophysiology of peripheral neuropathic pain: immune cells and molecules. *Anesth Analg.* (2007) 105:838–47. doi: 10.1213/01.ane.0000275190.42912.37
54. Clark AK, Old EA, Malcangio M. Neuropathic pain and cytokines: current perspectives. *J Pain Res.* (2013) 6:803–14. doi: 10.2147/JPR.S53660
55. Berta T, Qadri Y, Tan PH, Ji RR. Targeting dorsal root ganglia and primary sensory neurons for the treatment of chronic pain. *Expert Opin Ther Targets.* (2017) 21:695–703. doi: 10.1080/14728222.2017.1328057
56. Denk F, Crow M, Didangelos A, Lopes DM, McMahon SB. Persistent alterations in microglial enhancers in a model of chronic pain. *Cell Rep.* (2016) 15:1771–81. doi: 10.1016/j.celrep.2016.04.063
57. Whitehead KJ, Smith CG, Delaney SA, Curnow SJ, Salmon M, Hughes JP, et al. Dynamic regulation of spinal pro-inflammatory cytokine release in the rat *in vivo* following peripheral nerve injury. *Brain Behav Immun.* (2010) 24:569–76. doi: 10.1016/j.bbi.2009.12.007
58. Scholz J, Woolf CJ. The neuropathic pain triad: neurons, immune cells and glia. *Nat Neurosci.* (2007) 10:1361–8. doi: 10.1038/nn1992
59. Scheller J, Schuster B, Hölscher C, Yoshimoto T, Rose-John S. No inhibition of IL-27 signaling by soluble gp130. *Biochem Biophys Res Commun.* (2005) 326:724–8. doi: 10.1016/j.bbrc.2004.11.098
60. Wang S, Miyazaki Y, Shinozaki Y, Yoshida H. Augmentation of antigen-presenting and Th1-promoting functions of dendritic cells by WSX-1(IL-27R) deficiency. *J Immunol.* (2007) 179:6421–8. doi: 10.4049/jimmunol.179.10.6421
61. Alexander GM, van Rijn M, van Hilten JJ, Perreault MJ, Schwartzman RJ. Changes in cerebrospinal fluid levels of pro-inflammatory cytokines in CRPS. *Pain.* (2005) 116:213–9. doi: 10.1016/j.pain.2005.04.013
62. Backonja MM, Coe CL, Muller DA, Schell K. Altered cytokine levels in the blood and cerebrospinal fluid of chronic pain patients. *J Neuroimmunol.* (2008) 195:157–63. doi: 10.1016/j.jneuroim.2008.01.005
63. Ledeboer A, Jekich BM, Sloane EM, Mahoney JH, Langer SJ, Milligan ED, et al. Intrathecal interleukin-10 gene therapy attenuates paclitaxel-induced mechanical allodynia and proinflammatory cytokine expression in dorsal root ganglia in rats. *Brain Behav Immun.* (2007) 21:686–98. doi: 10.1016/j.bbi.2006.10.012
64. Wagner R, Janjigian M, Myers RR. Anti-inflammatory interleukin-10 therapy in CCI neuropathy decreases thermal hyperalgesia, macrophage recruitment, and endoneurial TNF-alpha expression. *Pain.* (1998) 74:35–42. doi: 10.1016/S0304-3959(97)00148-6
65. Alaaeddine N, Di Battista JA, Pelletier JP, Kiansa K, Cloutier JM, Martel-Pelletier J. Inhibition of tumor necrosis factor alpha-induced prostaglandin E2 production by the antiinflammatory cytokines interleukin-4, interleukin-10, and interleukin-13 in osteoarthritic synovial fibroblasts: distinct targeting in the signaling pathways. *Arthritis Rheum.* (1999) 42:710–718. doi: 10.1002/1529-0131(199904)42:4<710::AID-ANR14>3.0.CO;2-4
66. Helmark IC, Mikkelsen UR, Børglum J, Rothe A, Petersen MC, Andersen O, et al. Exercise increases interleukin-10 levels both intraarticularly and peri-synovially in patients with knee osteoarthritis: a randomized controlled trial. *Arthritis Res Ther.* (2010) 12:R126. doi: 10.1186/ar3064
67. Janes K, Esposito E, Doyle T, Cuzzocrea S, Tosh DK, Jacobson KA, et al. A3 adenosine receptor agonist prevents the development of paclitaxel-induced neuropathic pain by modulating spinal glial-restricted redox-dependent signaling pathways. *Pain.* (2014) 155:2560–7. doi: 10.1016/j.pain.2014.09.016
68. Kwilasz AJ, Ellis A, Wieseler J, Loram L, Favret J, McFadden A, et al. Sustained reversal of central neuropathic pain induced by a single intrathecal injection of adenosine A2A receptor agonists. *Brain Behav Immun.* (2018) 69:470–9. doi: 10.1016/j.bbi.2018.01.005
69. Wu HY, Mao XF, Tang XQ, Ali U, Apryani E, Liu H, et al. Spinal interleukin-10 produces antinociception in neuropathy through microglial β-endorphin expression, separated from antineuroinflammation. *Brain Behav Immun.* (2018) 73:504–19. doi: 10.1016/j.bbi.2018.06.015
70. Shen KF, Zhu HQ, Wei XH, Wang J, Li YY, Pang RP, et al. Interleukin-10 down-regulates voltage gated sodium channels in rat dorsal root ganglion neurons. *Exp Neurol.* (2013) 247:466–75. doi: 10.1016/j.expneurol.2013.01.018
71. Moore KW, de Waal Malefyt R, Coffman RL, O'Garra A. Interleukin-10 and the interleukin-10 receptor. *Annu Rev Immunol.* (2001) 19:683–765. doi: 10.1146/annurev.immunol.19.1.683
72. Rostami A, Ciric B. Role of Th17 cells in the pathogenesis of CNS inflammatory demyelination. *J Neurol Sci.* (2013) 333:76–87. doi: 10.1016/j.jns.2013.03.002
73. Sasaoka T, Ito M, Yamashita J, Nakajima K, Tanaka I, Narita M, et al. Treatment with IL-27 attenuates experimental colitis through the suppression of the development of IL-17-producing T helper cells. *Am J Physiol Gastrointest Liver Physiol.* (2011) 300:G568–76. doi: 10.1152/ajpgi.00329.2010
74. Zimmermann M. Ethical guidelines for investigations of experimental pain in conscious animals. *Pain.* (1983) 16:109–10. doi: 10.1016/0304-3959(83)90201-4

Conflict of Interest: The authors declare that the research was conducted in the absence of any commercial or financial relationships that could be construed as a potential conflict of interest.

frontiers in Immunology

ORIGINAL RESEARCH
published: 28 July 2020
doi: 10.3389/fimmu.2020.01442

Secreted Osteoclastogenic Factor of Activated T Cells (SOFAT) Is Associated With Rheumatoid Arthritis and Joint Pain: Initial Evidences of a New Pathway

Marcelo Henrique Napimoga[1†], Weslley Danny Dantas Formiga[1], Henrique Ballassini Abdalla[1], Carlos Antônio Trindade-da-Silva[1], Camila Motta Venturin[2], Elizabeth Ferreira Martinez[2], Ana Carolina Rossaneis[3], Waldiceu A. Verri Jr.[3] and Juliana Trindade Clemente-Napimoga[1]*

[1] Laboratoy of Neuroimmune Interface of Pain Research, Faculdade São Leopoldo Mandic, Instituto de Pesquisas São Leopoldo Mandic, Campinas, Brazil, [2] Faculdade São Leopoldo Mandic, Instituto São Leopoldo Mandic, Campinas, Brazil, [3] Departamento de Ciências Patológicas, Universidade Estadual de Londrina, Londrina, Brazil

Rheumatoid arthritis (RA) has an inflammatory milieu in the synovial compartment, which is regulated by a complex cytokine and chemokine network that induces continuously degenerative and inflammatory reactions. The secreted osteoclastogenic factor of activated T cells (SOFAT) is a unique cytokine and represents an alternative pathway for osteoclast activation. In this study, we examined whether SOFAT is able to induce joint pain and investigated the presence of SOFAT in a Collagen-induced Arthritis (CIA) model and in human subjects. Here, we found that an intra-articular stimulation with SOFAT (1, 10, 100, or 1,000 ng/10 μl) in the knee joint significantly decreases the mechanical threshold in the hind paw of mice ($p < 0.05$). Moreover, after a second injection of SOFAT, the mechanical threshold decrease was sustained for up to 8 days ($p < 0.05$). In the CIA model, the immunohistochemical assay of knee joint showed positivity stained for SOFAT, and the mRNA and protein expression of SOFAT were significantly higher in the affected-group ($p < 0.05$). Besides, the mRNA of RANKL, IL-1β, IL-6, and IL-15 were significantly higher in the affected-group ($p < 0.05$). Finally, SOFAT was detected in the synovial fluid of RA patients, but not in OA patients ($p < 0.05$). In conclusion, SOFAT is up regulated in inflammatory milieu such as RA but not in non-inflammatory OA. SOFAT may be a novel molecule in the complex inflammatory phenotype of RA.

Keywords: inflammation, SOFAT, rheumatoid arthritis, pain, osteoclast

OPEN ACCESS

Edited by:
Annalisa Del Prete, University of Brescia, Italy

Reviewed by:
Christoph Baerwald, Leipzig University, Germany
Nadia Lampiasi, Institute of Biomedicine and Molecular Immunology Alberto Monroy (IBIM), Italy

****Correspondence:***
Marcelo Henrique Napimoga
marcelo.napimoga@slmandic.edu.br; marcelo.napimoga@gmail.com

†ORCID:
Marcelo Henrique Napimoga
orcid.org/0000-0003-4472-365X

Specialty section:
This article was submitted to Cytokines and Soluble Mediators in Immunity, a section of the journal Frontiers in Immunology

Received: *05 March 2020*
Accepted: *03 June 2020*
Published: *28 July 2020*

Citation:
Napimoga MH, Dantas Formiga WD, Abdalla HB, Trindade-da-Silva CA, Venturin CM, Martinez EF, Rossaneis AC, Verri WA Jr and Clemente-Napimoga JT (2020) Secreted Osteoclastogenic Factor of Activated T Cells (SOFAT) Is Associated With Rheumatoid Arthritis and Joint Pain: Initial Evidences of a New Pathway. Front. Immunol. 11:1442. doi: 10.3389/fimmu.2020.01442

INTRODUCTION

The term arthritis is used to refer to a group of diseases that affect the joints with varied degrees of inflammation in sterile and septic forms (1, 2). According to the Centers for Disease Control and Prevention (CDC) and Arthritis Foundation, around 54 million people have any kind of arthritis in the USA. Despite the well-recognized burdens of arthritis, such as pain, swelling, and stiffness, 60% of arthritis-affected report limitations in their daily activities (3). The decline in quality of life as well as the risk of comorbid illness (obesity, diabetes, and heart disease) represent an individual

and society public cost since a high percentage of occurrence is in the working-age population (18–64 years old) (4, 5). Within this set of diseases commonly called arthritis, osteoarthritis (OA) represents the highest incidence; however, rheumatoid arthritis (RA), gout, and fibromyalgia are equally relevant (6).

The immune system fails to recognize the self in RA. The continuously degenerative and inflammatory reactions result from an abnormal innate and adaptive immune responses primarily affecting the joints but also extra-articular tissues (7). Failure of therapy treatment could lead to an irreversible stage of joint destruction and consequently disability of daily activities (8). Intense joint pain is a clinical symptom that profoundly decreases the quality of life of RA patients (9). OA is a degenerative disease (10) primarily characterized by progressive cartilage degeneration and secondarily by synovial inflammation. Although OA was initially considered as a non-inflammatory disease, associated especially with obesity, evidence demonstrates an important role of the chondrocytes phenotype in cartilage breakdown (10). In summary, RA or OA present destruction of cartilage and underlying bone despite their different etiologies and biological mechanism.

In this scenario, activated T cells stood out for their modulatory activity of bone turnover and by representing an important source of osteoclastogenic cytokines (11), including in RA (12, 13). Moreover, T cells induce osteoclast formation through RANKL (receptor activator of nuclear factor kappa-B ligand) and TNF-α (tumor necrosis factor-α) (14). Also, IL-1 and IL-6 (interleukin) are released by T cells, leading to RANKL expression by osteoblast (15). IL-15 recruits and activates T cells, which will produce TNF-α in RA. TNF-α, IL-1β, IL-6, and IL-15 induce pain in RA (16, 17).

A novel activated human T-cell-secreted cytokine, named as the secreted osteoclastogenic factor of activated T cells (SOFAT), has been characterized (11). Interestingly, SOFAT can induce bone loss in a RANKL-independent manner in periodontal disease (18, 19) as well as directly stimulate IL-6 by human osteoblasts (11), modulate osteoblast activities sustaining the inflammatory environment (20), and, finally, represent a putative marker for osteoclast in bone lesions (21).

In the present study, we examined whether SOFAT could induce joint pain. Other than this, we investigated the presence of SOFAT in collagen-induced arthritis (CIA) model. We therefore investigated whether the increase of SOFAT is an observed factor in patients previously diagnosed with RA or OA.

METHODS

Animals Approved and Care

Male Swiss mice (25–30 grams) and male DBA/1J mice (6–9 weeks) were used in this study. Animals were randomly assigned and housed in plastic cages ($n = 5$/per cage) in a temperature-controlled room (23 ± 1°C) at a 12:12 light cycle with access to water and food *ad libitum*. All animal experiment procedures and protocols were approved by the Committee on Animal Research of Faculdade São Leopoldo Mandic, Brazil (No. 2019/019) or Committee on Animal Research of Universidade Estadual de Londrina (approval under the number CEUA-UEL 28016.2014.91) and are in accordance with the guidelines by the National Council for Control of Animal Experimentation (CONCEA), ARRIVE (22), and the International Association for the Study of Pain (IASP) for the study of pain in conscious animals (23). All efforts were made to minimize animal suffering and to reduce the number of animals used. Each experimental group had a number of six animals in each experiment, and all experimental procedures were repeated twice.

Mechanical Hyperalgesia

A mechanical hyperalgesia test was performed by an electronic version of von Frey's filaments, as previously described (24). During the light phase (between 9:00 a.m. and 5:00 p.m.), the test was carried out in a quiet, temperature-controlled room. Mice were placed in acrylic cages with wire grid floors 30 min before the experiment for acclimatization with the new environment. The assessment of knee joint hyperalgesia in the femur–tibial joint consist of an electronic pressure meter with a force transducer fitted with polypropylene tip (Insight instruments, Ribeirão Preto, SP, Brazil). The articular pain was evaluated with a large tip (4.15 mm^2) due to the exclusion factor of cutaneous nociception. A progressive pressure was applied to a central area of plantar surface of hind paw to induce flexion of the femur–tibial joint and subsequent hind paw withdrawal. The pressure intensity of the withdrawal threshold (in grams) was automatically recorded. Investigators were blinded to the groups.

For this study, mice were treated with an intra-articular injection on knee joint, in different concentrations of SOFAT (1, 10, 100, or 1,000 ng/10 μl) as a noxious challenge or vehicle (saline 10 μl). The intensity of mechanical hyperalgesia at the intervals of 1, 3, 5, 7, 24, 48, 72, 96, and 120 h after the stimulus was evaluated. A two-injection assay was carried out. The first injection was performed in the baseline period (0 days), and the second injection on the fifth day. The mechanical hyperalgesia was then evaluated daily for 10 days.

Collagen-Induced Arthritis (CIA) in DBA/1J Mice

CIA protocol was induced in mice as previously described by Su and collaborators (25). Concisely, male DBA/1J mice (6–9 weeks) were immunized intradermally at 1.5 cm from the tail base with 100 μg of chicken sternal hyaline Collagen type 2 (CII) (Sigma, #C9301), dissolved in 100 μl acetic acid (0.05 mol/l), and mixed with an equal volume of Freund's Complete Adjuvant (CFA) (Difco Laboratories, Detroit, MI, USA). Twenty-one days later, animals were boosted with 100 μg of CII and emulsified in incomplete Freund's adjuvant (IFA). Mice were examined daily for signs of arthritis as described (25). By the end of 15 days, all groups were anesthetized with xylalizine and ketamine intraperitoneal and sacrificed by cervical dislocation. Knee and paw joints were collected for histological analyses, western blot, and RT-qPCR.

Subjects

Seven individuals diagnosed with rheumatoid arthritis (RA) ($n = 4$) or with osteoarthritis (OA) ($n = 3$), were selected from the General Hospital of the Medical School of Ribeirão Preto of the

University of São Paulo (HCFMRP-USP). The subjects with an indication for articular puncture were invited to participate of this study. All admitted subjects signed their informed consent. The Ethics Committee in Human Research at Ribeirão Preto General Hospital and Ribeirão Preto Medical School (protocol 38156414.4.0000.5374) previously approved this study protocol.

Synovial Liquid Collection

Patients previously diagnosed with AR or OA who also displayed indications of an articular puncture in the knee joint were selected. The procedure was performed under aseptic and antiseptic patterns (Povidone-iodine, PVP-I). The intra-articular puncture was performed with a 10 ml syringe coupled with a 25 × 7 needle. The synovial liquid was immediately stored in ice until the sample processing could occur.

Sample Preparation and Protein Extraction

Knee and paw samples for Western Blotting analysis (CIA protocol) were homogenized in 500 μl of the appropriate buffer containing protease inhibitors (Ripa Lysis Buffer, Santa Cruz, Biotechnology, Dallas, Texas, USA) using a specific sample homogenizer (BeadBlaster™ 24, Benchmark, Triple-Pure High Impact Zirconium Beads, Beads, Ø: 1.0 mm). After four cycles of 30 s with resting period of 40 s, the samples were centrifuged for 10 min/10,000 rpm/4°C. The total amount of extracted proteins was colorimetrically measured using the micro bicinchoninic acid (BCA) protein assay kit (Thermo Scientific, Rockford, IL, USA). The supernatants were stored at −20°C until further analysis.

Samples used for quantitative PCR (knee and paw joint mice; CIA protocol) were homogenized in TRIzol® reagent (ThermoFisher, MA, USA) with the homogenizer as previously detailed. Total RNA was extracted according to manufacturer's directions and stored at −70°C. The RNA concentration for each sample was determined by optical density using a micro-volume spectrophotometer (Nanodrop 1000, Nanodrop Technologies LLC, Wilmington, NC, USA).

Synovial liquid samples were immediately stored in ice after the intra-articular puncture. At the end of the surgical procedure, samples were centrifuged for 5 min/10,000 rpm/4°C, and the supernatant was collected and stored. The protein concentrations were determined using the bicinchoninic acid protein assay kit (Thermo Scientific, Rockford, IL, USA).

Reverse Transcription and Quantitative Polymerase Chain Reaction (RT-qPCR)

Reverse transcription of total RNA to cDNA was performed using DNase (Turbo DNA-frees, Ambion Inc., Austin, TX, USA). The reaction was carried out using the First-Strand cDNA synthesis kit (Roche Diagnostic Co., Indianapolis, IN, USA) following the manufacturer's recommendations. The qPCR was performed using GoTaq® 2-Step RT-qPCR System (Promega Corporation, WI, USA) and specific primers (Applied Biosystems®, ThermoFisher, MA, USA). The mRNA level of glyceraldehyde 3-phosphate dehydrogenase (GAPDH) was used as a reference gene.

Western Blotting

Equal amounts of protein (30 μg) from human synovial liquid or mice samples were loaded onto 10% SDS/PAGE gel and transferred to a nitrocellulose membrane. The membranes were blocked in TBS (20 mM Tris-HCl, 150 mM NaCl, and 1% Tween 20, pH 7.53) containing 5% non-fat dry milk for at least 2 h. Membranes were incubated with specific primary antibodies—anti-SOFAT (Rheabiotech), 1:500, overnight and GAPDH (Cell Signaling), 1:1,000, for 2 h. After incubation period, the membranes were rinsed with TBS, and subsequently incubated for 1 h with the secondary antibody, peroxidase-conjugated anti-rabbit IgG (Vector Laboratories, Burlingame, CA, USA). The bands of the membranes were visualized using the enhanced chemiluminescence (ECL) solution for 3 min (Amersham Biosciences, Piscataway, NJ, USA), and the digital image was obtained by CCD camera imaging for chemiluminescence (ImageQuant LAS 4000 mini, GE Healthcare Life Sciences, Pittsburgh, PA, USA). The program Image J (National Institutes of Health, Bethesda, USA) was applied to measure the optical density of the bands.

Enzyme-Linked Immunosorbent Assay (ELISA)

Levels of SOFAT were quantified in capture enzyme-linked immunosorbent assays (ELISA) as previously described (19). Briefly, microtiter plates (Costar 3590, Corning, NY) were incubated for 24 h at 4°C with 5 μg/ml of rabbit IgG anti-human SOFAT in carbonate–bicarbonate buffer, pH 9.6, following the manufacturer instructions. All antibody reagents were affinity purified and obtained from (Rheabiotech Laboratory, Campinas, SP, Brazil). After incubation period, plates were washed and blocked for 1 h at room temperature with 0.1% of BSA (bovine serum albumin). The washed process was repeated, and synovial liquid samples were pipetted. The plate was incubated for 2 h at room temperature. The assay included serial dilutions (500, 250, 125, 62.5, 31.25, 15.62, 7.81, and 3.90 lg/ml) of a standard sample of human SOFAT antibody (Rheabiotech). The secondary antibody was biotin-conjugated rabbit IgG anti-human SOFAT (Rheabiotech) at a dilution of 1:1,000. After incubation with a solution of avidin–peroxidase (30 min) at room temperature, a new series of washes was performed and substrate solution (TMB) was added and incubated for 15 min. The reaction was stopped with Stop Solution and read immediately in a spectrophotometer (Epoch, Biotek, Winooski, VT, USA) at 450 nm. Negative controls included an uncoated, no synovial liquid sample and no primary antibody wells. The total amounts of SOFAT were determined in nanograms per ml of synovial liquid sample. The assay was carried out in a blind fashion.

Histological Sections

For histological analysis, the knee joints of mice (CIA protocol) were used. The samples were fixed in 10% buffered neutral formalin (48 h) and decalcified in a solution of 10% EDTA. Knee samples were washed in running water, dehydrated, and embedded in paraffin wax. For hematoxylin-eosin staining, sections of 3 μm were sliced and dyed. For immunohistochemical staining, a previously standardized protocol was used as reference

(21). Briefly, samples sections (3 μm) were incubated with primary antibody of anti-SOFAT (1:300; Rheabiotech), followed by EnVision polymer HRP and Envision+ (Dako, SA, Denmark) for 1 h at 37°C. Ten minutes were used for developing at 37 with 3.3′-diaminobenzidine tetrahydrochloride and counterstained with Mayer hematoxylin (3 min; room temperature). Digital photomicrographs were taking from representative areas (Zeiss Axioskop 2 plus microscope, Carl Zeiss, Gottingen, Germany).

Statistical Analysis

The statistical analyses were performed using a software program (GraphPad Prism 6.0, La Jolla, CA, USA). To determine if there were significant differences ($P < 0.05$) among groups, the data were analyzed using the Student *t*-test. Data are presented in figures as mean ± standard deviation (SD).

RESULTS

SOFAT Induce Mechanical Hyperalgesia in the Knee Joint

First, we investigated whether intra-articular injection of SOFAT in the knee joint could induce mechanical hyperalgesia in mouse (**Figure 1**). For that, titrated doses of SOFAT (1, 10, 100, or 1,000 ng/10 μl) were injected in the knee joint. Mechanical hyperalgesia was evaluated at the intervals of 1, 3, 5, 7, 24, 48, 72, 96, and 120 h after the stimulus (**Figure 1A**). We demonstrated here that intra-articular injection 1 and 10, 100, and 1,000 nanograms of SOFAT induce mechanical hyperalgesia 5 and 3 h later, respectively (**Figure 1A**). The hyperalgesia lasted until 96 h when the mechanical threshold returned to normal values. In a repetitive injection protocol, SOFAT induced hyperalgesia over 4 days upon the first administration, and, on the fifth day in which the hyperalgesia vanished, an additional administration of SOFAT induced enhanced hyperalgesia, which lasted up to the eighth day ($p < 0.05$; **Figure 1B**).

Collagen-Induced Arthritis Augments SOFAT Levels

Given the capacity of SOFAT to induce joint pain, we next assessed the presence of SOFAT in a CIA model of arthritis. Histological sections with HE-staining were made in the knee joint of affected- or naive-group (**Figure 2**). Intense leukocyte infiltrates, pannus formation, cartilage, and bone breakdown were observed in the CIA model (**Figures 2D,E**) but not in the naive group (**Figures 2A,B**). Subsequently, immunohistochemistry for SOFAT exhibits high positive stain in the leukocyte infiltrate (**Figure 2F**). On the other hand, a weak or no stain was observed in the naive group (**Figure 2C**). In agreement with this, mRNA (**Figure 2G**) and protein expression of SOFAT (**Figure 2H**) showed statistical higher values ($p < 0.05$) in the CIA model when compared to the naive group.

Collagen-Induced Arthritis Enhances Inflammatory and RANK/RANKL/OPG Axis

Once it was demonstrated that CIA model augments the expression of SOFAT and leads to cartilage and bone breakdown,

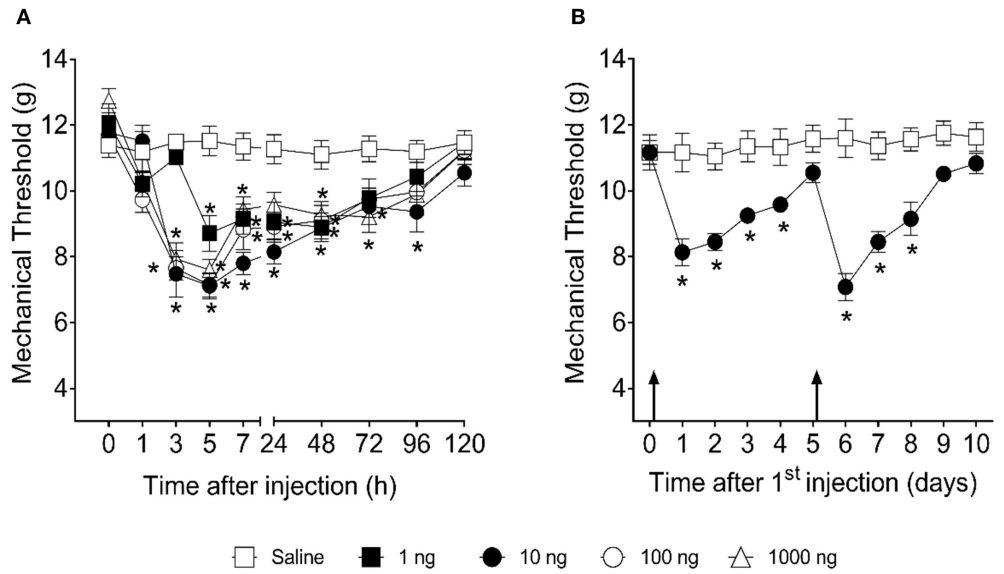

FIGURE 1 | SOFAT inhibits mechanical hyperalgesia in mice. Mice received intra-articular stimulation with SOFAT (1, 10, 100, or 1,000 ng/10 μl) and mechanical hyperalgesia was evaluated at the intervals of 1, 3, 5, 7, 24, 48, 72, 96, and 120 h after the stimulus **(A)**. The effect of two intra-articular injections of SOFAT (10 ng/10 μl) on mechanical hyperalgesia was evaluated daily for 10 days. Mice received the first injection immediately after baseline measurement (Time 0) and the second injection immediately after the fifth day measurement, as indicated by the arrows **(B)**. Results are expressed as mean ± SEM ($n = 6$ per group per experiment, representative of two experiments). The symbol (*) means difference compared to saline group ($P < 0.05$: Two-way ANOVA, Tukey's test).

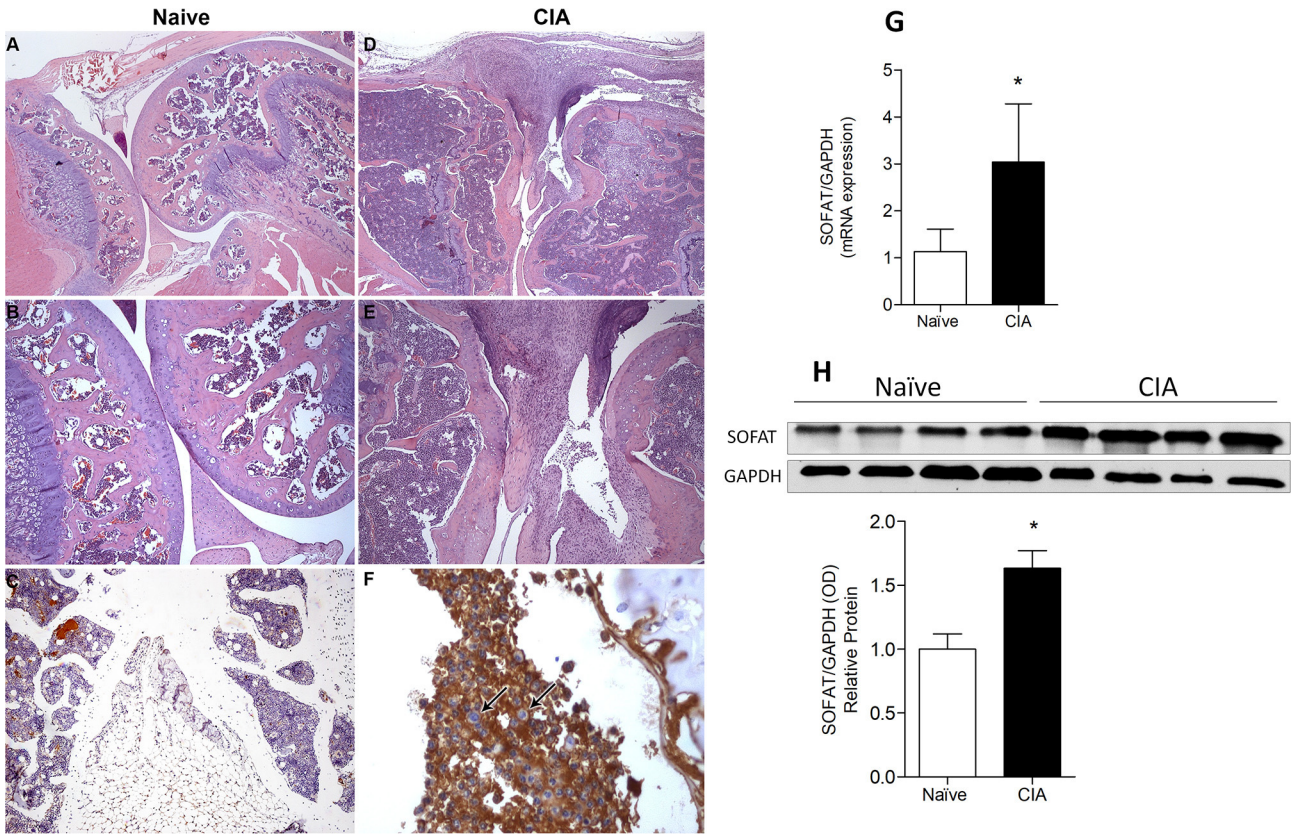

FIGURE 2 | Collagen-induced arthritis showed a positive stain for SOFAT in the knee joint of mice. Histological sections of the knee joint were staining with hematoxylin-eosin (HE). Magnification of 20x **(A,D)** and 40x **(B,F)** were used. Images were taken from the naïve group, demonstrating no leukocyte infiltrate and bone or cartilage breakdown **(A,B)**. Images were taken from the CIA group showing vast leukocyte infiltrate and bone or cartilage disrupted **(D,E)**. Immunohistochemical staining of SOFAT in the knee joint. Magnification of 40x **(C)** and 40X **(F)** were used. The arrows demonstrate leukocytes in the inflammatory infiltrate into the synovium. Naïve group does not show positive stained for SOFAT **(C)** and the CIA group shown positive stained for SOFAT **(F)**. SOFAT mRNA expression in joints of mice induced or not by CIA protocol **(G)**. Representative bands of Western Blotting and protein fold changed **(H)** of SOFAT. The data are expressed as mean ± *SD* ($n = 6$ per group per experiment, representative of two experiments). The symbol (*) means mRNA or protein expression significantly higher than the naive group ($P < 0.05$: *T*-test, Tukey's test).

we investigated the presence of pro inflammatory mediators and RANK/RANKL/OPG axis markers (**Figure 3**). Our results showed a statistical increase ($p < 0.05$) in mRNA expression for RANKL (**Figure 3A**), RANKL/OPG ratio (**Figure 3C**), IL-6 (**Figure 3D**), IL-15 (**Figure 3E**), and IL-1β (**Figure 3F**) in affected groups when compared to the naive group. Only mRNA expression of OPG (**Figure 3B**) did not show a statistical difference between naïve and CIA groups.

SOFAT Is Highly Expressed in Patients With Rheumatoid Arthritis (RA) but Not Osteoarthritis (OA)

Given the present animal model mimics RA, we investigated the presence of SOFAT in the synovial liquid of the knee joint of patients previously diagnosed with RA and OA (**Figure 4**). Our results demonstrated that the protein levels of SOFAT were significantly higher ($p < 0.05$) in patients diagnosed with RA than OA (**Figures 4A,B**).

DISCUSSION

Rheumatoid arthritis is a chronic inflammatory disease characterized by a vast lymphocyte infiltrate in the synovial membrane over the joints (8). RA probably arises from multiple hits, whereby an initial combination of lifestyle, environmental, and stochastic insults occurring in a genetically predisposed individual leads to breach of immunological tolerance (3). In the past decade, a new cytokine was described, namely, Secreted Osteoclastogenic Factor of Activated T cells (SOFAT), which is capable of inducing osteoclast formation in a RANKL-independent manner (11). Previously, we demonstrated that SOFAT is an important elicitor of bone breakdown when directly injected in mice, and elevated levels of SOFAT were found in inflamed gingival tissue from chronic periodontitis patients (19). Considering that periodontal disease has an important immunological feature in disease progression such as arthritis, we speculate that SOFAT could be involved in arthritic conditions.

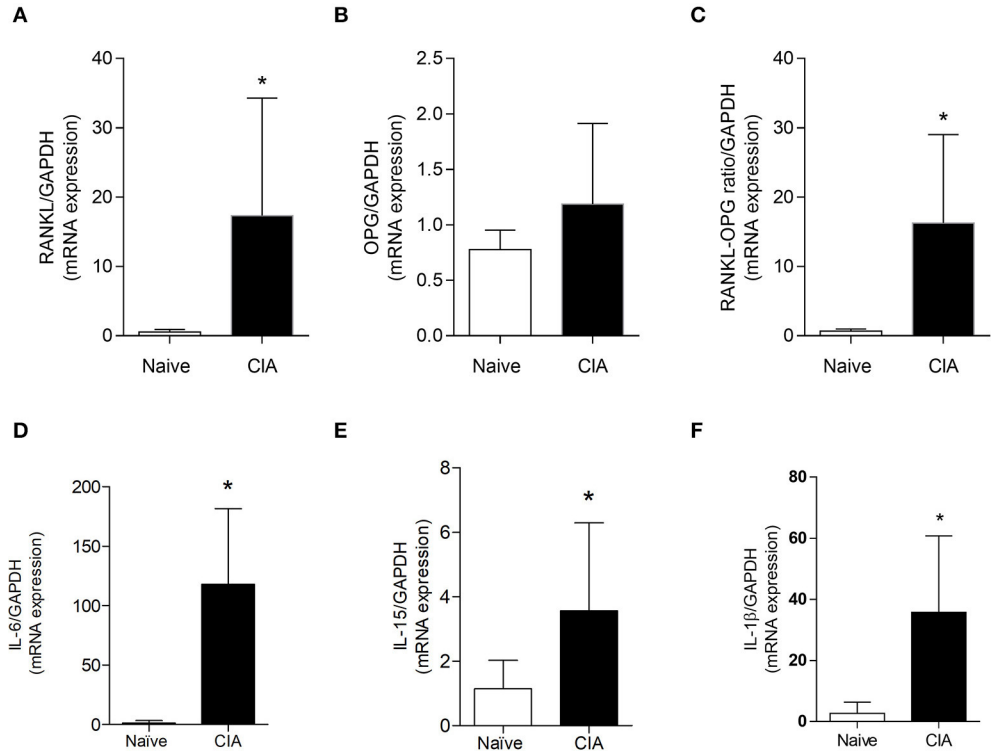

FIGURE 3 | Collagen-induced arthritis enhances inflammatories and osteolytic markers. mRNA expression of RANKL **(A)**, OPG **(B)**, RANKL/OPG ratio **(C)**, IL-6 **(D)**, IL-15 **(E)**, and IL-1β **(F)** were performed in joints mice. The data are expressed as mean ± SD ($n = 6$ per group per experiment, representative of two experiments). The symbol (*) means mRNA significantly higher than the naive group ($P < 0.05$: *T*-test, Tukey's test).

First, we investigate the noxious effect of SOFAT on mechanical hyperalgesia response in the knee joints of mice. We demonstrated that intra-articular injection of SOFAT in the knee joint induces mechanical hyperalgesia. Specifically, this nociceptive response initiates after 3 h of injection, and the two injections assay sustained this nociceptive stage for up to 8 days. The delay to initiate the mechanical hyperalgesia response could be associated with the fact that SOFAT does not stimulate neuronal fibers directly. SOFAT induces IL-6 synthesis by synovium osteoblast, promotes osteoclast formation, and triggers the activation of the nuclear factor of activated T cells (NFAT) signal transduction pathway (11, 19). Depending on the inflammatory molecule, it can activate the nociceptor sensory neurons generating pain behavior and/or sensitize the nociceptor sensory neurons facilitating neuronal depolarization upon mechanical or thermal stimulation. Nociceptor sensory neurons sensitization accounts for chronic pain (26).

Inflammatory bone disease, such as arthritis, is characterized by massive lymphocyte infiltrate as a consequence of the initial and uncontrolled inflammatory environment (3). Subsequently, a variety of factors exacerbate inflammation, which, in turn, is responsible for an irrecoverable bone loss and pain. Persistent pain in arthritis can continue without signs of peripheral inflammation due to altered expression of TNF-α in the dorsal root ganglia with nociceptor sensory neurons activation (27). In this sense, the CIA model was conducted to investigate the expression of SOFAT in a specific model that resembles rheumatoid arthritis. SOFAT was previously described in patients with chronic periodontitis (19) and is associated with RA (11, 28) since a feedback mechanism between T cells and osteoblasts was observed.

The cellular composition of synovitis in rheumatoid arthritis includes innate immune cells and adaptive immune cells, including T and B cells. It is known that both cells are important sources of pro-inflammatory cytokines (8) as well as major RANKL producer (29). Previously data revealed that B cells, in addition to T cells, are also important cellular sources of bone destructive factors SOFAT besides RANKL (18). Thus, it is possible to suggest that SOFAT may have a role, not yet fully understood, in the inflammatory loop of RA.

Our data showed positive stain and high expression of the mRNA and protein of SOFAT in the CIA group associated with bone pits in the knee joint and aberrant leukocyte infiltrate. In agreement with this, mRNA expression of RANKL, OPG, IL-6, IL-15, and IL-1β was also found to be high in CIA. RA is a chronic autoimmune disease that attacks multiple joints (8). The RANK/RANKL/OPG is a well-known signaling pathway for osteoclast activation and the ratio between RANKL and OPG is pivotal to drive osteoclastic activation (14) as well as IL-1β and IL-6 (30). IL-6 and IL-β are innate immunity

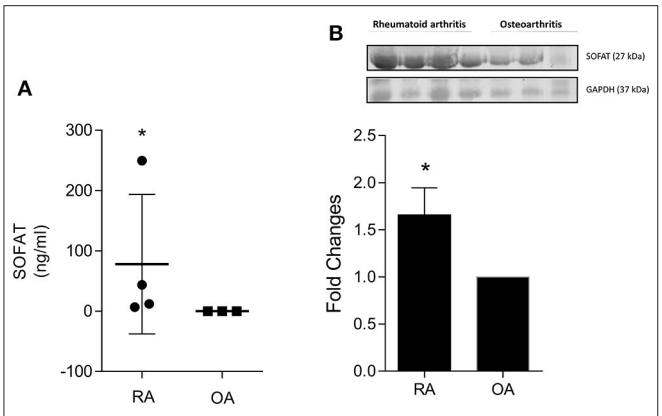

FIGURE 4 | SOFAT is highly expressed in patients with Rheumatoid Arthritis (RA) but not Osteoarthritis (OA). The protein level of SOFAT **(A)** was analyzed in the synovial liquid of knee patients using ELISA. Representative bands and protein expression **(B)** of SOFAT were analyzed in the synovial liquid of knee patients using Western Blotting. The data are expressed as mean ± SD. The symbol (*) means protein level or expression significantly higher than the naive group ($P < 0.05$: *T*-test, Tukey's test).

cytokines which have an important role in the pathogenesis of arthritis, by their chemotaxis and osteolytic capacities (31). For this reason, inhibitors of IL-6 and TNF-α were proposed as therapeutic strategies. However, around 50% are unresponsive to treatment as well as biologics targeting these cytokines increase the incidence of infection (8, 32). IL-15 contributes to RA physiopathology by stimulating T-cell development and survival, delaying the apoptosis of fibroblast-like synoviocytes as well as by recruiting neutrophils and lymphocytes to the inflammatory foci (17, 33, 34). A phase I-II clinical trial using a human IgG1 monoclonal antibody to target IL-15 reduced the disease activity according to the American College of Rheumatology criteria by 20% (ACR20) in 63% of patients, ACR50 in 38% of patients, and ACR70 in 25% of patients (35). This proof-of-concept study confirms experimentally in a clinical setting the relevance of IL-15 to RA disease. Considering that TNF-α, IL-1β, IL-6, and IL-15 induce pain in RA (16, 17), it is conceivable that in the CIA inflammatory context, SOFAT might also be an important hyperalgesic molecule. Of note, the hyperalgesia caused by TNF-α, IL-1β, IL-6, or IL-15 at 10 ng or a similar dose does not last in the same way as that induced by SOFAT. Thus, although these are proven hyperalgesic cytokines (16, 17), the 4 days of hyperalgesia upon a single injection of 10 ng of SOFAT is unforeseen.

Finally, we addressed the presence of SOFAT in patients previously diagnosed with RA and OA. This study presents some limitations due to the small number of subjects and the necessity for deeper understanding of the role of SOFAT in RA disease. However, this pilot study showed newsworthy findings and support the previous animal data. SOFAT protein was detected in the synovial liquid of patients diagnosed with RA for the first time. Our results showed a higher intensity of bands in immunoblotting for SOFAT in patients with RA compared to OA. ELISA assay also showed higher protein levels in RA samples than OA samples in which SOFAT was undetectable. Interestingly, patients with RA have OPG in increased levels, leading to augment in the OPG/RANKL ratio. Thus, these results reinforced the concept that SOFAT could be not only a possible therapeutic target but also a biological marker for RA and disease progression. Several new therapeutics are currently being developed on the basis of immunopathogenic insights and are being tested in trials. However, the main goal is to develop cause-directed, curative therapies, but this will not be possible without better understanding of the physiopathological mechanisms of rheumatoid arthritis.

In conclusion, this study adds a novel molecule in the complex inflammatory phenotype of RA. SOFAT induces pain *per se* and is expressed in the rheumatoid arthritis condition in an experimental mouse model and human samples.

DATA AVAILABILITY STATEMENT

The datasets generated for this study are available on request to the corresponding author.

ETHICS STATEMENT

The studies involving human participants were reviewed and approved by the Ethics Committee in Human Research at Ribeirão Preto General Hospital and Ribeirão Preto Medical School (protocol 38156414.4.0000.5374). The patients/participants provided their written informed consent to participate in this study. This animal study was reviewed and approved by Committee on Animal Research of Faculdade São Leopoldo Mandic, Brazil (No. 2019/019) or Committee on Animal Research of Universidade Estadual de Londrina (approval under the number CEUA-UEL 28016.2014.91).

AUTHOR CONTRIBUTIONS

MN, JC-N, EM, and WV contributed to the study concept and design. CT-S, WD, HA, CV, MN, AR, and WV contributed to data acquisition and interpretation. CT-S, HA, JC-N, MN, and WV wrote de manuscript. All authors critically revised the manuscript and approved the submitted version.

FUNDING

This study was financially supported by São Paulo Research Foundation, FAPESP (#2013/09524-2 and 2017/22334-9), Nacional de Desenvolvimento Científico e Tecnológico (CNPq) (Research Productivity Fellowships were awarded to MN, JC-N, EM, and WV), Coordenação de Aperfeiçoamento de Pessoal de Nível Superior, CAPES (#001), PPSUS Grant (agreement 041/2017, protocol 48.095); Programa de Apoio a Grupos de Excelência (PRONEX) grant supported by SETI (Secretaria da Ciência, Tecnologia e Ensino Superior)/Araucária Foundation and MCTI (Ministério da Ciência, Tecnologia e Inovação)/CNPq; and Paraná State Government (agreement 014/2017, protocol 46.843), Brazil.

REFERENCES

1. Staurengo-Ferrari L, Ruiz-Miyazawa KW, Pinho-Ribeiro FA, Domiciano TP, Fattori V, Mizokami SS, et al. The nitroxyl donor Angeli's salt ameliorates *Staphylococcus aureus*-induced septic arthritis in mice. *Free Radic Biol Med.* (2017) 108:487–99. doi: 10.1016/j.freeradbiomed.2017.04.016
2. Smolen JS, Aletaha D, Barton A, Burmester GR, Emery P, Firestein GS, et al. Rheumatoid arthritis. *Nat Rev Dis Primers.* (2018) 4:18001. doi: 10.1038/nrdp.2018.1
3. Smolen JS, Aletaha D, McInnes IB. Rheumatoid arthritis. *Lancet.* (2016) 388:2023–38. doi: 10.1016/S0140-6736(16)30173-8
4. Cross M, Smith E, Hoy D, Carmona L, Wolfe F, Vos T, et al. The global burden of rheumatoid arthritis: estimates from the global burden of disease 2010 study. *Ann Rheum Dis.* (2014) 73:1316–22. doi: 10.1136/annrheumdis-2013-204627
5. Kitas GD, Gabriel SE. Cardiovascular disease in rheumatoid arthritis: state of the art and future perspectives. *Ann Rheum Dis.* (2011) 70:8–14. doi: 10.1136/ard.2010.142133
6. The Lancet. Managing arthritis in the USA. *Lancet*. (2017) 389:1076. doi: 10.1016/S0140-6736(17)30765-1
7. Firestein GS, McInnes IB. Immunopathogenesis of rheumatoid arthritis. *Immunity.* (2017) 46:183–96. doi: 10.1016/j.immuni.2017.02.006
8. Miyabe Y, Lian J, Miyabe C, Luster AD. Chemokines in rheumatic diseases: pathogenic role and therapeutic implications. *Nat Rev Rheumatol.* (2019) 15:731–46. doi: 10.1038/s41584-019-0323-6
9. Fattori V, Amaral FA, Verri WA Jr. Neutrophils and arthritis: role in disease and pharmacological perspectives. *Pharmacol Res.* (2016) 112:84–98. doi: 10.1016/j.phrs.2016.01.027
10. Pap T, Korb-Pap A. Cartilage damage in osteoarthritis and rheumatoid arthritis–two unequal siblings. *Nat Rev Rheumatol.* (2015) 11:606–15. doi: 10.1038/nrrheum.2015.95
11. Rifas, L. Weitzmann MN. A novel T cell cytokine, secreted osteoclastogenic factor of activated T cells, induces osteoclast formation in a RANKL-independent manner. *Arthritis Rheum.* (2009) 60:3324–35. doi: 10.1002/art.24877
12. Ogawa Y, Ohtsuki M, Uzuki M, Sawai T, Onozawa Y, Nakayama J, et al. Suppression of osteoclastogenesis in rheumatoid arthritis by induction of apoptosis in activated CD4+ T cells. *Arthritis Rheum.* (2003) 48:3350–58. doi: 10.1002/art.11322
13. Fournier C. Where do T cells stand in rheumatoid arthritis? *Joint Bone Spine.* (2005) 72:527–32. doi: 10.1016/j.jbspin.2004.12.012
14. Yasuda H, Shima N, Nakagawa N, Yamaguchi K, Kinosaki M, Mochizuki S, et al. Osteoclast differentiation factor is a ligand for osteoprotegerin/osteoclastogenesis-inhibitory factor and is identical to TRANCE/RANKL. *Proc Natl Acad Sci USA.* (1998) 95:3597–602. doi: 10.1073/pnas.95.7.3597
15. Gillespie M.T. Impact of cytokines and T lymphocytes upon osteoclast differentiation and function. *Arthritis Res. Ther.* (2007) 9:103. doi: 10.1186/ar2141
16. Verri WA Jr, Guerrero AT, Fukada SY, Valerio DA, Cunha TM, Xu D, et al. IL-33 mediates antigen-induced cutaneous and articular hypernociception in mice. *Proc Natl Acad Sci USA.* (2008) 105, 2723–8. doi: 10.1073/pnas.0712116105
17. Verri WA Jr, Cunha TM, Parada CA, Wei XQ, Ferreira SH, Liew FY, et al. IL-15 mediates immune inflammatory hypernociception by triggering a sequential release of IFN-gamma, endothelin, and prostaglandin. *Proc Natl Acad Sci USA.* (2006) 103:9721–5. doi: 10.1073/pnas.0603286103
18. Jarry CR, Martinez EF, Peruzzo DC, Carregaro V, Sacramento LA, Araújo VC, et al. Expression of SOFAT by T- and B-lineage cells may contribute to bone loss. *Mol Med Rep.* (2016) 13:4252–8. doi: 10.3892/mmr.2016.5045
19. Jarry CR, Duarte PM, Freitas FF, de Macedo CG, Clemente-Napimoga JT, Saba-Chujfi E, et al. Secreted osteoclastogenic factor of activated T cells (SOFAT), a novel osteoclast activator, in chronic periodontitis. *Hum Immunol.* (2013) 74:861–6. doi: 10.1016/j.humimm.2013.04.013
20. Napimoga MH, Demasi AP, Jarry CR, Ortega MC, de Araújo VC, Martinez EF. In vitro evaluation of the biological effect of SOFAT on osteoblasts. *Int Immunopharmacol.* (2015) 26:378–83. doi: 10.1016/j.intimp.2015.04.033
21. Cândido-Soares LE, Martinez EF, de Araújo VC, Araújo NS, Freitas NS, Napimoga MH. SOFAT as a putative marker of osteoclasts in bone lesions. *Appl Immunohistochem Mol Morphol.* (2019) 27:448–53. doi: 10.1097/PAI.0000000000000648
22. Kilkenny C, Browne WJ, Cuthill IC, Emerson M, Altman DG. Improving bioscience research reporting: the ARRIVE guidelines for reporting animal research. *PLoS Biol.* (2010) 8:e1000412. doi: 10.1371/journal.pbio.1000412
23. Zimmermann M. Ethical guidelines for investigations of experimental pain in conscious animals. *Pain.* (1983) 16:109–10. doi: 10.1016/0304-3959(83)90201-4
24. Ruiz-Miyazawa KW, Staurengo-Ferrari L, Pinho-Ribeiro FA, Fattori V, Zaninelli TH, Badaro-Garcia S, et al. 15d-PGJ2-loaded nanocapsules ameliorate experimental gout arthritis by reducing pain and inflammation in a PPAR-gamma-sensitive manner in mice. *Sci Rep.* (2018) 8:13979. doi: 10.1038/s41598-018-32334-0
25. Su Z, Shotorbani SS, Jiang X, Ma R, Shen H, Kong F, et al. A method of experimental rheumatoid arthritis induction using collagen type II isolated from chicken sternal cartilage. *Mol Med Rep.* (2013) 8:113–7. doi: 10.3892/mmr.2013.1476
26. Verri WA Jr., Cunha TM, Parada CA, Poole S, Cunha FQ, Ferreira SH. Hypernociceptive role of cytokines and chemokines: targets for analgesic drug development? *Pharmacol Ther.* (2006) 112:116–38. doi: 10.1016/j.pharmthera.2006.04.001
27. Gonçalves WA, Rezende BM, de Oliveira MPE, Ribeiro LS, Fattori V, da Silva WN, et al. Sensory ganglia-specific TNF expression is associated with persistent nociception after resolution of inflammation. *Front Immunol.* (2020) 10:3120. doi: 10.3389/fimmu.2019.03120
28. Weitzmann MN, Cenci S, Rifas L, Haug J, Dipersio J, Pacifici R. T cell activation induces human osteoclast formation via receptor activator of nuclear factor kappaB ligand-dependent and -independent mechanisms. *J Bone Miner Res.* (2001) 16:328–37. doi: 10.1359/jbmr.2001.16.2.328
29. Weitzmann M, Ofotokun I. Physiological and pathophysiological bone turnover — role of the immune system. *Nat Rev Endocrinol.* (2016) 12:518–32. doi: 10.1038/nrendo.2016.91
30. Lacey DL, Boyle WJ, Simonet WS, Kostenuik PJ, Dougall WC, Sullivan JK, et al. Bench to bedside: elucidation of the OPG-RANK-RANKL pathway and the development of denosumab. *Nat Rev Drug Discov.* (2012) 11:401–19. doi: 10.1038/nrd3705
31. Garlet GP. Destructive and protective roles of cytokines in periodontitis: a reappraisal from host defense and tissue destruction viewpoints. *J Dental Res.* (2010) 89:1349–63. doi: 10.1177/0022034510376402
32. Ogata A, Kato Y, Higa S, Yoshizaki K. IL-6 inhibitor for the treatment of rheumatoid arthritis: a comprehensive review. *Mod. Rheumatol.* (2019) 29:258–67. doi: 10.1080/14397595.2018.1546357
33. Jin Y, Chen X, Gao Z, Liu K, Hou Y, Zheng J. Expression levels of IL-15 and IL-17 in synovial fluid of rheumatoid arthritis animal model. *Exp Ther Med.* (2018) 16:3377–82. doi: 10.3892/etm.2018.6643
34. Verri WA Jr., Cunha TM, Ferreira SH, Wei X, Leung BP, Fraser A, et al. IL-15 mediates antigen-induced neutrophil migration by triggering IL-18 production. *Eur J Immunol.* (2007) 37:3373–80. doi: 10.1002/eji.200737488
35. Baslund B, Tvede N, Danneskiold-Samsoe B, Larsson P, Panayi G, Petersen J, et al. Targeting interleukin-15 in patients with rheumatoid arthritis: a proof-of-concept study. *Arthritis Rheum.* (2005) 52:2686–92. doi: 10.1002/art.21249

Conflict of Interest: The authors declare that the research was conducted in the absence of any commercial or financial relationships that could be construed as a potential conflict of interest.

frontiers in Immunology

ORIGINAL RESEARCH
published: 26 January 2021
doi: 10.3389/fimmu.2020.539086

Experimental *Trypanosoma cruzi* Infection Induces Pain in Mice Dependent on Early Spinal Cord Glial Cells and NFκB Activation and Cytokine Production

*Sergio M. Borghi[1,2], Victor Fattori[1], Thacyana T. Carvalho[1], Vera L. H. Tatakihara[1], Tiago H. Zaninelli[1], Felipe A. Pinho-Ribeiro[1], Camila R. Ferraz[1], Larissa Staurengo-Ferrari[1], Rubia Casagrande[3], Wander R. Pavanelli[1], Fernando Q. Cunha[4], Thiago M. Cunha[4], Phileno Pinge-Filho[1] and Waldiceu A. Verri[1]**

[1] Department of Pathology, Center of Biological Science, State University of Londrina, Londrina, Brazil, [2] Center for Research in Health Science, University of Northern Paraná—Unopar, Londrina, Brazil, [3] Departament of Pharmaceutical Sciences, Health Sciences Center, University Hospital, Londrina State University, Londrina, Brazil, [4] Department of Pharmacology, Ribeirão Preto Medical School, University of São Paulo, Ribeirão Preto, Brazil

The neglected tropical infirmity Chagas disease (CD) presents high mortality. Its etiological agent *T. cruzi* is transmitted by infected hematophagous insects. Symptoms of the acute phase of the infection include fever, fatigue, body aches, and headache, making diagnosis difficult as they are present in other illnesses as well. Thus, in endemic areas, individuals with undetermined pain may be considered for CD. Although pain is a characteristic symptom of CD, its cellular and molecular mechanisms are unknown except for demonstration of a role for peripheral TNF-α in CD pain. In this study, we evaluate the role of spinal cord glial cells in experimental *T. cruzi* infection in the context of pain using C57BL/6 mice. Pain, parasitemia, survival, and glial and neuronal function as well as NFκB activation and cytokine/chemokine production were assessed. *T. cruzi* infection induced chronic mechanical and thermal hyperalgesia. Systemic TNF-α and IL-1β peaked 14 days postinfection (p.i.). Infected mice presented increased spinal gliosis and NFκB activation compared to uninfected mice at 7 days p.i. Glial and NFκB inhibitors limited *T. cruzi*–induced pain. Nuclear phosphorylated NFκB was detected surrounded by glia markers, and glial inhibitors reduced its detection. *T. cruzi*–induced spinal cord production of cytokines/chemokines was also diminished by glial inhibitors. Dorsal root ganglia (DRG) neurons presented increased activity in infected mice, and the production of inflammatory mediators was counteracted by glial/NFκB inhibitors. The present study unveils the contribution of DRG and spinal cord cellular and molecular events leading to pain in *T. cruzi* infection, contributing to a better understanding of CD pathology.

Keywords: *Trypanosoma cruzi*, pain, glial cells, NFκB, cytokine

OPEN ACCESS

Edited by:
Joanna Cichy, Jagiellonian University, Poland

Reviewed by:
Xuehong Liu, Shaoxing University, China
Ana Rosa Pérez, Consejo Nacional de Investigaciones Científicas y Técnicas (CONICET), Argentina

****Correspondence:***
Waldiceu A. Verri
waldiceujr@yahoo.com.br; waverri@uel.br

Specialty section:
This article was submitted to Cytokines and Soluble Mediators in Immunity, a section of the journal Frontiers in Immunology

Received: *28 February 2020*
Accepted: *08 December 2020*
Published: *26 January 2021*

Citation:
Borghi SM, Fattori V, Carvalho TT, Tatakihara VLH, Zaninelli TH, Pinho-Ribeiro FA, Ferraz CR, Staurengo-Ferrari L, Casagrande R, Pavanelli WR, Cunha FQ, Cunha TM, Pinge-Filho P and Verri WA (2021) Experimental Trypanosoma cruzi Infection Induces Pain in Mice Dependent on Early Spinal Cord Glial Cells and NFκB Activation and Cytokine Production. Front. Immunol. 11:539086. doi: 10.3389/fimmu.2020.539086

INTRODUCTION

According to the World Health Organization, more than 1.5 billion people worldwide are infected with neglected tropical diseases. Among them, 8 million people have Chagas disease (CD; American trypanosomiasis) with a mortality rate reaching 10,000 deaths per year (1). More than 25 million people are at risk of infection in endemic areas, and globalization contributes to the propagation of CD to other areas besides America (1). There are two well-established phases of CD upon infection, beginning with an acute phase that starts 6–10 days after infection with the parasite *Trypanosoma cruzi* (*T. cruzi*) and lasts for about 4–8 weeks, depending on mouse strain and parasite load and strain (2). In the present experimental condition, the parasitemia ends by the 28th day postinfection (p.i.) as demonstrated by previous studies by our group (3). During the acute phase of CD, high numbers of parasites are found in the bloodstream and tissues, and after this period, the parasite and the host reach an immunological balance and a chronic phase settles in. In the chronic phase of CD, parasitemia is substantially reduced, and patients become asymptomatic until major organ pathology develops, affecting, for instance, the heart (1, 2).

Immunoregulatory events found in the acute phase of CD include an intense inflammatory response with high production of inflammatory cytokines and nitric oxide (NO), which are important to orchestrate immune cells to eliminate the parasite (1, 4). These are key mediators in controlling infection because, for instance, tumor necrosis factor-α deficient $(TNF\text{-}\alpha)^{-/-}$ and inducible nitric oxide synthase deficient $(iNOS)^{-/-}$ mice are highly susceptible to *T. cruzi* infection (1, 5).

Clinical and epidemiological studies of patients with CD in the acute phase report pain and inflammation as major symptoms (6–11). In studies conducted in endemic areas of Brazil, fever (98%), headache (92.3%), myalgia (80%), swelling of the lower limbs (57.9%), facial edema (57.5%), abdominal pain (54.1%), and painful lumps (17%) were the most reported symptoms (7, 8). However, the cellular and molecular mechanism underlying the pain in CD remains unknown. There is evidence of high levels of peripheral TNF-α in CD (12). TNF-α has a well-established function in triggering hyperalgesia (13). Interleukin (IL)-1β is another hyperalgesic cytokine (14) that is speedily produced in response to *T. cruzi* infection (12, 15). Thus, the systemic elevations in TNF-α and IL-1β production during *T. cruzi* infection may account for the nociceptor neuron sensitization/activation and consequent prominent pain observed in CD patients. Further reinforcing this concept, targeting TNF-α in experimental CD reduces mechanical allodynia during the first week after infection (16). C-X_3-C motif chemokine ligand 1 (CX_3CL1) is another important molecule related to neuroinflammation and the central sensitization processes leading to pain, which is crucial for the neuron–glia interface during nervous system pathology (17). Its serum concentration is increased in the acute phase of CD (18); however, whether its signaling *via* C-X_3-C motif chemokine receptor 1 (CX_3CR1) in the central nervous system (CNS) has a role in CD pathology is unknown.

In addition to high serum levels of hyperalgesic cytokines, chronic phase CD patients may present severe neurological manifestations, resulting in elevated morbidity and mortality rates (19). Amastigote forms and *T. cruzi* granular antigens (this last one restricted to inflamed foci) can be abundantly detected in CNS (cortex and basal nuclei) in the chronic phase of CD in inbred mice, suggesting potential local actions (20, 21). There seems to occur an active interaction between *T. cruzi* and the immune/nervous system because the *T. cruzi* parasite can be found infecting mouse peripheral glial cells (22–24); brain astrocytes (25–27); and spinal cord astrocytes, microglia, and macrophages (24, 28) as well as human peripheral glial cells (29), astrocytes (25, 30), and neurons (29). In immunocompromised humans, such as patients with human immunodeficiency virus (HIV) and cancer, *T. cruzi* infection results in brain and spinal cord lesions, neurological abnormalities, and parasite detection in the brain and cerebrospinal fluid (25, 31). During the chronic phase of CD, CNS parasitism may rise by reentry of blood parasites or migration of infected macrophages (25). Spinal cord neuropathology occurs with the presence of *T. cruzi*–enhanced disease in mice lacking the IL-12p40 gene compared to wild type (28). Cultured dorsal root ganglia (DRG) and spinal cord neurons of mice infected with *T. cruzi* show altered morphology and can evolve to death that occurs probably by phagocyte overt inflammation in response to parasitism (24, 27). However, the neuro-immune interactions in the spinal cord leading to pain during *T. cruzi* infection are still unaddressed. This lack of information impairs the comprehension of central immune inflammatory events in CD considering that the spinal cord plays a pivotal role in the integrative mechanisms of pain processing.

Our group recently demonstrated the role of spinal cord astrocytes and microglia in neuroinflammation and central processing of pain in another neglected tropical disease, leishmaniasis, contributing to advance in the understanding of neuroimmune interactions that occur in the host in response to the parasite (32). However, although the evidence described above strongly suggests that systemic immune and inflammatory profiles of CD may account for the pain-related symptoms observed in human patients, the central pathophysiological mechanisms of the nociceptive activity in *T. cruzi* infection remains poorly explored. Therefore, the present study investigates the participation of spinal cord glial cells (microglia and astrocytes) in the pathology of experimental CD-induced pain using C57BL/6 mice.

METHODS

Animals

The experiments were performed on male C57BL/6 mice, 7–13 weeks, resistance prototype to *T. cruzi* infection, weighing between 20 and 30 g from TECPAR (Paraná Technology Institute), PR, Brazil. The choice of exclusively male mice for the study is based on previous findings indicating gender dimorphism in nociception and no effect of glial inhibitors in females in this specie (32). Pathogen-free mice were housed in standard clear plastic cages appended to a

ventilated rack (Alesco Indústria e Comércio LTDA, Monte Mor, Sao Paulo, Brazil) with free access to water and food, a light/dark cycle of 12/12 h, and controlled temperature. Shaving and feed provision for the animals was always controlled by a sterilization process. The mice were separated into a maximum of five per cage and were maintained in the vivarium of the Department of Pathology at the State University of Londrina for at least 2 days before the experiments. Mice were used only once and were acclimatized to the testing room at least 1 hour before the experiments, which was conducted during the light cycle. At the end of the experiments, mice were anesthetized with isoflurane 5% only once by inhalation overdose, and terminally euthanized by cervical dislocation followed by decapitation. Animals were monitored regarding welfare-related assessment before, during, and after the experiments. Clinical signs of severe illness, including changes in body weight, erection of the back hairs (reflecting irritation or agitation), diarrhea, lethargy, rapid/shallow breathing, and paralysis, were also properly recorded. Animals presenting clinical signs of severe disease before the end of the model were immediately euthanized using isoflurane 5% followed by cervical dislocation as per the guidelines of the Ethics Committee on Animal Use (CEUA) of the State University of Londrina. The euthanasia process used in the study for sample collection also followed the protocol of anesthesia of animals with isoflurane 5% followed by cervical dislocation according to the CEUA guidelines. Efforts were maintained to narrowly minimize the total number of animals used and their discomfort or suffering.

Drugs

Isoflurane was obtained from Abbot Park (Lake Bluff, IL, USA). L-2-aminoadipic acid (α-aminoadipate; A7275), minocycline hydrochloride (M9511), ammonium pyrrolidine dythiocarbamate (PDTC; P8765), dimethyl sulfoxide (DMSO; D8418), and tween 80 (P5188) were purchased from Sigma-Aldrich (St. Louis, MO, USA). Mouse neutralizing antibody anti-CX_3CL1 (AF472) was obtained from R&D System (Minneapolis, MN, USA). Etanercept was obtained from Wyeth (Enbrel®, São Paulo, SP, Brazil). IL-1 receptor antagonist was obtained from the National Institute for Biological Standards and Control (IL-1ra; NIBSC, South Mims, Hertfordshire, UK). Vehicle was obtained from LBS Laborasa (sodium chloride 0.9%; São Paulo, SP, Brazil). α-aminoadipate, minocycline, PDTC, etanercept, IL-1ra, antibody anti-CX_3CL1, and vehicle were injected only once by the intrathecal route (L_4-L_6 segment) in a final volume of 5 μL to obtain a local effect. We avoid repeated intrathecal injections because they cause increased nociceptive response *via* prostanoid production (33) and could, thus, interfere with the analysis of the present model. Doses of treatments used in the present model were chosen because they have analgesic effects as demonstrated previously (32). Intrathecal injections were performed in animals under a brief period of anesthesia induced by inhalation of isoflurane 5%.

T. cruzi Infection Protocol, Blood Parasite Count, and Survival Rate Analysis

Protozoan parasite *T. cruzi* (Kinetoplastea; Trypanosomatida; Trypanosomatidae; *Trypanosoma*) infection was induced using Y strain (*TcII*) and was maintained by weekly intraperitoneal inoculation in Swiss mice with $2x10^5$ blood trypomastigotes as described previously (34). Briefly, the blood of animals infected anteriorly was obtained by cardiac puncture under anesthesia without the use of anticoagulants. Samples were then centrifuged followed by standing in 37°C, and serum supernatant containing most parasites was centrifuged again for the resuspension of the pellet using appropriate culture and compounds (GIBCO, Grand Island, NY, USA). Trypomastigotes were derived from the supernatant of *T. cruzi*–infected LLC-Mk2 culture cells (ATCC CCL-7; American Type Culture Collection, Rockville, MD, USA) and grown in appropriate culture (GIBCO, Grand Island, NY, USA). Subconfluent cultures of LLC-Mk2 were infected with $5x10^6$ trypomastigotes. Free parasites were removed after 24 h, and cultures were maintained in medium. Five days after infection, free trypomastigote forms could be found in the cell supernatant, and the infection of animals was performed between the 7th and 8th days afterward by the intraperitoneal route. Blood parasitemia was assessed under standardized conditions by direct microscopic observation at 400x magnification of 50 fields. Counting the number of circulating parasites was performed in a volume of 5 μL of blood collected from the tail vein of infected animals. This result was expressed as the number of parasites per mL^{-1} in the blood samples. Blood parasitemia was evaluated every 7 days, starting on the 7th day of infection, and survival rates were monitored daily. Infection outcomes in mice were monitored daily to assess their health conditions during the experimental period.

General Experimental Procedures

Mice were infected with *T. cruzi* ($5x10^3$ infective trypomastigotes) by one intraperitoneal inoculation, and the following parameters at the respective time points evaluated in comparison to uninfected mice are described in sequence. Mechanical hyperalgesia and thermal hyperalgesia were assessed every 2 days for a period of 28 days. Survival of infected animals was recorded daily, and survival rate plotted every 2 days as a percentage. Blood parasite load was monitored every 7 days (7, 14, 21, and 28 days). Blood of the animals was also used to determine TNF-α and IL-1β protein levels on the same days described for the assessment of parasitemia. Temporal profile (7–28 days p.i.) of glial fibrillary acidic protein (*Gfap*) and ionized calcium-binding adapter molecule 1 (*Iba1*) mRNA expression or protein levels/staining (Western blot and immunofluorescence) were evaluated in spinal cord samples of uninfected and infected mice. The 7th day was selected because, at this time point, we could evaluate the participation of astrocytes (GFAP) and microglia (Iba-1) at the same time using all three approaches if necessary as per the results section. Next, infected animals were treated with vehicle, glial (α-aminoadipate and minocycline), and NFκB (PDTC) inhibitors by the intrathecal route for the evaluation of *Gfap* and *Iba1* mRNA expression, blood parasitemia, and mechanical and thermal hyperalgesia (1–7 h after the treatments) on day 7 p.i.; survival percentage was also assessed during this period to ensure that no animals died during the spinal treatment protocol, so certifying intrathecal treatments would not be harmful to the

animals. We opted to evaluate drug treatment effects during 1–7 h because we have previously standardized this approach to study the acute effect of treatments in ongoing hyperalgesia (32). Posteriorly, the effects of intrathecal treatments described above (most effective dose of each inhibitor) upon NFκB activation (7 h after the treatments) as well as double immunofluorescence analysis using antiglial and -p-NFκB antibodies 7 days p.i. were performed. The evaluation of the temporal profile of *Cx3cr1*, *Tnfα*, and *Il1β* mRNA expression in the spinal cord were conducted 7–28 days after the infection. In another round of experiments, mice were treated by the intrathecal route with vehicle, antibody anti-CX_3CL1, etanercept, and IL-1ra and mechanical and thermal hyperalgesia (1–7 h after the treatments), and parasitemia was investigated at day 7 after the infection; again, survival percentage was assessed during this period to ensure that no animals died during the spinal treatment protocol and that the intrathecal treatments would not be harmful to the animals. After this measurement, infected animals were treated with vehicle, glial (α-aminoadipate and minocycline), and NFκB (PDTC) inhibitors (most effective doses) by the intrathecal route to be evaluated; this time, the *Cx3cr1*, *Tnfα*, and *Il1β* mRNA expression in the spinal cord samples at the 7th day p.i. 7 h after the treatments. The activation of DRG neurons in response to infection alone and co-stimulus with capsaicin were examined using the calcium influx test through confocal microscopy as well as mRNA expression of *Trpv1* (transient receptor potential cation channel subfamily V member 1) at the 7th day p.i. The effects of intrathecal treatments with vehicle, glial (α-aminoadipate and minocycline), and NFκB (PDTC) inhibitors (most effective doses) were also evaluated over *Cx3cl1*, *Cx3cr1*, *Gfap*, *Tnfα*, *Il1β*, and *Cox2* mRNA expression in DRG cells at the day 7 after infection 7 h after the treatments.

Evaluation of Mechanical Hyperalgesia

Mechanical hyperalgesia was tested in mice as previously described (35). Briefly, in a quiet room, mice were placed in acrylic cages (12 X 10 X 17 cm) with wire grid floors, for at least 30 min before the test for adequate environmental adaptation. Stimulations were performed only when the animals were quiet without exploratory movements or defecation and not resting on their paws. The test consisted of evoking a hind paw flexion reflex with a hand-held force transducer (electronic von Frey esthesiometer; Insight, Ribeirão Preto, SP, Brazil), adapted with a 4.15-mm^2 (referred to as large probe) contact area polypropylene tip (35). The experimenter applies the probe perpendicularly to the central area of the hind paw with a gradual increase of pressure. The applied pressure to the hind paw surface induces movement of the ankle and knee joints, evoking stretching and/or shortening of leg muscles, promoting a muscle contraction response, which is enough to trigger muscle nociceptive activity (movement-induced hyperalgesia) when the latter is sensitized. The end point was characterized by the removal of the hindlimb followed by clear flinch movements. The measurements were standardized to be always measured on the right paw of the mice. The electronic pressure meter apparatus automatically recorded the intensity of the pressure applied when the paw was withdrawn. The value for the response was an average of three measurements. Only one experimenter started and ended the same test in order to avoid differences in the application of the pressure transducer force. The experimenter was always blinded to the experimental groups. The results are expressed by mechanical threshold in grams (g).

Evaluation of Thermal Hyperalgesia

The mensuration of thermal hyperalgesia in mice was conducted as described previously (32). Mice were positioned on the heated surface of a hot plate apparatus isolated by containment of a transparent acrylic material (EFF 361, Insight, Ribeirão Preto, SP, Brazil). The temperature on the surface was always maintained at 55 ± 1°C. The reaction time was registered using a conventional chronometer when the mouse presented the behaviors of licking or flinching one of the hind paws. A time limit of 15 s of maximum latency was defined as a cutoff with the intention of avoiding potential tissue injuries. The assessment of thermal hyperalgesia was performed before and after the infection process. The experimenter was always blinded to the experimental groups. The results were expressed by thermal threshold in seconds (s).

Assessment of Cytokine Levels

The blood of infected mice was collected in sterile microtubes containing the anticoagulant ethylenediamine tetraacetic acid (EDTA) by cardiac puncture following anesthetization with isoflurane 5%. Samples were then centrifuged for separation of plasma, and the resultant supernatant was separated for the tests. TNF-α and IL-1β levels were determined through an enzyme-linked immunosorbent assay (ELISA) test using paired antibodies following the manufacturer's instructions (eBioscience Inc.; Thermo Fisher Scientific, Waltham, MA, USA) (36). In summary, 96-well plates were first coated overnight in a refrigerator mixed with an immunoaffinity-purified polyclonal sheep antibody specifically for each cytokine. Plates were then blocked for 2 h. Subsequently, recombinant murine TNF-α and IL-1β standards were added to the plates using a serial dilution protocol for the standard curve. For sample testing, 100 μL of samples in duplicate were added and incubated for 1 h at room temperature followed by the addition of rabbit biotinylated immunoaffinity-purified antibodies anti-TNF-α and anti-IL-1β and incubation for 1 h at room temperature. In the next step, 50 μL of avidin-HRP reagent were added to each well in a dilution of 1:5000 for 30 min of incubation at room temperature. Plates were then washed, and the o-phenylenediamine dihydrochloride substrate was added to the plates at a volume of 200 μL per well to produce measurable signals. Finally, after 15 min, the reaction was interrupted with 1 M H_2SO_4 and measured spectrophotometrically at 450 nm. The detection limit of TNF-α (cat. no. 147325) and IL-1β (cat. no. 147012) kits is 8 picograms (pg)/milliliter (mL). The results were expressed as pg of target cytokine per mL of plasma (32).

Reverse Transcription and Quantitative Polymerase Chain Reaction (RT-qPCR) Assay

RT-qPCR was carried out following the protocol as described previously (32). Spinal cord (L_4-L_6 entire segments) and DRG (bilateral L_4-L_6) samples were collected using TRIzol™ reagent (#15596026, Invitrogen; Thermo Fisher Scientific, Waltham, MA, USA) 7–28 days after the infection, depending on the experiment. The purity of total RNA was measured with a spectrophotometer (MultiSkan GO Microplate Spectrophotometer, ThermoScientific, Vantaa, Finland), and the wavelength absorption ratio (260/280 nm) was between 1.8 and 2.0 for all preparations. Reverse transcription of total RNA to cDNA and qPCR were performed using the Go Taq® 2-Step RT-qPCR system (Promega Corporation, Madison, WI, USA) according to the manufacturer's guidelines. The relative gene expression was measured using the comparative $2^{-(\Delta\Delta Cq)}$ method. The expression of *β-actin* RNA was used as a reference gene to normalize data. The mouse primer pairs used were as follows:

β-actin fwd: 5'-AGCTGCGTTTTACACCCTTT-3'
β-actin rev: 5'-AAGCCATGCCAATGTTGTCT-3'
Gfap fwd: 5′-GCGCTCAATGCTGGCTTCA-3′
Gfap rev: 5′-TCTGCCTCCAGCCTCAGGTT-3′
Iba1 fwd: 5′-TGGAGTTTGATCTGAATGGAAAT-3′
Iba1 rev: 5′-CAGGGCAGCTCGGAGATAGCTTT-3′
Cx3cr1 fwd: 5′-CACCATTAGTCTGGGCGTCT-3′
Cx3cr1 rev: 5′-GATGCGGAAGTAGCAAAAGC-3′
Tnfα fwd: 5′-TCTCATCAGTTCTATGGCCC-3′
Tnfα fwd: 5′-GGGAGTAGACAAGGTACAAC-3′
Il1β fwd: 5′-GAAATGCCACCTTTTGACAGTG-3′
Il1β rev: 5′-TGGATGCTCTCATCAGGACAG-3′
Cx3cl1 fwd: 5′-ATTGGAAGACCTTGCTTTGG-3′
Cx3cl1 rev: 5′-GCCTCGGAAGTTGAGAGAGA-3′
Cox2 fwd: 5′-GTGGAAAAACCTCGTCCAGA-3′
Cox2 rev: 5′-GCTCGGCTTCCAGTATTGAG-3′
Trpv1 fwd: 5′- TTCCTGCAGAAGAGCAAGAAGC-3′
Trpv1 rev: 5′-CCCATTGTGCAGATTGAGCAT-3′

Western Blot Assay

Western blot analyses of the spinal cords were processed according to the previous study by our group (32). L_4–L_6 entire segments of spinal cord were accurately dissected at the 7th day after the infection, and the whole samples were homogenized in radioimmunoprecipitation assay (RIPA) buffer containing a protease and phosphatase inhibitor cocktail (100X, #5872S, Cell Signaling Technology, Danvers, MA, USA). The lysates were then homogenized and centrifuged. The protein extracts were separated by SDS-PAGE and transferred onto a nitrocellulose membrane (GE Healthcare-Amersham, Pittsburgh, PA, USA). Membranes were then incubated in blocking buffer 95% nonfat milk in Tris-buffered saline with Tween 20 or 1% bovine serum albumin (BSA) for different times for each antibody at 4°C in the presence of the primary antibody. β-actin and GFAP were purchased from Cell Signaling Technology (Danvers, MA, USA). Iba-1 and the secondary antibody were purchased from Thermo Fischer Scientific (Waltham, MA, USA). Catalog numbers of products are indicated below. The antibodies and dilutions used were β-actin (#4970, Cell Signaling Technology, 1:1000) and blocked with 5% BSA; GFAP (#12389, Cell Signaling Technology, 1:10,000) on 8% gel and blocked with 5% BSA; and Iba-1 (#16-20001, Wako Chemicals, 1:800) on 15% gel and blocked with 5% BSA. The molecular masses of protein were confirmed by Precision Plus Protein Standards (Bio-Rad, Hercules, CA, USA). After washing in tris buffered saline (TBS) with Tween 20, the membrane was incubated with secondary antibody (peroxidase-conjugated AffiniPure goat anti-rabbit IgG (H+L), #111-035-003, Jackson Immuno Research, 1:5000) on 5% BSA in TBS-T for 2 h at room temperature. Protein was visualized by chemiluminescence with an enhanced chemiluminescence ECL detection reagent (Luminata™ Forte, Millipore, USA). The membranes were stripped and re-probed with an antibody against β-actin for use as a loading control in addition to loading the same amount of protein in the case of Iba-1 protein. For GFAP protein analysis, a separate membrane using an equivalent mirror gel was prepared for the quantification of β-actin because the chemiluminescent signal for GFAP was still detected after the stripping phase as the stripping buffer failed to completely remove the GFAP antibody and ECL reagent from the membrane in the tested dilutions (dilution between 1:1000 and 1:10,000). Results are presented as the mean of six animals per group and compare noninfected and *T. cruzi*–infected groups at each time point (7–14 days) because experiments were performed separately. The images and analyses were performed in Image Lab 6.1 software (Bio-Rad Laboratories).

Spinal Cord Immunofluorescence

The spinal cord immunofluorescence assay was performed at the 7th day of infection. For this, mice were perfused through the ascending aorta with phosphate buffered saline (PBS) followed by 4% of paraformaldehyde (PFA), and L_4–L_6 segments of the spinal cord were accurately dissected out and postfixed in PFA 4% for 24 h. After this period, samples were replaced with 30% saccharose solution for 3 additional days. The spinal cord segments were then washed with PBS and embedded in optimum cutting temperature (O.C.T.) using Tissue-Tek® reagent (Sakura® Finetek USA, Torrance, CA), and 10-micrometers (μm) sections were cut in a cryostat (CM1520, Leica Biosystem, Richmond, IL, USA) and processed for immunofluorescence (four slides per mouse/four animals per group). All the sections were initially blocked with a buffer solution (500 μL per slide containing PBS plus 0.1% tween 20 plus 5% BSA) for 2 h at room temperature and subsequently incubated overnight at -4°C with a solution containing primary antibodies against the target protein. Next, a new incubation with secondary antibodies was performed for 1 h at room temperature. For double immunofluorescence, a mixture of primary antibodies for target proteins as well as secondary conjugated antibodies following the same sequence was

performed. GFAP (#180063; 1:500 dilution; Invitrogen, Life Technologies, Carlsbad, CA, USA), Iba-1 (#PA5-27436; 1:500 dilution, Invitrogen, Life Technologies, Carlsbad, CA, USA), and phosphorylated NFκB p65 subunit (sc-136,548, 1:200 dilution, Santa Cruz Biotechnology, Dallas, TX, USA) primary antibodies, and Alexa Fluor 488 (#A-110088, 1:1000 dilution, Thermo Fischer Scientific, Waltham, MA, USA) and Alexa Fluor 647 (#A28181, 1:1000 dilution, Thermo Fischer Scientific, Waltham, MA, USA) secondary antibodies were used in the study. The slide assembly was conducted using ProLong™ Gold Antifade Mountant with 4',6-diamidino-2-phenylindole, dihydrochloride (DAPI) melting media (#P36931, Thermo Fischer Scientific, Waltham, MA, USA). Analysis using slides with secondary antibodies alone was conducted in parallel with the controls to ensure that unspecified staining did not occur. Immunofluorescence analyses were performed in the dorsal horn of the spinal cord at a magnification of 20x. The images and analysis were performed using a confocal microscope (TSC SP8, Leica Microsystems, Mannheim, Germany) (32, 37). Results of the fluorescence quantification in the samples (control noninfected versus 7-day infected animals) are presented as the mean of four animals per group.

NFκB Activation Test

The evaluation of NFκB activation in spinal cord samples was performed following the protocol as described previously (32). For this objective, spinal cord samples (L_4–L_6 entire segments) were collected at the 7th day after the infection and the whole sample homogenized in ice-cold lysis buffer (Cell Signaling Technology, Beverly, MA, USA). The homogenates were centrifuged for 10 min (16,000 g and 4°C), and the resultant supernatants used to assess the levels of total and phosphorylated (p) NFκB p65 subunits by ELISA using two PathScan kits (Cell Signaling Technology, Beverly, MA, USA) specific for total and phosphorylated forms of NFκB p65 according to the manufacturer's instructions. The test indicates the proportion between total NF-kB and p-NF-kB in the analyzed samples. A low ratio indicates a great amount of p-NF-kB relative to total NF-kB, which indicates NF-kB activation. On the other hand, a high ratio indicates lessened activation because there is less p-NF-kB relative to total NF-kB. The results were expressed as a total-p65/phospho-p65 ratio measured spectrophotometrically (MultiSkan GO Microplate Spectrophotometer, ThermoScientific, Vantaa, Finland).

Calcium Imaging

The dissection and culture of DRG neurons for calcium imaging was performed as previously described (38). Bilateral DRGs (six mice per group) were dissected at the 7th day p.i. into neurobasal-A medium (Life Technologies, Thermo Fisher Scientific) and dissociated in collagenase A (1 mg·ml−1)/ dispase II (2.4 U·ml−1; RocheApplied Sciences, Indianapolis, IN, USA) in HEPES-buffered saline (Millipore Sigma) for 70 min at 37°C. After trituration with glass Pasteur pipettes of decreasing size, DRG cells were centrifuged over a 10% BSA gradient and plated on laminin-coated cell culture dishes. DRGs were then loaded with 1.2 μM of Fluo-4AM in neurobasal-A medium, incubated for 30 min at 37°C, washed with HBSS, and imaged in a Confocal Microscope (TCS SP8, Leica Microsystems, Mannheim, Germany). To assess TRPV1 activation, DRG plates were recorded for 6 min, which was divided into 2 min of initial reading (0-s mark, baseline values), followed by stimulation with TRPV1 agonist capsaicin for 2 min at the 120-s mark (1 μM) and KCl for 2 min at the 240-s mark (40 mM, activates all neurons). Calcium flux was analyzed from the mean fluorescence intensity measured with the LAS X Software (Leica Microsystems, Mannheim, Germany).

Statistical Analysis

Results are presented as means ± SEM of measurements made on four to six mice in each group, depending on the analysis, per experiment, and are representative of two independent experiments. ANOVA (two-way analysis of variance) was always used for comparison between groups and different doses when responses were measured at varied times after the parasite or treatments and/or stimulus injection. Analyzed factors were treatments, time, and time vs. treatment interaction, and when interaction was significant, one-way ANOVA preceded by Tukey's *post hoc* was performed for each time point. Differences between responses were evaluated by one-way ANOVA followed by Tukey's *post hoc* for data of a single time point. Differences between two groups were analyzed by *t*-test. Statistical differences were considered significant when $P < 0.05$.

RESULTS

Experimental *T. cruzi* Infection Induces Chronic Mechanical and Thermal Hyperalgesia Independent of Blood Parasitemia as Well as Induces a Transient Increase in Systemic TNF-α and IL-1β Levels

Mice were infected with *T. cruzi* and mechanical hyperalgesia, thermal hyperalgesia, blood parasitemia, survival, and TNF-α and IL-1β levels were evaluated from 2 to 28 days p.i. (**Figure 1**). Increased mechanical and thermal hyperalgesia in infected mice were detected from the 2nd to the 28th days p.i. (**Figures 1A, B**). The peak of blood parasitemia occurred at the 7th day p.i. with a gradual decrease in subsequent days, and at the 28th day, the parasites were no longer detected in the blood (**Figure 1C**). Interestingly, in infected mice, the hyperalgesia persists even with the decline of parasites in the blood (**Figures 1A, B**), suggesting that not only the parasites per se are responsible for the pain behavior, but possibly plastic changes are involved in the prolonged hyperalgesia. No animals died during the experiment due to *T. cruzi* infection, which is an expected outcome due to the use of a nonlethal parasite load for the C57BL/6 mouse strain (**Figure 1D**). TNF-α plasma levels were not significant at the 7th day p.i. (**Figure 1E**). TNF-α plasma levels were significant at the 14th day with a gradual reduction from the 14th day onward; however, they remained significant until the 28th day p.i. compared to uninfected animals

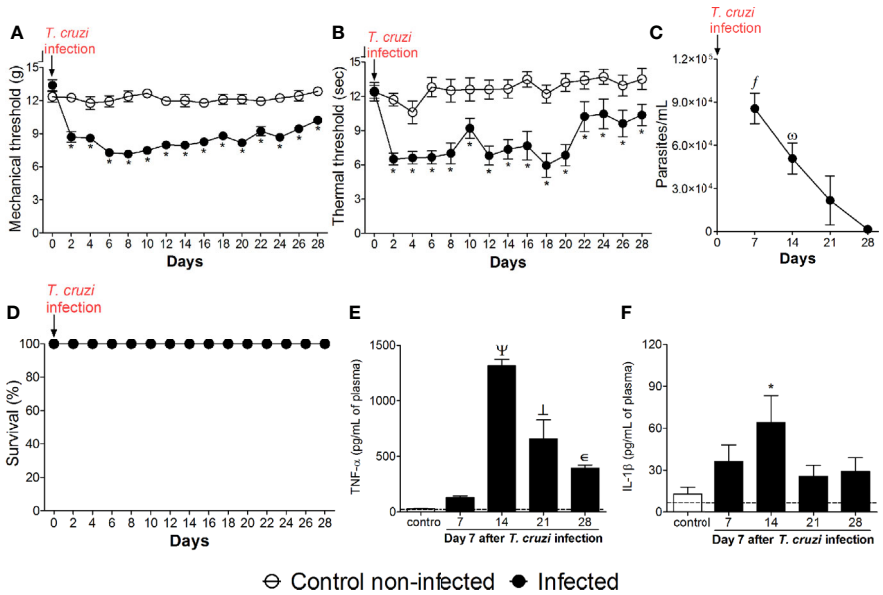

FIGURE 1 | Experimental *T. cruzi* infection induces chronic pain. Mechanical hyperalgesia **(A)**, thermal hyperalgesia **(B)**, blood parasitemia **(C)**, survival **(D)**, and plasma levels of TNF-α **(E)** and IL-1β **(F)** were determined. Hyperalgesia tests were evaluated for 28 days p.i. every 2 days. Blood parasitemia and cytokine plasma levels were evaluated 7–28 days p.i. every 7 days. Survival rate was monitored daily over the model. Results are presented as mean ± SEM of six mice per group per experiment and are representative of two separated experiments. *$p < 0.05$ compared to control noninfected mice; *f*$p < 0.05$ compared to days 21 and 28; ω$p < 0.05$ compared to day 28; Ψ $p < 0.05$ compared to all groups; ⊥ $p < 0.05$ compared to control noninfected mice and day 7 (two-way ANOVA followed by Tukey's posttest for panels **(A, B)**; and one-way ANOVA followed by Tukey's posttest for panels **(C, E, F)**. Dashed lines in panels **(E, F)** delimits the sensitivity of kits used for analysis.

(**Figure 1E**). IL-1β plasma levels were significant at the 14th day without significant levels in the other time points (**Figure 1F**). Altogether, these results indicate that *T. cruzi* infection at the tested dose induces chronic pain. However, factors other than solely blood parasite load and circulating levels of TNF-α and IL-1β might explain *T. cruzi* infection-induced pain overtime.

Experimental *T. cruzi* Infection Activates Astrocytes and Microglia in the Spinal Cord

We evaluated whether *T. cruzi* infection activates glial cells in the spinal cord of mice. First, we determined the temporal profile of *Gfap* and *Iba1* mRNA expression (7–28 days p.i.; **Figures 2A–F**), which are used as markers of astrocytes and microglial activation in the spinal cord, respectively. The activation profile of these two cells did not occur in a similar manner. *Gfap* mRNA presented a biphasic increase, and for *Iba1* mRNA time-dependent upregulation was observed until the 21st day p.i., when it reached its peak (**Figures 2A, F**). At the 7th day, infected mice presented increased *Gfap* and *Iba1* expression when compared to uninfected mice. However, thenceforward *Gfap* expression returned to the control level at days 14 and 21 p.i. and increased again at day 28 (**Figure 2A**). Instead, *Iba1* mRNA expression presented a sustained upregulation until the 21st day p.i., decreasing and ceasing to be significant compared to uninfected animals at day 28 p.i. (**Figure 2F**). A time course of GFAP and Iba-1 protein levels was also performed by Western blot analysis (**Supplementary Figure S1**), which showed that GFAP was significantly upregulated in the infected group at the 7th day (**Figures 2 B–G**). GFAP was also upregulated at days 21 and 28, thus, partially aligning with the mRNA data (**Supplementary Figure S1A**). A contrast between mRNA and protein data for GFAP was observed at the 21st day in which mRNA was not induced, but protein was increased (**Supplementary Figure S1A**). Iba-1 protein was increased in the infection group at all time points (**Supplementary Figure S1B**) contrasting with the mRNA data in which, at the 28th day, no upregulation was observed in the infected group (**Figure 2F**). An immunofluorescence assay in spinal cord samples for GFAP and Iba-1 was also conducted and showed a classical morphology of activated astrocytes and microglia in infected animals 7 days p.i., which was not observed in uninfected animals (**Figures 2C–E, H–J**, respectively). Time-response analysis (7–28) of GFAP and Iba-1 immunofluorescence detected significant activation of both glial cells in infected animals when compared to those uninfected at all evaluated times (**Supplementary Figures S2A, B**). Considering that concomitant activation of astrocytes and microglia was observed at the 7th day p.i. for all tests used (RT-qPCR, Western blot, and immunofluorescence), this time point was chosen for the next experiments to focus on the contribution of spinal cord glial cells to *T. cruzi* infection-induced pain in mice. These methods (RT-qPCR, Western blot, and immunofluorescence) quantitate different parameters (mRNA vs. protein), and the methods' sensibilities are different, which might explain the variations observed and that mRNA and protein data did not exactly align in the same way.

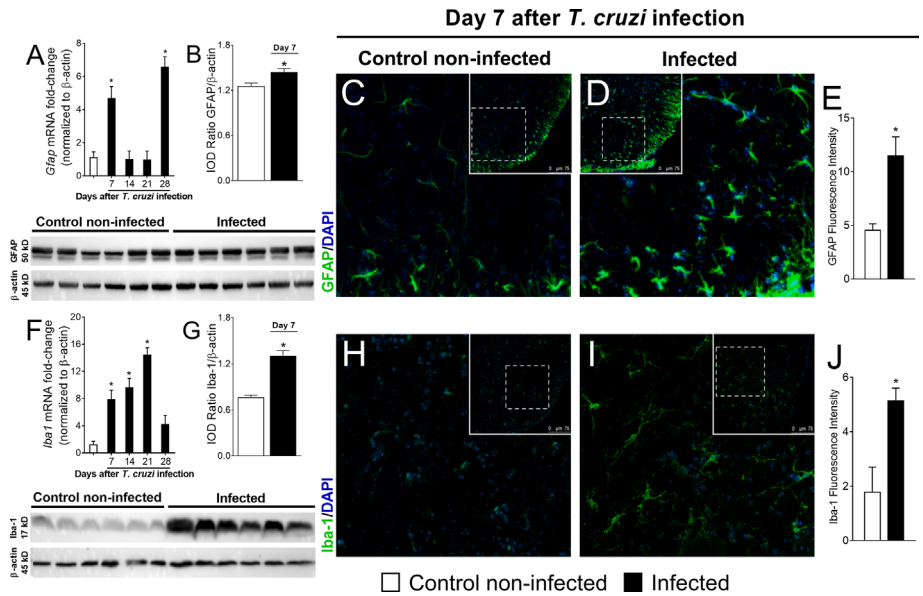

FIGURE 2 | Experimental *T. cruzi* infection induces spinal cord astrocytes **(A–E)** and microglial **(F–J)** activation. *Gfap* and *Iba1* mRNA expression was determined in control noninfected and infected mice 7–28 days p.i. every 7 days by RT-qPCR **(A, F**, respectively). At day 7 p.i. (peak of *Gfap* and *Iba1* mRNA expression), Western blot analysis of the spinal cord was performed to confirm GFAP **(B)** and Iba-1 **(G)** expression. Next, 7-day spinal cord samples were stained with antibodies for astrocytes **(C–E)** and microglia **(H–J)** (GFAP and Iba-1, respectively; green) and regular nucleus (DAPI, blue) detection. Representative immunostainings of the spinal cord of control noninfected and infected mice are shown in panels **(C, D, H, I)**, respectively (20x magnification, scale bar 75 μm with zoom). Panels **(E, J)** show the percentage of GFAP and Iba-1 fluorescence intensity in each experimental group, respectively. Results are presented as mean ± SEM of six **(A, B, F, G)** or four mice **(E, J)** per group per experiment and are representative of two separate experiments. *$p < 0.05$ compared to control noninfected mice (one-way ANOVA followed by Tukey's posttest).

Spinal Treatment With Glial Inhibitors Reduces *T. cruzi*–Induced Mechanical and Thermal Hyperalgesia

To investigate whether inhibiting spinal cord glial cells reduces *T. cruzi*–induced hyperalgesia, mice were treated by the intrathecal route with vehicle (saline); a selective astrocyte inhibitor, α-aminoadipate (30–100 nmol); or a selective microglial inhibitor, minocycline (50–150 μg), at day 7 after *T. cruzi* infection, and mechanical and thermal hyperalgesia were measured 1–7 h after the treatment (**Figure 3**). To validate α-aminoadipate and minocycline effects, mRNA expression of *Gfap* and *Iba1* were also evaluated at the 7th day p.i. The two doses of α-aminoadipate inhibited *Gfap* mRNA expression; on the other hand, only the highest dose of minocycline inhibited *Iba1* mRNA expression (**Figures 3A–D**). The doses of 30 and 100 nmol of α-aminoadipate inhibited mechanical hyperalgesia for up to 7 h after the treatment; however, the effect of the dose of 100 nmol was significantly higher than 30 nm between 3 and 7 h (**Figure 3B**). On thermal hyperalgesia, both doses of α-aminoadipate presented similar activity and inhibited thermal sensitivity at 5 and 7 h after treatment (**Figure 3C**). A similar profile was observed by the treatment with the microglia selective inhibitor, minocycline, regarding mechanical (**Figure 3E**) and thermal (**Figure 3F**) hyperalgesia. The fact that the lowest dose of minocycline did not inhibit the mRNA expression of Iba-1 in the spinal cord but inhibited hyperalgesia can be explained by the fact that Iba-1 or even GFAP are used as markers of glial cell activation and are not necessarily activity measures. Further, α-aminoadipate and minocycline are inhibitors of glial cell metabolism (39, 40), and it is reasonable that a higher dose will have faster activity than a lower dose as well as that makers of activation might change after actual downregulation of activity. Intrathecal treatments with the tested doses of glial inhibitors did not affect blood parasitemia (**Figure 3G**), and no animal died due to infection or treatment protocols (**Figure 3H**). These data corroborate the results presented in **Figure 2** and reinforce the concept of a role for spinal cord astrocytes and microglia in *T. cruzi*–induced hyperalgesia.

Targeting Spinal Cord NFκB Inhibits *T. cruzi*–Induced Glial Activation and Hyperalgesia as Well as Glial Inhibitors Reduce NFκB Activation in the Spinal Cord

The participation of the transcription factor NFκB in *T. cruzi*–induced spinal cord glial activation and hyperalgesia was evaluated. Mice were treated by the intrathecal route with vehicle (saline) or NFκB inhibitor PDTC (300 μg) at day 7 after *T. cruzi* infection, and mRNA expression of glial markers and mechanical and thermal hyperalgesia were measured. Additionally, the effects of glial inhibitors upon spinal cord NFκB activation and double staining using the phosphorylated (p) NFκB p65 subunit and glial markers in spinal cord samples were also performed (**Figure 4**). PDTC inhibited the increased expression of *Gfap* and *Iba1* in infected animals (**Figure 4A**) as

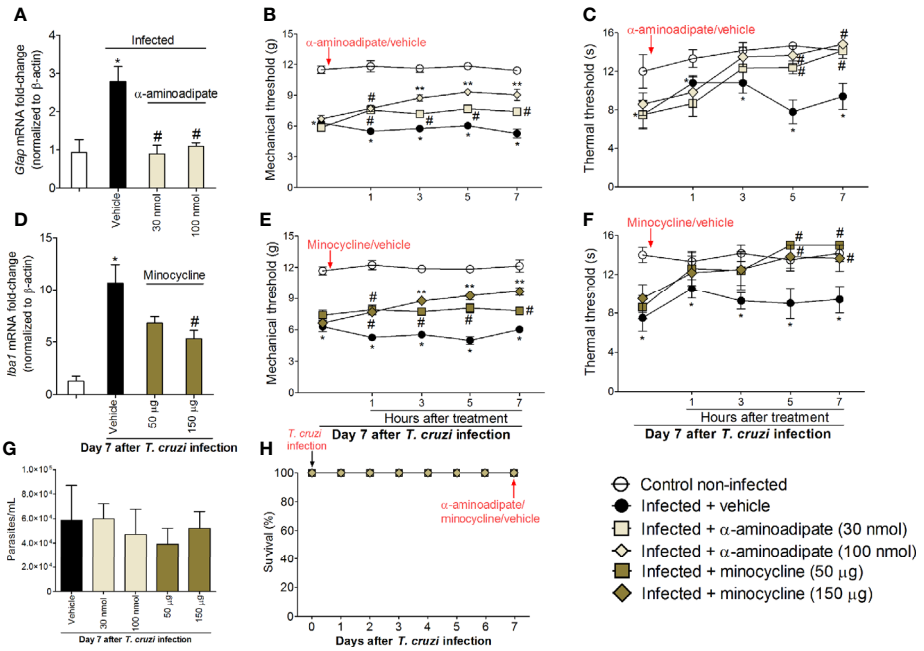

FIGURE 3 | Targeting spinal cord glial cells with α-aminoadipate and minocycline intrathecal treatments inhibits *T. cruzi*–induced hyperalgesia. Panels **(A–C)** show RT-qPCR data for *Gfap* mRNA expression and mechanical and thermal hyperalgesia after vehicle and α-aminoadipate treatments (30 and 100 nmol) at the 7th day p.i. Mensuration of hyperalgesia occurred 1–7 h after the treatments. Panels **(D–F)** show RT-qPCR data for *Iba1* mRNA expression and mechanical and thermal hyperalgesia after vehicle and minocycline treatments (50 and 150 μg) at the 7th day p.i. Panel **G** presents blood parasitemia at the 7th day p.i. 7 h after the treatments. Panel **H** presents survival rates during the experimental protocol. Results are presented as mean ± SEM of six mice per group per experiment and are representative of two separate experiments. $^{*}p < 0.05$ compared to control noninfected mice; $^{\#}p < 0.05$ compared to infected mice treated with vehicle; $^{**}p < 0.05$ compared to infected mice treated with the lowest doses of α-aminoadipate and minocycline (one-way ANOVA followed by Tukey's posttest for panels **A**, **D**; and two-way ANOVA followed by followed by Tukey's posttest for panels **B**, **C**, **E**, **F**).

well as the mechanical and thermal hyperalgesia at all time points evaluated (1–7 h) upon *T. cruzi* infection (**Figures 4B, C**). PDTC treatment did not affect blood parasitemia (**Figure 4D**). Furthermore, no animal died due to infection or treatment protocols (**Figure 4E**). Extending these experiments, we notice that the most effective doses of glial inhibitors (100 nmol of α-aminoadipate and 150 μg of minocycline) inhibited *T. cruzi*–induced NFκB activation in the spinal cord (demonstrated here by the ratio between total p65 subunits per phosphorylated p65 subunit), reaching similar levels of inhibition as positive control PDTC (**Figure 4F**). Finally, using a confocal immunofluorescence assay, we showed the concomitant expression of GFAP (**Figure 4G**, two top rows) or Iba-1 (**Figure 4G**, two lower rows) and phosphorylated pNFκB p65 (**Figure 4G**, last two columns on the right and respective inserts) in infected animals, which was not observed in uninfected mice (**Figure 4G**). As GFAP and Iba-1 are cell membrane molecules, they do not co-localize with NFκB, which has cytoplasmic or, in case of phosphorylation, nuclear localization. The 3-D images (inserts in **Figure 4G**) and videos (**Videos S1** and **S2**) allow visualization that part of pNFκB is surrounded by GFAP and Iba-1 staining. Further supporting that NFκB activation aligns with glial cell activation, increased fluorescence intensity of glial markers and pNFκB were detected in infected animals when compared to those uninfected (**Figures 4H, I**). Therefore, these results evidence that *T. cruzi* infection induces NFκB activation in spinal cord astrocytes and microglia, contributing to hyperalgesia as a result of the disease.

Temporal Profile of Spinal Cord *Cx3cr1*, *Tnfα*, and *Il1β* Expression in Response to Experimental *T. cruzi* Infection

NFκB is a central transcription factor in regulating cytokine production as they are important signaling molecules in neuro-immune regulation and pain (17). The chemokine receptor and cytokine mRNA expression profile were investigated between 7 and 28 days after *T. cruzi* infection (**Figure 5**). *T. cruzi* infection induced a progressive increase in mRNA expression of the chemokine receptor *Cx3cr1* (**Figure 5A**) and pro-inflammatory/hyperalgesic cytokines *Tnfα* (**Figure 5B**) and *Il1β* (**Figure 5C**) until the 21st day p.i. with a statistical difference compared to those uninfected. After this period, their expression declined and returned close to the baseline values (day 28) (**Figures 5A–C**). These data, together with the glial and NFκB activation (Figs. 2–4), depict spinal cord neuroinflammation in response to *T. cruzi* infection. Microglia is the main cell expressing CX_3CR1 in the spinal cord, and both astrocytes and microglia are well known sources of cytokines in the spinal cord (17).

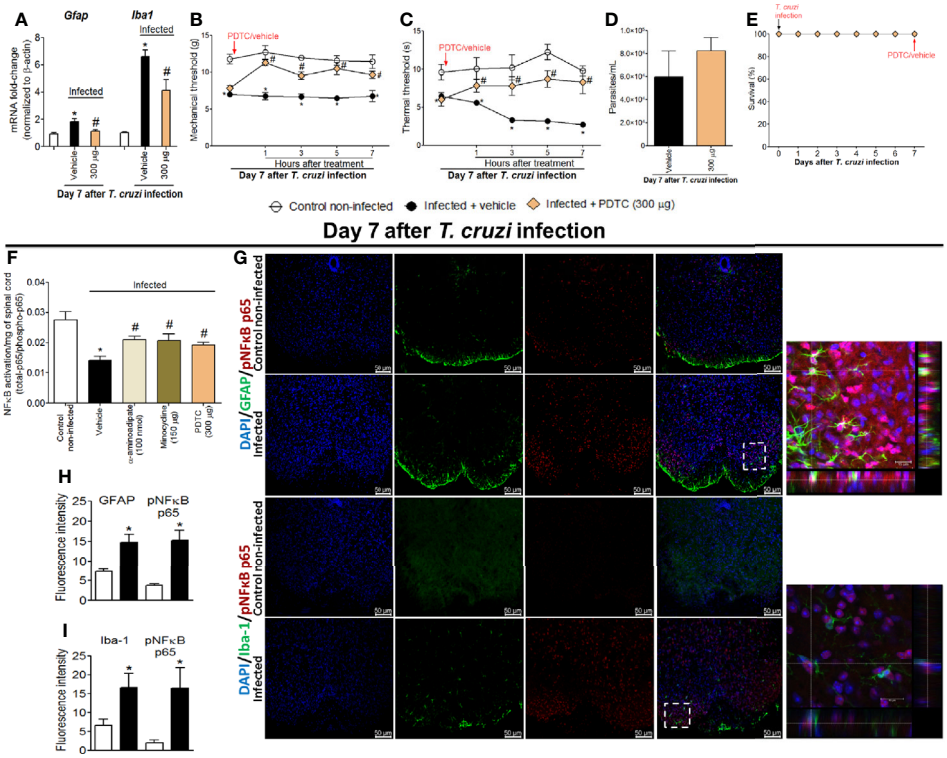

FIGURE 4 | Targeting spinal cord NFκB with PDTC intrathecal treatment inhibits *T. cruzi*–induced glial activation and hyperalgesia as well as targeting glial cells with α-aminoadipate and minocycline reduced spinal cord NFκB activation. Panels **(A–C)** show RT-qPCR data for *Gfap* and *Iba1* mRNA expression and mechanical and thermal hyperalgesia after vehicle and PDTC treatments (300 µg) at the 7th day p.i. Panel **(D)** presents blood parasitemia at the 7th day p.i. 7 h after the treatments. Panel **(E)** presents survival rates during the experimental protocol. The effects of targeting spinal cord glial cells with α-aminoadipate and minocycline upon NFκB activation at the 7th day p.i. 7 h after the treatments are presented in panel **(F)**. Representative immunostainings of triple immunofluorescence (DAPI/pNFκB p65/GFAP and DAPI/pNFκB p65/Iba-1) of the spinal cord of control noninfected and infected mice are shown in **(G)** (20x magnification, scale bar 50 µm). 3-D images with zoom demonstrating pNFκB p65 staining surrounded by GFAP or Iba-1 are shown in inserts. Panels H and I demonstrate the fluorescence intensity (%) of GFAP and pNFκB p65, and Iba-1, and pNFκB p65, respectively. Results are presented as mean ± SEM of six **(A–F)** or four mice **(G–I)** per group per experiment and are representative of two separate experiments. $^{*}p < 0.05$ compared to control noninfected mice; $^{\#}p < 0.05$ compared to infected mice treated with vehicle (one-way ANOVA followed by Tukey's posttest for panels **(A**, **F)**; and two-way ANOVA followed by followed by Tukey's posttest for panels **B**, **C**).

Targeting Spinal Cord CX_3CL1, TNF-α, and IL-1β Reduces *T. cruzi*–Induced Mechanical and Thermal Hyperalgesia

In addition to the mRNA expression data, we wanted to ascertain the physiopathological contribution of spinal cord CX_3CL1/CX_3CR1 signaling, TNF-α, and IL-1β in *T. cruzi*–induced hyperalgesia. For this purpose, mice were treated by the intrathecal route with vehicle (saline), anti-CX_3CL1 antibody (0.25–2.5 mg), soluble decoy receptor (sTNFR2) etanercept (3-10 ng) and Interleukin-1 receptor antagonist (IL-1ra, 30-100 pg) at day 7 after *T. cruzi* infection. Mechanical and thermal hyperalgesia were measured 1–7 h after the treatment (**Figure 6**). The dose of 0.25 mg of anti-CX_3CL1 antibody did not affect mechanical or thermal hyperalgesia; however, treatment with the dose of 2.5 mg inhibited mechanical hyperalgesia between 3 and 7 h and thermal hyperalgesia between 5 and 7 h after the treatment (**Figures 6A, B**). The dose of 3 ng of etanercept inhibited only thermal hyperalgesia at 5 h without presenting effects on mechanical hyperalgesia. On the other hand, treatment with the dose of 10 ng of etanercept inhibited both mechanical and thermal hyperalgesia from 3 to 7 h after the treatment (**Figures 6C, D**). Treatment with the dose of 30 pg of IL-1ra inhibited only mechanical hyperalgesia at 1 h without showing effects upon thermal hyperalgesia, and the anti-hyperalgesic effect of the dose of 100 pg of IL-1ra was detected between 1 and 7 for mechanical hyperalgesia and between 5 and 7 for thermal hyperalgesia (**Figures 6E, F**). All doses of the compounds tested in these experiments did not affect blood parasitemia (**Figure 6G**), and no animal died as a result of infection or treatment protocols (**Figure 6H**). These data (**Figure 6**) line up well with the mRNA expression results presented in **Figure 5** and demonstrate a role for CX_3CL1/CX_3CR1 signaling, TNF-α, and IL-1β in hyperalgesia induced by *T. cruzi* infection.

Targeting Spinal Cord Astrocytes, Microglia, and NFκB Inhibits *Cx3cr1*, *Tnfα*, and *Il1β* Expression in the Spinal Cord

The results of Figs. 1–6 show that *T. cruzi* infection induces pain that is amenable by inhibition of spinal cord glial cells,

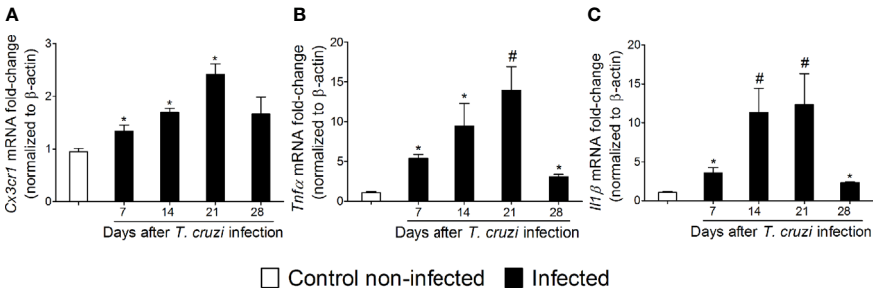

FIGURE 5 | Experimental *T. cruzi* infection induces spinal cord *Cx3cr1* **(A),** *Tnfα* **(B)**, and *Il1β* **(C)** mRNA expression. Time-course expressions of mRNA were evaluated 7–28 days p.i. every 7 days. Results are presented as mean ± SEM of six mice per group per experiment and are representative of two separate experiments. *$p < 0.05$ compared to control noninfected mice; #$p < 0.05$ compared to infected mice treated with vehicle (one-way ANOVA followed by Tukey's posttest).

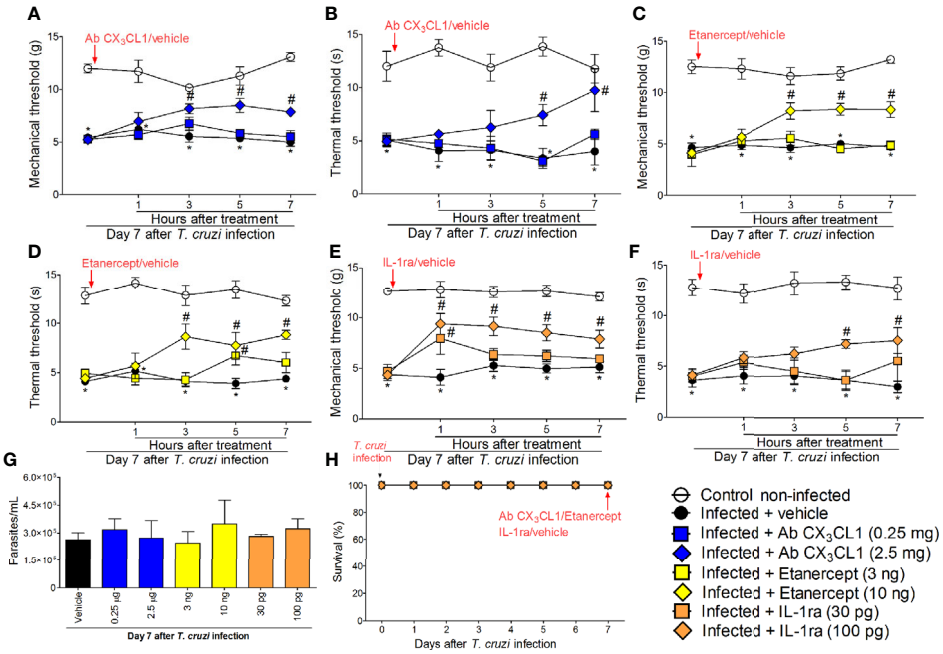

FIGURE 6 | Targeting spinal cord CX_3CL1, TNF-α, and IL-1β with neutralizing antibody anti-CX_3CL1, etanercept, and IL-1ra intrathecal treatments, respectively, inhibits *T. cruzi*–induced hyperalgesia. Mechanical hyperalgesia **(A, C, E)** and thermal hyperalgesia **(B, D, F)** were evaluated at the 7th day p.i., after vehicle, neutralizing antibody anti-CX_3CL1 (0.25 and 2.5 mg), etanercept (3 and 10 ng), and IL-1ra (30 and 300 pg) intrathecal treatments, 1–7 h after the treatments. Panel **(G)** presents blood parasitemia at the 7th day p.i. 7 h after the treatments. Panel **(H)** presents survival rates during the experimental protocol. Results are presented as mean ± SEM of six mice per group per experiment and are representative of two separate experiments. *$p < 0.05$ compared to control non-infected mice; #$p < 0.05$ compared to infected mice treated with vehicle (two-way ANOVA followed by followed by Tukey's posttest).

NFκB, chemokines, and cytokines and that the activation of glial cells is NFκB dependent. In this section, we addressed whether chemokine and cytokine expression would be dependent on NFκB and glial cells (**Figure 7**). Mice were treated by the intrathecal route with vehicle (saline) or the most effective dose of each inhibitor tested earlier, which include 100 nmol of α-aminoadipate, 150 µg minocycline, and 300 µg of PDTC. Treatments with all inhibitors significantly reduced *T. cruzi*–induced mRNA expression of *Cx3cr1* (**Figure 7A**), *Tnfα* (**Figure 7B**), and *Il1β* (**Figure 7C**) in the spinal cord. These data corroborate the results presented in Figs. 3–6 and indicate that spinal cord astrocytes, microglia, and NFκB activation are responsible for the production of major molecules related to the sensitization and activation process of nociceptor sensory neurons in *T. cruzi* infection.

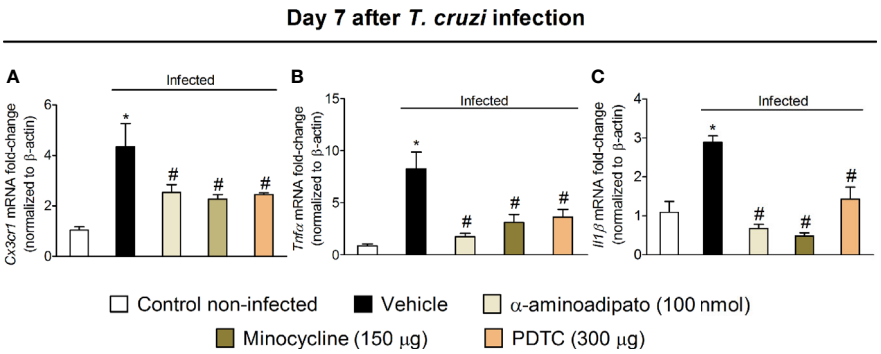

FIGURE 7 | Targeting spinal cord glial cells and NFκB with α-aminoadipate, minocycline, and PDTC intrathecal treatment inhibits *T. cruzi*–induced spinal cord *Cx3cr1* **(A),** *Tnfα* **(B)**, and *Il1β* **(C)** increased mRNA expression. Evaluations were performed at the 7th day p.i. after vehicle, α-aminoadipate (100 nmol), minocycline (150 μg), and PDTC (300 μg) intrathecal treatments, 7 h after the treatments. Results are presented as mean ± SEM of six mice per group per experiment and are representative of two separate experiments. $^{*}p < 0.05$ compared to control noninfected mice; $^{\#}p < 0.05$ compared to infected mice treated with vehicle (one-way ANOVA followed by Tukey's posttest).

Experimental *T. cruzi* Infection Increases Activation of DRG Neurons

The response of DRG neurons to experimental *T. cruzi* infection was evaluated through calcium imaging and *Trpv1* mRNA expression (an ion channel involved in nociceptor neuron activation). DRG neurons from infected mice presented a higher baseline level of calcium influx as well as a higher response to capsaicin than DRG neurons of uninfected mice (**Figures 8A–H**). In addition to a higher calcium baseline, DRG neurons of infected mice presented a higher intensity of response and higher percentage of responsive neurons upon capsaicin stimulation than DRG neurons of uninfected mice (**Figures 8H, I**). An explanation for a higher baseline and response to capsaicin is that DRG neurons of infected mice presented increased *Trpv1* mRNA expression compared to DRG neurons of uninfected mice (**Figure 8J**). Therefore, the behavioral responses triggered by *T. cruzi* infection parallel with activation of TRPV1-sensitive DRG neurons further confirming the nociceptive nature of behavioral responses.

Intrathecal Treatments With Inhibitors of Astrocytes, Microglia, and NFκB Downregulates the mRNA Expression of Inflammatory Molecules in the DRG Microenvironment

Intrathecal treatments reach the DRG, indicating that these treatments could affect DRG cells (41) and spinal cord neuroinflammation causes retrograde nociceptor neuron sensitization (42), indicating that spinal cord treatments can affect DRG cells through neuronal signaling. Therefore, we evaluated whether intrathecal treatments with α-aminoadipate, minocycline, and PDTC would affect DRG neuroinflammation. Mice were treated by the intrathecal route with vehicle (saline) or the same doses of glial and NFκB inhibitors used in **Figure 7** experiments (100 nmol of α-aminoadipate, 150 μg minocycline, and 300 μg of PDTC). The mRNA expression for *Cx3cl1*, *Cx3cr1*, *Gfap* (marker for satellite glial cells activity), *Tnfα*, *Il1β*, and *Cox2* mRNA expression were quantitated (**Figure 9**). Intrathecal treatments targeting spinal cord astrocytes, microglia, and NFκB reduced *T. cruzi*–induced *Cx3cl1* (**Figure 9A**), *Cx3cr1* (**Figure 9B**), *Gfap* (**Figure 9C**), and *Tnfα* (**Figure 9D**) mRNA expression in DRG samples. Regarding *Il1β*, only treatments with minocycline and PDTC inhibited its mRNA expression (**Figure 9E**). There was a trend toward inhibition ($P = 0.1236$) by α-aminoadipate. This result indicates that α-aminoadipate that selectively targets astrocytes could not significantly affect *Il1β* mRNA expression. We did not observe significant changes of *Cox2* mRNA expression in the DRG (**Figure 9F**). These data indicate that intrathecal treatments targeting astrocytes, microglia, and NFκB result in reduced DRG neuroinflammation after *T. cruzi* infection.

DISCUSSION

The infection of resistant mouse strain C57BL/6 with a nonlethal load of *T. cruzi* resembles human acute CD (43). We show that it induces another important symptom of human CD in mice: pain (7–10). *T. cruzi* induced chronic mechanical and thermal hyperalgesia for up to 28 days p.i. The hyperalgesia could not be explained by simply correlating with blood parasite load, suggesting that plastic changes might be responsible for maintaining pain at later time points when blood parasitemia declined and/or fluctuated drastically as in the chronic phase of the infection, similarly to human CD. The investigation of changes that would explain the disease pain phenotype led to unveiling novel physiopathological mechanisms of *T. cruzi* infection-induced pain.

TNF-α and IL-1β are well-known hyperalgesic molecules that induce sensitization of nociceptors (13, 14, 17, 44, 45). High peripheral levels of these cytokines can account for the observed

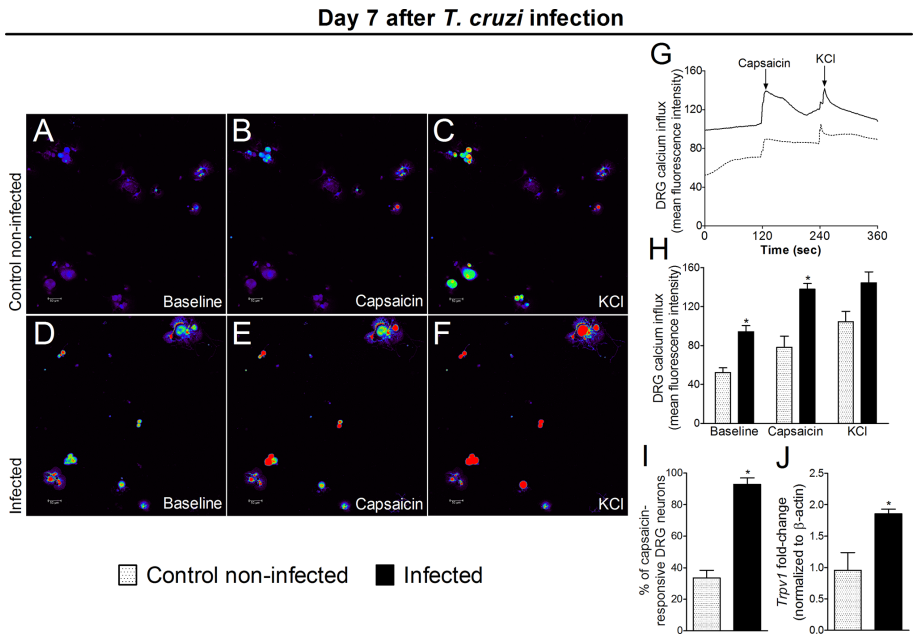

FIGURE 8 | Experimental *T. cruzi* infection induces the activation of DRG neurons. Seven days after the infection, DRGs were dissected for calcium imaging using Fluo-4AM **(A–I)** and mRNA expression by RT-qPCR **(J)**. Panels **(A–F)** display representative fields of DRG neurons from control noninfected **(A, C)** and infected **(D–F)** mice. Panels **(A, D)**: baseline fluorescence (first column); panels **(B, E)** fluorescence after capsaicin (second column); and panels **(C, F)** after KCl control (third column). Panel **G** displays the mean fluorescence intensity traces of calcium influx from the representative DRG fields **(A–F)** throughout the 6 min of recording. The representative traces show that DRG neurons of infected mice presented higher calcium levels in the baseline than those DRG neurons of control noninfected mice. Panel **(H)** shows the mean fluorescence intensity of calcium influx of the baseline (0-s mark) and that following the stimulus, either capsaicin (120-s mark, TRPV1 agonist) or KCl (240-s mark, activates all neurons). Panels **(I, J)** shows the capsaicin-responsive DRG cells and RT-qPCR data, demonstrating that infected mice present an increased percentage of responsive cells and *Trpv1* mRNA expression, respectively. Results are expressed as mean ± SEM; $n = 4$ DRG plates (each plate is a neuronal culture pooled from six mice) per group per experiment, and RT-qPCR used $n = 6$ DRG per group per experiment and are representative of two separate experiments. *$p < 0.05$ compared to control noninfected mice (one-way ANOVA followed by Tukey's posttest).

mechanical and thermal hyperalgesia. Recently, it was reported that bacterial infections may activate silent nociceptors *via* cytokine production (including TNF-α and IL-1β), resulting in bladder hyperalgesia (46). Thus, it is also likely that this is a contributing mechanism to *T. cruzi* infection-induced pain because there are high levels of TNFα and IL-1β in this disease (47). However, peripheral TNFα and IL-1β do not explain, alone, the peripheral component of *T. cruzi* infection-induced pain because hyperalgesia started by the 2nd day, and the production of these cytokines peaked at the 14th day of infection without significant levels at the 7th day p.i. These results raise the possibility that other peripheral cytokines/molecules might also be involved in *T. cruzi* pain. For instance, IFN-γ is a hyperalgesic cytokine (17, 48, 49). IFN-γ levels increase in the serum of mice at the 2nd day of *T. cruzi* infection (12), and spleen cells rapidly produce IFN-γ in response to *T. cruzi* (50). IL-12 is a well-known inducer of IFN-γ and also a hyperalgesic cytokine (51). IL-12 levels increase in response to *T. cruzi* in mice (52). Future studies might exhaustively investigate the mechanistic contribution of other peripheral cytokines to *T. cruzi* infection-induced pain.

We demonstrate here that experimental *T. cruzi* infection induces an early acute activation (7th day p.i.) of spinal cord astrocytes and microglia in an NFκB-dependent manner. A previous study also showed the activation of mouse brain astrocytes after *T. cruzi* (Colombian strain) infection in the acute phase of the disease (26), indicating this phenomena is not restricted to spinal cord astrocytes. Temporal differences in microglia and astrocyte activation have been reported in neuropathic and inflammatory pain (53, 54). We observed some discrepancies in the temporal profile between mRNA and protein data regarding glial cell activation. Overall, astrocyte and microglia activation could be detected at all time points by at least two techniques (RT-qPCR, Western blot, or immunofluorescence) except by GFAP at the 14th day, which was not increased in the infection group compared to the uninfected group as per RT-qPCR and Western blot results. These variations between the techniques may reflect the different sensitivity of each test for each target molecule. Additional studies that go beyond the current aims of the present work are necessary to elucidate this unique profile, its consequences, and relation to disease phenotype. In *Leishmania amazonensis* (*L. amazonensis*) infection, we observed a different profile of spinal cord glial cell activation. Both astrocytes and microglia were activated by the 30th day p.i (32). This difference is certainly explained by the characteristic pathology of each disease. *L. amazonensis* infection in BALB/c strain mice induces a chronic infection with pain up to 40 days. After this time

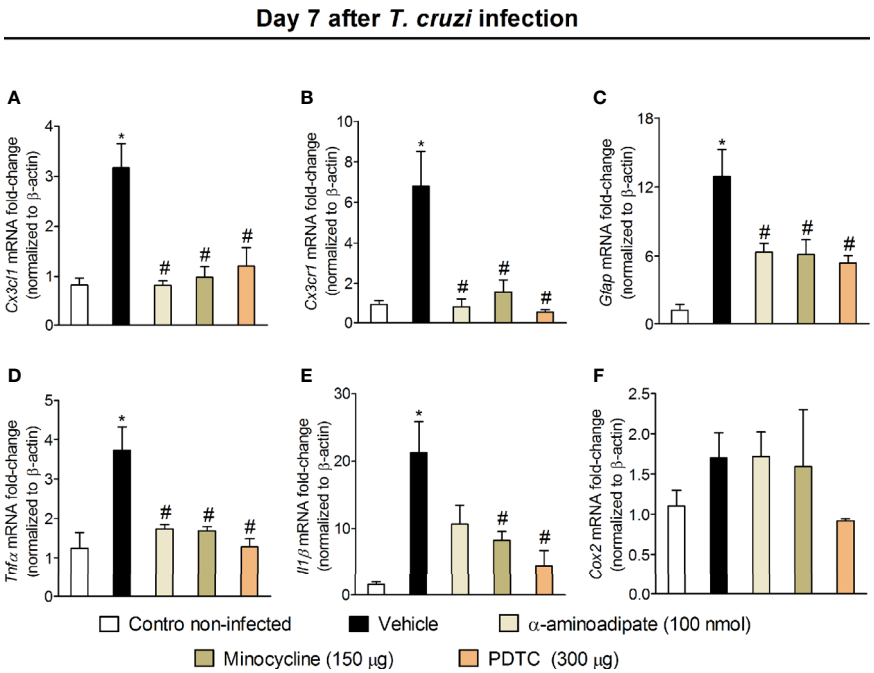

FIGURE 9 | Effect of intrathecal treatment with α-aminoadipate, minocycline, and PDTC against *T. cruzi*-induced DRG *Cx3cl1* **(A)**, *Cx3cr1* **(B)**, *Gfap* **(C)**, *Tnfα* **(D)**, *Il1β* **(E)**, and *Cox2* **(F)** mRNA expression. Evaluations were performed at the 7th day p.i. after vehicle, α-aminoadipate (100 nmol), minocycline (150 μg), and PDTC (300 μg) intrathecal treatments, 7 h after the treatments. Results are presented as mean ± SEM of six mice per group per experiment and are representative of two separate experiments. * $p < 0.05$ compared to control noninfected mice; # $p < 0.05$ compared to infected mice treated with vehicle (one-way ANOVA followed by Tukey's posttest).

point, there is development of ulcerating skin lesions that become painless (55). *L. amazonensis* infection presents this contrast of an initial prolonged painful phase followed by painless ulcer formation with reports of pain in other sites of the body in the case of humans (32, 56). We opted to study the spinal cord events in a CD mouse model at the 7th day p.i., considering astrocytes and microglia could be studied at the same time, reducing the number of animals.

Astrocytes, microglia, and the transcription factor NFκB are essential for hyperalgesic cytokine production in the spinal cord, contributing to central sensitization (17, 37). Indeed, *T. cruzi* infection increased spinal cord mRNA expression of *Cx3cr1*, *Tnfα*, and *Il1β*, and inhibiting spinal gliosis and NFκB activation as well as targeting NFκB-related spinal cord hyperalgesic mediators (CX_3CL1, TNF-α, and IL-1β) reduced *T. cruzi*–induced hyperalgesia. Moreover, treatment with glial and NFκB inhibitors also counteracted the increased expression of *Cx3cr1*, *Tnfα*, and *Il1β* mRNA expression in the spinal cord. Thus, expression and functional data support the contribution of spinal cord glial cells to pain in *T. cruzi* infection *via* cytokine production. CX_3CL1 release by nociceptor neurons in the spinal cord microenvironment acts on its receptor in microglia, leading to the production of TNF-α and IL-1β by these cells. These sequential events contribute to central sensitization (17). In addition to inducing microglia activation, CX_3CL1 can directly mediate neuronal hyper-responsiveness (57). TNFα makes a priming of astrocytes, enhancing their susceptibility to *T. cruzi* infection creating a cycle of infection and neuroinflammation because astrocytes are producers of TNFα in the spinal cord (25). Treatment with etanercept, a soluble p75/TNFR2 receptor reduces experimental CD pain (16), further corroborating the concept that cytokines, such as TNFα, have a role in immune cell activation during CD, but also as a hyperalgesic function. IL-1β can both activate and facilitate neuronal depolarization depending on disease context and chronicity (58, 59); however, this is the first evidence that it has a hyperalgesic role in CD.

DRG neurons of *T. cruzi*–infected mice showed increased baseline levels of intracellular calcium as well as responded more effectively to the stimulation with the TRPV1 agonist capsaicin than DRG neurons of uninfected mice. The percentage of capsaicin-responsive fibers and mRNA expression of *Trpv1* in DRG neurons of infected mice were also higher than those of uninfected mice. The enhanced *Trpv1* mRNA expression explains, at least in part, the DRG neuron activity representing the activation of the primary afferent neurons (17). The peripheral inflammation with immune response and parasite burden is certainly a contributing mechanism to the activation of these neurons. Spinal cord neuroinflammation also induces a retrograde neuronal sensitization (42). In this sense, we questioned whether the intrathecal treatments that inhibited spinal cord neuroinflammation would also diminish DRG activation because intrathecal delivery of drugs may also reach

spinal nerve roots and DRG exerting its effects directly in this site (41). The intrathecal treatments with α-aminoadipate, minocycline, and PDTC inhibited the *T. cruzi* infection-induced mRNA expression of *Cx3cl1*, *Cx3cr1*, *Gfap* (marker of satellite glial cells activation in the DRG), *Tnfα*, and *Il1β* (except by α-aminoadipate). In models, such as paclitaxel-induced neuropathy, infiltrating macrophages produce IL-1β in the DRG site (60), and the glycoprotein 120 of HIV-1 induces enhanced production of IL-1β in satellite glial cells (61). Moreover, minocycline reduced the activation of microglial and satellite glial cells in a model of visceral pain induced by colitis (62). Thus, infiltrating macrophages and satellite glial cells may produce IL-1β in the DRG, depending on disease context and minocycline effect, which seems to be more pronounced in satellite glial cells than α-aminoadipate possibly explaining the significant inhibition of *Il1β* expression by minocycline and not α-aminoadipate. The participation of DRG-neuron derived CX_3CL1 in the maintenance of nociceptor neuron sensitization during inflammatory pain was previously shown and occurs as a result of a paracrine circuit that involves its interaction with its receptor CX_3CR1 in satellite glial cells, which, in turn, produces additional TNF-α, IL-1β, and prostanoids that act directly on neurons perpetuating the hyperalgesic state (63). For instance, indomethacin is a COX-1/2 inhibitor (64, 65) that diminished CX_3CL1-induced pain and PGE_2 production by satellite glial cells (63). In the present model, *T. cruzi* infection did not increase the mRNA expression of *Cox2* as well as the intrathecal treatment with glial and NFκB inhibitors had no effect on its expression. Thus, suggesting that prostanoids are not major players in the neuronal sensitization in the DRG upon *T. cruzi* infection at the 7th day p.i. It is possible that the different stimulus applied in the models dictates which mediators will be released in greater or lesser quantity and their contribution to the physiopathology of disease.

In summary, the present data reveals the role of spinal cord astrocytes, microglia, NFκB, and cytokines/chemokines in experimental *T. cruzi* infection-induced pain. Glial reactivity is already detected in the acute phase (7 days) of infection. An early combined contribution of spinal cord astrocytes and microglia that persists until the end of the experimental protocol (28 days p.i.) was observed. To our knowledge, this is the first report unveiling such cellular and molecular pain mechanisms in *T. cruzi* infection. This study opens a novel venue for future studies investigating pain mechanisms and analgesic therapies to improve the quality of life of CD patients. **Figure 10** shows a schematic figure proposing the pathophysiological mechanisms involving *T.cruzi* infection-induced hyperalgesia.

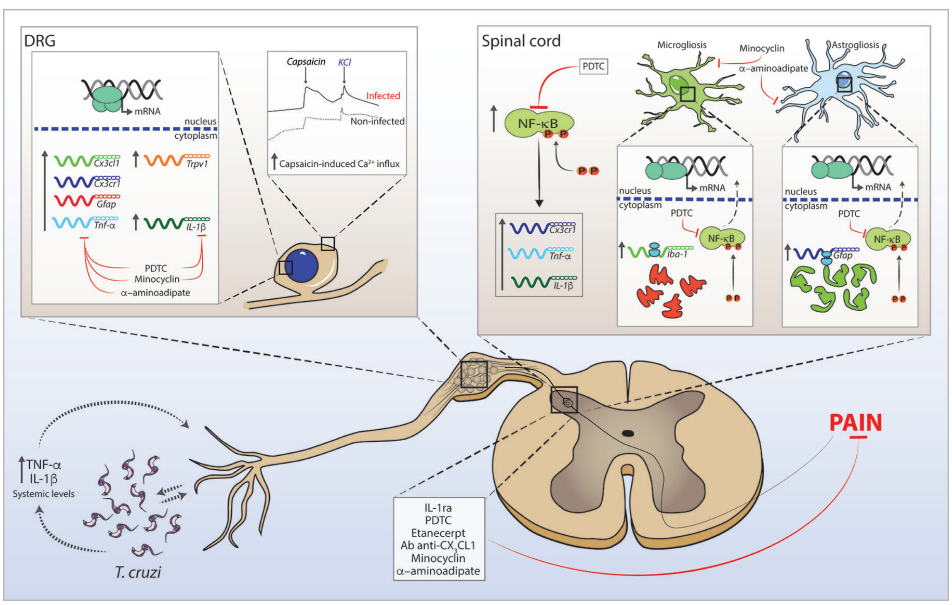

FIGURE 10 | Schematic proposition for *T. cruzi* infection-induced hyperalgesia-related mechanisms in mice. *T. cruzi* infection induces upregulation of systemic levels of TNF-α and IL-1β (and yet undetermined hyperalgesic mediators). The interface between *T. cruzi* parasites and pro-inflammatory cytokines may sensitize nociceptor neurons in peripheral tissue initiating nociceptive neurotransmission. Infection activates DRG cells and promotes increase in mRNA expression of *Cx3cl1*, *Cx3cr1*, *Gfap*, *Tnf-α*, *Il-1β*, and *Trpv1* at this site. In the spinal cord, *T. cruzi* infection leads to the activation of NFκB and increases mRNA expression of *Cx3cr1*, *Tnf-α*, and *Il-1β*. NFκB activation accounts for the gliosis in the spinal cord. These neuroinflammatory events contribute to central sensitization, resulting in increased pain in infected animals. In DRG, treatments with α-aminoadipate, minocycline, and PDTC inhibit the increased mRNA expression of hyperalgesic molecules with the exception of α-aminoadipate that did not inhibit the increase of *Il-1β* mRNA expression. In the spinal cord, α-aminoadipate, minocycline, and PDTC inhibit glial- and NFκB-dependent activities as well as increased mRNA expression of hyperalgesic molecules *Cx3cr1*, *Tnf-α*, and *Il-1β*. Confirming the data of DRG and spinal cord hyperalgesic molecule expression, spinal treatments with Ab anti-CX_3CL1, etanercept, IL-1ra, α-aminoadipate, minocycline, and PDTC inhibit *T. cruzi*-induced hyperalgesia in infected animals.

DATA AVAILABILITY STATEMENT

The datasets generated for this study are available on request to the corresponding author.

ETHICS STATEMENT

The animals were used respecting the protocols evaluated and approved by the CEUA (the Animal Welfare Ethical Review Board) of the State University of Londrina (process number 1067.2015.64). Animal care and handling tasks were performed following the Brazilian Council on Animal Experimentation (CONCEA), the Directive 2010/63/EU for animal experiments, and in agreement with the International Association for Study of Pain (IASP) guidelines.

AUTHOR CONTRIBUTIONS

SB designed the study and conducted most experiments, analyzed the data, and wrote the manuscript. VF, TTC, VT, TZ, FP-R, CF, and LS-F designed and performed experiments. RC, WP, FC, TMC, and PP-F contributed with reagents, analytical tools, and expert intellectual support for the study. WV conceived and designed the study, supervised the project, analyzed the data, and wrote the paper. All authors contributed to the article and approved the submitted version.

FUNDING

This work was supported by grants to purchase reagents, equipment, and consumable products and bursaries for students from Conselho Nacional de Desenvolvimento Científico e Tecnológico (CNPq), Coordenação de Aperfeiçoamento de Pessoal de Nível Superior (CAPES; finance code 001), FAPESP under grant agreements 2011/19670-0 (Thematic Project) and 2013/08216-2 (Center for Research in Inflammatory Disease), Programa de Apoio a Grupos de Excelência (PRONEX) grant supported by SETI/Fundação Araucária and MCTI/CNPq, and Governo do Estado do Paraná (agreement 014/2017, protocol 46.843), and Programa de Pesquisa Básica e Aplicada da UEL—PBA 2016 grant from Fundação Araucária, Secretaria de Saúde do Estado do Paraná (SESA) and Governo do Estado do Paraná (Brazil). The confocal microscope was acquired by a project supported by Financiadora de Estudo e Projetos (FINEP)—Apoio à Infraestrutura (CT-INFRA 01/2011; process 01.13.0049.00). SB received postdoctoral fellowships from CAPES and CNPq (process 152792/2016-3), and Fundação Nacional de Desenvolvimento do Ensino Superior Particular (FUNADESP; grant number 5301159) research fellowship during nonoverlapping periods of development of this study. RC, WP, FC, TMC, PP-F, and WV acknowledge the CNPq Productivity fellowship.

ACKNOWLEDGMENTS

The authors kindly thank TECPAR (Paraná Technology Institute), Curitiba, Paraná, Brazil, for providing the C57BL/6 mice for the study. The authors also appreciate the helpful technical assistance of Maria Rosana Ferreira de Paula during the experiments. The authors gratefully acknowledge the support of Central Multiusuário de Laboratórios de Pesquisa (CMLP) facility of State University of Londrina, Londrina, Paraná, Brazil, which provided access to equipment used in this study without charge.

SUPPLEMENTARY MATERIAL

The Supplementary Material for this article can be found online at: https://www.frontiersin.org/articles/10.3389/fimmu.2020.539086/full#supplementary-material

SUPPLEMENTARY VIDEO 1 | 3D representation showing that nuclear NFκB is surrounded by membrane GFAP staining.

SUPPLEMENTARY VIDEO 2 | 3D representation showing that nuclear NFκB is surrounded by membrane Iba-1 staining.

REFERENCES

1. Dutra WO, Menezes CA, Magalhaes LM, Gollob KJ. Immunoregulatory networks in human Chagas disease. *Parasite Immunol* (2014) 36(8):377–87. doi: 10.1111/pim.12107
2. Steverding D. The history of Chagas disease. *Parasit Vectors* (2014) 7:317. doi: 10.1186/1756-3305-7-317
3. da Silva RV, Malvezi AD, Augusto Lda S, Kian D, Tatakihara VL, Yamauchi LM, et al. Oral exposure to Phytomonas serpens attenuates thrombocytopenia and leukopenia during acute infection with Trypanosoma cruzi. *PloS One* (2013) 8(7):e68299. doi: 10.1371/journal.pone.0068299
4. Teixeira MM, Gazzinelli RT, Silva JS. Chemokines, inflammation and Trypanosoma cruzi infection. *Trends Parasitol* (2002) 18(6):262–5. doi: 10.1016/s1471-4922(02)02283-3
5. Silva JS, Vespa GN, Cardoso MA, Aliberti JC, Cunha FQ. Tumor necrosis factor alpha mediates resistance to Trypanosoma cruzi infection in mice by inducing nitric oxide production in infected gamma interferon-activated macrophages. *Infect Immun* (1995) 63(12):4862–7. doi: 10.1128/IAI.63.12.4862-4867.1995
6. ElMunzer BJ, Sallach SM, McGuire DK. Cardiac chagas disease masquerading as an acute myocardial infarction. *Cardiol Rev* (2004) 12(2):69–72. doi: 10.1097/01.crd.0000091840.92246.21
7. Pinto AY, Valente SA, Valente Vda C, Ferreira Junior AG, Coura JR. [Acute phase of Chagas disease in the Brazilian Amazon region: study of 233 cases from Para, Amapa and Maranhao observed between 1988 and 2005]. *Rev Soc Bras Med Trop* (2008) 41(6):602–14. doi: 10.1590/s0037-86822008000600011
8. Barros HD, Beltraõ M, Cerroni MDP, Roberto D, Freitas CD, Pinto AYDN, et al. Investigation of two outbreaks of suspected oral transmission of acute Chagas disease in the Amazon region, Pará State, Brazil, in 2007. *Trop DOCTOR* (2009) 39:231–2. doi: 10.1258/td.2009.090035
9. Souza-Lima Rde C, Barbosa M, Coura JR, Arcanjo AR, Nascimento Ada S, Ferreira JM, et al. Outbreak of acute Chagas disease associated with oral transmission in the Rio Negro region, Brazilian Amazon. *Rev Soc Bras Med Trop* (2013) 46(4):510–4. doi: 10.1590/0037-8682-1367-2013

10. Coura JR, Vinas PA, Brum-Soares LM, Sousa AS, Xavier SS. Morbidity of Chagas heart disease in the microregion of Rio Negro, Amazonian Brazil: a case-control study. *Mem Inst Oswaldo Cruz* (2013) 108(8):1009–13. doi: 10.1590/0074-0276130425
11. Bestetti RB, Restini CB. Precordial chest pain in patients with chronic Chagas disease. *Int J Cardiol* (2014) 176(2):309–14. doi: 10.1016/j.ijcard.2014.07.112
12. Ferreira BL, Ferreira ER, de Brito MV, Salu BR, Oliva MLV, Mortara RA, et al. BALB/c and C57BL/6 Mice Cytokine Responses to Trypanosoma cruzi Infection Are Independent of Parasite Strain Infectivity. *Front Microbiol* (2018) 9:553. doi: 10.3389/fmicb.2018.00553
13. Cunha FQ, Poole S, Lorenzetti BB, Ferreira SH. The pivotal role of tumour necrosis factor alpha in the development of inflammatory hyperalgesia. *Br J Pharmacol* (1992) 107(3):660–4. doi: 10.1111/j.1476-5381.1992.tb14503.x
14. Ferreira SH, Lorenzetti BB, Bristow AF, Poole S. Interleukin-1 beta as a potent hyperalgesic agent antagonized by a tripeptide analogue. *Nature* (1988) 334 (6184):698–700. doi: 10.1038/334698a0
15. Petersen CA, Burleigh BA. Role for interleukin-1 beta in Trypanosoma cruzi-induced cardiomyocyte hypertrophy. *Infect Immun* (2003) 71(8):4441–7. doi: 10.1128/iai.71.8.4441-4447.2003
16. Rodriguez-Angulo H, Thomas LE, Castillo E, Cardenas E, Mogollon F, Mijares A. Role of TNF in sickness behavior and allodynia during the acute phase of Chagas' disease. *Exp Parasitol* (2013) 134(4):422–9. doi: 10.1016/j.exppara.2013.05.006
17. Pinho-Ribeiro FA, Verri WAJr., Chiu IM. Nociceptor Sensory Neuron-Immune Interactions in Pain and Inflammation. *Trends Immunol* (2017) 38 (1):5–19. doi: 10.1016/j.it.2016.10.001
18. Martins RF, Martinelli PM, Guedes PM, da Cruz Padua B, Dos Santos FM, Silva ME, et al. Protein deficiency alters CX3CL1 and endothelin-1 in experimental Trypanosoma cruzi-induced cardiomyopathy. *Trop Med Int Health* (2013) 18(4):466–76. doi: 10.1111/tmi.12071
19. Cordova E, Maiolo E, Corti M, Orduna T. Neurological manifestations of Chagas' disease. *Neurol Res* (2010) 32(3):238–44. doi: 10.1179/016164110X12644252260637
20. Guarner J, Bartlett J, Zaki SR, Colley DG, Grijalva MJ, Powell MR. Mouse model for Chagas disease: immunohistochemical distribution of different stages of Trypanosoma cruzi in tissues throughout infection. *Am J Trop Med Hyg* (2001) 65(2):152–8. doi: 10.4269/ajtmh.2001.65.152
21. Yarbuh ALD, Araujo S, Colasant C, Alarcón M, Moreno E. Effects of Acute Chagas' Disease on Mice Central Nervous System. *Parasitol Latinoam* (2006) 61:3–11. doi: 10.4067/S0717-77122006000100001
22. de Almeida-Leite CM, Silva IC, Galvao LM, Arantes RM. Sympathetic glial cells and macrophages develop different responses to Trypanosoma cruzi infection or lipopolysaccharide stimulation. *Mem Inst Oswaldo Cruz* (2014) 109(4):459–65. doi: 10.1590/0074-0276130492
23. Tafuri WL. Pathogenesis of lesions of the autonomic nervous system of the mouse in experimental acute Chagas' disease. Light and electron microscope studies. *Am J Trop Med Hyg* (1970) 19(3):405–17. doi: 10.4269/ajtmh.1970.19.405
24. Tanowitz HB, Brosnan C, Guastamacchio D, Baron G, Raventos-Suarez C, Bornstein M, et al. Infection of organotypic cultures of spinal cord and dorsal root ganglia with Trypanosoma cruzi. *Am J Trop Med Hyg* (1982) 31(6):1090–7. doi: 10.4269/ajtmh.1982.31.1090
25. Silva AA, Silva RR, Gibaldi D, Mariante RM, Dos Santos JB, Pereira IR, et al. Priming astrocytes with TNF enhances their susceptibility to Trypanosoma cruzi infection and creates a self-sustaining inflammatory milieu. *J Neuroinflammation* (2017) 14(1):182. doi: 10.1186/s12974-017-0952-0
26. Silva RR, Mariante RM, Silva AA, dos Santos AL, Roffe E, Santiago H, et al. Interferon-gamma promotes infection of astrocytes by Trypanosoma cruzi. *PloS One* (2015) 10(2):e0118600. doi: 10.1371/journal.pone.0118600
27. Da Mata JR, Camargos MR, Chiari E, Machado CR. Trypanosoma cruzi infection and the rat central nervous system: proliferation of parasites in astrocytes and the brain reaction to parasitism. *Brain Res Bull* (2000) 53 (2):153–62. doi: 10.1016/s0361-9230(00)00326-9
28. Bombeiro AL, Goncalves LA, Penha-Goncalves C, Marinho CR, D'Imperio Lima MR, Chadi G, et al. IL-12p40 deficiency leads to uncontrolled Trypanosoma cruzi dissemination in the spinal cord resulting in neuronal death and motor dysfunction. *PloS One* (2012) 7(11):e49022. doi: 10.1371/journal.pone.0049022
29. Weinkauf C, Salvador R, Pereiraperrin M. Neurotrophin receptor TrkC is an entry receptor for Trypanosoma cruzi in neural, glial, and epithelial cells. *Infect Immun* (2011) 79(10):4081–7. doi: 10.1128/IAI.05403-11
30. Vargas-Zambrano JC, Lasso P, Cuellar A, Puerta CJ, Gonzalez JM. A human astrocytoma cell line is highly susceptible to infection with Trypanosoma cruzi. *Mem Inst Oswaldo Cruz* (2013) 108(2):212–9. doi: 10.1590/0074-0276108022013014
31. Lury KM, Castillo M. Chagas' disease involving the brain and spinal cord: MRI findings. *AJR Am J Roentgenol* (2005) 185(2):550–2. doi: 10.2214/ajr.185.2.01850550
32. Borghi SM, Fattori V, Pinho-Ribeiro FA, Domiciano TP, Miranda-Sapla MM, Zaninelli TH, et al. Contribution of spinal cord glial cells to L. amazonensis experimental infection-induced pain in BALB/c mice. *J Neuroinflammation* (2019) 16(1):113. doi: 10.1186/s12974-019-1496-2
33. Almeida FR, Schivo IR, Lorenzetti BB, Ferreira SH. Chronic intrathecal cannulation enhances nociceptive responses in rats. *Braz J Med Biol Res* (2000) 33(8):949–56. doi: 10.1590/s0100-879x2000000800011
34. Malvezi AD, da Silva RV, Panis C, Yamauchi LM, Lovo-Martins MI, Zanluqui NG, et al. Aspirin modulates innate inflammatory response and inhibits the entry of Trypanosoma cruzi in mouse peritoneal macrophages. *Mediators Inflammation* (2014) 2014:580919. doi: 10.1155/2014/580919
35. Guerrero AT, Verri WAJr., Cunha TM, Silva TA, Rocha FA, Ferreira SH, et al. Hypernociception elicited by tibio-tarsal joint flexion in mice: a novel experimental arthritis model for pharmacological screening. *Pharmacol Biochem Behav* (2006) 84(2):244–51. doi: 10.1016/j.pbb.2006.05.008
36. Ono K, Nimura S, Hideshima Y, Nabeshima K, Nakashima M. Orally administered sodium 4-phenylbutyrate suppresses the development of dextran sulfate sodium-induced colitis in mice. *Exp Ther Med* (2017) 14 (6):5485–90. doi: 10.3892/etm.2017.5251
37. Zarpelon AC, Rodrigues FC, Lopes AH, Souza GR, Carvalho TT, Pinto LG, et al. Spinal cord oligodendrocyte-derived alarmin IL-33 mediates neuropathic pain. *FASEB J* (2016) 30(1):54–65. doi: 10.1096/fj.14-267146
38. Chiu IM, Heesters BA, Ghasemlou N, Von Hehn CA, Zhao F, Tran J, et al. Bacteria activate sensory neurons that modulate pain and inflammation. *Nature* (2013) 501(7465):52–7. doi: 10.1038/nature12479
39. Voss LJ, Harvey MG, Sleigh JW. Inhibition of astrocyte metabolism is not the primary mechanism for anaesthetic hypnosis. *Springerplus* (2016) 5(1):1041. doi: 10.1186/s40064-016-2734-z
40. Tikka T, Fiebich BL, Goldsteins G, Keinanen R, Koistinaho J. Minocycline, a tetracycline derivative, is neuroprotective against excitotoxicity by inhibiting activation and proliferation of microglia. *J Neurosci* (2001) 21(8):2580–8. doi: 10.1523/JNEUROSCI.21-08-02580.2001
41. Ferrari LF, Cunha FQ, Parada CA, Ferreira SH. A novel technique to perform direct intraganglionar injections in rats. *J Neurosci Methods* (2007) 159 (2):236–43. doi: 10.1016/j.jneumeth.2006.07.025
42. Ji RR, Nackley A, Huh Y, Terrando N, Maixner W. Neuroinflammation and Central Sensitization in Chronic and Widespread Pain. *Anesthesiology* (2018) 129(2):343–66. doi: 10.1097/ALN.0000000000002130
43. Chatelain E, Konar N. Translational challenges of animal models in Chagas disease drug development: a review. *Drug Des Devel Ther* (2015) 9:4807–23. doi: 10.2147/DDDT.S90208
44. Binshtok AM, Wang H, Zimmermann K, Amaya F, Vardeh D, Shi L, et al. Nociceptors are interleukin-1beta sensors. *J Neurosci* (2008) 28(52):14062–73. doi: 10.1523/JNEUROSCI.3795-08.2008
45. Jin X. Gereau RWt. Acute p38-mediated modulation of tetrodotoxin-resistant sodium channels in mouse sensory neurons by tumor necrosis factor-alpha. *J Neurosci* (2006) 26(1):246–55. doi: 10.1523/JNEUROSCI.3858-05.2006
46. Brierley SM, Goh KGK, Sullivan MJ, Moore KH, Ulett GC, Grundy L. Innate immune response to bacterial urinary tract infection sensitises high-threshold bladder afferents and recruits silent nociceptors. *Pain* (2020) 161(1):202–10. doi: 10.1097/j.pain.0000000000001692
47. Gold MS, Gebhart GF. Nociceptor sensitization in pain pathogenesis. *Nat Med* (2010) 16(11):1248–57. doi: 10.1038/nm.2235
48. Verri WA Jr., Cunha TM, Parada CA, Wei XQ, Ferreira SH, Liew FY, et al. IL-15 mediates immune inflammatory hypernociception by triggering a sequential release of IFN-gamma, endothelin, and prostaglandin. *Proc Natl Acad Sci USA* (2006) 103(25):9721–5. doi: 10.1073/pnas.0603286103

49. Verri WAJr., Cunha TM, Parada CA, Poole S, Liew FY, Ferreira SH, et al. Antigen-induced inflammatory mechanical hypernociception in mice is mediated by IL-18. *Brain Behav Immun* (2007) 21(5):535–43. doi: 10.1016/j.bbi.2006.11.005
50. Canavaci AM, Sorgi CA, Martins VP, Morais FR, de Sousa EV, Trindade BC, et al. The acute phase of Trypanosoma cruzi infection is attenuated in 5-lipoxygenase-deficient mice. *Mediators Inflammation* (2014) 2014:893634. doi: 10.1155/2014/893634
51. Verri WAJr., Molina RO, Schivo IR, Cunha TM, Parada CA, Poole S, et al. Nociceptive effect of subcutaneously injected interleukin-12 is mediated by endothelin (ET) acting on ETB receptors in rats. *J Pharmacol Exp Ther* (2005) 315(2):609–15. doi: 10.1124/jpet.105.089409
52. Galvao da Silva AP, de Almeida Abrahamsohn I. Interleukin-12 stimulation of lymphoproliferative responses in Trypanosoma cruzi infection. *Immunology* (2001) 104(3):349–54. doi: 10.1046/j.1365-2567.2001.01311.x
53. Blaszczyk L, Maitre M, Leste-Lasserre T, Clark S, Cota D, Oliet SHR, et al. Sequential alteration of microglia and astrocytes in the rat thalamus following spinal nerve ligation. *J Neuroinflammation* (2018) 15(1):349. doi: 10.1186/s12974-018-1378-z
54. Lee S, Zhao YQ, Ribeiro-da-Silva A, Zhang J. Distinctive response of CNS glial cells in oro-facial pain associated with injury, infection and inflammation. *Mol Pain* (2010) 6:79. doi: 10.1186/1744-8069-6-79
55. Cangussu SD, Souza CC, Castro MS, Vieira LQ, Cunha FQ, Afonso LC, et al. The endogenous cytokine profile and nerve fibre density in mouse ear Leishmania major-induced lesions related to nociceptive thresholds. *Exp Parasitol* (2013) 133(2):193–200. doi: 10.1016/j.exppara.2012.11.015
56. Borghi SM, Fattori V, Conchon-Costa I, Pinge-Filho P, Pavanelli WR, Verri WAJr. Leishmania infection: painful or painless? *Parasitol Res* (2017) 116(2):465–75. doi: 10.1007/s00436-016-5340-7
57. Owolabi SA, Saab CY. Fractalkine and minocycline alter neuronal activity in the spinal cord dorsal horn. *FEBS Lett* (2006) 580(18):4306–10. doi: 10.1016/j.febslet.2006.06.087
58. Liu X, Quan N. Microglia and CNS Interleukin-1: Beyond Immunological Concepts. *Front Neurol* (2018) 9:8. doi: 10.3389/fneur.2018.00008
59. Takeda M, Tanimoto T, Kadoi J, Nasu M, Takahashi M, Kitagawa J, et al. Enhanced excitability of nociceptive trigeminal ganglion neurons by satellite glial cytokine following peripheral inflammation. *Pain* (2007) 129(1-2):155–66. doi: 10.1016/j.pain.2006.10.007
60. Jia M, Wu C, Gao F, Xiang H, Sun N, Peng P, et al. Activation of NLRP3 inflammasome in peripheral nerve contributes to paclitaxel-induced neuropathic pain. *Mol Pain* (2017) 13:1744806917719804. doi: 10.1177/1744806917719804
61. Zhao S, Zhou Y, Fan Y, Gong Y, Yang J, Yang R, et al. Involvement of purinergic 2X4 receptor in glycoprotein 120-induced pyroptosis in dorsal root ganglia. *J Neurochem* (2019) 151(5):584–94. doi: 10.1111/jnc.14850
62. Kannampalli P, Pochiraju S, Bruckert M, Shaker R, Banerjee B, Sengupta JN. Analgesic effect of minocycline in rat model of inflammation-induced visceral pain. *Eur J Pharmacol* (2014) 727:87–98. doi: 10.1016/j.ejphar.2014.01.026
63. Souza GR, Talbot J, Lotufo CM, Cunha FQ, Cunha TM, Ferreira SH. Fractalkine mediates inflammatory pain through activation of satellite glial cells. *Proc Natl Acad Sci USA* (2013) 110(27):11193–8. doi: 10.1073/pnas.1307445110
64. Blanco FJ, Guitian R, Moreno J, de Toro FJ, Galdo F. Effect of antiinflammatory drugs on COX-1 and COX-2 activity in human articular chondrocytes. *J Rheumatol* (1999) 26(6):1366–73.
65. Warner TD, Giuliano F, Vojnovic I, Bukasa A, Mitchell JA, Vane JR. Nonsteroid drug selectivities for cyclo-oxygenase-1 rather than cyclo-oxygenase-2 are associated with human gastrointestinal toxicity: a full in vitro analysis. *Proc Natl Acad Sci USA* (1999) 96(13):7563–8. doi: 10.1073/pnas.96.13.7563

Conflict of Interest: The authors declare that the research was conducted in the absence of any commercial or financial relationships that could be construed as a potential conflict of interest.

frontiers in Immunology

ORIGINAL RESEARCH
published: 01 April 2021
doi: 10.3389/fimmu.2021.584097

HMGB1 Promotes the Release of Sonic Hedgehog From Astrocytes

Yifan Xiao[1,2,3], Yan Sun[4,5], Wei Liu[1,3], FanFan Zeng[2], Junyu Shi[2], Jun Li[2], Huoying Chen[6], Chang Tu[7], Yong Xu[2], Zheng Tan[2], Feili Gong[2], Xiji Shu[1,3] and Fang Zheng[2,8]**

[1] Department of Pathology and Pathophysiology, School of Medicine, Jianghan University, Wuhan, China, [2] Department of Immunology, School of Basic Medicine, Tongji Medical College, Huazhong University of Science and Technology, Wuhan, China, [3] School of Medicine, Institutes of Biomedical Sciences, Jianghan University, Wuhan, China, [4] Wuhan Institute for Neuroscience and Neuroengineering, South-Central University for Nationalities, Wuhan, China, [5] Department of Neurobiology, College of Life Sciences, South-Central University for Nationalities, Wuhan, China, [6] Department of Laboratory Medicine, The Second Affiliated Hospital of Guilin Medical University, Guilin, China, [7] Department of Orthopedics, Renmin Hospital of Wuhan University, Wuhan, China, [8] Key Laboratory of Organ Transplantation, Ministry of Education, NHC Key Laboratory of Organ Transplantation, Key Laboratory of Organ Transplantation, Chinese Academy of Medical Sciences, Wuhan, China

High mobility group box 1 protein (HMGB1) is known to be a trigger of inflammation in experimental autoimmune encephalomyelitis (EAE), an animal model of multiple sclerosis (MS). However, it may play a different role in some way. Here we investigated the effect of HMGB1 on promoting sonic hedgehog (shh) release from astrocytes as well as the possible signal pathway involved in it. Firstly, shh increased in astrocytes after administration of recombinant HMGB1 or decreased after HMGB1 was blocked when stimulated by homogenate of the onset stage of EAE. Moreover, the expression of HMGB1 receptors, toll-like receptor (TLR) 2 and receptor for advanced glycation end products (RAGE) increased after HMGB1 administration in primary astrocytes. However, the enhancing effect of HMGB1 on shh release from astrocytes was suppressed only after RAGE was knocked out or blocked. Mechanistically, HMGB1 functioned by activating RAGE-mediated JNK, p38, stat3 phosphorylation. Moreover, HMGB1 could induce shh release in EAE. Additionally, intracerebroventricular injection of recombinant shh protein on the onset stage of EAE alleviated the progress of disease and decreased demylination, compared to the mice with normal saline treatment. Overall, HMGB1 promoted the release of shh from astrocytes through signal pathway JNK, p38 and stat3 mediated by receptor RAGE, which may provide new insights of HMGB1 function in EAE.

Keywords: sonic hedgehog (shh), HMGB1, astrocytes, experimental autoimmune encephalomyelitis (EAE), receptor for advanced glycation end products (RAGE)

OPEN ACCESS

Edited by:
Larissa Garcia Pinto, King's College London, United Kingdom

Reviewed by:
Alberto Javier Ramos, Consejo Nacional de Investigaciones Científicas y Técnicas (CONICET), Argentina
Yam Nath Paudel, Monash University Malaysia, Malaysia

***Correspondence:**
Fang Zheng
zhengfangtj@hust.edu.cn
Xiji Shu
shuxiji@sina.com

Specialty section:
This article was submitted to Cytokines and Soluble Mediators in Immunity, a section of the journal Frontiers in Immunology

Received: *16 July 2020*
Accepted: *15 March 2021*
Published: *01 April 2021*

Citation:
Xiao Y, Sun Y, Liu W, Zeng F, Shi J, Li J, Chen H, Tu C, Xu Y, Tan Z, Gong F, Shu X and Zheng F (2021) HMGB1 Promotes the Release of Sonic Hedgehog From Astrocytes. Front. Immunol. 12:584097. doi: 10.3389/fimmu.2021.584097

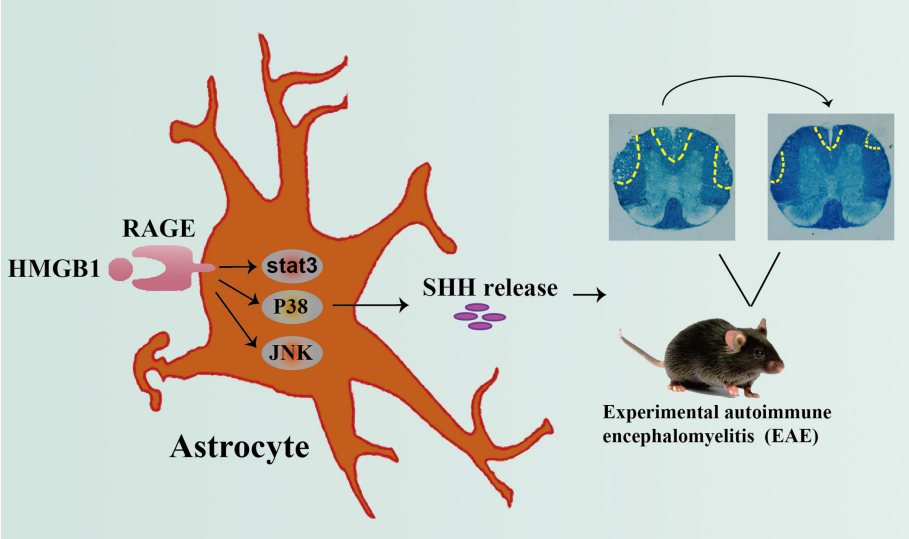

GRAHPICAL ABSTRACT | Graphical abstract depicting the effect of HMGB1 on promoting shh release from astrocytes through signal pathway JNK, p38 and stat3 mediated by receptor RAGE, which may provide new insights of HMGB1 function in EAE.

INTRODUCTION

High-mobility group box 1 protein (HMGB1) is a typical damage-associated molecular pattern (DAMP) found in the nucleus of nearly all eukaryotic cells (1). In physiological conditions, HMGB1 is located in the nucleus, binding to DNA and participating in the transcription, replication, and repair of DNA. When cells die or get injured in disease, HMGB1 is released outside the cells, binding to different receptors, participating in innate or adaptive immune responses, and repairing damaged tissue (2–4). Moreover, the three main receptors implicated in HMGB1 are the receptor for advanced glycation end products (RAGE), toll-like receptor (TLR) 2 and TLR4 (5, 6). In recent years, HMGB1 has brought much interest for its pro-inflammatory role in diseases related to spinal cord injury, such as multiple sclerosis (MS) and related animal models-experimental autoimmune encephalomyelitis (EAE) (5). We previously confirmed that the level of HMGB1 in the brain of mice varied during different stages of EAE and became the highest on onset stage (7). The released HMGB1 in CNS can initiate neuro-inflammation and drive the progress of EAE (1).

Despite growing number of publications that describe pro-inflammatory effects of HMGB1, less is known about the role of HMGB1 in the repair of spinal cord injury (8). In fact, HMGB1 is also known as amphoterin, playing an important role in the early development of organism (9, 10). In zebrafish embryos, both forebrain neurons and brain size were significantly reduced after down-regulating HMGB1 expression (11). In cerebral ischemia, over-expression of HMGB1 in astrocytes promotes the repair of neurovascular units, while low expression of HMGB1 decreases the density of microvessels around the infarct and inhibits the repair of motor neurons (12).

The role of HMGB1 is flexible because its sulfhydryl in C23, C45 and C106 are easily oxidized by active oxygen in external environment. As reported, all-thiol-HMGB1 can form a complex with CXCL12. Then HMGB1-CXCL12 binds to CXCR4 and exerts its chemotaxis function. At the same time, the main biological effect of HMGB1 after binding to RAGE is promoting cells migration through the expression of adhesion molecules VCAM-1 and ICAM-1 or the secretion of CXCL12 (13, 14). Therefore, some studies indicate that all-thiol-HMGB1 mainly recognizes RAGE (15, 16). After the sulfydryl at C23 and C45 are oxidized to form a disulfide bond, disulfide (ds)-HMGB1 can specifically bind to myeloid differentiation factor 2 (MD2)-TLR4, promoting the secretion of chemokines and inflammatory factors (17, 18). Since HMGB1 may play different roles through different receptors, the exact role of HMGB1 in spinal cord injury remains to be further investigated. And until now, the underlying mechanism for the effects of HMGB1 remains unclear.

Astrocytes, the most abundant cell population in the central nervous system (CNS), are essential for normal neurological function. They respond to all forms of CNS damage and disease by undergoing cellular, molecular and functional changes. Astrocyte roles in CNS disorders exhibit diversity and a better understanding of this diversity has the potential to impact on the understanding and treatment of CNS injury and disease (19). In MS/EAE, astrocytes not only recruit lymphocytes and contribute to tissue damage but also confine inflammation and promote lesion repair (20). Understanding the emerging roles of astrocytes in MS/EAE will open up a new therapeutic opportunity.

Sonic hedgehog (Shh), a highly conserved secreted glycoprotein, is a member of the Hedgehog protein family in vertebrates (21, 22). It can activate the transcription of downstream target genes by downstream signaling pathway

(21, 22). In MS/EAE, shh was upregulated in astrocytes and involved in promoting blood brain barrier (BBB) integrity or supporting neural stem cell (NSC) differentiation toward neurons and oligodendrocytes, facilitating remyelination and controlling axon growth (23–26). These results affirmed the important role of shh in improving functional recovery in MS/EAE. But the regulation mechanism of shh release is deficient. Among the limited researches, *Hmgb1* gene was reported to regulate the embryonic development partly by Shh signaling. However, the study was performed in the level of *Hmgb1* gene and non-pathological status. Together with the role of HMGB1 and Shh in neural injury (8, 25, 27), the limited understandings drive us to further characterize the relation of HMGB1 and shh. To validate the hypothesis, we design the experiment to investigated the relationship of HMGB1 and shh as well as the possible signal pathways involved in it.

MATERIAL AND METHODS

Ethics Statement

All animal experiments in this study were performed in strict accordance with the Institutional Animal Care and Use Committee, Tongji Medical College, Huazhong University of Science and Technology. All efforts were made to minimize animal suffering.

Mice

Wild type (WT) C57BL/6 mice were purchased from SLAC Laboratory Animal Co. Ltd. (Shanghai, China) and maintained in a SPF facility for further used. $TLR2^{-/-}$ mice were purchased from Nanjing Biomedical Research Institute of Nanjing University (Nanjing, China). $TLR4^{-/-}$ mice were given as a gift from Hui Wang professor in Tongji Medical College, Huazhong University of Science and Technology, Wuhan, Hubei, PR China. $RAGE^{-/-}$ mice were made by the loxp/cre recombinase system. $RAGE^{Loxp/Loxp}$ and cre mice were given as a gift from Chongyi Wang professor in the Organ Transplantation Institute of Tongji Hospital, Tongji Medical College, Huazhong University of Science and Technology, Wuhan, Hubei, PR China.

EAE Induction and Clinical Evaluation

Female C57BL/6J mice (8-9-week-old) were used for active induction of EAE, as described previously (7, 28, 29). Briefly, the mice were subcutaneously (s.c.) immunized with 200μg of MOG35-55 (CL Bio-Scientific Co. LTD., Xian, China), emulsified in Freund's complete adjuvant containing 5 mg/mL of Mycobacterium tuberculosis (strain H37Ra; Difco Laboratories, Detroit, MI, USA). In addition, 200 ng pertussis toxin (Sigma, St. Louis, MO, USA) was intraperitoneally (i.p.) injected at day 0 and 2 post immunization. The mice were scored daily, according to the clinical symptoms. The criteria were as follows: 0, asymptomatic; 0.5, loss of the distal half of tail tone; 1, loss of entire tail tone; 2, hind limb weakness; 2.5, hind limb paraplegia; 3, both hind limb paraplegia;3.5, forelimb weakness and hind limb paraplegia; 4, forelimb and hind limb paraplegia; 5, moribund or death.

GL Administration

The treatment of glycyrrhizin (Minophagen Pharmaceutical Co., Tokyo, Japan) was described previously (30). Briefly, a single intra-peritoneal (i.p.) dose of 25 mg/kg glycyrrhizin (GL) was administrated every other day from days 12 to 22 after induction of EAE.

Interstitial Fluid Preparation

Brains from EAE were weighed and homogenized in sterile PBS (100 mg tissue per 1 mL of 1×PBS) containing a protease inhibitor 4-(2-Aminoethyl) benzenesulfonyl fluoride hydrochloride (AEBSF, 0.1mM, Sigma, St. Louis, MO, USA) on ice, then centrifuged at 12000 rpm for 20 min at 4°C. The supernatant was removed in a new tube and the protein concentration was detected using the BCA Protein Assay Kit (Thermo Fisher).

Intracerebroventricular Injection

The procedure was performed as described previously (29). Briefly, after anesthetized intraperitoneally, a 26-gauge guide cannula (RWD life science, Shenzhen, China) was oriented into the left lateral ventricle using the following coordinates from Bregma: 0.5 mm posterior, 1.0 mm lateral, and 2.0 mm ventral. The guide cannula was secured by dental cement, anchored by stainless steel screws fixed to the skull, and sealed with a stainless steel wire to prevent occlusion. EAE induction was conducted 7 days later. During intracerebroventricular injection, a 30-gauge injection cannula connected to a 10-μL Hamilton syringe by a PE-20 catheter was filled with drug solution and inserted into the guide cannula extending 0.5 mm beyond the guide cannula tip. Recombinant mouse sonic hedgehog (Shh) protein (R&D system, Minneapolis, MN, USA) in 10 μL saline or 10 μL saline was delivered over a 2-min period every day from day 11 to day 19 post immunization.

The Culture of Primary Astrocytes

The primary astrocytes were obtained from cerebral cortices of C57BL/6 mouse pups (P1-P2) as described previously (29, 31). Briefly, cerebral cortices were isolated, minced, and digested in 0.25% trypsin–0.01% EDTA for 45 minutes. Then 10% FBS was used to terminate the digestion and the samples were passed through a 70μm filter. The mixed cortical cells were plated in 25 cm^2 (T25) culture flasks with DMEM/F12 medium (Gibco, Waltham, MA, USA) supplemented with 10% FBS (NATOCOR, Córdoba, Argentina) and cultured at 37°C in 5% CO_2. Medium was changed one day after plating the mixed cortical cells and all 3 days thereafter. After 7 to 8 days, when astrocytes reached confluence, the T25 flasks were shaked at 250 rpm for 24h on an orbital shaker to remove microglia and oligodendrocyte precursor cells (OPC). Floating cells were removed and the remaining confluent astrocyte layer were digested by 0.25% trypsin–0.01% EDTA and plated in T75 culture flasks. 12-14 days after the first split, astrocytes were plated in an appropriate cell concentration 24 hour before performing the experiment. The purity of astrocytes was identified by immunofluorescence and flow cytometry.

Flow Cytometry

After digested by 0.25% trypsin–0.01% EDTA and washed by 1×PBS-0.5%BSA, cells were incubated with anti-CD16/32 (BD Bioscience) for 15 minutes at room temperature to block the Fcγ receptors.

Staining of Cell Surface Antigens

All cells were resuspended in 1×PBS-0.5%BSA containing adequate antibody and incubated for 45 minutes at room temperature. The cells were then centrifuged for 5 min at 1000 rpm after washed by cold 1×PBS-0.5%BSA.

Intracellular Staining

The cells were permeabilized with Perm/Fix solution (BD Bioscience) and incubated with mouse anti-GFAP for 45min at room temperature. This was followed by a 30-min secondary incubation in FITC-anti mouse IgG (all diluted in 1×permwash). Cells were then washed by cold 1×PBS-0.5%BSA prior to FACS analysis by BD LSR II (BD Biosciences).

Astrocytes Treatment

Astrocytes were plated at 1.7×10^5 cells/well in 48-wells culture plates and cultured for 18h-24h before experiment. Then they were stimulated with HMGB1 (1-2μg/mL, Sigma, St. Louis, MO, USA) or interstitial fluid (100μg/mL) with/without the combination of antibody (HMGB1 Ab or IgG: 5 μg/mL) for 24 h. The culture supernatants were collected for ELISA while the remaining cells were performed for the following RT-PCR or Western blot assay.

Blocking agents for TLR4 (100nM TAK-242, Milipore, Temecula, CA, USA) or RAGE (148nM FPS-ZM1, Milipore, Temecula, CA, USA) in 10% FBS-DMEM/F12 medium were incubated with astrocytes for 2h at 37°C, 5%CO2 incubator. Inhibitor agents for p38 (3μM SB203580, MedChemExpress, Monmouth Junction, NJ,USA), ERK (2μM SCH772984, MedChemExpress, Monmouth Junction, NJ,USA), JNK (5μM SP600125, MedChemExpress, Monmouth Junction, NJ,USA) and stat3 (10μM SH-4-54, MedChemExpress, Monmouth Junction, NJ,USA) in 10% FBS-DMEM/F12 medium were incubated with astrocytes for appointed time at 37°C, 5%CO_2 incubator. Subsequently appropriate HMGB1 were used to reach to the final concentration 1-2μg/mL. The remaining steps are the same as before.

ELISA

The level of shh in the cell culture medium of astrocytes was measured by a mouse ELISA kit (R&D system, Minneapolis, MN, USA) according to the manufacturer's instructions.

Western Blot

The cells were lysed in RIPA buffer containing protease and phosphatase inhibitors on ice. The lysed cells were collected by cell scraper and then centrifuged for 30 min at 12000 rpm, 4°C. After that, the concentration of protein in supernatant was quantified using BCA Protein Assay Kit. Finally protein samples were mixed with 5 × SDS loading buffer, boiled for 5 min and stored in -80°C for further use.

Spinal cords from EAE were washed for three times using 1×PBS on ice to remove superficial blood, then single cell suspension were obtained after mechanical shear and grind in 1×PBS on ice followed by centrifuging (4000 rpm, 5 min, 4°C). The cell deposits were gathered and washed by 1×PBS on ice followed by centrifuging (4000 rpm, 2 min, 4°C). After that, cytoplasmic protein and nuclear protein were separated by cytoplasmic and nuclear protein extraction kit (Beyotime Biotechnology, ShangHai, China) according to the manufacturer's instructions.

The protein was separated by 10%-12% SDS–PAGE and blotted onto polyvinylidene fluoride (PVDF) membranes (Hybond Inc., Escondido, CA, USA) as described (7). Blots were visualized by an ECL system (Pierce Bio-Technology, Rockford, IL) after incubating with horseradish peroxidase (HRP) conjugated secondary antibody (Thermo, Massachusetts, USA), and quantified by densitometry using the Biorad GelDoc XR Image analysis system (Bio Rad, Hercules, California, USA).

Antibodies

Primary antibodies include rat anti-shh antibody (Abcam, UK), and mouse anti-β-actin antibody (EASYBIO, Beijing, China), mouse anti-GAPDH antibody (EASYBIO, Beijing, China), goat anti-RAGE polyclonal antibody (R&D system, USA), rabbit anti-AGER polyclonal antibody (Abcam, UK), rat anti-shh polyclonal antibody (Abcam, UK), mouse anti-GAPDH monoclonal antibody (EASYBIO, Beijing, China), mouse anti-GFAP monoclonal antibody (Millipore, USA), mouse anti-HMGB1 monoclonal neutralizing antibody (Institute of Biophysics, Chinese Academy of Sciences, Beijing, China), mouse IgG (Santa Cruz, USA), rabbit anti phosphorylation-ERK antibody (CST, USA), rabbit anti phosphorylation-p38 antibody (CST, USA), rabbit anti phosphorylation-JNK antibody (CST, USA), rabbit anti phosphorylation-stat3 antibody (Abcam, UK), rabbit anti total-ERK antibody (CST, USA), rabbit anti total-p38 antibody (CST, USA), rabbit anti total-JNK antibody (CST, USA), rabbit anti total-stat3 antibody (Abcam, UK). The antibodies for flow cytometry include PE-anti-mouse-TLR2 (eBioscience, San Diego, CA; clone: 6C2), PE-cy7-anti-mouse-TLR4 (Biolegend, San Diego, USA; clone: MTS510).

Statistical Analysis

Experimental data are expressed as the mean ± standard deviation (SD). The data for more than two groups was analyzed with one-way analysis of variance (ANOVA) followed by Tukey's multiple comparison test. Other data were analyzed using two-tailed unpaired Student's t-test. A P value of <0.05 was considered to be statistically significant (*P< 0.05, **P< 0.01, ***P< 0.001).

RESULTS

HMGB1 Promotes the Expression and Release of Shh in Primary Astrocytes

To investigate the effects of HMGB1 on shh expression and release in astrocytes, western blot analysis and ELISA were performed. The expression and release of Shh by astrocytes

significantly increased, after HMGB1 (1μg/ml) stimulation for 24h (**Figures 1A, B**). There was no significant change in cell viability after HMGB1 stimulation, and cell survival controls have been supplied in **Supplemental Figure 1**. To simulate the microenvironment in EAE, we obtained the interstitial fluid of brain from the onset stage of EAE, during which the level of HMGB1 reached to the highest as described in our previous study (7). We found that shh levels increased in astrocytes when simulated by the interstitial fluid (100μg/ml) compared to medium group. And the effect was reversed after HMGB1 antibody (5μg/ml) treatment. Moreover, when treated with control IgG (5μg/ml) instead of HMGB1 antibody, the shh levels remained unchanged (**Figure 1C**). It is worth mentioning that shh in EAE homogenate (cell-free) group was less than 2pg/ml, which was much lower than that of the medium group. The shh in EAE homogenate would not affect the result. The data above indicated that HMGB1 could promote shh expression and release in astrocytes.

The Effect of HMGB1 on Shh Release From Astrocytes Is Mainly Through Receptor RAGE

To investigate which receptor is changed in astrocytes after HMGB1 (2μg/ml) stimulation, flow cytometry was performed. The surface TLR2 and RAGE increased significantly while TLR4 remained unchanged (**Figure 2A**). Considering that TLR4 may internalized into endosomes after stimulation (32, 33), we checked the change of total TLR4 protein in astrocytes. The result demonstrated that total TLR4 protein significantly increased in astrocytes after HMGB1 (2μg/ml) stimulation (**Supplemental Figures 2A, B**). Although HMGB1 receptors increased, it could not illuminate which receptor is crucial for the effect of HMGB1 on shh release from astrocytes.

To further explore the possible mechanism for shh release, we next knocked out TLR2, TLR4 and RAGE respectively. Compared to wild type astrocytes, the levels of shh in $TLR2^{-/-}$, $TLR4^{-/-}$ and $RAGE^{-/-}$ astrocytes decreased (**Figure 2B**). We found that spontaneous shh release in astrocytes existed in medium group, the phenomenon reminded us spontaneous shh release was dependent on TLR2, TLR4 and RAGE. But as for HMGB1, the effect on shh release was weakened only after receptor RAGE was knocked out. To further prove this conclusion, we next introduced the blocking agents FPS-ZM1 and TAK-242, which could block RAGE and TLR4 respectively. As shown in **Figure 2C**, the levels of shh increased under the stimulation of HMGB1 (1μg/ml) comparing to that in medium group when TLR4 was blocked. But the levels of shh had no statistically significant increase after HMGB1 stimulation comparing to that in medium group when RAGE was blocked. It implied that HMGB1 promoted shh release in astrocytes mainly through receptor RAGE.

p38, JNK, and stat3 Are Involved in the Effect of HMGB1 on Promoting Shh Release From Astrocytes Through Receptor RAGE

The downstream signal pathway for RAGE included MAP kinases (p38, ERK, JNK) and stat3. In our results, the phosphorylation of p38, ERK, JNK and stat3 significantly increased after HMGB1 (1μg/ml) stimulation for 10 minutes (**Figure 3A**, **Supplemental**

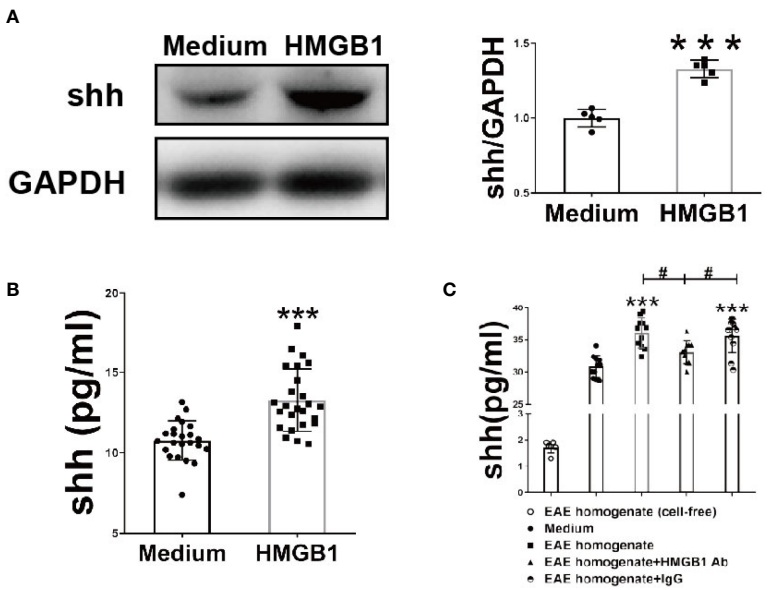

FIGURE 1 | The effect of HMGB1 on expression and release of shh in astrocytes. **(A)** The protein from astrocytes was obtained and detected by western blot (1μg/ml recombinant HMGB1 was used). **(B)** The level of shh in supernatant from astrocytes after recombinant HMGB1 (1μg/ml) or **(C)** brain homogenate of EAE onset stage (100μg/ml) with/without HMGB1 Ab/IgG (5μg/ml) stimulation for 24h were detected by ELISA. EAE homogenate (cell-free) group here indicates interstitial fluid (100μg/ml) from the onset stage of EAE mice without cultured astrocytes. All the data are shown as mean ± SD (***$P < 0.001$ compared with medium; $^{\#}P < 0.05$ compared with each other).

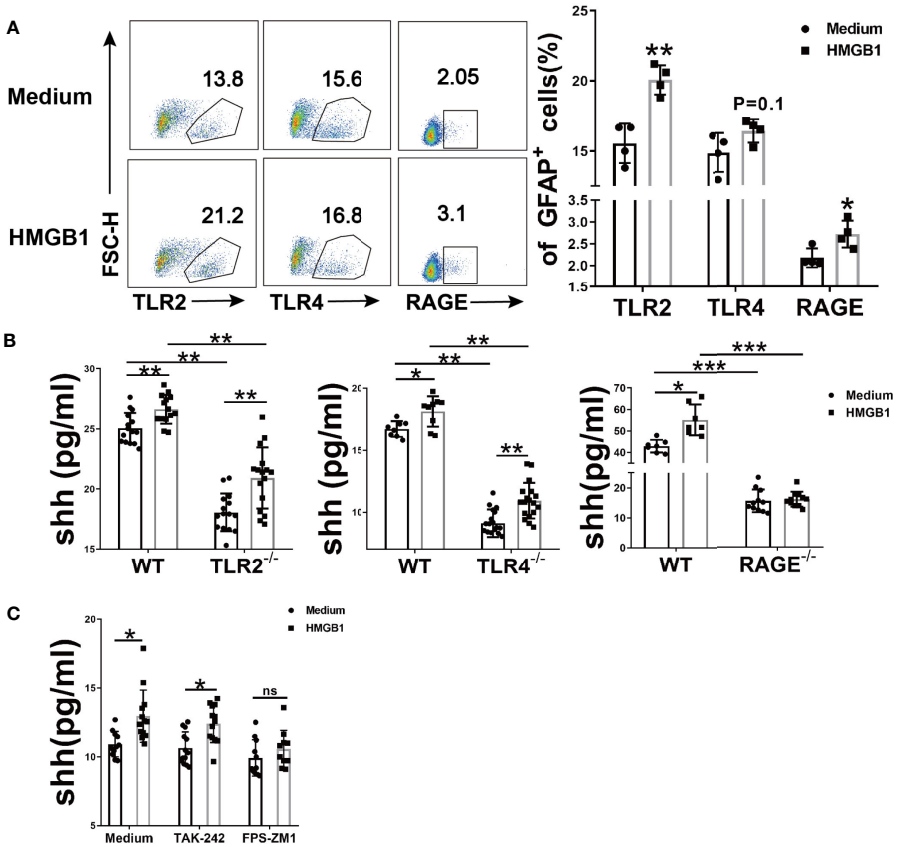

FIGURE 2 | The effect of HMGB1 receptors on the release of shh in astrocytes. **(A)** Three surface receptors for HMGB1 were analyzed by flow cytometry after HMGB1 stimulation (2μg/ml) in astrocytes. **(B)** The release of shh from astrocytes was detected after TLR2, TLR4 and RAGE were knocked out (2μg/ml and 1μg/ml recombinant HMGB1 was used in TLR2, TLR4 and RAGE knockout astrocytes respectively). **(C)** The effect of TLR4 blocker (TAK-242: 100nM) and RAGE blocker (FPS-ZM1: 148nM) on the release of shh in astrocytes (1μg/ml recombinant HMGB1 was used). Data are shown as mean ± SD (*$P < 0.05$, **$P < 0.01$, ***$P < 0.001$). ns, no significance.

Figure 3). We next explored the effect of inhibitors for stat3 and MAPK on shh release from astrocytes. As shown in **Supplemental Figure 4**, 5μM SP600125 (JNK blocker), 10μM SH-4-54 (stat3 blocker), 2μM SCH772984 (ERK blocker), 3μM SB203580 (p38 blocker) were chosen according to our preliminary experiment. When signal pathway JNK and stat3 were blocked, the level of shh had no significant change after HMGB1 (1μg/ml) stimulation for 10min. (**Figure 3B**). At the same time, when signal pathway ERK was blocked, shh release from astrocytes decreased, but the level of shh could still increase after HMGB1 (1μg/ml) stimulation for 10 min. When signal pathway p38 was blocked, shh release from astrocytes decreased and the level of shh did not increase after HMGB1 stimulation (1μg/ml) for 10 min (**Figure 3C**). The results indicated that the signal pathway involved in shh release after HMGB1 stimulation were closely related to stat3, JNK and p38. However, whether the above signal pathways depend on RAGE remained unknown. To furtherly illuminate it, we next detected the change of p-p38, p-JNK and p-stat3 in $RAGE^{-/-}$ astrocytes. The result displayed that phosphorylation of p38, JNK and stat3 in $RAGE^{-/-}$ astrocytes were weakened after HMGB1 (1μg/ml) stimulation for 10 min (**Figures 3D–G**). The above data revealed that the effect of HMGB1 on promoting shh release from astrocytes was through signal pathway stat3, JNK and p38 mediated by receptor RAGE.

HMGB1 Promote Shh Expression in EAE

However, whether HMGB1 could induce shh expression in EAE is unknown. Next we use glycyrrhizin (GL), a HMGB1 inhibitor, to further detect it *in vivo*. Based on our previous study (34), dose of 25 mg/kg glycyrrhizin (GL) was used in this study. As shown in **Figure 4**, GL (25mg/kg) treatment by intraperitoneal (i.p.) on the onset stage of EAE restrained shh expression compared to normal saline group (**Figures 4A, B**). The data indicated that HMGB1 could promote shh expression in EAE.

Shh Treatment Alleviated the Progress of EAE

In MS/EAE, shh can act on endothelial cells to repair blood brain barrier (BBB). In our study, the progress of EAE was alleviated when recombinant shh protein by intracerebroventricular injection was performed from onset to peak stage of EAE

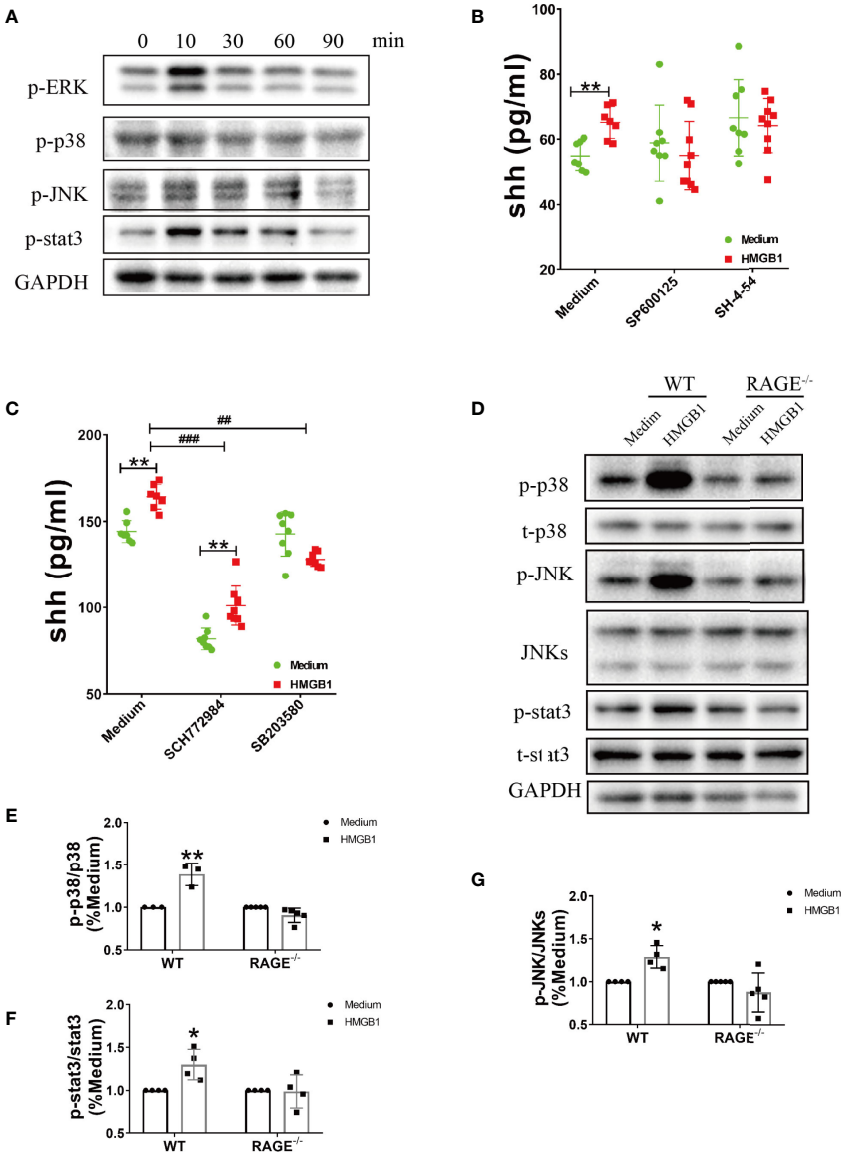

FIGURE 3 | The signal pathways involved in the effect of HMGB1 on promoting shh release from astrocytes through receptor RAGE. **(A)** The change of phosphorylation-ERK, p38, JNK and stat3 after HMGB1 (1μg/ml) stimulation. **(B, C)** The effect of JNK blocker (5μM SP 600125), stat3 blocker (10μM SH-4-54), ERK blocker (2μM SCH 772984) and p38 blocker (3μM SB 203580) on shh release from astrocytes after HMGB1 (1μg/ml) stimulation for 10 min. **(D)** The change of phosphorylation-p38, JNK and stat3 after HMGB1 (1μg/ml) stimulation for 10 min in RAGE$^{-/-}$ astrocytes comparing to WT astrocytes. **(E–G)** Data analysis for panel **(D)**. Data are shown as mean ± SD (*$P < 0.05$, **$P < 0.01$ compared with medium; $^{\#\#}P < 0.01$, $^{\#\#\#}P < 0.001$ compared with each other).

(**Figure 5A**). Besides, demyelination during chronic stage was ameliorated in shh group, compared to saline group (**Figure 5B**). The data indicated that shh played a protective role in EAE.

DISCUSSION

Multiple sclerosis (MS) and related animal models-experimental autoimmune encephalomyelitis (EAE) is an autoimmune disease of the central nervous system (CNS), during which damaged neurons can release large amounts of HMGB1 (7). In 1999, Wang et al. found that HMGB1 played an important role as a late mediator of endotoxin lethality (35). Since then, numerous researches focused on the pro-inflammatory effects of HMGB1 in various diseases, including MS/EAE. However, increasing studies indicated that DAMPs are not only dangerous signals after tissue damage, but also proteins that can repair tissue (9, 13, 14). It has been demonstrated that HMGB1 can promote the regeneration of new tissues by recruiting stem cells after its pro-inflammatory activity in some diseases (36–39). Therefore, the exact role of HMGB1 remains to be further explored.

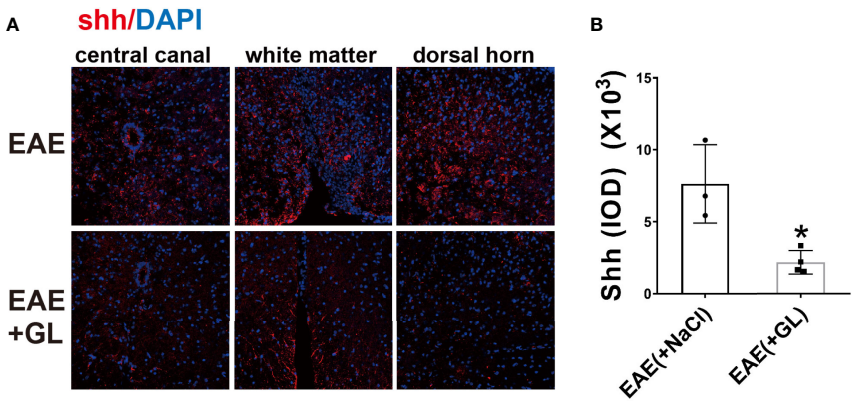

FIGURE 4 | The effect of HMGB1 inhibitor (glycyrrhizin, GL) on the expression of shh in EAE. GL (25mg/kg) was injected intraperitoneally (i.p.) on the onset stage of EAE and the spinal cord tissues were collected on the peak stage. **(A)** Immunofluorescence was used to detect the expression of shh in CNS. Images are representative of 3 or 4 mice in each group and **(B)** data are shown as mean ± SD. (*$P < 0.05$).

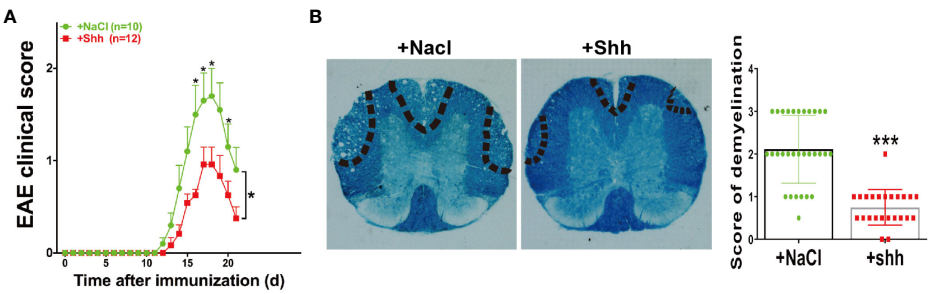

FIGURE 5 | The effect of shh on the progress of EAE. **(A)** Shh protein treatment was applied on the onset stage of EAE and the clinical score was observed across the progress of EAE. Data are shown as mean ± SEM. **(B)** LFB staining was used to study the demyelination of the spinal cord sections. The sections were obtained on the remission stage of EAE (images are representative of 4-5 mice in each group). The bar denotes 200 μm. Data (n = 3-5 mice in each group, and 5–6 sections from each mouse were used for LFB staining and scoring) are shown as mean ± SD. (*$P < 0.05$, ***$P < 0.001$).

In MS/EAE, abundance of immune cells infiltrate into CNS, accompanied by demyelination, axonal damage, and local inflammation (40). As we know, the peripheral immune cells can infiltrate into CNS only when blood brain barrier (BBB) was damaged (41). The BBB is composed of capillary endothelial cells, basement membrane, and glial boundary membrane (the terminal protuberance of astrocytes adhere to the capillary wall to form a glial boundary membrane) (42). The connection between endothelial cells directly determines the permeability of BBB (43). For astrocytes, it not only forms a secondary barrier that further restricts entry of peripheral immune cells into CNS, but also maintains the integrity of BBB through self-secreting cytokines (43–46). When encountering disease, astrocytes can promote the differentiation of endothelial cells by secreting cytokines such as TGF-β, GNDF, bFGF, VEGF, angiopoietin, and then promote tissue repair furtherly (38, 47–51). In MS/EAE, sonic hedgehog (shh) was largely expressed in astrocytes (24, 52) and shh from astrocytes can act on endothelial cells by receptor ptch1, reducing their permeability and repairing BBB (53, 54). In our study, we were the first to demonstrate that HMGB1 could promote shh release in astrocytes.

Due to its sulfhydryl in C23, C45 and C106 are easily oxidized by active oxygen, HMGB1 has different isoforms. In EAE, the level of reactive oxygen increased on the peak stage and decreased on the chronic stage (55, 56), indicating it was highly possible that the redox state of HMGB1 varied in EAE. HMGB1 under different redox state would bind to different receptors and play different roles (13, 14). To further investigate the underling mechanism of shh release promoted by HMGB1, we used gene knockout mice. We noticed that spontaneous shh release from astrocytes existed and the level of shh in wild type astrocytes was higher than that in $TLR2^{-/-}$, $TLR4^{-/-}$, $RAGE^{-/-}$ astrocytes. It indicated that the spontaneous release of shh was dependent on TLR2, TLR4 and RAGE. But the effect of HMGB1 on shh release was weakened only when RAGE receptor was knockout. Considering that gene knockout may bring unknown side effects, we further verified the above result using receptor blocking agents. Consistently, HMGB1 could not promote shh release after receptor RAGE was blocked. The result implied

that the promoting effect of shh release from astrocytes *via* HMGB1 was mediated by RAGE. Together with other study that HMGB1 promoted axon growth by binding to RAGE in spinal cord injury (57), HMGB1 may play a protective role in disease *via* promoting shh release through receptor RAGE.

As for the possible signal pathway involved in HMGB1-RAGE axis, MAP kinases (JNK, p38, ERK) and stat3 were activated (58). In our results, only the addition of inhibitors for p38, JNK and stat3 could furtherly suppress the release of shh from astrocytes after HMGB1 administration. And the phosphorylation of p38, JNK and stat3 was inhibited in $RAGE^{-/-}$ knockout astrocytes, compared to wild type astrocytes. The results indicated that the effect of HMGB1-RAGE-shh axis may be closely related with p38, JNK and stat3. Moreover, NF-κB signal pathway was also involved in HMGB1-RAGE axis in CNS and participated in neuroinflammation (59–61). It provided another possibility for HMGB1-RAGE-shh axis in astrocytes. Further researches are needed to explore the possibility.

In other reports, some agents attenuating MS/EAE was related to increased shh (62), we further proved it *via* shh protein treatment in EAE mice. Accordingly, shh treatment alleviated the progress of EAE, providing a direct evidence for its protective role in EAE. Considering the phenomenon of HMGB1 promoting shh release, HMGB1 may play a protective role in some way during the course of EAE. However, numerous study proved that HMGB1 exerted negative effects in EAE overall. Our data suggest a novel effect of HMGB1, providing a new understanding of DAMPs.

CONCLUSION

HMGB1 promoted shh release from astrocytes through RAGE and its downstream (p38, JNK and stat3), which may indicated a new role of HMGB1 in EAE.

DATA AVAILABILITY STATEMENT

The raw data supporting the conclusions of this article will be made available by the authors, without undue reservation.

ETHICS STATEMENT

The animal study was reviewed and approved by the Institutional Animal Care and Use Committee, Tongji Medical College, Huazhong University of Science and Technology.

AUTHOR CONTRIBUTIONS

FZ worked on conception and design. YFX performed the majority of the experiments. YS assisted to make EAE animal mode. WL, FFZ, JS, JL, HC, CT, YX, ZT, and FG contributed to the experimentation. YFX wrote the paper. FZ supervised the project, revised the manuscript, and financed the study. All authors contributed to the article and approved the submitted version.

FUNDING

This work was supported by the grant awarded by the National Natural Science Foundation of China (Grant No. 31670876, 31470852) to FZ, and National Natural Science Foundation of China (Grant No. 82001281) to YFX.

SUPPLEMENTARY MATERIAL

The Supplementary Material for this article can be found online at: https://www.frontiersin.org/articles/10.3389/fimmu.2021.584097/full#supplementary-material

Supplementary Figure 1 | The effect of HMGB1 (2μg/ml) stimulation on cell viability. Data are shown as mean ± SD.

Supplementary Figure 2 | The change of total TLR4 protein expression in astrocytes after HMGB1 (2μg/ml) stimulation was analyzed by Western blot. Data are shown as mean ± SD (***$P < 0.001$).

Supplementary Figure 3 | The variation tendency of phosphorylation-**(A)** ERK, **(B)** stat3, **(C)** p38 and **(D)** JNK after HMGB1 (1μg/ml) stimulation for different time. Data are shown as mean ± SD (*$P < 0.05$ compared with 0 min).

Supplementary Figure 4 | The blocking effect of JNK blocker (SP 600125), stat3 blocker (SH-4-54), ERK blocker (SCH 772984) and p38 blocker (SB 203580) in different concentrations after HMGB1 (1μg/ml) stimulation for 10 min.

REFERENCES

1. Robinson AP, Caldis MW, Harp CT, Goings GE, Miller SD. High-mobility group box 1 protein (HMGB1) neutralization ameliorates experimental autoimmune encephalomyelitis. *J Autoimmun* (2013) 43:32–43. doi: 10.1016/j.jaut.2013.02.005
2. Lu B, Antoine DJ, Kwan K, Lundbäck P, Wähämaa H, Schierbeck H, et al. JAK-STAT1 signaling promote HMGB1 hyperacetylation and nuclear translocation. *PNAS* (2014) 111:6. doi: 10.1073/pnas.1316925111
3. Zhang Q, Wang Y. HMG modifications and nuclear function. *Biochim Biophys Acta (BBA) - Gene Regul Mech* (2010) 1799(1-2):28–36. doi: 10.1016/j.bbagrm.2009.11.009
4. Bonaldi T, Talamo F, Scaffidi P, Ferrera D, Porto A, Bachi A, et al. A Agresti and M EBianchi. Monocytic cells hyperacetylate chromatin protein HMGB1 to redirect it towards secretion. *EMBO* (2003) 22:10. doi: 10.1093/emboj/cdg516
5. Andersson A, Covacu R, Sunnemark D, Danilov AI, Dal Bianco A, Khademi M, et al. Pivotal advance: HMGB1 expression in active lesions of human and experimental multiple sclerosis. *J Leukoc Biol* (2008) 84(5):1248–55. doi: 10.1189/jlb.1207844
6. Rosciszewski G, Cadena V, Murta V, Lukin J, Villarreal A, Roger T, et al. Toll-Like Receptor 4 (TLR4) and Triggering Receptor Expressed on Myeloid Cells-2 (TREM-2) Activation Balance Astrocyte Polarization into a Proinflammatory Phenotype. *Mol Neurobiol* (2018) 55(5):3875–88. doi: 10.1007/s12035-017-0618-z
7. Sun Y, Chen H, Dai J, Zou H, Gao M, Wu H, et al. HMGB1 expression patterns during the progression of experimental autoimmune encephalomyelitis. *J Neuroimmunol* (2015) 280:29–35. doi: 10.1016/j.jneuroim.2015.02.005
8. Fang P, Pan HC, Lin SL, Zhang WQ, Rauvala H, Schachner M, et al. HMGB1 contributes to regeneration after spinal cord injury in adult zebrafish. *Mol Neurobiol* (2014) 49(1):472–83. doi: 10.1007/s12035-013-8533-4

9. Rong LL, Gooch C, Szabolcs M, Herold KC, Lalla E, Hays AP, et al. RAGE: a journey from the complications of diabetes to disorders of the nervous system - striking a fine balance between injury and repair. *Restor Neurol Neurosci* (2005) 23(5-6):355–65.
10. Taguchi A, Blood DC, del Toro G, Canet A, Lee DC, Qu W, et al. Blockade of RAGE-amphoterin signalling suppresses tumour growth andmetastases. *Nature* (2000) 405:7. doi: 10.1038/35012626
11. Zhao X, Kuja-Panula J, Rouhiainen A, Chen YC, Panula P, Rauvala H. High mobility group box-1 (HMGB1; amphoterin) is required for zebrafish brain development. *J Biol Chem* (2011) 286(26):23200–13. doi: 10.1074/jbc.M111.223834
12. Hayakawa K, Pham LD, Katusic ZS, Arai K, Lo EH. Astrocytic high-mobility group box 1 promotes endothelial progenitor cell-mediated neurovascular remodeling during stroke recovery. *Proc Natl Acad Sci U S A* (2012) 109 (19):7505–10. doi: 10.1073/pnas.1121146109
13. Venereau E, Ceriotti C, Bianchi ME. DAMPs from Cell Death to New Life. *Front Immunol* (2015) 6:422. doi: 10.3389/fimmu.2015.00422
14. Bianchi ME, Crippa MP, Manfredi AA, Mezzapelle R, Rovere Querini P, Venereau E. High-mobility group box 1 protein orchestrates responses to tissue damage via inflammation, innate and adaptive immunity, and tissue repair. *Immunol Rev* (2017) 280(1):74–82. doi: 10.1111/imr.12601
15. Tang D, Billiar TR, Lotze MT. A Janus tale of two active high mobility group box 1 (HMGB1) redox states. *Mol Med* (2012) 18:1360–2. doi: 10.2119/molmed.2012.00314
16. Zhu L, Ren L, Chen Y, Fang J, Ge Z, Li X. Redox status of high-mobility group box 1 performs a dual role in angiogenesis of colorectal carcinoma. *J Cell Mol Med* (2015) 19(9):2128–35. doi: 10.1111/jcmm.12577
17. Balosso S, Liu J, Bianchi ME, Vezzani A. Disulfide-containing high mobility group box-1 promotes N-methyl-D-aspartate receptor function and excitotoxicity by activating Toll-like receptor 4-dependent signaling in hippocampal neurons. *Antioxid Redox Signal* (2014) 21(12):1726–40. doi: 10.1089/ars.2013.5349
18. Yang H, Wang H, Ju Z, Ragab AA, Lundback P, Long W, et al. MD-2 is required for disulfide HMGB1-dependent TLR4 signaling. *J Exp Med* (2015) 212(1):5–14. doi: 10.1084/jem.20141318
19. Khakh BS, Sofroniew MV. Diversity of astrocyte functions and phenotypes in neural circuits. *Nat Neurosci* (2015) 18(7):942–52. doi: 10.1038/nn.4043
20. Ponath G, Park C, Pitt D. The Role of Astrocytes in Multiple Sclerosis. *Front Immunol* (2018) 9:217. doi: 10.3389/fimmu.2018.00217
21. Hooper JE, Scott MP. Communicating with Hedgehogs. *Nat Rev Mol Cell Biol* (2005) 6(4):306–17. doi: 10.1038/nrm1622
22. De Luca A, Cerrato V, Fuca E, Parmigiani E, Buffo A, Leto K. Sonic hedgehog patterning during cerebellar development. *Cell Mol Life Sci* (2016) 73(2):291–303. doi: 10.1007/s00018-015-2065-1
23. Alvarez JI, Dodelet-Devillers A, Kebir H, Ifergan I, Fabre PJ, Terouz S, et al. The Hedgehog pathway promotes blood-brain barrier integrity and CNS immune quiescence. *Science* (2011) 334(6063):1727–31. doi: 10.1126/science.1206936
24. Wang Y, Imitola J, Rasmussen S, O'Connor KC, Khoury SJ. Paradoxical dysregulation of the neural stem cell pathway sonic hedgehog-Gli1 in autoimmune encephalomyelitis and multiple sclerosis. *Ann Neurol* (2008) 64(4):417–27. doi: 10.1002/ana.21457
25. Seifert T, Bauer J, Weissert R, Fazekas F, Storch MK. Differential expression of sonic hedgehog immunoreactivity during lesion evolution in autoimmune encephalomyelitis. *J Neuropathol Exp Neurol* (2005) 64(5):404–11. doi: 10.1093/jnen/64.5.404
26. Zhang J, Chen J, Li Y, Cui X, Zheng X, Roberts C, et al. Niaspan treatment improves neurological functional recovery in experimental autoimmune encephalomyelitis mice. *Neurobiol Dis* (2008) 32(2):273–80. doi: 10.1016/j.nbd.2008.07.011
27. Akazawa C, Tsuzuki H, Nakamura Y, Sasaki Y, Ohsaki K, Nakamura S, et al. The upregulated expression of sonic hedgehog in motor neurons after rat facial nerve axotomy. *J Neurosci Off J Soc Neurosci* (2004) 24(36):7923–30. doi: 10.1523/JNEUROSCI.1784-04.2004
28. Stromnes IM, Goverman JM. Active induction of experimental allergic encephalomyelitis. *Nat Protoc* (2006) 1(4):1810–9. doi: 10.1038/nprot.2006.285
29. Chen H, Sun Y, Lai L, Wu H, Xiao Y, Ming B, et al. Interleukin-33 is released in spinal cord and suppresses experimental autoimmune encephalomyelitis in mice. *Neuroscience* (2015) 308:157–68. doi: 10.1016/j.neuroscience.2015.09.019
30. Sun Y, Chen H, Dai J, Wan Z, Xiong P, Xu Y, et al. Glycyrrhizin Protects Mice Against Experimental Autoimmune Encephalomyelitis by Inhibiting High-Mobility Group Box 1 (HMGB1) Expression and Neuronal HMGB1 Release. *Front Immunol* (2018) 9:1518. doi: 10.3389/fimmu.2018.01518
31. Giulian D, Baker TJ, Shih LC, Lachman LB. Interleukin 1 of the central nervous system is produced by ameboid microglia. *J Exp Med* (1986) 164 (2):594–604. doi: 10.1084/jem.164.2.594
32. Li TL, Qin KW, Li N, Han CF, Cao XT. An endosomal LAPF is required for macrophage endocytosis and elimination of bacteria. *P Natl Acad Sci USA* (2019) 116(26):12958–63. doi: 10.1073/pnas.1903896116
33. Rosadini CV, Kagan JC. Early innate immune responses to bacterial LPS. *Curr Opin Immunol* (2017) 44:14–9. doi: 10.1016/j.coi.2016.10.005
34. Sun Y, Chen HY, Dai JP, Wan ZJ, Xiong P, Xu Y, et al. Glycyrrhizin Protects Mice Against Experimental Autoimmune Encephalomyelitis by Inhibiting High-Mobility Group Box 1 (HMGB1) Expression and Neuronal HMGB1 Release. *Front Immunol* (2018) 9:1518. doi: 10.3389/fimmu.2018.01518
35. Wang H. HMG-1 as a Late Mediator of Endotoxin Lethality in Mice. *Science* (1999) 285(5425):248–51. doi: 10.1126/science.285.5425.248
36. Zhang X, Jiang H, Gong Q, Fan C, Huang Y, Ling J. Expression of high mobility group box 1 in inflamed dental pulp and its chemotactic effect on dental pulp cells. *Biochem Biophys Res Commun* (2014) 450(4):1547–52. doi: 10.1016/j.bbrc.2014.07.027
37. Meng E, Guo Z, Wang H, Jin J, Wang J, Wang H, et al. High mobility group box 1 protein inhibits the proliferation of human mesenchymal stem cells and promotes their migration and differentiation along osteoblastic pathway. *Stem Cells Dev* (2008) 17(4):805–13. doi: 10.1089/scd.2007.0276
38. Tamai K, Yamazaki T, Chino T, Ishii M, Otsuru S, Kikuchi Y, et al. PDGFRalpha-positive cells in bone marrow are mobilized by high mobility group box 1 (HMGB1) to regenerate injured epithelia. *Proc Natl Acad Sci U.S.A.* (2011) 108(16):6609–14. doi: 10.1073/pnas.1016753108
39. Ranzato E, Patrone M, Pedrazzi M, Burlando B. Hmgb1 promotes wound healing of 3T3 mouse fibroblasts via RAGE-dependent ERK1/2 activation. *Cell Biochem Biophys* (2010) 57(1):9–17. doi: 10.1007/s12013-010-9077-0
40. Rossi B, Constantin G. Live Imaging of Immune Responses in Experimental Models of Multiple Sclerosis. *Front Immunol* (2016) 7:506. doi: 10.3389/fimmu.2016.00506
41. Muldoon LL, Alvarez JI, Begley DJ, Boado RJ, Del Zoppo GJ, Doolittle ND, et al. Immunologic privilege in the central nervous system and the blood-brain barrier. *J Cereb Blood Flow Metab* (2013) 33(1):13–21. doi: 10.1038/jcbfm.2012.153
42. Banks WA. From blood-brain barrier to blood-brain interface: new opportunities for CNS drug delivery. *Nat Rev Drug Discovery* (2016) 15 (4):275–92. doi: 10.1038/nrd.2015.21
43. Almutairi MM, Gong C, Xu YG, Chang Y, Shi H. Factors controlling permeability of the blood-brain barrier. *Cell Mol Life Sci* (2016) 73(1):57–77. doi: 10.1007/s00018-015-2050-8
44. Kuchler-Bopp S, Delaunoy JP, Artault JC, Zaepfel M, Dietrich JB. Astrocytes induce several blood-brain barrier properties in non-neural endothelial cells. *Neuroreport* (1999) 10(6):1347–53. doi: 10.1097/00001756-199904260-00035
45. Janzer RC, Raff MC. Astrocytes induce blood-brain barrier properties in endothelial cells. *Nature* (1987) 325(6101):253–7. doi: 10.1038/325253a0
46. Willis CL, Nolan CC, Reith SN, Lister T, Prior MJ, Guerin CJ, et al. Focal astrocyte loss is followed by microvascular damage, with subsequent repair of the blood-brain barrier in the apparent absence of direct astrocytic contact. *Glia* (2004) 45(4):325–37. doi: 10.1002/glia.10333
47. Abbott NJ, Rönnbäck L, Hansson E. Astrocyte–endothelial interactions at the blood–brain barrier. *Nat Rev Neurosci* (2006) 7(1):41–53. doi: 10.1038/nrn1824
48. Liddelow S, Barres B. SnapShot: Astrocytes in Health and Disease. *Cell* (2015) 162(5):1170– e1. doi: 10.1016/j.cell.2015.08.029
49. Jia Y, Wu D, Zhang R, Shuang W, Sun J, Hao H, et al. Bone marrow-derived mesenchymal stem cells expressing the Shh transgene promotes functional recovery after spinal cord injury in rats. *Neurosci Lett* (2014) 573:46–51. doi: 10.1016/j.neulet.2014.05.010
50. Li Y, Xia Y, Wang Y, Mao L, Gao Y, He Q, et al. Sonic hedgehog (Shh) regulates the expression of angiogenic growth factors in oxygen-glucose-deprived astrocytes by mediating the nuclear receptor NR2F2. *Mol Neurobiol* (2013) 47(3):967–75. doi: 10.1007/s12035-013-8395-9
51. He QW, Xia YP, Chen SC, Wang Y, Huang M, Huang Y, et al. Astrocyte-derived sonic hedgehog contributes to angiogenesis in brain microvascular

endothelial cells via RhoA/ROCK pathway after oxygen-glucose deprivation. *Mol Neurobiol* (2013) 47(3):976–87. doi: 10.1007/s12035-013-8396-8
52. Seifert T, Bauer J, Weissert R, Fazekas F, Storch MK. Differential Expression of Sonic Hedgehog Immunoreactivity During Lesion Evolution in Autoimmune Encephalomyelitis. *J Neuropathol Exp Neurol* (2005) 64(5):8. doi: 10.1093/jnen/64.5.404
53. Ivan Alvarez J, Dodelet-Devillers A, Kebir H, Ifergan I, Fabre PJ, Terouz S, et al. The Hedgehog Pathway Promotes Blood-Brain Barrier Integrity and CNS Immune Quiescence. *Science* (2011) 334:5. doi: 10.1126/science.1206936
54. Wang Y, Jin S, Sonobe Y, Cheng Y, Horiuchi H, Parajuli B, et al. Interleukin-1beta induces blood-brain barrier disruption by downregulating Sonic hedgehog in astrocytes. *PloS One* (2014) 9(10):e110024. doi: 10.1371/journal.pone.0110024
55. Dimitrijevic M, Kotur-Stevuljevic J, Stojic-Vukanic Z, Vujnovic I, Pilipovic I, Nacka-Aleksic M, et al. Sex Difference in Oxidative Stress Parameters in Spinal Cord of Rats with Experimental Autoimmune Encephalomyelitis: Relation to Neurological Deficit. *Neurochem Res* (2017) 42(2):481–92. doi: 10.1007/s11064-016-2094-7
56. Wang D, Li SP, Fu JS, Zhang S, Bai L, Guo L. Resveratrol defends blood-brain barrier integrity in experimental autoimmune encephalomyelitis mice. *J Neurophysiol* (2016) 116(5):2173–9. doi: 10.1152/jn.00510.2016
57. Wang H, Mei X, Cao Y, Liu C, Zhao Z, Guo Z, et al. HMGB1/Advanced Glycation End Products (RAGE) does not aggravate inflammation but promote endogenous neural stem cells differentiation in spinal cord injury. *Sci Rep* (2017) 7(1):10332. doi: 10.1038/s41598-017-10611-8
58. Taguchi A, Blood DC, del Toro G, Canet A, Lee DC, Qu W, et al. Blockade of RAGE-amphoterin signalling suppresses tumour growth and metastases. *Nature* (2000) 405(6784):354–60. doi: 10.1038/35012626
59. Rosciszewski G, Cadena V, Auzmendi J, Cieri MB, Lukin J, Rossi AR, et al. Detrimental Effects of HMGB-1 Require Microglial-Astroglial Interaction: Implications for the Status Epilepticus -Induced Neuroinflammation. *Front Cell Neurosci* (2019) 13:380. doi: 10.3389/fncel.2019.00380
60. Han R, Liu Z, Sun N, Liu S, Li L, Shen Y, et al. BDNF Alleviates Neuroinflammation in the Hippocampus of Type 1 Diabetic Mice via Blocking the Aberrant HMGB1/RAGE/NF-kappaB Pathway. *Aging Dis* (2019) 10(3):611–25. doi: 10.14336/AD.2018.0707
61. Huang M, Guo M, Wang K, Wu K, Li Y, Tian T, et al. HMGB1 Mediates Paraquat-Induced Neuroinflammatory Responses via Activating RAGE Signaling Pathway. *Neurotox Res* (2020) 37(4):913–25. doi: 10.1007/s12640-019-00148-1
62. Zhang J, Zhang ZG, Li Y, Ding X, Shang X, Lu M, et al. Fingolimod treatment promotes proliferation and differentiation of oligodendrocyte progenitor cells in mice with experimental autoimmune encephalomyelitis. *Neurobiol Dis* (2015) 76:57–66. doi: 10.1016/j.nbd.2015.01.006

Conflict of Interest: The authors declare that the research was conducted in the absence of any commercial or financial relationships that could be construed as a potential conflict of interest.

frontiers in Neurology

ORIGINAL RESEARCH
published: 01 June 2021
doi: 10.3389/fneur.2021.540660

Nerve Growth Factor Enhances Tooth Mechanical Hyperalgesia Through C-C Chemokine Ligand 19 in Rats

Rui Guo[1,2], Yiyin Chen[1], Lu Liu[1], Jing Wen[1], Hong Yang[1], Yafen Zhu[1], Meiya Gao[1], Hengyan Liang[1], Wenli Lai[1] and Hu Long[1]**

[1] State Key Laboratory of Oral Diseases and National Clinical Research Center for Oral Diseases and Department of Orthodontics, West China Hospital of Stomatology, Sichuan University, Chengdu, China, [2] Beijing Stomatological Hospital, School of Stomatology, Capital Medical University, Beijing, China

The nerve growth factor (NGF) plays an important role in the regulation of neuropathic pain. It has been demonstrated that calcitonin gene-related peptide (CGRP), a well-known contributor to neurogenic inflammation, increases neuroinflammatory pain induced by NGF. The inflammatory mediator that NGF most strongly induces is C-C chemokine ligand 19 (CCL19), which can recruit inflammatory cells by binding to the receptor CCR7 followed by promoting the response of neuroinflammation. However, the regulatory mechanism of NGF and CCL19 in tooth movement orofacial pain and the interaction between both are still unclear. In this study, male Sprague–Dawley rats were used to study the modulation of NGF on orofacial pain through CCL19 and the role of each in tooth movement pain in rats. The expression levels of CCL19 mRNA and protein were determined by real-time PCR and immunofluorescence, respectively. Pain levels were assessed by measuring the rats' bite force, which drops as pain rises. Meanwhile, by verifying the relationship between CGRP and CCL19, it was laterally confirmed that NGF could modulate tooth movement-induced mechanical hyperalgesia through CCL19. The results showed that the expression level of CCL19 rose with the increased NGF, and neurons expressing CGRP can express stronger CCL19. Compared with the baseline level, the bite force for all rats dropped sharply on day 1, reached its lowest level on day 3, and recovered gradually on day 5. All results indicated that NGF played an important role in tooth movement orofacial pain *via* positively regulating CCL19 expression in the trigeminal ganglia of rats. Additionally, CCL19 increased the sensitivity to experimental tooth movement orofacial pain. NGF can regulate CCL19 expression, although it may regulate other inflammatory pathways as well. This is the first report on the interactions and modulations of tooth movement orofacial pain by NGF through CCL19 in rats.

Keywords: nerve growth factor, tooth movement pain, C-C chemokine ligand 19, trigeminal ganglion, rat

OPEN ACCESS

Edited by:
Waldiceu A. Verri, State University of Londrina, Brazil

Reviewed by:
Koichi Iwata, Nihon University, Japan
Gilson Goncalves Dos Santos, University of California, San Diego, United States
Olga Anna Korczeniewska, The State University of New Jersey, United States

***Correspondence:**
Wenli Lai
wenlilai@scu.edu.cn
Hu Long
hlong@scu.edu.cn

Specialty section:
This article was submitted to Multiple Sclerosis and Neuroimmunology, a section of the journal Frontiers in Neurology

Received: *05 March 2020*
Accepted: *29 March 2021*
Published: *01 June 2021*

Citation:
Guo R, Chen Y, Liu L, Wen J, Yang H, Zhu Y, Gao M, Liang H, Lai W and Long H (2021) Nerve Growth Factor Enhances Tooth Mechanical Hyperalgesia Through C-C Chemokine Ligand 19 in Rats. Front. Neurol. 12:540660. doi: 10.3389/fneur.2021.540660

INTRODUCTION

Maxillofacial inflammatory pain caused by orthodontics presents as discomfort, dull pain, and hypersensitivity of the teeth. It is generated by the gradual tooth movement induced by orthodontic forces and the ensuing inflammatory reaction of periodontal tissue (1–3). In response to the periodontal inflammation, numerous leucocytes and inflammatory cells are recruited to and

activated in periodontal tissues where they release abundant inflammatory mediators, chemokines, and cytokines including but not limited to nerve growth factor (NGF), tumor necrosis factor-alpha3, interleukin-1 (IL-1), IL-6, prostaglandins, interferon-gamma, and macrophage-colony stimulating factors, and ultimately result in tooth movement along with pain (4–8). Among these mediators, NGF is a target-derived neurotrophic factor that is mainly distributed within peripheral nerve tissue (9). It plays a critical role in the sensitization of sensory neurons to pain induced by peripheral nerve injury, especially in the trigeminal ganglion (TG) (10–12). In the course of the inflammatory reaction of periodontal tissue, activated mast cells release a massive amount of NGF that binds to tyrosine kinase A (TrkA). The NGF–TrkA complex is retrogradely transported to the TG and activates neurons as well as satellite glial cells (SGC) through interstitial links followed by upregulating NGF expression (13, 14). Elevated NGF augments maxillofacial pain by changing the expression of ion channels and neuropeptides in the TG (15, 16). Blocking NGF function by periodontal injection of anti-NGF antibody can completely abolish the orthodontic pain, whereas periodontal administrations of NGF can mimic the pain (17). All these findings indicate that NGF plays an important role in the pain regulation caused by tooth movement during orthodontic treatment.

In a previous study, we found that NGF participated in the modulation of orofacial pain (17). The ensuing periodontal tissue inflammation is accompanied by upregulated expression of a series of inflammatory mediators including CC chemokine ligand 19 (CCL19), chemokine (C-X-C motif) ligand 17 (CXCL17), CCL12, CXCL10, CXCL12, IL-15, CCL11, CXCL1, and IL-5 as identified both by isobaric tags for relative and absolute quantitation and by Bio-Plex bead microarray analysis. Among these meditators, CCL19 is expressed at the highest level (18). CCL19 is a small cytokine in the CCL chemokine family that is thought to maintain homeostasis in the internal environment of cells (19). It is usually involved in various inflammatory disorders and recognized as one of the pain-causing chemokines that promote neuroinflammatory responses and regulate pain by recruiting inflammatory cells after binding to its receptor, CCR7 (20, 21).

It is well-known that calcitonin gene-related peptide (CGRP) is evidenced to participate in the initiation and maintenance of inflammatory pain (22). Our previous study has demonstrated that CGRP participates in orthodontic pain following experimental tooth movement (6). Recent research has also proved that increased nociceptive neuropeptide expression is most certainly involved as NGF has been associated with the upregulation of CGRP, leading to neuroinflammatory pain response (23, 24). At present, relatively little is known about the relationship between CCL19 and NGF expression in oral and maxillofacial pain, and the role of NGF in combination with CCL19 in tooth movement pain is still unclear. However, if we can verify that CCL19 and CGRP have the same variation trend with NGF in tooth movement pain when exploring the relationship between CCL19 and NGF, we may hypothesize that NGF modulates tooth movement-induced mechanical hyperalgesia through CCL19. Therefore, in the current study, we extend our original observations in rats across multiple time points by inoculating NGF or anti-NGF antibody, NGF plus anti-CCL19 antibody, and anti-NGF antibody plus CCL19, respectively, to study the role of CCL19 in the regulation of orthodontic pain caused by NGF.

MATERIALS AND METHODS

Animals

Two hundred and thirty-two male Sprague–Dawley rats with body mass of 200–250 g were obtained from the Animal Experimental Center at Sichuan University. They were maintained in the animal facility in an air-conditioned room at 21°C with a 12-h light–dark cycle. Standard rat chow and water were provided *ad libitum*. Animal experiments were performed in accordance with protocols that were approved by the Ethics Committee of the State Key Laboratory of Oral Diseases, Sichuan University (protocol no. WCHSIRB-D-2016-201).

As shown in **Supplementary Figure 1**, in our first study, to determine the effect of NGF injected into the TGs on CCL19 expression in the TGs after tooth movement, a total of 132 rats were used. Of these, 108 were randomly assigned to three groups of 36 each for the detection of CCL19 mRNA expression by quantitative polymerase chain reaction (qPCR): force + NGF (group 1), force + anti-NGF antibody (group 2), and force + normal saline (group 3). The remaining 24 rats were randomly divided into two groups of 12 each for the measurement of CCL19 protein expression by immunofluorescence: force + NGF (group 4) and force + normal saline (group 5). In the second study, to determine the functional role and contribution of elevated CCL19 levels on pain induced by tooth movement, 24 rats were randomly assigned to three groups of 8 rats each: force + CCL19 (group 6), force + anti-CCL19 antibody (group 7), and force + normal saline (group 8) (**Supplementary Figure 2**). In the third study, to investigate the effect of NGF on CCL19 expression following tooth movement, as displayed in **Supplementary Figure 3**, 40 rats were randomly assigned to five groups of 8 rats each: force + NGF (group 9), force + anti-NGF antibody (group 10), force + NGF + anti-CCL19 antibody (group 11), force + anti-NGF antibody + CCL19 (group 12), and force + normal saline (group 13). Moreover, to verify by immunofluorescence that NGF modulates tooth movement-induced mechanical hyperalgesia through CCL19, 36 rats were randomly divided into 6 groups: force + NGF (group 14), force + anti-NGF antibody (group 15), force + normal saline (group 16), pseudo-force + NGF (group 17), pseudo-force + anti-NGF antibody (group 18), and pseudo-force + normal saline (group 19) (**Supplementary Figure 4**). To induce tooth movement, every rat was anesthetized with intraperitoneal injection of 7% chloral hydrate in normal saline solution at 0.06 $ml \cdot g^{-1} \cdot$body weight, after which a Ni–Ti alloy closed-coil spring was fixed in place with ligation wires (0.2 mm in diameter) between the left maxillary first molar and the upper incisor. The fixed spring in all force groups delivered a 40 g force as measured by a force meter (Xinya, Hangzhou, China) to simulate steady orthodontic forces inducing tooth movement, while a 0 g force was used for all the pseudo-force groups. Rats in groups 1–13

were euthanized by decapitation after being anesthetized with pentobarbital sodium (50 mg·kg^{-1}·body weight) on days 0, 1, 3, 5, 7, and 14 ($n = 6$ per group per day), while rats in groups 14–19 were all sacrificed on day 3. Those rats that were euthanized on day 0 without receiving any interventions serve as the baseline controls for each study. All sections of this report adhere to the ARRIVE guidelines for reporting animal research (25).

TG Injection

A microsyringe with a dose of 20 μl was used in trigeminal ganglion injection. The injection point was located at the midpoint of the line between the rat's left condylar and the posterior edge of the ascending ramus of the left mandible. The trigeminal ganglion was reached 9 mm after the injection needle was inserted at the injection site. Specific injection procedures have been reported in the previous literature (26).

For the study of NGF effects on CCL19 in the TGs, 10 μl aliquots of recombinant murine β-NGF (Peprotech, USA) and anti-NGF antibody (Abcam, UK) solutions at concentrations of 0.1 μg/μl in phosphate buffered saline (PBS, pH 7.1) for each were inoculated into the TG in groups 1 (force + NGF), 2 (force + anti-NGF antibody), and 3 (force + normal saline), respectively, on days 1, 3, 5, 7, and 14 following the experimental tooth movement. Meanwhile, animals in each group that were neither injected reagents nor had force on day 0 were used as the baseline controls. On each injection day, all rats in these three groups were injected, and six rats in each group were euthanized 6 h after inoculation on days 0, 1, 3, 5, 7, and 14. TGs were harvested and rapidly placed in liquid nitrogen for PCR and immunofluorescence assay. For the study of CCL19 effects on tooth movement-induced pain, the baseline bite force for all animals in groups 6 (force + CCL19), 7 (force + anti-CCL19 antibody), and 8 (force + normal saline) was measured before spring fixation. This was followed by inoculations into the TGs of 10 μl of 0.6 μg/μl recombinant rat CCL19 beta protein (R&D Systems, USA) in PBS, 10 μl of 0.6 μg/μl rat CCL19 beta antibody (R&D Systems, USA) in PBS, or 10 μl of normal saline solution on days 1, 3, 5, 7, and 14. For the study of the activation of CCL19 expression by NGF as well as the interactions between both, rats in groups 9 (force + NGF), 10 (anti-NGF antibody), 11 (force + NGF + anti-CCL19 antibody), 12 (force + anti-NGF antibody + CCL19), and 13 (force + normal saline) received TG inoculations of 10 μl of NGF solution, 10 μl of anti-NGF antibody solution, 10 μl of NGF solution plus 10 μl of anti-CCL19 antibody solution, 10 μl of anti-NGF antibody solution plus 10 μl of CCL19 solution, or 10 μl of normal saline, respectively, on days 1, 3, 5, 7, and 14 after a baseline of bite force testing on day 0 followed by applying the orthodontic force to induce tooth movement. It should be noted that the injection of either anti-CCL19 antibody in group 11 or CCL19 in group 12 was given 2 h after either NGF or anti-NGF antibody injection. Lastly, for the study of NGF regulating tooth movement pain through CCL19, rats in groups 14 (force + NGF), 15 (force + anti-NGF antibody), 16 (force + normal saline), 17 (pseudo-force + NGF), 18 (pseudo-force + anti-NGF antibody), and 19 (pseudo-force + normal saline) received TG injections of 10 μl of NGF solution, 10 μl of anti-NGF antibody solution, or 10 μl normal saline on days 1 and 3, respectively, after the establishment of the tooth movement model.

Real-Time RT-PCR Assay

Total RNA was extracted from TGs using TaKaRa Minibest Universal RNA Extraction Kit (Takara, Shiga, Japan) according to the manufacturer's protocols. Then, cDNA was reverse transcribed using the PrimeScript^{TM} RT reagent kit with gDNA Eraser (Perfect Real Time) kit (TaKaRa, Shiga, Japan) following the manufacturer's recommendations.

Rat CCL19 mRNA expression was quantified in TG samples using triplex RT-PCR performed in a LightCycler480 (Roche, Switzerland) RT-PCR platform with TB Green^{TM} Premix Ex Taq (Perfect Real Time, TaKaRa, Dalian, China) according to the manufacturer's protocol. To quantify specific mRNA expression in the samples, a standard curve was generated for normal rat TG samples, and GAPDH served as an internal standard, using specific primers for rat GAPDH (forward primer CCAGCAAGGATACTGAGAGCAAG, reverse primer TGATGGTATTCGAGAGAAGGGAGG, expected size: 114 bp) and CCL19 (forward primer TAACGATGCGGAAGACTGCT, reverse primer CTGGTAGCCCCTTAGTGTGG, expected size: 139 bp). The final 20 μl reaction volume consisted of 10 μl of TB Green^{TM} Premix Ex Taq, 0.8 μl of the 10 μM primer mix, 4 μl of the reverse transcription nucleic acid template, and 5.2 μl of RNase-free H_2O. The thermal profile was set at 95°C for 30 s and 95°C for 5 s, followed by 40 cycles at 60°C for 30 s and 72°C for 30 s. Relative mRNA transcript level calculations were performed using the comparative CT method (ΔΔCT). The average CT values of the three complex holes for each sample were calculated and marked as CT_{CCL19} and CT_{GAPDH}, $\Delta\Delta CT = N(CT_{CCL19} - CT_{GAPDH}) - (CT_{CCL19} - CT_{GAPDH})$.

Immunofluorescence Assay

For CCL19 protein detection, TGs embedded in OCT were cut at 10 μm thickness along the TG long axis in a freezing microtome (Thermo Shandon, USA). The sections were rinsed with Tris-buffered saline Tween (TBST) three times for 5 min, underwent microwave-based antigen retrieval, and blocked with blocking buffer (Cell Signaling Technology, USA) for 60 min. Thereafter, the sections were stained with a primary mouse anti-CCL19/MIP-3 beta antibody (R&D Systems, USA) and incubated overnight at 45°C followed by rinsing with PBS (pH 7.1) three times for 5 min. The sections were further stained with an immunofluorescent rabbit anti-goat IgG secondary antibody (Bioss, Beijing, China), incubated for 1 h at 37°C, rinsed with PBS, and finally mounted onto slides for observation under a fluorescence microscope (Carl Zeiss, Goettingen, Germany). Images were taken by a Nikon Eclipse E400 microscope (Tokyo, Japan) and ImageJ 1.51 software was employed to analyze the average gray scale of each immunofluorescence image as the expression of CCL19 protein in the TG. The gray level of fluorescence immunoreactivity for CCL19 protein in the TG was taken as the mean of three measurements from three different areas of the slide.

Meanwhile, we used the same immunofluorescence protocols mentioned above to verify that the neurons expressing CGRP

protein can also express CCL19 protein. The sections of TG tissues obtained from groups 14 to 19 were stained with primary rabbit anti-CGRP (D5R8F)/mAb antibody (Cell Signaling Technology, USA) and primary mouse anti-CCL19/MIP-3 beta antibody (R&D Systems, USA), respectively.

Bite Force Measurement

The bite force of rats was determined following the protocols described previously (17). Briefly, after 1 week of acclimatization to the animal facility, rats were trained to bite the sensor (Nanjing, China) to obtain the baseline bite force. The next day, the spring to induce tooth movement was fixed in place. Thereafter, bite force was measured 6 h after inoculation of reagents into the TG on days 1, 3, 5, 7, and 14 following spring fixation, with triplicate measurements made for each rat. Changes in average bite force of triplicate measurements for each rat between prior and after inoculation interventions were recorded.

Statistical Analyses

Statistical analyses were performed using SPSS 16.0 (SPSS, Chicago, Illinois, USA) and GraphPad Prism 7.0 software (GraphPad Software, San Diego, USA). The results are presented as mean ± standard deviation (SD). Student's *t*-test was used to compare the average gray scale of CGRP and CCL19 immunofluorescence in different groups at the same time point. A two-way ANOVA and a *post hoc* test were used to examine the effects of time (0, 1, 3, 5, 7, and 14 days) on the expression of CCL19 or bite force in the same group, the effects of different injections on the expression of CCL19 or bite force at the same time point, and the interactions with both time and the injection of reagents. For the two-group comparisons at each time interval, the Bonferroni *post hoc* test was used if the pretest for normality was not rejected at the 0.05 significance level. p-values < 0.05 were considered statistically significant.

RESULTS

NGF Upregulates CCL19 Expression in Trigeminal Ganglia

As displayed in **Figure 1**, a two-way ANOVA with repeated measures revealed that the expression levels of CCL19 mRNA were significantly influenced by group ($p = 0.0021 < 0.01$), time ($p = 0.0121 < 0.05$), and interactions ($p = 0.0001 < 0.01$). The level of CCL19 mRNA expression in rats' TG on day 0 (1.000 ± 0.000) obtained following the tooth movement pain model development was used as the baseline control. The mRNA expression level of CCL19 in rats injected with NGF increased sharply on day 1 (2.120 ± 0.085, $p = 0.0001 < 0.001$), remained at a high level on day 3 (2.060 ± 0.453, $p = 0.0001 < 0.001$), and decreased to the baseline level on day 5 (1.170 ± 0.042, $p > 0.05$), day 7 (1.345 ± 0.106, $p > 0.05$), and day 14 (0.980 ± 0.099, $p > 0.05$). By contrast, the mRNA expression level of CCL19 in rats' TG injected with anti-NGF antibody was significantly lower than the baseline level on the 1st day (0.280 ± 0.057, $p = 0.0006 < 0.001$), the 3rd day (0.605 ± 0.304, $p = 0.0332 < 0.05$), the 5th day (0.445 ± 0.007, $p = 0.0042 < 0.01$), the 7th day (0.190 ± 0.104, $p = 0.0003 < 0.001$), and the 14th day (0.565 ± 0.021, $p = 0.0196 < 0.05$). Meanwhile, the mRNA expression level of CCL19 in rats' TG in the control group injected with normal saline also showed a decreasing trend, falling on the 1st day (0.665 ± 0.163, $p = 0.0736 > 0.05$), reached to the lowest on the 3rd day (0.425 ± 0.007, $p = 0.0033 < 0.01$), briefly on the 5th day (1.090 ± 0.212, $p = 0.9107 > 0.05$), declined again on the 7th day (0.535 ± 0.191, $p = 0.013$, $p < 0.05$), and finally returned to the baseline level on the 14th day (1.015 ± 0.106, $p = 0.9998 > 0.05$).

Comparing CCL19 mRNA levels on days following NGF injections vs. normal saline injections, expression was significantly higher on days 1 ($p = 0.0001 < 0.01$), 3 ($p = 0.0001 < 0.01$), and 7 ($p = 0.0002 < 0.01$), but not different on days 5 and 14 ($p > 0.05$). On the other hand, comparing CCL19 mRNA levels on days following anti-NGF injections vs. normal saline injections, expression was significantly lower on days 5 ($p = 0.0019 < 0.01$) and 14 ($p = 0.0276 < 0.05$). Finally, comparing CCL19 mRNA levels on days following NGF injections vs. anti-NGF injections, expression was significantly higher on every injection day ($p = 0.0001 < 0.05$ for days 1–7, $p = 0.0434 < 0.05$ for day 14) (**Table 1**).

Immunofluorescent staining demonstrated the localization of CCL19 protein expression in TGs. Relative to the weak staining of CCL19 in group 5 (force + normal saline) saline-injected TGs, many CCL19-positive neurons were present in the TG in

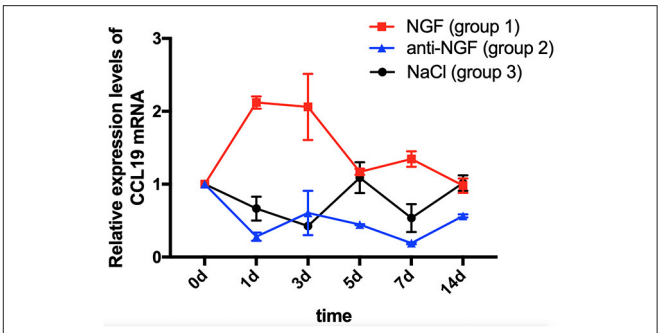

FIGURE 1 | Time course of C-C chemokine ligand 19 (CCL19) mRNA expression in rats' TGs following the injection of nerve growth factor (NGF)-related reagents. (The statistical analysis results related to the image are shown in **Table 1**).

TABLE 1 | *p*-value of C-C chemokine ligand 19 (CCL19) mRNA expression in rats' TGs following the injection of nerve growth factor (NGF)-related reagents.

Time intervals	Group 1 (NGF) vs. group 2 (anti-NGF)	Group 1 (NGF) vs. group 3 (NaCl)	Group 2 (anti-NGF) vs. group 3 (NaCl)
0 day	ns	ns	ns
1 day	<0.0001****	<0.0001****	ns
3 days	<0.0001****	<0.0001****	ns
5 days	0.0006***	ns	0.0019**
7 days	<0.0001****	0.0002***	ns
14 days	<0.0434*	ns	0.0276*

*$p < 0.05$, **$p < 0.01$, ***$p < 0.001$, ****$p < 0.0001$, ns: $p > 0.05$.
The variation tendency related to the statistical analysis results is shown in ***Figure 1****.*

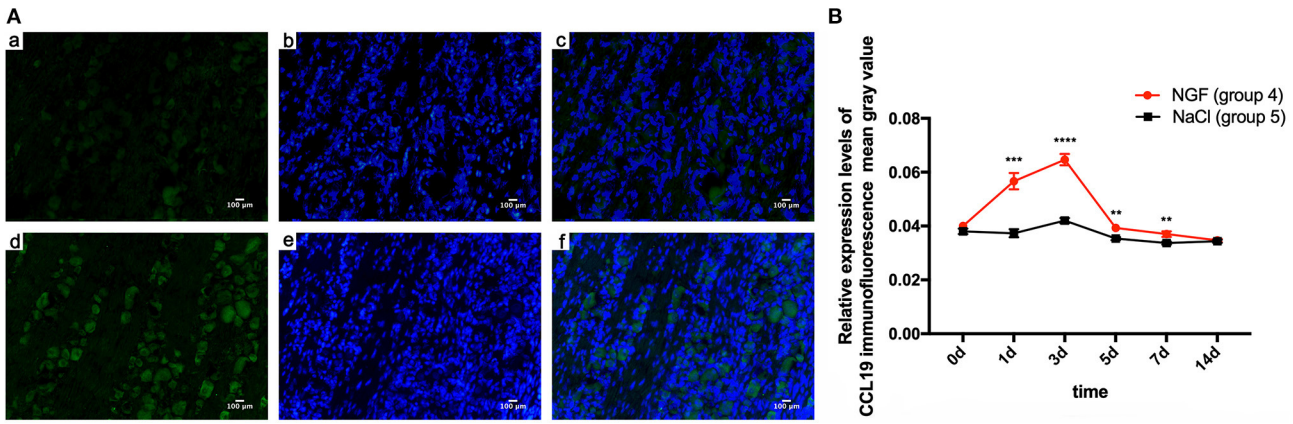

FIGURE 2 | (**A**) Immunofluorescence results of CCL19 protein expression after injection of NGF or normal saline into rats' trigeminal ganglia (TGs) 3 days after initiation of tooth movement. (**a**) Neurons expressing CCL19 (green) after injection of normal saline on day 3 after initiation of tooth movement. (**b**) Nuclei (blue) after injection of normal saline on day 3. (**c**) Overlap of (**A**) and (**B**). (**d–f**) The same labeling as in (**a–c**) but after injection of NGF on day 3. (**B**) Time course of CCL19 protein expression in TGs following the injection of NGF or normal saline after experimental tooth movement. $^{*}p < 0.05$, $^{**}p < 0.01$, $^{***}p < 0.001$, $^{****}p < 0.0001$.

group 4 (force + NGF) NGF-injected TGs on days 1 and 3, with intensity being the highest on day 3 (**Figure 2A**). Two-way ANOVA revealed that CCL19 immunoreactivity in the TG was significantly influenced by group ($p = 0.0001 < 0.01$), time ($p = 0.0001 < 0.01$), and interaction ($p = 0.0001 < 0.01$).

Taking the mean gray value of immunofluorescence of CCL19 protein in rats' TG receiving NGF injection (group 4) on day 0 (0.040 ± 0.000) as the baseline, CCL19 immunoreactivity increased sharply on day 1 (0.057 ± 0.003, $p = 0.0001 < 0.01$), reached to its peak on day 3 (0.065 ± 0.002, $p = 0.0001 < 0.01$), then quickly declined on day 5 (0.039 ± 0.001, $p = 0.9768 > 0.05$), day 7 (0.037 ± 0.001, $p = 0.0450 < 0.05$), and day 14 (0.035 ± 0.001, $p = 0.0003 < 0.001$). On the other hand, the immunoreactivity of CCL19 protein in TG for saline-injected rats (group 5) was similar to the baseline on day 1 (0.037 ± 0.002, $p = 0.9768 > 0.05$), slightly increased on day 3 (0.042 ± 0.001, $p = 0.0050 < 0.01$), gradually decreased on days 5 (0.035 ± 0.001, $p = 0.0891 > 0.05$), and then dropped below baseline on day 7 (0.034 ± 0.001, $p = 0.0024 < 0.01$) and day 14 (0.034 ± 0.001, $p = 0.0106 < 0.05$). Further comparison analysis between group 4 and group 5 showed that the CCL19 protein fluorescence intensity in group 4 was significantly higher than that of group 5 on days 1 ($p = 0.0006 < 0.001$), 3 ($p < 0.0001$), 5 ($p = 0.0058 < 0.01$), and 7 ($p = 0.0075 < 0.01$) (**Figure 2B**). Hence, CCL19 protein in TGs with NGF inoculation was significantly higher than that with saline injection, consistent with the findings for CCL19 mRNA expression.

In our previous studies, we found that the orthodontic tooth movement-induced pain was most notable on the 3rd day following tooth movement (17, 27). Therefore, we conducted a further study on the expression of CGRP and CCL19 in the trigeminal ganglion of rats specifically on the 3rd day after tooth movement. As shown in **Figure 3A**, the expression level of CGRP was significantly higher in the force + NGF group (group 14) than in the force + anti-NGF group (group 15) and the force + saline group (group 16) ($p < 0.0001$). The expression of CGRP in group 15 and group 16 was also statistically significant ($p = 0.0134 < 0.05$). Immunoreactivity of CGRP protein in TGs for pseudo-forced rats in the pseudo-force + NGF group (group 17) was much higher than that of rats in the pseudo-force + anti-NGF group (group 18) ($p < 0.0001$) and the pseudo-force + saline group (group 19) ($p = 0.0005 < 0.001$), while the expression level of CGRP in group 18 was lower than that of rats in group 19 ($p = 0.0011 < 0.01$). In the meantime, the immunofluorescence protein expression of CGRP in rats in the forced group 14 was higher than that of rats in the pseudo-forced group 17 ($p = 0.0003 < 0.001$), as well as in group 15 and group 18 ($p = 0.0026 < 0.01$).

The trend of immunofluorescence expression of CCL19 in rats' trigeminal ganglia was similar to that of CGRP, as displayed in **Figure 3B**. The mean gray value of immunofluorescence observed in rats' trigeminal ganglia was the highest in group 14 among groups 14–19 ($p < 0.0001$ for group 14 vs. group 15, $p = 0.0001 < 0.001$ for group 14 vs. group 16, and $p = 0.0201 < 0.05$ for group 14 vs. group 17). Furthermore, the expression level of CCL19 immunofluorescence in forced rats' TGs injected with anti-NGF antibody in group 15 was significantly lower than that of rats injected with normal saline in group 16 ($p = 0.0271 < 0.05$). Similarly, rats in pseudo-forced group 17 with NGF injection expressed more CCL19 protein than the rats in group 18 ($p = 0.0293 < 0.05$) and group 19 ($p = 0.0334 < 0.05$).

One-way ANOVA showed that CGRP immunoreactivity in the TG of different groups on day 3 was statistical different among groups 14–19 ($p = 0.0022 < 0.01$) and the p-value of CCL19 protein expression was $0.0051 < 0.01$. Meanwhile, using two-way ANOVA with repeated measures, it can be observed that the immunofluorescence expression levels were significantly influenced by groups ($p < 0.0001$) and target stain protein ($p < 0.0001$). It is worth noting that on the 3rd day, the mean gray value of immunofluorescence of CCL19 protein in trigeminal ganglion of rats was higher than that of CGRP protein in groups 14–19 (all $p < 0.0001$) (**Figure 3C**).

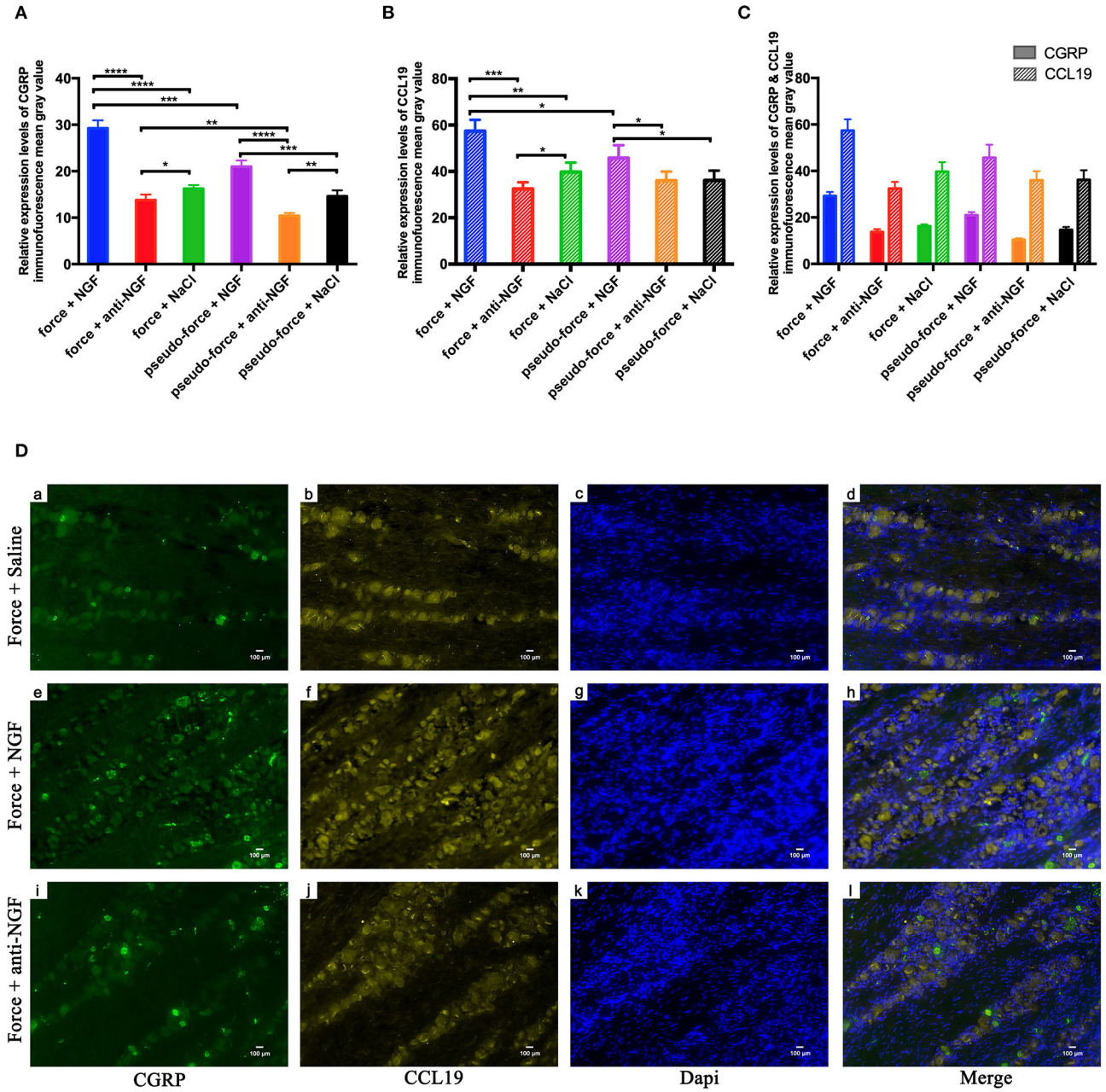

FIGURE 3 | (**A**) Calcitonin gene-related peptide (CGRP) protein expression levels in TGs following different interventions after experimental tooth movement. (**B**) CCL19 protein expression levels in TGs following different interventions after experimental tooth movement. (**C**) Comparison of immunofluorescence mean gray value of CGRP and CCL19 relative expression. (**D**) Immunofluorescence results of protein expression after injection on NGF, anti-NGF antibody, and normal saline into forced rats' TGs on the 3rd day after tooth movement. (**a, e, i**) Neurons expressing CGRP (green) after injection of related reagents. (**b, f, j**) Neurons expressing CCL19 (yellow). (**c, g, k**) Nuclei (blue) after injection of related reagents on day 3. (**d, h, l**) Overlap of (**a + b + c**), (**e + f + g**), and (**i + j + k**). $^{*}p < 0.05$, $^{**}p < 0.01$, $^{***}p < 0.001$, $^{****}p < 0.0001$.

It can be seen in **Figure 3D** that the neurons stained with CGRP also express CCL19. Meanwhile, it can also be observed that the expression intensity of CCL19 and CGRP in the trigeminal ganglion of rats injected with NGF was significantly higher than that of rats injected with anti-NGF antibody and normal saline.

Effect of CCL19 in Rats' TG on Orofacial Pain Induced by Tooth Movement

Bite force was employed to assess the level of mechanical hyperalgesia in teeth as recorded by an occlusal force tester (Nanjing, China) and expected to decrease to the degree when biting induces pain. A two-way repeated measures ANOVA

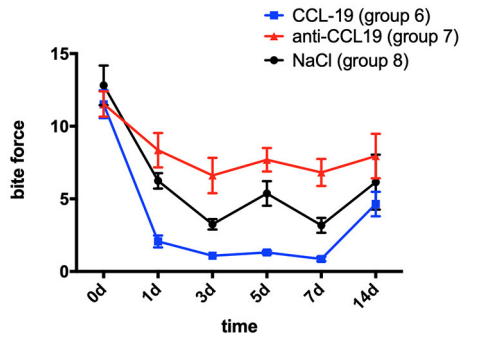

FIGURE 4 | Changes in pain expressed as the bite force of rats over time after injection of CCL19 and anti-CCL19 antibody. (The statistical analysis results related to the image are shown in **Table 2**).

TABLE 2 | *p*-value of bite force of rats over time after injection of CCL19 and anti-CCL19 antibody.

Time intervals	Group 6 (CCL19) vs. group 7 (anti-CCL19)	Group 6 (CCL19) vs. group 8 (NaCl)	Group 7 (anti-CCL19) vs. group 8 (NaCl)
0 day	ns	ns	ns
1 day	<0.0001****	0.0065**	ns
3 days	0.0002***	ns	0.0361*
5 days	<0.0001****	0.0084**	ns
7 days	<0.0001****	ns	0.0208*
14 days	0.0399*	ns	ns

*$p < 0.05$, **$p < 0.01$, ***$p < 0.001$, ****$p < 0.0001$, ns: $p > 0.05$.
*The variation tendency related to the statistical analysis results is shown in **Figure 4**.*

showed that bite force in all groups was significantly influenced by group ($p = 0.0001 < 0.01$), time ($p = 0.0001 < 0.01$), and interactions ($p = 0.0144 < 0.05$).

In comparison with the baseline level measured on day 0 (11.512 ± 2.692), the bite force of rats with CCL19 inoculation (group 6) plummeted on day 1 (2.069 ± 1.155, $p < 0.0001$) and continued to decrease on day 3 (1.086 ± 0.658, $p < 0.0001$), slightly rose on day 5 (1.308 ± 0.366, $p < 0.0001$), reached its lowest level on day 7 (0.864 ± 0.445, $p < 0.0001$), and then recovered but still lower than the baseline on day 14 (4.463 ± 2.375, $p < 0.0001$) (**Figure 4**). Regarding the bite force of rats in group 7 (force + anti-CCL19 antibody), it dropped sharply on the 1st day (8.351 ± 3.360, $p = 0.0482 < 0.0001$), declined to its lowest level on the 3rd day (6.608 ± 3.435, $p = 0.0006 < 0.01$), increased slightly on the 5th day (7.689 ± 2.288, $p = 0.0111 < 0.05$), decreased a little on the 7th day (6.819 ± 2.638, $p = 0.0012 < 0.01$), and gradually raised to near the baseline on the 14th day (7.950 ± 4.334, $p = 0.0203 < 0.05$) in comparison with the baseline of bite force measured on day 0 (11.512 ± 2.460). In the meantime, the bite force of rats in group 8 (force + normal saline) significantly decreased on day 1 (6.244 ± 1.501, $p < 0.0001$), dropped to the lowest on day 3 (3.249 ± 1.016, $p < 0.0001$), increased slightly on day 5 (5.371 ± 2.403, $p < 0.0001$), continued to decrease on day 7 (3.179 ± 1.443, $p < 0.0001$), and then rose but still below the baseline on day 14 (6.152 ± 5.351, $p < 0.0001$), compared with those of baseline on day 0 (12.815 ± 3.863). Representative bite patterns are shown in **Supplementary Figure 5**.

Rats with anti-CCL19 antibody inoculation (group 7) shared similar trends of bite force with rats in group 6 but at a much higher level ($p < 0.0001$ for days 1, 5, and 7, respectively, $p = 0.0002 < 0.05$ for day 3, and $p = 0.0399 < 0.05$ for day 14). Additionally, as displayed in **Figure 4**, the bite force in group 6 was significantly lower than that of the saline controls (group 8) on day 1 ($p = 0.0065 < 0.01$) and day 5 ($p = 0.0084 < 0.01$). Therefore, the lowest bite force following tooth movement was found in rats inoculated with CCL19, while the highest one was found in rats with anti-CCL19 antibody inoculation. It is noteworthy that elevated bite force was seen in rats injected with anti-CCL19 antibody as compared with saline on day 3 ($p = 0.0361 < 0.05$) and day 7 ($p = 0.0208 < 0.05$). All these results illustrate that CCL19 has a positive sensitization to experimental tooth movement pain in rats. Details of significant statistical differences are shown in **Table 2**.

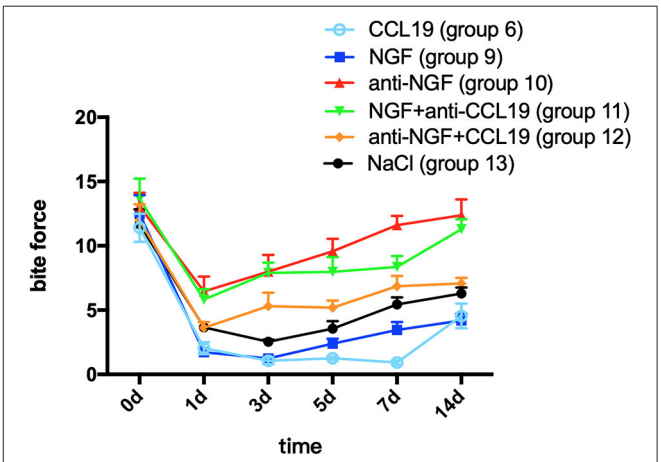

FIGURE 5 | Changes in pain expressed as the bite force modulated by NGF *via* CCL19 over time. (The statistical analysis results related to the image are shown in **Table 3**).

Regulation of CCL19 Expression and Its Interaction With NGF Following Tooth Movement

A two-way repeated measures ANOVA analysis showed that bite force in groups 9 (force + NGF), 10 (force + anti-NGF antibody), 11 (force + NGF + anti-CCL19 antibody), 12 (force + anti-NGF antibody + CCL19), and 13 (force + normal saline) was significantly influenced by group ($p < 0.0001$), time ($p < 0.0001$), and interactions ($p = 0.0016 < 0.01$). In comparison with baseline bite force measured before spring fixation on day 0, the bite force of rats in group 9 with NGF inoculation decreased sharply on day 1 (1.719 ± 0.816, $p = 0.0001 < 0.01$), declined to a minimum on day 3 (1.248 ± 0.364, $p = 0.0001 < 0.01$), and

slightly increased on day 5 (2.390 ± 1.107, $p = 0.0001 < 0.01$), day 7 (3.466 ± 1.740, $p = 0.0001 < 0.01$), and day 14 (4.194 ± 1.495, $p = 0.0001 < 0.01$) although still well-below baseline. As shown in **Figure 5**, similar trends in bite force were observed across study days for rats injected with anti-NGF (group 10), NGF + anti-CCL19 (group 11), and anti-NGF antibody + CCL19 (group 12). Compared with the baseline on day 0 (13.054 ± 3.052), the bite force of rats injected with anti-NGF (group 10) dropped to its lowest value on the 1st day (6.459 ± 3.234, $p < 0.0001$), increased slightly on the 3rd day (7.997 ± 3.664, $p = 0.0002 < 0.001$) and the 5th day (9.568 ± 2.731, $p = 0.0252 < 0.05$), and returned to the baseline level on the 7th day (11.607 ± 2.021, $p = 0.7869 > 0.05$) and the 14th day (12.372 ± 3.500, $p = 0.9901 > 0.05$). For rats injected with NGF + anti-CCL19 antibody in group 11, the bite force measured on each time interval was 5.820 ± 2.254 ($p < 0.0001$) for the 1st day, 7.894 ± 2.243 ($p < 0.0001$) for the 3rd day, 7.971 ± 3.286 ($p < 0.0001$) for the 5th day, 8.364 ± 2.388 ($p < 0.0001$) for the 7th day, and 11.287 ± 2.216 ($p = 0.2853 > 0.05$) for the 14th day, respectively, in comparison with the baseline level of 13.646 ± 4.472 obtained on day 0. For rats injected with anti-NGF antibody + CCL19 in group 12, the bite force decreased sharply on day 1 (3.631 ± 1.271, $p < 0.0001$) and continued to increase on day 3 (5.309 ± 2.972, $p < 0.0001$), day 5 (5.191 ± 1.550, $p < 0.0001$), day 7 (6.860 ± 2.252, $p = 0.0001 < 0.001$), and day 14 (7.081 ± 1.199, $p = 0.0003 < 0.001$) but still well-below the baseline level of 11.971 ± 3.549 measured on day 0.

In terms of the regulation of CCL19 expression by NGF in experimental tooth movement pain, a two-way repeated measures ANOVA revealed that the bite force of rats injected with NGF alone (group 9) was much lower than that of rats injected with NGF + anti-CCL19 (group 11) on day 1 ($p = 0.0096 < 0.01$), day 3 ($p = 0.0001 < 0.01$), day 5 ($p = 0.0001 < 0.01$), day 7 ($p = 0.0010 < 0.01$), and day 14 ($p = 0.0001 < 0.01$). Meanwhile, the bite force of rats injected with anti-NGF alone (group 10) was significantly higher than that of rats injected with anti-NGF antibody + CCL19 (group 12) on day 5 ($p = 0.0046 < 0.01$), day 7 ($p = 0.0016 < 0.01$), and day 14 ($p = 0.0003 < 0.01$). In addition, it can be found that the bite force of rats injected with anti-NGF antibody + CCL19 (group 12) was much higher than that of rats injected with CCL19 alone (group 6) on day 1 ($p = 0.0222 < 0.05$), day 3 ($p = 0.0015 < 0.01$), day 5 ($p < 0.0001$), day 7 ($p < 0.0001$), and day 14 ($p = 0.0213 < 0.05$), respectively (**Table 3**). Also, as shown in **Figure 5**, rats injected with NGF (group 9) and rats injected with CCL19 (group 6) both expressed low level bite force measurement values, but there was no statistical difference between these two groups. Therefore, NGF, at least but not unique, is involved in the pain signaling pathways activated by orthodontic treatment *via* regulation of CCL19 expression.

TABLE 3 | *p*-value of bite force of rats over time after injection of CCL19/NGF-related reagents.

Time intervals	Group 9 (NGF) vs. group 11 (NGF + anti-CCL19)	Group 10 (anti-NGF) vs. group 12 (anti-NGF + CCL19)	Group 6 (CCL19) vs. group 12 (anti-NGF + CCL19)
0 day	ns	ns	ns
1 day	0.0096**	ns	0.0222*
3 days	<0.0001****	ns	0.0015**
5 days	0.0001***	0.0046**	<0.0001****
7 days	0.0010***	0.0016**	<0.0001****
14 days	<0.0001****	0.0003***	0.0213*

*$p < 0.05$, **$p < 0.01$, ***$p < 0.001$, ****$p < 0.0001$, ns: $p > 0.05$.
The variation tendency related to the statistical analysis results is shown in ***Figure 5****.*

DISCUSSION

Orthodontic pain arising from the periodontal inflammatory responses induced by orthodontic forces is a very common complaint. Previous studies have shown that the trigeminal ganglion can produce a large number of inflammatory factors following tooth movement pain (28, 29). These inflammatory factors alter the biological activity of the neurons in the trigeminal ganglia, increasing excitability of neurons (30, 31), leading to thermal and mechanical sensitivity to pain (32, 33). Increased expression of chemokines including CCL2, CXCL9, and CXCL10 is of particular interest because they promote synovial inflammation by stimulating leukocyte migration and are known to be involved in orofacial neuropathic pain (34, 35). A positive correlation between their concentration in the TGs and orofacial pain induced by orthodontic treatment has been reported (36). To our best knowledge, this is the first report of CCL19 expression and regulation as well as its functional role in tooth movement-induced pain generation in a rat model.

CCL19, also known as macrophage inflammatory protein-3β and EBI-1 ligand chemokine, is a small cytokine belonging to the C-C chemokine family. Increased expression of CCL19 can promote inflammatory responses (37). Our data emphasize that inoculation of CCL19 into the TG after spring fixation aggravates tooth movement-induced pain, whereas the anti-CCL19 antibody can reduce the pain. Specifically, elevation of CCL19 mRNA and protein levels following spring fixation-induced tooth movement was significantly associated with increased pain as reflected in reduced bite force, while injections of anti-CCL19 provided pain relief. Thus, CCL19 plays a crucial role in nervous system sensitization in inflammation-associated tooth movement-induced orofacial pain.

As a protein involved in the growth of neurons and the repair of nerve tissues, NGF plays an important role in pain regulation. The expression of this protein can be upregulated by damage to peripheral axons and retrogradely transported to the central processes of sensory neurons (13). Specifically, in the process of experimental tooth movement in rats, trigeminal nerve endings of the periodontal ligament were damaged, followed by the upregulation of NGF expression in rats' periodontal membrane (38). The signals were then transmitted in reverse to the trigeminal ganglia, which activated the neurons located in the trigeminal ganglia. The neurons then activated the satellite glial

cells and led to upregulated NGF expression in TG (14). NGF mRNA and protein are expressed in the neurons and satellite glial cells of the TGs as can be seen with *in situ* hybridization and immunocytochemistry, respectively.

There are many biological mechanisms of NGF-induced trunk mechanical hyperalgesia. Recent studies have shown that NGF is related to the upregulation of CGRP in dorsal root ganglion and spinal dorsal horn (23). CGRP is a well-known contributor to persistent neurogenic inflammation (22). Activation of CGRP receptors located at the terminals of primary afferent neurons can reduce the activation threshold of secondary neurons, increasing the synaptic strength between nociceptors and spinal dorsal horn neurons, which ultimately promote mechanical and thermal sensitization. Eventually, these changes in intracellular signaling pathways contribute to persistent hyperalgesia. Therefore, by studying the relationship between CCL19 and CGRP, the interaction between CCL19 and NGF in tooth movement pain in rats can be laterally verified.

Our previous study found that NGF may regulate tooth movement pain in the trigeminal ganglia through the pro-neuroinflammatory response pathway (18). The expression of multiple inflammatory mediators was upregulated by NGF-induced tooth movement pain. Regarding the interactions between NGF and CCL19 expression, pairwise comparison showed that expression of CCL19 mRNA and protein in rats in the presence of NGF is significantly higher than in controls, while the expression of CCL19 mRNA and protein in rats with anti-NGF inoculation was much lower than in controls. Similarly, our published data also indicate that rats show a significantly reduced "functional status" of bite force due to tooth movement pain compared with their controls (17). In this experiment, we also found that the expression levels of CCL19 in the force groups were higher than those in the pseudo-force groups. Meanwhile, after the injection of NGF and CCL19, respectively, the corresponding rats both showed extremely low level of bite force measurement values. All these results suggest that CCL19 is specifically linked to orofacial pain induced by tooth movement. In addition to the above research findings, the experimental results of groups 14–19 showed that the immunofluorescence expression intensity of CCL19 changed with the injection of NGF-related reagents. Besides, CCL19 can be expressed in the trigeminal ganglion neurons of rats with CGRP expression, and the immunoactivity of the former was stronger than that of the latter, indicating that NGF can modulate tooth movement-induced mechanical hyperalgesia through CCL19. These results further validate our hypothesis that the increased NGF can significantly upregulate the expression of inflammatory mediator CCL19 in rats' TG. The increased CCL19 expression further facilitates the response to neuroinflammation and releases more inflammatory factors, amplifying and augmenting the pain induced by tooth movement. Therefore, neutralization of NGF or CCL19 will be an option for the relief of pain induced by orthodontic tooth movement.

Moreover, rats injected with NGF + anti-CCL19 antibody (group 11) present significantly higher bite force than those injected with NGF alone (group 9). This indicates that tooth movement pain sensitized by NGF can be alleviated by blocking CCL19. Thus, we can suppose that CCL19 is a downstream signaling pathway of NGF and NGF regulates tooth movement pain through CCL19. Meanwhile, CCL19 may also be regulated by other inflammatory factors that affect tooth movement pain. This hypothesis was proposed owing to the fact that the bite force of rats injected with NGF + anti-CCL19 antibody should be consistent with that of rats injected with normal saline because the antibody against CCL19 neutralized the pain caused by NGF, if CCL19 is only regulated by NGF. Actual results contrary to the above speculation obtained in the present study suggest that the expression of CCL19 may also be regulated by other inflammatory factors other than NGF. Similarly, by comparing the bite force of rats injected with anti-NGF antibody (group 10), anti-NGF antibody + CCL19 (group 12), and NS (group 13), we can conclude that the modulation of tooth movement pain by NGF may also be through other pathways besides CCL19.

Limitations of this study include the lack of *in vitro* study with cells. Further studies are needed to determine the relationship between the expression of this chemokine with the postoperative prognosis of orthodontic treatment, as well as to determine whether NGF regulates not only CCL19 but also other related molecular pathways that mediate tooth movement pain.

In conclusion, this study investigated the molecular mechanism of pain induced by tooth movement based on a rat model. Firstly, CCL19 expression levels in rats' TGs were studied by qPCR and immunofluorescence. It was confirmed that NGF positively regulated CCL19 expressions. Secondly, CCL19 in TGs plays an important role in tooth movement-induced orofacial pain in rats measured by bite force, which can objectively reflect the changes of pain levels. Finally, we continue to use this test as an indicator to elucidate the modulation mechanisms of experimental tooth movement orofacial pain by NGF through CCL19 pathway in rats.

DATA AVAILABILITY STATEMENT

All datasets generated for this study are included in the article/**Supplementary Material**.

ETHICS STATEMENT

The animal study was reviewed and approved by the ethical committee of the state key laboratory of oral diseases, Sichuan University.

AUTHOR CONTRIBUTIONS

RG, JW, HY, YZ, MG, and HLi carried out the experiment. RG, YC, and HLo analyzed the data, discussed the results, and drafted the manuscript in consultation with WL. HLo offered domain knowledge in the design of the system. WL conceived the study and was in charge of overall direction and planning.

RG, LL, HLo, and WL critically revised and commented on the manuscript. All authors contributed to the article and approved the submitted version.

FUNDING

This work was supported by Sichuan Science and Technology Program (Nos. 2021YJ0428, 2018JY0558, and 2018SZ0232) and by the National Natural Science Foundation of China (Nos. 82071147, 81571004, and 81500884).

SUPPLEMENTARY MATERIAL

The Supplementary Material for this article can be found online at: https://www.frontiersin.org/articles/10.3389/fneur.2021.540660/full#supplementary-material

REFERENCES

1. Asiry MA, Albarakati SF, Al-Marwan MS, Al-Shammari RR. Perception of pain and discomfort from elastomeric separators in saudi adolescents. *Saudi Med J*. (2014) 35:504–7.
2. Kavaliauskiene A, Smailiene D, Buskiene I, Keriene D. Pain and discomfort perception among patients undergoing orthodontic treatment: Results from one month follow-up study. *Stomatologija*. (2012) 14:118–25.
3. Long H, Wang Y, Jian F, Liao LN, Yang X, Lai WL. Current advances in orthodontic pain. *Int J Oral Sci.* (2016) 8:67–75. doi: 10.1038/ijos.2016.24
4. d'Apuzzo F, Cappabianca S, Ciavarella D, Monsurro A, Silvestrini-Biavati A, Perillo L. Biomarkers of periodontal tissue remodeling during orthodontic tooth movement in mice and men: overview and clinical relevance. *Sci World J*. (2013) 2013:105873. doi: 10.1155/2013/105873
5. Gameiro GH, Schultz C, Trein MP, Mundstock KS, Weidlich P, Goularte JF. Association among pain, masticatory performance, and proinflammatory cytokines in crevicular fluid during orthodontic treatment. *Am J Orthod Dentofacial Orthop*. (2015) 148:967–73. doi: 10.1016/j.ajodo.2015.05.029
6. Long H, Liao L, Gao M, Ma W, Zhou Y, Jian F, et al. Periodontal cgrp contributes to orofacial pain following experimental tooth movement in rats. *Neuropeptides*. (2015) 52:31–7. doi: 10.1016/j.npep.2015.06.006
7. Luppanapornlarp S, Kajii TS, Surarit R, Iida J. Interleukin-1beta levels, pain intensity, and tooth movement using two different magnitudes of continuous orthodontic force. *Eur J Orthod*. (2010) 32:596–601. doi: 10.1093/ejo/cjp158
8. Qiao H, Zhou H, Zhu YJ, Gao YN. The change of calcitonin gene- related peptide in periodontal tissue during orthodontic tooth movement. *Shanghai Kou Qiang Yi Xue*. (2012) 21:606–11.
9. Levi-Montalcini R, Skaper SD, Dal Toso R, Petrelli L, Leon A. Nerve growth factor: From neurotrophin to neurokine. *Trends Neurosci*. (1996) 19:514–20. doi: 10.1016/S0166-2236(96)10058-8
10. Hefti FF, Rosenthal A, Walicke PA, Wyatt S, Vergara G, Shelton DL, et al. Novel class of pain drugs based on antagonism of NGF. *Trends Pharmacol Sci*. (2006) 27:85–91. doi: 10.1016/j.tips.2005.12.001
11. Zhang X, Huang J, McNaughton PA. NGF rapidly increases membrane expression of trpv1 heat-gated ion channels. *EMBO J*. (2005) 24:4211–23. doi: 10.1038/sj.emboj.7600893
12. Zhu W, Galoyan SM, Petruska JC, Oxford GS, Mendell LM. A developmental switch in acute sensitization of small dorsal root ganglion (drg) neurons to capsaicin or noxious heating by NGF. *J Neurophysiol*. (2004) 92:3148–52. doi: 10.1152/jn.00356.2004
13. Kurata S, Goto T, Gunjigake KK, Kataoka S, Kuroishi KN, Ono K, et al. Nerve growth factor involves mutual interaction between neurons and satellite glial cells in the rat trigeminal ganglion. *Acta Histochem Cytochem*. (2013) 46:65–73. doi: 10.1267/ahc.13003
14. Shinoda M, Asano M, Omagari D, Honda K, Hitomi S, Katagiri A, et al. Nerve growth factor contribution via transient receptor potential vanilloid 1 to ectopic orofacial pain. *J Neurosci*. (2011) 31:7145–55. doi: 10.1523/JNEUROSCI.0481-11.2011
15. Diogenes A, Akopian AN, Hargreaves KM. NGF up-regulates trpa1: Implications for orofacial pain. *J Dent Res*. (2007) 86:550–5. doi: 10.1177/154405910708600612
16. Mamet J, Lazdunski M, Voilley N. How nerve growth factor drives physiological and inflammatory expressions of acid-sensing ion channel 3 in sensory neurons. *J Biol Chem*. (2003) 278:48907–13. doi: 10.1074/jbc.M309468200
17. Long H, Shan D, Huang R, Liu H, Zhou Y, Gao M, et al. Bite force measurements for objective evaluations of orthodontic tooth movement-induced pain in rats. *Arch Oral Biol*. (2019) 101:1–7. doi: 10.1016/j.archoralbio.2019.02.002
18. Huang RH. *The Effect of Periodontal Blockade of Nerve Growh Factor Signaling on Tooth Movement Pain in rats*. Doctorate thesis, Sichuan University, Chengdu (2017).
19. Wang Q, Ou C, Wei X, Yu Y, Jiang J, Zhang Y, et al. Cc chemokine ligand 19 might act as the main bursal t cell chemoattractant factor during ibdv infection. *Poult Sci*. (2019) 98:688–94. doi: 10.3382/ps/pey435
20. Nair A, Gan J, Bush-Joseph C, Verma N, Tetreault MW, Saha K, et al. Synovial chemokine expression and relationship with knee symptoms in patients with meniscal tears. *Osteoarthritis Cartilage*. (2015) 23:1158–64. doi: 10.1016/j.joca.2015.02.016
21. Schmitz K, Pickert G, Wijnvoord N, Haussler A, Tegeder I. Dichotomy of ccl21 and cxcr3 in nerve injury-evoked and autoimmunity-evoked hyperalgesia. *Brain Behav Immun*. (2013) 32:186–200. doi: 10.1016/j.bbi.2013.04.011
22. Malon JT, Cao L. Calcitonin gene-related peptide contributes to peripheral nerve injury-induced mechanical hypersensitivity through CCL5 and p38 pathways. *J. Neuroimmunol*. (2016) 297:68–75. doi: 10.1016/j.jneuroim.2016.05.003
23. Reed WR, Little JW, Lima CR, Sorge RE, Yarar-Fisher C, Eraslan M, et al. Spinal mobilization prevents ngf-induced trunk mechanical hyperalgesia and attenuates expression of cgrp. *Front Neurosci*. (2020) 14:385. doi: 10.3389/fnins.2020.00385
24. Liang H, Hu H, Shan D, Lyu J, Yan X, Wang Y, et al. CGRP Modulates Orofacial Pain through Mediating Neuron-Glia Crosstalk. *J Dent Res*. (2021) 100:98–105. doi: 10.1177/0022034520950296
25. Kilkenny C, Browne WJ, Cuthill IC, Emerson M, Altman DG. Improving bioscience research reporting: The arrive guidelines for reporting animal research. *J Pharmacol Pharmacother*. (2010) 1:94–99. doi: 10.4103/0976-500X.72351
26. Long H, Liao L, Zhou Y, Shan D, Gao M, Huang R, et al. A novel technique of delivering viral vectors to trigeminal ganglia in rats. *Eur J Oral Sci*. (2017) 125:1–7. doi: 10.1111/eos.12326
27. Liao L, Long H, Zhang L, Chen H, Zhou Y, Ye N, et al. Evaluation of pain in rats through facial expression following experimental tooth movement. *Eur J Oral Sci*. (2014) 122:121–24. doi: 10.1111/eos.12110
28. Guo R, Zhou Y, Long H, Shan D, Wen J, Hu H, et al. Transient receptor potential Vanilloid 1-based gene therapy alleviates orthodontic pain in rats. *Int J Oral Sci*. (2019) 11:11. doi: 10.1038/s41368-019-0044-3
29. Yang Z, Luo W, Wang J, Tan Y, Fu R, Fang B. Chemokine ligand 2 in the trigeminal ganglion regulates pain induced by experimental tooth movement. *Angle Orthod*. (2014) 84:730–6. doi: 10.2319/090213-643.1
30. Lyu J, Wen J, Guo R, Zhu Y, Liang H, Gao M, et al. Botulinum toxin A alleviates orofacial nociception induced by orthodontic tooth movement through nociceptin/orphanin-FQ pathway in rats. *Arch Oral Biol*. (2020) 117:104817. doi: 10.1016/j.archoralbio.2020.104817
31. Meng J, Ovsepian SV, Wang J, Pickering M, Sasse A, Aoki KR, et al. Activation of trpv1 mediates calcitonin gene-related peptide release, which excites trigeminal sensory neurons and is attenuated by a retargeted

botulinum toxin with anti-nociceptive potential. *J Neurosci*. (2009) 29:4981–92. doi: 10.1523/JNEUROSCI.5490-08.2009
32. Sood M, Bhatt P, Sessle BJ. Mechanical and thermal hypersensitivities associated with orthodontic tooth movement: A behavioral rat model for orthodontic tooth movement-induced pain. *J Oral Facial Pain Headache*. (2015) 29:60–69. doi: 10.11607/ofph.1336
33. Yang H, Shan D, Jin Y, Liang H, Liu L, Guan Y, et al. The role of acid-sensing ion channel 3 in the modulation of tooth mechanical hyperalgesia induced by orthodontic tooth movement. *Neuroscience*. (2020) 442:274–85. doi: 10.1016/j.neuroscience.2020.06.023
34. Jiang BC, He LN, Wu XB, Shi H, Zhang WW, Zhang ZJ, et al. Promoted interaction of c/ebpalpha with demethylated cxcr3 gene promoter contributes to neuropathic pain in mice. *J Neurosci*. (2017) 37:685–700. doi: 10.1523/JNEUROSCI.2262-16.2016
35. Xie F, Wang Y, Li X, Chao YC, Yue Y. Early repeated administration of cxcr4 antagonist amd3100 dose-dependently improves neuropathic pain in rats after l5 spinal nerve ligation. *Neurochem Res*. (2016) 41:2289–99. doi: 10.1007/s11064-016-1943-8
36. Zhang ZJ, Jiang BC, Gao YJ. Chemokines in neuron-glial cell interaction and pathogenesis of neuropathic pain. *Cell Mol Life Sci*. (2017) 74:3275–91. doi: 10.1007/s00018-017-2513-1
37. Noor S, Wilson EH. Role of c-c chemokine receptor type 7 and its ligands during neuroinflammation. *J Neuroinflammation*. (2012) 9:77. doi: 10.1186/1742-2094-9-77
38. Mizumura K, Murase S. Role of nerve growth factor in pain. *Handb Exp Pharmacol*. (2015) 227:57–77. doi: 10.1007/978-3-662-46450-2_4

Conflict of Interest: The authors declare that the research was conducted in the absence of any commercial or financial relationships that could be construed as a potential conflict of interest.

Advantages of publishing in Frontiers

OPEN ACCESS
Articles are free to read for greatest visibility and readership

FAST PUBLICATION
Around 90 days from submission to decision

HIGH QUALITY PEER-REVIEW
Rigorous, collaborative, and constructive peer-review

TRANSPARENT PEER-REVIEW
Editors and reviewers acknowledged by name on published articles

Frontiers
Avenue du Tribunal-Fédéral 34
1005 Lausanne | Switzerland

Visit us: www.frontiersin.org
Contact us: frontiersin.org/about/contact

REPRODUCIBILITY OF RESEARCH
Support open data and methods to enhance research reproducibility

DIGITAL PUBLISHING
Articles designed for optimal readership across devices

FOLLOW US
@frontiersin

IMPACT METRICS
Advanced article metrics track visibility across digital media

EXTENSIVE PROMOTION
Marketing and promotion of impactful research

LOOP RESEARCH NETWORK
Our network increases your article's readership